ISSN 0021-9673
Period.

VOL. 476 AUGUST 4, 1989
COMPLETE IN ONE ISSUE

8th Int. Symp. on HPLC of proteins, peptides and polynucleotides Copenhagen, Oct. 31–Nov. 2, 1988

JOURNAL OF CHROMATOGRAPHY

INTERNATIONAL JOURNAL ON CHROMATOGRAPHY, ELECTROPHORESIS AND RELATED METHODS

SYMPOSIUM VOLUMES

ELSEVIER

JOURNAL OF CHROMATOGRAPHY

Scope. The *Journal of Chromatography* publishes papers on all aspects of chromatography, electrophoresis and related methods. Contributions consist mainly of research papers dealing with chromatographic theory, instrumental development and their applications. The section *Biomedical Applications*, which is under separate editorship, deals with the following aspects: developments in and applications of chromatographic and electrophoretic techniques related to clinical diagnosis or alterations during medical treatment; screening and profiling of body fluids or tissues with special reference to metabolic disorders; results from basic medical research with direct consequences in clinical practice; drug level monitoring and pharmacokinetic studies; clinical toxicology; analytical studies in occupational medicine.

Submission of Papers. Papers in English, French and German may be submitted, in three copies. Manuscripts should be submitted to: The Editor of *Journal of Chromatography*, P.O. Box 681, 1000 AR Amsterdam, The Netherlands, or to: The Editor of *Journal of Chromatography, Biomedical Applications*, P.O. Box 681, 1000 AR Amsterdam, The Netherlands. Review articles are invited or proposed by letter to the Editors. An outline of the proposed review should first be forwarded to the Editors for preliminary discussion prior to preparation. Submission of an article is understood to imply that the article is original and unpublished and is not being considered for publication elsewhere. For copyright regulations, see below.

Subscription Orders. Subscription orders should be sent to: Elsevier Science Publishers B.V., P.O. Box 211, 1000 AE Amsterdam, The Netherlands, Tel. 5803 911, Telex 18582 ESPA NL. The *Journal of Chromatography* and the *Biomedical Applications* section can be subscribed to separately.

Publication. The *Journal of Chromatography* (incl. *Biomedical Applications*) has 37 volumes in 1989. The subscription prices for 1989 are:

J. Chromatogr. + *Biomed. Appl.* (Vols. 461–497):
Dfl. 6475.00 plus Dfl. 999.00 (p.p.h.) (total *ca.* US$ 3737.00)

J. Chromatogr. only (Vols. 461–486):
Dfl. 5200.00 plus Dfl. 702.00 (p.p.h.) (total *ca.* US$ 2951.00)

Biomed. Appl. only (Vols. 487–497):
Dfl. 2200.00 plus Dfl. 297.00 (p.p.h.) (total *ca.* US$ 1248.50).

Our p.p.h. (postage, package and handling) charge includes surface delivery of all issues, except to subscribers in Argentina, Australia, Brasil, Canada, China, Hong Kong, India, Israel, Malaysia, Mexico, New Zealand, Pakistan, Singapore, South Africa, South Korea, Taiwan, Thailand and the U.S.A. who receive all issues by air delivery (S.A.L. — Surface Air Lifted) at no extra cost. For Japan, air delivery requires 50% additional charge; for all other countries airmail and S.A.L. charges are available upon request. Back volumes of the *Journal of Chromatography* (Vols. 1–460)are available at Dfl. 195.00 (plus postage). Claims for missing issues will be honoured, free of charge, within three months after publication of the issue. Customers in the U.S.A. and Canada wishing information on this and other Elsevier journals, please contact Journal Information Center, Elsevier Science Publishing Co. Inc., 655 Avenue of the Americas, New York, NY 10010. Tel. (212) 633-3750.

Abstracts/Contents Lists published in Analytical Abstracts, ASCA, Biochemical Abstracts, Biological Abstracts, Chemical Abstracts, Chemical Titles, Chromatography Abstracts, Current Contents/Physical, Chemical & Earth Sciences, Current Contents/Life Sciences, Deep-Sea Research/Part B: Oceanographic Literature Review, Excerpta Medica, Index Medicus, Mass Spectrometry Bulletin, PASCAL-CNRS, Referativnyi Zhurnal and Science Citation Index.

See inside back cover for Publication Schedule, Information for Authors and information on Advertisements.

0021-9673/89/$03.50

Printed in The Netherlands

For contents see p. VII.

For Superior Chiral Separation

CHIRALCEL, CHIRALPAK and CROWNPAK are now available from DAICEL and include 15types of HPLC columns which provide superior resolution of racemic compounds.

Drugs directly resolved on our DAICEL columns are given as follows;

SUBSTANCE	α	column
Alprenolol	3.87	OD
Amphetamine	1.2	CR
Atenoloi	1.58	OD
Atropine	1.62	OD
Baclofen	1.39	CR
Carbinoxamine	1.39	OD
Carteolol	1.86	OD
Chlophedianol	2.82	OJ
Chlormezanone	1.47	OJ
Cyclopentolate	2.47	OJ
Diltiazem	1.46	OD
	2.36	OF
	1.75	OG
Disopyramide	2.46	OF
Ethiazide	1.54	OF
Ethotoin	1.40	OJ
Fenoprofen	1.35	OJ
Glutethimide	2.48	OJ

SUBSTANCE	α	column
Gauifenesin	2.40	OD
Hexobarbital	1.7	CA-1
Homatropine	3.13	OD
Hydroxyzine	1.17	OD
Indapamide	1.58	OJ
Ketamine	complete resolution	CA-1
Ketoprofen	1.46	OJ
Mephobarbital	5.9	OJ
	2.3	CA-1
Methaqualone	2.8	CA-1
	7.3	OJ
Methsuximide	2.68	OJ
Metoprolol	complete resolution	OD
Mianserin	1.75	OJ
Nilvadipine	complete resolution	OT

SUBSTANCE	α	column
Oxapadol	complete resolution	CA-1
Oxazepan	4.36	OC
Oxazolam	1.67	OF
Oxprenolol	6.03	OD
Perisoxal	1.33	OF
	1.27	OD
Pindolol	5.07	OD
Piprozolin	1.7	CA-1
Praziquantal	complete resolution	CA-1
Propranolol	2.29	OD
Rolipram	complete resolution	CA-1
Sulconazole	1.68	OJ
Suprofen	1.6	OJ
Trimebutine	1.81	OJ
Warfarin	1.96	OC

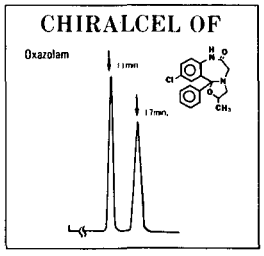

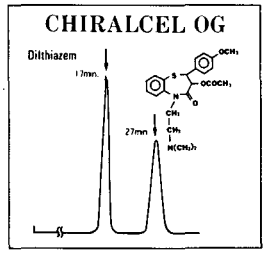

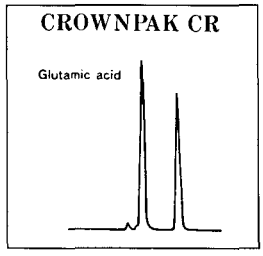

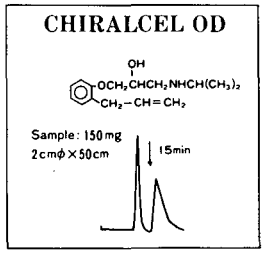

In addition to the drugs listed above, our chiral columns permit resolution also of the following: FMOC amino acids and Carboxylic acids, and Pesticides, for example Isofenfos, EPN and Acephate, and Synthetic intermediate 4-hydroxy cyclophentenone etc, Many other compounds besides these can be readily resolved.

▶ *Separation Service*

- A pure enantiomer separation in the amount of 100g~10kg is now available.
- Please contact us for additional information regarding the manner of use and application of our chiral columns and how to procure our separation service.

For more information about our Chiral Separation Service and Columns, please contact us!

DAICEL CHEMICAL INDUSTRIES, LTD.

Tokyo
8-1, Kasumigaseki 3-chome,
Chiyoda-ku, Tokyo 100, Japan
Phone: 03(507)3151, 3189
Telex: 222-4632 DAICEL J
FAX: 03(507)3193

DAICEL (U.S.A.) INC.
Fort Lee Executive Park
Two Executive Drive Fort Lee,
New Jersey 07024
Phone: (201)461-4466
FAX: (201)461-2776

DAICEL (U.S.A.), INC.
611 west 6th Street, Room 2152
Los Angeles California 90017
Phone: (213)629-3656
Telex: 215515 DCIL UR
FAX: (213)629-2109

DAICEL (EUROPA) GmbH
Königsallee 92a.
4000 Düsseldorf 1, F.R. Germany
Phone: (0211)134158
Telex: (41)8588042 DCEL D
FAX: (0211)879-8329

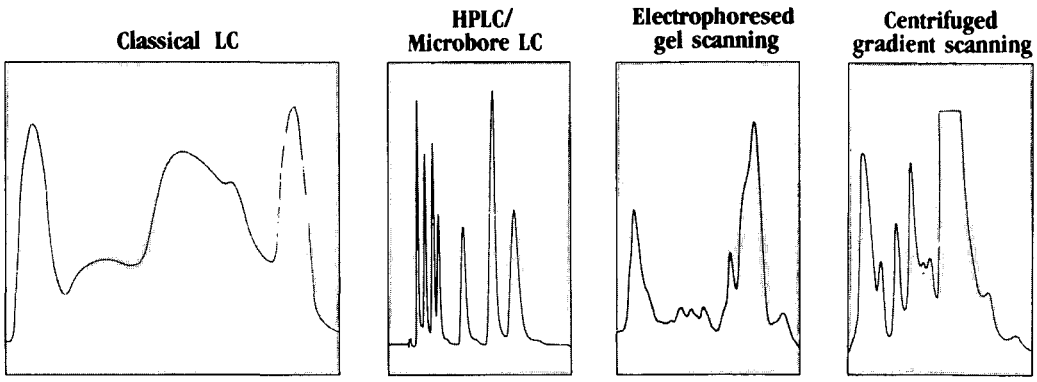

When your research expands, so should your instruments.

Primarily, the UA-5® is a sensitive absorbance detector for LC and HPLC. But it's also the key part of a multifunction instrument system for life-science research. Accessories turn the UA-5 into a fluorescence detector, a gel scanner, or a fractionator for centrifuged density gradients.

But the UA-5 is still the best all-around LC detector. Fifteen flow cells suit processes from production LC to microbore HPLC. A selection of 18 wavelengths means you can detect peptides at 214 nm, chlorophylls at 660 nm, and nearly everything else in between.

A UA-5 gives you a built-in recorder, simultaneous monitoring of two columns or two wavelengths, automatic scale expansion, and peak collection. But it costs no more than a single-purpose detector.

Learn more about what a UA-5 can do for you—send for your Isco catalog today. In the U.S.A., call **(800)228-4250.** Outside the U.S.A., contact your Isco dealer listed below.

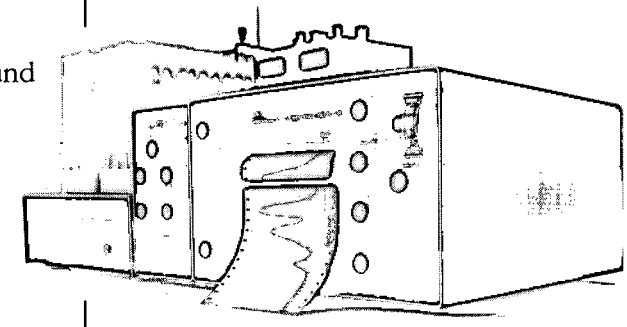

Isco Inc., P.O. Box 5347,
Lincoln NE 68505, U.S.A.
Isco Europe AG, Brüschstr. 17,
CH-8708 Männedorf, Switzerland

ISCO

Distributors • The Netherlands: Beun-de Ronde B.V. Abcoude 02946-3119 • **Hungary:** Lasis Handelsges. mbH Wien 82 01 83 • **Spain:** Iberlabo, s.a. Madrid 01 251 1491 • **W. Germany:** Colora Messtechnik GmbH Lorch, Württ. 07172 1830 • **France:** Ets. Roucaire, S.A. Velizy (1) 39469633 • **Italy:** Gio. de Vita e C. s.r.l. Roma 4950611 • **U.K.:** Life Science Laboratories, Ltd. Luton (0582) 597676 • **Norway:** Dipl. Ing. Houm A.S. Oslo 02 15 92 50 • **Finland:** ETEK OY, Helsinki 0 729 2748 • **Sweden:** SAVEN AB, Taby 8 792 1100 • **Switzerland:** IG Instrumenten-Gesellschaft AG Zurich 01 4613311 • **Belgium:** SA HVL NV Bruxelles (02) 720 48 30 • **Denmark:** Mikrolab Aarhus A/S Højbjerg 06-2961 11 • **Austria:** Neuber Gesellschaft mbH Wien 42 62 35 •

JOURNAL OF CHROMATOGRAPHY

VOL. 476 (1989)

JOURNAL *of* CHROMATOGRAPHY

INTERNATIONAL JOURNAL ON CHROMATOGRAPHY,
ELECTROPHORESIS AND RELATED METHODS

SYMPOSIUM VOLUMES

ELSEVIER
AMSTERDAM — OXFORD — NEW YORK — TOKYO

J. Chromatogr., Vol. 476 (1989)

Copenhagen (then named Hafnia) in 1690

0021-9673/89/$03.50

Printed in The Netherlands

SYMPOSIUM VOLUME

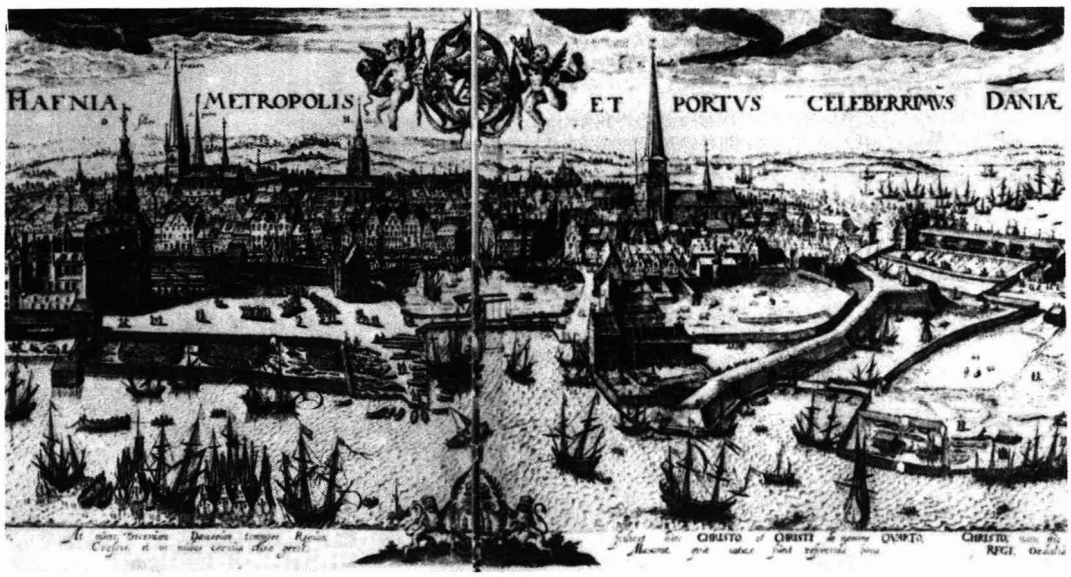

EIGHTH INTERNATIONAL SYMPOSIUM ON HIGH-PERFORMANCE LIQUID CHROMATOGRAPHY OF PROTEINS, PEPTIDES AND POLYNUCLEOTIDES

Copenhagen (Denmark), October 31–November 2, 1988

Guest Editors

JOSEPH J. DeSTEFANO
(Wilmington, DE, U.S.A.)

MILTON T. W. HEARN
(Melbourne, Australia)

JAN-CHRISTER JANSON
(Uppsala, Sweden)

FRED E. REGNIER
(West Lafayette, IN, U.S.A.)

KLAUS K. UNGER
(Mainz, F.R.G.)

VOL. 476 JOURNAL OF CHROMATOGRAPHY AUGUST 4, 1989

CONTENTS

8TH INTERNATIONAL SYMPOSIUM ON HIGH-PERFORMANCE LIQUID CHROMATOGRAPHY OF PROTEINS, PEPTIDES AND POLYNUCLEOTIDES, COPENHAGEN, OCTOBER 31–NOVEMBER 2, 1988

Journal of Chromatography, 476 (1989) 1
Elsevier Science Publishers B.V., Amsterdam — Printed in The Netherlands

FOREWORD

The *Eighth International Symposium on High-Performance Liquid Chromatography of Proteins, Peptides and Polynucleotides* was held at the Hotel Scandinavia Congress Centre, in Copenhagen, Denmark from October 31 to November 2, 1988. In common with earlier symposia in the series, this meeting was extremely successful, providing a stimulating forum for attendee participation and scientific contact. Discussion focused on the current status of developments related to high-resolution analysis and purification of biomacromolecules. The international basis of the substantial research effort in this important field of separation science was highlighted repeatedly throughout the symposium by the 400 attendees from 18 countries. In over 140 oral and poster presentations, the interlinked aspects of modern biopolymer analysis and/or preparative separation was addressed through consideration of the concepts and practical application of advances in column technology and support materials, protein biorecognition and conformation, retention processes, preparative chromatography, affinity chromatography, purity and quality control of proteins and glycoproteins, analysis of nucleic acids, analytical applications of high-performance electrophoresis and microanalytical techniques addressed to specific problems in the characterisation of biomacromolecules. The vigorous discussion sessions complemented the formal scientific programme whilst light relief with the opportunity for continued stimulating dialogues with colleagues was provided by the informal receptions well attended by scientists from academic, commercial or government laboratories keen to exchange information and ideas on recent developments and applications.

My symposium co-chairmen (J. J. DeStefano, J.-C. Janson, F. E. Regnier and K. K. Unger) and myself would like to express our appreciation for the lively and thought-provoking manner with which the oral and poster presentations were made. We also appreciated the smooth running of the symposium, ably managed by Bengt Österlund. Thanks are also due to Dr. Erich Heftmann for his tireless and meticulous efforts in the preparation of the proceedings volume. The generous sponsorship of the receptions by E. I. du Pont de Nemours and Co. Inc., Pharmacia LKB Biotechnology AB and Tosoh Corp., is also acknowledged. With the participation of E. I. du Pont de Nemours and Co., Inc. as one of the sponsors for this and subsequent symposia in the series, a new phase of development has commenced. To the retiring Scientific Committee member, C. Tim Wehr, the Scientific Committee would like to express its appreciation for his dedicated commitment to earlier symposia. Finally, we would like to thank all the scientists who came to Copenhagen, braved the rigours of a relatively mild three days of a Scandinavian autumn, and through their active participation in the oral, poster and discussion sessions made this symposium a success.

MILTON T. W. HEARN

Journal of Chromatography, 476 (1989) 3–19
Elsevier Science Publishers B.V., Amsterdam — Printed in The Netherlands

CHROMSYMP. 1626

FAST SEPARATION OF BIOLOGICAL MACROMOLECULES ON NON-POROUS, MICROPARTICULATE COLUMNS

GERARD P. ROZING* and HEINZ GOETZ
Hewlett-Packard GmbH, Waldbronn Analytical Division, P.O. Box 1280, D-7517 Waldbronn 2 (F.R.G.)

SUMMARY

The use of high-performance liquid chromatographic columns for the separation of proteins and nucleic acids is gradually increasing in biochemical laboratories. The efficiency of these columns for such separations has been much lower than that achievable for the separation of smaller molecules. Non-porous microparticulate packings are the logical answer one arrives at after consideration of the chromatographic behaviour of proteins. Non-porous stationary phases are described for the separation of proteins, peptides and nucleic acids. The stationary phases used are TSK-Gel NPR-C_{18}, TSK-Gel NPR-DEAE, TSK-Gel NPR-SP and HYTACH MicroPell C_{18}. A number of fundamental properties of columns based on these sorbents were evaluated, such as permeability, retention behaviour towards small and large molecules, load capacity and stability. Instrumental requirements for these columns are discussed and some applications described.

INTRODUCTION

High-performance liquid chromatographic (HPLC) separations of mixtures of biological macromolecules, such as proteins, on macroporous, microparticulate packings seem to be much poorer than the separation of mixtures of small molecules on the same column material. The lower performance is reflected in the increased zone broadening of the sample components and, therefore, in reduced efficiency and resolution. At the same time, only a much lower speed of separation is possible and longer separation times are necessary than for small-molecule separations.

HPLC separations of biological macromolecules on macroporous, microparticulate supports suffer from a few additional limitations relative to small molecule separations. Recovery of mass and/or biological activity is not quantitative in many instances. The mechanism of separation of macromolecules is not yet understood[1] as well as that of small molecules. Finally, the reproducibility of separations from column to column, even for the same brand of stationary phase, is much poorer in protein separations than for small-molecule separations. Reasons for all these problems can be classified as kinetic factors and thermodynamic factors.

0021-9673/89/$03.50

Kinetic factors

It should be emphasized that for zone broadening to be minimal, the reduced velocity, v ($v = ud_p/D_i$, where u is the velocity of the mobile phase, d_p is the particle size and D_i is the diffusion coefficient of the solute molecule in the mobile phase), must be optimum. Now, if the diffusion coefficient of the solute decreases, because of its higher molecular weight (MW) and/or because diffusion is hindered, the reduced velocity increases. Thus, if the flow-rate through the column, and therefore the mobile phase velocity u, are maintained at typical values for small-molecule separations, the reduced velocity will be too high to achieve optimum values of v for separations of high-molecular-weight substances. Counteracting this by reducing the linear velocity reduces zone broadening, but at the expense of a longer residence time of the solute with adverse consequences for separation time and recovery.

Although it is clear that, for the successful separation of biological macromolecules on HPLC materials, the pores must be enlarged (to > 300 Å), it should be pointed out that in many instances this will not be sufficient. The simple concept that biological macromolecules will assume a globular shape and therefore have a minimum surface/volume ratio is not valid in practice. Proteins have particular shapes, which are required for their biological functions, *e.g.*, phosphorylase *b* has a rectangular prism shape of $6.3 \times 6.3 \times 11.6$ nm^2. Therefore, the orientation of the macromolecule relative to the topography of the pore will have a large influence on its diffusion into the pores. Moreover, when the distance between the binding sites on the molecule and the interface decreases, the path of approach may become highly energetic, because the molecule has to be deformed for good binding.

Thermodynamic factors

In addition to kinetic causes, slow binding can be due to chemical reasons. A number of ancillary equilibria will play a role in the overall binding process, and each of these will have its own time requirement. In addition, large molecules will have multiple, similar interactions with the stationary phase and interactions of a different nature due to the heterogeneity of the stationary phase. Further, as it is the aim of a chromatographic separation of, *e.g.*, proteins to separate as much mass as possible, a high load capacity is desirable. This is achieved by improving the phase ratio of the stationary phase by increasing the surface area and ligand density. However, as a consequence, the number of solute–surface interactions increases, with detrimental effects on zone broadening.

Finally, in addition to all the solute–surface interactions, the macromolecules show many conformational and secondary chemical equilibria in the dissolved state. All these conformers and states have their own kinetics and constants of binding, in addition to time requirements for their interconversion. Hence more terms contribute to the overall broadening process than with small molecules.

A chromatographic approach that obviates these disadvantageous processes is the reduction of particle size, which counteracts the increase in reduced velocity. One could imagine pores that have an "infinite diameter" in addition to surfaces that are convex rather than concave, so that the steric hindrance during surface binding is minimized. Reduction of the phase ratio will minimize the number of interactions, while increased temperature will speed up the attainment of equilibria so that the

effects of slow kinetics in the sorption–desorption processes and in the mobile phase equilibria are minimized. Moreover, the favourable geometry of the packing material will also allow a much better coating of the stationary phase to provide a more homogeneous layer with uniform retention.

Non-porous, microparticulate packings have the potential to provide these improvements, especially when they are used at elevated temperature[3–12]. However, a number of questions arise concerning the applicability of these materials to HPLC separations of macromolecules. Reduction of the particle size will have consequences for the permeability of the columns and the column pressure drop. Does this become a practical limitation? Even if the design of the stationary phase is simple, does this help in understanding the separation mechanism better? Is the load capacity of these materials sufficient? What is the lifetime of these columns when they are operated at elevated temperature? What are the instrumental requirements for operating these columns successfully? Finally, for what kind of applications are these columns useful?

The purpose of this work was to investigate the applicability of non-porous, microparticulate columns to the separation of proteins, peptides and nucleic acids, together with the questions formulated above. In addition, a number of practical examples are described.

EXPERIMENTAL

Materials

All experiments were carried out on an HP 1090 Series M LC (Hewlett-Packard, Waldbronn, F.R.G.), equipped with a binary DR5 solvent-delivery system, a variable-volume injector with a 25- or a 250-μl loop installed, and equipped with a cooled sample compartment, a thermostated column compartment with integrated mobile-phase preheater (capillary 100 mm × 0.12 mm I.D., cast in the aluminium heater block). The built-in diode-array detector had a heat exchanger (capillary 550 mm × 0.12 mm I.D., cast in an aluminium block mounted on the detector sheet metal parts and a short 0.12 mm I.D. capillary cast in a small aluminium block mounted on the side of the flow cell) in front of the flow cell. The detection wavelength was set at 214 nm with a band width of 4 nm and the reference wavelength was set at 450 nm with a band width of 100 nm, unless stated otherwise. Control of the chromatographic system and data evaluation were achieved with Series HP 79994A Chemstation computer software.

The columns used were TSK-Gel NPR-C_{18}, -DEAE and -SP (35 mm × 4.6 mm I.D.), packed with 2.5-μm particles (Tosoh, Yamaguchi, Japan) and HYTACH MicroPell C_{18} (30 mm × 4.6 mm I.D. and 75 mm × 4.6 mm I.D.), packed with 1.5-μm particles (Glycotech, New Haven, CT, U.S.A.). For comparison, a 5-μm, 300-Å pore size VYDAC TP C_{18} column (250 mm × 4.6 mm I.D.) (Separations Group, Hesperia, CA, U.S.A.) and a TSK-Gel 5PW-SP column (75 mm × 7.5 mm I.D.), 10 μm, were used. All columns except the MicroPell columns were obtained from Hewlett-Packard.

TSK-gel is a non-porous, polymeric material, based on the well known PW material from Tosoh, which is a hydrophilic polymer. The NPR-PW gels are modified with the same coatings that are available in the porous 4PW and 5PW series, such as octadecyl, diethylaminoethyl and sulphopropyl for reversed-phase, weak anion-

exchange and strong cation-exchange chromatography, respectively[6]. HYTACH MicroPell C_{18} is a non-porous silica-based material which is modified by conventional coating procedures with materials having the octadecyl functionality. This material has been described in detail by Kalgathi and Horváth[12].

Details of experimental conditions are given in the Figure legends.

Ribonuclease A (RNAse), insulin (INS), lysozyme (LYS), bovine serum albumin (BSA) and ovalbumin (OVA) were purchased from Sigma (Deisenhofen, F.R.G.) and used without further purification. DNA restriction fragments were purchased from New England Biolabs (Schwalbach, F.R.G.).

The isocratic column test was carried out with a standard test sample containing dimethyl phthalate (DMP), diethyl phthalate (DEP), biphenyl (BP) and *o*-terphenyl (*o*-TER), 0.1% (w/v) in methanol.

Trifluoroacetic acid (TFA) used in the mobile phase was of Sequanal grade from Pierce (Rockford, IL, U.S.A.). All buffer salts were of analytical-reagent grade and obtained from E. Merck (Darmstadt, F.R.G.). Water used for the mobile phases was purified with an HP 661 water purification system (Hewlett-Packard). All other solvents for mobile phase preparation were of chromatographic grade.

Methods

Phototropically grown cells from the photosynthetic purple bacterium *Rhodopseudomonas viridis* were broken by sonification (buffer: 20 m*M* Tris–HCl–0.1% EDTA–0.02% sodium azide, pH 7.0, 4°C). After centrifugation for 40 min at 16 000 *g*, the samples were adjusted to pH 5 by addition of 2 *M* HCl for cation-exchange chromatography. The samples were centrifuged for 5 min at 1500 *g* prior to injection on to the column.

A 1-mg amount of recombinant human interferon was incubated with L-1-tosylamide-2-phenylethyl chloromethyl ketone (TCPK)-treated trypsin (Sigma) in 0.1 *M* ammonium hydrogencarbonate buffer–0.01 *M* calcium chloride (pH 8) at 37°C for 8 h using an enzyme/protein ratio of 1:30 (w/w). The reaction was stopped by adjusting the pH of the solution to 2 with 1 *M* hydrochloric acid.

RESULTS AND DISCUSSION

Separation performance

Fig. 1a and b illustrate the separation efficiency that can be achieved with non-porous, microparticulate columns. Both chromatograms were obtained with the 35 × 4.6 mm I.D. TSK-Gel NPR-C_{18} column. The resolution in Fig. 1a is very high, so that by increasing the flow-rate and gradient speed, a much faster separation is possible. These conditions were chosen in Fig. 1b. The peak widths at the base are 3–5 s.

The real separation power of this type of column is illustrated in Fig. 2. Here, identical elution conditions were used for the separation of the protein test mixture on a TSK-Gel NPR-C_{18} column and on a macroporous, reversed-phase type of column (VYDAC C_{18}, 5 μm, 250 mm × 4.6 mm I.D.). Although a comparable speed of separation and zone broadening are achieved on the VYDAC column, the resolution is much better on the NPR column. Moreover, in Fig. 2b, BSA starts to show broadening due to some of the factors described in the Introduction. The combined effect of the

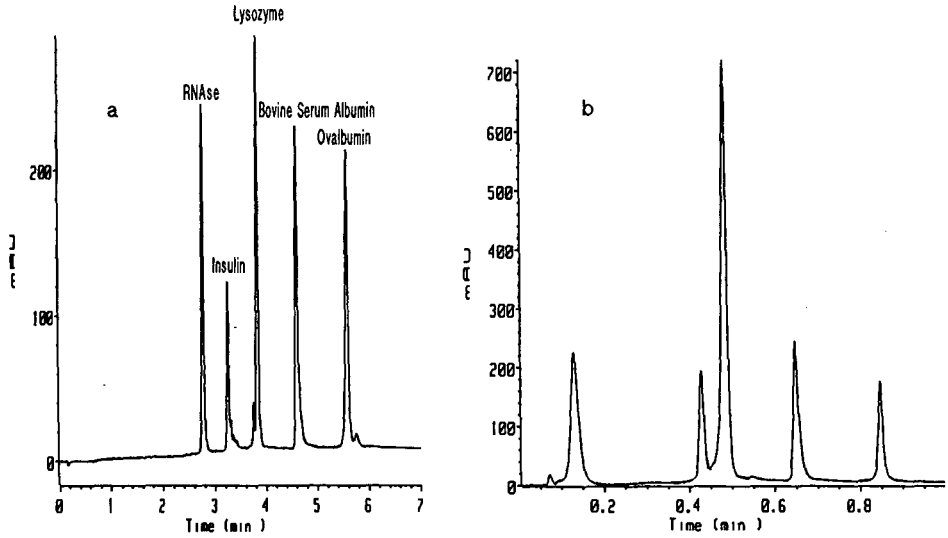

Fig. 1. Fast reversed-phase separation of protein test mixture on TSK-Gel NPR-C_{18} column by gradient elution. Column, 35 × 4.6 mm I.D., 2.5 μm; injection volume, 2 μl (1 mg/ml of each protein); eluent A, 0.1% aqueous TFA; eluent B, 0.1% TFA in acetonitrile. (a) Flow-rate, 1.5 ml/min; gradient from 10 to 60% B in 10 min; column temperature, 40°C. (b) Flow-rate, 3.0 ml/min; gradient from 20 to 60% B in 0.4 min; column temperature, 80°C.

low volume of the NPR column and the intrinsic efficiency of the small particles is responsible for the improved performance. Comparable resolution can be obtained on the VYDAC column, but at a much lower gradient speed.

In Fig. 3, a similar comparison is made between a non-porous and a porous strong cation exchanger (TSK-Gel 5PW-SP, 75 mm × 7.5 mm I.D., 10 μm *vs.*

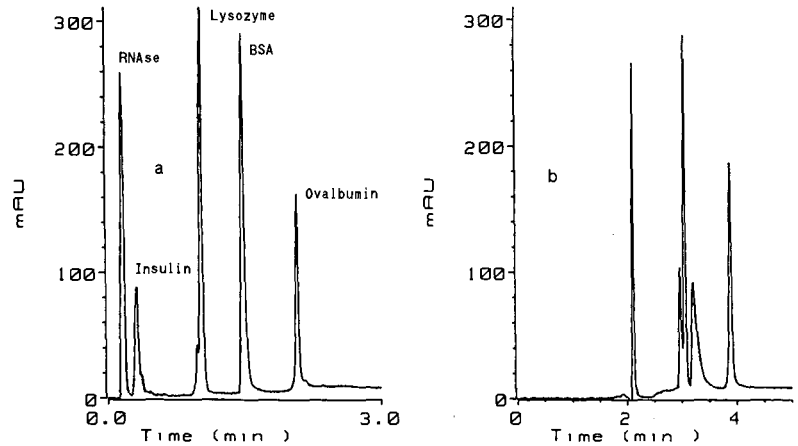

Fig. 2. Comparison of fast reversed-phase gradient elution of protein test mixture on TSK-Gel NPR-C_{18} and VYDAC C_{18} columns. Experimental conditions as in Fig. 1, except flow-rate, 1.5 ml/min; gradient from 27.5 to 57.5% B in 2 min; column temperature, 40°C. (a) Column, TSK-Gel NPR-C_{18}, 35 × 4.6 mm I.D., 2.5 μm; (b) column, VYDAC C_{18}, 250 × 4.6 mm I.D., 5 μm.

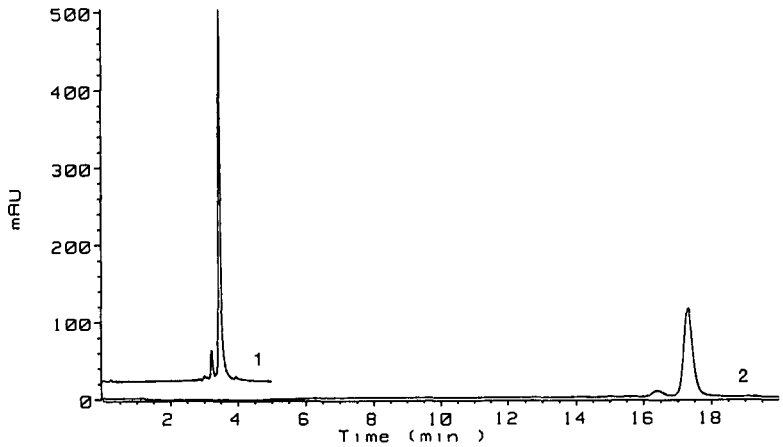

Fig. 3. Purification of a crude lysozyme preparation on porous and non-porous TSK-Gel Sulfopropyl columns. Flow-rate, 1.0 ml/min; eluent A, 0.02 *M* aqueous KH_2PO_4 (pH 6); eluent B, same as A but containing 0.5 *M* NaCl; column temperature, 50°C; sample, 4.5 μg crude lysozyme. (1) Column, TSK-Gel NPR-SP, 35 × 4.6 mm I.D., 2.5 μm; gradient from 0 to 100% B in 5 min; (2) column, TSK-Gel 5PW-SP, 75 × 7.5 mm I.D., 10 μm; gradient from 0 to 100% B in 20 min.

TSK-Gel NPR-SP, 35 mm × 4.6 mm I.D., 2.5 μm). A crude lysozyme preparation was used as a test sample. A five-fold improvement in separation speed and in peak height (solute concentration) is obtained through the combined effect of the low volume of the NPR column, faster gradient and intrinsic efficiency of the packing material. At the same time, it may be observed that the selectivity of the NPR packing is identical with that of the porous support, as illustrated by the elution of the impurities in front of the main peak.

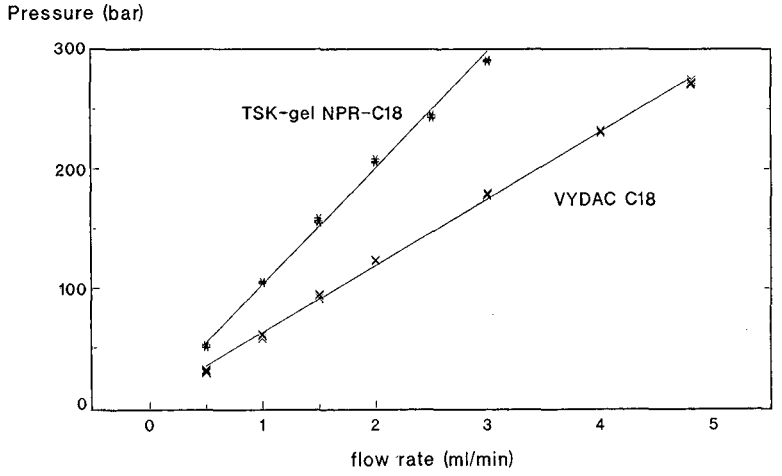

Fig. 4. Column pressure *vs.* flow-rate. Mobile phase, acetonitrile; temperature, ambient. *, TSK-Gel NPR-C_{18} column, 35 × 4.6 mm I.D., 2.5 μm; regression coefficient, 0.9973, permeability, 0.0032 μm^2; column resistance factor, 1950. ×, VYDAC C_{18} column, 250 × 4.6 mm I.D., 5 μm; regression coefficient, 0.9980; permeability, 0.0339 μm^2; column resistance factor, 737.

Column permeability

The permeability of the TSK-Gel NPR-C_{18} column was calculated by the Darcy equation[13] from the slope of the plot of column pressure *vs.* flow-rate (Fig. 4). For reference, the permeability of a VYDAC C_{18} column was obtained in the same way. VYDAC C_{18} is a porous, silica-based reversed-phase material. The column permeability was normalized as the dimensionless column resistance factor. This eliminates the influence of particle size on the permeability and allows the assessment of the influence of packing density and particle shape.

Values of the column resistance factor between 500 and 700 are regarded as optimum for spherical particles[14]. The VYDAC column showed an almost optimum value of 737. The TSK-Gel NPR C_{18} column showed a value three times higher. There may be several reasons for this result, *e.g.*, presence of fines, a smaller nominal particle size or a reduction of the interparticulate space. The last reason proved to be the correct one, as is illustrated in the scanning electron microscope (SEM) picture of particles from an unpacked column in Fig. 5. Some particles have been squeezed together so that only a minimal interparticulate space remained. However, the pressure–flow curve is linear, and no hysteresis was observed. This indicates a very stable column bed, and this was corroborated by the results of the stability tests.

Separation of small molecules

We were interested in verifying whether the high separation efficiency of the TSK-Gel NPR-C_{18} column for proteins could also be useful for small-molecule separations. For this purpose, a simple isocratic column test was carried out, and the result was compared with that for the VYDAC C_{18} and the HYTACH Micro-Pell C_{18} columns (Fig. 6).

The VYDAC column showed excellent efficiency for the four aromatic test solutes (Fig. 6b). Obviously, a lower organic solvent content of the mobile phase is needed in order to achieve a retention on the NPR columns comparable to that on the VYDAC column (8% and 30% acetonitrile *vs.* 70% acetonitrile). However, the peak

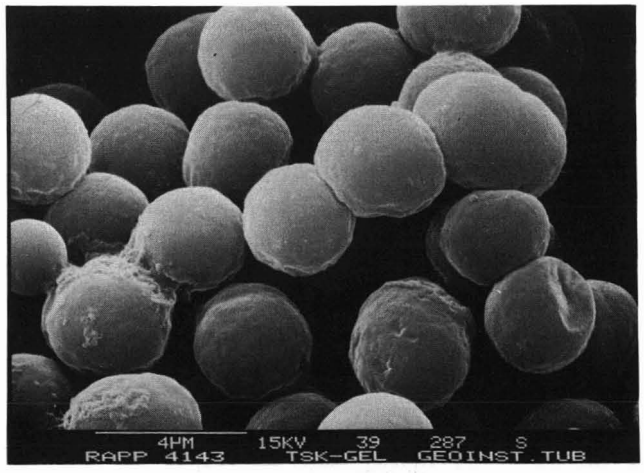

Fig. 5. Scanning electron micrograph of TSK-Gel NPR-C_{18} particles after unpacking a column.

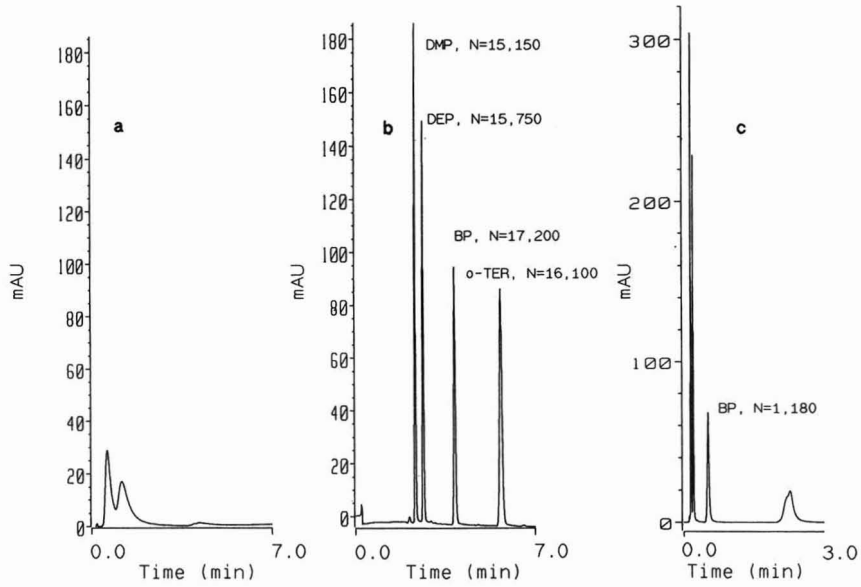

Fig. 6. Comparison of column performance with low-molecular-weight solutes. Flow-rate, 1.5 ml/min; sample, isocratic test sample; injection volume, 1 μl; detection, 254 nm; column temperature, 40°C. (a) Column, TSK-Gel NPR-C_{18}, 35 × 4.6 mm I.D., 2.5 μm; eluent 8% aqueous acetonitrile. (b) Column, VYDAC C_{18}, 250 × 4.6 mm I.D., 5 μm; eluent, 70% aqueous acetonitrile. (c) Column, HYTACH MicroPell C_{18}, 30 × 4.6 mm I.D., 1.5 μm; eluent, 30% aqueous acetonitrile.

shape was very poor and only two peaks were eluted on the TSK-Gel NPR-C_{18} column (Fig. 6a).

Our interpretation is that only DMP and DEP were eluted and that the BP and *o*-TER peaks were broadened so much that they were indistinguishable from the baseline. This is indicative of very poor kinetics of partitioning for the small molecules. The poor kinetics can be caused by the presence of small cracks in the NPR beads or by intercalation of the small-solute molecules in the reticular structure of the polymer. Whatever reason applies, larger molecules will not be subject to these problems and will partition only at the outside of the particle.

In contrast to this observation, the HYTACH MicroPell C18 columns showed good peak shapes for the first three eluting substances (Fig. 6c). The fourth test analyte, *o*-TER, however, is broadened substantially. Moreover, it is striking that on this column, a relatively high concentration of acetonitrile in the mobile phase compared with the TSK-Gel NPR-C_{18} column is necessary to cause elution. Both observations are consistent with the conclusion that the silica-based NPR material is not really "non-porous" for small solutes.

Load capacity

In order to determine whether NPR columns can be used for the separation of larger amounts of proteins, the mass of the solutes injected was varied systematically (Fig. 7). A two-component sample was prepared, and the sample volume was increased. Two observations were made: first, the band width increases with increased

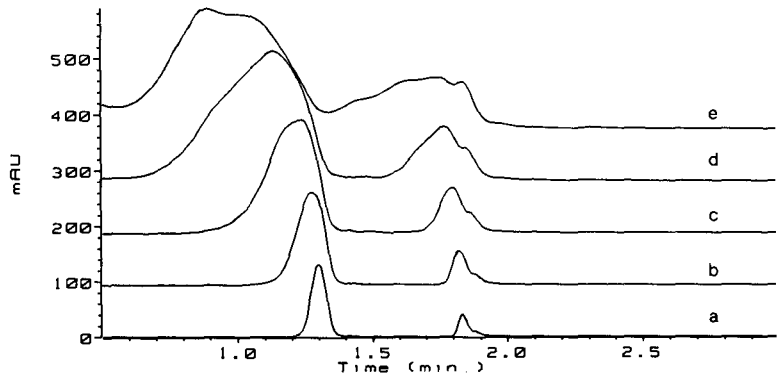

Fig. 7. Load capacity of NPR columns for proteins. Flow-rate, 1.5 ml/min; eluent A, 0.1% aqueous TFA; eluent B, 0.1% TFA in acetonitrile; gradient from 20 to 60% B in 3 min; column, TSK-Gel NPR-C_{18}, 35 × 4.6 mm I.D., 2.5 μm; column temperature, 80°C. (a) Injection volume 5 μl, 13 μg lysozyme, 12 μg BSA; (b) injection volume 10 μl, 26 μg lysozyme, 24 μg BSA; (c) injection volume 20 μl, 52 μg lysozyme, 48 μg BSA; (d) injection volume 40 μl, 104 μg lysozyme, 96 μg BSA; (e) injection volume 75 μl, 195 μg lysozyme, 180 μg BSA.

load, but in a way very similar to the empirical and theoretical models developed by Snyder *et al.*[15] and Ghodbane and Guiochon[16] for small molecules; and second, the small shoulder on the BSA peak stays partly resolved when the load is increased, demonstrating the high efficiency of the column.

The available surface area on the NPR material amounts to 1750 cm^2 per unit column volume (assuming an interparticulate porosity of 0.25). This means that at the lowest load (trace a in Fig. 7) the overall BSA concentration at the surface of the bead is approximately 0.1 pmol/cm^2. Monolayer coverage of BSA on a surface amounts to a surface concentration of 1 pmol/cm^2 (ref. 17). The available stationary phase surface is thus used very efficiently in these columns, providing still reasonable resolution at high load conditions. In fact, the question of load capacity as a stationary phase property becomes relatively unimportant. The proper question to ask for preparative work on these columns is, "how much resolution can be sacrificed in order to improve the throughput?"

Recovery studies

It was expected from the considerations described in the Introduction that NPR columns would show improved recovery. This was verified quantitatively (Fig. 8). The benchmark protein separation was repeated three times, and a blank run was performed immediately afterwards (Fig. 8a and b). As can be seen, a trace of BSA and a relatively large ovalbumin peak were produced. The recovery, based on peak-area measurement, was 64% for ovalbumin. This is corroborated by data published by Kato *et al.*[6]. Ovalbumin is a relatively hydrophobic protein, known to give poor recovery from reversed-phase columns.

The column could be easily cleaned up by injection of glacial acetic acid (Fig. 8c). The low column volume, combined with the low surface area per column, allows for efficient cleaning of the column merely by injection of small volumes of cleaning liquids rather than pumping these, in most instances, very aggressive solvents with the expensive HPLC pump.

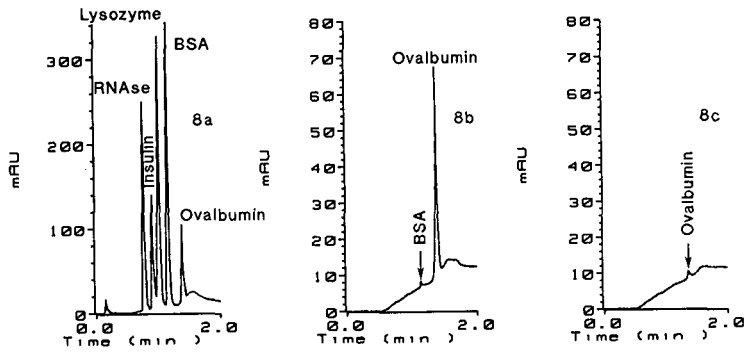

Fig. 8. Protein recovery on NPR columns. Conditions as in Fig. 7, except gradient from 20 to 60% B in 1 min; column temperature, 40°C; sample, protein test mixture; injection volume, 2 μl.

In a separate series of experiments with increased column temperature and increased mobile phase flow-rate, the recovery of ovalbumin was quantitative. These conditions were applied in the precision studies detailed in Table I. Because excellent repeatability of peak heights and peak areas was obtained, it can be asserted that the recovery was quantitative in this test.

Column stability

The elevated temperatures used to operate these columns render the mobile phase highly aggressive, generating concern about the stability of the column bed and also potential bleeding of the C_{18} coating from the bead surface. This would have consequences for the separation efficiency and retention behaviour of the solutes, and bleeding of the coating would contaminate the collected fractions. Therefore, the stability of the columns was investigated. Two procedures were used for the test. In the first, a slow gradient from 10:90 to 90:10 eluent A (0.1% aqueous TFA)–eluent B (0.1% TFA in acetonitrile) at a low flow-rate of 1.0 ml/min was applied at 75°C for 36 h. The efficiency of the column was checked before and after the test (Fig. 9a and b).

TABLE I

QUANTITATIVE PRECISION ON TSK-Gel NPR-C_{18} COLUMN

Experimental conditions: column, 35 mm × 4.6 mm I.D.; flow-rate, 3.0 ml/min; eluent A, 0.1% aqueous TFA; eluent B, 0.1% TFA in acetonitrile; gradient from 20 to 60% B in 2 min; column temperature, 80°C; injection volume, 2 μl; No. of replicates, 9.

Solute	*Relative standard deviation (%)*		
	Retention time	*Peak height*	*Peak area*
RNAse	1.1	2.0	0.5
Insulin	0.1	1.7	7.0
Lysozyme	0.2	1.1	0.4
BSA	0.1	1.3	1.8
Ovalbumin	0.1	1.1	1.3

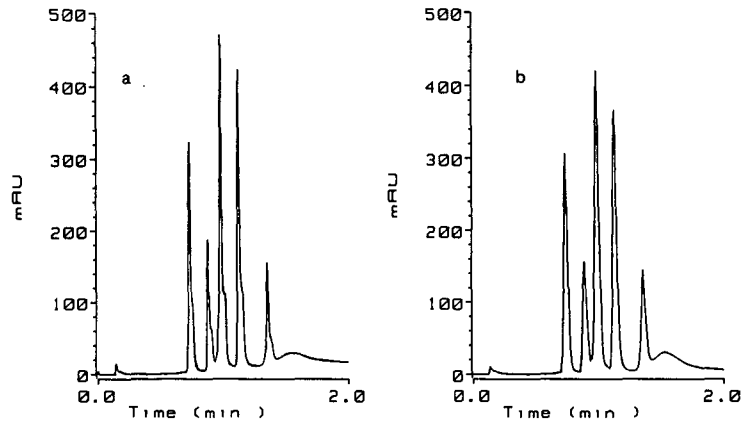

Fig. 9. Stability test of TSK-Gel NPR-C_{18}. Comparison of performance before and after stress test. Stress test conditions: eluent A, 0.1% aqueous TFA; eluent B, 0.1% TFA in acetonitrile; gradient from 10 to 90% B in 90 min; flow-rate, 1.0 ml/min; column temperature, 75°C. Performance test conditions: identical with those in Fig. 8. (a) Starting chromatogram; (b) after 36 h of stress test.

After this test, the same column was operated under faster conditions, with a flow-rate of 1.5 ml/min and a gradient from 80:20 to 40:60 A–B in 3 min, at a column temperature of 80°C, and the protein test mixture was injected continuously (Fig. 10a–c). The overall duration of the test was 7 days, during which time 40 000 column volumes of mobile phase were flushed through the column. As a separation takes 10–20 column volumes to be complete, this is equivalent to 2000–4000 injections. The experiments were carried out with the TSK-Gel NPR-C_{18} column. No sign of column deterioration was observed. The peak shape even improved slightly during the test (compare Fig. 10b and c), whereas none of the peak retention times changed significantly.

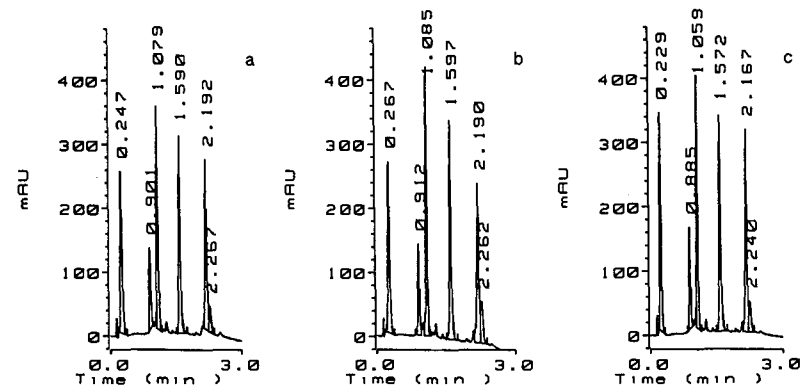

Fig. 10. Stability test of TSK-Gel NPR-C_{18} by repetitive injection of the protein test mixture. Conditions as in Fig. 7, except test sample, protein test mixture; injection volume, 2 μl. (a) First injection; (b) after 186 injections; (c) after 311 injections.

Instrumental requirements

The low column volume and high intrinsic efficiency of the NPR columns place strict demands on the instrumentation used to operate these columns successfully. A number of these requirements were investigated here.

It has been reported[18] that mere thermostating of HPLC columns at high temperature is inadequate. The large temperature difference between the incoming mobile phase and the column itself readily destroys the separation efficiency because of the temperature gradients that are generated. This can be overcome by heating the mobile phase to the column temperature prior to entering the column. Most modern HPLC instruments provide this facility. The effect of omitting mobile phase preheating is demonstrated in Fig. 11. The expanded part of the trace shows the ovalbumin peak, which is doubled in Fig. 11b (as are all the other peaks).

After leaving the column, the temperature of the mobile phase will be substantially different from the temperature of the detector flow cell. As a consequence, temperature-mediated refractive index effects will be transmitted to the detector, leading to apparent light absorption and noise. This is illustrated in Fig. 12b. Efficient mobile phase thermostating to the temperature in the detector is required. This is achieved by an efficient, dual-stage, passive heat exchanger, which consists of a large stage with a high capacity and a small, fast heat exchanger, mounted directly on the flow cell to eliminate fast, low-amplitude temperature fluctuations. The beneficial effect of this adjustment is seen in Fig. 12a. The noise in this instance is down to 0.1 mAU, whereas without thermostating a 20–50-fold higher noise level is observed. The overall volume of this heat exchanger is approximately 6 μl, and no performance loss due to band spreading is observed.

The fast gradients used have consequences for the ability of the pumping system to generate these mobile phase compositions in a reproducible, linear and rapid manner. A low dead volume between the mixing point and the head of the column is required to allow rapid transfer of the gradient profile and to avoid excessive spreading and rounding of the gradient profile. The actual profile was checked by normal HPLC

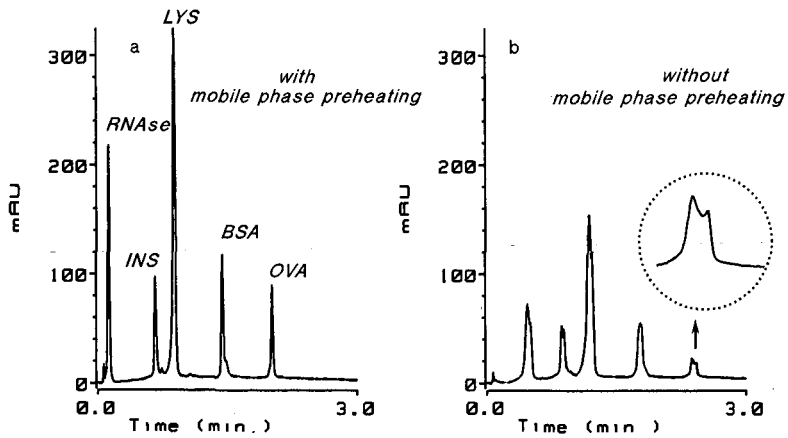

Fig. 11. Influence of mobile phase preheating on column performance. Conditions as in Fig. 7, except test sample is protein test mixture; injection volume, 2 l. (a) With mobile phase preheating; (b) without mobile phase preheating.

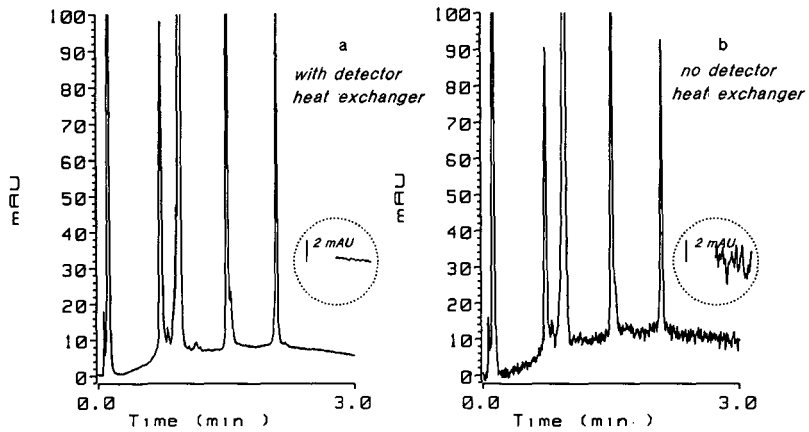

Fig. 12. Influence of mobile phase thermostating on detector performance. Conditions as in Fig. 7, except test sample is protein test mixture. (a) With detector heat exchanger; (b) without detector heat exchanger.

pump performance verification tests in which the TFA was eliminated from eluents A and B, and 0.5% (v/v) acetone was used as a tracer in eluent B. In the pump test no column was used. The profile that is generated now is easily monitored (Fig. 13). A small delay volume, 510 μl, of which *ca.* 300 μl originates from the sample loop, was found. Low rounding at the points where the gradient starts and ends indicates a slight spreading in the delay volume. Even at the highest speed (100% change per minute) the major part of the trace was linear.

Applications

Soluble cytochrome *c*2 is present in the supernatant of the purple bacterium *Rhodopseudomonas viridis*, described under Experimental. Direct injection of 50 μl of the supernatant into a TSK-Gel NPR-SP column allows the isolation of 0.5 μg of the pure cytochrome *c*2 directly (Fig. 14). Previously, chromatographic isolation of this

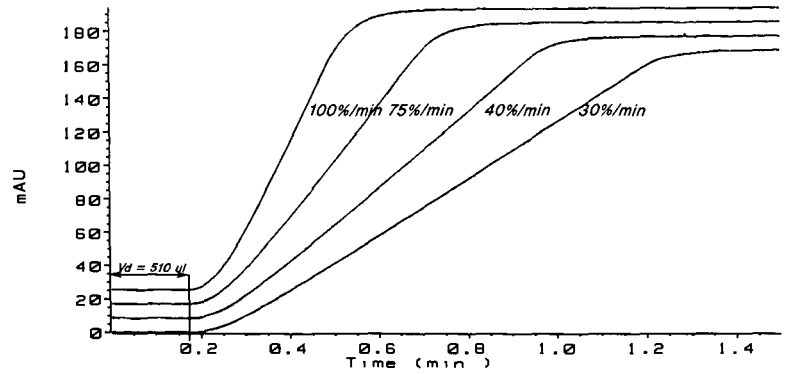

Fig. 13. Demonstration of pump performance for fast gradient elution. Conditions: flow-rate, 3.0 ml/min; eluent A, water; eluent B, 0.5% acetone in acetonitrile; gradient from 27.5 to 57.5% B, without column, detection at 275 nm.

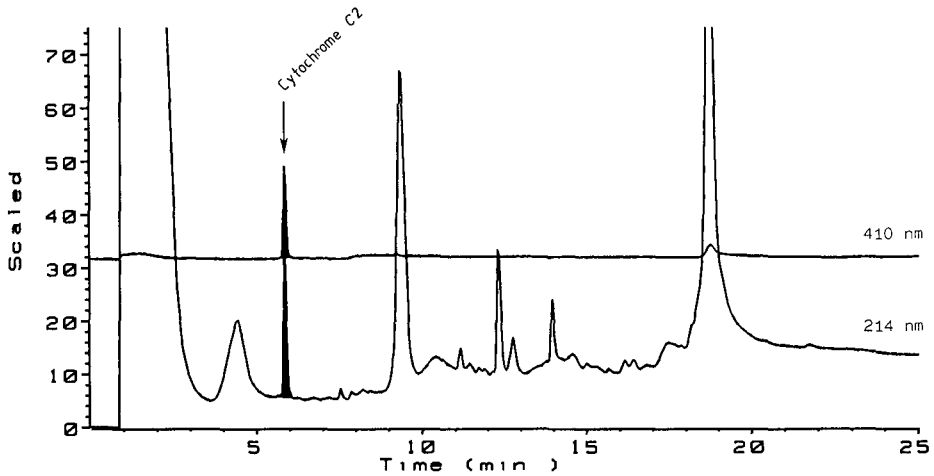

Fig. 14. Isolation of cytochrome *c*2 from the supernatant of a *Rhodopseudomonas viridis* cell culture. Conditions: flow-rate, 1.5 ml/min; eluent A, 0.01 *M* NaH_2PO_4 (pH 5); eluent B, same as A but with 0.5 *M* NaCl; gradient from 0 to 100% A in 20 min; column, TSK-Gel NPR-SP, 35 × 4.6 mm I.D., 2.5 μm; injection volume, 50 μl of supernatant; total protein concentration, 1.5 mg/ml; amount isolated, 0.5 μg cytochrome *c*2.

protein was carried out by low-pressure chromatography on a weak anion-exchange column (Whatman DE-52, diethylaminoethylcellulose), followed by chromatofocusing on a PBE 94 gel with Polybuffer (Pharmacia), and took over 1 day. With the NPR-SP column, the protein was available for further work within a few minutes after centrifugation and injection on to the column.

The structure of small DNA molecules, such as plasmids and viral and bacteriophage DNA, is well known nowadays. Restriction enzymes clip these molecules and provide fragments that are known exactly. These fragments serve as

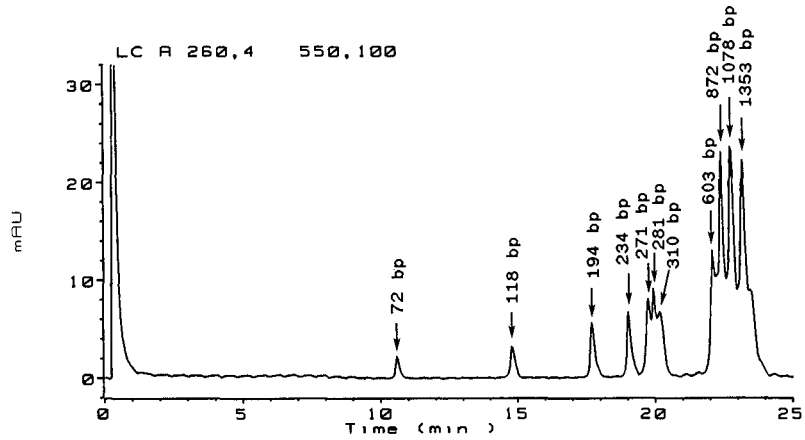

Fig. 15. Separation of restriction fragments of φX174 RF Phage DNA digested with HaeIII. Conditions: flow-rate, 0.9 ml/min; eluent A, 6 *M* urea in 0.03 *M* NaH_2PO_4 (pH 6); eluent B, same as A but with 1 *M* NaCl; gradient from 30 to 50% B in 25 min; column, TSK-Gel NPR-DEAE, 2.5 μm, 35 × 4.6 mm I.D.; injection volume, 10 μl (1 mg/ml). bp = base pairs.

molecular-weight markers in the electrophoresis of unknown DNA restriction fragments. The potential of NPR-DEAE columns for separating high-molecular-weight nucleotides was illustrated with these fragments (Fig. 15). A salt gradient with a high concentration of urea in the mobile phase suffices to obtain an excellent separation of all the fragments present in the sample. In fact, electrophoresis showed the separation of only eight fragments whereas the HPLC analysis showed all eleven fragments.

The favourable separation efficiency of these columns can also be used for the rapid separation of peptides[4], as illustrated by Fig. 16. For this work, a longer column having a higher peak capacity, or more chromatographic space for positioning peaks, is required. Therefore, the HYTACH MicroPell C_{18} column (75 × 4.6 mm I.D.) was used for this work and compared with the VYDAC C_{18} column (250 × 4.6 mm I.D.). The top chromatogram (Fig. 16) shows the VYDAC C_{18} column and the analysis of the trypsin digest of genetically engineered human interferon. A gradient of from 0 to 55% in 2 h was applied in order to achieve almost baseline separation of most peptides. The middle trace in Fig. 16 shows the chromatogram of the same sample on the TSK-Gel NPR-C_{18} column. In order to keep the conditions on both columns the same, the gradient time was reduced by the same factor as the ratio of the lengths of the two columns. It can be seen that the number of peaks separated on the NPR-C_{18} column is much smaller than that on the VYDAC column.

A separation that is comparable to that on the VYDAC column was obtained when the tryptic peptide sample was injected into the HYTACH MicroPell C_{18} column and the same gradient range but with a gradient time of 36 min was used. The overall analysis time on this column was 34 min, compared with 100 min on the VYDAC column. In order to obtain a better visual comparison of the separation efficiency and selectivity of the HYTACH column relative to the VYDAC column, the time axis of the lower trace in Fig. 16 was stretched so that the interferon peaks

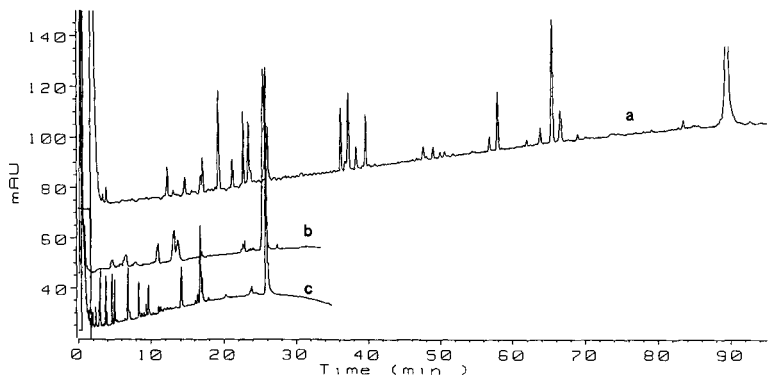

Fig. 16. Comparison of separation performance of non-porous reversed-phase columns with porous reversed-phase columns. Conditions: flow-rate, 1.0 ml/min; eluent A, 0.1% aqueous TFA; eluent B, 0.1% TFA in acetonitrile, gradient from 0 to 55% in 120, 16.8 and 36 min in chromatograms a, b and c, respectively. Sample, recombinant human interferon digested with trypsin as described under Experimental. (a) Column, VYDAC C_{18}, 250 × 4.6 mm I.D., 5 μm; column temperature, 40°C. (b) Column, TSK-Gel NPR-C_{18}, 35 × 4.6 mm I.D., 2.5 μm; column temperature, 40°C. (c) Column, HYTACH MicroPell C_{18}, 75 × 4.6 mm I.D., 1.5 μm; column temperature, 55°C.

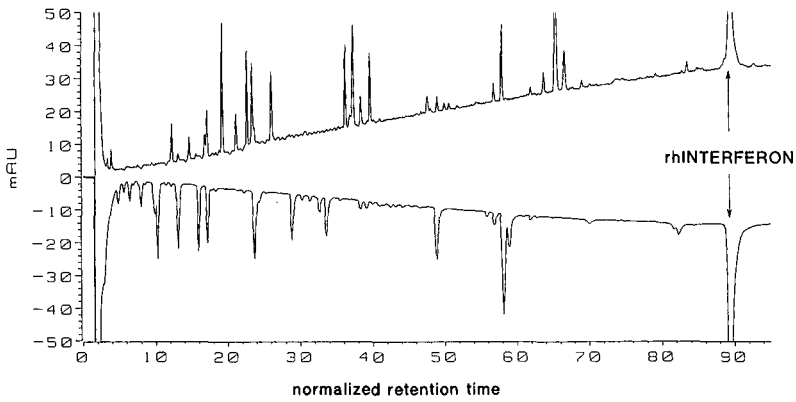

Fig. 17. Comparison of VYDAC and HYTACH MicroPell columns for tryptic map analysis. Conditions as in Fig. 16. Upper trace, VYDAC column; inverse trace, HYTACH MicroPell C_{18} column.

matched in both chromatograms (Fig. 17). As can easily be seen, the same peak clusters can be identified in both traces. However, the relative peak-height ratios within each peak trace are different. This indicates differences in the recoveries from the two columns.

Although the number of major peaks separated was 20 on the MicroPell column and 23 on the VYDAC column, it must be taken into account that the gradient conditions were not fully optimized for the HYTACH column. The excellent reproducibility of this system is illustrated in Fig. 18, which is an overlap of five consecutive runs of the trypsin digest of the interferon sample.

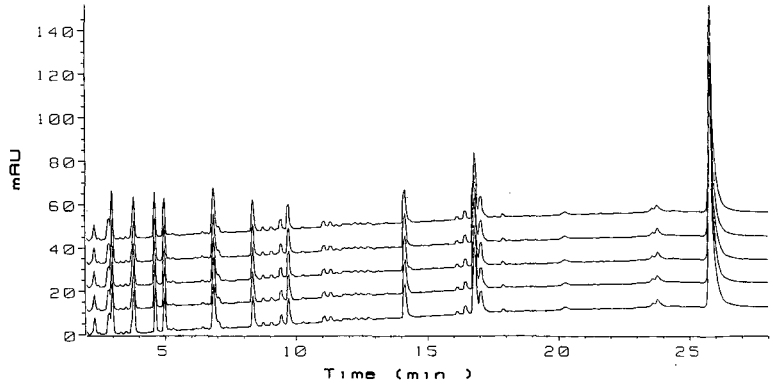

Fig. 18. Five consecutive injections of tryptic digest of rh-interferon onto a HYTACH MicroPell C_{18} column, 75 × 4.6 mm I.D., 1.5 μm. Conditions as in Fig. 16.

CONCLUSIONS

Non-porous, microparticulate columns have considerable potential for rapid, high-resolution separations of proteins. This is effected in short, low-volume, columns operated at elevated temperature. At the same time, the TSK-Gel NPR-C_{18} columns showed excellent bed stability, demonstrated by the linearity of the pressure *vs.* flow-rate curve and by the results of the stability stress test. However, the permeability of these columns needs to be improved. Small molecules permeate the "non-porous" beads, giving rise to poor separations. The applicability of these columns is limited by molecular weight and by molecular structure. High protein loads are feasible while maintaining chromatographic resolution and recovery on the NPR-C_{18} column. If the columns become fouled, they can be easily cleaned by injection of small volumes of a cleaning agent such as acetic acid. Instrumental requirements for operating these columns, although demanding, can be met by modern HPLC equipment.

The main applicability of these columns will be for rapid micropreparative-scale separations (< 200 μg), for verification of the homogeneity of recombinant proteins (deamidated forms, mutants and degraded forms) and for fast tryptic mapping. In the last application, on the MicroPell column, the number of resolvable peptides will be limited by the peak capacity of the relatively short column (75 mm).

ACKNOWLEDGEMENTS

The authors acknowledge the help of Dr. Friedrich Lottspeich of the Max Planck Institute for Biochemistry, Munich, F.R.G., in generating some of the chromatograms, Dr. Wolfgang Rapp, Laboratory for Organic Chemistry, University of Tübingen, Tübingen, F.R.G., for generating the SEM picture and Dr. Virginia Curtis, Hewlett-Pachard, Waldbronn, F.R.G., for critically reading the manuscript.

REFERENCES

1 L. R. Snyder and M. A. Stadelius, in Cs. Horváth (Editor), *HPLC — Advances and Perspectives*, Vol. 4, Academic Press, London, 1986, pp. 195–312.
2 N. L. Johnson, N. B. Madsen, J. Mosely and K. S. Wilson, *J. Biol. Chem.*, 90 (1974) 703.
3 J. K. Duncan, A. J. C. Chen and C. J. Siebert, *J. Chromatogr.*, 397 (1987) 1.
4 D. J. Burke, J. K. Duncan, L. C. Dunn, L. Cummings, C. Siebert and G. S. Ott, *J. Chromatogr.*, 353 (1986) 425.
5 D. J. Burke, J. K. Duncan, C. Siebert and G. S. Ott, *J. Chromatogr.*, 359 (1986) 533.
6 Y. Kato, T. Kitamura, A. Mitsui and T. Hashimoto, *J. Chromatogr.*, 398 (1987) 327.
7 Y. Kato, T. Kitamura, A. Mitsui, Y. Yamasaki, T. Hashimoto, T. Murotsu, S. Fukushige and K. Matsubara, *J. Chromatogr.*, 447 (1988) 212.
8 K. K. Unger, G. Jilge, J. N. Kinkel and M. T. W. Hearn, *J. Chromatogr.*, 359 (1986) 61.
9 R. Janzen, K. K. Unger, H. Giesche, J. N. Kinkel and M. T. W. Hearn, *J. Chromatogr.*, 397 (1987) 91.
10 Y. F. Maa and Cs. Horváth, *J. Chromatogr.*, 445 (1988) 71.
11 M. A. Rounds and F. E. Regnier, *J. Chromatogr.*, 447 (1988) 73.
12 K. Kalgathi and Cs. Horváth, *J. Chromatogr.*, 398 (1987) 335.
13 H. Darcy, *Les Fontaines Publiques de la Ville de Dijon*, Dalmont, Paris, 1856.
14 K. K. Unger, *Porous Silica (Journal of Chromatography Library*, Vol. 16), Elsevier, Amsterdam, 1979.
15 L. R. Snyder, G. B. Cox and P. E. Antle, *J. Chromatogr.*, 444 (1988) 303.
16 S. Ghodbane and G. Guiochon, *J. Chromatogr.*, 444 (1988) 275.
17 F. E. Regnier, personal communication.
18 H. Schrenker, *J. Chromatogr.*, 213 (1981) 243.

Journal of Chromatography, 476 (1989) 21–35
Elsevier Science Publishers B.V., Amsterdam — Printed in The Netherlands

CHROMSYMP. 1582

NEW POROUS ORGANIC MICROSPHERES FOR HIGH-PERFORMANCE LIQUID CHROMATOGRAPHY

RICHARD W. STOUT*, HENRY J. LEIBU, ALBERT T. ROUSAK and RICHARD C. WRIGHT
E. I. du Pont de Nemours & Co., Inc., Medical Products Department, Glasgow Site, Wilmington, DE 19898 (U.S.A.)

SUMMARY

A process for producing spherical porous organic microspheres, based on urea–formaldehyde (UF) polymer, has been developed. These microspheres exhibit exceptional mechanical strength and resiliency and have minimal tendency toward shrinking or swelling in aqueous, organic, or hydroorganic media. The geometric parameters of the microspheres are conveniently adjusted by process variables, which allow precise control of pore and particle dimensions. The surface of the UF microsphere contains organic functional groups suitable for chemical modification so that ligands of choice may be covalently attached for operation in the anion-exchange or hydrophobic interaction modes.

INTRODUCTION

Considerable effort has been expended on the design of stationary phases for high-performance liquid chromatography (HPLC). The first requirement for a suitable support involves consideration of a set of geometric parameters. These parameters include mean particle diameter, mean pore diameter, specific pore volume and other factors. These parameters are optimally held within narrow range specifications in order to allow a packed column with a regular, well-defined geometry to be obtained. A regular, controlled geometry is essential to maintaining high theoretical plate efficiency. The mean diameter of the particles which comprise the bed dictates the system operating pressure during use with flowing mobile phases and also influences the column packing procedure. This sets an upper limit on the number of theoretical plates attainable. The dual requirements of small particles and regular geometry of the support place restrictions on the manufacture and mechanical stability of the support. Not all chromatographic supports fulfill these essential requirements. Silica gel has been utilized to a far greater extent than other substances that could ostensibly serve as alternatives.

Silica gel is unique among numerous substances in its ability to fulfill so many requirements as a chromatographic stationary phase. Its cubic expansion is essentially zero under normal operating temperatures. Several convenient processes are available for the manufacture of porous microspheres with narrow size distribution and

0021-9673/89/$03.50

well-defined spatial geometry. The silica surface is conveniently modified to suit the various chromatographic requirements by the introduction of covalently attached ligands. The pore size and specific pore volume may be adjusted by several techniques to permit separation of substances of varying molecular dimensions. Silica gel is an admirable stationary phase for the separation of small molecules having a wide range of chemical functional groups.

Silica gel is less useful with water-rich hydroorganic eluents, since the surface of the gel slowly dissolves in water at all pH levels. The dissolution process eventually causes the bonded phase to hydrolyze. The rate at which this occurs becomes rapid above pH 8 but is less of a problem at lower pH levels. Several measures to prevent rapid destruction of the silica surface have been incorporated, but none are completely satisfactory when sterilizing agents, such as dilute alkali solutions, are pumped through the columns. Thus, the question becomes: Can organic substances be conveniently substituted for silica gel as chromatographic supports and is it possible to keep their geometric parameters within narrow limits?

The literature contains numerous descriptions of organic chromatographic supports which can function in most operating modes[1–15], and most of these may be obtained commercially. The available supports may be conveniently divided into two broad categories. The first group[1–9] consists of supports that are vinyl polymers. The second group[10–15] includes substrates derived from agarose, dextrans, polypeptides, or substances other than polymers.

Porous organic microspheres may be produced from vinyl monomers, polymers, and other ingredients by using suspension or emulsion polymerization techniques. The patent literature discloses some aspects of the methods of producing organic microspheres. The pores are introduced by allowing the polymerization to proceed around an inert substance, such as toluene, which is washed away after polymerization is terminated. Polystyrene–divinyl benzene (PS–DVB) is the most common type; it is described in some detail by Helfferich[16].

While not labile in the presence of strong bases in most cases, the organic substrates suffer from other problems. Their most serious disadvantages over their silica counterpart are swelling and insufficient mechanical strength. Organic eluents, commonly employed in the practice of HPLC, will solvate many polymers and thus induce undesirable changes in particle and pore geometries. The swelling effects may be minimized by employing cross-linking agents in varying amounts. A high degree of cross-linking ensures mechanical strength, while a low degree usually produces a particle which has insufficient mechanical strength to withstand the pressure necessary for packing into columns or for sustained operation at the usual pressures. The cross-linking agents may cause additional difficulties by introducing secondary surface interactions, which, in turn, lead to band-broadening or irreversible adsorption. These factors frequently limit the lower boundary of the mean particle size, which dictates the highest number of theoretical plates that can be achieved. Thus, large particle diameters are preferred for separations when such materials are utilized, and lower efficiency and long separation time must be tolerated.

Several porous organic microspheres described in the literature are reported to perform about as well as silica analogues in terms of mechanical parameters. Most of these supports are copolymers of vinyl monomers. Ugelstad[1] has patented processes for the production of monodisperse microspheres. Vlacil *et al.*[2,3] and Kas *et al.*[4]

described porous organic microspheres, based on hydroxyethyl methacrylate copolymers. Hirata *et al.*[5] and Hanai *et al.*[6] worked with similar materials based on polyvinyl alcohol (PVA). Wojaczynska and Kolarz[7] reported on particles made from copolymers of acrylonitrile and DVB. Tanaka *et al.*[8] used particles of 5–7 μm diameter, produced from copolymers of stearyl methacrylate and ethylene dimethacrylate. Dawkins *et al.*[10,11] described microspheres based on polyacrylamide. Most manufacturers disclose little or nothing concerning the exact composition of their chromatographic products produced from vinyl compounds. However, swelling and mechanical strength are routinely discussed. These properties must be tested in detail, since they are the cause of the two most important deficiencies in organic packing materials.

Another group of chromatographic substrates is based on the use of agarose, dextrans, or other naturally occurring substances[12–14]. The sugar-based supports are widely used for separations of numerous biochemical substances. The chief advantage of agarose lies in the very low non-specific adsorption properties of the complex sugars that form the backbone of the structure. The disadvantages are the lack of mechanical strength and undesirable interactions introduced by the cross-linking agents used to circumvent such problems. Supports based on polypeptides have recently been introduced by Ihara *et al.*[15].

This paper reports on the use of urea–formaldehyde (UF) polymer as an alternative to vinyl-, dextran-, or polypeptide-based supports. The process for producing these microspheres permits convenient selection and control of the most important geometric parameters, such as particle diameter, pore diameter, and specific pore volume. In addition, this polymer exhibits high resiliency and marked resistance toward shrinking and swelling in the presence of organic solvents and is stable up to pH 13.

EXPERIMENTAL

Instruments

Chromatographic experiments were conducted with several instruments, depending on the type of chromatography required. For size-exclusion chromatography (SEC) a Model 8800 HPLC apparatus (E. I. du Pont & Co., Wilmington, DE, U.S.A.), equipped with a fixed photometer, operating at 254 nm, was used. Samples were injected with a Rheodyne Model 7125 injector (Rheodyne, Cotati, CA, U.S.A.). Ion-exchange experiments were performed with a fast protein liquid chromatography (FPLC) system (Pharmacia, Piscataway, NJ, U.S.A.), which included an LCC-500 controller, two P-500 pumps, a mixer, a motor-valve MV-7 injector, a UV-1 single-path monitor with an HR-10 flow-cell and 280-nm filter, and a REC-482 recorder. Analog data were digitized and archived with a Nelson Analytical Model 760 Series interface (Cupertino, CA, U.S.A.), which was interfaced with an HP Series 220 microcomputer (Hewlett-Packard, Fort Collins, CO, U.S.A.). Nelson Analytical software was modified to include calculations for theoretical plates, retention, and skew or peak asymmetry. Archived data were treated with non-linear curve fitting routines by the use of the software package MINSQ (MicroMath Scientific Software, Salt Lake City, UT, U.S.A.).

Chemicals

Tetrahydrofuran (THF) and acetonitrile of HPLC grade were obtained from J. T. Baker (Phillipsburg, NJ, U.S.A.) and used as received. Deionized water was produced in a Continental Water System Unit (North Wales, PA, U.S.A.). Tris(hydroxymethyl)aminomethane (Tris), ammonium sulfate, dipotassium hydrogenphosphate, and sodium chloride were obtained from Aldrich (Milwaukee, WI, U.S.A.). The buffer pH levels were adjusted with reagent-grade hydrochloric acid or sodium hydroxide, as appropriate.

Mobile phases and samples

Buffered mobile phase solutions were prepared in single batches and consisted of 2.0 *M* ammonium sulfate or 1.0 *M* sodium chloride, 0.02 *M* dipotassium hydrogen phosphate or 0.05 *M* Tris, and 0.05–0.10% (w/v) sodium azide. The pH of the buffers was adjusted with 1 *M* sodium hydroxide or hydrochloric acid, as appropriate. The protein samples were mixtures prepared from proteins as received by dissolving them gently in the mobile phase and filtering through a 0.45-μm cellulose acetate sterile filter (Nalge Company, Rochester, NY, U.S.A.). Size-exclusion samples were prepared by dissolving polystyrene molecular weight standards in neat THF at concentrations of *ca.* 1 mg/ml.

Carbonic anhydrase, lysozyme, myoglobin, ovalbumin, soybean trypsin inhibitor, and transferrin were obtained from Sigma (St. Louis, MO, U.S.A.). Polystyrene molecular weight standards (PS MW) were obtained from Du Pont.

UF microspheres and columns

UF microspheres were produced by treating coacervated spheres, described elsewhere[17], with ammonium bifluoride in water at ambient temperature. The product was washed with deionized water and the UF surface was chemically modified to introduce chromatographic ligands by proprietary procedures.

UF microspheres were packed into stainless-steel columns of 250 mm × 4.6 or 9.4 mm I.D. by proprietary procedures. Column inlet pressures varied from about 1000 to 10000 p.s.i. with a variety of different organic solvents. Alternately, UF microspheres were slurry-packed in deionized water into glass columns, 100 mm × 10 mm or 300 mm × 10 mm I.D. at ambient pressure.

Rigidity and resilience experimental protocol

A column of 250 mm × 4.6 mm I.D. was packed with UF microspheres of 3 μm nominal particle diameter and 60 Å pore size. The HPLC pump was directly connected to the inlet of the test column with capillary tubing. The system was thoroughly flushed with THF at a flow-rate of 1.0 ml/min, and the column was purged with this mobile phase for *ca.* 10 column volumes (30 ml). The pump flow-rate was set to 0.25 ml/min. This flow-rate was maintained for 2–3 min or until the pressure reading indicated steady-state operation. This reading was recorded, and the flow-rate was increased in 0.25 ml/min increments with pressure readings being taken at each new step until the inlet pressure approached 350 bar. The flow-rate was then decreased by the same procedure in reverse, and pressure readings were again recorded until the final flow-rate was 0.25 ml/min. These data are shown in Table I.

Occasionally the flow-rate was set to some arbitrary, previously recorded level

TABLE I
RESULTS OF RIGIDITY AND RESILIENCE EXPERIMENTS

Flow-rate, F	*THF*		*Water*		*Acetonitrile*	
(ml/min)	Pa^a *(bar)*	Pd^b *(bar)*	Pa^a *(bar)*	Pd^b *(bar)*	Pa^a *(bar)*	Pd^b *(bar)*
0.25	26	26	53	53	19	20
0.50	53	53	106	106	40	41
0.75	81	81	159	158	61	62
1.00	110	108	209	209	83	83
1.25	138	137	258	255	104	104
1.50	165	164	301	299	125	125
1.75	193	191	344	341	145	145
2.00	220	219			165	165
2.25	247	246			185	185
2.50	274	272			206	205
2.75	293	294			225	225
3.00	323	320			244	244
3.25					264	263
3.50					280	280
3.75					300	300
4.00					318	319
4.25					330	332
4.00					317	317
3.75					299	298
3.50					279	279
3.25					262	261
3.00					241	240
2.75	291	293			223	223
2.50	270	268			204	205
2.25	243	242			184	184
2.00	216	215			164	165
1.75	190	188			145	145
1.50	162	162	294	295	125	125
1.25	136	135	250	249	104	104
1.00	108	108	204	203	84	84
0.75	81	81	155	155	62	62
0.50	53	53	105	104	41	41
0.25	26	26	53	53	20	20

[a] Ascending pressure readings.
[b] Descending pressure readings.

(data not shown) to check for hysteresis effects. The entire procedure was repeated in order to produce additional data for a single mobile phase. The pump was then flushed with the second solvent at a flow-rate of 1.0 ml/min, the column was purged with this mobile phase for *ca.* 10 column volumes, and the entire process was repeated. Finally, a third solvent was used to complete the data set.

THEORY

Synthesis of UF microspheres

Iler patented a process[17] for the production of uniform oxide microspheres. Urea (U) or melamine and formaldehyde (F) are combined with an aqueous silica sol under acidic conditions so that polymerization of the organic constituents produces coacervation of the components into microspheres. The silica sol particles are trapped within the coacervate matrix. The microspheres are dried and heated in air to oxidize the urea–formaldehyde (UF) polymer portion of the matrix, leaving behind porous silica microspheres (PSM). The PSM material is sold commercially as Zorbax™. This paper deals with the organic portion of the coacervate matrix, which is retained while the silica is discarded. This is opposite to the Iler process.

The reaction proceeds according to the following equation

$$n\mathrm{U} + n\mathrm{F} + \mathrm{SiO_2} \rightarrow (\mathrm{UF})_n\text{–}\mathrm{SiO_2}$$

where the term on the right represents the composite organic–inorganic coacervate matrix.

The silica is conveniently removed to leave behind a porous organic microsphere, which contains imprints of the silica sol. The pore size is determined by the diameter of the silica sol analogous to that of Zorbax with several significant differences. While the pore in the silica microsphere is determined by the cavity surrounded by sol particles in a random close-packed arrangement with a coordination number of 5, the situation is different in the porous organic microsphere. The UF matrix is not "solid", in contrast to the silica counterpart, but seems to be a foam. Other investigators have reported on similar microporous substances. Nevejans and Verzele[18] have studied microporosity in detail for the case of PS–DVB copolymers. Intrinsic porosity in the UF material is similar to that of the vinyl analogues and consists of two types: (1) micropores of probably 3–12 Å and (2) some "channels" within this microporous foam. Thus, pores are interconnected by a network of channels. The channel structure facilitates the removal of silica with ammonium bifluoride in a few minutes, and the UF material yields essentially no residue when burned in air. The sol particles are not surrounded by the foam structure in such a way as to limit the effective pore size by some aperture effect (*e.g.*, no 13-Å porous barrier or isolated sol particles). The average pore size is determined by the mean particle diameter of the sol.

Particle and column volumes

The internal volume V_c, of a packed column is given by[19]

$$V_c = V_o + V_s + V_p + V_l \tag{1}$$

where V_o is the interstitial volume outside the microspheres, V_s is the volume of the solid support, V_p is the pore volume, and V_l is the volume of any bonded or coated ligand on the surface of the pores. The volume of spheres when random close-packed into any container is about 0.6 of the volume of the container. Thus, V_o will have a nominal value of 0.4 V_c.

For cases where no ligand is present

$$V_o = 0.4\ V_c \quad (2)$$
$$V_m = V_o + V_p \quad (3)$$
$$V_m = V_c[1-0.6(1-\Phi)] \quad (4)$$

where Φ is the porous fraction and is defined as the ratio of the pore volume to the total volume of the support[20].

$$\Phi = V_p/(V_s + V_p) \quad (5)$$

According to SEC theory, as described by Yau *et al.*[19], the retention volume, V_R, is given by

$$V_R = V_o + V_p(K_D) \quad (6)$$

where K_D is the distribution constant. Eqn. 6 is combined with eqn. 3 to give the following expression in convenient chromatographic volume terms

$$K_D = (V_R - V_o)/(V_m - V_o) \quad (7)$$

Permeability and inlet pressure

The Darcy equation[21,22] predicts the column inlet pressure from eqn. 8

$$U = K_o\ d_p^2\ P/\eta L \quad (8)$$

where U is the linear velocity, K_o is a constant related to the column permeability, d_p is the mean microsphere diameter, P is the pressure drop across the column, η is the viscosity of the mobile phase, and L is the column length.

Since the linear velocity[21]

$$U = L/t_o \quad (9)$$

where t_o is the column breakthrough time and

$$t_o = V_m/F \quad (10)$$

where F is the flow-rate, by combining eqns. 8–10, we obtain

$$P = \Omega\eta L^2 F/V_m d_p^2 \quad (11)$$

where $\Omega = 1/K_o$.

A packed column has fixed values of d_p, L, and V_m and will experience a pressure drop that is controlled only by changes in F and η, provided the physical properties of the packing material do not change when the mobile phase is changed or the elastic or plastic deformation limits are exceeded. Then the invariant terms may become

a constant, and eqn. 12 holds for the following units: P (bar), η (N s/m^2), L (mm), F (ml/min), V_m (ml), and d_p (μm).

$$\varepsilon = 6\ V_m\ d_p^2/L^2 \tag{12}$$

or

$$\varepsilon P = \Omega \eta F \tag{13}$$

A plot of εP *vs.* ηF will be a straight line with a slope equal to Ω.

RESULTS AND DISCUSSION

Pore size

Three lots of UF microspheres were produced from three different sol sizes. Nominal sol sizes of 5, 15, and 30 nm were employed to give UF-60 (60 Å), UF-150 (150 Å), and UF-300 (300 Å) porous organic microspheres, respectively. These lots were analyzed by SEC to verify that changing the sol size did directly influence the final pore size. The chromatographic retention volumes for macromolecular polystyrene standards are shown in Table II. Values of the particle porous fraction Φ were calculated from eqn. 5. This gives 0.57, 0.57, and 0.54 for the three packings,

TABLE II
SIZE-EXCLUSION RESULTS FOR UF-60, -150, AND -300

PS MW (daltons)	*UF-60*		*UF-150*		*UF-300*	
	V_R (cm^3)	K_D[a]	V_R (cm^3)	K_D[a]	V_R (cm^3)	K_D[a]
9 000 000	–	–	–	–	5.80	0.000
1 800 000	5.68	0.000	6.97	0.000	6.01	0.019
900 000	6.11	0.065	7.07	0.010	6.04	0.034
233 000	6.39	0.107	7.17	0.027	6.19	0.063
200 000	6.52	0.126	7.21	0.034	–	–
100 000	6.64	0.144	7.26	0.043	–	–
97 200	6.70	0.153	7.32	0.053	6.50	0.113
50 000	6.81	0.170	7.35	0.058	7.00	0.194
35 000	7.03	0.202	7.56	0.094	7.88	0.327
20 000	–	–	7.94	0.158	8.36	0.413
17 500	7.25	0.236	8.29	0.218	8.54	0.442
10 000	7.59	0.287	9.23	0.287	9.00	0.516
9000	7.87	0.329	9.36	0.329	9.27	0.560
4000	8.89	0.482	10.36	0.482	9.79	0.644
2100	9.76	0.613	11.04	0.613	10.12	0.697
800	10.39	0.788	12.29	0.788	10.75	0.798
92[b]	12.34	1.000	12.89	1.000	11.98	1.000

[a] Calculated from eqn. 7.
[b] Toluene.

respectively. When V_o is calculated from eqn. 2, the values are similar and yield 0.52, 0.57, and 0.48. This indicates that the columns are nearly optimally packed, since the porosity should not be altered during these experiments. The porous fraction Φ may be varied independently (not reported here) by changing process variables. Fig. 1 shows a plot of the logarithm of polystyrene molecular weight standards *versus* K_D, which was calculated from eqn. 7 by using the retention volumes from Table II. Fig. 2 shows a typical SEC chromatogram on UF-60, lot 1, which separates polystyrene molecular weight standards according to accepted theory. The results indicate that the pore size is controlled to a first approximation by the sol mean particle diameter.

Columns were packed by high-pressure slurry techniques in a manner similar to that used for silica packing materials. No obvious deformation was observed that could be attributed to collapse of the packing material under these conditions. No packing collapse was observed in further studies with solvents such as methanol, THF, and similar solvents commonly used for slurry packing. Even when the inlet pressure exceeded 8000 p.s.i., there was no significant rise in column inlet pressure with time, although the initial operating pressures were higher with higher packing pressure. Column steady-state operating pressures remained constant or returned to their

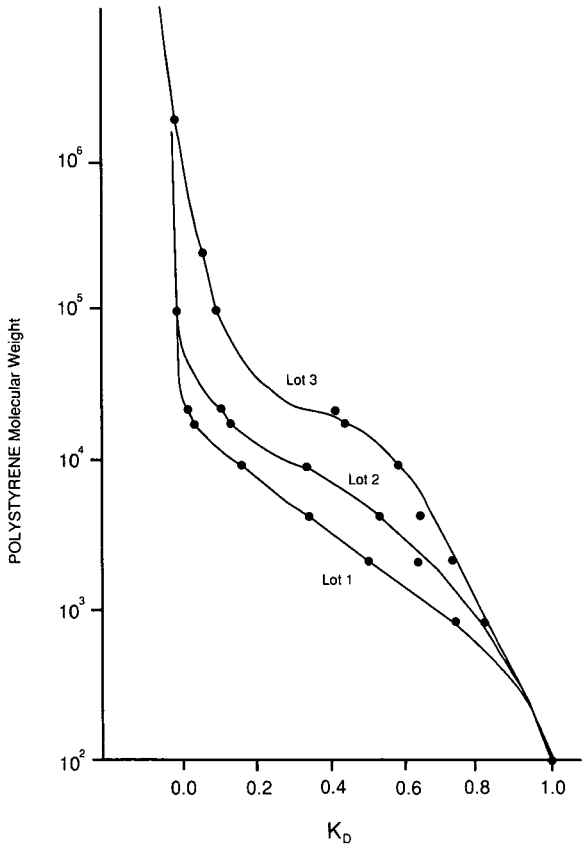

Fig. 1. Plot of log molecular weight *vs.* K_D for polystyrene standards. Lot 1, 60 Å; lot 2, 150 Å; lot 3, 300 Å.

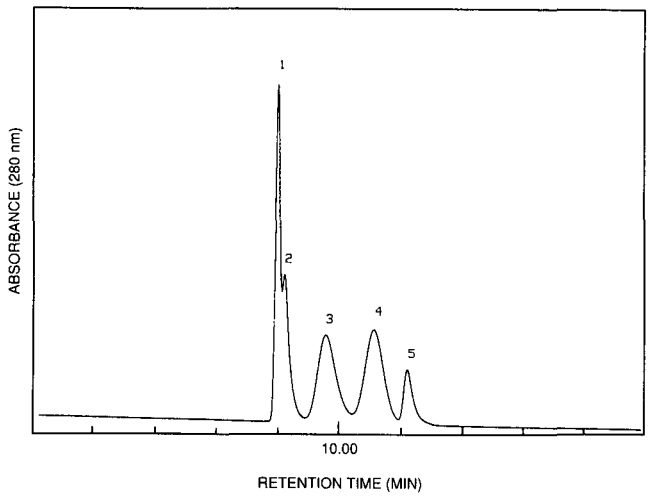

Fig. 2. Typical size-exclusion chromatogram of UF-60. Conditions: column, 250 × 9.4 mm I.D.; particle diameter, 3 μm; mobile phase, THF; flow-rate, 1.0 ml/min; detector, 254 nm, 0.2 a.u.f.s.; inlet pressure, 12 bar. Peak identities: 1 = polystyrene 97 200; 2 = 17 500; 3 = 4000; 4 = 800; 5 = 92 (toluene).

original levels during various evaluation episodes, even though several different mobile phases of neat or hydroorganic composition were employed.

More systematic experiments were designed to investigate the swelling phenomenon of these UF microspheres, since there was no indication in the literature that they had previously been utilized as a chromatographic column material, nor was there any indication of how UF would behave in an environment such as a packed column under pressure.

Swelling of porous supports

Swelling of porous organic particles has been reported by several researchers. In fact, controlled swelling is the basis for the synthesis of some patented processes for the production of monodisperse microspheres[1]. Hirata *et al.*[5] studied hydrophilic gels, derived from copolymers of vinyl alcohol (VA). They used the theoretical plate efficiency as a parameter for estimating the magnitude of swelling effects of organic particles in packed columns. The VA gels maintained a rather consistent efficiency when methanol, ethanol, or dimethylformamide (DMF) were used as the mobile phase but significant decreases in efficiency were observed when acetonitrile, THF, or chloroform were used. When several VA gels were subjected to these tests, these materials were generally observed to shrink in organic solvents. Wojaczynska and Kolarz[7] performed similar experiments on porous particles derived from copolymers of acrylonitrile (AN) and DVB. Maa and Horváth[23] studied non-porous, highly cross-linked microspheres of 3 μm particle diameter and assessed their mechanical stability by performing flow and pressure experiments. Their results indicated that the nominal value of the interstitial volume fraction V_o/V_c (usually 0.4) decreased from 0.38 to 0.24, depending on which solvents were selected for mobile phases. This change was calculated to correspond to a 7.8% increase in particle diameter, and this

corresponds to a 25% increase in the volume of the particles in the packed column. The specific permeability was found to be greatest with water.

Thus, even "solid" (described as non-porous in this case) or highly cross-linked vinyl copolymers appear to swell to some extent in the presence of organic solvents. Most researchers will agree that swelling of organic particles in packed columns is highly complicated where linear or predominantly linear vinyl polymers and copolymers are concerned.

The situation is similar in the case of agarose, except that the mobile-phase systems are predominantly aqueous and nearly always buffered. Hjertén[13,14] described highly cross-linked agarose beads with particle diameters between 3 and 10 μm. These materials were deformed during column packing, and a microscopic examination showed that the original spherical shape was restored on the microscope slide after a short period of time. In addition, the cross-linking reagents interfered with the chromatographic process unless suitable precautions to mask their effects were taken. These materials are not equivalent to "linear polymers" in the sense of vinyl copolymers. The chief problem with these packing materials is insufficient rigidity and resilience.

Rigidity and resilience of UF microspheres

UF porous microspheres probably belong to a different classification scheme in that they are undoubtedly highly cross-linked, not linear, and not very well solvated by commonly used organic solvents. The exact nature of the UF matrix is unknown and somewhat controversial[24].

Marvel *et al.*[25] suggested that their structure consists of rings formed by the reaction of urea with amino acid amide. In our experiments of surface modifications we found nothing to support this assumption. Even the mole ratio of urea and formaldehyde in UF polymers is in question, since the methods to determine this parameter are laborious and imprecise[26,27].

Experiments were conducted on 3-μm diameter, 60-Å pore-size UF microspheres, since the small particle diameter would offer the highest resistance to flow, a concomitantly high pressure drop, and a high propensity toward plastic or elastic deformation. A column of 250 mm × 4.6 mm I.D. was packed and used at several different flow-rates with different mobile phases. The inlet pressure was recorded under fixed conditions of mobile phase and operating pressure, and then the flow-rate was increased and the new pressure level was recorded after the system was sufficiently equilibrated. Table I shows the results of this experiment with three different solvents, and a plot of the pressure *versus* flow-rate is shown in Fig. 3. The results indicate that the packed column is resistant to geometric changes up to 300 bar with three different solvents commonly used in HPLC. The open circles indicate ascending pressure readings, while the solid triangles indicate descending pressure readings. In addition, random flow-rate selections were made during the experiments (not shown) to verify the absence of any hysteresis effects. Note that the linearity is good, as Horváth[23] and others have previously shown, and the intercept of the line is zero within the experimental error. When slight deviations from linearity are observed, such as points where levels exceed 280 bar, the deviation is seen to be negative with respect to pressure. This negative deviation is probably caused by heat generated by the system. Heat works on the packed column to lower the viscosity of the mobile phase. If the

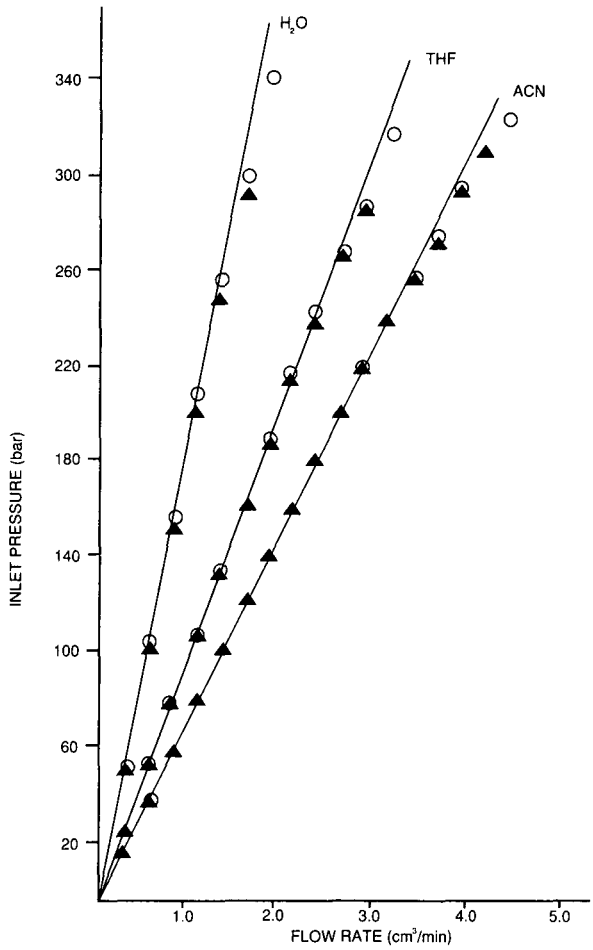

Fig. 3. Plot of inlet pressure *vs.* flow-rate for 3-μm UF-60. For conditions see Experimental section. (○) Ascending pressure readings; (▲) descending pressure readings. ACN = Acetonitrile.

deviation had been observed to occur in the opposite direction and hysteresis effects had been noted, the UF particles would be shrinking, swelling, or changing in shape in some irreversible manner. The chromatographic theory states[22] that there should be some flow resistance parameter, Ω, with a nominal value of 500 for spherical particles. The theory further predicts that the magnitude of this value is invariant with stable packed columns, as is the case for silica, provided the pressure limit of the particles is not exceeded. For this experiment, the constant ε from eqn. 14 has a value of $2.557 \cdot 10^{-3}$, when P is in units of bar, L in mm, V_m in ml and d_p in μm,

$$\varepsilon = 6V_m d_p^2/L^2 \tag{14}$$

and the viscosities of water, acetonitrile, and THF were taken as 0.993, 0.370, and 0.550 N s/m^2, respectively[28]. According to the Theory section from eqn. 13

$$\varepsilon P = \Omega \eta F$$

where Ω should remain invariant, with a constant value of about 500, while the mobile phase composition is altered. Fig. 4 shows a plot of εP *vs.* ηF with a slope of 535. This experiment clearly shows that UF microspheres exhibit exceptional resistance to swelling and particle deformation in organic solvents. Maintenance of the Ω value of about 500 in various solvents at high pressures shows that, if elastic deformation or other phenomena are occurring, the effects are reversible and a stable packed column is maintained.

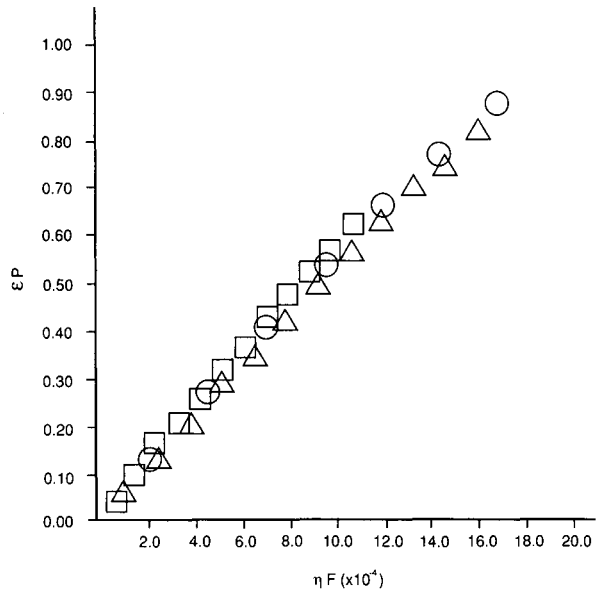

Fig. 4. Normalized plot of inlet pressure *vs.* flow-rate for 3-μm UF-60. For conditions see Experimental section. (○) Water; (□) acetonitrile; (△) THF.

Bonded phases

The surface of the UF matrix is probably complex in terms of chemical functional groups. There are doubtlessly numerous varieties of substituted urea and other similar substructures in this polymer[24]. Nevertheless, the surface may be chemically modified to introduce ligands suitable for use in the interactive modes of HPLC. For example, ionogenic ligands can be covalently attached to the surface so that ion-exchange (electrostatic interaction) chromatography can be performed. A strong anion-exchange packing (SAX) was prepared on a UF matrix by a proprietary process and studied experimentally to determine its suitability for the fractionation of some common proteins. This particular packing material had 300-Å pores and a nominal particle diameter of 10 μm. Fig. 5 shows the separation of several proteins under classical ion-exchange conditions.

Hydrophobic interaction chromatography (HIC) is frequently preferred as a separation technique, since the conditions are mild, and denaturation of precious substances is minimized. The UF surface was chemically modified to produce a weakly hydrophobic environment, such that proteins and other macromolecular substances

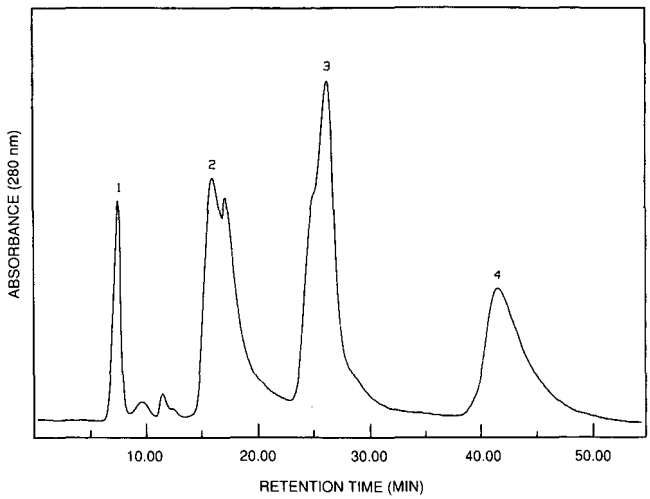

Fig. 5. Typical chromatogram of proteins on UF-300 SAX. Conditions: column, 300 × 10 mm I.D.; particle diameter, 9.5 μm; mobile phase system: (A) 0.01 *M* Tris (pH 8.0)–0.05% (w/v) sodium azide, (B) 0.01 *M* Tris–1.0 *M* sodium chloride (pH 8.0)–0.05% (w/v) sodium azide; gradient: 0% to 100% B linear in 50 min; flow-rate, 2.0 ml/min; detector, 280 nm, 0.1 a.u.f.s.; inlet pressure, 20 bar. Peak identities: 1 = myoglobin (cetine), 2 = carbonic anhydrase, 3 = ovalbumin (hen egg) and 4 = soybean trypsin inhibitor.

can be sorbed under mobile-phase conditions of high salt concentration and desorbed at lower concentrations. Fig. 6 shows a separation of myoglobin, carbonic anhydrase, and lysozyme. The linear gradient runs from a 2.0 *M* salt concentration, held constant

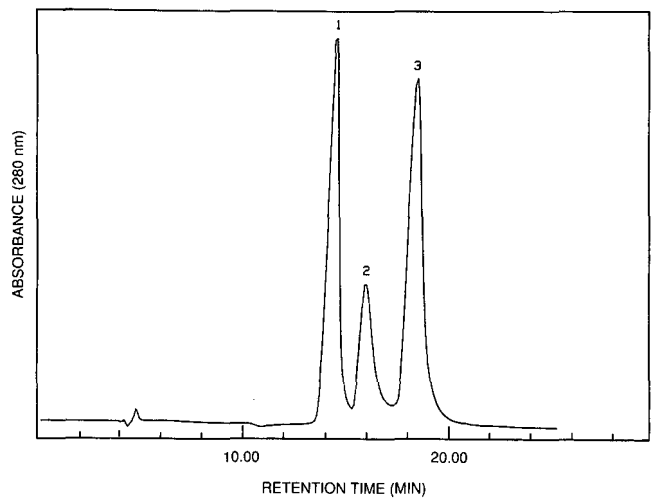

Fig. 6. Typical chromatogram of proteins on UF-300 HIC. Conditions: column, 300 × 10 mm I.D.; particle diameter, 9.5 μm; mobile phase system: (A) deionized water (pH 7.00)–0.05% (w/v) sodium azide, (B) 2.0 *M* ammonium sulfate–0.02 *M* potassium phosphate (pH 7.00)–0.05% (w/v) sodium azide; gradient, 100% to 0% B linear in 10 min, hold at 0% B for 15 min; flow-rate, 3.7 ml/min; detector, 280 nm, 0.1 a.u.f.s.; inlet pressure, 45 bar (at 100% B). Peak identities: 1 = myoglobin (equine), 2 = transferrin and 3 = lysozyme (hen egg).

for 5 min to ensure the sample was loaded, to 0.0 *M* in 15 min. The eluted substances were detected at 280 nm. Nominal 10-μm diameter particles with 300-Å pores were used for this separation.

CONCLUSIONS

The results of this work indicate that UF polymer may be quite suitable for use as a chromatographic support for HPLC. This material is easily formed into spherical microparticles by a well-established process, and the pore size is conveniently controlled by merely selecting silica sols of different sizes. The microspheres resist shrinking or swelling when contacted with common HPLC mobile phases. Furthermore, the UF microspheres exhibit no elastic or plastic deformation when subjected to inlet operating pressures ranging from ambient to levels in excess of 300 bar. The surface can be chemically modified by several procedures to provide for separations of proteins.

REFERENCES

1 J. Ugelstad, *U.S. Pat.*, 4,530,956 (1985); 4,186,120 (1980); 4,113,687 (1978).
2 F. Vláčil and I. Vinš, *J. Chromatogr.*, 391 (1987) 133.
3 F. Vláčil, I. Vinš and J. Čoupek, *J. Chromatogr.*, 391 (1987) 119.
4 J. Káš, M. Marek, J. Beronová and F. Švec, *J. Chromatogr.*, 376 (1986) 269.
5 N. Hirata, M. Kasai, Y. Yanagihara and K. Noguchi, *J. Chromatogr.*, 396 (1987) 115.
6 T. Hanai, Y. Arai, M. Kirukawa, K. Noguchi and Y. Yanagihara, *J. Chromatogr.*, 349 (1985) 323.
7 M. Wojaczyńska and B. Kolarz, *J. Chromatogr.*, 358 (1986) 129.
8 Y. Tanaka, H. Sato, K. Miyazaki and Y. Yamada, *J. Chromatogr.*, 407 (1987) 197.
9 Y. Kato, T. Kitamura and T. Hashimoto, *J. Chromatogr.*, 333 (1985) 93.
10 J. V. Dawkins, N. P. Gabbott, M. Montenegro, L. L. Lloyd and F. P. Warner, *J. Chromatogr.*, 371 (1986) 283.
11 J. V. Dawkins, L. L. Lloyd and F. P. Warner, *J. Chromatogr.*, 352 (1986) 157.
12 T. Anderson and L. Hagel, *Anal. Biochem.*, 141 (1984) 461.
13 S. Hjertén, B.-L. Wu and J.-L. Liao, *J. Chromatogr.*, 396 (1987) 101.
14 S. Hjertén, Z.-Q. Liu and D. Yang, *J. Chromatogr.*, 296 (1984) 115.
15 H. Ihara, T. Yoshinaga and C. Hirayama, *J. Chromatogr.*, 362 (1986) 197.
16 F. Helfferich, *Ion Exchange*, McGraw-Hill, New York, 1962.
17 R. K. Iler, *U.S. Pat.*, 4,010,242 (1977).
18 F. Nevejans and M. Verzele, *J. Chromatogr.*, 406 (1987) 325.
19 W. Yau, J. Kirkland and D. Bly, *Modern Size-Exclusion Chromatography*, Wiley, New York, 1979.
20 R. Stout, G. Cox and T. Odiorne, *Chromatographia*, 24 (1987) 602.
21 P. A. Bristow, *Liquid Chromatography in Practice*, hetp, Cheshire, 1976.
22 L. R. Snyder and J. J. Kirkland, *Introduction to Modern Chromatography*, Wiley, New York, 2nd ed., 1979.
23 Y.-F. Maa and Cs. Horváth, *J. Chromatogr.*, 445 (1988) 71.
24 W. R. Sorenson and T. W. Campbell, *Preparative Methods of Polymer Chemistry*, Wiley, New York, 2nd ed., 1968.
25 C. S. Marvel, J. R. Elliott, F. E. Boettner and H. Yuska, *J. Am. Chem. Soc.*, 68 (1946) 1681.
26 P. P. Grad and R. J. Dunn, *Anal. Chem.*, 25 (1953) 1211–1213.
27 J. C. Morath and J. T. Woods, *Anal. Chem.*, 30 (1958) 1437–1440.
28 R. C. Weast (Editor), *Handbook of Chemistry and Physics*, The Chemical Rubber Co., Cleveland, OH, 50th ed., 1969.

Journal of Chromatography, 476 (1989) 37–48
Elsevier Science Publishers B.V., Amsterdam — Printed in The Netherlands

CHROMSYMP. 1632

EVALUATION OF ADVANCED SILICA PACKINGS FOR THE SEPARATION OF BIOPOLYMERS BY HIGH-PERFORMANCE LIQUID CHROMATOGRAPHY

VI. DESIGN, CHROMATOGRAPHIC PERFORMANCE AND APPLICATION OF NON-POROUS SILICA-BASED ANION EXCHANGERS

G. JILGE, K. K. UNGER* and U. ESSER
Institut für Anorganische Chemie und Analytische Chemie, Johannes Gutenberg-Universität, D-6500 Mainz (F.R.G.)
H.-J. SCHÄFER and G. RATHGEBER
Institut für Biochemie, Johannes Gutenberg-Universität, D-6500 Mainz (F.R.G.)
and
W. MÜLLER
Chemical Reagents Division, R&D Chromatography, E. Merck, D-6100 Darmstadt (F.R.G.)

SUMMARY

The linear solvent strength model of Snyder was applied to describe fast protein separations on 2.1-μm non-porous, silica-based strong anion exchangers. It was demonstrated on short columns packed with these anion exchangers that (i) a substantially higher resolution of proteins and nucleotides was obtained at gradient times of less than 5 min than on porous anion exchangers; (ii) the low external surface area of the non-porous anion exchanger is not a critical parameter in analytical separations and (iii) μg-amounts of enzymes of high purity and full biological activity were isolated.

INTRODUCTION

The replacement of soft organic packings by microparticulate rigid macroporous organic polymers and wide-pore bonded silicas has substantially improved the separation performance in all modes of interactive chromatography of proteins and polynucleotides[1,2]. However, the results obtained so far indicate that the enhancement in resolution, speed, and biorecovery was not as high as expected. Several factors responsible for this observation are related to two intrinsic properties of porous packings: the tortousity and connectivity of pores and the heterogeneity of the surface. As a consequence, the kinetics of mass transfer of analytes can be slow, due to restricted intraparticle diffusion of polymers, and the remaining active surface sites can give rise to undesired interactions. All together, the effects cause additional peak dispersion and often considerable losses in recovery of biological activity.

0021-9673/89/$03.50

The logical solution to this problem is the use of non-porous packings, which offer a number of advantages, such as (i) fast mass transfer kinetics due to lack of restricted pore diffusion; (ii) absence of the enthalpic and entropic exclusion of solutes occurring in porous packings; (iii) maximum surface accessibility; (iv) maximum ligand utilization by appropriate ligand design and adjustment of ligand density and topography; (v) preservation of biological activity, due to short residence time of solutes in the column and (vi) fast column regeneration, due to the absence of an internal column volume.

The use of non-porous supports has some disadvantages also. Due to the lack of porous and internal surface, the external surface area of non-porous particles is extremely low. Assuming a solid density of 2.2 g/ml, the external surface area is calculated to 5.5 m^2/g at d_p (particle diameter) = 0.5 μm, 2.7 m^2/g at d_p = 1.0 μm, and 0.55 m^2/g at d_p = 5 μm. It is seen that the surface area of non-porous packings is about two orders of magnitude lower than that of porous packings. As a result, the solute retention and the mass loadability of packings decreases in the same proportion. To compensate for this drawback, the use of non-porous particles of 1–2 μm is recommended. They have a surface area of 2–4 m^2/ml of packing, comparable to that of a 200-nm pore-size packing. Particles much smaller than 1 μm are difficult to pack into columns and to operate with a conventional high-performance liquid chromatography (HPLC) system.

In 1984 we introduced 1.5-μm non-porous, monodisperse silica beads as packings for affinity chromatography with binding capacities for proteins comparable to those of 100- to 200-nm pore-size silicas[3]. Phillips *et al.*[4] have described the use of non-porous glass beads with $d_p > 10$ μm in affinity chromatography. Since that time, a number of non-porous packings have been developed and their outstanding chromatographic properties have been demonstrated[5–12].

In this paper, we describe the investigation of the potential of 2-μm silica-based non-porous strong anion exchangers in fast high-resolution separation and micropreparative isolation of biopolymers.

EXPERIMENTAL

Materials and methods

Non-porous monodisperse 2.1-μm silica and LiChrospher Si-300 -1000 and -4000 (10 μm) silicas were from Merck (Darmstadt, F.R.G.). Polyethylenimine-6 (PEI-6; molecular weight *ca.* 600) was purchased from Polysciences (Warrington, PA, U.S.A.). Glyceryltriglycidyl ether and pentaerythritol triglycidyl ether for crosslinking were from Grillonit, Ems-Werke AG (Domat/Ems, Switzerland). Methyl iodide, inorganic salts and solvents were of analytical grade or comparable quality.

Samples

Pure proteins, soybean trypsin inhibitor (STI), bovine serum albumin (BSA), catalase (CAT) and alcoholdehydrogenase (ADH) were from Merck; conalbumin (CON), ovalbumin (OVA) and human transferrin (TRA) from Serva (Heidelberg, F.R.G.); human serum albumin (HSA) from Behring-Werke (Marburg, F.R.G.) and horse heart myoglobin from Sigma (St. Louis, MO, U.S.A.). All 5′-mono, di- and triphosphate nucleotides were also purchased from Sigma. The DNA restriction

fragments were a gift of Prof. Müller (Merck). The enzyme F_1-ATPase from *Micrococcus luteus* was prepared in our laboratory.

Synthesis of anion exchangers

The method of Alpert and Regnier[13], modified by Kopaciewicz *et al.*[14], was applied for polyethylenimine coating and crosslinking of the porous and non-porous silicas with a minor variation. A 3-g amount of the non-porous silica was weighed into a 100-ml round-bottom flask, and 50 ml of a 10% (w/v solution of PEI-6 in methanol were added. The flask was sonicated, degassed briefly and kept at room temperature for 48 h. The coated silica was collected in a sintered glass funnel with a G4 frit and dried under vacuum for 2 h. Crosslinking was performed by suspending the coated silica in 50 ml of a solution of 10% (v/v) glyceryldiglycidyl ether (pentaerythritol triglycidyl ether) in methanol. The flask was sonicated, evacuated shortly and left at room temperature for 72 h. The product was isolated on a sintered glass funnel, washed with methanol and water and dried under vacuum. The porous particles were modified as described by Kopaciewicz *et al.*[14]. For quaternization the PEI-coated silicas were methylated using methyl iodide[15].

As the PEI loading of porous as well as non-porous silicas could not be assessed by elemental analysis due to the low nitrogen content, the solute retention served as a relative measure of mass of the load.

Packing procedure

The PEI-coated packing materials were slurry-packed into columns of 33 × 8 mm I.D. (Bischoff Analysentechnik und -geräte, Leonberg, F.R.G.) with 2-propanol–cyclohexanol (3:2, v/v) mixtures at constant flow-rates under maximum pressures of 60 MPa for the 2.1-μm non-porous particles and 40 MPa for the porous silicas. Alternatively, the anion exchangers were also packed with a 0.01 *M* Tris–HCl buffer (pH 8), yielding the same column performance as those packed with 2-propanol/cyclohexanol mixtures. The end fittings were made of paper filters (porosity $\leq$ 0.2 μm), supplied by Schleicher & Schüll (Dassel, F.R.G.) and supported by metal (porosity $<$ 2 μm) frits from Bischoff Analysentechnik und -geräte.

HPLC instrumentation

All chromatographic procedures were performed with a high-pressure gradient LC system, consisting of two Model 2150 HPLC pumps and a Model 2152 HPLC controller (Pharmacia-LKB Biotechnology, Uppsala, Sweden). All measurements were monitored at 280 nm for proteins and 254 nm for nucleotides using a Shimadzu SPD 6VA detector (Kyoto, Japan) with a 0.6-μl cell. The response time of 50 ms of the detector was sufficient to monitor fractions eluted a few seconds apart. The dwell time at a flow-rate of 1 ml/min amounted to 16.2 s. Two manual injection systems from Rheodyne (Cotati, CA, U.S.A.) were employed, equipped with a 1-μl and a 20-μl sample loop. Dead volume of all connecting tubing (0.125 mm I.D.) was kept at a minimum. The mobile phases were filtered through 0.45-μm porosity filters and degassed. For proteins and DNA fragments linear gradient elution was carried out with 0.01 *M* Tris–HCl buffer at pH 8 (eluent A) and 0.5 and 1 *M* sodium chloride in Eluent A (eluent B). The 5′-phosphate nucleotides were chromatographed by gradient elution, using a potassium phosphate buffer (0.01–0.5 *M*, pH 8).

Protein mass recovery

For the assessment of the mass recovery the column was loaded with a solution of 1 or 5 mg of pure protein in 0.01 *M* Tris–HCl (pH 8) and then eluted with 0.4 *M* sodium chloride in eluent A. In a second experiment the sample was directly injected into the detector. The collected volumes of samples eluted with and without the column were measured spectrophotometrically at 280 nm. Mass recovery of the following proteins were examined: OVA, BSA, CON, TRA, CAT, ADH, HSA and STI.

Recovery of the enzymatic activity

The activity of CAT[16] was determined by monitoring the decrease of the hydrogen peroxide concentration at 240 nm (UV) during the first 2 min of the reaction. CAT was injected at four different concentrations (2364 – 26 000 U) and eluted with 0.5 *M* in eluent A. Again, the experiments were repeated without the column, *i.e.*, by direct connection of the injector with the detector.

RESULTS AND DISCUSSION

Application of the linear solvent strength (LSS) model of Snyder to anion-exchange chromatography of proteins on non-porous packings

For the application of non-porous packings in interactive HPLC of proteins it is useful to predict operating conditions and to optimize the separation with respect to resolution, speed, and recovery. Recently, Snyder and co-workers[17–20] have developed a general model applicable to the chromatographic separations of large molecules in size-exclusion, reversed-phase, hydrophobic interaction and ion-exchange chromatography. To check the general validity of the linear solvent strength model of Snyder, it was applied to fast protein separations on the non-porous 2.1-μm anion exchangers. First isocratic retention parameters were calculated by means of two gradient runs. In isocratic ion-exchange chromatography the solute capacity factor is a function of salt concentration, c, of the mobile phase as

$$\log k' = \log K - m \log c \tag{1}$$

where K is the ion-exchange distribution constant and m the effective charge of the solute. Furthermore the average k' value of the solute during elution can be calculated by

$$\bar{K} = 1/1.15 \cdot b \tag{2}$$

where b is the gradient steepness parameter (eqn. 4). $\bar{K}$ corresponds to the k' value of the migrating band at the halfway point along the column. The concentration, $\bar{c}$, at the column midpoint is obtained by

$$\bar{c} = c_0 + [t_g - t_0 - t_D - 0.3(t_0/b)]\Delta c/t_G \tag{3}$$

where c_0 and c_f are the initial and final salt concentrations ($\Delta c = c_f - c_0$), t_g the retention time in gradient elution, t_0 the column dead-time, t_D the dwell-time and t_G the gradient time. The gradient steepness parameter, b, is given by

$$b = V_m \log(c_f/c_0)/t_G f_v \tag{4}$$

where f_v is the volume flow-rate and V_m the column dead-volume. It should be emphasized that b is not constant over the entire gradient. Hence, an average value of $b(b_0)$ is defined by

$$b_0 = rb \tag{5}$$

where r is

$$r = \Delta c/2.3\bar{c} \log(c_f/c_0) \tag{6}$$

A more reliable method for calculating isocratic retention data is based on the equation

$$b_1 = (t_0 \log \beta)/[t_{g1} - (t_{g2}/\beta) - (t_0 + t_D)(\beta - 1)/\beta] \tag{7}$$

when b_2 is equal to

$$b_2 = b_1/\beta \tag{8}$$

with

$$b_2/b_1 = \beta = t_{G2}/t_{G1} \tag{9}$$

Values of $\bar{K}$ *vs.* $\bar{c}$ are calculated from gradient elution data for proteins and compared with the experimental results obtained isocratically (k' *vs.* c).

Furthermore, the chromatographic performance, can be expressed by the resolution, R_s, as

$$R_s = 1.176 \frac{t_{g2} - t_{g1}}{[w_{0.5}]_1 + [w_{0.5}]_2} \tag{10}$$

where t_{g1} and t_{g2} are the retention times of the proteins and $[w_{0.5}]_1$ and $[w_{0.5}]_2$ the bandwidths at half-height of the peak. From the experimental data the b values were calculated for the 0.5- and 1.0-min gradients at a flow-rate of 4 and 5 ml/min and for the 1-, 2- and 5 min gradient at a flow-rate of 1.5 ml/min. Values of $\bar{K}$ against $\bar{c}$ were plotted for TRA, OVA and STI and compared with the experimental data, obtained isocratically from the plots of k' against c. Fig. 1 shows a relatively good agreement between the data obtained from isocratic elution and gradient runs. Note that the average $\bar{K}$ values are mostly $\ll 1$, caused by the smaller differences between the retention times of proteins on the non-porous anion exchanger. It was shown that the LSS model is applicable to fast separations on non-porous packings.

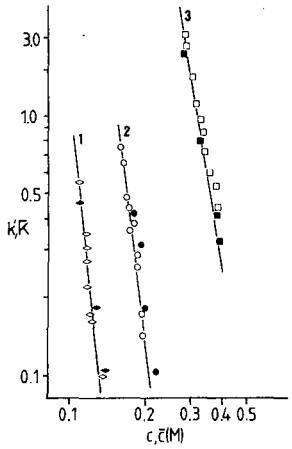

Fig. 1. Correlation of retention data from isocratic (◆, ●, ■) and gradient elution (◇, ○, □). Ion-exchange chromatography of (1) transferrin, (2) ovalbumin and (3) soybean trypsin inhibitor on a non-porous strong anion-exchange column; conditions and equations as described in text.

Fast high-resolution separations of proteins and polynucleotides

Tests have been performed to compare the resolution of proteins in anion-exchange chromatography on non-porous 2.1-μm packings and 10-μm silicas of graduated pore diameter. All products were PEI coated and quaternized.

In Fig. 2 the chromatographic resolution R_s for OVA–STI is plotted against the gradient time, t_G, obtained from separations of proteins on non-porous and porous anion exchangers. It is obvious that the porous anion exchanger based on LiChrospher

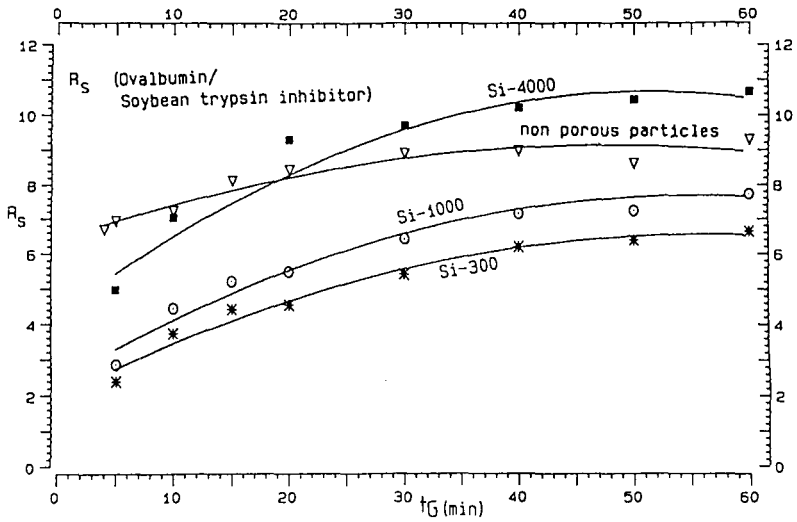

Fig. 2. Chromatographic resolution, R_s, of OVA–STI on PEI-coated porous and non-porous strong anion-exchange columns as a function of gradient time, t_G, at a constant flow-rate of 1.5 ml/min. Gradient: 0–0.5 *M* sodium chloride.

Si-4000 provides a better resolution at larger gradient times of about 20 min than the non-porous anion exchangers. Higher R_s values are the result of larger retention differences between t_{g1} and t_{g2} for the porous packing. However, the highest resolutions at $t_G < 20$ min were achieved on columns packed with the non-porous anion exchangers. Although there is a difference in particle size between 2.1-μm (non-porous) and 10-μm (porous), all porous anion exchangers gave a higher band-broadening due to the intraparticulate mass transfer. Nearly the same results were achieved by Duncan *et al.*[7], comparing 10-μm polymer-based, porous and non-porous ion exchangers. The difference in resolution for high-speed separations becomes much more pronounced at high flow-rates and very short gradient times (see Fig. 3A and B). But it must be noticed, that the linear velocity, u, is nearly double as high for the non-porous particles as for porous packings, caused by the absence of the pore volume for the non-porous anion exchanger. So the difference between the curves of Lichrospher Si-4000 and the non-porous packing decreases, when the resolution is plotted against the linear velocity (not shown). A comparison of the chromatograms

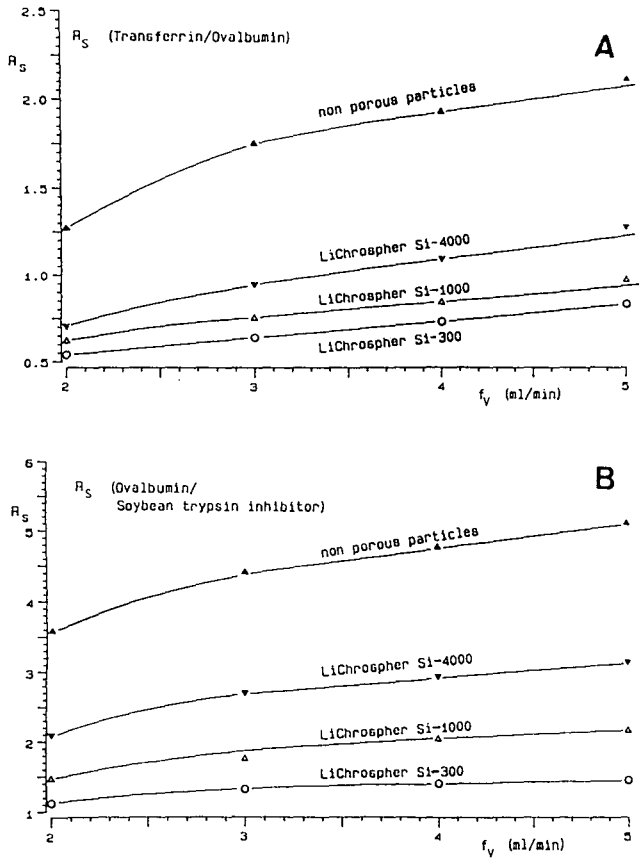

Fig. 3. Chromatographic resolution, R_s, of (A) TRA–OVA and (B) OVA–STI on porous and non-porous strong anion-exchange columns as a function of volume flow-rate, f_v. Gradient: 1 min, linear (0–0.5 *M* sodium chloride).

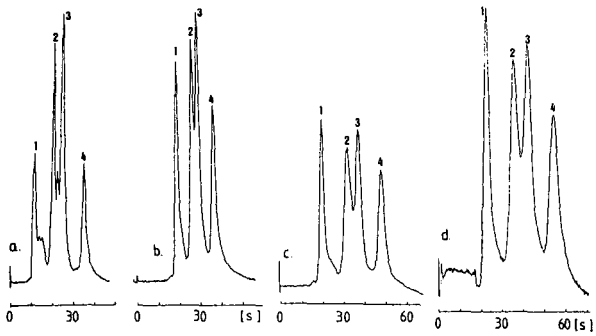

Fig. 4. Fast separation of (1) MYO, (2) TRA, (3) OVA and (4) STI on PEI-coated silica-based strong anion-exchange columns (33 mm × 8 mm I.D.). (a) Non-porous 2.1-μm particles, (b) LiChrospher Si-4000, (c) LiChrospher Si-1000, (d) LiChrospher Si-300. Gradient time: 0.5 min, linear (0–0.5 *M* sodium chloride). Flow-rate; 5 ml/min.

obtained with different anion exchangers demonstrate the advantage of the non-porous material (Fig. 4). In case of the non-porous anion exchanger (Fig. 4a) the prepeak of OVA (see arrow) was detected. Furthermore, the retention times and peak width of proteins are seen to become larger with decreasing the pore size (Fig. 4b–d).

Protein mass and enzymatic activity recoveries

Mass recoveries of ⩾97% were achieved for OVA, BSA, CON, TRA, CAT, ADH, HSA and STI on the non-porous anion exchanger (Table I). With the exception of CON and TRA, recoveries were generally superior to those obtained from the porous packings under identical conditions. Especially with LiChrospher Si-300 larger amounts of proteins were irreversibly adsorbed on the surface of the silica.

TABLE I

PROTEIN MASS RECOVERIES USING POROUS AND NON-POROUS STRONG ANION EXCHANGERS

Columns (33 mm × 8 mm I.D.): (a) non-porous particles, (b) LiChrospher Si-4000, (c) LiChrospher Si-1000 and (d) LiChrospher Si-300. For conditions, see text.

Proteins	*Mass recovery (%)*			
	Column			
	a	*b*	*c*	*d*
OVA	98	97	97	96
BSA	98	97	97	94
CON	99	99	98	99
TRA	99	99	99	99
CAT	98	97	97	89
ADH	98	98	98	94
HSA	98	96	95	93
STI	97	96	95	89

A similar result was achieved for the recovery of the enzymatic activity of CAT. Although CAT is a tenaciously retained protein, with the non-porous anion exchanger the activity recovery was 97–98% for all concentrations. With porous packing the values were lower, *i.e.*, between 90 and 95% were obtained. Possibly the decrease of the biological activity of catalase on porous anion exchangers is caused by the multisite solute surface interactions in the pores of the silica.

Temperature effects

While shorter retention times of proteins have been observed at elevated column temperatures in reversed-phase chromatography, the retention times for strong anion exchangers increased with increasing temperature. Raising the temperature from 298 to 333 K resulted in an increase in the retention time of DNA-fragments with a non-porous anion exchanger by 70%. According to Helfferich[21], it is assumed that with increasing temperature the diffusion coefficient in ion exchangers increases, the matrix becomes more flexible and the diameter of the ions decreases because solvation is reduced. The resolution of protein separation was nearly doubled at a temoerature of 328 K, caused mainly by longer retention times and, to a minor extent, by a small decrease in peak bandwidth at higher temperatures. But above 328 K, resolution could no more be calculated because strong band broadening and dramatic losses of mass recovery occurred. To avoid denaturation at higher temperatures, it is necessary to minimize the contact time between protein and stationary phase. Only non-porous particles, allow to separate proteins with a very short contact time due to their capacity, the low column dead-volume and the absence of pore diffusion.

High-resolution separations of 5′-phosphate nucleotides

Significant differences in resolution between non-porous and porous anion exchangers were also observed for smaller molecules like 5′-mono, di- and tri-phosphate nucleotides. A comparison of the chromatograms in Fig. 5 shows, that all 12 nucleotides were well separated on the non-porous anion exchanger within 2 min. Resolution on porous packings is decreased by pore diffusion and larger particle sizes. Best results in nucleotide separations were obtained with LiChrospher Si-4000 especially for longer gradient times. But there were no significant differences between the porous materials varying the pore size. Fig. 6 demonstrates that all nucleotides can actually be resolved in less than 90 s on the non-porous (2.1-μm) anion exchanger.

Furthermore, on the non-porous anion exchanger the nucleotides can also be resolved isocratically on the non-porous anion exchanger. The plate numbers calculated from separations of 5′-mono- and diphosphate nucleotides using the non-porous packing show that they do not change significantly. This is probably due to the lack of pore diffusion, which minimizes the mass transfer effects, *e.g.*, expressed in the Van Deemter *C* Term. The highest plate numbers of nearly 140 000 plates/m were achieved at a flow-rate of 2.0 ml/min.

Fast micropreparative fractionation of crude F_1-ATPase

A crude extract of F_1-ATPase (molecular weight *ca.* 400 000) from *Micrococcus luteus* was fractionated by anion-exchange chromatography using the non-porous strong anion-exchange packing. Fig. 7 shows a 10-min gradient (0–1 *M* sodium chloride) of the sample at a load of *ca.* 200 μg. Six subfractions were collected. Fraction

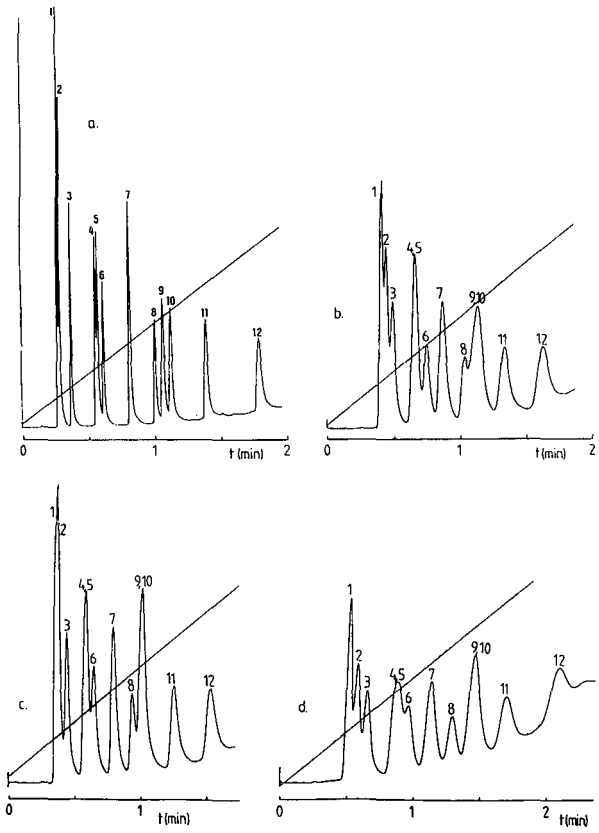

Fig. 5. Separation of 5′-mono-, di- and triphosphate nucleotides. Columns: PEI-coated strong anion exchangers. (a) Non-porous particles, (b) LiChrospher Si-4000, (c) LiChrospher Si-1000, (d) LiChrospher Si-300. Gradient time: 2 min, linear, 0.01–0.5 *M* KH_2PO_4 (pH 6.3). Flow-rate: 5 ml/min. Peak identification: 1 = UMP; 2 = CMP; 3 = AMP; 4 = GMP; 5 = UDP; 6 = CDP; 7 = ADP; 8 = UTP; 9 = CTP; 10 = GDP; 11 = ATP; 12 = GTP.

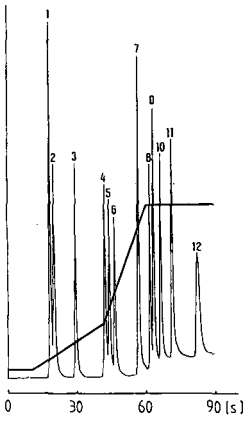

Fig. 6. Fast high-resolution separation of 5′-mono-, di- and triphosphate nucleotides. Column: non-porous (2.1-μm) packing, PEI-coated strong anion exchanger. Flow-rate; 5 ml/min. Gradient: 0 min (0.01 *M* KH_2PO_4, pH 6.3), 0.2 min (0.01 *M* KH_2PO_4), 0.7 min (0.14 *M* KH_2PO_4), 1.0 min (0.5 *M* KH_2PO_4). The elution sequence of the nucleotides is given in Fig. 5.

4 contained the pure protein (*ca.* 60 μg). The purity was checked by electrophoretic monitoring (Fig. 8). The sodium dodecyl sulfate polyacrylamide gel electrophoresis (SDS-PAGE) of the six subfractions showed a superior purity compared to the reference purified by Shephadex A-25 (Pharmcia-LKB Biotechnology). The enzymatic activities of subfraction 4 and the reference sample were comparable. Limited loadability of the non-porous anion exchanger due to the low surface area, hence, low ion-exchange capacity became notable when the mass load exceeded *ca.* 200 μg of crude extract. At higher loads, the purity as well as the recovery of enzymatic activity decreased.

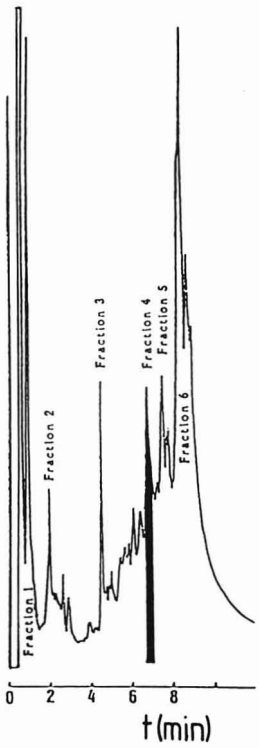

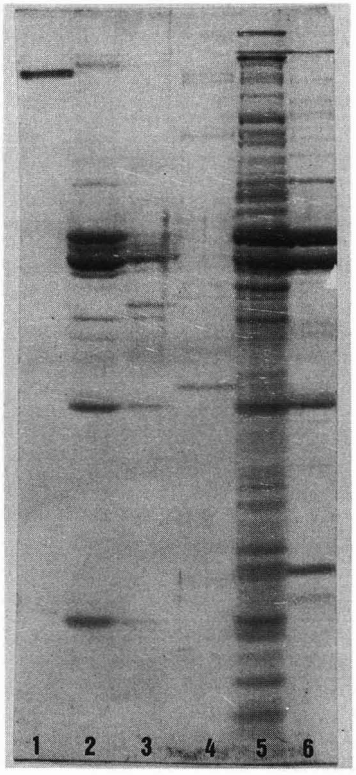

Fig. 7. Fractionation of F_1-ATPase crude extract from *Micrococcus luteus* (molecular weight *ca.* 400 000) on a PEI-coated, non-porous, strong anion-exchange column (33 mm × 8 mm I.D.). Buffer: 0.01 *M* Tris–HCl (pH 8). Gradient time: 10 min (0–1.0 *M* sodium chloride). Flow-rate: 1.5 ml/min. Sample volume: 20 μl. Detection: UV at 280 nm. Six subfractions were taken. Fraction 4 contains the pure protein (*ca.* 60 μg/injection).

Fig. 8. SDS-PAGE electrophoretic monitoring of the chromatographic separation shown in Fig. 7. Lane 1, fractions 1–3; lane 2, fraction 4; lane 3, fraction 5; lane 4, fraction 6; lane 5, crude extract; lane 6, reference sample purified by DEAE-Sephadex A-25.

CONCLUSION

We have demonstrated that non-porous (2.1-μm) silica-based anion exchangers are well suited for fast high-resolution analytical separations and for the fast micropreparative isolation of proteins and polynucleotides. It was also shown that low-molecular-weight substances such as nucleotides, can be separated in *ca.* 1 min on short columns of 33 mm × 8 mm I.D. packed with non-porous anion exchanger.

Furthermore, the linear solvent strength model of Snyder has been applied to the non-porous anion exchanger, separating proteins with very short gradient times and high flow-rates. Comparison of the calculated isocratic retention for TRA, OVA and STI from gradient runs shows a good agreement with measured isocratic retention data.

The column temperature also plays a significant role in anion-exchange chromatography of proteins. With increasing temperature the solvation decreases, the protein retention times increase strongly and the resolution becomes better. But the longer contact time between protein and anion-exchange surface leads to denaturation of biologically active products.

REFERENCES

1 K. K. Unger, R. Janzen and G. Jilge, *Chromatographia*, 24 (1987) 144.
2 F. E. Regnier, *Chromatographia*, 24 (1987) 241.
3 F. B. Anspach, K. K. Unger, H. Giesche and M. T. W. Hearn, *presented at the Fourth International Symposium on HPLC of Proteins, Peptides and Polynucleotides, Baltimore, MD, December 1984*, paper 103.
4 T. M. Phillips, W. D. Queen, N. S. More and A. M. Thompson, *J. Chromatogr.*, 327 (1985) 213.
5 D. J. Burke, J. K. Duncan, L. C. Dunn, L. Cummings, C. Siebert and G. S. Ott, *J. Chromatogr.*, 353 (1986) 425.
6 D. J. Burke, J. K. Duncan, C. Siebert and G. S. Ott, *J. Chromatogr.*, 359 (1986) 533.
7 J. N. Duncan, A. J. C. Chen and C. J. Siebert, *J. Chromatogr.*, 397 (1987) 1.
8 Y. Kato, T. Kitamura, A. Mitsui and T. Hashimoto, *J. Chromatogr.*, 398 (1987) 327.
9 M. A. Rounds and F. E. Regnier, *J. Chromatogr.*, 447 (1988) 73.
10 Y. Kato, T. Kitamura, A. Mitsui, Y. Yamasaki, T. Hashimoto, T. Murotsu, S. Fukushige and K. Matsubara, *J. Chromatogr.*, 447 (1988) 212.
11 K. K. Unger, G. Jilge, J. N. Kinkel and M. T. W. Hearn, *J. Chromatogr.*, 359 (1986) 61.
12 R. Janzen, K. K. Unger, H. Giesche, J. N. Kinkel and M. T. W. Hearn, *J. Chromatogr.*, 397 (1987) 91.
13 J. Alpert and F. E. Regnier, *J. Chromatogr.*, 185 (1979) 75.
14 W. Kopaciewicz, M. A. Rounds and F. E. Regnier, *J. Chromatogr.*, 318 (1985) 157.
15 M. A. Rounds, W. Kopaciewicz and F. E. Regnier, *J. Chromatogr.*, 362 (1986) 187.
16 *Biochemica Catalog*, E. Merck, Darmstadt, 1986.
17 M. A. Stadalius, H. S. Gold and L. R. Snyder, *J. Chromatogr.*, 296 (1984) 31.
18 M. A. Stadalius, H. S. Gold and L. R. Snyder, *J. Chromatogr.*, 327 (1985) 27.
19 R. W. Stout, S. I. Sivakoff, R. D. Ricker and L. R. Snyder, *J. Chromatogr.*, 353 (1986) 439.
20 L. R. Snyder and M. A. Stadalius, in Cs. Horvath (Editor), *High-Performance Liquid Chromatography, Advances and Perspectives*, Vol. 4, Academic Press, New York, 1986, p. 195.
21 F. Helfferich, *Ion-Exchange*, McGraw-Hill, New York, 1962.

Journal of Chromatography, 476 (1989) 49–57
Elsevier Science Publishers B.V., Amsterdam — Printed in The Netherlands

CHROMSYMP. 1576

POLYMER SUPPORT SYNTHESIS

XV[a]. BEHAVIOUR OF NON-POROUS SURFACE-COATED SILICA GEL MICROBEADS IN OLIGONUCLEOTIDE SYNTHESIS

HARTMUT SELIGER*, UDO KOTSCHI and CAROLINE SCHARPF
Universität Ulm, Sektion Polymere, Oberer Eselsberg, D-7900 Ulm (F.R.G.)
RAINER MARTIN
Universtät Ulm, Sektion Elektronenmikroskopie, Oberer Eselsberg, D-7900 Ulm (F.R.G.)
FRIEDHELM EISENBEISS and JOCHEN N. KINKEL
E. Merck, Abt. Reagenzienforschung, Frankfurter Str. 250, D-6100 Darmstadt (F.R.G.)
and
KLAUS K. UNGER
Institut für Anorganische Chemie und Analytische Chemie, Johannes Gutenberg-Universität, D-6500 Mainz (F.R.G.)

SUMMARY

Non-porous silica gel microbeads of diameter 1.5 μm have been investigated as supports for oligonucleotide synthesis. In the preparation of oligothymidylates of chain length up to 150 bases, with 5′-di-*p*-anisylphenylmethyl-3′-phosphoramidite as an intermediate, the average yields per chain elongation were up to 99%. Lower overall yields were observed in the case of a support which developed a strong tendency towards aggregation after the build up of an oligonucleotide coating.

INTRODUCTION

For the automated solid-phase synthesis of oligonucleotides, non-swellable porous inorganic carriers, like silica gel or controlled-pore glass (CPG), are currently the most widely used support materials. The growth of oligonucleotide chains on such supports can be seen as the controlled build up of an organic coating on the surface of the inorganic matrix. During the preparation of very long oligonucleotide chains (more than 100 bases) on a support with an average pore diameter 750 Å, the chain growth was found to come to nearly a complete stop after the attainment of a certain length[1]. This was attributed to steric problems created by the filling up of the pores. As a consequence of this observation and of experiments on yield optimization carried out in our laboratory[2], carriers with wide pores of narrow size distribution, *e.g.*,

[a] For Part XIV, see ref. 3

0021-9673/89/$03.50

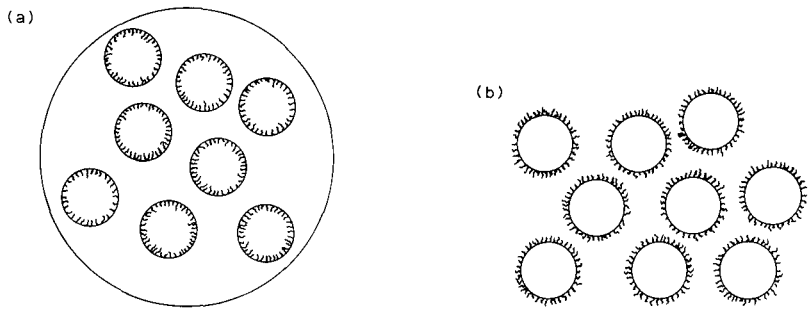

Fig. 1. Schematic representation of (a) a macroporous polymer support with internal organic coating of the pores, and (b) a non-porous microbead support of similiar surface area with external organic coating.

CPG 3000 Å, were found to be suitable for oligonucleotide preparations. Additionally, we have recently found that oligonucleotides grafted onto CPG 3000 also become available for reactions catalyzed by a variety of enzymes, such as polynucleotide kinase, DNA or RNA ligase, DNA polymerase, restriction enzymes or exonucleases[3].

Yet, if one wishes to construct very long polynucleotide chains, it can be envisaged that steric problems will arise, even with these wide pore materials. Therefore, if the accessibility of oligonucleotides inside the pores of the support is a limitation of further chain growth, an advantageous alternative should be found in non-porous microbeads, where the organic coating is on the outer surface only, the oligonucleotide chains being able to extend into the void volume of the resin bed (Fig. 1). The idea of improving the accessibility of support-bound oligonucleotide chains by using microreticular support materials was first suggested by Köster[4,5] about 16 years ago. However, the microgels described in his papers did not find application to oligonucleotide preparations. We have now exploited this concept and tested the performance of non-porous silica gel microbeads, originally prepared as stationary phases for high-performance liquid chromatography (HPLC)[6], in the automated solid-phase synthesis of oligonucleotides.

EXPERIMENTAL

Chemicals

Nucleoside phosphoramidites were products of Applied Biosystems (Foster City, CA, U.S.A.). 3-Aminopropyltriethoxysilane, benzoyl chloride, dichloroacetic acid, 4-(N,N-dimethyl)aminopyridine, acetic anhydride, 1-methylimidazole and trimethylchlorosilane were obtained from Fluka (Buchs, Switzerland). Silica gel 60 H for column chromatography as well as most solvents were obtained from E. Merck (Darmstadt, F.R.G.). Dichloromethane was obtained from Hedinger (Stuttgart, F.R.G.), 4,4'-Dimethoxytrityl chloride from Aldrich (Steinheim, F.R.G.) and [γ-^{32}P]ATP from Amersham, Buchler (Braunschweig, F.R.G.). Acetonitrile (HPLC grade) was supplied by J. T. Baker (Phillipsburgh, NJ, U.S.A.). Tetrazole was prepared from 5-aminotetrazole by a literature procedure[7]. Most solvents were purified and dried according to the literature.

Apparatus

Oligonucleotide synthesis was carried out using automated synthesizers 381 A (Applied Biosystems) and SAM I (Biosearch, San Rafael, CA, U.S.A.). The reaction column of the latter synthesizer was replaced by the Autofix System (E. Merck) as described previously[2,8]. HPLC was performed with a solvent delivery system 1400 A (Applied Biosystems). Polyacrylamide gel electrophoresis (PAGE) was carried out on an LKB Macrophor (LKB, Bromma, Sweden). For scanning electron microscopy a Philips SEM 500 (Eindhoven, The Netherlands) was used. For this purpose, the dry samples were coated by sputtering with gold or palladium.

Supports

Two species of monodisperse silica gel microbeads, prepared as described previously[9–11], were used (supports I and II). Each had a diameter of 1.5 μm (surface area 2.5 m^2/g). Support I in contrast to II had a residual content of very small pores (average diameter *ca.* 4 Å).

Loading of supports

The supports were functionalized by reaction with (1) aminopropyltriethoxysilane and (2) 5′-di-*p*-anisylphenylmethylthymidine-3′-*p*-nitrophenylsuccinate, as described in the literature[12,13]. The major part of the material was treated further with 50% aqueous methanol for 16 h at room temperature[2]. This removes more loosely bonded organic material and reduces the load to roughly one-half. However, the stability of the immobilized oligonucleotides is greatly increased.

Oligonucleotide synthesis

The oligonucleotide synthesis started with immobilized thymidine, the protected monomer for further elongation was di-*p*-anisylphenylmethylthymidine-3′-β-cyanoethoxyphosphoramidite[14]. Cycle times were approximately 10.3 min. After completion of all cycles, small samples of support material were withdrawn from the columns and their contents of target oligonucleotide estimated by spectroscopy at 498 nm in a 0.1 *M* toluenesulphonic acid solution in acetonitrile. The further work-up included standard deblocking and release from the support[12,13], followed by reversed-phase (RP) HPLC and/or PAGE.

RESULTS

The first reaction, which was performed on the surface of the silica gel microbeads, was the aminopropylation with aminopropyltriethoxysilane, followed by addition of 5′-di-*p*-anisylphenylmethylthymidine as 3′-terminal nucleoside via its *p*-nitrophenylsuccinate. The nucleoside load capacity was 2–3 μmol/g (see Table I).

Several test syntheses of oligothymidylates of chain lengths up to 100 bases were done with support I, using automated nucleotide synthesizers. Appropriately protected nucleoside phosphoramidites were used as intermediates. The reaction cycle proceeded mainly as described[12,13]. We found, however, that good results in the preparation of long oligonucleotides required a prolongation of the detritylation step. The reactions and conditions for chain elongation are listed in Table II.

The results, summarized in Table III, show that yields obtained with this sup-

TABLE I

CONDITIONS FOR AND RESULTS OF NUCLEOSIDE LOADING OF DIFFERENT MICROBEAD AND MACROPOROUS SUPPORTS

Support	*Surface area* (m^2/g)	*Capacity, NH_2*				*Capacity, DMTrdT*			
		$\mu mol/g$		$\mu mol/m^2$		$\mu mol/g$		$\mu mol/m^2$	
		a	*b*	*a*	*b*	*a*	*b*	*a*	*b*
Microbeads I	2.5	11.0	6.1	4.4	2.4	4.2	3.1	1.7	1.2
Microbeads II	2.5	8.0	3.7	3.2	1.5	3.1	2.1	1.2	0.8
CPG 1400	17.3	87.0	46.0	5.0	2.6	14.1	15.6	0.8	0.9
CPG 3007	6.9[c]	34.0	16.0	4.9	2.3	7.7	5.8	1.1	0.8
Fractosil 2500	8.0	29.0	8.0	3.6	1.0	7.5	6.5	0.9	0.8

[a] Untreated.

[b] Treated with 50% aqueous methanol.

[c] Value obtained from W. Haller (Chevy Chase, MD, U.S.A.).

TABLE II

REACTION CYCLE FOR OLIGONUCLEOTIDE CHAIN ELONGATION USING MICROBEAD SUPPORTS

Function	*Time (s)*
Acetonitrile to column	240
Phosphoramidite and tetrazole to column	27
Capping reagent to column	13
Iodine to column	17
Dichloroacetic acid to column	160

TABLE III

RESULTS OF OLIGONUCLEOTIDE SYNTHESES PERFORMED WITH MICROBEAD SUPPORTS I AND II

Oligonucleotide	*Support*	*Capacity ($\mu mol/g$)*		*Yield after completion of cycles (OD_{260})*[b]	*Average yield per condensation (%)*
		Initial	*Terminal*		
$(dT)_{30}$	Microbeads I	3.1	1.60	1.5	97.8
$(dT)_{50}$	Microbeads I	3.1	0.82	4.3	98.6
$(dT)_{100}$	Microbeads I	3.1	0.64	2.7	98.4
$(dT)_{50}$	Microbeads I[a]	2.1	1.00	4.4	97.8
$(dT)_{50}$	CPG 1400[a]	23.1	18.40	32.6	99.5
$(dT)_{50}$	Microbeads II	2.1	1.30	11.9	99.0
$(dT)_{150}$	Microbeads II	2.1	0.55	7.1	99.1

[a] Syntheses performed simultaneously in the SAM I/Autofix system[2,15]. All other syntheses were performed in the Synthesizer 381 A (Applied Biosystems).

[b] One OD_{260} unit is $1/\varepsilon$ mmol/mol of a dissolved chromophore, measured at 260 nm (ε = absorption coefficient).

port were somewhat lower than usual, being 97–98% per cycle. This was obviously independent of the batch of nucleoside phosphoramidite, since different preparations were used. In order to exclude the possibility that this yield decrease might be due to machine failure or inadequate purity of solvents or reagents, we compared support I with CPG, using a set up of two stacked cartridges in the SAM I/Autofix system described earlier[2,15]. The result of this comparison is also shown in Table III. Obviously, under stringently identical conditions, the performance of the CPG support in the preparation of $(dT)_{50}$ was significantly better, the latter giving average yields of *ca.* 99% per elongation. Incomplete yields in the case of support I were also reflected in the appearance of a significant ladder of truncated sequences on gel electrophoresis of the solid-phase products (Fig. 2) and in a tailing observed on separation of DMTr-$(dT)_{30}$ [DMTr = di-(*p*-anisyl)phenylmethyl-] in RP-HPLC[14].

Recently, a new type of microbead support has become available in which the residual content of micropores is completely eliminated (support II). A first test synthesis of $(dT)_{50}$ with this new support (Table III) indicated a significant improvement in yields. This stimulated us to prepare $(dT)_{150}$, as an example of a very long oligonucleotide. This synthesis was accomplished with an average yield per chain elongation of 99.1%, a result which compares well to previous syntheses of oligonucleotides of 140–175 bases, performed with CPG of average pore diameter 1000–2000 Å (refs. 1, 15 and 17). The products, after release from the support, were subjected to PAGE (Fig. 3). The correct lengths of the various oligothymidylates were checked by the simultaneous electrophoresis of authentic polynucleotide samples of known sizes.

In order to explore possible reasons for the relatively low yields with support I, scanning electron microscopy of supports I and II was performed prior to synthesis, after loading with di-*p*-anisylphenylmethylthymidine and after completion of an oligonucleotide synthesis. From these electron microscopic images it appears that considerable agglomeration of microbeads occurs when the organic coating builds up on support I. This agglomeration effect is not seen in the case of support II where the appearance of the material in scanning electron microscopy is similar before synthesis and after 150 cycles.

DISCUSSION

Non-porous silica gel microbeads can be surface-loaded with nucleosides according to standard procedures to produce polymer supports useful for machine-aided oligonucleotide synthesis. Loads are in the range of 2–3 μmol nucleoside per g support, *i.e.*, 0.8–1.2 μmol nucleoside per m^2 of surface area. Although this is lower than the capacity usually used in solid-phase oligonucleotide synthesis, we do not see this as a disadvantage, since the amount of material needed for biological experiments is generally very small, and both the microbeads and wide-pore CPG will produce enough material for biological experiments if yields are sufficiently high. The capacity of these microbead supports is compared in Table I with those of two species of wide-pore CPG[2]. Although the nucleoside load, measured in μmol/g support, is higher in the case of CPG supports owing to the higher specific surface area, the capacity, calculated in μmol/m^2 surface area, is the same. From this and the following results of oligonucleotide syntheses it is evident that the microbead supports, in accordance with Fig. 1, behave very much like CPG pores "turned inside out".

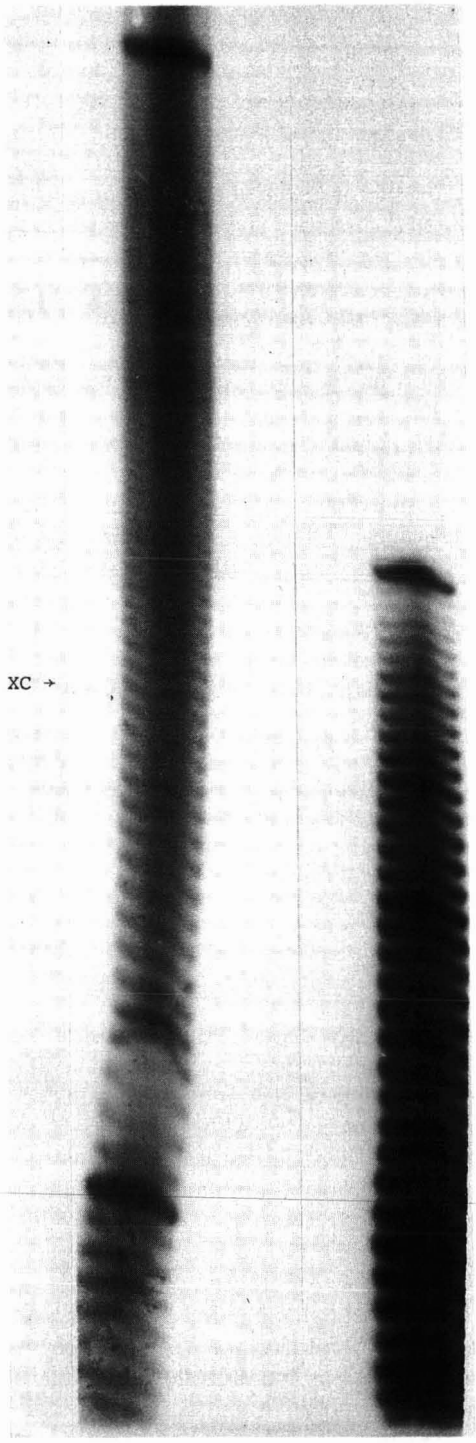

Fig. 2. Autoradiogram of the PAGE separations of crude $(dT)_{100}$ (left lane) and $(dT)_{50}$ (right lane) prepared on support I (12% denaturing polyacrylamide gel; XC = xylene cyanol marker corresponds to the length of *ca.* 48 bases[16].

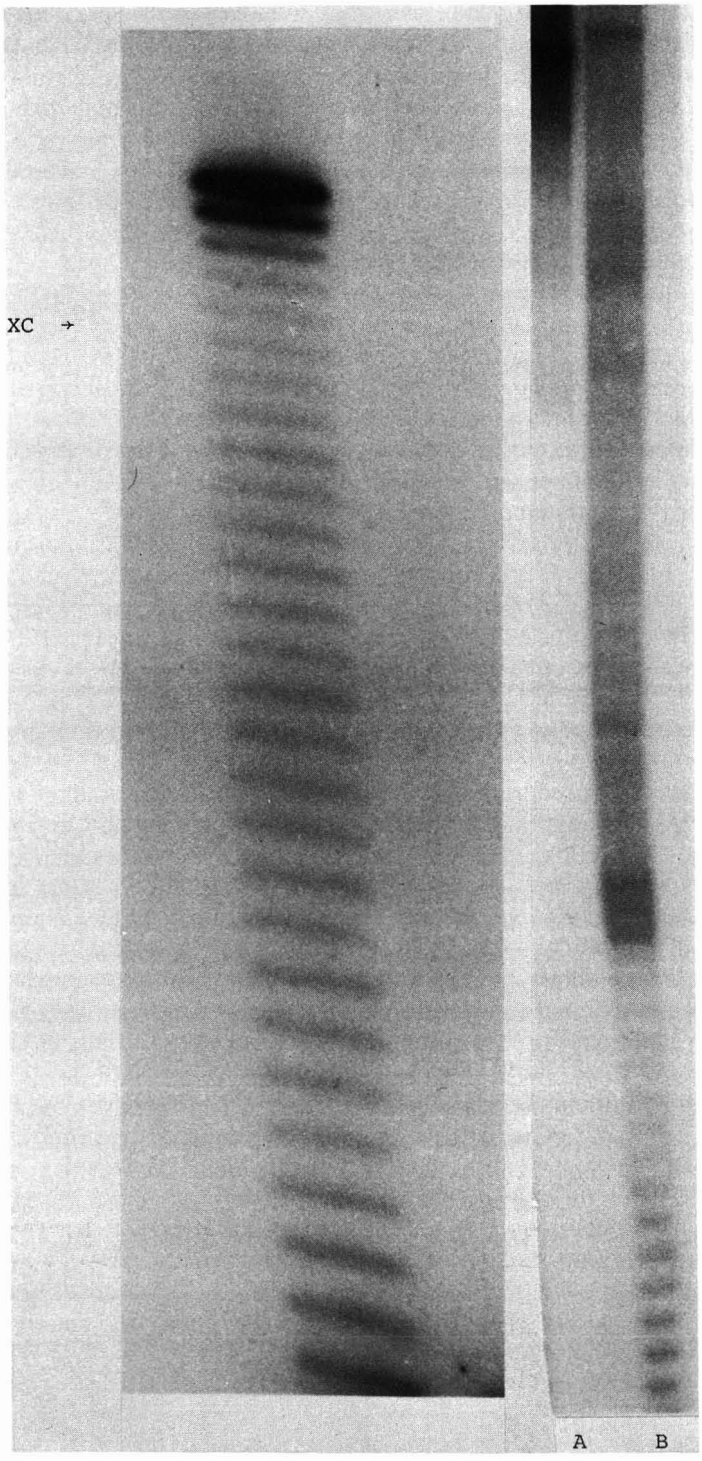

Fig. 3. Autoradiogram of the PAGE separations of crude $(dT)_{50}$ (left panel) and $(dT)_{150}$ (right panel), prepared on support II and 12% denaturing polyacrylamide gels. The left panel contains xylene cyanol (XC) as a marker. The right panel contains as a marker in lane A an authentic sequenced gene fragment of 146 bases[17]. The sample of $(dT)_{150}$ is shown in lane B.

The yields of the oligonucleotide chain elongations in the case of support II may be raised to levels comparable to those obtained with the best macroporous support systems. Thus, microbead supports are suitable for the preparation of long oligonucleotides up to 150 bases. This chain length is not the limit for chemical elongation[1], however it is near the maximum length for which a purification can be achieved by HPLC[15,17,a]. The full advantage of the microbead supports over macroporous resins is expected to be revealed on further enzyme-catalyzed lengthening of the chemically synthesized oligonucleotides. Studies along these lines are now being performed in parallel with CPG[6] and support II in our laboratory.

The slightly inferior yields with support I compared to support II and CPG supports still remain to be explained. From our studies two yield-decreasing factors may be envisaged. First, support I has an high tendency to agglomerate. Inside the chunks that are thus formed the growing oligonucleotide chains are less readily accessible to reagents and washing solutions. Secondly, Ogilvie and co-workers[18] recently observed that small pores on the surface may be opened up during repeated acid detritylations. If this observation applies also to microbead materials, one can imagine that the very small pores of support I might be widened, thus allowing water molecules to be adsorbed. This adsorbed water may then be a source of reagent hydrolysis and yield decrease.

The exposure of the surface layer of oligonucleotide to shearing during the flow of reagent and washing solutions through the column packing was also considered as a possible problem. However, although long polynucleotides are known to be susceptible to chain disruption by mechanical forces, this does not seem to be a significant yield-decreasing process in our case, particularly in view of the highly satisfactory results obtained with support II.

The handling of such microbead supports of very small particle size in automated oligonucleotide synthesizers requires some precautions, although it does not create major difficulties. Standard reaction columns as parts of commercial synthesizers, as well as the reaction cartridges we described earlier for simultaneous syntheses of multiple oligonucleotides[2,15], can be used. However, it is recommended that filters with appropriately small pore size or a double filter layer be used. We have observed that, with suitable reaction columns, the loss of support material was less than 5%, even during the 149 cycles required to prepare $(dT)_{150}$. This loss may perhaps be further reduced by an additional careful sizing of the silica gel microbeads after loading them with nucleoside. No build up of back pressure was observed with the apparatus and under the conditions described here.

The application of the microbead support system to the preparation of various oligonucleotides, containing different constituents, is presently under investigation in our laboratory.

ACKNOWLEDGEMENTS

Financial aid for work done at the University laboratories from the Deutsche Forschungsgemeinschaft is gratefully acknowledged. We are greatly indebted to W. Haller (Chevy Chase, MD, U.S.A.) for gifts of samples of CPG materials.

[a] PAGE shows a resolution of ±2 bases at a chain length of 150 bases (see ref. 1).

REFERENCES

1 J. W. Efcavitch, L. J. McBride and J. S. Eady, in K. S. Bruzik and W. Stec (Editors), *Biophosphates and Their Analogues, Synthesis, Structure, Metabolism and Activity,* Elsevier, Amsterdam, 1987, p. 65.
2 H. Seliger, A. Herold, U. Kotschi, J. Lyons and G. Schmidt, in K. S. Bruzik and W. Stec (Editors), *Biophosphates and Their Analogues, Synthesis, Structure, Metabolism and Activity,* Elsevier, Amsterdam, 1987, p. 43.
3 G. Gröger and H. Seliger, *Nucleosides Nucleotides,* 7 (1988) 773.
4 H. Köster, *Tetrahedron Lett.,* 16 (1972) 1527.
5 H. Köster and S. Geussenhainer, *Angew. Chem.,* 84 (1972) 712.
6 K. K. Unger, G. Jilge, J. N. Kinkel and M. T. W. Hearn, *J. Chromatogr.,* 359 (1986) 61.
7 R. A. Henry and W. G. Finnegan, *J. Am. Chem. Soc.,* 76 (1954) 290.
8 H. Seliger, A. Herold, U. Kotschi, J. Lyons, G. Schmidt and F. Eisenbeiss, *Nucleosides Nucleotides,* 6 (1987) 137.
9 K. Unger, H. Giesche and J. Kinkel, *Ger. Pat. Appl.,* DE 3534143 (1985).
10 W. Stöber, A. Fink and E. Bohn, *J. Colloid Interface Sci.,* 26 (1968) 62.
11 W. Stöber and H. Flachsbart, *J. Colloid Interface Sci.,* 30 (1969) 568.
12 M. D. Matteucci and H. M. Caruthers, *J. Am. Chem. Soc.,* 103 (1981) 3185.
13 H. Seliger, S. Klein, C. K. Narang, B. Seemann-Preising, J. Eiband and N. Hauel, in H. G. Gassen and A. Lang (Editors), *Chemical and Enzymatic Synthesis of Gene Fragments,* Verlag Chemie, Weinheim, 1982, pp. 81ff.
14 N. D. Sinha, J. Biernat, J. McManus and H. Köster, *Nucleic Acids Res.,* 12 (1984) 4539.
15 H. Seliger and G. Schmidt, *J. Chromatogr.,* 397 (1987) 141.
16 T. Maniatis, E. F. Fritsch and J. Sambrook, *Molecular Cloning —A Laboratory Manual,* Cold Spring Harbor Laboratory, Cold Spring Harbor, NY, 1982.
17 G. Schmidt, R. Schlenk and H. Seliger, *Nucleosides Nucleotides,* 7 (1988) 795.
18 R. T. Pon, N. Usman and K. K. Ogilvie, *Biotechniques,* 6 (1988) 768.

Journal of Chromatography, 476 (1989) 59–72
Elsevier Science Publishers B.V., Amsterdam — Printed in The Netherlands

CHROMSYMP. 1623

BLOTTING OF PROTEINS ONTO IMMOBILON MEMBRANES *IN SITU* CHARACTERIZATION AND COMPARISON WITH HIGH-PERFORMANCE LIQUID CHROMATOGRAPHY

THEODORA CHOLI, ULRIKE KAPP and BRIGITTE WITTMANN-LIEBOLD*
Max-Planck-Institut für Molekulare Genetik, Abteilung Wittmann, D-1000 Berlin 33 (Dahlem) (F.R.G.)

SUMMARY

The electrophoretic transfer from polyacrylamide gels to Immobilon [poly(vinylidene difluoride)] membranes of various proteins differing in molecular masses from 14 000 to 200 000 was performed, using both a semi-dry blotting apparatus and a standard blotting chamber. The blotted proteins were analyzed and sequenced with and without staining, and the initial yields of the degradation were examined. Furthermore, protein purification by blotting after one- and two-dimensional gel electrophoresis was compared with conventional HPLC methods. Optimum blotting conditions for *in situ* enzymatic or chemical cleavages of the proteins on the blots are described, and for the *in situ* hydrolysis followed by amino acid analysis and cysteine determination.

INTRODUCTION

Over the past 10 years, blotting procedures have become an essential element in the biochemical analysis of nucleic acids, proteins and lipids. Several articles have been published on various technical aspects of these methods, and different blotting procedures have been proposed as means for studying biological problems.

Blotting or transfer of electrophoretically resolved proteins to immobilizing matrices, followed by specific detection, has become a routine procedure for the biochemical characterization of these macromolecules. For optimum results the following criteria must be met: (i) proteins must be transferred efficiently from the gel to the matrix; (ii) they must be quantitatively bound; (iii) the detection must be specific and sensitive and (iv) the blotted substances must allow senstitive analysis and characterization by appropriate micro methods. The combined use of sodium dodecyl sulphate (SDS) with polyacrylamide gel electrophoresis (PAGE) and discontinuous buffer systems[1,2] allows evaluation of the purity or the complexity of protein mixtures, the resolution of which has been increased by the development of two-dimensional gel electrophoresis[3–5]. Further improvement was made when blot techniques for the analysis of DNA[6] were applied to proteins[7–9]. Recently, methods for protein microsequence analysis have been described which employ the electrotransfer of pro-

0021-9673/89/$03.50

teins onto sequencer-stable supports, such as modified glass fibres (GFs) or poly(vinylidene difluoride) (PVDF) membranes[10–15].

However, many proteins cannot be sequenced by Edman degradation, due to blockage of the NH_2-terminal amino acid. Furthermore, modified NH_2-terminal amino acids cannot easily be determined. Sequence information for these proteins is obtained by cleavage of the polypeptide chain and purification of the peptides derived. As has been reported[16,17], proteins blotted onto various membranes can be cleaved enzymatically or chemically, and the peptides released can be separated by reversed-phase high-performance liquid chromatography (HPLC).

In this paper, we describe the enzymatic digestions of standard proteins *in situ* on PVDF membranes under different conditions, including the use of organic solvents, which were reported[18] to lead to an efficient elution of the polypeptides from the membranes. The activity of trypsin under these conditions was tested and the initial yields from stained or non-stained protein blots were examined. Furthermore, the advantages and applications of protein blotting *versus* purification by reversed-phase HPLC methods for complex protein mixtures are demonstrated on examples of ribosomal protein mixtures.

EXPERIMENTAL

Materials

PVDF membranes (Immobilon Transfer) of pore size 0.45 μm were obtained from MilliGen (Division of Millipore, Bedford, MA, U.S.A.). Poly(vinylpyrrolidone) with an average M_r of 40 000 (PVP-40) was obtained from Sigma Chemie (Deisenhofen, F.R.G.), polybrene from Applied Biosystems (Foster City, CA, U.S.A.), trypsin, TPCK (L-1-tosylamido-2-phenylethylchloromethyl ketone)-treated trypsin from Boehringer (Mannheim, F.R.G.), sodium dodecyl sulphate (SDS), N,N′-methylenediamine and ammonium persulphate from Bio-Rad (Heidelberg, F.R.G.), 2-mercaptoethanol, methanol, glycine, tris(hydroxymethyl)aminomethane (Tris), Amido Black, thioglycolic acid, hydrochloric acid and dithiothreitol from Merck (Darmstadt, F.R.G.). Unless stated otherwise, all chemicals were of analytical grade or better quality. The marker proteins were from Bethesda Research Laboratories (BRL) (Gaithersburg, MD, U.S.A.). Vydac column packings, C_4 (300 Å, 5 μm) and C_{18} (201 Total Porous Beads), were obtained from the Separation Group (Hesperia, CA, U.S.A.). The columns were packed in our laboratory.

Methods

SDS-PAGE. Samples of 500 pmol β-lactoglobulin B were loaded onto gels (16 cm × 10 cm), which were subjected to pre-electrophoresis overnight at 20 V prior to sample application. Thioglycolate (0.1 m*M*) was added to the buffer. The polyacrylamide concentration was 15%, and the gels were prepared according to Laemmli[1].

The gels used for blotting of standard proteins in the two different blotting chambers (the semi-dry and conventional tank buffer system described below) were 5-15% gradient gels or 10% discontinuous polyacrylamide gels and were prepared as described above. The electric potentials were 60 V for the stacking gel and 100 V for the separation gel.

Electrophoretic transfer. Two blotting systems were used: the semi-dry appara-

tus from H. Hölzel (Dorfen, F.R.G.) and the conventional blotting chamber of standard design[8] with an interelectrode distance of 10.5 cm.

For SDS gels, the transfer buffer in both blotting systems consisted of 25 m*M* Tris–HCl (pH 8.4)–0.5 m*M* dithioerythritol (DTE)–0.02% SDS and was degassed before use. Transfer for the semi-dry apparatus was conducted for 1–2.5 h at 0.5–0.8 mA/cm^2. Transfer with our conventional system[15] was conducted for 1 h at 120–150 mA and then for 4–6 h at 650 mA. For electroblotting from two-dimensional gels in urea, the composition of the transfer buffer was 1% acetic acid and 0.5 m*M* DTE. In this case, the blotting was conducted at 4°C for 1 h with 650 mA, using the conventional tank buffer system.

In all cases, two PVDF membranes were sandwiched for blotting. After transfer, the membranes were washed thrice with HPLC-grade water (MilliQ system of Millipore, Eschborn, F.R.G.) for *ca.* 10–15 min with *ca.* 20 ml water per 10 cm × 10 cm membrane. The protein bands were excised and either sequenced immediately or stored at −20°C under nitrogen in sealed Eppendorf tubes. In cases where the membranes were stained, they were treated either with 0.1% R-250 in 50% methanol for 5 min and destained in 50% methanol for 5–10 min at room temperature[13] or with Amido Black in 0.1% in 50% methanol for 5 min and destained in 30% methanol for 5–10 min at room temperature. The protein bands that were not stained were detected as grayish areas while the membrane became white upon drying.

Sequencing of immobilized proteins. The excised bands were arranged as pieces in a single layer on top of a Polybrene-treated glass fibre disk in the upper cartridge block of an Applied Biosystems (Weiterstadt, F.R.G.) Model 477A sequencer, equipped with a Model 120 phenylthiohydantoin (PTH)-amino acid analyzer. The glass-fibre filters were pre-treated with trifluoroacetic acid, loaded with 2 mg Polybrene, and twice precycled, as instructed by Applied Biosystems. Sequencing and analysis of PTH derivatives were performed by standard procedures. Initial coupling yields were determined from recovery of the NH_2-terminal residue and are presented with respect to the amount of sample loaded onto the gels.

In situ tryptic digestion. Tryptic digests were performed on dot blots of β-lactoglobulin on PVDF membranes, which were prepared as follows. Small pieces of a PVDF membrane were immersed in 100% methanol. Before the membranes became dry, 10 μl of β-lactoglobulin (1 nmol) were spotted onto it, and the membranes were dried overnight in open test-tubes.

Each membrane, containing 1 nmol protein, was incubated for 30 min at room temperature in 1 ml 0.2% PVP-40, dissolved in 100% methanol, in order to prevent adsorption of the protease on the PVDF membrane during digestion[16,17]. Prior to enzymatic digestion, the excess of poly(vinylpyrrolidone) (PVP-40) was removed by extensive washing with water, at least three times.

The protein samples were digested as follows: 100 m*M* N-methylmorpholine acetate buffer (pH 8.1) was used as the digestion buffer, and the digestion was performed for 20 h at 37°C with gentle stirring. The enzyme/protein ratio was 1:20. The peptides were separated by reversed-phase HPLC on a Vydac C_{18} 201 TPB column (250 mm × 4 mm) with an acetonitrile gradient in 0.1% aqueous trifluoroacetic acid. A complete removal of PVP-40 prior to HPLC analysis is essential, because it absorbs strongly in the UV region.

In situ chemical cleavage with CNBr. A 500-pmol amount of β-lactoglobulin

was loaded onto SDS polyacrylamide gel, which was subjected to pre-electrophoresis. Electroblotting onto PVDF membranes was carried out by using the transfer buffer and the apparatus described above. After blotting, the membranes were washed, and after inspection the spots were excised and collected in a small test-tube. The protein was cleaved with CNBr in 70% formic acid with 2 μl β-mercaptoethanol (ME) for 48 h in the dark under nitrogen at ambient temperature or, alternatively, in 70% formic acid, 2 μl ME and 20% acetonitrile under the same conditions. A 200-μl volume of the solution was added per cm^2 of excised membrane. After cleavage, the solution was diluted in water, the membrane taken out and the solution was lyophilized. The peptides were dissolved in 20 μl water, separated by reversed-phase HPLC (C_{18}, 5-μm packing). Sequencing and analysis of the PTH derivatives released were performed by standard procedures.

Total hydrolysis. The membrane pieces containing blotted β-lactoglobulin or insulin B (oxidized) were immersed in 250 μl of 5.7 *M* HCl and hydrolyzed for 24 h at 110°C in precleaned, evacuated, sealed test-tubes. After hydrolysis, the membranes were removed and the hydrolysate was dried in a desiccator or in a Savant (München, F.R.G.) Speed-Vac centrifuge for about 2 h. The amino acids were determined after precolumn derivatization with *o*-phthaldialdehyde (OPA) by reversed-phase HPLC, as described in ref. 19.

Cysteine determination. Lysozyme, insulin B and ribonuclease (each 1 nmol), respectively, were electroblotted in the semi-dry apparatus described above. In this case, the SDS-PAGE pre-electrophoresis of the SDS-polyacrylamide gel was not used. After blotting, the protein bands were rinsed with methanol for about 1 s, collected in hydrolysis tubes and 200 μl 98% formic acid was added to each tube. A 1-ml volume of 98% formic acid was mixed with 0.1 ml H_2O_2 and kept at room temperature for about 1 h. After cooling to 4°C, 40 μl of the performic acid solution were added to each protein blot in 200 μl 98% formic acid, and oxidation at −20°C was carried out for 2–4 h. The excess of performic acid was destroyed by the addition of 400 μl ice–water. The solution was evaporated in the Savant Speed-Vac centrifuge. Cysteines were determined as cysteic acid after acid hydrolysis, as described above.

RESULTS AND DISCUSSION

Electrophoretic transfer

As described under Methods, the electrotransfer of high- and low-molecular-weight (200 000 and 14 000) proteins was performed in a tank of buffer[15] or in a semi-dry apparatus[20], employing two sandwiched PVDF membranes (see Fig. 1A). The transfer buffer in both systems was the same, containing 25 m*M* Tris (pH 8.4)–0.5 m*M* DTE–0.02% SDS[15]. However, different blotting times and electric potentials were used in the two devices (see Methods). The transfer buffer was prechilled, and blotting was conducted at 4°C. Fig. 2 shows the transfer of several proteins from a gradient of 5–15% PAGE, using the tank buffer[15] under the conditions described above. From this Figure it is obvious that proteins with relative low molecular masses, such as β-lactoglobulin (18 400) or lysozyme (14 300), are transferred faster than the high-molecular-weight components. They almost totally penetrate the first membrane and are trapped on the second PVDF layer. Three of the other proteins, with M_r 29 000 (carbonic anhydrase), 43 000 (ovalbumin) and 68 000 (bovine serum albu-

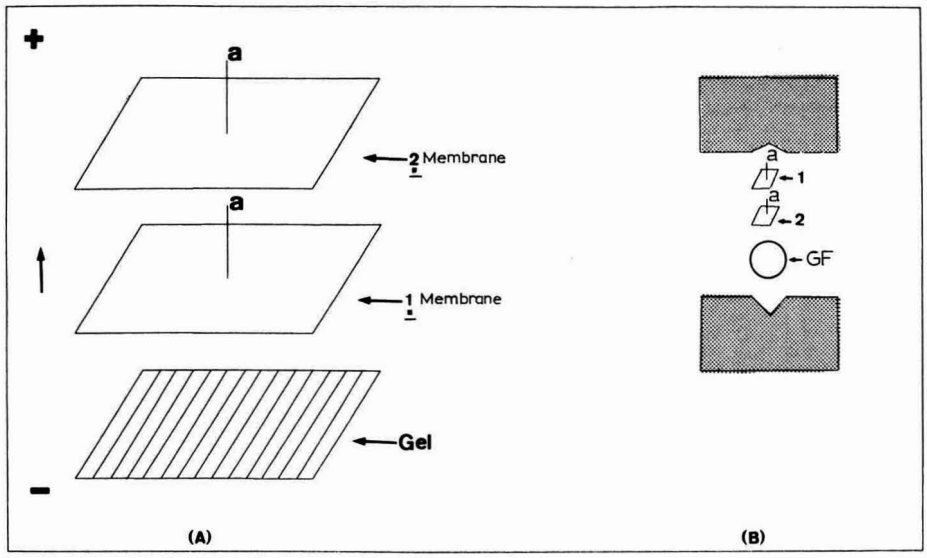

Fig. 1. (A) Electrotransfer from a SDS gel onto PVDF membranes. The arrow indicates the blot direction and "a" shows the membrane surface on which most of the protein was detected. (B) Arrangement of the PVDF pieces in the reactor. Numbers 1 and 2 show the first and second PVDF membrane, respectively; GF represents the glass-fibre disk, pre-treated with TFA, and precycled with Polybrene.

min), were partially transferred to the second PVDF layer. The high-molecular-weight components phosphorylase B and myosin (H-chain), with M_r of 97 000 and 200 000, respectively, were transferred in only poor yields.

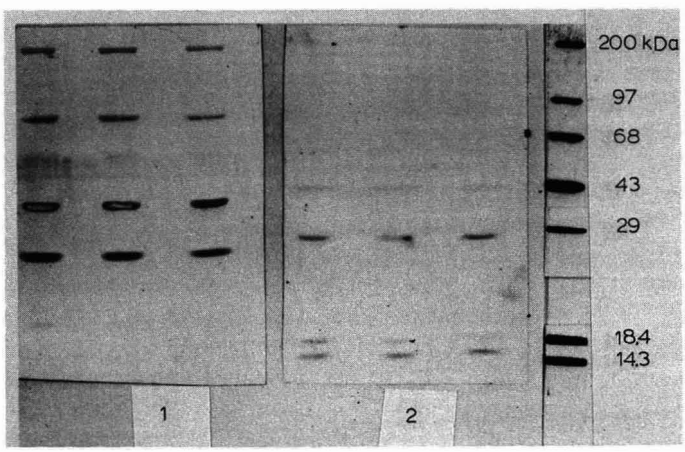

Fig. 2. Electrotransfer of various proteins onto PVDF membranes from a 5–15% gradient gel with the conventional tank buffer system. The transfer buffer consisted of 25 m*M* Tris (pH 8.4)–0.5 m*M* DTE–0.02% SDS. Numbers 1 and 2 represent the first and the second membrane, respectively. Blotting was conducted at 4°C, 150 mA for 1 h and 650 mA for 4 h. The membranes were weakly stained with Coomassie Blue for 5 min.

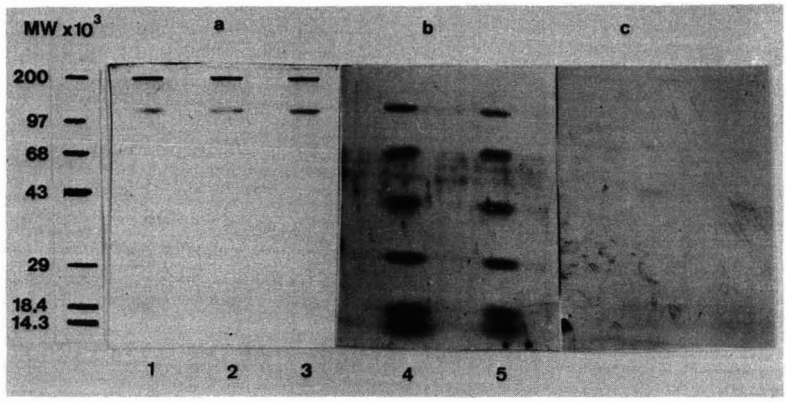

Fig. 3. Electrotransfer of proteins onto PVDF membranes from a 10% polyacrylamide gel by the semi-dry method. The transfer buffer was the same as in Fig. 2. Blotting was conducted at 4°C for 1 h with 0.8 mA/cm². The membranes were weakly stained with Coomassie Blue. "a" shows the remaining proteins in the gel, "b" and "c" the blotted proteins on the first and second membrane, respectively. Lanes: 1–4, loaded with the proteins described in Materials; 5, identical to 4.

Figs. 3 and 4 show the protein transfer from 10 and 5–15% PAGE, respectively, by the semi-dry method[20], which was used at 4°C for 1 h with 0.8 mA/cm². Problems with heating of the buffer during the transfer at 4°C were negligible under these conditions. Again, a poor transfer of the high-molecular-weight components (200 000 and 97 000) was observed, which necessitates the use of more SDS in the buffer system or a longer transfer time. On the other hand, the low-molecular-weight proteins were better transferred by using the homogeneous 10% gel which has bigger sizes of pores.

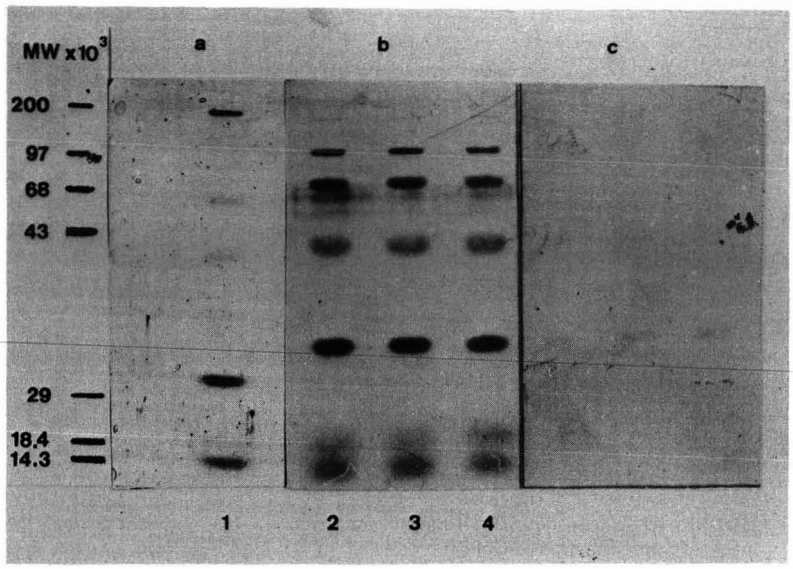

Fig. 4. Electrotransfer of proteins onto PVDF membranes from a 5–15% gradient gel by the semi-dry method. Blotting conditions and abbreviations as in Fig. 3.

Comparison of the transfers with the conventional tank system and the semi-dry apparatus shows that the lower-molecular-weight proteins blotted by the semi-dry method were transferred sufficiently and almost quantitatively to the first PVDF layer, independent of the size or charge of the proteins. These transfers, in which a flat electrode system with short distances between the electrodes and filter-paper reservoirs for the buffers, is used, offer advantages over the blotting in tanks in terms of homogeneous voltage fields and high voltage gradients, which produce rapid, efficient, safe and convenient electrotransfer. On the other hand, high-molecular-weight proteins need more time for the transfer, if the same transfer buffer is used. Therefore, for complex protein mixtures containing various sizes of proteins, such as ribosomal proteins, two layers of PVDF should be sandwiched to make sure that all the proteins can be trapped. Furthermore, an optimum transfer time must be found.

Sequencing of immobilized protein

A 500-pmol amount of β-lactoglobulin was loaded on a 15% polyacrylamide gel, which was subjected to pre-electrophoresis prior to protein application. The electrotransfer was conducted at 4°C in the conventional tank buffer system[15]. After transfer, the Immobilon membranes were quickly rinsed in water of HPLC grade for removal of glycinate ions, which interfere with sequencing, and for reduction of the SDS level, in order to prevent blockage of the HPLC injection line in the sequencer. The proteins were detected by weak staining with Coomassie Blue or Amido Black. They can also be detected without staining as grayish areas on the surrounding white membrane during drying. With further drying, the protein-containing areas are easily seen as zones more intensely white than the surrounding ones when transilluminated with white light. The bands were excised with a razor blade, dried overnight at room temperature and stored in sealed Eppendorf tubes under nitrogen at −20°C.

The arrangement of the Immobilon pieces in the reactor is shown in Fig. 1B. At first, the membrane surface onto which the protein is blotted (showing the highest intensity) is placed in the upper cartridge in upside-down position. Secondly, the second PVDF membrane piece is placed on top of the first one, and thirdly, both are kept in place by covering them with a trifluoroacetic acid (TFA)-treated glass filter, pretreated with 2 mg Polybrene, and precycled in a normal sequencing program. The upper cartridge is then turned over and screwed on to the lower cartridge part, so that the "protein face" is on top. At the R_3 delivery and wash stages, the blotted protein is transferred and trapped on the pretreated glass filter. Thus, the blotted proteins or peptides are degraded by this technique mainly in the glass filter, and incomplete coupling due to insufficient penetration of the aqueous base into the PVDF membrane pieces is prevented. Table I shows the difference between blotted unstained β-lactoglobulin samples, which were arranged either with the "protein face" in the cartridge on top as described above, or randomly arranged. The initial yields of 40% in the first case and 21.8% in the second case demonstrate that the correct placement of the protein side of the PVDF membranes is very important.

In order to demonstrate that blotted proteins easily become NH_2-terminally blocked, not only during electrophoresis and electrotransfer[21], but also during staining, even if all the chemicals used are of high-purity grade, we sequenced 500 pmol of blotted β-lactoglobulin, either stained with Coomassie Blue or Amido Black or unstained, using identical conditions for electrophoresis, transfer and sequencing (see

TABLE I

EFFECT OF THE POSITION OF THE PROTEIN BLOTS IN THE CARTRIDGE BLOCK ON INITIAL SEQUENCING YIELDS (SEE FIG. 1B)

β-Lactoglobulin samples (500 pmol) were applied onto the gel and blotted after electrophoresis. Initial yields were determined for the NH_2-terminal residues. The values shown are the percentages of the amounts of protein loaded onto the gel. The yields are average values from three experiments.

Detection	*Arrangement*	*Yield (%)*
Coomassie Blue[a]	Protein face[b]	24.1
Amido Black[a]	Protein face	15.0
Non-stained	Protein face	40.0
Non-stained	Random	21.8

[a] Weakly staining for 5 min.
[b] The "protein face" arrangement is described in Fig. 1B and in the text.

Table I). The Coomassie-stained samples gave 24.1% initial yield, and the Amido Black-stained yielded 15.0%, while the non-stained samples gave 40% for the "protein face" arrangement and 21.8% for a random arrangement.

Cleavage with CNBr

The cyanogen bromide cleavage *in situ* on the Immobilon was used to obtain internal sequences of known blocked proteins. The mixture of the peptides was dissolved in about 20–30 μl water, then applied on a TFA-pretreated glass filter, and sequenced according to the standard programs. For cleavage of small polypeptides with a M_r of about 6000, addition of acetonitrile to the cleavage solution was unnecessary, whereas for cleavage of larger proteins, such as β-lactoglobulin (18 400), this was very useful (final concentration, 20% acetonitrile). The presence of an organic solvent helps to wet the PVDF membrane, facilitating cleavage of the protein and extraction of the peptides from the membrane. The use of Triton X-100 or other detergents was found unnecessary in case of the proteins tested.

Employing this technique, we studied a fragment of ribosomal protein L12 from *Sulfolobus acidocaldarius*, produced during autolysis of the protein. Since the intact L12 protein is NH_2 -terminally blocked (by acetylmethionine)[22], this fragment with a molecular mass of about 6000 was isolated by SDS-PAGE. The gel was subjected to pre-electrophoresis, and the fragment (1–2 nmol) was blotted in the tank buffer system. After *in situ* cyanogen bromide cleavage of the fragment on the PVDF membrane, we were able to determine the sequence of 58 residues[23]. This cleavage was performed without the addition of acetonitrile.

After chemical cleavage of a protein, *e.g.*, by CNBr *in situ*, on the blot, it is very important to dilute the generated peptide solution in water and to dry it several times. Multiple washing and drying removes the excess of CNBr and reaction products, which could block the delivery and injection lines of the sequencer.

Cysteine determination

The cysteine content was estimated for insulin B and for a ribosomal protein of *Bacillus stearothermophilus*. The blots were stained with Coomassie Blue and Amido

Black. The amount of protein loaded onto the gel was 2 and 1 nmol, respectively. The ribosomal protein was blotted from two-dimensional gels[5] by using the conventional tank buffer system[15]. The number of cysteines found for blotted oxidized lysozyme and ribonuclease was lower than that calculated from their sequences. Four cysteines were found for ribonuclease (theoretical value 8.0) and five for lysozyme (theoretical value 8.0). In part, this is to be expected after oxidation and hydrolysis. Likely, cysteine residues in blotted proteins need a longer oxidation time, and they are partially destroyed during electrophoresis and transfer. On the other hand, proteins with low molecular weights, such as insulin B (3400) and the ribosomal protein (*ca.* 6000), gave better results. The number of cysteines determined for the blotted insulin B was 1.67, and for the non-blotted protein it was 2.0. This is in good agreement with the number of cysteine residues present (two residues) in this polypeptide chain.

Tryptic digestion

The ability to perform *in situ* chemical or enzymatic cleavage of proteins blotted on PVDF membranes, followed by reversed-phase HPLC of the peptide fragments released, obviates many problems. In order to prevent adsorption of the protease on the membrane during digestion, the blotted pieces were pretreated with PVP-40, as described in ref. 16, with some modifications. We used a concentration of 0.2% in 100% methanol (see Methods). The cleavage was performed with an enzyme/protein ratio of 1:20, at 37°C in 100 m*M* N-methylmorpholine acetate buffer at pH 8.1.

Fig. 5a shows the HPLC separation of the tryptic peptides released from 1 nmol β-lactoglobulin without blotting, and Fig. 5b shows the separation of the same peptides produced *in situ* after gel electrophoresis and blotting. Fig. 6a and b illustrate the HPLC separation of the tryptic digest made in 100 m*M* N-methylmorpholine acetate buffer (pH 8.1) with 20% methanol and 10% acetonitrile, respectively. According to the results of these experiments, the enzymatic cleavage is optimal under the conditions used in Fig. 5b, with the N-methylmorpholine buffer and without addition of any organic solvent. Under the cleavage conditions described in ref. 16, we obtained a smaller release of fragments. Obviously, the activity of the enzyme is decreased more by the presence of acetonitrile than by methanol, and pretreatment of the membrane with PVP-40 is superior. (See Experimental.)

Comparison HPLC versus blotting

HPLC, mainly reversed-phase chromatography, is highly suitable for rapid purification of minute amounts of protein. Very complex protein mixtures are well resolved, *e.g.*, the many proteins extracted from ribosomal particles[24]. Furthermore, reversed-phase HPLC is frequently applied to peptide mixtures derived from enzymatic or chemical fragmentation of such proteins, where 20–30 peptides are generated. Other advantages of HPLC are that volatile buffers can be used with the addition of preservatives for protection of the free NH_2-terminal amino groups. This allows direct microsequencing and amino acid analysis of the dried peptide and protein fractions.

However, the usual high recoveries of peptides and proteins by reversed-phase HPLC decrease drastically with increased size and hydrophobicity of the proteins and drop further with acidic hydrophobic proteins, which are poorly resolved[15,25]. Proteins of M_r greater than 30 000 are usually trapped on top of the column. Losses of

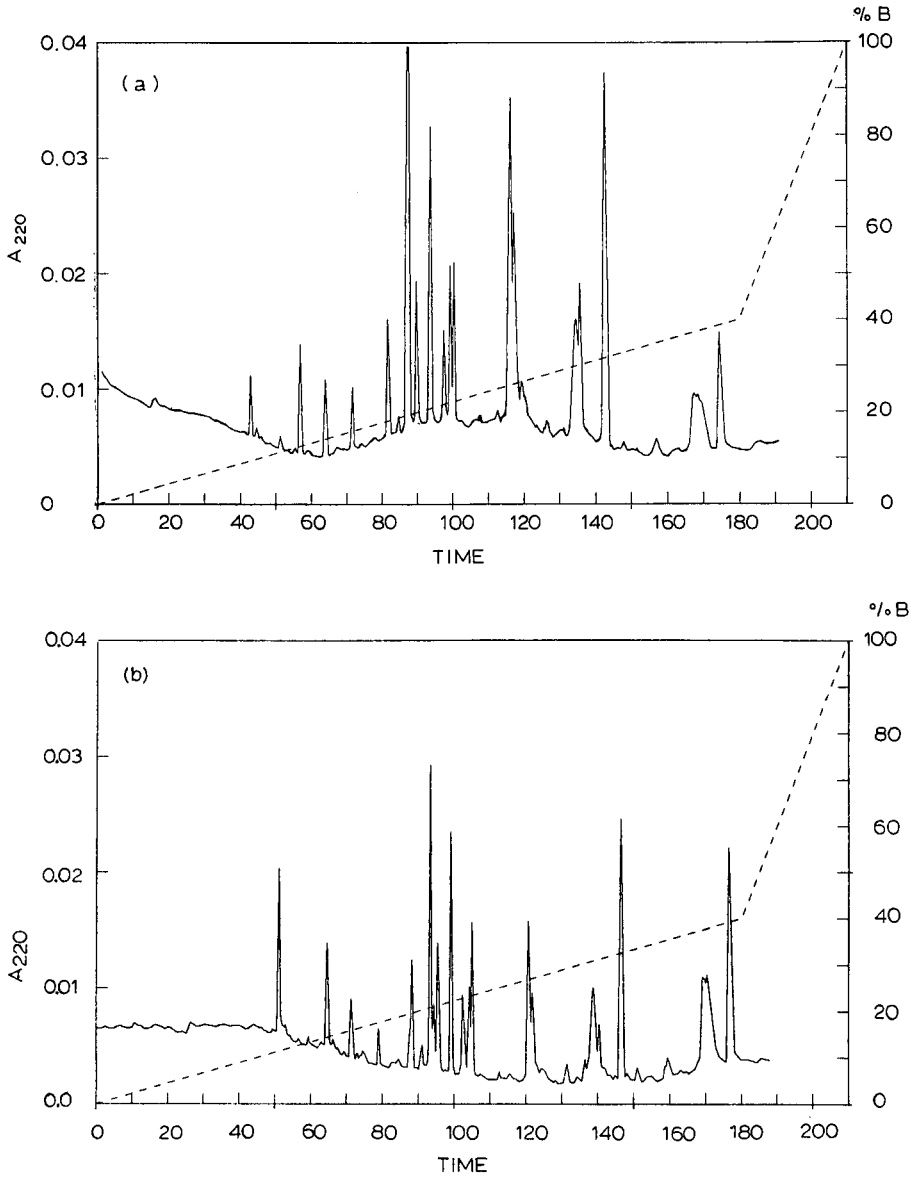

Fig. 5. (a) Tryptic peptides released from 1 nmol of β-lactoglobulin (without blotting) separated by HPLC on a Vydac C_{18} column (250 mm × 4 mm). Eluents: A, 0.1% TFA; B, acetonitrile containing 0.1% TFA; flow-rate, 0.5 ml/min. Paper speed: 2 mm/min. Sensitivity: 0.04 a.u.f.s. The digestion took place in 100 m*M* aqueous N-methylmorpholine acetate (pH 8.1) at 37°C for 20 h. (b) Separation of tryptic peptides, produced by *in situ* digestion of 1 nmol blotted β-lactoglobulin under te same conditions as in (a). The PVDF membrane was treated with PVP-40, as described in Methods. The peptides released were separated by HPLC under the same conditions as in (a).

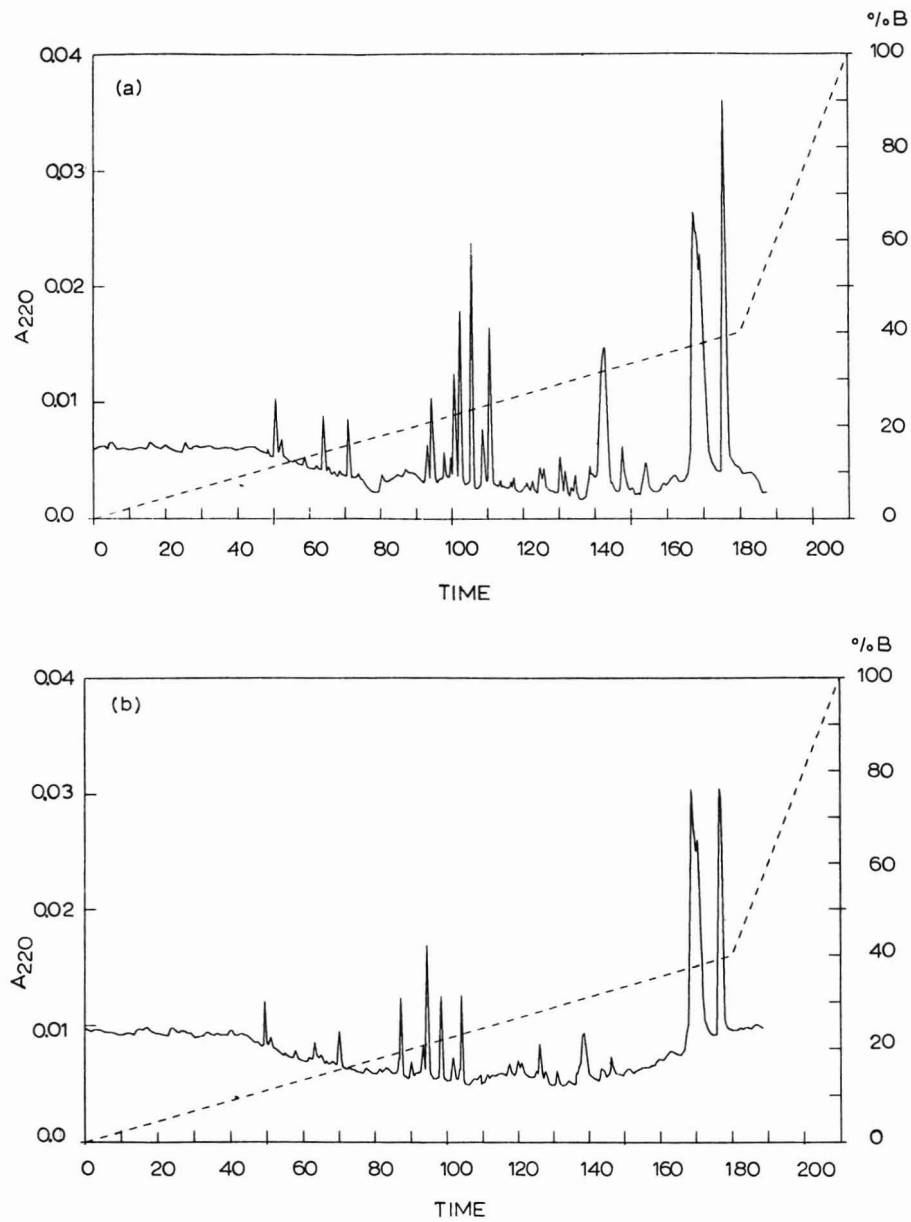

Fig. 6. (a) Separation of tryptic peptides produced by *in situ* digestion of 1 nmol blotted β-lactoglobulin. Digestion conditions as in Fig. 5, but the buffer contained 20% methanol in 100 m*M* N-methylmorpholine acetate at pH 8.1. The peptides were separated by HPLC, as in Fig. 5a. (b) Separation of tryptic peptides derived by *in situ* digestion of 1 nmol blotted β-lactoglobulin. Digestion conditions as in Fig. 5, but the digestion buffer contained 10% acetonitrile in 100 m*M* N-methylmorpholine acetate (pH 8.1). HPLC was performed as in Fig. 5a.

precious material might also occur during processing of the HPLC fractions, or due to dilution of the sample. In addition, problems are encountered due to variations in sorbents. Different batches and products from different manufacturers may show changes in the elution of diverse proteins.

Although the chromatograms often yield sharp and distinct peaks, the proteins may be contaminated with each other (*cf.*, *e.g.*, Fig. 7a and b). As an example, in Fig. 7a the protein indicated by an arrow is still not purified (*cf.*, Fig. 7b). Therefore, the purity of protein-containing fractions must be tested by rechromatography or by one- and two-dimensional gel electrophoresis. These disadvantages of HPLC are circumvented by the two-dimensional gel electrophoresis separation methods, which have an

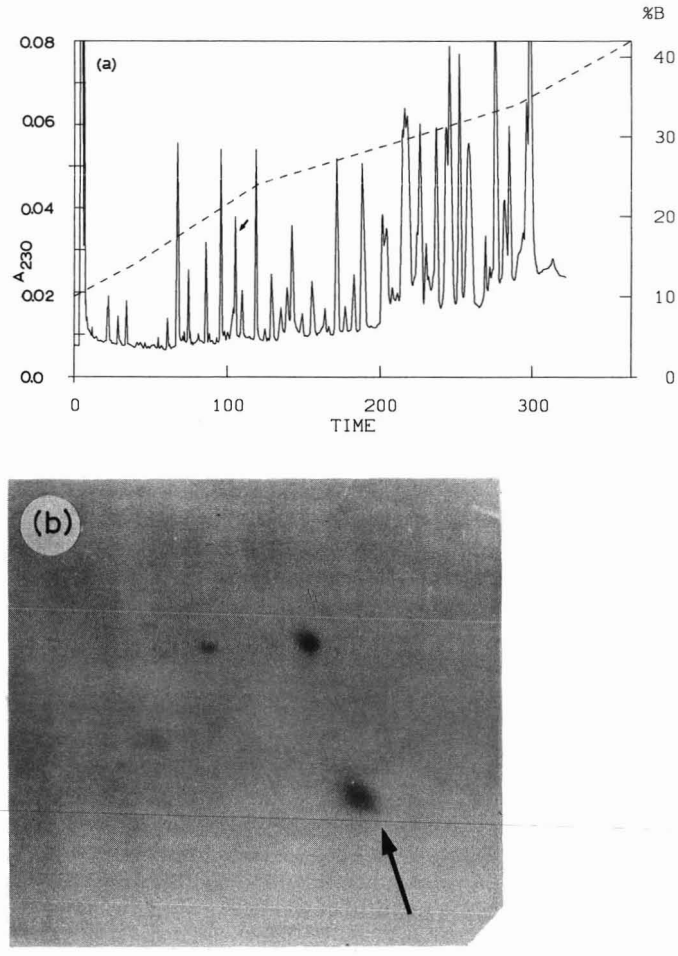

Fig. 7. (a) Separation of the protein mixture (2.7 mg) extracted from *Bacillus stearothermophilus* 50S ribosomes by reversed-phase HPLC on a Vydac C_4 column (250 mm × 4 mm) with a 2-propanol gradient in 0.1% TFA. Flow-rate: 0.5 ml/min. Paper speed: 1 mm/min. Sensitivity: 0.16 a.u.f.s. (b) Blotted proteins after two-dimensional gel electrophoresis of the peak in (a) indicated by an arrow. This peak contains one main and three minor components.

extremely high resolving power for complex protein mixtures[4] and are easy to perform without sophisticated equipment. In combination with protein blotting from these gels onto membranes suitable for sequencing, these methods have recently become an excellent alternative to HPLC. The blotting procedures complement HPLC in cases where the latter gives low resolution and low recoveries or where high-molecular-weight proteins are present in the mixture. Sequencing of the blotted proteins can successfully be applied provided that high-quality chemicals are used for gel electrophoresis and that necessary precautions to prevent blockage or destruction of labile amino acids are taken[15].

In this article, we have described transfer conditions that allow blotting of low- and high-molecular-weight proteins in the same experiment. Without removing the proteins from the membrane, direct microsequencing, enzymatic or chemical fragmentation or hydrolysis for amino acid analysis can be carried out. This procedure, especially when combined with two-dimensional gel electrophoresis, is a very powerful and efficient method for isolation and microsequencing of proteins in complex protein mixtures and may replace HPLC techniques.

ACKNOWLEDGEMENTS

We thank Professor H. G. Wittmann for support of this work, Andreas Ney for performing some of the one-dimensional gel electrophoreses and Mrs. Renate Hasenbank for providing the material shown in Fig. 7b.

REFERENCES

1 U. K. Laemmli, *Nature (London)*, 227 (1970) 600.
2 D. M. Neville, Jr., *J. Biol. Chem.*, 246 (1971) 6328.
3 E. Kaltschmidt and H. G. Wittmann, *Anal. Biochem.*, 36 (1970) 401.
4 P. H. O'Farrell, *J. Biol. Chem.*, 250 (1975) 4007.
5 D. Geyl, A. Böck and K. Isono, *Mol. Gen. Genet.*, 181 (1981) 309.
6 E. M. Southern, *J. Mol. Biol.*, 98 (1975) 503.
7 H. M. Ehrlich, J. R. Levinson, S. N. Cohen and H. O. McDevitt, *J. Biol. Chem.*, 254 (1979) 12 240.
8 H. Towbin, T. Staehelin and J. Gordon, *Proc. Natl. Acad. Sci. U.S.A.*, 76 (1979) 4350.
9 J. Renart, J. Reiser and G. R. Stark, *Proc. Natl. Acad. Sci. U.S.A.*, 76 (1979) 3116.
10 J. Vandekerckhove, G, Bauw, P. Puype, J. Van Damme and M. Van Montague, *Eur. J. Biochem.*, 152 (1985) 9.
11 R. H. Aebersold, D. B. Teplow, L. E. Hood and S. B. H. Kent, *J. Biol. Chem.*, 261 (1986) 4229.
12 G. Bauw, M. De Loose, M. Van Montaque and J. Vandekerckhove, *Proc. Natl. Acad. Sci. U.S.A.*, 84 (1987) 4806.
13 P. Matsudaira, *J. Biol. Chem.*, 262 (1987) 10035.
14 R. Aebersold, G. Pipes, H. Nika, L. Hood and S. Kent, *Biochemistry*, 27 (1988) 6860.
15 M. Walsh, J. McDougall and B. Wittmann-Liebold, *Biochemistry*, 27 (1988) 6867.
16 R. Aebersold, J. Laevitt, R. Saevedra, L. Hood and S. Kent, *Proc. Natl. Acad. Sci. U.S.A.*, 84 (1987) 6970.
17 G. Bauw, M. Van den Bulcke, J. Van Damme, M. Puype, M. Van Montaque and J. Vandekerckhove, *J. Prot. Chem.*, 7, No. 3 (1988) 194.
18 B. Szewczyk and D. Summers, *Anal. Biochem.*, 168 (1988) 48.
19 K. Ashman and A. Bosserhof, in H. Tschesche (Editor), *Modern Methods in Protein Chemistry*, Vol. 2, Walter de Gruyter, Berlin, 1985, p. 155.
20 J. Andersen-Kyhse, *J. Biochem. Biophys. Methods*, 10 (1984) 203.
21 M. Moos, N. Y. Nguyen and T. Y. Lin, *J. Biol. Chem.*, 263 (1988) 6005.

22 A. T. Matheson, K. A. Louie and A. Böck, *FEBS Lett.*, 231 (1988) 1.
23 P. Henning, T. Choli and R. Reinhardt, manuscript in preparation.
24 R. M. Kamp and B. Wittmann-Liebold, *Methods Enzymol.*, 164 (1988) 542.
25 R. M. Kamp, in B. Wittmann-Liebold, J. Salnikow and V. A. Erdmann (Editors), *Advanced Methods in Protein Microsequence Analysis*, Springer, Heidelberg, New York, 1986, pp. 8 and 21.

Journal of Chromatography, 476 (1989) 73–82
Elsevier Science Publishers B.V., Amsterdam — Printed in The Netherlands

CHROMSYMP. 1615

AUTOMATED ENANTIOSEPARATION OF AMINO ACIDS BY DERIVATIZATION WITH *o*-PHTHALDIALDEHYDE AND N-ACYLATED CYSTEINES

HANS BRÜCKNER* and ROBERT WITTNER
Institute of Food Technology, University of Hohenheim, D-7000 Stuttgart 70 (F.R.G.)
and
HERBERT GODEL
Hewlett-Packard, Research and Development Division, D-7517 Waldbronn 2 (F.R.G.)

SUMMARY

The enantioseparation of standard mixtures composed of protein DL-amino acids was performed by reversed-phase high-performance liquid chromatography of the corresponding diastereomeric isoindolyl derivatives, formed by automated precolumn derivatization with *o*-phthaldialdehyde (OPA) and a series of N-acyl-L-cysteines (Acyl-Cys). A photodiode-array detector, operating at 338 nm, was used for detection. In order to evaluate systematically the influence of the structures of the acyl group in the chiral thiol reagents, a series of novel N-acyl-L-cysteines was synthesized [acyl = *n*-butyryl, isobutyryl (*i*-But), pivaloyl, benzoyl) and the chromatographic behaviour of the diastereomers formed was compared with those of already known reagents, N-acetyl-L-cysteine and N-*tert.*-butyloxycarbonyl-L-cysteine. All Acyl-Cys derivatives of DL-amino acids were resolved. In particular, *i*-But-Cys gave the highest resolutions for most of the amino acid enantiomers in comparison with the other Acyl-Cys. Investigation of yoghurt using OPA–acetyl-Cys demonstrated the applicability of the method to a complex food matrix and the occurrence of D-Asp, D-Glu and D-Ala in this dairy product.

INTRODUCTION

It has been shown that the enantioseparation of mixtures of DL-amino acids can be performed by reversed-phase high-performance liquid chromatography (RP-HPLC) by converting them to the diastereomeric isoindolyl derivatives formed by pre-column derivatization with *o*-phthaldialdehyde (OPA) and chiral thiols, such as N-acetyl-L-cysteine (Ac-Cys)[1–5], N-*tert.*-butyloxycarbonyl-L-cysteine[2] and N-acetyl-D-penicillamine[4]. This successful approach has been extended to the enantioseparation of chiral amino alcohols[4], non-protein α-alkyl-α-amino acids[6,7] and α-hydroxymethyl-α-amino acids[7,8]. An intriguing aspect of this method is that an HPLC instrument dedicated to quantitative amino acid analysis by means of OPA and non-chiral thiols, such as 2-mercaptoethanol[9] or 3-mercaptopropionic acid[10], can also permit the chiral separation of amino acid enantiomers by simple changes of the reagent and the gradient programme. From the structures of the diastereomeric

0021-9673/89/$03.50

isoindolyl derivatives[3], it is also evident that the selection of appropriate chiral thiols is most important for the enantioseparation and that, with N-acyl-L-cysteines (Acyl-Cys), the structures of the acyl groups will influence drastically the elution behaviour of amino acid enantiomers. We were interested in the question of how systematically modified acyl groups in Acyl-Cys will alter and possibly improve the enantioseparation of amino acid standard mixtures containing a large number of DL-amino acids and whether the selection of suitable derivatives and chromatographic conditions will permit the detection and quantification of the D-amino acids assumed to occur in complex matrices such as fermented foods.

EXPERIMENTAL

Instruments

For HPLC an HP 1090 LC system, equipped with a photodiode-array detector and an autosampler with a device for automated precolumn derivatization of amino acids, was used. The workstation consisted of a Series 9000 computer, Model 300, with fixed disk and floppy disk, Model 9153 B, and a plotter, ColorPro Model 7440 A (all from Hewlett-Packard, Waldbronn, F.R.G.).

Chromatography

HPLC was performed using Spherisorb ODS II (3 μm) (Phase Separations, Queensferry, U.K.) as stationary phase, packed in a 125 mm × 4.6 mm I.D. column, connected to a 20 mm × 4.6 mm I.D. precolumn (Novogrom system; Grom, Herrenberg, F.R.G.); the buffer compositions and gradient programmes, are given in the legend to Fig. 1.

Chiral thiol reagents

N-Acetyl-L-cysteine (Ac-Cys) was purchased from Fluka (Buchs, Switzerland) and N-*tert.*-butyloxycarbonyl-L-cysteine (Boc-Cys) from Novabiochem (Läufelfingen, Switzerland). Other Acyl-Cys [*n*-butyryl (*n*-But), isobutyryl (*i*-But), pivaloyl (Piv) and benzoyl (Bz)] were synthesized by Schotten–Baumann bisacylation of L-cystine (Fluka), dissolved in 2 *M* sodium hydroxide solution, by addition of the respective acyl chlorides (1.1 equiv. for each amino group) at 0°C and stirring for 1 h. The solutions were acidified to pH 2.5, the bisacyl-L-cystines were extracted with ethyl acetate and the organic phase was dried with anhydrous sodium sulphate and evaporated to dryness. The oily residues were reduced to the Acyl-Cys by treatment with zinc powder in 2 *M* hydrochloric acid for 1 h[11]. After extraction with ethyl acetate and drying over sodium sulphate, the organic phases were evaporated to dryness and the Acyl-Cys were obtained as solids or oils (for *i*-But-Cys and Bz-Cys). The components were characterized by their mass spectra and had purities of ⩾95% according to thin-layer chromatography [pre-coated silica plates (Merck), solvent system chloroform–methanol–water–acetic acid (65:25:4:3)].

Chemicals and composition of amino acid standards

DL-Amino acids were of analytical-reagent grade and purchased from Sigma (St. Louis, MO, U.S.A.). Standard mixtures were composed of (a) 0.5 m*M* amino acids (*cf.*, Table I) in 0.01 *M* hydrochloric acid, (b) 2 m*M* His and (c) 2 m*M* Asn, Gln and Trp

in 20% aqueous methanol. For storage, (a) and (b) were kept in a freezer and (c) was kept at +4°C. When *i*-But-Cys and *n*-But-Cys were used for enantioseparation, 2 μl of (a), 1 μl of (b) and 0.5 μl of (c) were mixed automatically with the derivatizing reagents (see derivatization procedures). When Ac-Cys, Piv-Cys and Bz-Cys were used, 2 μl of (a) and 1 μl of (b) were mixed, and for Boc-Cys 2 μl of (c) were used.

Acetonitrile was a Baker analyzed HPLC reagent with a 190-nm UV cut-off (J. T. Baker, Deventer, The Netherlands) and sodium acetate trihydrate of *pro analysi* grade was from Merck (Darmstadt, F.R.G.). Water was doubly distilled and eluents were degassed by sonification prior to use.

Derivatization procedures

A volume of 4 μl (5 μl for Bz-Cys) of 0.133 *M* borate buffer, pH 10.4 (Pierce, Rotterdam, The Netherlands), 2 μl of OPA reagent (5 mg of OPA in 1 ml of borate buffer), 2 μl of Acyl-Cys (1 μl of Bz-Cys) reagent and appropriate amounts of standards (see above) were mixed automatically by the mixing device of the autosampler, programmed for six mixing cycles (twelve for *n*-But-Cys and *i*-But-Cys), which required approximately 3 and 6 min, respectively. Acyl-Cys reagents were prepared freshly every day by dissolving the following amounts of Acyl-Cys in borate buffer: Ac-Cys, 8; *i*-But-Cys, 20; *n*-But-Cys, 20; Piv-Cys, 10; Boc-Cys, 11; and Bz-Cys, 22 mg/ml.

For the study with yoghurt, a commercial product from the Dairy Factory of the University of Hohenheim, manufactured by the use of lyophilized starter cultures composed of *Lactobacillus bulgaricus, Lactobacillus acidophilus* and *Streptococcus thermophilus* (Laboratorium Wiesby, Niebüll, F.R.G.), was used. A 15-g amount of yoghurt and 45 ml of 80% aqueous methanol were stirred for 10 min and then centrifuged at 1630 *g*. The supernantant was evaporated *in vacuo* to a volume of *ca.* 10 ml, then 10 ml of a saturated solution of picric acid were added for deproteinization. After centrifugation at 1630 *g*, the supernatant was poured into a separating funnel and defatted twice with 20-ml portions of light petroleum (b.p. 40–60°C)–diethyl ether (1:1, v/v). The aqueous phase was passed through a Dowex 50W-X8 cation exchanger with a bed volume of 5 cm × 1 cm I.D. After washing with water, the amino acids were eluted with *ca.* 30 ml of 2 *M* aqueous amonia. The effluent was evaporated to dryness, the residue was dissolved in 0.5 ml of 0.133 *M* borate buffer and aliquots were subjected to HPLC analysis.

RESULTS AND DISCUSSION

The chiral resolution of standard mixtures, composed of the non-chiral Gly and thirteen DL-amino acids (fourteen when His was included and seventeen when His, Asn, Gln and Trp were included) by the use of various Acyl-Cys are shown in Fig. 1a–f, and the retention times and calculated resolutions of the respective pairs of amino acids are given in Table I. (It is understood in this context and in the following discussion that actually the diastereomeric isoindolyl derivatives formed from amino acids are separated by RP-HPLC.) As can be seen from the chromatograms, in principle all Acyl-Cys reagents employed resulted in the separation of the amino acid enantiomers. When the resolutions resulting from the use of the various reagents are compared, the resolutions of the individual pairs of DL-amino acids and the overall

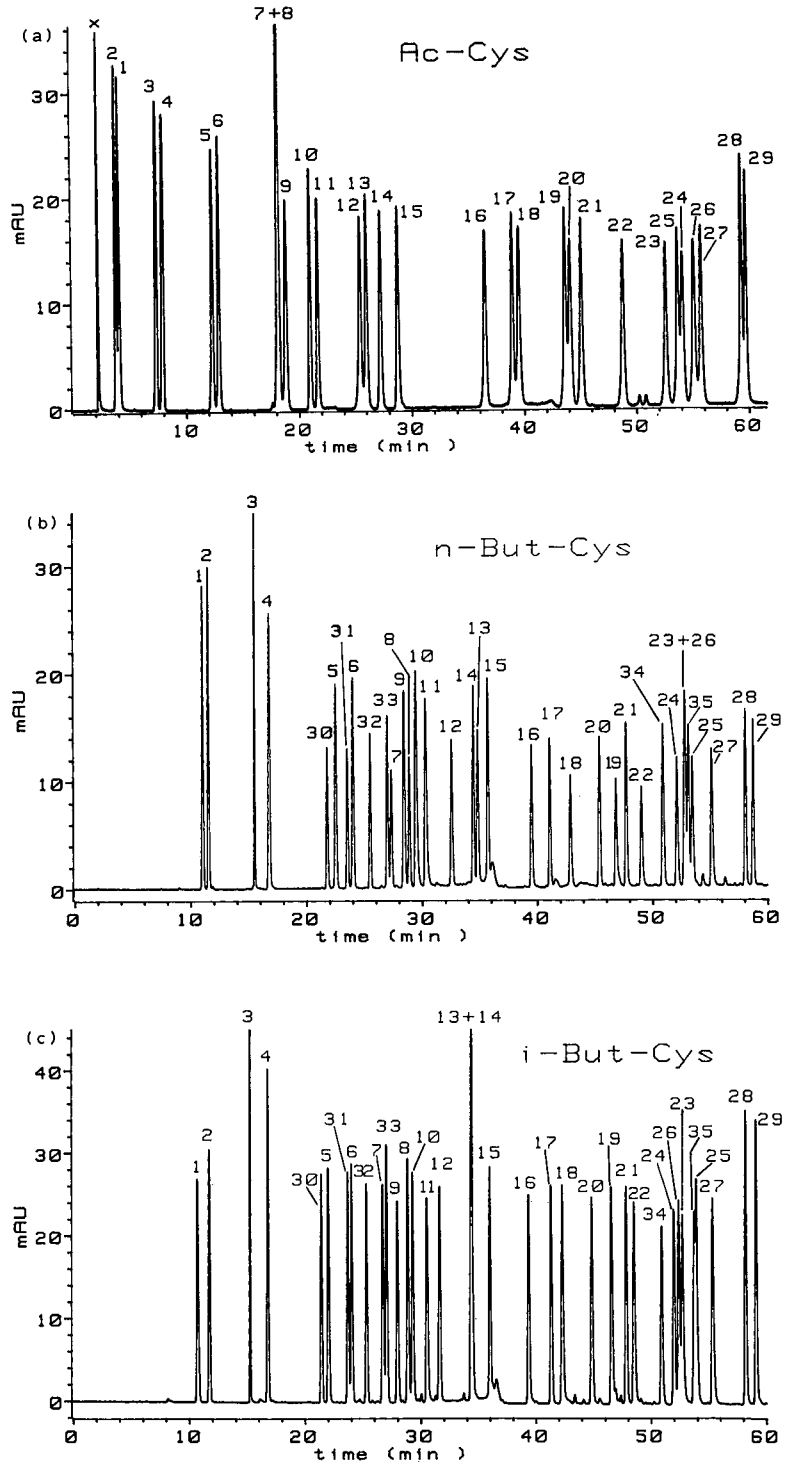
(a)
Ac-Cys
mAU
time (min)
(b)
n-But-Cys
mAU
time (min)
(c)
i-But-Cys
mAU
time (min)

Fig. 1.

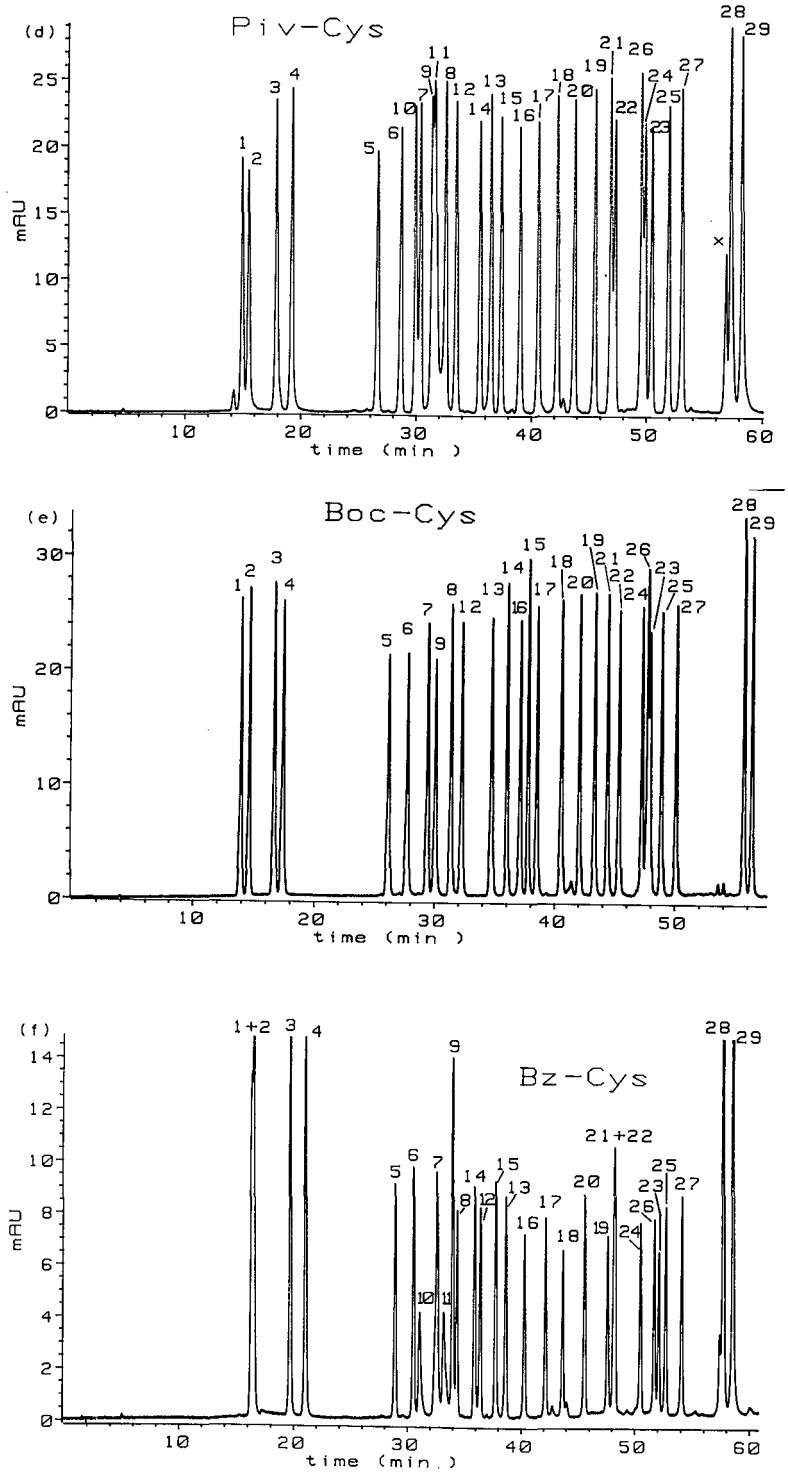

Fig. 1.

(continued on p. 78)

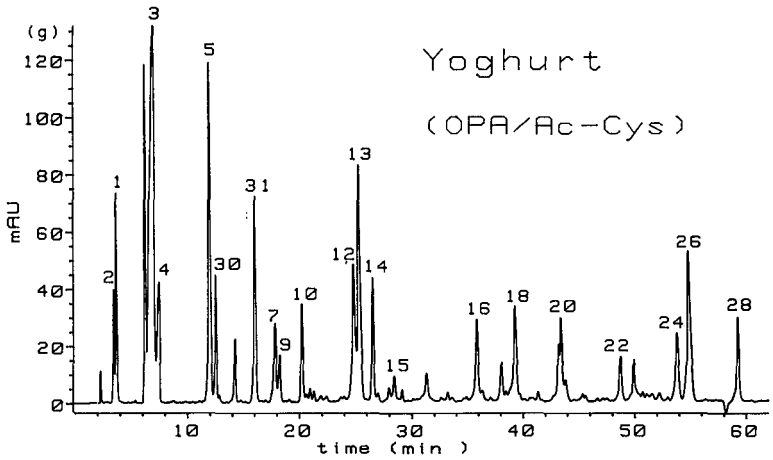

Fig. 1. Enantioseparation of diastereomeric derivatives of (a)–(f) standard mixtures of DL-amino acids and (g) yoghurt after pre-column derivatization with OPA and (a), (g) Ac-Cys, (b) *n*-But-Cys, (c) *i*-But-Cys, (d) Piv-Cys, (e) Boc-Cys and (f) Bz-Cys. Buffer gradients (a)–(g): eluent A, (a), (g) 40 m*M* sodium acetate (pH 6.5); (b) 30 m*M* sodium acetate (pH 6.5); (c) 30 m*M* sodium acetate (pH 6.5); (d) 75 m*M* sodium acetate (pH 7.5); (e) 30 m*M* sodium acetate (pH 7.2); (f) 100 m*M* sodium acetate (pH 7.2); eluent B, (a)–(g), 100% acetonitrile; linear gradient, in 60 min to *x*% B; (a), (g) 18% B; (b) 23.5% B; (c) 23% B; (d) 27.5% B; (e), (f) 29% B; column temperature, (a), (g) 26°C; (b), (c), (f) 25°C; (d) 30°C; (e) 35°C; flow-rate (a)–(g), 0.9 ml/min. pH values of the buffers were adjusted by addition of 1% acetic acid; for other abbreviations, derivatization procedures, and chromatographic conditions, see Experimental. For numbers of amino acids and assignment of the elution order and configuration, see Table I; peaks marked by x originate from reagents; mAU = milli-absorption units.

resolution of complex mixtures of DL-amino acids must be considered. Frequently, optimization of the enatioseparation of individual pairs resulted in poorer separations or peak overlap of other pairs of DL-amino acids in the chromatograms. Further, when the resolutions of amino acids due to the various Acyl-Cys reagents are compared, it must be taken into account that, owing to the different hydrophobicities of the diastereomers formed, the same buffer compositions and gradients cannot be employed. Each of the chromatograms shown in Fig. 1a–f therefore represents the most satisfactory result of about fifteen attempts to optimize the overall resolution of the respective DL-amino acid mixture. In general, it can be said that the more lipophilic the acyl group in Acyl-Cys, the higher the temperature, pH and proportion of the organic modifier and the lower the molarity of the buffer that should be in order to obtain acceptable and comparable elution times. In the present cases, the conditions were adjusted such that the last-eluted amino acid, *i.e.*, Lys, was eluted after *ca.* 60 min. The buffer conditions are given in the legend to Fig. 1.

Fig. 1a–f show the chromatograms of amino acid standard mixtures composed of thirteen (Fig. 1e), fourteen (Fig. 1a, d and f) and seventeen (Fig. 1b and c) pairs of DL-amino acids and, in addition, the non-chiral Gly. Nimura and Kinoshita[3] separated thirteen pairs of DL-amino acids by use of OPA–Ac-Cys, but failed to resolve DL-Lys. They used a combination of three gradient and two isocratic elution programs. Fig. 1a shows the enantioseparaton of thirteen pairs of DL-amino acids, including DL-Lys, with OPA–Ac-Cys using a linear gradient. However, DL-Thr is not resolved

TABLE I

ELUTION ORDER OF ENANTIOMERS OF AMINO ACIDS AFTER PRE-COLUMN DERIVATIZATION WITH OPA/ACYL-L-CYS REAGENTS

Retention times (min) of the first- (t_{R_1}) and second-eluted (t_{R_2}) enantiomers and resolution (R) are given; n.d., not determined.

Amino acid[a,b]	*Reagent*																	
	Ac-Cys[b]			*n-But-Cys*			*i-But-Cys*			*Piv-Cys*			*Boc-Cys*			*Bz-Cys*		
	t_{R_1}	t_{R_2}	R[c]	t_{R_1}	t_{R_2}	R	t_{R_1}	t_{R_2}	R	t_{R_1}	t_{R_2}	R	t_{R_1}	t_{R_2}	R	t_{R_1}	t_{R_2}	R
1,2 LD-Asp	–	–	–	11.1	11.6	2.1	10.7	11.8	3.6	14.9	15.5	1.4	14.0	14.7	2.3	16.3	16.5	0.5
2,1 DL-Asp[b]	3.8	4.1	1.1	–	–	–	–	–	–	–	–	–	–	–	–	–	–	–
3,4 LD-Glu	7.4	8.0	1.5	15.6	16.8	5.9	15.3	16.8	7.8	17.9	19.2	3.2	16.7	17.4	2.2	19.7	21.0	4.0
5,6 LD-Ser	12.3	12.9	1.7	22.6	24.1	5.0	22.0	24.0	6.5	26.7	28.7	4.7	26.2	27.8	4.4	28.9	30.5	4.7
7,8 LD-Thr	18.2	18.2	0.0	27.4	28.9	4.9	26.7	28.9	6.8	30.4	32.6	5.3	29.5	31.4	6.0	32.6	34.3	4.5
9 Gly	18.4	–	–	28.5	–	–	28.0	–	–	31.4	–	–	30.1	–	–	34.0	–	–
10,11 LD-His	21.0	21.6	1.9	29.5	30.3	2.1	29.3	30.5	3.4	30.0	31.6	3.4	n.d.	n.d.	–	31.1	33.2	4.1
12,13 LD-Ala	25.4	26.0	1.2	32.6	34.8	6.9	31.6	34.4	7.9	33.5	36.5	7.4	32.3	34.8	7.2	36.4	38.6	6.6
14,15 LD-Arg	27.2	28.8	3.3	34.5	35.7	3.9	34.4	36.0	4.6	35.6	37.4	4.4	36.0	37.8	5.9	35.9	37.7	4.9
16,17 LD-Tyr	36.5	38.9	5.1	39.5	41.1	5.1	39.4	41.3	5.8	39.0	40.6	3.9	37.1	38.5	4.5	40.3	42.1	5.6
18,19 LD-Val	39.5	43.6	8.0	42.9	46.8	11.2	42.3	46.5	11.8	42.3	45.5	8.2	40.6	43.3	8.6	43.6	47.6	12.4
20,21 LD-Met	44.1	45.1	1.9	45.4	47.7	6.9	44.9	47.8	8.4	43.7	46.9	8.0	42.1	44.4	7.7	45.5	48.2	6.9
22,23 LD-Ile	48.8	52.6	7.4	49.0	52.8	10.1	48.5	52.7	11.2	47.3	50.5	8.1	45.4	47.9	8.3	48.2	52.1	10.1
24,25 LD-Phe	–	–	–	52.1	53.5	4.0	52.0	53.9	5.1	49.9	51.9	5.4	47.3	38.9	5.0	50.5	52.7	6.5
25,24 DL-Phe[b]	53.6	54.1	0.8	–	–	–	–	–	–	–	–	–	–	–	–	–	–	–
26,27 LD-Leu	55.1	55.7	1.2	52.8	55.1	6.1	52.4	55.3	8.0	49.6	53.1	8.7	47.7	50.1	7.5	51.7	54.1	7.3
28,29 LD-Lys	59.3	59.7	0.9	58.1	58.7	2.0	58.2	59.1	2.8	57.3	58.3	2.2	55.7	56.4	2.2	57.7	58.5	2.4
30,31 LD-Asn	12.7	13.7	2.3	21.8	23.6	6.5	21.4	23.7	8.0	25.7	27.5	4.0	25.7	27.2	4.4	27.1	28.3	3.1
32,33 LD-Gln	16.5	18.0	3.2	25.5	27.0	5.2	25.3	27.1	6.0	28.8	30.3	3.4	28.0	29.4	4.0	29.8	31.6	4.5
34,35 LD-Trp	51.5	53.2	2.7	50.9	53.1	6.3	50.9	53.7	8.8	48.7	51.1	5.2	45.4	47.6	6.5	49.3	51.6	5.7

[a] Peak numbers 1–35 refer to the elution order of amino acids in the chromatograms shown in Fig. 1a–g.

[b] Exceptions to the elution order of amino acids (L before D) are Asp and Phe when Ac-Cys is used as reagent; only in these instances is the respective D-amino acid eluted before the L-amino acid.

[c] Resolution R is calculated according to the formula $R = (t_{R_1} - t_{R_2})/(w_1 + w_2)$, where w_1 and w_2 are the peak widths at half-height of the first- and second-eluted peaks of amino acid derivatives. Resolutions of amino acids not shown in the chromatograms were calculated from retention times determined in separate runs.

under these conditions. Employing linear gradient programmes, Buck and Krummen[2] separated five pairs of DL-amino acids using OPA–Ac-Cys, and ten pairs of DL-amino acids using OPA–Boc-Cys. Fig. 1e shows the separation of thirteen pairs of DL-amino acids with OPA–Boc-Cys reagent.

From the chromatograms shown in Fig. 1, it is also obvious that all the Acyl-Cys reagents used are capable of separating mixtures composed of a large number of DL-amino acids. Compared with Ac-Cys and Boc-Lys, Piv-Cys and Bz-Cys offer no advantage when applied to amino acid mixtures under the conditions used, although several pairs of amino acids (His, Val and Phe), derivatized with the latter reagent, show the highest resolutions (*cf.*, Table I).

Remarkably, when the various Acyl-Cys reagents are applied to DL-amino acids the highest resolution is found for DL-Val, with the exception that the use of Piv-Cys gives a slightly higher resolution for DL-Leu (*cf.*, Table I). Further, among the various Acyl-Cys reagents, in most instances *i*-But-Cys effects the highest resolutions for amino acid enantiomers (*cf.*, Table I). It is assumed, therefore, that the isopropyl group, which represents the valyl side-chain and is also part of the isobutyryl group, is responsible for this exceptionally high degree of chiral resolution. This is in agreement with the findings that suitably derivatized L-valine when bonded as a chiral selector to silica gel and used in liquid chromatography[12,13], or when attached to a polysiloxane matrix and used as the stationary phase in gas chromatography[14,15], or when valine is derivatized to so-called ureido phases[16], this amino acid shows a very high degree of chiral recognition. Further, when discussing the chiral resolution of amino acids, one must remember that very often the enantioseparation of a large number of amino acids is not necessary. For example, for proving the optical purity of amino acids, the detection of minor amounts of one enantiomer together in a large excess of the other is essential. In these instances, very high resolutions of the diastereomeric amino acid pairs are advantageous and, in order to obtain high accuracy, the minor enantiomers should be eluted first. In the cases investigated, the L-enantiomers of amino acids were eluted before the D-enantiomers. However, when Ac-Cys was used as the reagent, D-Asp and D-Phe were eluted before the respective L-enantiomers (*cf.*, Table I). As the elution order is reversed when Acyl-L-Cys is replaced with Acyl-D-Cys, the order of emergence of enantiomers is easily reversible by choosing the appropriate chiral reagent.

Application of the method to complex food samples, with Ac-Cys as a commercially available chiral reagent, is exemplified by yoghurt (Fig. 1g) and confirms[17,18] the presence of D-Asp (32.2%), D-Glu (16.4%) and D-Ala (62.0%), calculated with respect to the L-enantiomers. The relative amounts and the kinds of D-amino acids occurring in yoghurt depend on the manufacturing process and starter cultures used. The use of *n*-But-Cys for the determination of D-amino acids in yoghurt and the employment of capillary gas chromatography and the chiral stationary phase Chirasil-Val for the detection of D-amino acids in processed foodstuffs have been reported previously[17,18].

CONCLUSION

From the results it is clear that systematically modified acyl groups in Acyl-Cys, applied together with OPA to DL-amino acids, make it possible to adjust the

hydrophobicities and conformations of the resulting diastereomeric isoindolyl derivatives. Hence it is possible, by selection of appropriate reagents and chromatographic conditions, to optimize the enantioseparation of individual pairs of amino acids and also of complex mixtures consisting of a large number of amino acids, such as those occurring, *e.g.*, in foodstuffs or biomatrices.

It is expected by analogy that much more suitable Acyl-Cys, or N-substituted cysteines in general, will be found for the high-performance enantio separation of chiral amino components. The use of cysteine as a chiral thiol component has the advantage that both enantiomers are available as economic building blocks of high optical purity for derivatization procedures. Moreover, in this instance, the almost unlimited range of N-terminal protecting groups employed by peptide chemists[19] can be considered as candidates for the design of many more N-substituted cysteines suitable for the enantioseparation of amino acids.

The liquid chromatographic approach has the advantage, in contrast to gas chromatography[14], that acid-sensitive amino acids, such as asparagine, glutamine and tryptophan, or those requiring special derivatization conditions for gas chromatography, such as histidine and arginine, can be determined using the routine procedures described above, and that these derivatization procedures for chiral amino acid analyses are fully automated.

A disadvantage of the OPA–thiol approach is that no amino acids with secondary amino groups, such as proline or hydroxyproline, can be determined directly. This major drawback is overcome in the HP 1090 LC analyser (AminoQuant system) used for quantitative, non-chiral amino acid analysis with OPA–2-mercaptopropionic acid, by applying an additional derivatization with 9-fluorenyl chloroformate (Fmoc-Cl)[20]. However, by analogy it is assumed that use of chiral variations of this reagent, *e.g.*, (+)-1-(9-fluorenyl)ethyl chloroformate (Flec-Cl)[21], will overcome this shortcoming.

REFERENCES

1 D. W. Aswad, *Anal. Biochem.*, 137 (1984) 405.
2 R. H. Buck and K. Krummen, *J. Chromatogr.*, 315 (1984) 279.
3 N. Nimura and T. Kinoshita, *J. Chromatogr.*, 352 (1986) 169.
4 R. H. Buck and K. Krummen, *J. Chromatogr.*, 387 (1987) 255.
5 T. Takeuchi, T. Niwa and D. Ishi, *J. High Resolut. Chromatogr. Chromatogr. Commun.*, 11 (1988) 343.
6 H. Brückner, I. Bosch, S. Kühne and S. Zivny, in G. R. Marshall (Editor), *Peptides: Chemistry and Biology*, ESCOM Science Publishers, Leiden, 1988, pp. 195–197.
7 H. Brückner, S. Kühne, S. Zivny, M. Langer, Z. J. Kamiński and M. T. Leplawy, in A. Aubry, M. Marraud and B. Vitoux (Editors), *Second Forum on Peptides*, John Libbey Eurotext, London, 1988, pp. 291–295.
8 Z. J. Kamiński, M. T. Leplawy, A. Esna-Ashari, S. Kühne, S. Zivny, M. Langer and H. Brückner, in E. Bayer and G. Jung (Editors), *Peptides 1988*, Walter de Gruyter, Berlin, 1989, pp. 298–300.
9 S. L. Pentoney, X. Huang, D. S. Burgi and R. N. Zare, *Anal. Chem.*, 60 (1988) 2625; and references cited therein.
10 H. Godel, T. Graser, P. Földi, P. Pfaender and P. Fürst, *J. Chromatogr.*, 297 (1984) 49; and references cited therein.
11 L. Zervas and I. Photaki, *J. Am. Chem. Soc.*, 84 (1962) 3887.
12 S. Hara and A. Dobashi, *J. Chromatogr.*, 186 (1979) 543.
13 N. Ôi and H. Kithara, *J. Chromatogr.*, 285 (1984) 198.
14 H. Frank, G. J. Nicholson and E. Bayer, *J. Chromatogr.*, 167 (1978) 187.
15 W. A. König, *J. High Resolut. Chromatogr. Chromatogr. Commun.*, 5 (1982) 588.

16 B. Feibush, E. Gil-Av and T. Tamari, *J. Chem. Soc., Perkin Trans. 2,* (1972) 1197.
17 H. Brückner and M. Hausch, in H. Frank, B. Holmstedt and B. Testa (Editors), *Chirality and Biological Activity,* Alan R. Liss, New York, 1989, in press.
18 H. Brückner, R. Wittner, M. Hausch and H. Godel, *Fresenius' Z. Anal. Chem.*, 333 (1989) 775.
19 M. Bodansky, *Principles of Peptide Synthesis,* Springer, Berlin, Heidelberg, New York, Tokyo, 1984.
20 S. Einarsson, B. Josefsson, S. Lagerkvist, *J. Chromatogr.*, 282 (1983) 609.
21 S. Einarsson, B. Josefson, P. Möller and D. Sanchez, *Anal. Chem.*, 59 (1987) 1191.

Journal of Chromatography, 476 (1989) 83–92
Elsevier Science Publishers B.V., Amsterdam — Printed in The Netherlands

CHROMSYMP. 1617

LIQUID CHROMATOGRAPHIC ANALYSIS OF AMINO AND IMINO ACIDS IN PROTEIN HYDROLYSATES BY POST-COLUMN DERIVATIZATION WITH *o*-PHTHALALDEHYDE AND 3-MERCAPTOPROPIONIC ACID

ANTONIO FIORINO*, GIANCARLO FRIGO and EUGENIO CUCCHETTI
Ellem Research Centre, Viale dell'Industria 17, 20094 Corsico (Milan) (Italy)

SUMMARY

A method for the simultaneous determination of imino and amino acids is reported. The method, based on the derivatization of amino acids, separated by ion-exchange chromatography, by reaction with alkaline hypochlorite and *o*-phthalaldehyde–3-mercaptopropionic acid, increases the sensitivity towards imino acids to the picomole level. The use of 3-mercaptopropionic acid gives intensely fluorescent derivatives and improves the stability of primary and secondary amino acid fluorophores towards oxidation.

The accuracy and reproducibility of the method are increased by using three internal standards. The determination of all amino and imino acids present in protein hydrolysates, including tryptophan, in a single run is demonstrated.

INTRODUCTION

A great deal of interest has been focused on the development of methods for amino acid determination since the pioneering work of Moore and co-workers in the 1950s[1,2]. The original method, based on the post-column derivatization of separated amino acids with ninhydrin, was significantly modified in the 1970s with the advent of reversed-phase adsorbents. The new methods, involving pre-column derivatization and reversed-phase high-performance liquid chromatographic (HPLC) separation of amino acid derivatives, have dramatically improved the speed and sensitivity of analysis. Problems associated with the instability of derivatives have led many analysts to adopt the classical ion-exchange chromatography with post-column derivatization, because this approach offers the advantage of non-destructive separation of amino acids.

Most of the new ion-exchange analysers for HPLC instruments have improved the performance of amino acid analysis by reducing the time of analysis and the detection limits. In these systems, *o*-phthalaldehyde (OPA) has replaced the classical ninhydrin reagent, which suffers from the limitations of a slow reaction rate, which contributes to band broadening[3], and the need for dual-wavelength detectors for complete amino and imino acid monitoring.

Roth[4] first showed that OPA readily reacts with amino acids in the presence of 2-mercaptoethanol to give fluorescent compounds. As imino acids do not react with

0021-9673/89/$03.50

these reagents, oxidation steps have been developed in order to convert imino compounds to primary amines[5–8]. The related adducts showed poor fluorescence compared with the other amino acid derivatives.

Various thiols have been used in the derivatization reactions to improve the stability of fluorescent compounds [9,10]. Recently, Fujiwara *et al.*[11] reported the use of N-acetyl-L-cysteine (AcCys) as a thiol agent to increase the stability of adducts toward hypochlorite oxidation. The AcCys thiol showed excellent sensitivity in the detection of proline.

We have studied the amino acid composition of protein and peptide hydrolysates according to the Fujiwara method. Although AcCys gave quantitative, sensitive and reproducible results, it was often necessary to load different amounts of the sample in order to obtain greater accuracy for methionine and tyrosine, present in relatively small amounts in some hydrolysates. Therefore, we found this method to be insufficiently sensitive for these amino acids.

In order to obtain adducts of methionine and tyrosine with higher fluorescence and, at the same time, good sensitivity in the determination of secondary amino acids, we investigated other thiol compounds. The use of 3-mercaptopropionic acid (3-MPA), first investigated by Kucera and Umagat[12], yielded the desired results and allowed the simultaneous determination of primary and secondary amino acids.

In this work, the use of OPA–3-MPA as an alternative reagent for the determination of amino and imino acids in acidic hydrolysates of proteins and peptides is described. The use of three internal standards for monitoring variations in the analysis is also reported.

EXPERIMENTAL

Chemicals

Analytical-reagent grade chemicals and 3-MPA were purchased from Merck (Darmstadt, F.R.G.) and HPLC-grade water and OPA from Carlo Erba (Milan, Italy). Brij-35 (30%, w/v), chymotrypsinogen A (Type II, from bovine pancreas), the amino acid calibration mixture (AA-S-18) and individual amino acids were purchased from Sigma (St. Louis, MO, U.S.A.). The ultrafiltered milk protein sample (85% peptide content) (Ultimate, Saronno, Italy) and sodium hypochlorite (chlorine concentration 5–6%) (Procter & Gamble, Pomezia, Italy) were of commercial grade.

Apparatus

The analyses were performed with a Series 4 liquid chromatograph (Perkin-Elmer, Monza, Italy), equipped with a 650-10S fluorescence detector with an 18-μl flow cell (Perkin-Elmer), and data were quantitated by a Model 3600 computing integrator (Perkin-Elmer). Samples were injected into the mobile-phase stream via a Rheodyne (Cotati, CA, U.S.A.) 7125S valve with 25-, 50- and 100 μl filling loops. The stainless-steel column (170 × 4.6 mm I.D.), the reaction coils, the column oven and the two fluid metering pumps for post-column reactions were supplied by Jasco (Barzanò, Italy). The column packing consisted of 7–8-μm particles of MCI CK 10F gel (Mitsubishi, Tokyo, Japan), a strong cation-exchange resin composed of sulphonic acid groups attached to a styrene–divinylbenzene copolymer (cross-linkage, 10%).

The hypochlorite oxidation step was carried out in a 300 × 0.5 mm I.D. stain-

less-steel tube. The reaction coil for the derivatization step was made of the same tubing but with a length of 2.5 m.

Chromatographic conditions

The mobile phases consisted of (A) 0.2 *M* Na^+ and (B) 0.25 *M* Na^+. Eluent A contained sodium citrate dihydrate (15.78 g/l), sodium nitrate (3.4 g/l), phenol (1 g/l), 2-propanol (30 ml/l) and Brij-35 (0.2 ml/l). Eluent B contained the same amounts of sodium citrate, sodium nitrate and Brij-35 as in A, plus 9.54 g/l of sodium tetraborate decahydrate and 15 ml/l of 2-propanol. The buffers were adjusted to (A) pH 3.05 and (B) 10.45 with 20% nitric acid and 5 *M* sodium hydroxide. Citrate buffers are stable for 1 month if stored at room temperature.

The OPA reagent[4] was prepared by dissolving 3.2 g of OPA in 40 ml of anhydrous ethanol and mixing this solution with 1 l of degassed and filtered 0.35 *M* potassium borate buffer (pH 10.4). Amounts of 2.4 ml of 3-MPA and 2.0 ml of Brij-35 were then added. The sodium hypochlorite reagent, 0.2% (v/v) in borate buffer containing 1.5% (w/v) potassium sulphate, was stabilized overnight at 4°C before use. This solution, which is not stable, was not kept longer than 48 h. The OPA reagent kept in a nitrogen atmosphere for 1 week without appreciable change in response.

The column and reaction coils were thermostated in the column oven at 68°C. The mobile-phase flow-rate was set at 0.5 ml/min. The post-column reagents were delivered on-line by pumping the solutions into the reaction coils via two tee-valves, as described by Cunico and Schlabach[8]. The final flow-rate of each reactant was set at 0.35 ml/min. Peaks were detected by measurement at 360 nm excitation wavelength and 450 nm emission wavelength. The gradient conditions are summarized in Table I. The typical cycle time between two injections was 60 min.

TABLE I

GRADIENT PROGRAMME FOR CHROMATOGRAPHIC AMINO ACID ANALYSIS

Step	*Time (min)*	*Eluent A (%)*	*Eluent B (%)*	*Gradient profile*
Equilibration	14	100	–	–
1	13	80	20	Concave
2	15	65	35	Linear
3	14	–	100	Isocratic
Regeneration[a]	4	–	–	–

[a] With 0.2 *M* sodium hydroxide.

Amino acid standards

The amino acid calibration mixture and the individual amino acids were diluted in eluent A, containing the three internal standards (I.S. buffer). Each internal standard had a concentration of 10 μM. Standard solutions were stored refrigerated for 2 weeks. Stock solutions of individual amino acids in water were kept at −20°C before dilution.

Sample preparation

Chymotrypsinogen A was hydrolysed *in vacuo* with 4 *M* methanesulphonic acid containing tryptamine (2 mg/ml). Cysteines were converted to S-sulphocysteine (Cys-SO_3H) according to the method of Inglis *et al.*[13]. The same amount of protein was hydrolysed in 5.7 *M* hydrochloric acid (0.2% phenol) at 110°C for 22 h. Both hydrolysates were diluted with the I.S. buffer before conversion of the cysteines to Cys-SO_3H.

The ultrafiltered milk protein sample (5 mg) was hydrolysed with 1 ml of 4 *M* methanesulphonic acid (0.2% tryptamine) and diluted to 50 ml with the I.S. citrate buffer.

Leucotrofina, a therapeutic formulation of the calf thymus derivative Thymomodulin (Ellem, Milan, Italy)[14] in 35% (w/v) sorbitol was diluted with four volumes of I.S. buffer and injected (50 μl) into the HPLC system for free amino acid determination.

Calculations

Quantitative estimates of the amino acid content were based on internal standardization with homoserine (I.S.$_1$), norleucine (I.S.$_2$) and β-aminoisobutyric acid (I.S.$_3$).

RESULTS AND DISCUSSION

A typical HPLC separation of standard amino acids at the 250- and 40-pmol levels is shown in Fig. 1. Critical pairs of amino acids, Hyp–Asp, Thr–Ser, Ala–(Cys_2) and Leu–Nleu, are well separated with the gradient programme in Table I. Shorter programmes can affect the resolution of the Hyp–Asp pair. A 57-min gradient programme may be used for the analysis of hydrolysates lacking Hyp (Fig. 2) by shortening the equilibration time to 11 min. In this instance, the gradient slope of the first step must be lowered in order to maintain the performance of the separation.

The volume of the samples can seriously affect the resolution of the pairs Met (O)–Hyp and Hyp–Asp (Table II). Larger injection volumes are observed to contribute to the peak broadening in the acidic and hydroxyl amino acid zone. Very diluted peptide hydrolysates lacking Hyp can be injected in larger volumes without affecting the performance of the analysis. The internal standards (a) I.S.$_1$, (b) I.S.$_2$ and (c) I.S.$_3$ were used for the following three groups of amino acids, respectively: (a) $CysSO_3H$, Cya, Met(O), Hyp, Asp, Thr, Ser, Glu, Pro, Gly, Ala and $(Cys)_2$; (b) Val, Met, Ile, Leu, Tyr and Phe; (c) His, Trp, Lys and Arg.

The relative standard deviation (R.S.D.) of the retention time relative to that of the internal standards ranged between 0.2 and 1.0% for six replicate injections. The R.S.D. of the peak-area ratios ranged between 0.6 and 3.3 (Table III). The linearity of the assay was evaluated in the 0.1–2.5 nmole range. The linear correlation coefficients were higher than 0.985 ($n = 6$) for all amino acids except $(Cys)_2$ ($r = 0.955$), Met(O) ($r = 0.972$) and Hyp ($r = 0.982$).

The lowest limit of detection in this chromatographic procedure was 10 pmol for each amino acid (Fig. 1), but at this level of sensitivity the precision was low. The R.S.D. of the peak-area ratios at 40 pmol ranged between 3 and 7% for all of the amino acids except Hyp (8%), Cys (12%) and Trp (10%). The large variation of the

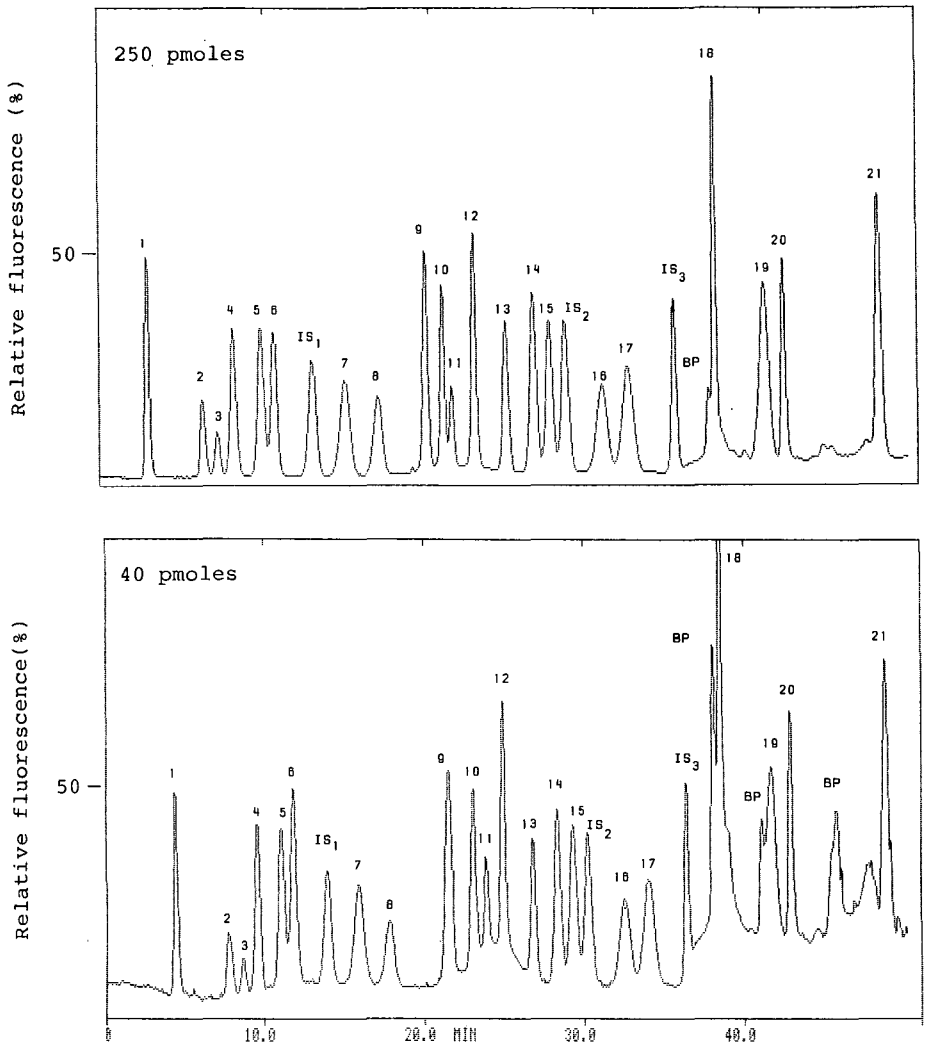

Fig. 1. HPLC and post-column detection of a standard mixture of amino acids. Conditions are summarized under Experimental. Gradient conditions of amino acids are given in Table I. Peaks: 1 = cysteic acid; 2 = Met(O); 3 = Hyp; 4 = Asp; 5 = Thr; 6 = Ser; 7 = Glu; 8 = Pro; 9 = Gly; 10 = Ala; 11 = $(Cys)_2$; 12 = Val; 13 = Met; 14 = Ile; 15 = Leu; 16 = Tyr; 17 = Phe; 18 = His; 19 = Trp; 20 = Lys; 21 = Arg. Amounts of Met(O) and Hyp were 125 pmol (above) and 20 pmol (below), and of $I.S._i$ was 250 pmol (above) and 40 pmol (below). BP = blank impurity peaks.

Trp peak-area ratio is caused by a blank impurity which is eluted in the Trp zone (Fig. 1). In the blank run this impurity ranged between 5 and 12 pmol, if evaluated as Trp. As its contribution is small, it can be subtracted from the Trp peak area.

The chromatograms show an impurity peak (BP) which is eluted in the His zone. This peak does not interfere in the His determination in the picomole range, but

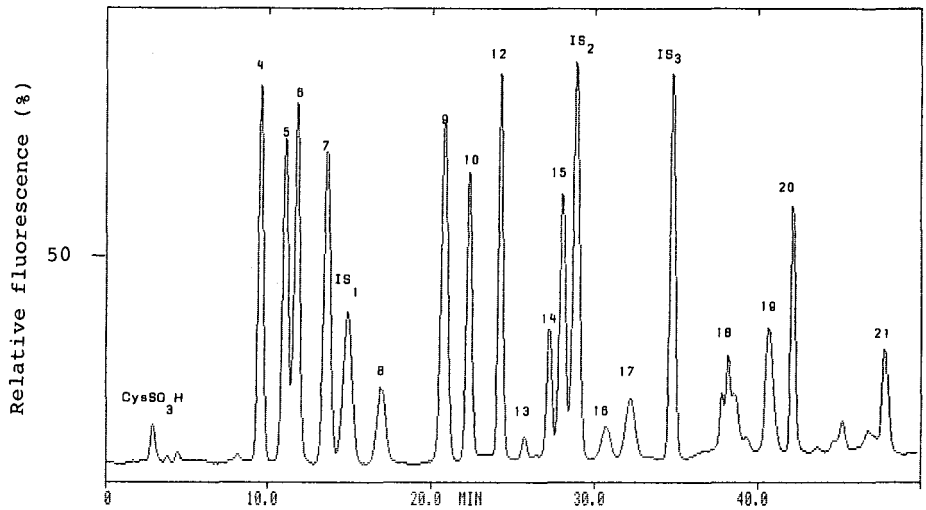

Fig. 2. Amino acid analysis of bovine chymotrypsinogen A hydrolysate performed with the methanesulphonic acid procedure. Peaks and conditions as in Fig. 1. $CysSO_3H$ = S-sulphocysteine. Amount of I.S.$_i$, 500 pmol.

TABLE II

INFLUENCE OF INJECTION VOLUME ON RESOLUTION FACTOR

Critical pair	*Injection volume (µl)*		
	25	*50*	*100*
Met(O)–Hyp	> 1.4	> 1.3	> 1.0
Hyp–Asp	> 1.3	> 1.2	< 1.0
Thr–Ser	> 1.1	> 1.1	> 1.0

TABLE III

REPRODUCIBILITY OF PEAK-AREA RATIOS OF AMINO ACIDS

The peak-area ratios (R) are average values of six replicate injections. Each value corresponds to 500 pmol.

Amino acid	*R*	*R.S.D. (%)*	*Amino acid*	*R*	*R.S.D. (%)*
Cysteic acid	1.046	1.4	Val	1.034	1.5
Met(O)	0.848	1.3	Met	0.751	1.4
Hyp	0.488	1.6	Ile	1.045	0.9
Asp	1.123	2.5	Leu	0.970	1.6
Thr	1.113	0.6	Tyr	0.848	0.9
Ser	1.165	2.6	Phe	1.067	0.7
Glu	1.108	0.8	His	1.620	3.3
Pro	0.768	1.8	Trp	1.782	2.6
Gly	1.410	0.8	Lys	1.074	2.6
Ala	0.975	1.8	Arg	1.721	1.2
$\frac{1}{2}(Cys)_2$	0.407	3.6			

it is not separated from His at the nanomole level. Impurity and buffer-change peaks were also reported for dedicated commercial buffers[15].

The two reaction steps, oxidation and derivatization, were carried out at 68°C, because the best ion-exchange separation was obtained at this temperature. The length of the two reaction coils was chosen in order to maintain the oxidation and derivatization steps in the ranges 4–5 and 20–30 s, respectively. The highest Pro, Met and Tyr responses were found with 0.2% hypochlorite and 0.32% OPA. The molar ratio of 3-MPA to OPA in the derivatizing solution was kept at 1:1, as suggested by Fujiwara *et al.*[11].

The influence of reaction time on the fluorescence response of Pro, Met and Tyr was studied at different flow-rates of the reactants (Table IV). Although the best results were obtained with prolonged reaction times, we delivered each post-column reagent at 0.35 ml/min, because at lower flow-rates the excessive decrease in resolution of critical pairs can interfere with their determination. Lower flow-rates also affect the reproducibility of amino acid determinations.

TABLE IV

INFLUENCE OF REACTION TIME ON FLUORESCENCE RESPONSE

The fluorescence response was monitored as the mean of the peak areas of two 500-pmol samples of amino acids. The data were obtained by delivering the reagents (sodium hypochlorite and OPA–3-MPA) at 0.25, 0.30, 0.35 and 0.40 ml/min, respectively. The two reactions were delivered at the same flow-rate in each trial.

Amino acid	*Reaction time (s)*			
	30	*27*	*25*	*23*
Pro	36 220	34 500	30 413	24 608
Met	32 913	31 035	28 950	27 576
Tyr	37 086	35 610	32 909	32 584

The good recovery shown by the fluorescence responses of Pro, Met and Tyr suggests that 3-MPA is a suitable reagent for the reliable simultaneous determination of amino and imino acids.

The method was extended to the determination of tryptophan in protein, hydrolysed with 4 *M* methanesulphonic acid (MSA)[13] containing 0.2% tryptamine. Fig. 2 shows the chromatogram of the MSA hydrolysate of bovine chymotrypsinogen A. Table V compares the results of determinations using the 5.7 *M* hydrochloric acid and the 4 *M* MSA hydrolysis methods. The 90% tryptophan recovery indicates that MSA hydrolysis, coupled with the two-step post-column derivatization method, is satisfactory for the determination of Trp in purified peptides. In our experiments, the MSA hydrolysis seemed to improve the recovery of Ser, whereas Ile and Val were more resistant to the cleavage. In spite of various attempts, low recoveries of S-sulphocysteine was obtained with both the hydrochloric acid and the MSA hydrolysis methods. Although the composition of chymotrypsinogen is unbalanced (low contents of Met, Tyr and Hys), the analysis demonstrated that the OPA–3-MPA method

TABLE V

RECOVERY OF AMINO ACIDS OF CHYMOTRYPSINOGEN A BY HYDROLYSIS WITH 5.7 *M* HCl AND 4 *M* MSA

Amino acid	*HCl*		*MSA*	*Amino acid*	*HCl*		*MSA*
$CysSO_3H$	7.68[a]	(10)[b]	6.70	Met	1.82	(2)	1.90
Asx	22.40	(23)	23.06	Ile	8.82	(10)	8.09
Thr	22.01	(23)	22.31	Leu	18.60	(19)	18.37
Ser	24.75	(28)	26.91	Tyr	3.94	(4)	3.62
Glx	15.69	(15)	15.56	Phe	5.86	(6)	5.89
Pro	9.34	(9)	9.29	His	2.30	(2)	1.70
Gly	22.82	(23)	23.41	Trp	–	(8)	7.22
Ala	22.20	(22)	22.00	Lys	13.72	(14)	14.07
Val	20.49	(23)	18.58	Arg	4.02	(4)	4.14

[a] The number of residues was normalized to the number of Ala residues found. The absolute recoveries of Ala were 82% (HCl) and 81% (MSA), assuming 100% purity of the reference protein sample. Experimental values are means of two determinations of each hydrolysate.

[b] The numbers in parentheses are the expected values based on the protein sequence analysis.

is suitable for the determination of each amino acid. A representative chromatogram of an MSA hydrolysate of ultrafiltered milk proteins (85% protein) is shown in Fig. 3.

Several workers have recommended restricting the use of sulphonic acids to protein samples that do not contain carbohydrates, because Trp is destroyed during acid hydrolysis in the presence of carbohydrates[13].

The OPA–3-MPA post-column method also improved the determination of proline and hydroxyproline. Fig. 1 shows a good fluorescence response of Hyp and Pro at the picomole level. As these amino acids usually indicate the presence of

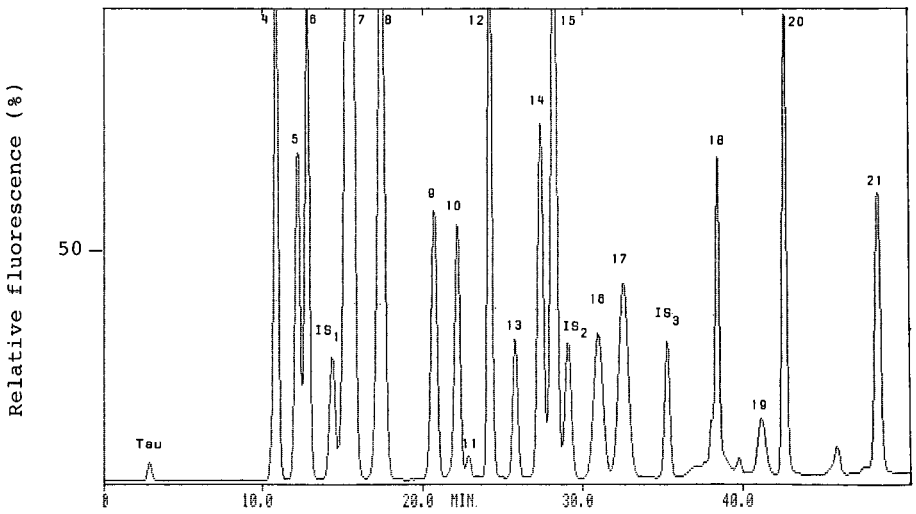

Fig. 3. Chromatogram of ultrafiltered milk protein after hydrolysis with 4 *M* MSA. Peaks and conditions as in Fig. 1. Tau = taurine. Amount of I.S.$_i$, 500 pmol.

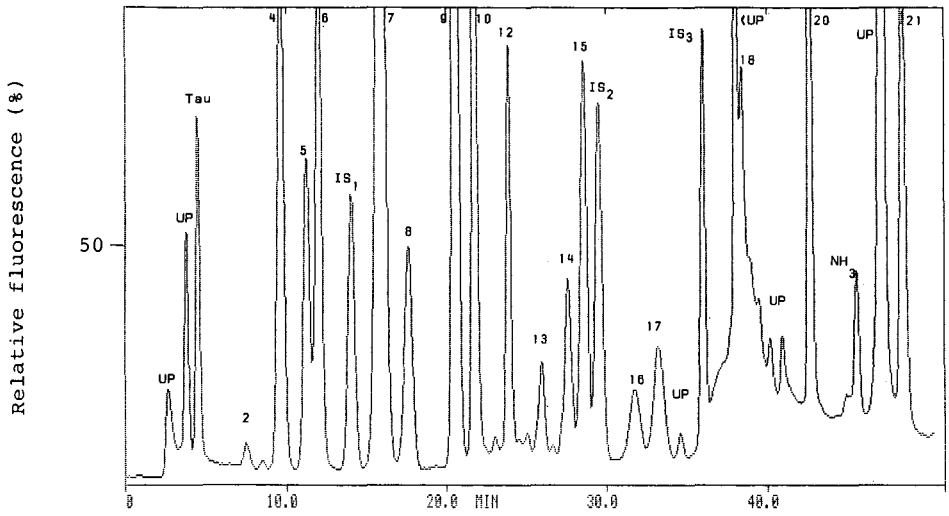

Fig. 4. Free amino acid analysis of a therapeutic formulation of the calf thymus derivative Thymomodulin. The sample syrup was diluted with I.S. buffer (see Experimental) and injected directly into the HPLC system. Peaks and conditions as in Fig. 1. UP = unknown peaks. Amount of I.S.$_i$, 500 pmol.

collagen in biological materials, the accurate determination of imino acids gives an estimate of the collagen content of the sample[16].

The chromatographic separation of free amino acids in the therapeutic formulation, Leucotrofina syrup, without previous purification is illustrated in Fig. 4. In this sample, the total free amino acids usually amount to 0.15–0.25 mg/ml. A complete assay is obtained simply by injecting the diluted sample directly into the HPLC system. The sorbitol in the sample (7%, w/v), does not interfere with the separation performance.

In conclusion, it has been shown that the use of OPA–3-MPA as the derivatizing agent, coupled with hypochlorite oxidation, in the HPLC and post-column detection of amino and imino acids is a useful tool for their quantitative determination.

ACKNOWLEDGEMENTS

We thank Dr. Giorgio Mazzola for suggesting the use of 3-MPA. We are also greatly indebted to Dr. Brunetto Brunetti for his support.

REFERENCES

1 S. Moore and W. H. Stein, *J. Biol. Chem.*, 211 (1954) 907.
2 S. Moore, D. H. Spackman and W. H. Stein, *Anal. Chem.*, 30 (1958) 1185.
3 R. F. Pfeifer and D. W. Hill, *Adv. Chromatogr.*, 22 (1982) 1.
4 M. Roth, *Anal Chem.*, 43 (1971) 880.
5 M. Weigele, S. De Bernardo and W. Leingruber, *Biochem. Biophys. Res. Commun.*, 50 (1973) 352.
6 D. G. Dresker and K. S. Lee, *Anal. Biochem.*, 84 (1978) 559.
7 P. Böhlen and M. Mellet, *Anal. Biochem.*, 94 (1979) 313.
8 R. L. Cunico and J. Schlabach, *J. Chromatogr.*, 266 (1983) 461.

9 S. S. Simons and D. F. Johnson, *Anal. Biochem.*, 82 (1977) 250.
10 L. A. Allison, G. S. Mayer and R. E. Shoup, *Anal. Chem.*, 56 (1984) 1089.
11 M. Fujiwara, Y. Ishida, N. Nimura, A. Toyama and T. Kinoshita, *Anal Biochem.*, 166 (1987) 72.
12 D. Kucera and H. Umagat, *J. Chromatogr.*, 255 (1983) 563.
13 A. S. Inglis, D. T. W. McMahon, C. M. Roxburgh and H. Takayanagi, *Anal. Biochem.*, 72 (1976) 86.
14 A. Fiocchi, E. Borella, E. Riva, D. Arensi, P. Travaglini, P. Cazzola and M. Giovannini, *Thymus*, 8 (1986) 331.
15 G. R. Barbarash and R. H. Quarles, *Anal. Biochem.*, 119 (1982) 177.
16 K. Yaegaki, J. Tonzetich and A. S. K. Ng, *J. Chromatogr.*, 356 (1986) 163.

Journal of Chromatography, 476 (1989) 93–98
Elsevier Science Publishers B.V., Amsterdam — Printed in The Netherlands

CHROMSYMP. 1612

HIGH-PERFORMANCE LIQUID CHROMATOGRAPHY FOR CYCLOSPORIN MEASUREMENT: COMPARISON WITH RADIOIMMUNOASSAY

MARIO PLEBANI, MAURIZIO MASIERO, CARLO D. PALEARI, LAURA SCIACOVELLI, DIEGO FAGGIAN and ANGELO BURLINA*

Cattedra di Chimica e Microscopia Clinica, Laboratorio Centrale di Analisi, Università di Padova, Via Giustiniani 2, 35128 Padova (Italy)

SUMMARY

The large inter-patient variability in cyclosporin pharmacokinetics coupled with the agent's narrow therapeutic index with adverse effects resulting from supra-therapeutic levels, necessitates individualization of drug dosage and therapeutic monitoring of cyclosporin blood levels. The performance of a liquid chromatographic method for the measurement of cyclosporin was evaluated and the results obtained by this method and by a specific radioimmunoassay were correlated. The method described is sensitive, selective, reproducible and easier to perform than other chromatographic methods. It is suitable for the daily measurement of cyclosporin in batches of up to 40 samples and the results correlate well with another chromatographic method and with the specific radioimmunoassay.

INTRODUCTION

Cyclosporin A (CsA) is widely used as an effective and potent immunosuppressant in organ transplantation[1,2] and treatment with CsA has greatly improved the results of kidney, heart, bone marrow and liver transplantation. However, the narrow therapeutic index and the wide variability in its pharmacokinetics necessitate individualized dosage adjustment[3]. Well known adverse effects of drug levels above that range include nephrotoxicity, neurotoxicity, hypertension, gingival hyperplasia, anorexia, nausea and ileus[4]. On the other hand, levels below the appropriate range are associated with an enhanced risk of graft rejection or graft *versus* host disease in bone marrow transplants. For these reasons, careful attention to the CsA concentration in blood is essential for optimization of therapy.

Several techniques [radioimmunoassay (RIA) with polyclonal and monoclonal antibodies, high-performance liquid chromatography (HPLC) and fluorescence polarized immunoassay (FPIA)] for therapeutic monitoring of CsA have been developed[5]. RIA with polyclonal antiserum and FPIA measure CsA together with some cross-reactive metabolites that appear in blood after the drug is administered. In contrast, HPLC and the new RIAs with monoclonal antibodies specifically measure the parent drug, independent of its metabolites. Specific measurement of CsA seems to

0021-9673/89/$03.50

be recommended, as suggested by recent papers[6]. The aim of this work was to evaluate the performance of isocratic HPLC for the measurement of CsA and to compare the results with those obtained by a specific radioimmunoassay.

EXPERIMENTAL

Samples

Whole-blood samples were taken from 80 renal and 60 heart transplant patients who had received immunotherapy with CsA. CsA (5–20 mg/kg body weight) was given orally, once or twice a day, and all blood specimens were collected before the next dose. Samples were collected in tubes containing EDTA-K3 (Merck-Bracco, Milan, Italy) as an anticoagulant and stored at −20°C until analysed. All samples were analysed by three different methods for CsA measurement (specific RIA, reference HPLC and described HPLC).

Chemical and reagents

Cyclosporin A (CsA) and the internal standard, cyclosporin D (CsD), were obtained from Sandoz (Basle, Switzerland). Acetonitrile, hexane, methanol and water (HPLC grade) were purchased from Merck-Bracco.

Instrumentation and chromatographic conditions

A Bio-Rad HPLC instrument was employed (Bio-Rad Labs., Segrate, Italy), including a Model 1330 HPLC dual piston pump, Model 1306 variable-wavelength UV detector, Model AS-48 autosampler and Model 3392 A integrator. The column used was a reversed-phase C_8 mini-column (high-performance RP mini-column, 30 × 4.6 mm I.D., particle size 5 μm, from Bio-Rad Labs.), maintained at 70°C with a column heater (Bio-Rad Labs.). The flow-rate of the mobile phase (20 m*M* ammonium phosphate buffer in 56% aqueous acetonitrile, pH 6.2) was 1.2 ml/min. The effluent from the column was monitored at 210 nm.

Preparation of extraction columns

The extraction of CsA involved the use of 1.0-ml disposable cyano extraction columns (40-μm mean particle size) (Analytichem International, Harbor City, CA, U.S.A.). These columns were prepared by washing with 3 ml of 15% acetonitrile under vacuum. A Vac-Elut SPS 24 vacuum chamber, designed to accept 24 extraction column simultaneously, was purchased from Analytichem International.

Procedure

We employed the method of Sivorinowsky *et al.*[7,8] for the HPLC measurement of CsA, with the following modifications. A 1.0-ml volume of of water and 2.0 ml of working internal standard solution (CsD in a 30% aqueous acetonitrile solution) are pipetted into 1.0 ml of whole-blood samples, controls and standards, followed by vortex mixing for 30 s and centrifugation for 10 min at 1000 *g* at 0°C. A 3.0-ml volume of blood supernatant is applied to the columns, which are drained under vacuum. Excess blood is washed off the column with 15% acetonitrile (three 1.0-ml volumes) and each column is rinsed with 4.0 ml of 50% acetonitrile to remove hydrophobic contaminants. The cyclosporins are eluted with 450 μl of ethanol into small

borosilicate test-tubes. The eluate is diluted with 200 μl of 10^{-3} *M* phosphoric acid and washed twice with 600 μl of hexane. After centrifugation (1 min at 500 *g*), the hexane is removed by aspiration and 100 μl of the eluate are injected into an isocratic HPLC system consisting of a reversed-phase C_8 minicolumn and the buffered acetonitrile mobile phase (pH 6.2) at 70°C. The quantitation is based on comparison of the CsA/CsD (internal standard) peak-height ratio in the unknown sample to the ratio in the whole-blood standard.

Interferences

We evaluated potential interferences in this analysis by chromatographing pure drug solutions and samples of whole blood from patients who had ingested various drugs.The drugs tested under these conditions were acetaminophen, aminotriptyline, caffeine, chloramphenicol, chlordiazepoxide, diazepam, ethosuximide, gentamicin, imipramine, pentobarbital, phenobarbital, phenytoin, primidone, salicylate, secobarbital, theophylline and cortisone analogues (prednisone, prednisolone and methylprednisolone). We also evaluated the interference of metabolite 17 of CsA (generously supplied by Dr. Maurer, Sandoz).

Recovery

CsA was added to a drug-free whole-blood pool in amounts equivalent to 100–1500 μg/l, and the analytical recovery was calculated.

Comparison methods

HPLC according to Carruthers *et al.*[9]. This method employs extraction with diethyl ether and chromatography on a 25 cm × 4.8 mm I.D. Ultrasphere-Octyl (5 μm) column (Beckman Analytical, Milan, Italy) maintained at 72°C.

RIA with monoclonal antibodies. We utilized a radioimmunoassay with a mice monoclonal antibody that did not react appreciably with the metabolites of CsA. The method utilizes an iodinated tracer and a double antibody for separating bound and free fractions (Cyclo-Trac sp, Incstar Corp., Stillwater, MN, U.S.A.).

Statistics

The comparison between methods was made by regression analysis with an *F*-test on variance; the difference in slope from unity was assessed by Student's *t*-test.

RESULTS

As shown in Fig. 1, the retention times of CsA and of the internal standard CsD are 6.0 and 8.5 min, respectively. No interfering peaks eluting at times that would interfere with the analysis were detected in samples from patients who had received CsA together with commonly used drugs. The precision of the method is shown in Table I. The results of the analytical recovery test carried out on samples spiked with CsA are illustrated in Table II. The lower limit of sensitivity (signal equal to twice the baseline noise) of our procedure is 25 μg/l.

In order to simplify the original method, we tried to eliminate the double extraction with hexane by introducing directly 1.0 ml of hexane (twice) into the extraction column. The results obtained were not significantly different from those

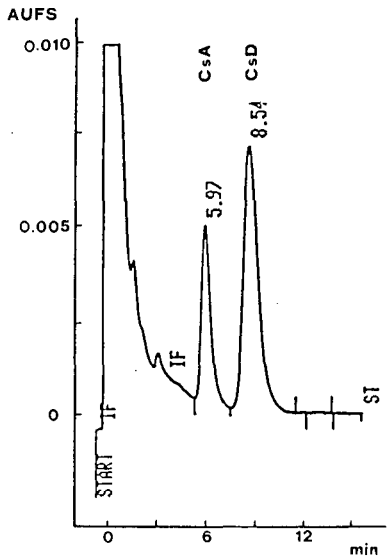

Fig. 1. Chromatogram of extracted whole-blood sample. CsA concentration, 460 μg/l.

TABLE I

REPRODUCIBILITY STUDIES

Parameter	$\bar{x}$ *(μg/l)*	*S.D. (μg/l)*	*Coefficient of variation (%)*
Within-run	150	3.5	2.3
precision	470	11.2	2.4
(n = 21)	805	21.7	2.7
Between-run	145	8.6	5.9
precision	468	23.8	5.1
(n = 11)	810	39.0	4.8

TABLE II

ANALYTICAL RECOVERY

Calculated value (μg/l)	*Observed value*[a] *(μg/l)*	*Recovery (%)*[b]
100.0	104.0 ± 4.0	104.0
200.0	205.0 ± 4.9	102.5
500.0	506.0 ± 13.4	101.0
1000.0	984.0 ± 26.4	98.4

[a] Mean of three determinations ± standard deviation.
[b] Mean value.

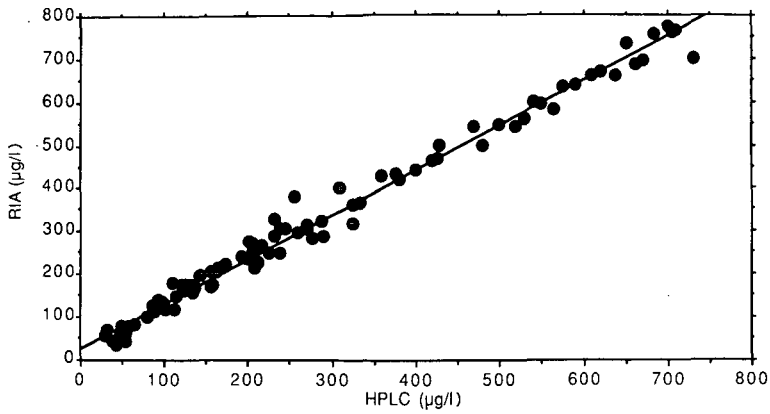

Fig. 2. Results of simultaneous analysis of whole-blood samples by HPLC and specific RIA [$n = 137$; $r = 0.974$ ($p < 0.0001$); $y = 1.037x + 27.17$ µg/l; $S_{y.x} = 27$; the slope was not different from 1 ($p = 0.11$; n.s.)].

given by the original method ($p > 0.05$). No interference from metabolite 17 and the drugs tested was observed. A high correlation between the results obtained by our method (y) and that of Carruthers *et al.*[9] (x) was observed [$n = 135$, $r = 0.989$, $p < 0.0001$; $y = 0.920x + 10.2$ µg/l; $S_{y.x} = 22$; the slope was not different from 1 ($p = 0.34$; n.s.)]. Moreover, a good correlation was found between our HPLC method and specific RIA with monoclonal antibodies (Fig. 2).

DISCUSSION

Numerous HPLC methods have been described for the measurement of CsA[10,11]. Despite their specificity, most HPLC determinations of CsA have definite disadvantages in comparison with RIA. In particular, long analysis times and difficulties in processing a large number of samples have been reported. Some procedures require time-consuming multi-step extractions; in some the extraction efficiency is poor; others have unsatisfactory detection limits. For these reasons, most laboratories prefere to monitor CsA by RIA.

The chromatographic method evaluated here is suitable for the daily measurement of CsA in batches up to 40 samples of whole blood. Whole blood was chosen because of the known problem of temperature-dependent separation[12,13] and because of recent recommendations of the National Academy of Clinical Biochemistry/American Association for Clinical Chemistry Task Force on Cyclosporin Monitoring[6]. The extraction is rapid and efficient, and chromatography is completed in 10 min per sample. With the use of a Vac-Elut chamber, designed to accept 24 extraction columns simultaneously, we are able to process 24 samples of whole blood in less than 30 min. The reproducibility is satisfactory, and 25 µg/l is an adequate sensitivity for therapeutic drug monitoring.

The principal advantage of our HPLC method is the rapid and simple extraction procedure compared with other published extraction procedures[10,11]. Moreover, the use of a mini-column is cost effective. The agreement observed between the results

obtained by our HPLC method and specific RIA demonstrates the accuracy of our method.

Although specific measurement of CsA is now recommended as a guide to therapy, some evidence exists that CsA metabolites are immunosuppressive[14] and even toxic[15]. Furthermore, differences exist in the metabolic handling of CsA in different groups of patients. The combination of specific and non-specific measurement of CsA provides a method for investigating the influence of metabolism on immunosuppressive therapy and its adverse effects[16]. Better information is derived from the concomitant identification and determination of CsA and its individual metabolites by HPLC. Recently, Lensmeyer *et al.*[17] described a chromatographic method for concomitant profiling of CsA and its metabolites in one assay. Preliminary results obtained with this selective measurement of CsA metabolites seems to prove the importance of such a determination for describing the interrelationship of CsA and its metabolites in therapy and toxicity[18]. We hope that new HPLC methods for concomitant measurement of CsA and its metabolites will soon be introduced into clinical practice.

REFERENCES

1 G. Opelz, *Prog. Allergy*, 38 (1986) 329.
2 T. Beveridge, *Prog. Allergy*, 38 (1986) 269.
3 G. J. Burckart, D. M. Canafax and G. C. Yee, *Drug Intell. Clin. Pharm.*, 20 (1986) 649.
4 H. Nogueira and R. Cutler, *Dialysis Transplant. Today*, Oct. (1985) 585.
5 D. W. Holt, J. T. Marsden and A. Johnston, *Transplant. Proc.*, 18 (1986) 101.
6 L. M. Shaw, L. Demers, D. Freeman, T. Moyer, A. Sanghui, H. Seltman and R. Vonkataramanan, *Clin. Chem.*, 33 (1987) 1269.
7 G. Sivorinowsky, S. R. Binder, M. J. Regalia and M. E. Biaggi, *Ann. Clin. Biochem.*, 24, Suppl. 2 (1987) 64.
8 *Bio-Rad Cyclosporin by HPLC Test, Instruction Manual*, Bio-Rad Clinical Division, Richmond, CA, 1986.
9 S. G. Carruthers, D. J. Freeman, T. G. Koepler, W. Howson, P. A. Keown, A. Laupacls and C. R. Stiller, *Clin. Chem.*, 29 (1983) 180.
10 T. P. Moyer, P. Johnson, S. M. Faynor and S. Sterioff, *Clin. Biochem.*, 19 (1986) 83.
11 S. J. Fletcher and R. A. Bacchus, *Ann. Clin. Biochem.*, 25 (1988) 510.
12 M. Wenk, F. Follath and E. Abish, *Clin. Chem.*, 29 (1983) 1865.
13 H. Dieperik, *Lancet*, i (1983) 416.
14 B. Freed, T. Rosano and N. Lempert, *Transplantation*, 43 (1987) 123.
15 A. Wood and M. Lemaire, *Transplant. Proc.*, 17 (1985) 27.
16 M. Plebani and A. Burlina, *Lancet*, ii (1988) 687.
17 G. Lensmeyer, D. A. Wiebe and I. H. Carlson, *Clin. Chem.*, 33 (1987) 1841.
18 G. Lensmeyer, D. A. Wiebe and I. H. Carlson, *Clin. Chem.*, 33 (1987) 1851.

Journal of Chromatography, 476 (1989) 99–112
Elsevier Science Publishers B.V., Amsterdam — Printed in The Netherlands

CHROMSYMP. 1596

ISOLATION OF RECOMBINANT PARTIAL *gag* GENE PRODUCT p18 (HIV-1_{Bru}) FROM *ESCHERICHIA COLI*

HANNO V. J. KOLBE*, FRANCINE JAEGER, PIERRE LEPAGE, CAROLYN ROITSCH, GEORGES LACAUD, MARIE-PAULE KIENY, JEAN SABATIE, STEPHEN W. BROWN and JEAN-PIERRE LECOCQ

Transgene SA, 11 Rue de Molsheim, 67000 Strasbourg (France)

and

MARC GIRARD

Pasteur Vaccins, 3 Avenue Pasteur, 92430 Marnes-la-Coquette (France)

SUMMARY

The membrane-associated structural protein, p18, of the human immunodeficiency virus (HIV-1), has been expressed in *Escherichia coli*. The recombinant protein was purified by cation-exchange chromatography on S Sepharose followed by cation-exchange high-performance liquid chromatography (HPLC) on Sulfoethyl Aspartamide. The isolation of 28.7 mg of recombinant p18 from 16.7 l of cell culture represents an overall yield of *ca.* 20%.

Recombinant p18 was characterized by sodium dodecyl sulphate polyacrylamide gel electrophoresis, reversed-phase HPLC, amino acid composition and amino acid sequence analysis of the N-terminus. Edman degradation of peptides generated by trypsin or *Staphylococcus aureus* V8 proteolytic digestion, including the C-terminus, confirmed the amino acid sequence to be that predicted from the cDNA. A C-terminally cleaved form of recombinant p18, p18LM, was separated in the cation-exchange HPLC step and was partially characterized in parallel with the intact molecule. By Western blotting it was shown that recombinant p18 in addition to the cleaved form p18LM is recognized by a monoclonal antibody which was generated against the natural protein from HIV-1.

INTRODUCTION

The *gag* gene of the human immodeficiency virus (HIV-1) codes for a precursor protein of 500 amino acids[1]. This precursor is processed by a protease which is coded by a region on the *pol* gene of HIV-1 to generate the structural proteins p18 (Met_1–Tyr_{132}, calculated molecular mass M_c = 14883 Da; calculated isoelectric point, pI_c = 9.23), p25 (Pro_{133}–Leu_{363}, M_c = 25580 Da, pI_c = 6.51), and p15 (Ala_{364}–Leu_{500}, M_c = 15497 Da, pI_c = 9.54). However, during processing of p18 in the mammalian host cell, Met_1 is cleaved off and Gly_2 is myristylated. Natural p18 thus shows a blocked N-terminus[2]. It is assumed that the myristate moiety anchors p18

0021-9673/89/$03.50

to the lipid membrane of the virus. This assumption is supported by the results of Gelderblom *et al.*[3], who localized p18 by electron microscopy after immunolabelling on the inner side of the lipid membrane of human immunodeficiency virus particles, showing that p18 forms a spherical shell around the inner core.

Quantitative Western blot analyses of sera from HIV-1-seropositive individuals showed that antibodies against the core proteins p25 and p18 are discovered predominantly before and during the early stages of the disease. The recession of anti-p25 and anti-p18 antibodies during the development of the disease can consequently be used to diagnose the clinical status of the patient[4,5].

Antigens for Western blots are usually prepared by growing HIV-1 in culture, inactivating the virus and separating the viral proteins by sodium dodecyl sulphate polyacrylamide gel electrophoresis (SDS-PAGE). Considering the potentially dangerous manipulation of live virus and the limited availability of these antigens, the advantages of using recombinant protein antigens in Western blot analysis become apparent[6].

Naylor *et al.*[7] have shown that p18 displays a 44% similarity in a stretch of 18 amino acids (Ile_{92}–Asn_{109}) when compared with the hormone peptide thymosin alpha-1 (Ile_{11}–Asn_{28}). Sera raised against thymosin alpha-1 recognized p18, isolated from HIV-1, and partially neutralized viral activity, as measured by inhibition of expression of p15, p25 and reversed transcriptase activity in the cell culture medium[8]. These findings make recombinant p18, or peptides thereof, interesting as potential components of an AIDS vaccine.

In this paper, we describe the purification of recombinant p18 from *E. coli*. The protein was characterized biochemically and appears suitable for tests in preliminary experiments regarding its diagnostic and immunological use.

EXPERIMENTAL

Chemicals

All buffers were prepared with Milli-Q water (Millipore-Waters, Milford, MA, U.S.A.). Cation-exchange high-performance liquid chromatographic (HPLC) buffers were filtered in a 0.45-μm Nalgene unit (Sybron/Nalge, Rochester, NY, U.S.A.). Acetonitrile and 1-propanol were from Carlo Erba (Milan, Italy) and trifluoroacetic acid (TFA) and heptafluorobutyric acid (HFBA) from Pierce (Rockford, IL, U.S.A.). All other chemicals were of analytical-reagent grade.

Plasmid construction and fermentation of E. coli

The complete *gag* gene of HIV-1_{Bru}[1] was constructed by juxtaposing the Hind III restriction fragments of plasmids pJ19-1, pJ19-13 and pJ19-17[9]. Using site-directed mutagenesis, a stop codon was introduced at the position of the C-terminal tyrosine of p18. This synthetic gene, coding for Met_1 to Asn_{131} (numerical order of amino acids taken from mature *gag* gene product precursor protein[1]) was inserted into a procaryotic expression vector under control of the bacteriophage lambda PL promoter. *E. coli*, strain TGE901, contains a temperature-sensitive cI repressor. *E. coli*, transformed with this construction (pTG-2153-HIV-1), was grown overnight in a 500-ml preculture in Luria–Bertani medium (+ ampicillin) at 30°C. A 20-l LSL-Biolafitte (St. Germain-en-Laye, France) bioreactor was inoculated to an absorbance of 0.1 (650 nm, 1-cm

cuvette). Cells were grown for 2.5 h at 30°C until the cell density reached an absorbance of 0.3. Expression of p18 was then induced by raising the temperature and maintaining it at 42°C. After 7 h, the absorbance had reached 2.4. From the final volume of 16.7 l, cells were harvested by a 10-min centrifugation at 5000 rpm (Sorvall RC-3B, H-6000A rotor; DuPont, Wilmington, DE, U.S.A.).

S Sepharose chromatography

The cell pellet (7.87 g of protein) was homogenized (hand-operated glass/glass homogenizer) in 300 ml of phosphate-buffered saline (PBS). Recombinant p18 was released from *E. coli* cells by first freezing the suspension at −80°C and then thawing it at 0–2°C. The supernatant was collected by a 20-min centrifugation at 10 000 rpm and 0–5°C (Sorvall RC-5B, GSA rotor). Broken cells were carried through another two cycles, as described above, and a second and third supernatant were recovered. The pool of the first and second supernatants (540 ml) was diluted with 540 ml of Milli-Q water, adjusted to pH 6.0 with hydrochloric acid and left overnight at 2–4°C. The resulting precipitate was removed by a 15-min centrifugation at 7000 rpm and 0–5°C (Sorvall RC-5B, GSA rotor), At room temperature, protein continued to precipitate. To avoid application of precipitate to the column, the sample was loaded at 200 ml/h from a reservoir, containing a magnetic stirrer, via tubing equipped with a 10-μm solvent filter (Gilson, Middleton, WI, U.S.A.) on to a column (10 cm × 4.4 cm I.D.) of S Sepharose Fast Flow (Pharmacia, Uppsala, Sweden). equilibrated with half-concentrated PBS (pH 6.0). Precipitate concentrated in the sample reservoir and was discarded. The column was washed successively with 50 ml of half-concentrated PBS (pH 6.0) and 200 ml of PBS and protein was eluted with 200 ml each of 40 mM sodium phosphate (pH 7.0) containing 0.2, 0.4, 0.6, 0.8 and 1 *M* sodium chloride. Absorbance was measured at 275 nm with a Model 2158 Uvicord SD instrument (2.5-mm flow cell, 70 μl, LKB, Bromma, Sweden). Eluted fractions were pooled according to the purity of recombinant p18 and concentrated at room temperature in an ultrafiltration cell on a YM5 membrane (Amicon, Danvers, MA, U.S.A.). The concentrated sample was thoroughly washed with CatEx-A buffer (see below).

Preparative high-performance liquid chromatography

Preparative HPLC was performed on a Beckman Model 421A gradient liquid chromatograph, equipped with two Model 110A solvent pumps, a Model 340 organizer/sample injector (Beckman Instruments, Palo Alto, CA, U.S.A.), a Uvicord 2158 SD absorbance detector (275 nm, 2.5-mm HPLC flow cell, 8 μl), a Model 2210 recorder and a Model 2112 Redirac fraction collector (LKB). The chromatographic unit consisted of a Sulfoethyl Aspartamide HPLC column (300 Å, 5 μm, 200 mm × 9.4 mm I.D.; Nest Group, Southborough, MA, U.S.A.) and a guard column (20 mm × 2 mm I.D.), dry-filled with Zorbax Diol WR955 (DuPont). Separation of proteins was performed at room temperature. Prior to sample loading, the column was equilibrated with a blank gradient (flow-rate, 1.3 ml/min); 100% CatEx-A buffer [20 m*M* sodium phosphate (pH 7.0)–40 m*M* sodium chloride] from 0 to 5 min, 0–70% CatEx-B buffer [40 m*M* sodium phosphate (pH 7.0)–1 *M* sodium chloride] from 5 to 20 min, 70–100% CatEx-B from 20 to 40 min, 100% CatEx-B from 40 to 45 min, 100% CatEx-B to 100% CatEx-A from 45 to 50 min, 100% CatEx-A from 50 to 70 min. The sample was loaded via pump A at 1.5 ml/min and, after rinsing the system with 20 ml of

CatEx-A, the above-described gradient was started. Fractions were collected automatically every 0.7 min. The salt concentration in the fraction was determined by conductimetry (CDM3 conductivity meter, Radiometer, Copenhagen, Denmark).

Proteolytic digestion

Trypsin digestion. Recombinant p18 and p18LM (100 μg each) were separately desalted by reversed-phase HPLC in system 1 (see below). The protein peak was collected and solvent was removed in a Speedvac concentrator (Savant Instruments, Framingdale, NY, U.S.A.). Trypsin (5 μg) (sequence grade, Boehringer, Mannheim, F.R.G.) was added in 100 m*M* N-ethylmorpholine (Janssen Chimica, Beerese, Belgium)–0.1 m*M* calcium chloride (pH 8.3) (final volume 400 μl) and digestion was performed for 6 h at 37°C. The reaction was stopped by addition of 2% (final concentration) TFA. Samples were kept at −20°C until analysed by reversed-phase HPLC.

V8 protease digestion. To recombinant p18 and p18LM (100 μg each), 20 μg of *S. aureus* V8 protease (Boehringer) were added in 50 m*M* sodium phosphate (pH 7.8) (final volume 500 μl) and digestion was performed for 24 h at 37°C. The reaction was stopped by addition of 4% (final concentration) acetic acid. Samples were kept at −20°C until analysed by reversed-phase HPLC.

Analytical reversed-phase high-performance liquid chromatography

Analytical reversed-phase HPLC was performed at room temperature on a Hewlett-Packard ChemStation 1090 M liquid chromatograph (500-μl sample loop) with a photodiode-array detector, connected to a Model 9000/300 computer with monitor, a Model 9122 disk drive unit, a ThinkJet and a ColorPro plotter. For editing of chromatograms Operating Software, Revision 4.05, was used (Hewlett-Packard, Avondale, PA, U.S.A.).

System 1. The chromatographic unit consisted of a Nucleosil (C_4) HPLC column (4000 Å, 7 μm, 150 mm × 4.6 mm I.D.; Macherey, Nagel & Co., Düren, F.R.G.). Separation of purified proteins was performed using the following gradient (flow-rate, 0.6 ml/min): 90% eluent RP1-A (0.1% TFA in Milli-Q water) at 0 min, 10–90% eluent RP1-B [0.1% TFA in acetonitrile–Milli-Q water (70:30, v/v)] from 0 to 14 min, 90% RP1-B from 14 to 21 min, 90% RP1-B to 90% RP1-A from 21 to 24 min, 90% RP1-A from 24 to 30 min. The absorbance was measured at 205 and 280 nm. Fractions were collected manually. Samples for amino acid sequence analysis were dried in a Speedvac concentrator.

System 2. The chromatographic unit consisted of a Vydac 218TP54 (C_{18}) HPLC column (300 Å, 5 μm, 4.6 mm × 250 mm I.D.; Separation Group, Hesperia, CA, U.S.A.). Separation of peptides after proteolytic digestion was performed using the following gradient (flow-rate, 0.6 ml/min): 99% eluent RP1-A (see above) from 0 to 2 min, 1–100% eluent RP1-B (see above) from 2 to 22 min, 100% RP1-B from 22 to 26 min, 100% RP1-B to 99% RP1-A from 26 to 29 min, 99% RP1-A from 29 to 35 min. The absorbance was measured at 205 and 280 nm. Fractions were collected manually. Samples for amino acid sequence were prepared as described above.

System 3. The chromatographic unit was the same as in System 2. Separation of protein and peptides was achieved with the following gradient (flow-rate, 0.6 ml/min): 99% eluent RP3-A (0.1% HFBA in Milli-Q water) from 0 to 2 min, 1–80% eluent

RP3-B [0.1% HFBA in acetonitrile–1-propanol–Milli-Q water (60:30:10, v/v/v)] from 2 to 62 min, 80% RP3-B from 62 to 66 min, 80% RP3-B to 99% RP3-A from 66 to 69 min, 99% RP3-A from 69 to 75 min. The absorbance was measured at 205 and 280 nm. Fractions were collected manually. Samples for amino acid sequence analysis were prepared as described above.

Protein quantitation

Depending on the amount and purity of the protein, the following quantitation methods were used: a modified biuret method[10], the Bio-Rad kit (Bio-Rad Labs., Richmond, CA, U.S.A.), based on the method of Bradford[11], and integration of absorbance at 205 nm in reversed-phase HPLC (system 1; see above) with bovine RNAse and BSA as standards.

Sodium dodecyl sulphate polyacrylamide gel electrophoresis and Western blotting

SDS-PAGE was performed in 13% gels [acrylamide–bisacrylamide (37:1); gel dimensions, 0.75 mm thick × 13 cm wide × 7 cm long] according to the method of Laemmli with modifications as described in ref. 12. Molecular mass markers were from Amersham (Amersham), U.K.): lysozyme, 14.3 kDa; trypsin inhibitor, 21.5 kDa; carbonic anhydrase, 30 kDa; ovalbumin, 46 kDa; bovine serum albumin, 69 kDa, phosphorylase *b*, 92.5 kDa and myosin 200 kDa. Coomassie Brilliant Blue-stained gels were dried between Cellophane sheets on a Model 1125 slab gel dryer (Bio-Rad Labs.). The dried gels were scanned with a Model CS-930 dual-wavelength TLC scanner, connected to a Model DR-2 data recorder (Shimadzu, Kyoto, Japan).

Electrotransfer of proteins to nitrocellulose (0.45 μm, Schleicher & Schüll, Dassel, F.R.G.) was achieved according to ref. 13. After saturation with 1% BSA–0.01% Tween 20, the membrane was incubated with the monoclonal anti-p18 antibody described in ref. 14, excess of antibody was washed off and direct immunostaining was performed with anti-mouse Ig, horseradish peroxidase-linked $F(ab')_2$ fragment from sheep (Amersham) and 4-chloro-1-naphthol (Bio-Rad Labs.) as substrate.

Amino acid sequence and composition

Amino acid sequence analysis was performed on an Applied Biosystems (Foster City, CA, U.S.A.) Model 470A or 477A protein sequencer, connected to a Model 120A PTH-amino acid analyser.

After hydrolysis of protein with 6 *M* hydrochloric acid under nitrogen for 24 h at 106°C in a PicoTag Workstation (Waters), the amino acid composition analysis was performed on an Applied Biosystems Model 420A derivatizer connected to a Model 130A separation system. To obtain a best fit for the composition data of p18LM, the sums of squared errors ($AA_{\text{theor.}} - AA_{\text{determ.}}$) were calculated for p18LM between 95 and 130 amino acids. A minimum was found for p18LM, corresponding to p18, missing 13 amino acids from the C-terminus.

Calculation of protein parameters by computer

Protein parameters, *i.e.*, molecular mass (M_c), isoelectric point (pI_c) and Hopp index of antigenicity, were calculated on an IBM AT computer, using the DNA-star program (Computer Systems for Molecular Biology, Madison, WI, U.S.A.).

RESULTS AND DISCUSSION

Extraction of *E. coli* cells (TGE901 pTG-2153-HIV-1) showed that recombinant p18 is a soluble protein and that it can be separated from cell fragments and aggregated proteins by collecting the supernatants of repetitive freezing–thawing cycles. Fig. 1 shows the SDS-PAGE analysis of successive homogenates (H1, H2 and H3) and the corresponding supernatants (S1, S2 and S3). Recombinant p18 is found in the first and second supernatants, which were pooled and adjusted to pH 6.0. On leaving the pool in the cold overnight, we observed a protein precipitate, which did not contain recombinant p18 (Fig. 1, lane PP). The clarified pool was applied to a column of S Sepharose. A soft gel cation-exchange sorbent was chosen because protein continued to precipitate during sample application and the regeneration of Sepharose was considered to be easier than the regeneration of a closed HPLC column.

SDS-PAGE analysis of the non-adsorbed fraction (Fig. 1, lane 1) shows a protein band with about the same mobility as recombinant p18 (M_r 17.4 kDa). This protein is not identical with recombinant p18, as will be shown below (Fig. 8, lane C). Fractions which were step-eluted from S Sepharose at different salt concentrations are shown in Fig. 1, lanes 2–9. Recombinant p18 appears in the first and second protein peaks at 400 m*M* sodium chloride (lanes 6 and 7) and is completely eluted with 600 m*M* sodium chloride (lane 8). The fractions in lanes 7 and 8 were pooled (pool A); the fraction in lane 6 was kept separately (pool B).

After ultrafiltration of pools A and B, we observed a contaminant derived from

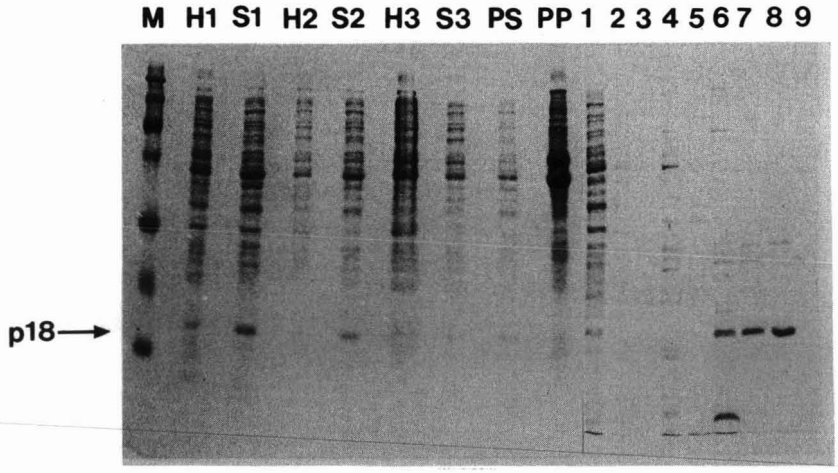

Fig. 1. Coomassie Brilliant Blue-stained SDS-polyacrylamide gel of recombinant p18 after extraction of protein from *E. coli* and after S Sepharose chromatography. M = molecular mass markers (see Experimental); H1 = *E. coli* cell suspension (first homogenate); S1 = first supernatant after freezing of *E. coli* cells; H2 = *E. coli* cell suspension (second homogenate); S2 = second supernatant after freezing of *E. coli* cells; H3 = *E. coli* cell suspension (third homogenate); S3 = third supernatant after freezing of *E. coli* cells; PS = pool of supernatants S1 and S2; PP = protein precipitate after adjusting PS to pH 6.0. Fractions 1–9 = S Sepharose chromatography: 1 = non-absorbed material; 2 and 3 = elution with half-concentrated PBS; 4 = PBS elution; 5 = 200 m*M* NaCl; 6 = 400 m*M* NaCl (first peak); 7 = 400 m*M* NaCl (second peak); 8 = 600 m*M* NaCl; 9 = 800 m*M* NaCl.

recombinant p18, namely p18LM, appearing with a lower molecular mass (15.1 kDA), as determined by SDS-PAGE. In different preparations of recombinant p18 we always found p18LM in the ultrafiltration step. For the following reasons we decided not to add protease inhibitors during this step; (1) purified recombinant p18 was to be used in animal experiments, and no potential health hazard to the animals could be tolerated; (2) as will be shown below, during cation-exchange HPLC recombinant p18 and p18LM could be separated; (3) the loss of *ca.* 13% C-terminally cleaved recombinant p18 (4.8 mg p18LM, Table I) was still considered tolerable; and (4) purified recombinant p18, stored in phosphate–sodium chloride buffer at −80°C, proved to be stable.

The concentrated pools A and B were separately chromatographed on a Sulfoethyl Aspartamide HPLC column. Fig. 2 shows the chromatographic separation of pool A. Elution of recombinant p18 was achieved with 32 m*M* sodium phosphate–635 m*M* sodium chloride and p18LM was eluted with 33 m*M* sodium phosphate–665 m*M* sodium chloride. The inset in Fig. 2 shows the SDS-PAGE analysis of the starting material (lane S) and of fractions A–L, as indicated in the chromatogram. Most of recombinant p18 is found in fractions E, F and G, whereas the majority of p18LM is eluted in fractions H and I. Pool B was analogously chromatographed. Fractions from both runs, containing either predominantly recombinant p18 or p18LM, were pooled separately and rechromatographed on the same column under identical conditions.

Table I summarizes the protein balance of recombinant p18 purification from *E. coli*. Scanning of Coomassie Brilliant Blue-stained SDS-polyacrylamide gels of the starting material (homogenate, *i.e.*, cell suspension before lysis of cells; see Experimental) and of purified recombinant p18 (Fig. 3, lane A) gives an estimate of about a 20% final yield. However, this value may be underestimated owing to the 17.4 kDa protein which co-migrates with recombinant p18 and which becomes visible in the S Sepharose flow-through (Fig. 1, lane 1), thus contributing to the scanned peak of recombinant p18 in the homogenate.

Purified recombinant p18 and p18LM were analysed by SDS-PAGE (Fig. 3) and

TABLE I

PROTEIN BALANCE OF RECOMBINANT p18 PURIFICATION FROM *E. COLI*

Analysed fraction[a]	*Total protein (mg)*	*Recovery of protein (%)*	*Purity (%)*[b]
Homogenate (*E. coli*, suspended in PBS)	7870	100.0	1.6
Pool of supernatants $S_1 + S_2$ after freezing–thawing	1440	18.3	6.2
Pool of supernatants before S Sepharose chromatography	367	4.7	N.D.
400 m*M* elution (1st peak)	16.2	0.21	23.0
400 m*M* elution (2nd peak)	13.9	0.18	67.3
600 m*M* elution	15.5	0.20	80.8
Purified recombinant p18	28.7	0.3	90.0
Purified p18LM	4.8	0.06	93.3

[a] For a detailed description, see Experimental.

[b] Coomassie Brilliant Blue-stained SDS-polyacrylamide gels were scanned, and the area corresponding to recombinant p18 (or p18LM) was expressed as a percentage of the total area scanned.

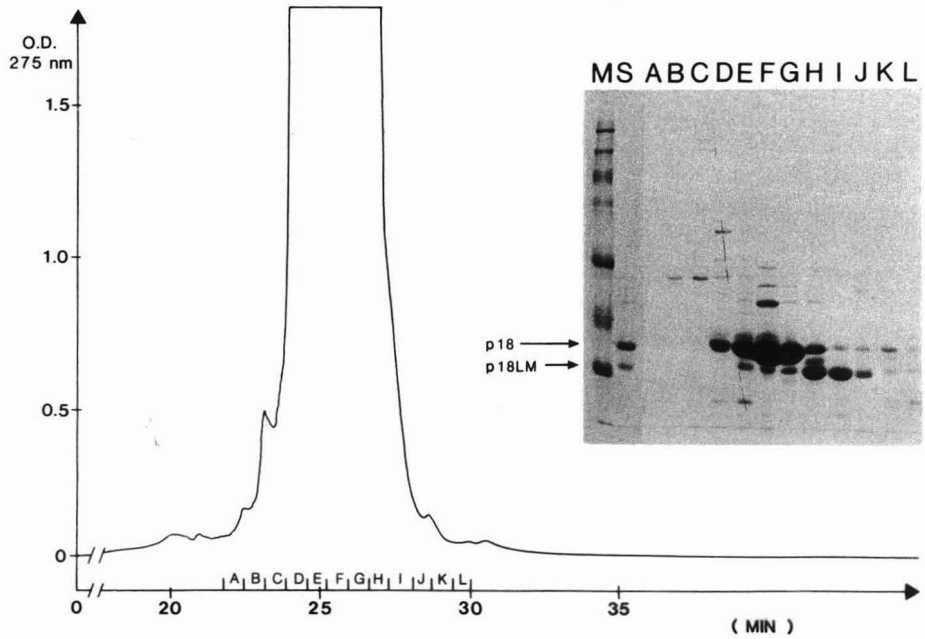

Fig. 2. Cation-exchange high-performance liquid chromatography of recombinant p18 and analysis of fractions by SDS-PAGE. Cation-exchange HPLC on Sulfoethyl Aspartamide was performed as described under Experimental. Protein (20 mg) was loaded in 40 ml of CatEx-A buffer. Inset: Coomassie Brilliant Blue-stained SDS-polyacrylamide gel, showing the analysis of fractions A–L. M = molecular mass markers (see Experimental). The positions of recombinant p18 and p18LM are indicated by arrows.

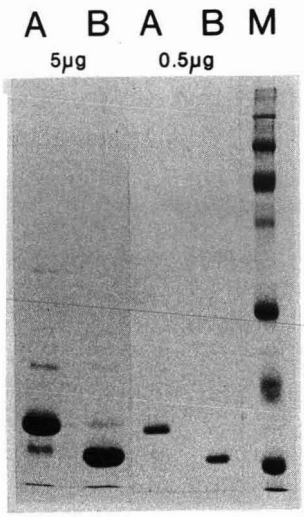

Fig. 3. Coomassie Brilliant Blue-stained SDS-polyacrylamide gel of purified recombinant p18 and p18LM at loadings of 5 and 0.5 μg per lane. A = Purified recombinant p18; B = purified p18LM; M = molecular mass markers (see Experimental).

showed purities of 90% and 93.3%, respectively. When the SDS-PAGE lanes were overloaded with 5 μg of protein per slot (width 2 mm), in addition to contamination of recombinant p18 with p18LM, and *vice versa*, faint protein bands of M_r 22.4 and 32.4 kDa could be detected (Fig. 3).

Analysis of purified recombinant p18 and p18LM by reversed-phase HPLC (Fig. 4) showed identical retention times for both proteins, despite the long gradient (system 3). Chromatography of a mixture of recombinant p18 and p18LM in system 3 showed no peak broadening but an increased peak height (not shown). The same result was obtained with reversed-phase system 1 (not shown), demonstrating the potential limitations of reversed-phase HPLC analysis of closely related proteins.

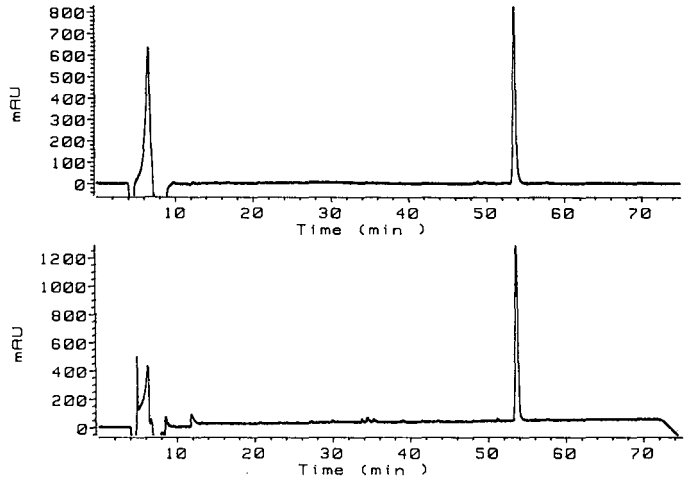

Fig. 4. Comparison of purified recombinant p18 and p18LM by reversed-phase HPLC in system 3, recorded at 205 nm. Upper panel, purified recombinant p18; lower panel, purified p18LM. Chromatograms are shown after baseline subtraction of a blank run. Retention times: recombinant p18, 53.644 min, p18LM, 53.687 min.

The same sequence (Gly–Ala–Arg) was obtained on N-terminal amino acid sequence determination of purified recombinant p18 and p18LM. Fig. 5 summarizes the amino acid sequence results obtained from tryptic and V8 proteolytic peptides of purified recombinant p18 and p18LM. The tryptic peptide of purified recombinant p18, eluted at a retention time of 19.4 min (Fig. 6, upper panel), represents the C-terminus of the protein (Table II) and is absent from the tryptic digest of p18LM (Fig. 6, lower panel). The same evidence of a missing C-terminus is obtained after V8 proteolysis: the peptide peak at retention time 11.8–12.2 min (Fig. 7, upper panel) of the recombinant p18 digest contains two successive C-terminal peptides (Table II), which are absent from the p18LM digest (Fig. 7, lower panel). The peptides eluted at retention time 16.1–16.6 min, displaying switched intensities of recombinant p18 and p18LM (Fig. 7, upper and lower panel), show an identical amino acid sequence. The different relative mobilities in reversed-phase HPLC may be due to differences in the oxidation state of Cys_{56} in recombinant p18 and p18LM. Table II identifies all sequenced peptides by their retention times in reversed-phase system 2 and/or system 3.

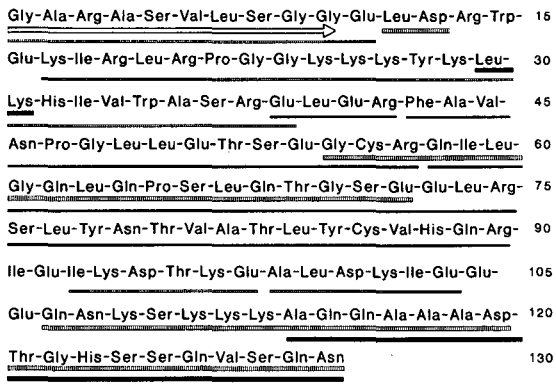

Fig. 5. Amino acid sequence of recombinant p18 and alignment of sequenced tryptic and V8 proteolytic peptides. Solid bars = tryptic peptides; hatched bars = V8 proteolytic peptides; thick bars = peptides obtained from recombinant p18 digests; thin bars = peptides obtained from p18LM; arrow = N-terminal amino acid sequence obtained from recombinant p18.

The amino acid composition of purified recombinant p18 and p18LM is shown in Table III. As identical N-termini were found for p18 and p18LM, we assumed that p18LM is a C-terminally cleaved form or a mixture of very similar C-terminally cleaved forms of p18, differing only in a few amino acids. We calculated for p18LM the sums of squared errors, comparing the theoretical amino acid composition of successive C-terminally cleaved molecules with the experimentally determined amino acid composition. A best fit was obtained for p18LM consisting of the first 117 amino acids (Gly_1–Ala_{117}) of recombinant p18. Calculation of the isoelectric point of this

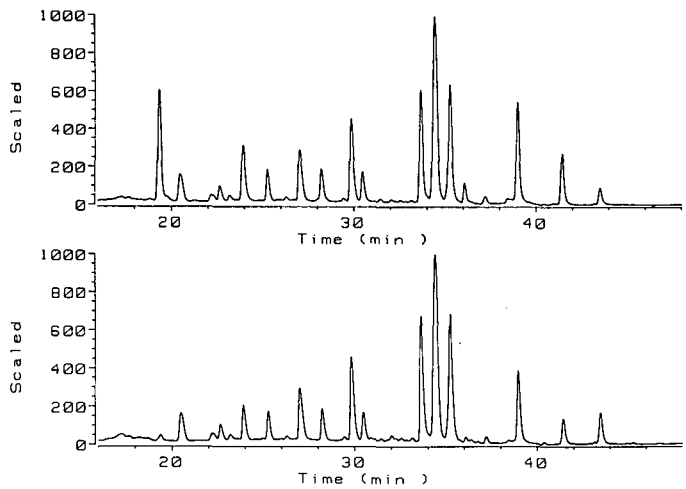

Fig. 6. Comparison of recombinant p18 and p18LM tryptic digests by reversed-phase HPLC in system 3, recorded at 205 nm. Upper panel, peptide map of recombinant p18; lower panel, peptide map of p18LM. Only the region containing peptide peaks is shown. To facilitate comparison, both chromatograms were normalized to the highest peak (value of 1000) at 34.4 min.

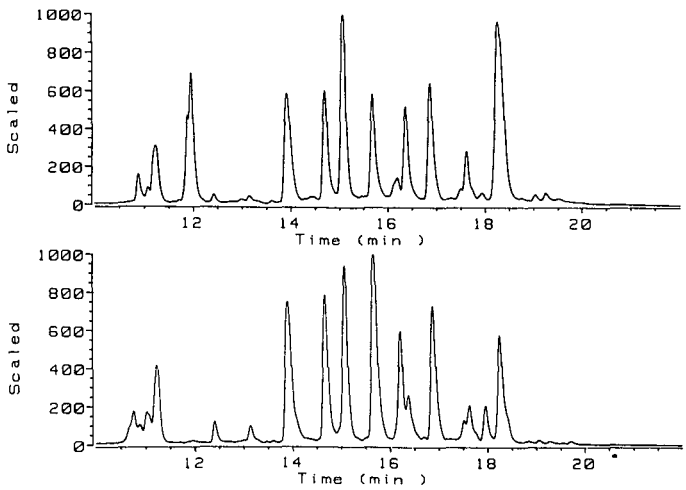

Fig. 7. Comparison of recombinant p18 and p18LM V8 protease digests by reversed-phase HPLC in systems 2, recorded at 205 nm. Upper panel, peptide map of recombinant p18; lower panel, peptide map of p18LM. Only the region containing peptide peaks is shown. To facilitate comparison, both chromatograms were normalized to the highest peak.

TABLE II

REVERSED-PHASE HPLC RETENTION TIMES OF TRYPTIC AND V8 PROTEOLYTIC PEPTIDES DERIVED FROM PURIFIED RECOMBINANT p18 AND p18LM

Peptide	*Retention time (min)*	
	System 2[a]	*System 3*[a]
Recombinant p18		
V8 protease: Leu_{12}–Asp_{13}	11.8–12.2	30.5
V8 protease: Gly_{55}–Glu_{72}	16.35	38.7
V8 protease: Gln_{107}–Asp_{120}	11.8–12.2	33.1
V8 protease: Thr_{121}–Asn_{130}	11.8–12.2	30.5
Trypsin: Leu_{30}–Lys_{31}	N.D.	36.2
Trypsin: Ala_{114}–Asn_{130}	N.D.	19.3
p18LM		
V8 protease: Gly_{1}–Glu_{11}	N.D.	28.7
V8 protease: Lys_{17}–Glu_{39}	N.D.	43.8
V8 protease: Gly_{55}–Glu_{72}	16.5	38.7
V8 protease: Ile_{93}–Glu_{98}	11.2	26.8
V8 protease: Ala_{99}–Glu_{104}	N.D.	28.7
Trypsin: Glu_{39}–Arg_{43}	N.D.	23.9
Trypsin: Phe_{43}–Arg_{57}	N.D.	34.4
Trypsin: Gln_{58}–Arg_{75}	N.D.	34.4
Trypsin: Ser_{76}–Arg_{90}	N.D.	43.4

[a] V8 proteolytic peptide separation of purified recombinant p18 and p18LM in system 2 is shown in Fig. 7. Tryptic peptide separation of purified recombinant p18 and p18LM in system 3 is shown in Fig. 6.

TABLE III

AMINO ACID COMPOSITION OF RECOMBINANT p18 AND p18LM

Amino acid	*Recombinant p18*	*p18LM*
Asp + Asn	8.0 (8)[a]	6.0 (6)[b]
Glu + Gln	24.8 (23)	21.8 (21)
Ser	10,4 (11)	8.1 (8)
Gly	9.9 (10)	9.7 (9)
His	3.0 (3)	2.0 (2)
Arg	10.4 (9)	10.1 (9)
Thr	6.0 (6)	5.2 (5)
Ala	10.1 (10)	8.8 (8)
Pro	3.0 (3)	3.1 (3)
Tyr	2.9 (3)	2.9 (3)
Val	5.4 (6)	4.4 (5)
Met	0.1 (0)	0.0 (0)
Cys	1.2 (2)	0.8 (2)
Ile	5.1 (6)	4.9 (6)
Leu	13.5 (14)	13.3 (14)
Phe	1.2 (1)	1.2 (1)
Lys	13.2 (13)	12.7 (13)
Trp	N.D. (2)	N.D. (2)
Total	130	117

[a] Values in parentheses correspond to the actual number of amino acids in recombinant p18.

[b] Values in parentheses correspond to the "best-fit" number of amino acids, as determined for p18LM (see Experimental).

protein gives a value of $pI_c = 9.47$, which is slightly more basic than the value of $pI_c = 9.23$ calculated for a complete recombinant p18. This finding correlates well with the fact that p18LM is eluted at higher salt concentrations than recombinant p18 from the Sulfoethyl Aspartamide HPLC column (Fig. 2).

Fig. 8 shows the immunostain (II) of purified recombinant p18 and p18LM obtained with a monoclonal antibody which was selected for binding to natural p18 after a mouse had been injected with whole HIV-1[14]. Recombinant p18 is recognized in *E. coli* homogenate (Fig. 8II, lane E), in supernatant after freezing–thawing cycles (Fig. 8II, lane D), and as the purified protein (Fig. 8II, lane B).

No immunostain was detected in *E. coli* wild-type homogenate (Fig. 8II, lane F) or in the non-adsorbed fraction of S Sepharose (Fig. 8II, lane C), thus showing that the 17.4-kDa protein in this fraction (visible in the Coomassie Brilliant Blue-stained SDS-polyacrylamide gel, Fig. 8I) is not identical with recombinant p18.

In spite of the missing C-terminus, p18LM still contains the epitope(s) which is/are recognized by the monoclonal antibody, as is shown by the immunostain (Fig. 8II, lane A). The calculated Hopp index for antigenicity shows a maximum for Glu_{104}–Lys_{112}. an amino acid sequence which, according to our analysis (amino acid composition, pI_c), is present in p18LM.

We have isolated recombinant p18 from *E. coli* in an overall yield of *ca.* 20% and a final purity of 90% as determined by SDS-PAGE and >95% as determined by reversed-phase HPLC. Owing to the absence of a post-translational myristylation

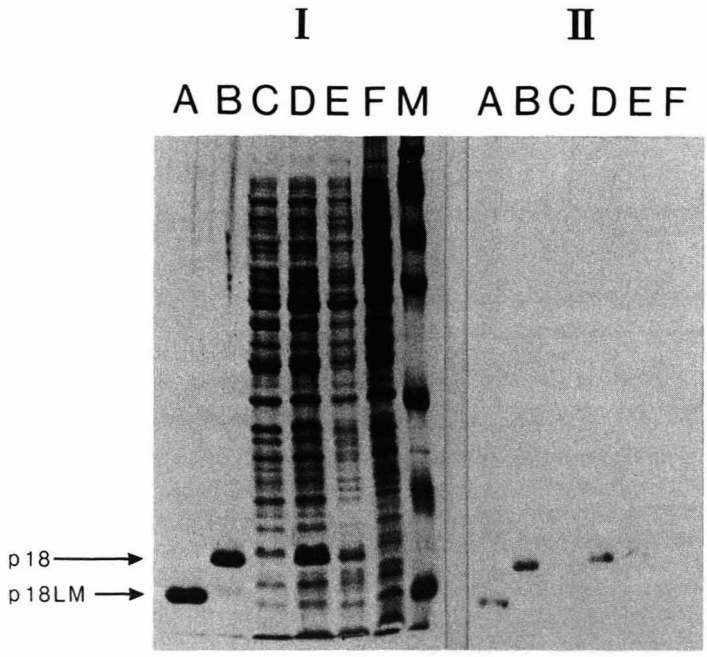

Fig. 8. Comparison of Coomassie Brilliant Blue-stained SDS-polyacrylamide gel (I) and immunostain after Western blotting (II). A = Purified p18LM; B = purified recombinant p18; C = S Sepharose flow-through; D = supernatant after freezing–thawing cycles; E = *E. coli* homogenate; F = *E. coli* wild-type homogenate; M = molecular mass markers (see Experimental).

pathway in *E. coli*, the protein lacks the myristic acid at the N-terminal glycine. As the codon UAC in position 611–613 of the *gag* gene[1] was point-mutated to generate a UAG stop codon, the C-terminal tyrosine of natural p18 is missing from recombinant p18. This was confirmed by amino acid sequence analysis (Fig. 5, Table II).

A monoclonal antibody, which had been generated against natural p18 from HIV-1, recognized purified recombinant p18, thus making the protein appear suitable for preliminary tests for diagnostic and immunological applications.

ACKNOWLEDGEMENTS

We thank J. C. Gluckman for a generous gift of anti-p18 monoclonal antibody, F. Daul for the photographic work and F. Vernon for the bibliography. This work was supported by Pasteur Vaccins and Diagnostics Pasteur.

REFERENCES

1 S. Wain-Hobson, P. Sonigo, O. Danos, S. Cole and M. Alizon, *Cell*, 46 (1986) 63.
2 M. G. Sarngadharan, F. D. Veronese, S. Oroszlan, S. Arya and R. C. Gallo, *Acquired Immunodeficiency Syndrome*, Elsevier, Paris, 1987, p. 43.
3 H. R. Gelderblom, E. H. S. Hausmann, M. Ozel, G. Pauli and M. A. Koch, *Virology*, 156 (1987) 171.
4 G. Schmidt, K. Amiraian, H. Frey, R. W. Stevens and D. S. Berns, *J. Clin. Microbiol.*, 25 (1987) 1993.

5 D. S. Burke, R. R. Redfield, P. Putman and S. S. Alexander. *J. Clin. Microbiol.*, 25 (1987) 81.
6 R. L. Shoeman, D. Young, R. Pottathil, J. Victor, R. R. Conroy, R. M. Crowl, T. Coleman, E. Heimer, C. Y. Lai, K. Ganguly, E. P. Reddy, A. M. Skalka, P. R. Pine, F. R. Kahn and H. Weissbach, *Anal. Biochem.*, 161 (1987) 370.
7 P. H. Naylor, C. W. Naylor, M. Badamchian, S. Wada, A. L. Goldstein, S. S. Wang, D. K. Sun, A. H. Thornton and P. S. Sarin, *Proc. Natl. Acad. Sci. U.S.A*, 84 (1987) 2951.
8 P. S. Sarin, D. K. Sun, A. H. Thornton, P. H. Naylor and A. L. Goldstein, *Science (Washington, D.C.)*, 232 (1986) 1135.
9 G. Rautmann, M.-P. Kieny, R. Brandely, K. Dott, M. Girard, L. Montagnier and J.-P. Lecocq, *Aids Research and Human Retroviruses*, (1989) in press.
10 B. Kadenbach, *Biochem. Z.*, 344 (1966) 49.
11 M. Bradford, *Anal. Biochem.*, 72 (1976) 248.
12 H. V. J. Kolbe, D. Costello, A. Wong, R. C. Lu and H. Wohlrab, *J. Biol. Chem.*, 259 (1984) 9115.
13 H. Towbin, T. Staehelin and J. Gordon, *Proc. Natl. Acad. Sci. U.S.A.*, 76 (1979) 4350.
14 J. Chassagne, P. Verrelle, C. Dionet, F. Clavel, F. Barre Sinoussi, J. C. Chermann, L. Montagnier, J. C. Gluckman and D. Klatzmann, *J. Immunol.*, 136 (1986) 1442.

Journal of Chromatography, 476 (1989) 113–123
Elsevier Science Publishers B.V., Amsterdam — Printed in The Netherlands

CHROMSYMP. 1598

HIGH-PERFORMANCE LIQUID CHROMATOGRAPHY OF AMINO ACIDS, PEPTIDES AND PROTEINS

XC[a]. INVESTIGATIONS INTO THE RELATIONSHIP BETWEEN STRUCTURE AND REVERSED-PHASE HIGH-PERFORMANCE LIQUID CHROMATOGRAPHY RETENTION BEHAVIOUR OF PEPTIDES RELATED TO HUMAN GROWTH HORMONE

A. W. PURCELL, M. I. AGUILAR and M. T. W. HEARN*
Department of Biochemistry, Monash University, Clayton, Victoria 3168 (Australia)

SUMMARY

The gradient elution behaviour of eight synthetic peptides encompassing residues [6–13] of human growth hormone, *i.e.* Leu[1]-Ser-Arg-Leu-Phe-Asp-Asn-Ala[8], has been investigated, by using an octadecylsilica, a butylsilica, and a polymeric fluorocarbon as stationary phases. Quantitative expressions, derived from the linear-solvent-strength theory and the general plate-height theory, were used to assess the influence of gradient time on the relative retention and bandwidths of these peptides. It was demonstrated that the chromatographic properties of the cyclised imide form involving Asp[6] are consistent with the formation of a highly stabilised amphipathic helix, while the open-chain α- and β-rearranged forms eluted as less rigid structures. The putative hydrophobic contact region consists of two leucine residues and one phenylalanine residue. From an analysis of the retention and bandwidth data obtained at pH 9, a surface-induced molecular reorientation of the β-linked peptides was observed, in which the repulsion of the aspartyl carboxyl group from the hydrophobic stationary phase directs the C-terminal moiety away from the sorbent surface. Furthermore, the fluorocarbon sorbent exhibited characteristics favourable for use in preparative purification of these peptides. The present results demonstrate the sensitivity of reversed-phase high-performance liquid chromatography (RP-HPLC) to monitor small changes in the interactive behaviour of peptides with hydrocarbonaceous ligands and aquo-organic solvent combinations in reversed-phase systems. These observations further illustrate the general utility of HPLC for investigating the conformational behaviour of peptides at solid–liquid interfaces.

[a] For Part LXXXIX see ref. 20.

0021-9673/89/$03.50

INTRODUCTION

Human growth hormone (hGH) is a member of the somatotropic family of structurally conserved pituitary and placental proteins, important for the regulation of growth and lactogenesis in mammals. Typically, these proteins contain *ca.* 190 amino acid residues with molecular weights of *ca.* 22 000. GHs exhibit several important physiological properties including the well-established growth-promoting activity, as well as significant effects on protein, lipid and carbohydrate metabolism. Numerous studies have been directed towards elucidating the relationship between the chemical structure and biological activity or immunoactivity of hGH[1,2]. In addition to the classical somatotropic and lactogenic activities of hGH, structure–function correlations have also been carried out by examining the biological activity of enzymatically and chemically modified derivatives, and by determining the relative affinities of hGH and its derivatives in radioimmuno assays and radioreceptor assays. Following the early report[3] that hGH, partially digested with chymotrypsin, retained significant somatotropic activity, considerable effort has been directed towards identifying a small fragment of hGH which retained potent biological activity[4,5]. To date this approach has been unsuccessful in segregating the somatotropic or lactogenic activities within the sequential structure of the protein. However, recent studies[6] on the hypoglycaemic and hyperglycaemic activities of hGH have identified an eight-residue segment at the amino terminus (residues [6–13]), which retains significant biological activity in terms of its insulin-potentiating properties. This sequence segment is located at the beginning of the first α-helical region (helix 1) of the protein, as predicted from our secondary-structure analysis[7] and confirmed by comparison with the recently reported X-ray structure of porcine GH[8]. Furthermore, it was found[9] that the cyclisation of the aspartyl residue at position 11 in the hGH sequence to give the imide derivative, is important for this biological activity. Two-dimensional NMR (COSY and NOESY) studies[9] of synthetic analogues to the peptide [6–13] have revealed that in solution the first five residues exist as an amphipathic helical structure which is then stabilised by the imide function.

The differences in the biological activity of the imide and the open chain α- and β-rearranged forms is related to the differences in molecular charge and conformation at the receptor surface[9]. Reversed-phase high-performance liquid chromatography (RP-HPLC) has been utilised in this laboratory as a physicochemical tool for the study of peptide behaviour at hydrophobic liquid–solid interfaces which mimic biological lipid bilayers. In particular, correlation of changes in retention and bandwidth behaviour over a range of chromatographic conditions with differences in primary and secondary structure has enabled us in earlier investigations to identify and characterise both the hydrophobic interaction sites and the existence of conformational equilibria with, for example, β-endorphin[10,11], luteinizing hormone-releasing hormone (LHRH)[12] and myosin kinase analogues[13]. The present paper provides a detailed analysis of the gradient elution behaviour of a set of eight peptides related to residues [6–13] of hGH. In particular, the retention and bandwidth behaviour under different pH values of the mobile phase and with different stationary phases has been analysed in terms of the relationship between molecular structure, hydrophobic contact area, and the predicted surface accessibility of the constituent amino acids. This approach also provides further insight into the important role that RP-HPLC data can play in

the design of peptide analogues of naturally occurring, biologically significant peptide hormones.

MATERIALS AND METHODS

Apparatus

All chromatographic measurements were performed with a Du Pont 8800 liquid chromatograph (Du Pont, Wilmington, DE, U.S.A.), coupled to a Valco 6-port HPLC injector (Valco, Houston, TX, U.S.A.) and a Waters M450 variable-wavelength UV detector (Waters Assoc., Milford, MA, U.S.A.). All measurements were routinely monitored at 215 nm and recorded with a Spectra-Physics SP4100 computing integrator (Spectra-Physics, San Jose, CA, U.S.A.). Reversed-phase chromatography was carried out with a Bakerbond widepore octadecylsilica and butylsilica stationary phase (J. T. Baker, Phillipsburg, NJ, U.S.A.), both with a nominal particle diameter of 5 μm and average pore size of 30 nm, packed into 25 × 0.46 cm I.D. columns, and a Du Pont Bio Series Poly F proprietary polymeric fluorocarbon HPLC packing with a 20-μm particle size and 30-nm pore size, packed into a 8 × 0.62 cm I.D. column. All injections were made with SGE (Melbourne, Australia) syringes, and pH measurements were performed with an Orion Model SA520 pH meter (Orion, Cambridge, MA, U.S.A.).

Chemicals and reagents

Acetonitrile (HPLC grade) was obtained from Mallinckrodt (Paris, KY, U.S.A.), trifluoroacetic acid (TFA) was obtained from Pierce (Rockford, IL, U.S.A.), and ammonium hydrogen carbonate (Bicarb; AnalaR) was obtained from BDH (Poole, U.K.). Water was distilled and deionised in a Milli-Q system (Millipore, Bedford, MA, U.S.A.). The peptide analogues were synthesised by established F-moc procedures and purified by RP-HPLC, by using semi-preparative TSK C_{18} columns (250 × 10 mm) eluted with a gradient of 0–65% water in acetonitrile containing 0.1% TFA of 30 min duration and flow-rate of 2 ml/min. Purity , as assessed by amino acid compositional analysis, two-dimensional paper electrophoresis, fast atom bombardment mass spectrometry (FAB-MS) and multidimensional RP-HPLC, for the synthetic peptides was >95%.

Chromatographic procedures

Bulk solvents and mobile phases were filtered and degassed under vacuum. Linear gradient elution was carried out with 0.1% TFA in water (eluent A) and 0.1% TFA in 50% aqueous acetonitrile (eluent B) over gradient times varying between 15 and 90 min. The influence of basic conditions on peptide retention was studied by using a linear gradient from 25 m*M* Bicarb in water (eluent C) and 35 m*M* Bicarb in 50% aqueous acetonitrile (eluent D). Peptide solutions were prepared by dissolving the peptides in the appropriate eluent (A or C) at a concentration of 1 mg/ml, and sample sizes varied between 5 and 20 μg. The column dead-time was taken as the retention time for sodium nitrate. The various chromatographic parameters used in the analysis of peptide retention and bandwidth behaviour were calculated using the Pek-n-ese program, written in BASIC language for a Hewlett-Packard HP86B computer, as previously described[10,11]. Iterative regression analyses were performed by statistical

packages on a Monash University Computer Centre VAX11780 mini-computer system.

RESULTS AND DISCUSSION

Retention and bandwidth relationships

Expressions based on the linear-solvent-strength (LSS) gradient model have provided a useful approach for investigating the intimate relationship between the chromatographic behaviour of peptides and proteins and their primary, secondary, and tertiary structures. A detailed description of the application of the LSS theory to peptide separations in RP-HPLC has been outlined previously[10,14]. Briefly, the retention time, t_g, for a peptide, separated under ideal LSS conditions, can be used to determine the gradient steepness parameter, b, through the expression

$$b = t_0 \log \beta/[t_{g1} - (t_{g2}/\beta) + t_0 (t_{G1} - t_{G2})/t_{G2}] \quad (1)$$

where t_{g1} and t_{g2} are the solute gradient retention times at gradient times t_{G1} and t_{G2}, respectively, β is the ratio of the gradient times (t_{G2}/t_{G1}), and t_0 is the column dead-time. Evaluation of b values from retention data then allows the calculation of the median capacity factor, $\bar{k}$, and the corresponding organic mole fraction, $\bar{\psi}$, according to the relationships

$$\bar{k} = 1/1.15\, b \quad (2)$$

$$\bar{\psi} = [t_{g1} - t_0 - (t_0/b) \log 2]/(t_G/\Delta\psi) \quad (3)$$

Under regular reversed-phase conditions, $\bar{k}$ and $\bar{\psi}$ can be empirically related through the expression

$$\log \bar{k} = \log k_0 - S\bar{\psi} \quad (4)$$

The S and $\log k_0$ values can then be obtained by linear regression analysis of plots of $\log \bar{k}$ *versus* $\bar{\psi}$. The value of the parameter S in RP-HPLC is related to the magnitude of the hydrophobic contact area and the number of interaction sites, established between the solute and the stationary phase ligands during the adsorption process. Furthermore, the magnitude of the $\log k_0$ value is a measure of the free-energy changes associated with the binding of the solute to the stationary phase in the absence of the organic modifier. The determination of these parameters for a range of closely related peptides under a range of chromatographic conditions therefore provides the basis for quantitative characterisation of peptide orientation at the stationary phase surface.

Further characterisation of the interactive properties of peptides at hydrophobic surfaces can be carried out through the analysis of bandwidth dependencies. The relationship between the bandwidth, σ_v, and $\bar{k}$ for linear solvent systems can be expressed, according to the general plate-height theory, by

$$\sigma_{v,calc} = [\bar{k}/2) + 1]GV_m N^{-0.5} \quad (5)$$

where G is the band-compression factor, which arises from the increase in solvent strength across the solute zone as the gradient develops along the column, and N is the plate number. The derivation of eqn. 5 is based on the assumption that the shape of the peptide solute of a defined molecular weight can be characterised in terms of a constant hydrodynamic shape throughout the chromatographic separation. Under ideal conditions, the normalised ratio of the experimentally observed bandwidths to the calculated bandwidths ($\sigma_{v,exp}/\sigma_{v,calc}$) should approach unity over the normal operational range of $\bar{k}$ values. However, slow, time-dependent solvent- or stationary-phase-induced changes in the secondary or tertiary structure of the peptide solute will lead to significant alterations in surface topography or molecular dimensions of the peptide. This behaviour results in changes in the diffusional or interactive properties of the solute, such that experimentally observed peak widths will be significantly different from those predicted by eqn. 5.

As part of further investigations on the relationship between peptide structure and retention behaviour in RP-HPLC, gradient elution data were collected for a series of eight synthetic peptides, related to the N-terminal region (Leu^6–Ala^{13}) of hGH, with the view to provide further supportive information on the secondary and tertiary structure of these peptides, both in solution and at a hydrophobic surface.

Dependence of peptide retention and bandwidth on the stationary phase ligand

Based on extensive *in vitro* and *in vivo* biological evaluation of families of synthetic peptides related to hGH residues [6–13][9], a set of peptide analogues with known biological activities was selected for these investigations. The amino acid sequences of these peptides are listed in Table I, and are related to the linear peptide corresponding to residues [6–13] of hGH, *i.e.* Leu^1-Ser-Arg-Leu-Phe-Asp-Asn-Ala^8. The peptide analogues contain substitutions $Asp^6 \rightarrow Glu^6$, addition of a C-terminal Gly, replacement of the L-amino acid at position Leu^4 by the D-isomer or deletion of the amino-terminal Leu-Ser-Arg residues. The peptides are also characterised by the configuration of the side chain at position Asp^6, which exists as the naturally occurring

TABLE I

SEQUENCE, S, AND LOG k_0 VALUES FOR PEPTIDES USED IN THIS STUDY

Abbreviations for amino acids were as follows: A = Ala = alanine, D = Asp = aspartic acid, E = Glu = glutamic acid, F = Phe = phenylalanine, G = Gly = glycine, L = Leu = leucine, R = Arg = arginine, S = Ser = serine.

Peptide No.	*Sequence*	*Link*	*C_{18}/0.1% TFA*		*C_4/0.1% TFA*		*Poly-F/0.1% TFA*		*C_{18}/Bicarb*	
			S	*Log k_0*	*S*	*Log k_0*	*S*	*Log k_0*	*S*	*Log k_0*
1	LSRLFDNA	β	13.1	2.3	12.8	1.8	9.2	1.6	10.1	2.5
2	LSRLFDNA	imide	7.2	3.6	7.8	3.5	8.8	3.7	6.3	3.0
3	LSRLFENAG	β	12.0	2.1	13.1	1.9	8.1	1.5	8.1	2.1
4	LSRLFENAG	α	11.4	3.0	11.1	2.5	7.6	1.9	–	–
5	LSRL[a]FDNA	imide	8.2	4.0	7.3	3.2	7.1	3.1	7.4	3.7
6	LFDNAG	α	11.2	1.8	12.7	1.4	8.7	1.3	13.0	2.5
7	LSRLFDN-G	β	12.8	1.7	10.6	1.0	10.5	1.1	8.3	1.8
8	LSRLFENAG	β	12.8	1.9	13.0	1.5	8.2	1.2	9.5	1.8

[a] D-amino acid.

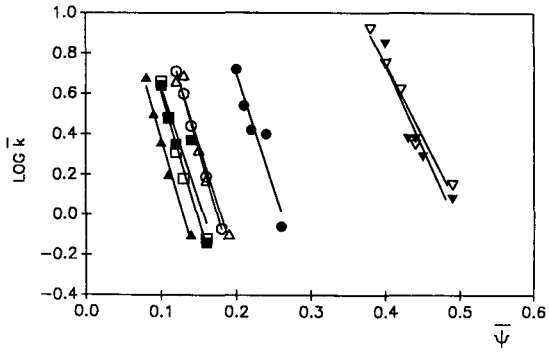

Fig. 1. Plots of log $\bar{k}$ *versus* $\bar{\psi}$ for hGH-related peptides **1–8**, separated on the C_{18} column at pH 2. The plots were derived from linear regression analysis of the data points (r^2 = 0.95–0.99), where t_G = 15, 30, 45, 60, and 90 min, and the flow-rate = 1 ml/min. See Table I for the derived S and log k_0 values and the Material and Methods section for other experimental details. Peptides: (○), **1**; (▽), **2**; (△), **3**; (●), **4**; (▼), **5**; (■), **6**; (▲), **7**; (□), **8**.

α-linkage, the cyclised imide form, or the β-linked peptide, which represents the alternative product obtained from imide cyclisation and subsequent hydrolysis. Peptides **1–8** were chromatographed, in the first instance, on a widepore octadecylsilica (C_{18}), by using a linear gradient from 0.1% TFA in water to 0.1% TFA in 50% aqueous acetonitrile. Chromatographic data were accumulated for t_G = 15, 30, 45, 60, and 90 min at a fixed flow-rate of 1 ml/min.

Fig. 1 represents plots of log $\bar{k}$ *versus* $\bar{\psi}$ for the GH peptide analogues separated on the C_{18} column, and shows that essentially linear dependencies of log $\bar{k}$ *versus* $\bar{\psi}$ were observed, with correlation coefficients for linear regression between 0.95 and 0.99. The corresponding S and log k_0 values are also listed in Table I. Even with this set of closely related peptides, in which the amino acid compositions vary only slightly, it can be seen that selectivity changes occur over the range of experimental conditions used. The dependence of peptide retention on eluotropic strength in RP-HPLC can be categorised[15] on the basis of the relative S and log k_0 values. Thus, while large log k_0 values will be observed for hydrophobic peptides and lower values for polar peptides, both classes of solutes can exhibit a range of S values. The present results therefore represent examples that are consistent with our earlier conclusions[15] on structure–retention relationships for peptides in RP-HPLC as manifested by the log k' *versus* ψ dependencies. In particular, the imide-containing analogues exhibited higher log k_0 values than the α- and β-peptide structures. On superficial inspection, based solely on the linear amino acid sequence without consideration of the hierarchical structure of the peptides, it could be concluded that cyclisation of the β-carboxyl group of the aspartyl residue to form the imide, results in decreased molecular polarity and would be expected to result in increased retention. However, as is evident from Table I, the S values for the imides (*e.g.* peptides **2** and **5**) were significantly smaller than those for the corresponding α- and β-forms. This suggests that the hydrophobic contact area is much smaller for the imides than for the open-chain peptides. The chromatographic results for these peptides are fully consistent with the formation of an amphipathic helix, as depicted in Fig. 2 for the naturally occurring sequence of [6–13] in hGH. This

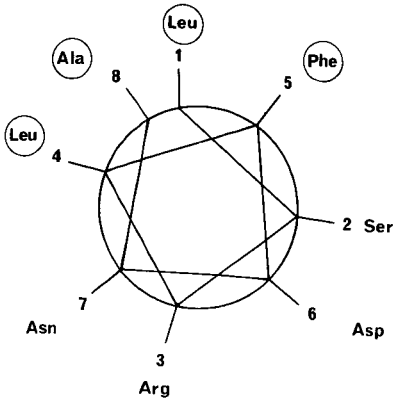

Fig. 2. Representation of the naturally occurring sequence of residues 6–13 of hGH on an Edmundson helical wheel.

helical structure results in the clustering of the hydrophobic residues Leu[1], Leu[4], Phe[5], and Ala[8] on one face of the helix of the open-chain peptide. This portion of the molecule would clearly represent the dominant interactive area in a reversed-phase system and would result in a high affinity for the hydrophobic ligands. The presence of a helical structure in solution has also been confirmed for the imide by two-dimensional NMR[9]. However, the formation of the imide bond between Asp[6] and Asn[7] inhibits extension of the helical structure through to the carboxy-terminal residues in the sequence and directs the Ala[8] residue away from the hydrophobic region of the peptide surface. The hydrophobic contact area of the imide peptides will therefore be diminished, as evidenced by lower S values. Therefore, the differences in the log k_0 values between the imides and the open chain peptides cannot be attributed to the relative polarity of the imide *versus* the aspartyl carboxyl group. Rather, two-dimensional NMR analysis[9] has revealed that the imide exerts an electron-polarising effect on the adjacent phenylalanine residue, thereby influencing the hydrophobicity of the interactive region of the peptide surface. Such constrained alignment of the hydrophobic residues on one face of the molecule clearly has important consequences as far as biological activity is concerned[9], *i.e.* the imide form of the peptide exhibits full activity in the glucose utilisation assay, whilst the α- and β-forms either lack activity or have very low activity. Generally, the β-peptides, which contain an additional methylene carbon in the peptide backbone, exhibited higher S values than the α-analogues but similar log k_0 values. Thus, it appears that the extra carbon atom has either been incorporated into the hydrophobic contact area or has caused a shift in the spatial disposition of the hydrophobic residues. The substitution of L-leucine for D-leucine (peptides **2** and **5**) did not result in any significant changes in the S and log k_0 values with this stationary phase. This suggests that the relative orientation of Leu[4] in the helical imide structure does not alter the interactive properties of the peptide. Furthermore, the substitution of Gly for Ala at position 8 (peptides **1** and **7**) resulted in a decreased log k_0, while the S value for these peptides was unaltered. This observation reflects the relative hydrophobicity of the two amino acids side chains and confirms the contribution of residue 8 to the retention process.

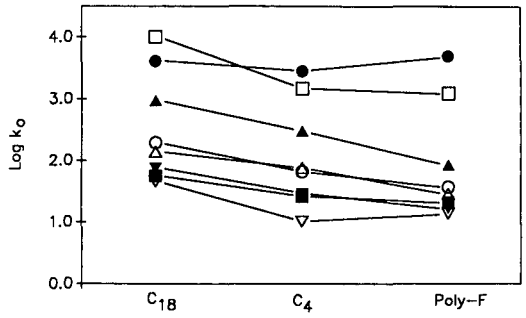

Fig. 3. Plot of log k_0 *versus* stationary phase ligand. See Table I for the log k_0 values. Peptides: (○), **1**; (●), **2**; (△), **3**; (▲), **4**; (□), **5**; (■), **6**; (▽), **7**; (▼), **8**.

There are several examples[16–18] where the presence of lipids have been found to enhance the formation and stability of amphipathic peptide helices in solution. Clearly, the nature of the hydrophobic C_{18} ligand may play a significant role in the equilibrium between the random coil and the helical structure of the GH-related analogues. Peptides **1–8** were therefore chromatographed on an *n*-butylsilica (C_4) stationary phase and a polymeric fluorocarbon (Poly F) packing material. The Poly F stationary phase is also a hydrophobic surface, yet it lacks the long carbon chains normally associated with reversed-phase packings. The log k_0 and S values obtained on both columns are listed in Table I and are also plotted against ligand type in Figs. 3 and 4. The log k_0 values for all peptides were lower on the C_4 than on the C_{18} column. However, while the S values for five of the peptides did not change significantly with the decrease in alkyl chain length, the S value on the C_4 phase increased for peptides **3** and **6** and decreased for peptide **7** relative to the results obtained on the octadecylsilica stationary phase. Hence, the different alkyl chain lengths change the way in which these three peptides interact with the surface. Previous studies[19] on the RP-HPLC of a group of peptides related to the paracelsins, separated on a series of sorbents with different alkyl chain lengths, revealed a discontinuity in the dependence of k' on the hydrophobic ligand carbon number when the chain length was C_4. It was postulated that the butyl chain existed as a more rigid unit than the longer chains and

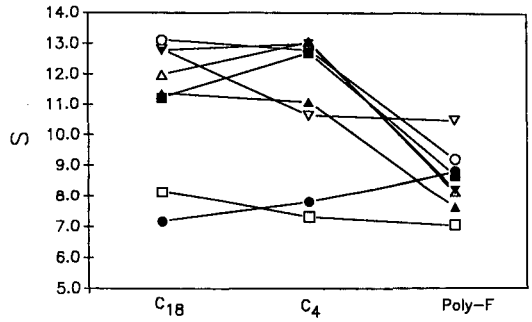

Fig. 4. Plot of log S *versus* stationary phase ligand. See Table I for the S values. Peptides: (○), **1**; (●), **2**; (△), **3**; (▲), **4**; (□), **5**; (■), **6**; (▽), **7**; (▼), **8**.

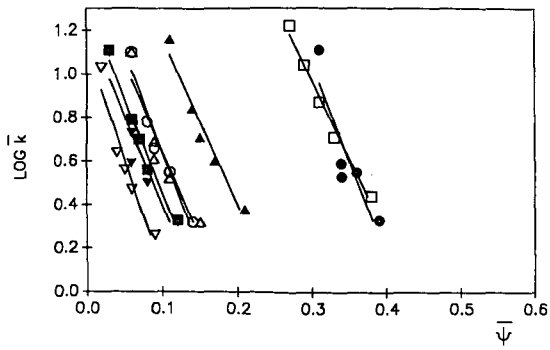

Fig. 5. Plots of log $\bar{k}$ *versus* $\bar{\psi}$ for peptides **1–8**, separated on the Poly F column at pH 2. See Fig. 1 for other experimental details. Peptides: (○), **1**; (●), **2**; (△), **3**; (▲), **4**; (□), **5**; (■), **6**; (▽), **7**; (▼), **8**.

induced some degree of preferred secondary structure in the peptide solutes. Clearly, a similar phenomenon could also be occurring with peptides **3**, **6** and **7**.

Plots of log $\bar{k}$ *versus* $\bar{\psi}$ for peptides **1–8**, separated on the Poly F column, are shown in Fig. 5. The S and log k_0 values for the imides (peptides **2** and **5**) when eluted from the octadecylsilica of Poly F sorbent essentially remained constant demonstrating that the interactive properties of these solutes with the Poly F sorbent are similar to that observed with the alkylsilica materials. Furthermore, these results indicate that the stability of the imide helix is unaffected by the presence or absence of alkyl chains bonded to the stationary phase surface. Conversely, both the S and log k_0 values for the α- and β-peptides decreased significantly with the Poly F column. These results indicate that a much smaller proportion of these peptides is involved in a weaker interaction with the fluorocarbon surface. The data also suggests that the interactive properties of the open-chain α-helix are strongly influenced by the physicochemical characteristics of the packing material, and further demonstrates the decreased conformational stability of these peptides relative to the imide-containing structures. These results are consequently consistent with the other observations and findings that the imide form of these peptides is fully constrained as a amphipathic helix whilst the α- and β-forms have significant flexibility in solution but can be induced to form a pseudo-helical conformation by an appropriate hydrophobic ligand.

The observed retention behaviour characterised by low S and log k_0 values for the Poly F column also represent properties suitable for the large-scale isolation of peptides and proteins. Under these conditions, lower amounts of organic solvent are required for elution and this, in the case of proteins, also minimises denaturation, reduces production costs, and increases the recovery of biological activity. While quantitative analysis by HPLC requires high peak capacity for all the components of interest, the preparative separation and recovery of pure compounds does not. In the present study, broader peak widths were generally observed on the Poly F phase than on the C_{18} material *e.g.* peak widths were approximately two-fold larger when comparable gradient conditions were employed. Under these circumstances, as long as the fraction collected between overlapping bands remains relatively small, peptides could be resolved to high purity. Thus, in addition to the increased pH stability of the stationary phase, the Poly F sorbent has significant potential for use in preparative HPLC.

Dependence of peptide retention and bandwidth on mobile phase pH

Two-dimensional NOESY NMR[9] of both the α- and imide forms of the peptide corresponding to residues [6–13] of hGH indicates that an ionic interaction occurs between Arg^3 and Asp^6 in the α-form and an ion–dipole interaction between the imide function and Arg^3 in the cyclised form. Inspection of a space-filling three-dimensional molecular model of the β-peptide reveals that for the ionic interaction to occur, a more strained configuration is required. As these interactions will be dependent on pH, the retention and bandwidth behaviour of peptides **1–8** at pH 2 (0.1% TFA) was compared with that at pH 9 (30 m*M* Bicarb) on the C_{18} stationary phase. The *S* and log k_0 values obtained are listed in Table I. The *S* and log k_0 values for the α-linked peptide **6** increased as the pH was increased. Thus, the ionisation of the aspartyl residue, which is located on the side of the helical structure directed away from the hydrophobic region, enhanced the affinity of the hydrophobic contact residues for the stationary phase ligands, presumably by bringing the Ala residue into closer proximity with the Leu and Phe residues. The most significant observation however, was a dramatic decrease in the *S* value for the β-linked peptides. Thus, as the peptide surface becomes more electrostatic due to potentially enhanced ion-bridging with the guanidinium group of the arginine residue or with the surrounding solvent, the COOH group effectively directs the C-terminal residues away from the stationary phase ligands, thereby reducing the interaction and decreasing the *S* value, *i.e.* the Ala^8 residue is no longer interacting with the hydrophobic stationary phase. This molecular reorientation at the surface appears to have relatively slow kinetics. Evaluation of the dependence of solute bandwidth on gradient steepness[11,12] for peptides **1–8** at pH 9 revealed that the bandwidth ratio for the β-peptides **1**, **3** and **7** were significantly higher with 30 m*M* Bicarb than with 0.1% TFA as the mobile phase, while the bandwidth ratio for the α- and imide peptides remained essentially constant.

The present study further demonstrates the utility of RP-HPLC for studying and characterising subtle changes in the interactive properties of biologically important peptides. Correlation of changes in the hydrophobic contact area and ligand affinity over a range of experimental conditions with differences in the amino acid sequence and composition has allowed the preferential orientational properties of these hGH-related peptides at hydrophobic surfaces to be studied. As documented elsewhere[9], the chromatographic properties of low *S* and high log k_0 values, which characterise the imide peptides, can be related to their biological potency as insulin-potentiating agents. The ability to correlate the influence of environmental and structural factors as monitored by chromatographic tools with the biological efficacy of peptides such as hGH residues [6–13] is thus expected to expand the utility of HPLC as a physicochemical technique in the design of peptide drugs and peptide derived vaccines.

ACKNOWLEDGEMENTS

The support of research grants to MTWH from the National Health and Medical Research Council of Australia, Australian Research Grants Committee and Monash University Special Research Fund is gratefully acknowledged. MIA is a recipient of a Monash University Postdoctoral Fellowship.

REFERENCES

1 C.S. Nicoll, G. L. Mayer and S. M. Russell, *Endocr. Rev.*, 7 (1986) 169.
2 M. Wallis, in B. Weinstein (Editor), *Chemistry and Biochemistry of Amino Acids, Peptides and Proteins. A Survey of Recent Developments*, Vol. 5, Marcel Dekker, New York, 1978, p. 213.
3 C. H. Li, *Fed. Proc., Fed. Am. Soc. Exp. Biol.*, 16 (1957) 775.
4 J. L. Kostyo, *Metabolism*, 23 (1974) 885.
5 J. L. Kostyo and A. E. Wilhelmi, *Metabolism*, 25 (1976) 105.
6 M. T. W. Hearn, F. M. Ng, M. F. O'Donoghue and I. M. Rae, *Patents PCT/AU*, 88/00421.
7 C. Turner, P. D. Cary, B. Grego, M. T. W. Hearn and G. E. Chapman, *Biochem. J.*, 213 (1983) 107.
8 S. S. Abdel-Meguid, H.-S. Shiel, W. W. Smith, H. E. Dayringer, B. N. Violand and L. A. Benthe, *Proc. Natl. Acad. Sci. U.S.A.*, 84 (1987) 6434.
9 M. F. O'Donoghue, M. T. W. Hearn and I. M. Rae, *Proc. 20th Eur. Pept. Symp. (Tubingen)*, 1989, in press.
10 M.-I. Aguilar, A. N. Hodder and M. T. W. Hearn, *J. Chromatogr.*, 327 (1985) 115.
11 M. T. W. Hearn and M. I. Aguilar, *J. Chromatogr.*, 352 (1986) 35.
12 M. T. W. Hearn and M. I. Aguilar, *J. Chromatogr.*, 359 (1986) 31.
13 M. T. W. Hearn and M. I. Aguilar, *J. Chromatogr.*, 392 (1987) 33.
14 L. R. Snyder, in Cs. Horváth (Editor), *High Performance Liquid Chromatography*, Vol. 1, Academic Press, New York, 1980, p. 208.
15 M. T. W. Hearn and M. I. Aguilar, in A. Neuberger and L. L. M. van Deenen (Editors), *Modern Physical Methods in Biochemistry*, Part B, Elsevier, Amsterdam, 1988, p. 113.
16 W. L. Mattice, J. M. Piser and D. S. Clark, *Biochemistry*, 15 (1976) 4264.
17 J. T. Yang, T. A. Bewley, G. C. Chen and C. H. Li, *Proc. Natl. Acad. Sci. U.S.A.*, 74 (1977) 3253.
18 J. B. Blanc and E. T. Kaiser, *J. Biol. Chem.*, 259 (1984) 9549.
19 K. D. Lork, K. K. Unger, H. Brückner and M. T. W. Hearn, *J. Chromatogr.*, 476 (1989) 135.
20 A. N. Hodder, M. I. Aguilar and M. T. W. Hearn, *J. Chromatogr.*, 476 (1989) 391.

Journal of Chromatography, 476 (1989) 125–133
Elsevier Science Publishers B.V., Amsterdam — Printed in The Netherlands

CHROMSYMP. 1580

HIGH-PERFORMANCE LIQUID CHROMATOGRAPHY OF AMINO ACIDS, PEPTIDES AND PROTEINS

XCI[a]. THE INFLUENCE OF TEMPERATURE ON THE CHROMATOGRAPHIC BEHAVIOUR OF PEPTIDES RELATED TO HUMAN GROWTH HORMONE

A. W. PURCELL, M. I. AGUILAR and M. T. W. HEARN*
Department of Biochemistry, Monash University, Clayton, Victoria 3168 (Australia)

SUMMARY

The influence of temperature on the gradient elution properties of synthetic peptides related to residues [6–13] of human growth hormone, *e.g.*, Leu[1]-Ser-Arg-Leu-Phe-Asp-Asn-Ala[8], has been studied by using both an octadecylsilica and a polymeric fluorocarbon stationary phase. Correlation of changes in the solute hydrophobic contact area and affinity for the stationary phase, as given by S and $\log k_0$ values respectively, revealed that the α- and imide forms are more conformationally stable than the β-linked peptide. In addition, negative values of the standard entropy change, ΔS^0_{assoc}, for the transfer of the solute to the stationary phase, were observed for both α- and β-linked peptides. These results are indicative of an increased ordering of the system upon solute adsorption and implies that the open-chain peptides exist in solution in more flexible conformations, while the helical structure of the cyclised imide is more rigid and constrained. The implications of the relative conformational stability of these peptides in their role as insulin-potentiating agents is also discussed.

INTRODUCTION

The exquisite nature of high-performance liquid chromatographic techniques as physicochemical tools in the analysis of peptide and protein surface interactions is rapidly gaining wide recognition. The ability of the stationary phase to act as a probe of the topographic surface of the peptide or protein solute has provided greater insight into the factors that control the mechanistic basis of chromatographic separations[1–3]. In a previous study[1], we reported the analysis of the retention behaviour of a number of peptide analogues related to the amino-terminus of human growth hormone (hGH), separated under reversed-phase high-performance liquid chromatography (RP-HPLC) conditions. It was found that these peptides, which are derived from a helical segment of the parent protein, also exhibited chromatographic properties that were

[a] For Part XC, see ref. 1.

0021-9673/89/$03.50

consistent with the formation of a helical structure at the stationary phase interface. Furthermore, comparison of solute hydrophobic contact area and affinity for the stationary phase, as expressed by S and log k_0 values, at different mobile phase pH values has revealed specific details of the factors that control the orientation of the peptides at the hydrophobic stationary phase. The differences in the biological activity of the Asp^6 imide and the open-chain Asp^6 α- and β-forms of the parent sequence Leu-Ser-Arg-Leu-Phe-Asp-Asn-Ala is clearly related to the difference in molecular charge distribution and peptide conformation, both in solution and at the site of biological action. As part of our studies on defining the conformational preferences of these peptides, the relative stability of the imide and α- and β-forms of these peptides was investigated through the analysis of the influence of temperature on chromatographic properties.

MATERIALS AND METHODS

Apparatus

All chromatographic measurements were performed with a Du Pont 8800 liquid chromatograph (Du Pont, Wilmington, DE, U.S.A.) coupled to a Valco HPLC 6-port injector (Valco, Houston, TX, U.S.A.) and a Waters M450 variable-wavelength UV detector (Waters Assoc., Milford, MA, U.S.A.). All measurements were routinely monitored at 215 nm and recorded with the aid of a Spectra-Physics SP4100 computing integrator (Spectra-Physics, San Jose, CA, U.S.A.). Chromatographic measurements at 5 and 25°C were made by immersing the column in a plastic column jacket, coupled to a recirculating cooler (FTS Systems, New York, U.S.A.), while a DuPont column oven was used for measurements at 50, 65 and 75°C. RP-HPLC was carried out with a Bakerbond widepore octadecylsilica (J. T. Baker, Phillipsburg, NJ, U.S.A.) with a nominal particle diameter of 5 μm and average pore size of 30 nm, packed into a 25 cm × 0.46 cm I.D. column, and a Du Pont Bio Series Poly F proprietary polymeric fluorocarbon HPLC packing with a 20-μm particle size and 30-nm pore size, packed into a 8 cm × 0.62 cm I.D. column. All injections were made with SGE (Melbourne, Australia) syringes, and pH measurements were performed with an Orion Model SA520 pH meter (Orion, Cambridge, MA, U.S.A.).

Chemicals and reagents

Acetonitrile (HPLC grade) was obtained from Mallinckrodt (Paris, KY, U.S.A.), and trifluoroacetic acid (TFA) was obtained from Pierce (Rockford, IL, U.S.A.). Water was distilled and deionised in a Milli-Q system (Millipore, Bedford, MA, U.S.A.). N-Acetyl-L-tryptophanamide and N-acetyl-L-phenylalanine methyl ester and penta-D-phenylalanine were all obtained from Sigma (St. Louis, MO, U.S.A.). The hGH-related peptide analogues were synthesised by established 9-fluorenylmethyloxycarbonyl (F-moc) group protection procedures and purified by RP-HPLC.

Chromatographic procedures

Bulk solvents and mobile phases were filtered and degassed under vacuum. Linear gradient elution was carried out with 0.1% TFA in water (buffer A) and 0.1% TFA in 50% aqueous acetonitrile (buffer B) over gradient times varying between 15

and 90 min and at a flow-rate of 1 ml/min. Peptide solutions were prepared by dissolving the peptide in 0.1% TFA at a concentration of 1 mg/ml, and sample sizes varied between 5 and 20 μg. All data points were derived from duplicate measurements with retention times typically varying by less then 1%. The column dead-time was taken as the retention time for sodium nitrate. The various chromatographic parameters used in the analysis of peptide retention and bandwidth behaviour were calculated using the Pek-n-ese program, written in BASIC language for a Hewlett-Packard HP86B computer, as previously described[2].

RESULTS AND DISCUSSION

Solute retention in adsorptive modes of HPLC is governed by the distribution equilibria established between the stationary phase and the mobile phase, and can be defined as

$$K = \frac{[P]_s}{[P]_m} \tag{1}$$

where $[P]_s$ and $[P]_m$ represent the solute concentration in the stationary phase and mobile phase, respectively.

The dependence of the median capacity factor, $\bar{k}$, of a solute, chromatographed under regular reversed phase conditions, on K, is then given by

$$\bar{k} = \phi K \tag{2}$$

where ϕ is equal to the ratio of the volume of the stationary phase, V_s, to the volume of the mobile phase, V_m.

The thermodynamic equilibrium constants can be equated with the overall standard unitary free-energy changes associated with the transfer of the solutes from the mobile phase to the stationary phase, such that

$$\log K = -\Delta G^0_{assoc}/RT \tag{3}$$

where R is the gas constant and T is the temperature. Solute retention can then be expressed as

$$\log \bar{k} = -\Delta G^0_{assoc}/RT + \log \phi \tag{4}$$

Thus, the dependence of $\bar{k}$ on T is given by

$$\log \bar{k} = \frac{-\Delta H^0_{assoc}}{RT} + \frac{\Delta S^0_{assoc}}{R} + \log \phi \tag{5}$$

where ΔH^0_{assoc} and ΔS^0_{assoc} are the standard enthalpy and entropy changes, respectively, for the transfer of the solute to the stationary phase.

The capacity factors of peptides in RP-HPLC are generally reduced with increased temperature. For peptides with no significant secondary or tertiary structure, higher temperatures will favour more rapid mass transfer of the solute and

TABLE I

PEPTIDE SEQUENCES AND S AND LOG k_0 VALUES OBTAINED AT DIFFERENT TEMPERATURES ON THE C_{18} COLUMN

Abbreviations for amino acids were as follows: A = Ala = alanine, D = Asp = aspartic acid, E = Glu = glutamic acid, F = Phe = phenylalanine, G = Gly = glycine, L = Leu = leucine, R = Arg = arginine, S = Ser = serine, W = Trp = tryptophan.

Peptide	*5°C*		*25°C*		*50°C*		*65°C*		*75°C*	
	S	*log* k_0	*S*	*log* k_0	*S*	*log* k_0	*S*	*log* k_0	*S*	*log* k_0
1 LSRLFDNA (imide)	8.8	4.2	7.2	3.6	7.0	3.4	8.2	3.8	8.5	3.8
2 LFDNAG (α)	10.6	1.8	11.2	1.8	11.3	1.5	10.9	1.3	11.5	1.3
3 LSRLFENAG (β)	11.7	1.9	12.8	1.9	11.6	1.5	11.9	1.4	15.5	1.6
4 $(Phe)_5$	8.7	3.6	9.6	4.0	8.0	3.3	12.7	4.6	19.5	6.6
5 F	6.9	2.1	6.8	2.0	5.4	1.6	6.2	1.7	9.0	1.9
6 W	7.8	1.4	9.5	1.4	7.9	1.0	9.6	0.9	–	–

lead to improved efficiencies. Recently, the influence of temperature on a first-order irreversible on-column reaction was investigated[4]. These studies revealed that, depending on the rate constant and activation energy for the reaction, the deleterious effects of, *e.g.*, protein denaturation are diminished due to the faster separation times and decreased exposure of the solute to the high temperatures.

The influence of temperature on the chromatographic behaviour of peptides and proteins can also be used to characterise conformational equilibria and stability of the solutes. The correlation of changes in the hydrophobic contact area and solute affinity, as given by the S and log k_0 values of the solute, can provide valuable insight into structural and environmental factors that influence chromatographic behaviour of peptides and proteins. The gradient elution behaviour of a set of peptides related to residues [6–13] of hGH has been recently studied. It was found that the closed-ring imide form and the open-chain α- and β-forms all chromatographed as an amphipathic helical structure with slight differences in the final conformation. The main factors contributing to the stabilisation of the amphipathic helical structure of the imide have been shown by 2D-NMR (NOESY) studies[5] to consist of the hydrophobic face of the helix and a dipolar interaction between an arginine residue (Arg^3) and the imide ring, in the open-chain forms. The influence of temperature on the reversed-phase gradient-elution properties of these peptides was therefore studied. Table I lists the peptides used in the present study. Gradient-elution data were accumulated at gradient times (t_G) of 15, 30, 45, 60, and 90 min and a flow-rate of 1 ml/min at temperatures of 5, 25, 50, 65, and 75°C. Samples were chromatographed, in the first instance, on a C_{18} stationary phase with a linear gradient from 0.1% TFA in water to 0.1% TFA in 50% aqueous acetonitrile. Plots of the median capacity factor, $\bar{k}$, *versus* the corresponding organic mole fraction, $\bar{\psi}$, were derived as described previously[2]. The S and log k_0 values for each temperature were obtained by linear regression analysis of the plots according to the relationship

$$\log \bar{k} = \log k_0 - S\bar{\psi} \qquad (6)$$

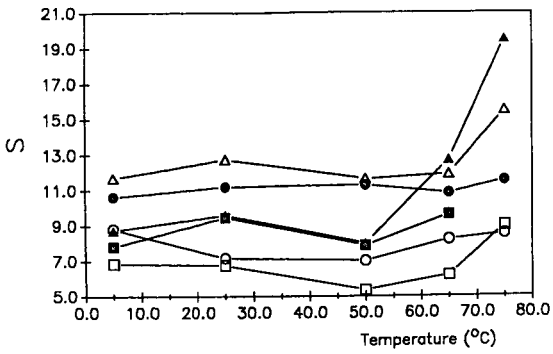

Fig. 1. Plot of *S versus* temperature (°C) for the peptides and amino acids listed in Table I. Experimental data points were derived from gradient retention data with t_G = 15, 30, 45, 60 and 90 min and a flow-rate of 1 ml/min, on a C_{18} column. See Materials and Methods section for other details. Peptides: (○), **1**; (●), **2**; (△), **3**; (▲), **4**; (□), **5**; (■), **6**.

The three hGH-related peptides included in this study represent examples of an imide, and an α- and β-linked peptide. In addition pentaphenylalanine [$(Phe)_5$] was used as a control as this peptide is known to exist as a helix in solution[6]. Data for the amino acid derivatives N-acetyl-L-tryptophanamide and N-acetyl-L-phenylalanine methyl ester were also determined as an example of non-interconverting solutes. The S and log k_0 values are listed in Table I and plotted against temperature in Figs. 1 and 2, respectively. Studies on the influence of temperature on the physical state of silica surfaces covered by alkylsiloxy layers have demonstrated[7] the existence of phase transitions which are characterised by an increase in the retention of molecular probes with increasing temperature. This conformational transition of the ligand is dependent on the carbon chain length, the ligand density and the nature of the mobile phase. While temperature-dependent stationary phase transitions may also occur with the octadecylsilica packing used in the present study, differences in the chromatographic properties of the peptide solutes will be related to the differences in amino acid composition and sequence. Further, the trends evident in these studies are expected to

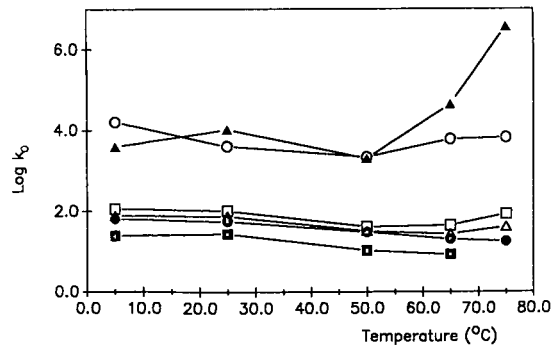

Fig. 2. Plot of log k_0 *versus* temperature (°C) for peptides **1–6** listed in Table I. See legend to Fig. 1 for experimental conditions. Peptides: (○), **1**; (●), **2**; (△), **3**; (▲), **4**; (□), **5**; (■), **6**.

apply to other well-manufactured *n*-alkylsilica stationary phases even in situations when small batch to batch variability may occur.

If a peptide existed in solution in an amphipathic helical conformation, then significant changes in the interactive properties would be anticipated as the operating temperature approaches and exceeds the melting temperature of an α-helix in the range 55–65°C[8]. As is evident in Fig. 1, the largest change in the S value over the range of temperatures was observed for $(Phe)_5$, which increased from 8 to 19.5 between 50 and 75°C, respectively. This clearly corresponds to the thermal denaturation of the peptide and was also associated with a significant increase in the log k_0 value (Fig. 2). These observations are a result of an increase in the number of residues that can simultaneously interact with the column when the peptide exists as the random coil structure. Of the remaining peptides, only the β-linked hGH peptide showed any significant increase in S value at the higher temperature. The S values for all other solutes remained essentially constant over the entire range of temperatures. This indicates that the α- and imide forms are more conformationally stable than the β-linked peptide. Detailed analysis of 2D-NMR NOESY spectra of the imide form[5] has revealed the existence of hydrogen bonding between the imide ring and the arginyl residue and the formation of the hydrophobic surface on one face of the helix. Preliminary evidence also suggests that the α-linked peptide also exists as an amphipathic helix, but the presence of the aspartyl residue results in an ionic interaction between the aspartyl carboxyl group and the arginyl residue. Clearly these interactions have resulted in a highly stabilised structure, while the additional carbon atom in the peptide backbone of the β-peptide appears to destabilise the amphipathic helix.

The ΔH^0_{assoc} and ΔS^0_{assoc} values for the peptides **1–4** were determined by linear regression analysis of plots of log $\bar{k}$ (at $\bar{\psi} = 0.3$) *versus* $1/T$, shown in Fig. 3, according to eqn. 5. The resulting values are listed in Table II. Two values of ΔH^0 and ΔS^0, corresponding to a high-temperature and a low-temperature value, were obtained for the β-linked peptide. Negative ΔH^0 values, as observed for the peptides used in this study, indicate that heat is released upon adsorption of the solute on the stationary phase. Positive values of ΔS^0 indicate that there is an increase in the disorder of the

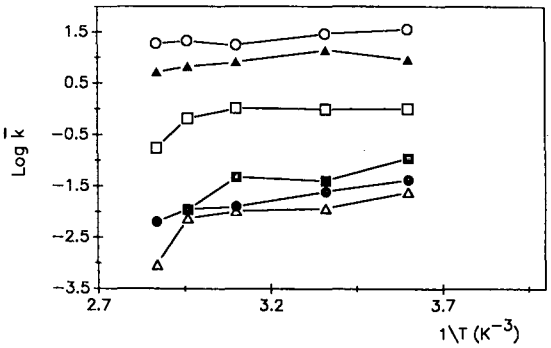

Fig. 3. Plot of log $\bar{k}$ versus $1/T$ (Van't Hoff plot) for peptides **1–6**, used to derive ΔH^0_{assoc} and ΔS^0_{assoc}, which are listed in Table III. Experimental log $\bar{k}$ values were derived at $\bar{\psi} = 0.3$. See legend to Fig. 1 for experimental conditions. Peptides: (○), **1**; (●), **2**; (△), **3**; (▲), **4**; (□), **5**; (■), **6**.

TABLE II

THERMODYNAMIC DATA FOR PEPTIDES SEPARATED ON THE C_{18} COLUMN

Peptide[a]	ΔH^0_{assoc} (*kJ mol*$^{-1}$)	ΔS^0_{assoc} (*J mol*$^{-1}$)
1 Imide	−3.3 ± 0.6	3.8 ± 0.6
2 α	−8.7 ± 0.3	−39.7 ± 1.2
3 β		
high T	−35.4 ± 8.9	−122.2 ± 30.6
low T	−6.1 ± 1.0	−32.8 ± 5.5
4 $(Phe)_5$	−3.3 ± 0.6	2.6 ± 1.1

[a] See Table I for amino acid sequence.

system during adsorption; two positive ΔS^0 values were observed for the imide and $(Phe)_5$. However, negative values were obtained for the α- and β-linked peptides. This indicates an increased ordering of the overall system. These results suggest that the open-chain peptides exist in solution in more flexible conformations, while the helical structure of the imide and $(Phe)_5$ are more rigid and constrained. This conclusion is also consistent with the COSY and NOESY NMR data[5]. The enthalpy and entropy values obtained in this study are also in the same range as other peptides including paracelsins[9] and insulin[10] which undergo conformational changes at the stationary phase.

The contribution of the hydrophobic ligands at the stationary-phase surface to conformational stability of the peptides was also investigated by comparing the chromatographic properties on the Poly F stationary phase. This packing material is a hydrophobic, polymeric fluorocarbon resin which does not contain the long alkyl-bond chains associated with more conventional reversed-phase materials. The S and $\log k_0$ values obtained for peptides **1–5**, separated on the Poly F column at 5, 25, 50, and 65°C, are listed in Table III. There was much more variability in both sets of values on the Poly F than observed with the octadecylsilica packing. In particular, there was a large change in the S value for the α-, and β-peptides between 5 and 25°C, followed by a large increase between 50 and 65°C for the open-chain peptides. This was associated with a steady decrease in the $\log k_0$ values of the α- and β-linked forms over

TABLE III

S AND LOG k_0 VALUES OBTAINED AT DIFFERENT TEMPERATURES WITH THE POLY F COLUMN

Peptide[a]	*5°C*		*25°C*		*50°C*		*65°C*	
	S	$\log k_0$	S	$\log k_0$	S	$\log k_0$	S	$\log k_0$
1 Imide	8.1	3.3	8.8	3.7	7.7	3.3	8.9	3.5
2 α	15.8	1.6	8.7	1.3	9.7	1.2	21.8	0.8
3 β	17.4	1.5	8.2	1.2	9.2	1.1	22.5	1.1
4 $(Phe)_5$	5.5	2.5	11.8	3.8	9.4	3.1	11.5	3.2
5 Phe	20.2	2.5	12.0	1.6	6.9	1.3	12.0	1.2

[a] See Table I for amino acid sequence.

the experimental temperature range while the value of S and log k_0 of the imide remained essentially constant. Clearly, the difference between the C_{18} ligands and the polymeric fluorocarbon surface is manifested as significantly altered interactive properties for these peptides. In particular, the high S values at low temperatures suggests that these peptides may have been trapped in the random-coil structure on the Poly F packing. As the temperature increases, the amphipathic helix can form, which then starts to unfold between 50 and 65°C. Furthermore, the S value for $(Phe)_5$ increased between 5 and 25°C and remained essentially constant at the higher temperatures. This contrasts with the results obtained for the octadecylsilica packing where increases in S value were observed between 50 and 65°C. This increase in S values, which is associated with helix denaturation at the lower temperature, indicates that the octadecylsilica packing material enhanced the stability of the $(Phe)_5$ helix. Similar ligand-induced behaviour is evident in stabilisation of the amphipathic helix of the hGH peptides presumably through interaction with the hydrophobic pocket containing Leu[1], Leu[4] and Phe[5]. These results are also relevant to the known pattern of biological activity of these peptides. It has been suggested[11] that the planar surface on one side of the molecule in which the imide ring is located, is the active side of the molecule in its role as an insulin-potentiating agent. The interaction of the hydrophobic face on the alternate side of the molecule with a complementary surface at the site of biological recognition may serve to anchor the peptide specifically at the receptor surface. Thus, while the α- and β-forms, which are inactive in the glucose utilisation assay, may be able to bind to the biological recognition surface, the absence of the precise structural factors provided by the correct juxtapositioning of the arginyl-imide moieties prevents the open-chain peptides from exhibiting any biological activity.

The analysis of chromatographic retention data obtained at different operating temperatures provides significant insight into the influence of both solute structure and the nature of the stationary-phase ligand on the preferred orientation of peptide solutes at the hydrocarbonaceous surfaces used in RP-HPLC. By analogy, similar methods are also pertinent to the manner in which peptides interact with both synthetic and biological surfaces. The present results also demonstrate the utility of RP-HPLC techniques in providing information on peptide topography which is clearly important in the rational design and development of therapeutic analogues to naturally occurring peptide hormones.

ACKNOWLEDGEMENTS

The support of research grants to MTWH from the National Health & Medical Research Council of Australia, Australian Research Grants Committee and Monash University Special Research fund is gratefully acknowledged. MIA is a recipient of a Monash University Postdoctoral Fellowship.

REFERENCES

1 A. W. Purcell, M. I. Aguilar and M. T. W. Hearn, *J. Chromatogr.*, 476 (1989) 113.
2 M.-I. Aguilar, A. N. Hodder and M. T. W. Hearn, *J. Chromatogr.*, 327 (1985) 115.
3 M. T. W. Hearn and M. I. Aguilar, *J. Chromatogr.*, 392 (1987) 33.
4 F. D. Antia and Cs. Horváth, *J. Chromatogr.*, 435 (1988) 1.

5 M. F. O'Donoghue, M. T. W. Hearn and I. M. Rae, *Proc. 20th Eur. Pept. Symp. (Tubingen)*, 1989, in press.
6 H. Neurath and K. Bailey (Editors), *The Proteins —Chemistry, Biological Activity and Methods*, Academic Press, New York, 1954, p. 892.
7 K. Jinno, T. Nagoshi, N. Tanaka, M. Okamoto, J. C. Fetzer and W. R. Biggs, *J. Chromatogr.*, 436 (1988) 1.
8 D. Freifelder, *Physical Biochemistry —Applications to Biochemistry and Molecular Biology*, Freeman, San Fracnsico, CA, 1976, p. 398 and 419.
9 K. D. Lork, K. K. Unger, H. Brücker and M. T. W. Hearn, *J. Chromatogr.*, 476 (1989) 135.
10 W. S. Hancock, D. R. Knighton, J. R. Napier, D. R. K. Harding and R. Venable, *J. Chromatogr.*, 367 (1986) 1.
11 M. T. W. Hearn, F. N. Ng, M. F. O'Donoghue and I. M. Rae, *Patents PCT/AU*, 88/00421.

Journal of Chromatography, 476 (1989) 135–145
Elsevier Science Publishers B.V., Amsterdam — Printed in The Netherlands

CHROMSYMP. 1634

RETENTION BEHAVIOUR OF PARACELSIN PEPTIDES ON REVERSED-PHASE SILICAS WITH VARYING *n*-ALKYL CHAIN LENGTH AND LIGAND DENSITY

K. D. LORK and K. K. UNGER*
Institut für Anorganische Chemie und Analytische Chemie, Johannes Gutenberg-Universität, J. J. Becher Weg 24, D-6500 Mainz (F.R.G.)
H. BRÜCKNER
Institut für Lebensmitteltechnologie, Universität Hohenheim, Garbenstrasse 25, D-7000 Stuttgart-70 (F.R.G.)
and
M. T. W. HEARN
Department of Biochemistry, Monash University, Clayton, Victoria 3168 (Australia)

SUMMARY

As part of further investigations on the characterization of the ligand-induced conformational stabilization of peptides, two series of *n*-alkyldimethylsilyl bonded silicas have been prepared. In series A the *n*-alkyl chain length, *n*, of the bonded phase was varied between 1 and 20 carbon atoms at a constant ligand density. In series B the ligand density, α_{exp}, was gradually changed from 0 to 4.1 μmol/m^2 on a C_1, C_4, C_6, C_8 and C_{18} bonded phase. The retention behaviour of four peptides of the paracelsin family were examined under isocratic conditions, using a ternary mobile phase of water–methanol–acetonitrile (22:39:39, v/v/v). Plots of k' *versus* n showed pronounced maxima between $n = 2$ and 4 carbon atoms, followed by a decrease by a factor of 3 at $n = 5$, whereas above 5 carbon atoms only a slight increase in k' was observed.

The selectivity behaviour of the paracelsins A–D can be mainly rationalized by interaction of the amphiphathic polypeptide $3.6_{13}(\alpha)$-helix with the hydrophobic ligand and protrusion of the key amino acid residues at positions 6 and 9 in the sequence. However, from experiments with a polystyrene stationary phase it is evident that hydrophobic interactions and different partition coefficients also contribute to the resolution of the paracelsin peptides. Furthermore, Van 't Hoff plots confirm significant free energy changes associated with retention. These observations provide the basis for evaluating the enthalpic and entropic changes associated with peptide interactions with *n*-alkyl silicas.

INTRODUCTION

The wide use of reversed-phase (RP) silica packings in high-performance liquid chromatographic (HPLC) separations of peptides and proteins has stimulated in-

0021-9673/89/$03.50

tensive studies on the stationary phase properties and on the properties of the peptide itself and their effects on retention and selectivity[1–3]. Numerous studies have shown[4] that the position of an amino acid within the peptide sequence and the neighbouring groups influence retention. For example, it is well known[4] that a series of peptides containing the same amino acids but with different sequence can be separated.

The influence of the mobile phase on the retention of peptides and proteins under reversed-phase conditions has been broadly investigated[1,2,5,6]. However, there is a lack of understanding of the molecular mechanism(s) of interaction between the hydrocarbonaceous surface representing the stationary phase and the peptides and proteins as solutes.

While the dependence of the retention and selectivity of polar and non-polar small size solutes on reversed-phase chain length and on ligand density has been the subject of several studies[7–16], no systematic investigations of the influence of these stationary phase parameters on the retention of peptides and proteins have been made. In a recent paper[7] it was shown that solute retention in reversed-phase chromatography (RPC) as a function of either *n*-alkyl chain length or ligand density both follows a linear relationship up to characteristic critical values whereby the dependencies progressively diverge and reach asymptotic limiting values. The critical chain length and the critical ligand density are dependent on the solute size for polar low-molecular-weight compounds: the larger the solute, the higher is the critical chain length, but the lower is the critical ligand density. These phenomena can be understood on the basis of a restricted intercalation of the solutes into the stationary phase.

However, peptides and proteins exhibit secondary and tertiary structures and can therefore behave differently. For large molecules, *e.g.*, proteins, the retention was found to be fairly independent of the chain length of an alkyl-bonded silica[17].

This paper aims to investigate the influence of ligand density, *n*-alkyl chain length and column temperature on the retention of peptides of the paracelsin family in RPC. These studies thus provide further evidence for the critical chain length concept, and demonstrate that enthalpy-driven processes play an important role in the retention of amphiphatic peptides on hydrocarbonaceous stationary phases.

EXPERIMENTAL

Reagents and procedures

A series of *n*-alkyldimethylchlorosilanes [X-Si$(CH_3)_2C_nH_{2n+1}$] with an *n*-alkyl chain length, *n*, varying from 1 to 20 carbon atoms were prepared by hydrosilylation of *n*-alkenes with dimethylchlorosilane by using hexachloroplatinic acid as catalyst. The physical properties of these silanes are listed in a recent paper[7]. The starting silica was LiChrospher Si-100-10 (Batch No. F 667512), a gift of Merck (Darmstadt, F.R.G.) with a specific surface area of a_s(BET) = 388 ± 5 m^2/g, a mean pore diameter of p_d = 10 nm and a mean particle diameter of d_p = 10 μm.

The silanization of the silicas was performed in dry dimethylformamide (50 ml) at a temperature of 426 K under gentle stirring, applying the prepared chlorosilane (30 mmol) and 2,6-lutidine (36 mmol) as catalyst. The silica samples (0.1 mol) were previously dried at 423 K under vacuum at $P \leqslant 30$ Pa for 16 h. The reversed-phase silica formed was washed with different solvents in succession and then dried at 353 K under vacuum overnight. The procedure has been described in detail elsewhere[7].

The ligand density (α_{exp}) of bonded *n*-alkyldimethylsilyl groups was determined by means of elemental analysis from the carbon content of the modified sample[7].

Chromatographic measurements

The reversed-phase silicas were packed into columns, 250 × 4.6 mm I.D. by means of the slurry packing technique. In addition, a polystyrene column PRP-1, 125 × 4 mm I.D., was used (Hamilton, Darmstadt, F.R.G.). The chromatographic measurements were performed on an LKB (Pharmacia-LKB Biotechnology, Freiburg, F.R.G.) liquid chromatograph with a Model 2150 HPLC pump and a Model 2151 variable-wavelength monitor. The chromatograms were recorded on a Shimadzu (Shimadzu, Duisburg, F.R.G.) Model CR-3A integrator. All columns were thermostated at a temperature of 301 K using an LKB 2155 column oven. In order to realize low column temperatures for the investigation of the influence of temperature on retention a Colora (Lorch, F.R.G.) WK 30 A cryostate filled with ethanol was employed.

The peptides used in this study were a mixture of the paracelsins A–D, dissolved in methanol at a concentration of 0.1 mg ml^{-1}. The mobile phase was water–methanol–acetonitrile (22:39:39). Methanol and acetonitrile were of chromatography grade, supplied by Merck and the water used was destilled and then additionally purified by means of Milli-Q water system (Millipore/Waters, Bedford, MA, U.S.A.). The injection loop had a volume of 20 µl, the flow-rate was 1 ml/min and the detection wavelength was 206 nm.

Properties of paracelsin

Paracelsin[18–20], a membrane-active polypeptide, is an antibiotic of the peptaibol class[21], excreted by the mould *Trichoderma reesi*. It exhibits a pronounced microheterogeneity, *i.e.*, it is composed of four peptides differing only in two positions (positions 6 and 9)[18–20]. The primary structures of the paracelsins A–D are given in Fig. 1, where the differences are indicated. The N-termini of these peptides are acetylated, and the C-termini linked in a peptide bond with phenylalaninol (Pheol). Furthermore, it is noteworthy that the paracelsins exhibit a high proportion of the uncommon α-aminoisobutyric acid (Aib). By means of circular dichroism and ^{13}C NMR spectroscopy Brückner *et al.*[18] have demonstrated the helical structure of the paracelsins. The presence of a mainly 3.6_{13} (α)-helical solute structure of paracelsin, and not a 3_{10}-helix, as found in certain Aib-peptides[22], is the most likely conformation since X-ray crystallographic and NMR spectroscopic investigations of the paracelsin analogues alamethicin[23] and trichorzianine[24] have shown that they have α-helical conformations.

1	2	3	4	5	6	7	8	9	10	11	12	13	14	15	16	17	18	19	20	
Ac-	Aib-	Ala-	Aib-	Ala-	Aib-	**Ala-**	Gln-	Aib-	**Val-**	Aib-	Gly-	Aib-	Aib-	Pro-	Val-	Aib-	Aib-	Gln-	Gln-	Pheol (A)
Ac-	Aib-	Ala-	Aib-	Ala-	Aib-	**Ala-**	Gln-	Aib-	**Leu-**	Aib-	Gly-	Aib-	Aib-	Pro-	Val-	Aib-	Aib-	Gln-	Gln-	Pheol (B)
Ac-	Aib-	Ala-	Aib-	Ala-	Aib-	**Aib-**	Gln-	Aib-	**Val-**	Aib-	Gly-	Aib-	Aib-	Pro-	Val-	Aib-	Aib-	Gln-	Gln-	Pheol (C)
Ac-	Aib-	Ala-	Aib-	Ala-	Aib-	**Aib-**	Gln-	Aib-	**Leu-**	Aib-	Gly-	Aib-	Aib-	Pro-	Val-	Aib-	Aib-	Gln-	Gln-	Pheol (D)

Fig. 1. Primary structure of the paracelsin peptides A–D.

RESULTS AND DISCUSSION

Retention of paracelsin

Despite the small differences between the four paracelsins (PCs), separation of all four components could be achieved under isocratic conditions[25]. A chromatogram of the paracelsin peptides on an octyldimethylsilyl bonded silica showing the characteristic elution profile is presented in Fig. 2.

In order to rationalize that the paracelsin peptides are separated in spite of their small molecular differences the following facts have to be taken into account. It is known from numerous examples that reversed phases are able to separate peptides according to their hydrophobicities and differences in their conformations. The most surprising effect in the case of the paracelsins is that an unexpectedly good separation of the microheterogenous peptides occurs. This is manifested in the k' values and resolution factors. However, no significant differences in the α-helical conformations of components A–D are to be expected. Since PC-A and PC-B, as well as PC-C and PC-D, differ from each other just by the insertion of one methylene group in an amino acid side chain (exchange of Val against Leu in position 6, *cf.* Fig. 1) the question arises whether the chromatographic separation is attributable solely to minor differences in hydrophobicities or not.

The differences in the numbers of methine, methylene, and methyl groups of the amino acids exchanged in the decisive positions 6 and 9 shown in Table I.

From the temperature-difference of the paracelsin peptides (*cf.* Fig. 3) it is obvious that the enthalpy values increase by 0.5–0.6 kJ/mol in the series PC-A to PC-D. These enthalpy differences are sufficient for the separation of paracelsin peptides, but the data describe a macroscopic phenomenon rather than providing a separation mechanism. Furthermore, in analogy to the structurally related trichotoxins, which partly have been separated by counter-current distribution[19], it is reasonable to assume that also the paracelsins differ in their partition coefficients. These coefficients also reflect the differences in the hydrophobicities of the peptides. The conclusions are supported by the ability of a polystyrene stationary phase to separate PC-A and PC-B from PC-C and PC-D, whereby the latter coelute (*cf.* Fig. 4). However, the above findings hardly explain the maxima of k' values of paracelsins found

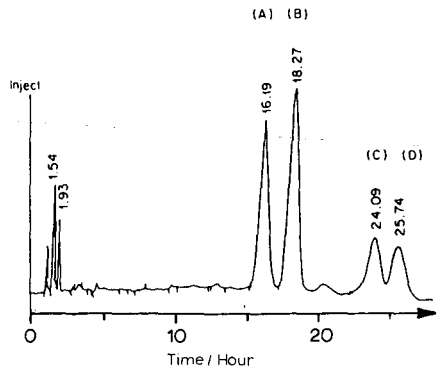

Fig. 2. Chromatogram of four paracelsin peptides on a LiChrospher Si-100 RP-8 column. 5 μm, 250 × 4.6 mm I.D. Eluent: water–methanol–acetonitrile (22:39:39, v/v/v).

TABLE I

NUMBERS OF CH, CH_2 AND CH_3 GROUPS OF AMINO ACIDS IN POSITIONS 6 AND 9 OF PARACELSIN A–D

Paracelsin compound	*Number of groups*		
	CH	*CH_2*	*CH_3*
A	1	0	3
B	1	1	3
C	1	0	4
D	1	1	4

for the C_4 phase, and to a lower extent, for the C_2 stationary phase (*cf.* Fig. 5). In the case of paracelsins it is therefore reasonable to assume a certain degree of conformational interaction between the stationary phases and the paracelsins, in particular with the alkyl side-chains of the peptide-bonded amino acids.

This is supported by recent results of Pfleiderer *et al.*[26] who performed cross polarization magic angle spinning (CP-MAS) NMR measurements on reversed-phase silicas with varying *n*-alkyl chain length. It was found that in particular *n*-butyl bonded silica (C_4) showed a minimum in mobility (or maximum in rigidity) compared to other *n*-alkyl bonded silicas. As a result of the restricted conformational degrees of freedom of the C_4 phase it is reasonable to assume an optimal interaction of this stationary phase with the alkyl side chains of peptides. With regard to paracelsins, in particular when restricting to the amino acid exchange positions, this interaction preferently takes place, with the isopropyl and isobutyl chains of Val and Leu, respectively, in position 9, and the methyl and geminal dimethyl group of Ala and Aib, respectively, in position 6 (*cf.* Fig. 1).

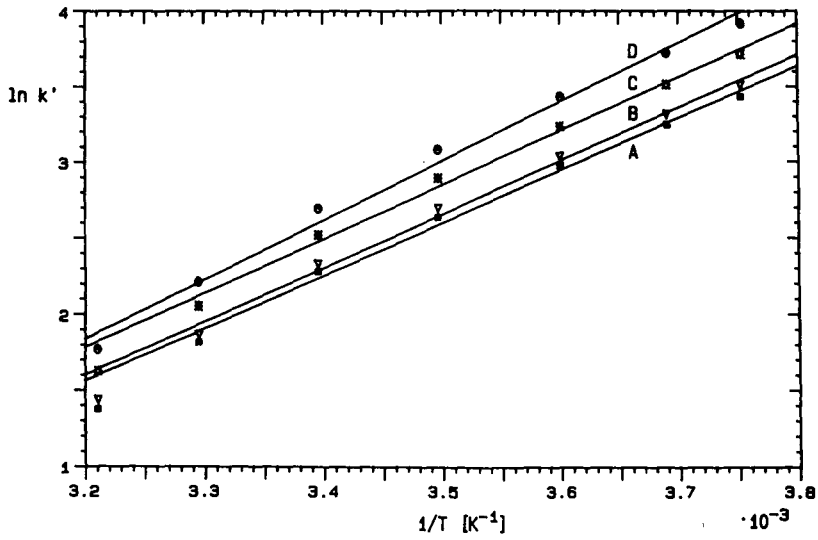

Fig. 3. Van 't Hoff plot of the separation of paracelsin A–D on a LiChrospher Si-100-10 RP-18 column.

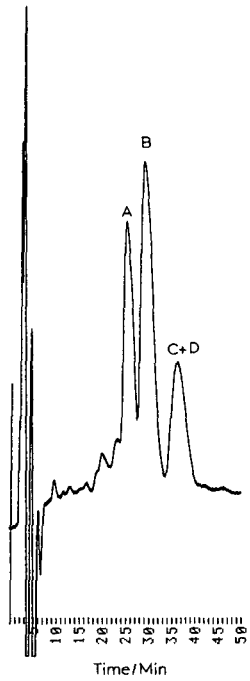

Fig. 4. Chromatogram of the natural mixture of paracelsins (A–D) on a polystyrene stationary phase (PRP-1). Column, 150 × 4.1 mm I.D. Eluent: water–methanol–acetonitrile (35:30:35, v/v/v); flow-rate: 0.4 ml/min; absorbance: 215 nm.

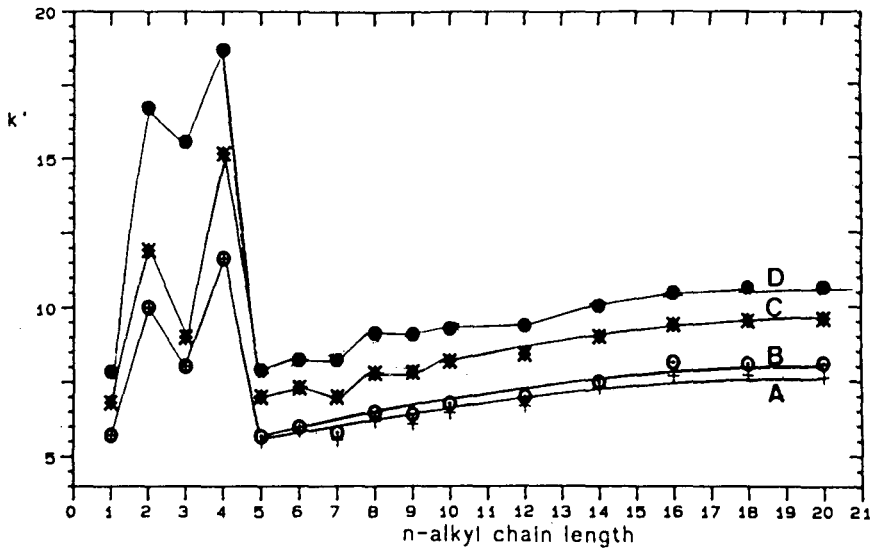

Fig. 5. Capacity factors, k', of paracelsin as a function of *n*-alkyl chain length of reversed-phase silicas at constant ligand density in water–methanol–acetonitrile (22:39:39, v/v/v).

Finally the question remains open whether the α-helical solute structures of the individual paracelsins contribute to their chromatographic separation. It should be emphasized that the α-helical conformations of paracelsins are not induced (but might be enforced) by interaction with the stationary phase since circular dichroitic measurements proved a high degree of helical conformation even in aqueous solvents such as water–methanol (30:70, v/v). Fig. 6 represents the axial α-helical wheel projection of paracelsins showing also the amino acid exchange positions. As can be seen these amino acids are located at the hydrophobic side of the helix. Since it is reasonable to assume that the hydrophobic regions (positions 1–17, *cf.* Fig. 1) of the amphipathic helices of paracelsins are directed towards the reversed phase, optimal side chain recognition should occur for the amino acids exchanged. The conformational interaction of the hydrophobic part of the amphipathic paracelsin helix and the C_4 stationary phase might contribute therefore to the highest k' values found for this phase and also to the unexpectedly good separation of the microheterogeneous paracelsins peptides by RP-HPLC.

Dependence of the retention of paracelsin on n-alkyl chain length and ligand density

In a series of experiments, the retention behaviour of the paracelsins on reversed-phase silicas with an *n*-alkyl chain length ranging from C_1 to C_{20} was investigated while the ligand density was kept constant ($\alpha_{exp} = 3.5 \pm 0.2$ μmol/m^2). The results are presented in Fig. 5. In an other series with trimethyl(C_1)-, *n*-butyl(C_4)-, *n*-hexyl(C_6)-, *n*-octyl(C_8)- and *n*-octadecyl(C_{18})-bonded reversed.phase silica, the ligand density was varied between 0 and 4.1 μmol/m^2. Fig. 7 shows the dependence of the capacity factor of paracelsins on the ligand density of the reversed-phase silica.

Testing small solutes (anilines and bencoic acid esters)[7] we found that the capacity factor did not markedly increase above a certain *n*-alkyl chain length, called the critical chain length, L_{crit}. This result is in agreement with earlier findings of Berendsen and De Galan[12,13]. Surprisingly, the plot showing the dependence of paracelsin retention on the *n*-alkyl chain length of the stationary phase (Fig. 5) exhibits two maxima, corresponding to an *n*-alkyl chain length between 2 and 4 carbon atoms.

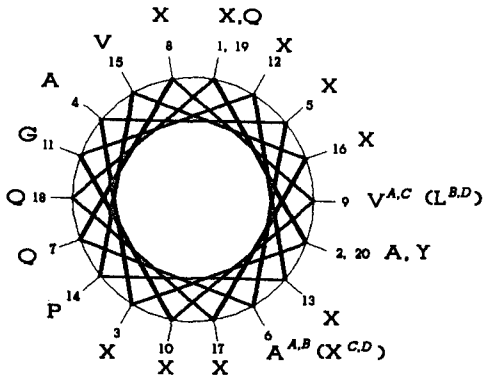

Fig. 6. Axial projection of the helical wheels of paracelsins A–D showing amino acid exchange in position 6 and 9 (superscripts of amino acids refer to paracelsin peptides A, B, C and D). One-letter nomenclature of amino acids: A = Ala, G = Gly, L = Leu, P = Pro, Q = Gln, V = Val, X = Aib, Y = Pheol (phenyl-alaninol).

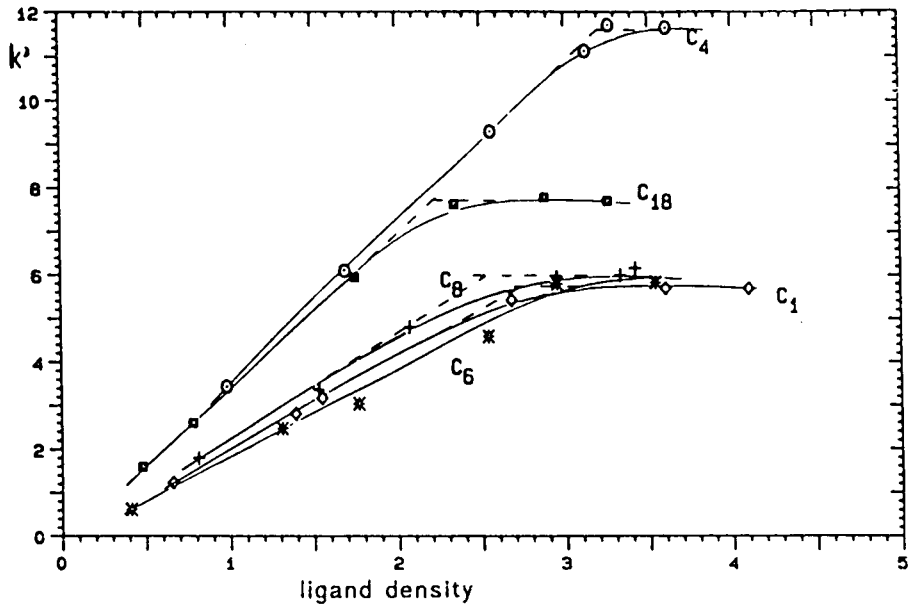

Fig. 7. Capacity factors, k', of paracelsin A as a function of ligand density of reversed-phase silicas at constant *n*-alkyl chain length in water–methanol–acetonitrile (22:39:39, v/v/v).

From 4 carbon atoms on, the capacity factors are three times lower but increase slowly and linearly up to a plateau, where the retention remains constant. The critical chain length found for paracelsin was about 14 carbon atoms.

The phenomenon of the critical chain length has been explained previously by Berendsen and De Galan[12,13] by means of the compulsory absorption model, where the solute is squeezed into spaces created between the bonded *n*-alkyl chains. This is the reason why the critical chain length increases with increasing size of the solute molecule.

Considering the plot in Fig. 7, it is evident that the capacity factors linearly increase with increasing ligand density of the reversed-phase silica up to a plateau, where the retention remains constant. This observation is in agreement with our recent results[7]. By interpolation of the straight lines in the plot of k' against the ligand density, a critical ligand density, α_{crit}, between 2.3 and 3.2 μmol/m^2 (depending on the *n*-alkyl chain length of the stationary phase) is found for paracelsin. These values are in the same range as those obtained for anilines and esters[7]. From the latter data the conclusion can be drawn that the retention of paracelsin is solely caused by hydrophobic effects and is therefore not influenced by residual silanol groups of the stationary phase. On the other hand, retention above a distinct ligand density is limited by the greatly reduced ability of the solute to penetrate into the stationary phase[3]. *n*-Alkyl groups that are packed together very closely loose the possibility of lateral evasion and this explains the critical ligand density.

Dependence of temperature on paracelsin retention

The significance of the influence of temperature on RPC is often underestimat-

ed[27,28]. Gilpin and Gangoda[29], Morel and Serpinet[30] and others have observed a distinct phase transition, depending on temperature, ligand density and *n*-alkyl chain length.

Fig. 3 shows the dependence of the separation of paracelsin peptides on temperature in the range 265–315 K. It is evident that in this range the dependence of retention on temperature is linear. Hancock *et al.*[31] and Hearn *et al.*[32] have shown, that a linear dependence means that the helical conformational structure is not significantly altered within the temperature range chosen.

In general, for chromatography of small molecules it has been observed that the retention time decreases with an increase in temperature[29,33]. This temperature effect is opposite to that observed for many biopolymers, for which an increase often results in strengthened hydrophobic interactions[31,34]. Such an increase is usually attributed to an entropy-driven process. Hearn *et al.*[32] and Hancock *et al.*[31] have observed that the retention of different peptides decreases with increasing temperature. The same trend is found for paracelsin: the Van 't Hoff plot exhibits a positive slope, corresponding to a decrease of retention with increasing temperature.

Hearn *et al.*[32] and Hancock and co-workers[31,35] have postulated when an amphipathic peptide adopts a nearly 100% helical structure during RPC, maximal hydrophobic interactions result between the stationary phase and the non-polar face of the amphipathic peptide. As shown previously, paracelsin exhibits a helical structure and even in aqueous organic solvents this conformation seems to be maintained during the chromatographic separation.

By means of eqn. 1, relating the capacity factor, k', the phase ratio, Φ, the absolute temperature, T, and the gas constant, R, it is possible to calculate the standard free enthalpy, ΔG^0, of the interaction between the solute and the stationary phase from the slope of the Van 't Hoff plot (Fig. 3):

$$\ln k' = \ln \Phi - \Delta G^0/RT \tag{1}$$

The following enthalpy values were found for the corresponding paracelsin peptides: paracelsin A, $\Delta G^0 = -30.8$ kJ/mol; paracelsin B, $\Delta G^0 = -31.3$ kJ/mol; paracelsin C, $\Delta G^0 = -31.8$ kJ/mol; paracelsin D, $\Delta G^0 = -32.4$ kJ/mol. Eqn. 1 can be expressed according to the Gibbs equation as follows:

$$\ln k' = -\Delta H^0/RT + \Delta S^0/R + \ln \Phi \tag{2}$$

Assuming that the entropy remains constant, the free standard enthalpy values are identical with the standard enthalpies.

The enthalpy values for paracelsins listed above are in the same range as those of other peptides undergoing conformational changes at the stationary phase surface (*ca.* -36 kJ/mol)[31,32]. Because the value of Φ is not available, the entropy cannot be calculated by means of eqn. 2. Comparing Fig. 3 and the Van 't Hoff plots of other peptides[31,32] it is evident that the intercepts for the paracelsin peptides in terms of entropy contributions have values in the same range. For example, Hancock *et al.*[31] showed that the association of the peptide LAP with the stationary phase is enthalpy-driven, in contrast to the association of insulin, which was found to be entropy-driven. By comparison with these and other results[32], the separation of paracelsin is

obviously enthalpy-driven. Finally, it should be pointed out that a difference in the enthalpy of *ca.* 0.5 kJ/mol is sufficient for a complete separation of the four paracelsin peptides.

CONCLUSION

This investigation with paracelsin peptides has demonstrated that solute retention in RPC as a function of *n*-alkyl chain length ($n > 4$) and ligand density follows linear relationships and reaches limiting values. This phenomenon can be understood on the basis of a restricted intercalation of the solutes into the stationary phase.

While basic and non basic small-sized solutes exhibit nearly the same pattern (*cf.* ref. 13), peptides having a tertiary structure behave quite differently. In this study, the family of paracelsin peptides, which possess an α-helical structure, showed a pronounced maximum in retention as a function of the *n*-alkyl chain length ($\alpha_{exp} < 5$). However, the retention of paracelsin as a function of the ligand density at constant chain length increased linearly up to a critical point, similar to that observed in the case of the anilines and esters. Furthermore, an exceptionally high selectivity was achieved under isocratic elution conditions, *i.e.*, 20-mer peptides were separated that differed only by one or two methylene groups, respectively.

It appears that the *n*-alkyl chains of the reversed-phase packing, depending on their length and conformation, have the ability to distinguish peptides with amino acid side chain residues differing by only one methine, methylene or methyl group. These investigations indicate that the effect of alkyl chain length and conformation on retention and selectivity are of critical importance for solutes with a secondary structure, such as peptides.

ACKNOWLEDGEMENTS

These studies were supported by the Deutsche Forschungsgemeinschaft, Bonn (F.R.G.) and by the National Health and Medical Research Council of Australia, whom are indepted for. We are also indepted to Dr. R. Weber for placing the PRP-1 column at our disposal.

REFERENCES

1 W. S. Hancock and D. R. K. Harding, in W. S. Hancock (Editor), *CRC Handbook of HPLC for the Separation of Amino Acids, Peptides and Proteins.* Vol. 2, CRC Press, Boca Raton, FL, 1984, pp. 3–21 and 303–312.
2 M. T. W. Hearn, *Adv. Chromatogr.*, 20 (1982) 1.
3 M. T. W. Hearn, in Cs. Horváth (Editor), *High Performance Liquid Chromatography–Advances and Perspectives,* Vol. 3, Academic Press, New York, 1980, p. 87.
4 M. T. W. Hearn and M. I. Aguilar, in A. Neuberger and L. L. M. van Deemter (Editors), *Modern Physical Methods in Biochemistry,* Elsevier, Amsterdam, 1988, pp. 113–189.
5 M. T. W. Hearn and B. Grego, *J. Chromatogr.*, 203 (1981) 349.
6 F. E. Regnier, *Anal. Chem.*, 55 (1983) 1299A.
7 KD. Lork and K. K. Unger, *Chromatographia,* 26 (1988) 115.
8 K. Karch, I. Sebestian, I. Halász and H. Engelhardt, *J. Chromatogr.* 122 (1976) 171.
9 H. Hemetsberger, P. Behrensmeyer, J. Henning and H. Ricken, *Chromatographia,* 12 (1979) 71.
10 H. Hemetsberger, W. Maasfeld and H. Ricken, *Chromatographia,* 9 (1976) 303.
11 P. Roumeliotis and K. K. Unger, *J. Chromatogr.*, 149 (1978) 211.

12 G. E. Berendsen and L. de Galan, *J. Chromatogr.*, 196 (1980) 21.
13 G. E. Berendsen, *PhD thesis*, Delft University, Delft; 1980.
14 D. E. Martire and R. E. Boehm, *J. Phys. Chem.*, 87 (1983) 1045.
15 M. Zakaria and Ph. R. Brown, *J. Chromatogr.*, 255 (1983) 151.
16 A. Tchapla, H. Colin and G. Guiochon, *Anal. Chem.*, 56 (1984) 621.
17 G. Jilge, R. Janzen, H. Giesche, K. Unger, J. N. Kinkel and M. T. W. Hearn, *J. Chromatogr.*, 397 (1987) 71.
18 H. Brückner, H. Graf and M. Bokel, *Experientia*, 40 (1984) 1189.
19 H. Brückner and M. Przybylski, *J. Chromatogr.*, 296 (1984) 263.
20 M. Przybylski, I. Dietrich, I. Manz and H. Brückner, *Biomed. Mass Spectrom.*, 11 (1984) 569.
21 H. Brückner and C. Reinecke, *J. High Resolut. Chromatogr. Chromatogr. Commun.*, 11 (1988) 735.
22 H. Brückner, in W. A. König and W. Voelter (Editors), *Chemistry of Peptides and Proteins*, Attempto Verlag, Tübingen, 1988, pp. 79–86; and references cited therein.
23 R. O. Fox and F. M. Richards, *Nature (London)*, 300 (1982) 325.
24 B. Bodo, S. Rebuffat, M. El Hajji and D. Davoust, *J. Am. Chem. Soc.*, 107 (1985) 6011.
25 K. K. Unger and K. D. Lork, *European Chromatogr. News*, 2 (1988) 14.
26 B. Pfleiderer, K. Albert, K. D. Lork, K. K. Unger, H. Brückner and E. Bayer, *Angew. Chem., Int. Ed. Engl.*, 28 (1989) 327.
27 G. Vigh and Z. Varga-Puchony, *J. Chromatogr.*, 196 (1980) 1.
28 D. Morel, J. Serpinet, J. M. Letoffe and P. Claudy, *Chromatographia*, 22 (1986) 103.
29 R. K. Gilpin and M. E. Gangoda, *Anal. Chem.*, 56 (1984) 1470.
30 D. Morel and J. Serpinet, *12th International Symposium on Column Liquid Chromatography, Washington, DC, June 1988.*
31 W. S. Hancock, D. R. Knighton, J. R. Napier, D. R. K. Harding and R. Venable, *J. Chromatogr.*, 367 (1986) 1.
32 M. T. W. Hearn, M. I. Aguilar and A. W. Purcell, *J. Chromatogr.*, in press.
33 H. Colin and G. Guiochon, *J. Chromatogr.*, 158 (1978) 183.
34 H. Lauffer, *Entropy-Driven Processes in Biology*, Springer Verlag, Berlin, 1975.
35 W. S. Hancock, D. R. Knighton and D. R. K. Harding, *Peptides 1984*, Almquist and Wiksell, Stockholm, 1984, p. 145.

Journal of Chromatography, 476 (1989) 147–158
Elsevier Science Publishers B.V., Amsterdam — Printed in The Netherlands

CHROMSYMP. 1590

SODIUM DODECYL SULPHATE–PROTEIN COMPLEXES

CHANGES IN SIZE OR SHAPE BELOW THE CRITICAL MICELLE CONCENTRATION, AS MONITORED BY HIGH-PERFORMANCE AGAROSE GEL CHROMATOGRAPHY

ERIK MASCHER and PER LUNDAHL*
Department of Biochemistry, Biomedical Center, University of Uppsala, P.O. Box 576, S-751 23 Uppsala (Sweden)

SUMMARY

We have determined the sodium dodecyl sulphate (SDS) concentration needed to complete the formation of SDS–protein complexes. A Superose-6 column was equilibrated with SDS for 7 h. A sample of a native protein or an SDS–protein complex was applied, and the elution volume, V_e, was determined. Then the SDS concentration, C_{SDS}, was changed, etc., *i.e.*, V_e was determined as a function of C_{SDS}. The critical micelle concentration of SDS (cmc_{SDS}) was 1.8 m*M* in the eluent (ionic strength 0.10 *M*). Native bovine carbonic anhydrase (BCA) formed an SDS complex above 0.2 m*M* SDS. As C_{SDS} was increased, V_e decreased gradually in two main transitions, (TI) at 0.2–1.0 m*M* and (TII) at 1.2–2.0 m*M* SDS. These concentrations are corrected for a lag in the column equilibration with SDS. SDS–BCA, pre-equilibrated at 1.6 m*M* SDS, showed transitions similar to those observed with native BCA, except that transition TII included a minor transition at 2.0–2.2 m*M* SDS. The SDS complexes of reduced and carboxamidomethylated bovine serum albumin, of N-5′-phosphoribosylanthranilate isomerase–indole-3-glycerol-phosphate synthase from *Escherichia coli* (PRAI–IGPS) and of two tryptic fragments of this enzyme behaved similarly. For SDS–PRAI–IGPS the major part of transition TII was completed at 1.6–1.7 m*M* SDS, as shown by analyses after 20-h column equilibrations with increasing as well as decreasing C_{SDS}. The SDS complex of an integral membrane protein, the glucose transporter from human red cells, was smaller or less elongated than the SDS complexes of water-soluble proteins of the same polypeptide length. The formation of all five SDS–protein complexes investigated was practically completed at cmc_{SDS}.

INTRODUCTION

One of the most powerful dissociating and denaturing detergents is sodium *n*-dodecyl sulphate (SDS). In pure water, SDS forms micelles at concentrations above 8 m*M* (refs. 1–3). These are of a spherical, fluctuating shape with an hydrophobic core

0021-9673/89/$03.50

of an average radius of 1.84 nm and they contain 74 SDS molecules each[4]. SDS is widely used in separations of proteins by gel electrophoresis[5–12] and gel chromatography on dextran gel beads[13], large-bead agarose and acrylamide gels[14], controlled-pore glass particles[15,16], silica gel particles[17–22], small- and medium-bead cross-linked agarose gels[23] and a small-bead cross-linked agarose gel[24]. The use of small agarose gel beads enhances resolution and reduces equilibration times, which was important in the present work.

The binding of SDS to proteins has been extensively studied (*cf.*, *e.g.*, refs. 12 and 25–30). Saturation is reported to occur below the critical micelle concentration (cmc) of SDS[12]. Some models for the structure of complexes between proteins and SDS have been proposed: (1) a rod-like particle model[27]; (2) the necklace model, where clusters of SDS are scattered along the free-draining polypeptide chain[30]; (3) a model in which α-helices are present, although parts of the polypeptide form a random coil[31] and (4) the flexible-helix model, in which the polypeptide chain is helically coiled around an alongated SDS micelle, attached by hydrogen bonds between sulphate group oxygens and peptide-bond nitrogen[32]. As early as in 1968–1969 some authors suggested that micellar structures form part of SDS–protein complexes[8,25].

We have studied the changes in the elution volume, V_e, of SDS–protein complexes upon binding or release of SDS by high-performance gel chromatography on a Superose-6 gel. A decrease in V_e with an increase in SDS concentration indicates an increase in size or an elongation of the complexes.

We have used five water-soluble proteins or protein fragments and one integral membrane protein to determine whether a final size and shape of the SDS–protein complex is reached at the cmc of the detergent, and we propose a model for the mechanism of complex formation.

MATERIALS AND METHODS

Materials

SDS was obtained from Merck (Darmstadt, F.R.G.; No. 13760, 'für biochemische Zwecke und Tensiduntersuchungen'). Carbonic anhydrase (No. C-7500) from bovine erythrocytes (BCA), bovine serum albumin (No. A-7030) (BSA), octyl glucoside (*n*-octyl-β-D-glucopyranoside) and dithioerythritol were obtained from Sigma (St. Louis, MO, U.S.A.). SDS complexes of N-5'-phosphoribosylanthranilate isomerase–indole-3-glycerol-phosphate synthase (PRAI–IGPS)[33,34] and of two tryptic fragments of this protein[33] were kindly provided by K. Kirschner and H. Szadkowski, Biozentrum, Basel, Switzerland (*cf.*, Discussion). Unless stated otherwise chemicals were of analytical grade. Human red cell concentrate (4–5 weeks old) was supplied by the Blood Bank of the University Hospital, Uppsala, Sweden. All solutions were passed through 0.2-μm filters (Sartorius, Göttingen, F.R.G.; SM 11107) and simultaneously degassed.

Methods

High-performance gel chromatography. High-performance gel chromatography experiments were performed with a prepacked 22-ml (28 cm × 1.0 cm) column of Superose-6 (V_o = 8.2 ml, V_t = 22.2 ml) for medium-pressure (0.5 MPa) chromatography at a flow-rate of 0.30 ml/min. This column was connected to two precision

pumps (P-500), a mixer, a sample injection valve (V-7) and an UV monitor set at 280 nm (UV-1). This system was controlled from a gradient programmer (GP-250) and an automatic injector (ACT-100). All these components were provided by Pharmacia LKB Biotechnology (Uppsala, Sweden). The same column was used for several hundreds of analyses, including those in refs. 24, 35 and 36. The samples were applied to the Superose-6 column from a 25- (Figs. 1–3, 6) or a 50-μl loop (Fig. 4). Unless otherwise stated, the column was equilibrated with SDS for 6.8 h with 122 ml of the eluent before sample application. The SDS concentration was changed in 0.2-m*M* increments at intervals of 8 h. The elution or retention volume, V_e, was determined by measuring the distance between the application mark and the peak maximum on the chart paper (speed, 2 mm/min) with a precision of ± 0.2 mm, *i.e.*, ± 0.2% or ± 30 μl at V_e = 15 ml. It was corrected for the sample volume. All column chromatography experiments were performed at 22.0–24.0°C.

Eluent. The eluent for gel chromatography was 50 m*M* sodium phosphate, pH 6.86, 1 m*M* Na_2EDTA, 0.2 m*M* dithioerythritol and 3.1 m*M* NaN_3 (solution W) with addition of SDS. Solution W was prepared by mixing equal volumes of 0.2 *M* Na_2HPO_4 and 0.2 *M* NaH_2PO_4 and then adding the other components and water, resulting in pH 6.86. In solution W (ionic strength, 0.10 *M*) the cmc of SDS is approximately 1.85 m*M* at 25°C (ref. 37), as determined by the drop number method, which corresponds to 1.80 m*M* at 23°C according to the temperature dependence graph, reported by Becker *et al.*[28]. There is a strong consensus for a cmc value of 1.76–1.80 m*M* at 22°C (dye solubilization measurements[39] and our unpublished light-scattering and electric conductivity data). The critical micelle temperature can be estimated as 20°C at the ionic strength of 0.10 *M* (*cf.*, ref. 40).

The chosen SDS concentrations in the eluent were obtained by automatic mixing of (A) solution W with appropriate fractions of (B) solution W containing 10.0 ± 0.4 m*M* SDS. The SDS concentration in (B) was checked by automated sulphur analysis[41,42] at the Department of Chemistry, Uppsala University, Uppsala. Briefly, the samples were freeze-dried and subjected to Schöniger flask combustion; the sulphite and the sulphur dioxide were converted into sulphate; the sulphate was reduced to sulphide by hydriodic and hypophosphorous acid in acetic acid solution, and the sulphide was treated with *p*-aminodimethylaniline and ferric iron to form methylene blue, which was determined photometrically.

Samples

Native carbonic anhydrase. BCA was dissolved in solution W to a concentration of 1 mg/ml and passed through a 0.2-μm Acrodisc-13 filter (Gelman Sciences, Ann Arbor, MI, U.S.A.). The BCA sample contained minor impurities of M_r 14 000–24 000, as judged by SDS-gel electrophoresis (not shown). BCA (M_r 29 000) contains Zn^{2+} but no disulphide bridge.

SDS–BCA. BCA (20 mg) was dissolved, together with 41.2 mg SDS, in 2 ml of solution W and was equilibrated with 1.6 m*M* SDS in solution W (W1.6) by passage through a 59 cm × 2.6 cm column of Sephacryl S-300 HR (Pharmacia LKB Biotechnology). This column had been equilibrated for 20 h with six column volumes of W1.6. The final BCA concentration was 1 mg/ml.

SDS–BSA. A 30-mg amount of BSA was reduced with 20 m*M* dithioerythritol for 5 min at 95°C, together with 65.8 mg SDS, in 2 ml of solution W. The protein was

then carboxamidomethylated and equilibrated with 1.6 m*M* SDS on a Sephacryl S-300 HR column as above. The product is denoted as SDS–RCAM-BSA. Native BSA (M_r 66 200) contains seventeen disulphides.

SDS–PRAI–IGPS and two fragments of this enzyme. Deuterated PRAI–IGPS (M_r 49 500, ref. 33) as well as two tryptic fragments of this protein (M_r 32 000 and 17 500, ref. 33) were dissolved with 1.6 mg SDS per mg protein in W1.6 and equilibrated, first by dialysis and then by gel chromatography on a Sephacryl S-300 column with 1.6 m*M* SDS (No. 10807 3J, AnalaR from BDH Chemicals, Poole, U.K.), otherwise as above. These preparations were made by K. Kirschner and H. Szadkowski (Biozentrum, Basel) (*cf.*, Discussion). PRAI–IGPS consists of two domains with triose-phosphate isomerase (TIM)-barrel structures[34]. The enzyme contains no disulphide[34].

Glucose transporter. Integral membrane proteins from human red cells were prepared as described earlier[43] and were solubilized at an initial protein concentration of 8 mg/ml with 75 m*M* octyl glucoside[36]. The glucose transporter (GT), as a complex with octyl glucoside, was then purified by fractionation of the solubilized integral membrane proteins on DEAE-cellulose (No. DE-52 from Whatman Bio-Systems, Maidstone, U.K.), in the presence of 75 m*M* octyl glucoside. This results in a preparation that probably contains mainly native GT monomers[35,36]. The final protein concentration was *ca.* 0.8 mg/ml (ref. 36).

The sample was kept on ice during the whole series of gel chromatography experiments. As in all other experiments, the Superose-6 column was kept at 22.0–24.0°C.

The GT is an heterogeneously glycosylated integral membrane protein with a polypeptide M_r of about 54 100 (*cf.*, ref. 44). Possibly, it contains twelve membrane-spanning α-helices and six cysteine residues (*cf.*, refs. 44 and 45). Cys 429 is exofacial[46], Cys 207 is endofacial[46] and Cys 347 is probably exposed at a binding site for glucose[46,47]. Two of the three remaining cysteine residues (Nos. 133, 201 and 421) might form a disulphide, although, to our knowledge, there is no evidence for this.

RESULTS

Accuracy and precision. In all of the gel chromatography experiments except those illustrated in Fig. 4 (below), the equilibration time before sample application was 6.8 h. The equilibration was not complete; a series of analyses with increasing SDS concentrations gave larger elution volumes than did a series with decreasing SDS concentrations (Fig. 1). The graphs in Fig. 1 indicate a lag in SDS monomer concentration of about 0.22 m*M*. This value was used to correct the SDS concentration scales in Figs. 2, 3 and 6 (below) for increasing as well as decreasing concentrations. Fig. 4 illustrates similar experiments with a much longer equilibration time, 20.5 h. In this case, the lag in SDS monomer concentration was 0.06 m*M* (see below).

The reproducibility of V_e, in different series of experiments, was ± 50 μl, similar to the precision of ± 30 μl in individual V_e values (see Methods). V_e ± 50 μl corresponds to K_d ± 0.7% (at K_d = 0.5) or M_r ± 300 (*cf.*, Fig. 5, below).

Carbonic anhydrase. Native BCA (N) bound SDS only at SDS concentrations above 0.2–0.3 m*M* (Fig. 2, *cf.* ref. 48). The graph of V_e for BCA as a function of increasing SDS concentrations showed two distinct transitions (TI, from N to CI; TII, from CI to CII, in Fig. 2).

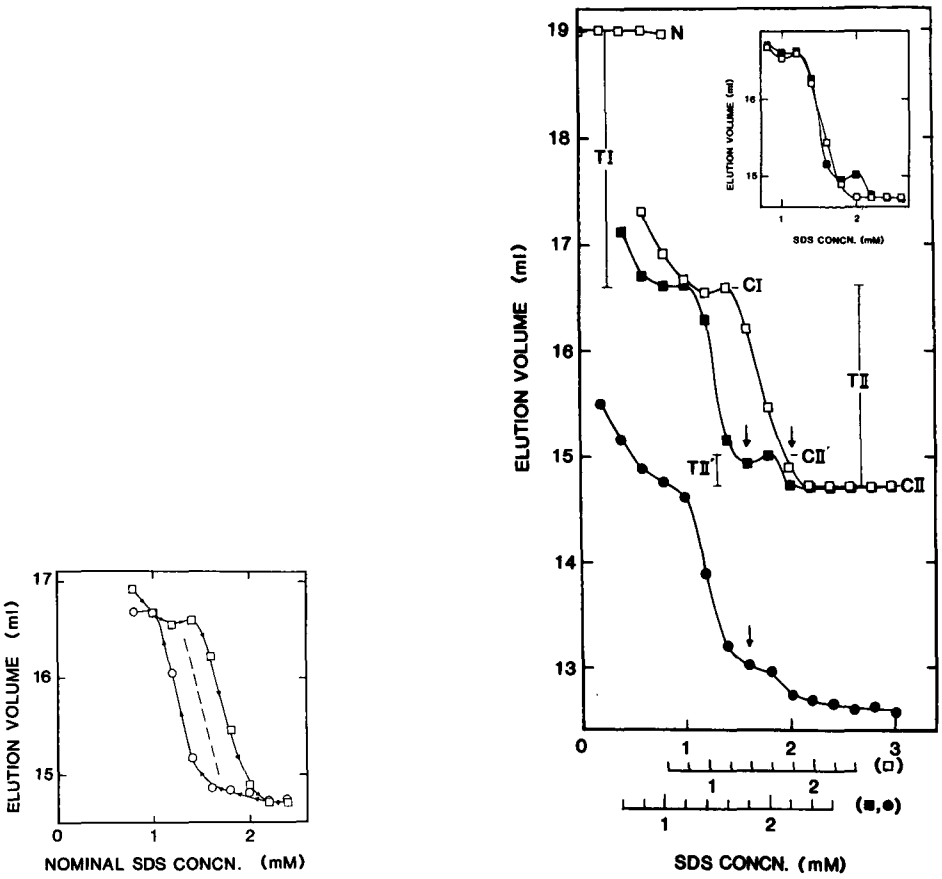

Fig. 1. Elution volumes for BCA upon high-performance gel chromatography on Superose-6 in the presence of SDS. Native enzyme was applied to the column (protein amount 12 μg). The SDS concentration in the eluent was either increased (□) or decreased (○) in steps of 0.2 m*M* SDS, at intervals of 8 h. The elution volumes observed at the same nominal SDS concentration differ, due to a lag in the column equilibration with SDS. The hatched line indicates the expected position of the graph at complete column equilibration. The displacement is ± 0.22 m*M* SDS. This value was used to correct the nominal SDS concentrations in later experiments (Figs. 2, 3 and 6).

Fig. 2. Elution volumes for native BCA (□) and SDS-denatured BCA (■) and reduced and carboxamidomethylated bovine serum albumin (RCAM-BSA) (●) upon high-performance gel chromatography on Superose-6 as a function of the SDS concentration in the column. SDS–BCA and SDS–RCAM-BSA were analyzed together. The SDS concentration was increased (□) or decreased (■, ●) as in Fig. 1. The corresponding corrected SDS concentration scales (*cf.*, Fig. 1) are given below the nominal scale and the cmc for SDS is indicated (arrows). The denatured proteins were equilibrated with 1.6 m*M* SDS before application to the Superose-6 column. Sample amount: 12 μg of each protein. Elution volumes for native BCA (N) as well as for the SDS complexes of BCA (CI, CII' and CII) are indicated as are the corresponding transitions (TI, TII' and TII). Insert: the graphs for native BCA (□) and SDS–BCA (■) plotted *vs.* the corrected SDS concentrations (see above).

Two main types of SDS–BCA complexes thus exist, one (CI) at 1.0–1.2 m*M* detergent (Fig. 2, corrected scale) and another (CII) above 2 m*M* SDS. At SDS concentrations from 1.2 to 2.0 m*M* the small-size complex, CI, was gradually converted into the large-size complex, CII (Fig. 2).

When a SDS–BCA complex (in equilibrium with 1.6 m*M* SDS, see Methods) was chromatographed on the Superos-6 column (with decreasing SDS concentrations) the V_e was constant between 2.8 and 2.2 m*M* detergent (Fig. 2, corrected scale). A minor transition, TII′ (from complex CII to complex CII′) was observed between 2.2 and 2.0 m*M* SDS. Below 1.8 m*M* SDS, the V_e increased with decreasing concentrations of SDS to 1.2 m*M* SDS and also below 0.9 m*M* (Fig. 2). The BCA and SDS–BCA graphs for increasing and decreasing SDS concentrations partly coincided when the V_e values were plotted against the corrected SDS concentrations (Fig. 2, insert; *cf.*, Fig. 1). The uptake of SDS by proteins or release of SDS from SDS–protein complexes thus occurred practically instantaneously on the column for the small protein amounts that were applied. At low SDS concentrations the SDS–BCA was not eluted. Probably, the polypeptides became entangled in the agarose gel matrix during refolding upon removal of the detergent from the complex. When the SDS concentration was increased, the protein was released and eluted (not shown).

Bovine serum albumin. The SDS–RCAM-BSA complex showed a two- or three-step increase in V_e with decreasing SDS concentrations (Fig. 2), as did the SDS–BCA complex. The 'plateau' regions, corresponding to complexes CI, CII and CII′, were not as distinct as for BCA. The V_e of the SDS–RCAM-BSA complex increased somewhat from 3 m*M* SDS to the cmc (*cf.*, ref. 12). The steepest increase was between 1.6 and 1.2 m*M* SDS, similar to the case of SDS–BCA (transition TII, Fig. 2, corrected scale).

The transition TII obviously corresponds to the steep change in binding of the detergent to the RCAM-BSA between 1.2 and 1.5 m*M* SDS as well as to the dramatic decrease in distribution coefficient on Sepharose 6B between 1.1 and 1.7 m*M* SDS, reported by Takagi *et al.*[12].

At low SDS concentrations the SDS–BSA was not eluted. This was also the case for SDS–BCA (see above).

N-5′-Phosphoribosylanthranilate isomerase–indole-3-glycerol-phosphate synthase. The SDS–PRAI–IGPS complex (equilibrated with 1.6 m*M* SDS) showed a considerable decrease in V_e on the Superose-6 column from about 0.4 to 1.4 m*M* detergent, whereas the decrease in V_e above 1.6 m*M* SDS was small (Fig. 3, corrected scale). The graph for the SDS complex of the large tryptic fragment (L) of PRAI–IGPS was similar, with a 'plateau' at about 0.8 m*M* SDS. The small tryptic fragment (S) showed a more gradual decrease in V_e for its SDS complex (Fig. 3). At 0.9 m*M* SDS the SDS complexes of L and S were eluted at the same V_e but had probably reached different stages of SDS binding. SDS-polyacrylamide gel electrophoresis (not shown) confirmed that the graphs do not cross each other at this point. At a corrected SDS concentration of 0.3 m*M*, the resolution of PRAI–IGPS and the fragments was lost, maybe due to re-association of the fragments, although this does not occur when the SDS is completely removed[33]. At other SDS concentrations, the components were well separated (*cf.*, Fig. 3, insert).

In a final series of experiments with PRAI–IGPS, the SDS concentration was increased in 0.2-m*M* steps, as earlier, and the column was equilibrated for 20.5 h with

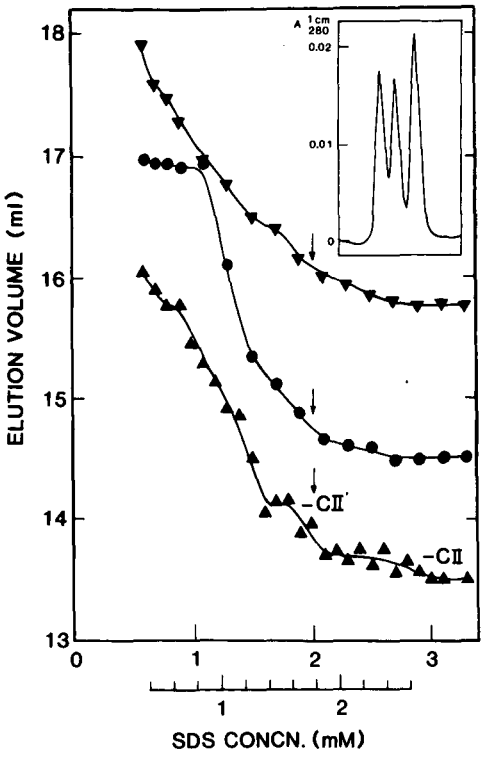

Fig. 3. Elution volumes for SDS complexes of PRAI–IGPS and of two tryptic fragments of this enzyme upon gel chromatography as in Fig. 2. (▲) PRAI–IGPS; (●) fragment of M_r 32 000 and (▼) fragment of M_r 17 500. The protein and the fragments were equilibrated with 1.6 m*M* SDS before application to the Superose-6 column. The SDS concentration was increased stepwise, and all three components were applied (8 μg of each) in a single sample at 0.7, 0.9... m*M* SDS. SDS–PRAI–IGPS alone was also applied (12 μg) in a separate series of analyses at 0.6, 0.8... m*M* SDS. A corrected SDS concentration scale is given as in Fig. 2. The elution volumes corresponding to the SDS complexes CII' and CII (*cf.* Fig. 2) for PRAI–IGPS are indicated. The cmc for SDS is indicated (arrows) using the corrected SDS concentration scale. Insert: gel chromatogram, illustrating the separation of the components at the nominal SDS concentration of 2.9 m*M*.

369 ml eluent before chromatography (Fig. 4). Also, the eluted material (SDS–PRAI–IGPS) was collected and rechromatographed, 2.5 h after the first sample application, at the same SDS concentration as used for the first chromatogram. The experiments were repeated with decreasing SDS concentrations. This time-consuming procedure resulted in an accurate determination of V_e *vs.* SDS concentration for SDS–PRAI–IGPS (Fig. 4). The lag in column equilibration with monomeric SDS was 0.06 m*M*. The equilibration with micellar SDS was slower. The results show that the SDS–PRAI–IGPS complex has nearly reached a final conformation at 1.6–1.7 m*M* SDS in our eluent. There is a minor transition at 1.7–2.4 m*M* SDS (or 1.9–2.2 m*M* SDS, as corrected for the micellar equilibration lag in Fig. 4).

A gradual slope of V_e *vs.* SDS concentration is also observed above the cmc (*cf.*, ref. 24). This might either reflect additional uptake of SDS or an interference of the

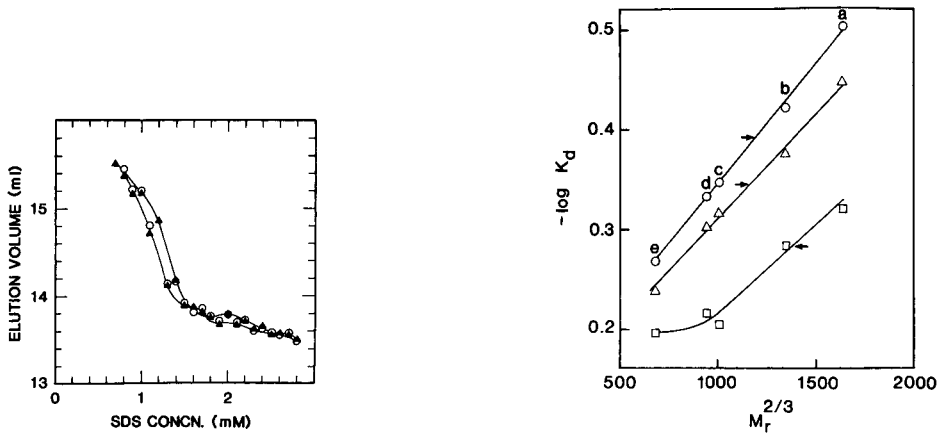

Fig. 4. Elution volumes for SDS–PRAI–IGPS (*cf.*, Fig. 3) on Superose-6 as a function of the SDS concentration. The column was equilibrated at each chosen SDS concentration for 20.5 h before sample application. The SDS concentration was changed in 0.2-m*M* steps at intervals of 24 h. (▲) SDS–PRAI–IGPS (50 μg) applied at an equilibration concentration of 1.6 m*M* SDS and collected. (○) Rechromatography of an aliquot of the collected SDS–PRAI–IGPS (2 μg). The analyses were carried out at increasing (0.8, 1.0... m*M*) as well as decreasing (2.7, 2.5... m*M*) SDS concentrations.

Fig. 5. Calibration diagram for SDS complexes of water-soluble proteins: $-\log K_d = f(M_r^{2/3})$ (see refs. 23 and 49), where $K_d = (V_e - 8.2)/14$, V_e in ml. The V_e values are taken from Figs. 2, 3 and 6. Corrected SDS concentrations: (○) 2.8; (△) 1.6; (□) 0.8 m*M*. The proteins were: (a) SDS–RCAM–BSA (M_r 66 200); (b) SDS–PRAI–IGPS (49 500); (c) SDS–PRAI–IGPS large fragment (32 000); (d) SDS–BCA (29 000); (e) SDS–PRAI–IGPS small fragment (17 500). The arrows denote the $-\log K_d$ values for SDS–GT.

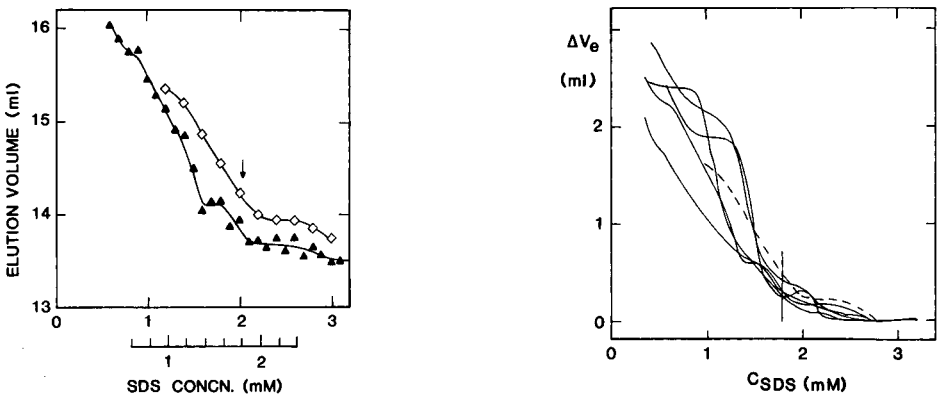

Fig. 6. Elution volumes for one amphiphilic and one water-soluble protein upon high-performance gel chromatography on Superose-6 as a function of the SDS concentration in the eluent. (◇) GT from human red cells, applied as an octyl glucoside complex (protein amount, 20 μg), and (▲) SDS–PRAI–IGPS (data from Fig. 3). The arrow denotes the cmc of SDS. Corrected SDS concentration scale as in Fig. 2.

Fig. 7. Comparison of the graphs for the SDS–protein complexes shown in Figs. 2, 3 and 6. The formation of the complexes was considered to be completed at the corrected SDS concentration, C_{SDS}, of 2.8 m*M* ($\Delta V_e = 0$). Hatched line: the glucose transporter. The vertical line indicates the cmc for SDS in the 0.10 *M* ionic strength eluent.

SDS micelles with the gel chromatography process. The equilibration of the column with SDS micelles is slow, due to the minimal micelle concentration gradients through the gel beads and the large micelle size.

The calibration diagrams, constructed from the V_e values for the above proteins at 2.8, 1.6 and 0.8 m*M* SDS, are shown in Fig. 5. The saturated complexes at 2.8 m*M* SDS as well as the nearly saturated ones at 1.6 m*M* SDS gave linear calibration graphs of $-\log K_d$ *vs.* $M_r^{2/3}$ (*cf.*, refs. 23 and 49), whereas the corresponding graph for non-saturated complexes (at 0.8 m*M* SDS) is non-linear. The calibration line for the complexes at 2.8 m*M* SDS shows the best fit to the points.

Glucose transporter. Purified human red cell glucose transporter (GT) in a complex with octyl glucoside was applied to the Superose-6 column, which had been equilibrated with given concentrations of SDS, as above. The V_e of the SDS–GT complex decreased steeply with the increase in SDS concentration between 1.0 and 2.0 m*M* SDS (Fig. 6, corrected scale). Above 2.4 m*M* SDS, a further small decrease was observed.

The amphiphilic GT shows the low apparent M_r of 40 000 (Fig. 5, 2.8 m*M* SDS) or, at high ionic strength, 37 000 (ref. 24). Its true polypeptide M_r is about 54 000 (*cf.*, ref. 43). The GT molecules also contain an oligosaccharide of heterogeneous size, representing up to 17% of the total weight[50]. The size of the SDS–GT complex is smaller (the V_e is larger) than that of the water-soluble enzyme PRAI–IGPS (M_r 49 500, ref. 33) over the range 1.0–2.8 m*M* SDS (Fig. 6).

DISCUSSION

The transition TII, in the formation of SDS–protein complexes, excluding transition TII′, became complete at or somewhat below cmc = 1.8 m*M* SDS for BCA, BSA and PRAI–IGPS. For the tryptic fragments of PRAI–IGPS and for GT the 'end-points' of the transitions were less distinct, but the increase in V_e was small above the cmc (see Figs. 2, 3 and 6).

For comparison of the proteins, the graphs from Figs. 2, 3 and 6 are shown together in Fig. 7. All of the proteins or fragments show a steep decrease in V_e with increasing SDS concentration up to the cmc, and a further small and gradual decrease above the cmc (Fig. 7). We have shown earlier that further, minor transitions may occur at much higher SDS concentrations[24], possibly as a result of slightly increased monomer concentrations. In addition, SDS micelles may affect the gel chromatography process. The final SDS–protein size was approached rapidly far below the cmc, during transition TII (Fig. 7; *cf.*, Fig. 2). At this stage, the SDS binding is probably a cooperative process (*cf.*, ref. 51), and interactions other than the hydrophobic effect may contribute to the stability of the complex. Hydrogen bonding between the peptide-bond nitrogens and oxygens of the sulphate group of the SDS molecules is a candidate for a stability-enhancing interaction below cmc[32].

A complex between a water-soluble protein and SDS is formed upon binding of SDS monomers to the protein. We propose that this process takes place as described below.

(1) The dodecyl chains of the detergent penetrate the surface of the protein and come into contact with the hydrophobic interior of the protein or the protein domains. (2) Polypeptide segments from the interior of the protein or protein domain become

displaced toward the surface of the complex, since they are less hydrophobic than the dodecyl chains. Many SDS molecules become locked in an inserted position by ion-pair formation and, mainly, by hydrogen bonding (*cf.*, ref. 32). (3) The increased hydrophobicity enables more SDS molecules to become included in the complex until a spherical SDS micelle is completed, around which the polypeptide is wound. (4) Any length of the polypeptide that, for steric reasons, cannot be accommodated in direct contact with this micelle forms the core for growth of another protein-covered micelle. This process is repeated until the whole polypeptide is coiled around adjacent SDS micelles that are linked with short polypeptide segments.

The proposal that adjacent, protein-decorated, spherical micelles are formed, rather than a cylindrical structure[32], is based on preliminary small-angle neutron scattering data for deuterated PRAI–IGPS in a complex with SDS at an equilibrium concentration of 1.6 m*M* SDS[52]. A report by Mazer *et al.* indicates that very elongated SDS micells are formed at an ionic strength of 0.3–0.6 *M*, but not at 0.10 *M*, which we have used. The above preliminary neutron scattering results have been confirmed and refined[53].

The mechanism for the formation of SDS–protein complexes proposed above is consistent with our present gel chromatography data. Transition TI (Fig. 2) may correspond to the initial swelling and rearrangement of the protein (1 and 2, above), whereas transition TII may correspond to the final formation of one or more protein-covered micells (3 and 4, above).

The glycosylated GT (polypeptide M_r 54 100) was eluted at a relatively large volume. The transporter may contain a single disulphide bridge. However, the small size of the SDS–GT complex is probably ascribable to the presence of hydrophobic α-helices in the protein (*cf*, ref. 44). Several of these α-helices may well travers the SDS micelle(s) in the complex, consistent with the flexible helix model[32] and with the neutron scattering results (see above). Reduced and deglycosylated GT polypeptide migrates as a water-soluble protein of M_r 45 000 (ref. 54) or 46 000 (ref. 55) in SDS gel electrophoresis, and this also indicates a compact structure for the complex.

However, the SDS–GT complex is eluted at a smaller V_e (13.75 ml at 2.8 m*M* SDS, see Fig. 6) than is the octyl glucoside complex (16.8 ml at 50 m*M*, ref. 35) or 16.1 ml at 75 m*M*, ref. 36, octyl glucoside) and is thus larger or more elongated than the octyl glucoside–GT complex. The V_e for the SDS–GT complex corresponds to that of a native globular protein of M_r 320 000 (calibration not shown).

CONCLUSION

The time needed for equilibration of a Superose-6 column with SDS monomers to within 0.06 m*M* of the desired concentration is long: at least 20 h for 0.2-m*M* increments. Equilibration with SDS micelles is slower. The observed changes in V_e for SDS–protein complexes in gel chromatography experiments as the SDS concentration in the column is changed indicate that the complexes have nearly reached their final shape and size, corresponding to saturation with SDS, at the cmc of the detergent. We observed two major transitions and an intermediate complex. The first transition may correspond to an uptake of SDS monomers with a displacement of protein segments from the hydrophobic interior of the protein by the dodecyl chains of the detergent monomers and the second transition to the formation of one or more detergent micelle(s) surrounded by the polypeptide.

An integral membrane protein showed a more compact complex than a water-soluble one of the same molecular weight, probably due to the incorporation of hydrophobic α-helices in one or more hydrophobic core(s) of the complex.

NOTE ADDED IN PROOF

Recent data from our laboratory indicate that the slow equilibration of Superose-6 with SDS at low SDS concentrations is partly related to adsorption of SDS to the cross-linked agarose gel matrix.

ACKNOWLEDGEMENTS

We are grateful to Kasper Kirschner and Halina Szadkowski (Biozentrum, Basel), for kindly providing the preparations of SDS–PRAI–IGPS and SDS–PRAI–IGPS fragments and, together with Konrad Ibel and Roland May (Institut Laue-Langevin, Grenoble), for valuable discussions as well as for permission to refer to preliminary neutron scattering data. We also thank Eva Greijer for valuable assistance and Hans Lindblom as well as Kurt Andersson (Pharmacia LKB Biotechnology, Uppsala) for the loan of an automatic sample application system. This work was supported by the Swedish Natural Science Research Council and the O.E. and Edla Johansson Science Foundation.

REFERENCES

1 K. J. Mysels and L. H. J. Princen, *J. Phys. Chem.*, 63 (1959) 1696.
2 P. Mukerjee and K. J. Mysels, in *Critical Micelle Concentrations of Aqueous Surfactant Systems*, National Bureau of Standards, NSRDS-NBS 36, Washington, D.C., 1971.
3 A. Helenius, D. R. McCaslin, E. Fries and C. Tanford, *Methods Enzymol.*, 56 (1979) 734.
4 B. Cabane, R. Duplessix and T. Zemb, *J. Physique*, 46 (1985) 2161.
5 A. L. Shapiro, E. Vinuela and J. V. Maizel, Jr., *Biochem. Biophys. Res. Commun.*, 28 (1967) 815.
6 J. V. Maizel, Jr., in K. Habel and N. P. Salzman (Editors), *Fundamental Techniques in Virology*, Academic Press, New York, 1969, p. 334.
7 K. Weber and M. Osborn, *J. Biol. Chem.*, 244 (1969) 4406.
8 A. K. Dunker and R. R. Rueckert, *J. Biol. Chem.*, 244 (1969) 5074.
9 D. M. Neville, Jr., *J. Biol. Chem.*, 246 (1971) 6328.
10 J. V. Maizel, Jr., in K. Maramorosch and H. Koprowski (Editors), *Methods in Virology*, Academic Press, New York, 1971, p. 179.
11 K. Weber and M. Osborn, in H. Neurath and R. L. Hill (Editors), *The Proteins*, Vol. 1, Academic Press, New York, 3rd ed., 1975, p. 179.
12 T. Takagi, K. Tsujii and K. Shirahama, *J. Biochem. (Tokyo)*, 77 (1975) 939.
13 M. Pagé and C. Godin, *Can. J. Biochem.*, 47 (1969) 401.
14 W. W. Fish, J. A. Reynolds and C. Tanford, *J. Biol. Chem.*, 245 (1970) 5166.
15 R. C. Collins and W. Haller, *Anal. Biochem.*, 54 (1973) 47.
16 R. J. Blagrove and M. J. Frenkel, *J. Chromatogr.*, 132 (1977) 399.
17 T. Imamura, K. Konishi, M. Yokoyama and K. Konishi, *J. Biochem. (Tokyo)*, 86 (1979) 639.
18 Y. Kato, K. Komiya, H. Sasaki and T. Hashimoto, *J. Chromatogr.*, 193 (1980) 29.
19 T. Takagi, K. Takeda and T. Okuno, *J. Chromatogr.*, 208 (1981) 201.
20 T. Takagi, *J. Chromatogr.*, 219 (1981) 123.
21 T. Konishi, *Methods Enzymol.*, 88 (1982) 202.
22 B. B. Gupta, *J. Chromatogr.*, 282 (1983) 463.
23 K.-O. Eriksson, *J. Biochem. Biophys. Methods*, 11 (1985) 145.

24 E. Mascher and P. Lundahl, *Biochim. Biophys. Acta*, 856, (1986) 505.
25 R. Pitt-Rivers and F. S. A. Impiombato, *Biochem. J.*, 109 (1968) 825.
26 J. A. Reynolds and C. Tanford, *Proc. Natl. Acad. Sci. U.S.A.*, 66 (1970) 1002.
27 J. A. Reynolds and C. Tanford, *J. Biol. Chem.*, 245 (1970) 5161.
28 C. A. Nelson, *J. Biol. Chem.*, 246 (1971) 3895.
29 P.-F. Rao and T. Takagi, *Anal. Biochem.*, 174 (1988) 251.
30 K. Shirahama, K. Tsujii and T. Takagi, *J. Biochem. (Tokyo)*, 75 (1974) 309.
31 W. L. Mattice, J. M. Riser and D. S. Clark, *Biochemistry*, 15 (1976) 4264.
32 P. Lundahl, E. Greijer, M. Sandberg, S. Cardell and K.-O. Eriksson, *Biochim. Biophys. Acta*, 873 (1986) 20.
33 K. Kirschner, H. Szadkowski, A. Henschen and F. Lottspeich, *J. Mol. Biol.*, 143 (1980) 395.
34 J. P. Priestle, M. G. Grütter, J. L. White, M. G. Vincent, M. Kania, E. Wilson, T. S. Jardetzky, K. Kirschner and J. N. Jansonius, *Proc. Natl. Acad. Sci. U.S.A.*, 84 (1987) 5690.
35 E. Mascher and P. Lundahl, *J. Chromatogr.*, 397 (1987) 175.
36 E. Mascher and P. Lundahl, *Biochim. Biophys. Acta*, 945 (1988) 350.
37 T. Takagi, K. Kubo and T. Isemura, *Biochim. Biophys. Acta*, 623 (1980) 271.
38 R. Becker, A. Helenius and K. Simons, *Biochemistry*, 14 (1975) 1835.
39 K. Kirschner, personal communication.
40 N. A. Mazer, G. B. Benedek and M. C. Carey, *J. Phys. Chem.*, 80 (1976) 1075.
41 L. Gustafsson, *Talanta*, 4 (1960) 227.
42 L. Gustafsson, *Talanta*, 4 (1960) 236.
43 P. Lundahl, E. Greijer, S. Cardell, E. Mascher and L. Andersson, *Biochim. Biophys. Acta*, 855 (1986) 345.
44 M. Mueckler, C. Caruso, S. A. Baldwin, M. Panico, I. Blench, H. R. Morris, W. J. Allard, G. E. Lienhard and H. F. Lodish, *Science (Washington, D.C.)* 229 (1985) 941.
45 S. A. Baldwin, J. M. Baldwin and G. E. Lienhard, *Biochemistry*, 21 (1982) 3836.
46 R. E. Abbott and D. Schachter, *Mol. Cell. Biochem.*, 82 (1988) 85.
47 A. R. Walmsley, *Trends Biochem. Sci.*, 13 (1988) 226.
48 J. Steinhardt and J. A. Reynolds, in *Multiple Equilibria in Proteins*, Academic Press, New York, 1970.
49 S. Hjertén, *J. Chromatogr.*, 50 (1970) 189.
50 D. C. Sogin and P. C. Hinkle, *J. Supramol. Struct.*, 8 (1978) 447.
51 M. N. Jones, *Biochem. J.*, 151 (1975) 109.
52 K. Kirschner, P. Lundahl, K. Ibel and R. May, *Report: Low-Resolution Structure of Protein–SDS Complexes,* Institut Max von Laue-Paul Langevin, Grenoble, 1988.
53 K. Ibel, R. May, K. Kirschner, H. Szadkowski and P. Lundahl, unpublished work.
54 F. Y. P. Kwong, S. A. Baldwin, P. R. Scudder, S. M. Jarvis, M. Y. M. Choy and J. D. Young, *Biochem. J.*, 240 (1986) 349.
55 G. E. Lienhard, J. H. Crabb and K. J. Ransome, *Biochim. Biophys. Acta*, 769 (1984) 404.

Journal of Chromatography, 476 (1989) 159–163
Elsevier Science Publishers B.V., Amsterdam — Printed in The Netherlands

CHROMSYMP. 1602

PROTEIN CONFORMATION CHANGES AS THE RESULT OF BINDING TO REVERSED-PHASE CHROMATOGRAPHY COLUMN MATERIALS

A. F. DRAKE, MICHELLE A. FUNG* and C. F. SIMPSON
Chemistry Department, Birkbeck College, University of London, 20 Gordon Street, London WC1H OAJ (U.K.)

SUMMARY

The conformational changes of the protein α-chymotrypsinogen which may take place on reversed-phase chromatographic material of differing hydrocarbon chain lengths *e.g.* C_4, C_6, C_8, C_{10} and phenyl, have been studied by circular dichroism as a function of 1-propanol concentration and pH of the solvent before and after binding to the reversed-phase material.

INTRODUCTION

Bovine chymotrypsinogen A is a pancreatic protein and is the inactive precursor of the chymotrypsin family. It is composed of 245 amino acid residues, arranged in a single polypeptide chain, cross-linked by five disulphide bridges. With the exception of a ten-residue segment of α-helix at the C-terminus, the overall folding of the polypeptide chain is very similar to α-chymotrypsin. The backbone chain is more or less fully extended and often doubles back on itself to form large sections of distorted anti-parallel pleated sheets[1].

Circular dichroism (CD) provides a convenient non-invasive and non-destructive method of determining the secondary structure of proteins. Accordingly, we have been successful in using this technique to assess the influence of the chromatographic eluent (1-propanol)[2] and pH on the secondary structure of α-chymotrypsinogen. UV and CD measurements have also been used to monitor solutions of the protein before and after binding to several reversed-phase materials.

The CD spectrum of a protein can be divided into three main regions[3,4]:

(1) 340–245 nm. Region of the lowest energy where the first π–π^* transition of the aromatic side-chains takes place. In this region some small signals due to the n–σ^* transition of the disulphide (S–S) bonds may also occur. The three major aromatics phenylalanine, tyrosine and tryptophan have fine structure in this area, which aids in their spectroscopic assignment.

(2) 260–220 nm. Region of the second π–π^* transition of the aromatic side-chains and a prominent disulphide-based transition.

(3) 230–185 nm. The characteristic region of the protein back-bone secondary structure (Fig. 1), assuming there are no contributions other than amide n–π^* and π–π^* excitations.

0021-9673/89/$03.50

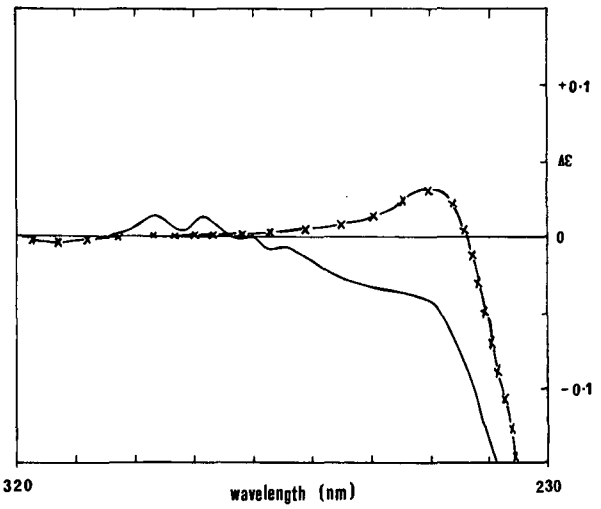

Fig. 1. Circular dichroism spectra of α-chymotrypsinogen. (——) Native protein and 40% 1-propanol; (×—×) protein taken off C_8 column material.

Ordinary absorption spectroscopy in the first region provides a monitor of protein concentration. We have measured CD and UV spectra throughout these regions during every step of our experiments.

Similar studies, using other techniques[2,5] *e.g.* fluorescence, electronic absorption spectroscopy and differential scanning calorimetry under reversed-phase high-performance liquid chromatographic (RP-HPLC) elution conditions, have also led to the proposal that protein conformation changes may occur as the result of variations in the eluent and/or binding of the protein to the stationary phase during HPLC. The observations reported here complement and confirm these findings.

EXPERIMENTAL

Preparation of bonded phases

The 20- and 7μm silica gel was obtained from Phase Sep. (Queensferry, U.K.) and Machery-Nagel (Düren, F.R.G.), respectively. Butyl-, hexyl-, octyl-, decyl- and phenylchlorosilanes were prepared by hydrosilation of the appropriate *n*-alkane (Aldrich, Gillingham, U.K.) with dimethylchlorosilane (Fluka, Glossop, U.K.) in the presence of the catalyst chloroplatinic acid[6] (Johnson Matthey Chemicals, London, U.K.).

The silica gel was dried in an oven at 200°C overnight before use. Before reaction, the apparatus was purged with dry nitrogen. An excess of the appropriate silane reagent was added dropwise to the suspension of silica gel in sodium dried toluene (BDH, Poole, U.K.) and pyridine (BDH). All reactions were refluxed for approximately 6 h. After reaction, the product was filtered and washed with toluene, tetrahydrofuran (THF, BDH), methanol (Fisons, Leics, U.K.) and finally with THF.

Elemental analysis were performed on the prepared bonded phases at the Microanalysis Labs., (University College, London, U.K.). The surface coverages were

TABLE I

CHARACTERISTICS OF THE BONDED PHASES

Alkyl group	*Carbon (%)*	*Surface coverage (μmole/m^2)*
Butyl	7.29	3.509
Hexyl	9.24	3.410
Octyl	12.96	3.970
Decyl	12.00	3.043
Phenyl	8.62	3.250

calculated using the Berendsen and De Galan equation[7]. The results are shown in Table I.

CD measurements

α-Chymotrypsinogen (Sigma, Poole, U.K.) in 0.1 *M* potassium phosphate buffer, pH 5.3 (Fisons) was incubated with C_4, C_6, C_8, C_{10} (20 μm) and phenyl (7 μm) reversed-phase material at the weight ratio of 1:20 (protein to reversed-phase material)[5] for 1 h at 25°C. The reversed-phase material was initially wetted with neat 1-propanol (99+% spectrophotometric grade, Aldrich) and the 1-propanol was subsequently removed from the column material with the buffer by centrifugation for 5 min at 5500 *g*. After the incubation period, the supernatant liquid containing any unbound protein was removed. The bound protein was then removed from the material by incubating with 40% 1-propanol for a further 1 h. UV and CD spectra were taken of the protein before and after binding to the reversed-phase material, using a JASCO J-40CS (Tokyo, Japan) recording spectropolarimeter. In particular, absorbance measurements were used to follow protein concentrations at the various steps.

RESULTS AND DISCUSSION

The CD spectrum of native α-chymotrypsinogen in 0.1 *M* phosphate buffer pH 5.3, is illustrated in Fig. 2. Progressive additions of 1-propanol affect this spectrum only at alcohol concentrations >30% (above 60%, precipitation occurs). A 1-propanol concentration in the range 30–40% induces a change in the β-sheet structure. Only the backbone CD region shows changes upon the addition of 1-propanol. The backbone of the structure appears to be pH-independent. The aromatic groups present in α-chymotrypsinogen are little affected by pH, but the disulphide region is seen to be affected to a small though detectable extent.

The CD of the solution in contact with C_8 column material is shown in Figs. 1 and 3 as the 40% 1-propanol spectrum. It can be clearly seen that the protein is modified after binding and releasing back into solution. The classical β-sheet contribution is enhanced, optical activity associated with the aromatic excitations is lost, and the disulphide CD is drastically changed. Similar results have been observed for the C_4, C_6, C_8, C_{10} and phenyl reversed-phases. We were not able to distinguish differences in the protein conformation between these materials. Thus, it appears that the conformation is independent of the alkyl chain length. Surprisingly, a micellular

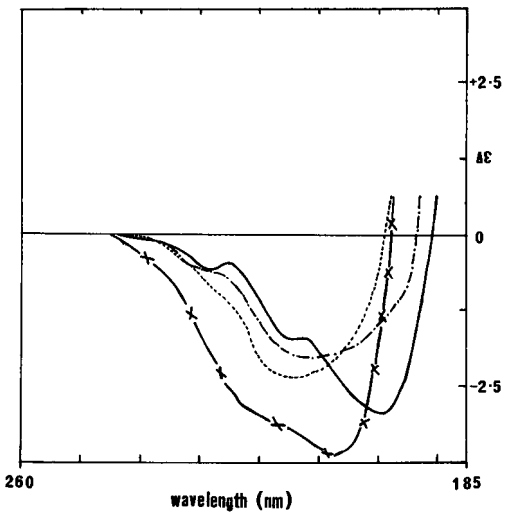

Fig. 2. Circular dichroism spectra of α-chymotrypsinogen. (——) Protein in 0.1 *M* phosphate buffer (pH 5.3); (– · –) protein in 30% 1-propanol; (-----) protein in 60% 1-propanol; (× — ×) protein in sodium dodecyl sulphate.

solution of sodium dodecyl sulphate does not mimic the changes induced by binding to reversed phases, rather, it promotes a 30% α-helical state.

Proteins dissolved in aqueous solution will bind to reversed-phase column materials by hydrophobic interactions. The processes taking place in RP-HPLC separations of proteins involves a complex series of equilibria between protein, surface, solvent and eluent[8–13]. The precise nature of the binding of the protein is not known

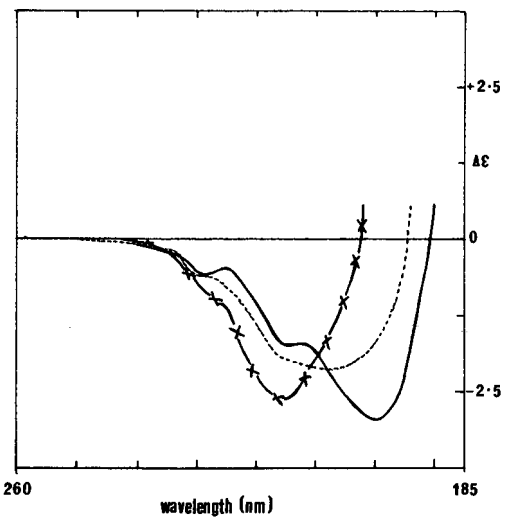

Fig. 3. Circular dichroism spectra of α-chymotrypsinogen. (——) Protein in 0.1 *M* phosphate buffer (pH 5.3); (-----) protein in 40% 1-propanol; (× — ×) protein taken off C_8 column material.

and cannot be determined from the experiments reported in this paper. However, it is possible to suggest the types of interactions which may take place. The hydrocarbonaceous layer of the reversed-phase material could penetrate into the protein's hydrophobic moeities, potentially causing protein conformational changes[8–13], or the reversed-phase material may bind to the hydrophobic moeities on the native protein's surface[14].

1-Propanol may cause a differential weakening of the protein–surface interaction forces and this is primarily responsible for the relative rates of elution of proteins. The amount of organic solvent required to remove proteins from reversed-phase materials varies and this is a function of the extent of the hydrophobic character associated with a particular protein. Thus, a potential mechanism for the desorption of the protein is a competition between the protein and the 1-propanol for the hydrophobic surface of the reversed-phase.

It is interesting to note that 35–40% 1-propanol gave the highest recovery for α-chymotrypsinogen from the reversed-phase, as determined from UV spectra. Below this value (10–15% 1-propanol) the protein was irreversibly bound. However, above 40% 1-propanol, the recoveries were reduced. It is possible that above the 40% 1-propanol concentration, the protein begins to precipitate and at 60% 1-propanol concentration, precipitation is complete.

The results presented in this paper give an indication of the adsorption strength of α-chymotrypsinogen on various reversed-phase materials. It is proposed to extend these studies on a dynamic basis using a combined LC–CD system. This work will be reported in due course.

ACKNOWLEDGEMENT

This work was supported by the Science and Engineering Research Council.

REFERENCES

1 S. T. Freer, J. Kraut, J. D. Robertus, H. T. Wright and Ng. H. Xuong, *Biochemistry*, 9 (1970) 4481.
2 A. J. Sadler, R. Micanovic, G. E. Katzenstein, R. V. Lewis and R. Middaugh, *J. Chromatogr.*, 317 (1984) 93.
3 A. F. Drake, M. J. Dufton and R. C. Hider, *Eur. J. Biochem.*, 105 (1980) 623.
4 R. C. Hider, A. F. Drake and N. Tamiya, *Biopolymers*, 27 (1988) 113.
5 G. E. Katzenstein, S. A. Vrona, R. J. Wechsler, B. L. Steadman, R. V. Lewis and C. R. Middaugh, *Proc. Natl. Acad. Acad. Sci. U.S.A.*, 83 (1986) 4268.
6 J. L. Speier, *Adv. Organomet. Chem.*, 17 (1979) 407.
7 G. E. Berendesen and L. de Galan, *J. Liq. Chromatogr.*, 1 (1978) 561.
8 S. A. Cohen, K. P. Benedek, S. Dong, Y. Taphui and B. L. Karger, *Anal. Chem.*, 56 (1984) 217.
9 S. A. Cohen, K. P. Benedek, Y. Taphui, J. C. Ford and B. L. Karger, *Anal. Biochem.*, 144 (1985) 275.
10 K. P. Benedek, S. Dong and B. L. Karger, *J. Chromatogr.*, 317 (1984) 227.
11 X. Geng and F. E. Reignier, *J. Chromatogr.*, 296 (1984) 15.
12 S. Y. M. Lau, A. K. Taneja and R. S. Hodges, *J. Chromatogr.*, 317 (1984) 129.
13 R. H. Ingraham, S. Y. M. Lau, K. Taneja and R. S. Hodges, *J. Chromatogr.*, 327 (1985) 77.
14 W. R. Melander and Cs. Horváth, *Chromatographia*, 15 (1982) 86.

Journal of Chromatography, 476 (1989) 165–174
Elsevier Science Publishers B.V., Amsterdam — Printed in The Netherlands

CHROMSYMP. 1567

STEREOCHEMICAL RECOGNITION OF ENANTIOMERIC AND DIASTEREOMERIC DIPEPTIDES BY HIGH-PERFORMANCE LIQUID CHROMATOGRAPHY ON A CHIRAL STATIONARY PHASE BASED UPON IMMOBILIZED α-CHYMOTRYPSIN

PHILIPPE JADAUD and IRVING W. WAINER*
St. Jude Children's Research Hospital, Memphis, TN 38105 (U.S.A.)

SUMMARY

A series of 24 enantiomeric and diastereomeric dipeptides were chromatographed on a chiral stationary phase (CSP) based upon immobilized α-chymotrypsin (ACHT). The ACHT-CSP was able to resolve stereochemically a number of the enantiomeric D,D- and L,L-dipeptides as well as the diastereomeric D,D-/L,L- and L,D-/D,L-dipeptides. The solutes were also chromatographed on a N-tosyl-L-phenylalanine chloromethyl ketone-deactivated form of the ACHT-CSP, where stereochemical separations were also achieved. The results of this study suggest that binding interactions between the dipeptides and the ACHT-CSP occur at the active site of the ACHT and at other hydrophobic sites on the ACHT molecule.

INTRODUCTION

The stereochemical purity of small peptides is an important and difficult problem in the development of a number of new drugs[1]. The complexity of the problem is illustrated by the simplest case, a dipeptide, where the molecule can exist in four stereoisomeric forms, *i.e.* two diastereomeric molecules, L,L/D,D and D,L/L,D, which are themselves enantiomeric pairs. The number of possible stereoisomers for a given peptide is 2^n where n is the number of constituent amino acids.

At the present time, the determination of the stereochemical composition of a peptide has been mainly limited to dipeptides. This problem has been approached by using enantioselective chromatographic techniques that utilized chiral stationary phases (CSPs) developed for high-performance liquid chromatography (HPLC) and thin-layer chromatography (TLC).

The most comprehensive study of the application of HPLC CSPs to the separation of peptide stereoisomers was carried out by Florance *et al.*[2]. This work involved the use of three different types of commercially available HPLC CSPs, based upon β-cyclodextrin (CD-CSP), (*R*)-N-(3,5-dinitrobenzoyl)phenylglycine (PG-CSP), and an unspecified amino acid derivative (WE-CSP).

Using the CD- and WE-CSPs, Florance *et al.*[2] were able to achieve the chromatographic resolution of diastereomeric dipeptides, such as L-Leu–L-Tyr/D-Leu–L-Tyr.

0021-9673/89/$03.50

The resolutions were accomplished without derivatization of the dipeptides and by the use of aqueous mobile phases. Diastereomeric cyclic dipeptides were also resolved on the CD- and PG-CSPs, enantiomeric dipeptides, such as L-Leu–L-Tyr/D-Leu–D-Tyr, were not.

Hyun *et al.*[3] have also used an HPLC CSP to resolve a series of enantiomeric dipeptides. The CSP was synthesized with (*S*)-1-(6,7-dimethyl-1-naphthyl)-isobutylamine as the chiral selector. However, to accomplish the separations, the dipeptides had to be first converted to the corresponding N-3,5-dinitrobenzoyl methyl esters. Chromatography was then carried out with a mobile phase composed of hexane–2-propanol (90:10, v/v). Using this method, all four stereoisomers of Leu–Ala and fourteen other dipeptides were resolved.

Pirkle *et al.*[4] have accomplished similar separations of enantiomeric di- and tripeptides on HPLC CSPs related to the one reported by Hyun *et al.*[3]. The peptides also had to be converted to the corresponding N-3,5-dinitrobenzoyl methyl esters.

The stereochemical resolution of enantiomeric dipeptides without derivatization has been reported by Günther[5]. These separations were accomplished by using enantioselective TLC on a commercially available TLC CSP, based upon (2*S*,4*R*,2′*RS*)-N-(2′-hydroxydodecyl)-4-hydroxyproline. The dipeptides were chromatographed with a mobile phase composed of methanol–water–acetonitrile (50:50:200, v/v/v). Under these conditions, enantiomeric dipeptides such, as D-Ala–L-Phe/L-Ala–D-Phe, could be stereochemically resolved. This method can also be used to resolve diastereomeric dipeptides[6].

Another possible approach to this problem has been suggested by the development of a HPLC CSP based upon the enzyme α-chymotrypsin (ACHT), the ACHT-CSP[7]. The CSP was synthesized by the immobilization of ACHT on a silica-based support containing covalently bonded glutaraldehyde. The immobilization produced a stationary phase which contains an active enzyme capable of binding and hydrolyzing natural substrates of ACHT, such as L-amino acid amides and esters[8]. Stereochemical resolutions of a number of enantiomeric compounds, including free and derivatized amino acids, were observed on this "active" form of the ACHT-CSP[7,8].

Another form of the CSP can be produced by inactivating the ACHT. This can be accomplished by blocking the active site of the enzyme with N-tosyl-L-phenylalanine chloromethyl ketone (TPCK)[9,10]. Thus, the "active" ACHT-CSP was treated with TPCK, resulting in an "inactive" ACHT-CSP[8]. The "inactive" form of the CSP was unable to resolve stereochemically most of the substrates separated on the "active" form of the CSP, although some enantiomeric amino acid esters were separated with higher stereoselectivity[8].

ACHT is an endopeptidase which stereoselectively hydrolyzes peptides at bonds involving the carboxyl groups of aromatic L-amino acids, particularly phenylalanine (Phe), tyrosine (Tyr) and tryptophan (Trp)[11]. Therefore, it is likely that the ACHT-CSP will be able to discriminate between the stereoisomers of dipeptides containing Phe, Tyr, and Trp. To test this hypothesis, we have chromatographed on the ACHT-CSP a series of dipeptides composed of leucine (Leu) and one of the three aromatic amino acids, *i.e.* Phe, Tyr, Trp. The results demonstrate that both enantioselective and diastereoselective resolutions can be achieved on both "active" and "inactive" forms of the CSP.

EXPERIMENTAL

Apparatus

The HPLC experiments with the ACHT-CSP were performed with two modular liquid chromatographs. One system was composed of a Beckman 116 solvent module pump (Beckman Instruments, Houston, TX, U.S.A.), a Beckman 160 absorbance detector (wavelength fixed at 254 nm) and a Shimadzu C-R6A Chromatopac integrator (Shimadzu Scientific Instruments, Columbia, MD, U.S.A.). The other system consisted of the same pump, a multiwavelength Beckman programmable UV detector module 166 and a Shimadzu C-R5A Chromatopac integrator. The pumps and the second detector were controlled by a NEC PC-8300 microcomputer (NEC Home Electronics U.S.A., Wood Dale, IL, U.S.A.). The 10 cm × 4.6 mm I.D. and 25 cm × 4.6 mm I.D. stainless-steel columns used in this study were packed with the ACHT-CSP by J. T. Baker (Phillipsburg, NJ, U.S.A.).

Chemicals

The α-chymotrypsin (Type VII, TLCK-treated), amino acids, amino acid derivatives, and TPCK were purchased from Sigma (St. Louis, MO, U.S.A.). The L,L-dipeptides were also obtained from Sigma. The other dipeptides were synthesized in the Department of Virology and Molecular Biology of St. Jude Children's Research Hospital.

The hydrophilic polymer-bonded silicas (particle diameters: 5 and 15 μm, pore diameter: 300 Å), containing covalently bonded glutaraldehyde, were obtained from J. T. Baker.

Chromatographic conditions

The standard mobile phases were composed of pure buffers, usually at pH 5.5–6.0. For the comparison of the retention on active and TPCK-deactivated ACHT-CSP, the mobile phase was an aqueous solution of sodium phosphate (0.123 *M*, pH 6.0, $I = 0.140$). Flow-rates of 0.3 ml/min and 0.6 ml/min were used for the 15-μm and 5-μm packing, respectively. All experiments were carried out at ambient temperature. The elution order of the isomers was established by chromatographing the solutes separately.

Synthesis of the ACHT-CSP

The synthesis of the ACHT-CSP has been reported elsewhere[7]. In brief, the synthesis was accomplished in three steps.

(1) The support was washed four times with phosphate buffer (0.1 *M*, pH 7.0).

(2) The support was added to a sodium borate solution (0.1 *M*, pH 8.7) at a rate of 2.5 ml per gram of support; the solution contained ACHT in an amount of at least 60 mg per gram of support. The mixture was stored at 5–6°C for at least 18 h.

(3) The mixture was filtered, and the solid phase was washed four times with phosphate buffer (0.1 *M*, pH 7.0).

The calculated concentration of ACHT on the support was 50–53 mg ACHT per gram of solid phase.

Deactivation of the ACHT-CSP

The deactivation of the ACHT-CSP (10 cm long column) was carried out by injecting 3.5 ml of a solution of TPCK [5.5 m*M* in phosphate buffer (0.1 *M*, pH 6.0)–acetonitrile (50:50, v/v)]. This volume of 3.5 ml corresponds to 35 injections with a 100-μl loop. The injection of D,L-tryptophanamide into this deactivated support showed a lack of hydrolysis and stereoselectivity[8].

RESULTS

The structure of the dipeptides used in this study are presented in Fig. 1. Table I summarizes the chromatographic results obtained with the "active" and "inactive" form of the ACHT-CSP. Some examples of chromatograms, for the pairs L,D-/L,L-Tyr–Leu, D,D-/L,L-Leu–Trp and L-Trp–D-Leu/L-Leu–D-Trp, are presented in Fig. 2a, b and c, respectively. The results of this study indicate that the relative retention of the dipeptides, *i.e.* the capacity factor, k', is a function of the hydrophobicity of the constituent aromatic amino acid, and of the interactions of this moiety with the active site of the enzyme. This is demonstrated by the retention of Leu–Phe and Leu–Tyr dipeptides on the "active" and "inactive" forms of the ACHT-CSP. Phe is more hydrophobic than Tyr[12] while Tyr has a higher affinity for ACHT[13]. On the active form of the CSP, the binding to the active site of the ACHT played an important role in the retention[7,8], and Tyr-containing dipeptides had higher k' values than the corresponding Phe-containing dipeptides. When the active site was blocked by TPCK, hydrophobic interactions played a dominant role in the retention[8], and the Phe-containing dipeptides had the higher k' values.

In addition, the observed retentions of the dipeptides were not the arithmetic sum of the k' values of the constituent amino acids. This was clearly demonstrated by the k' values for the dipeptides composed of Leu–Tyr and Leu–Trp. With regard to the stereoselectivity of the "active" and "inactive" forms of the ACHT-CSP, the following results were observed.

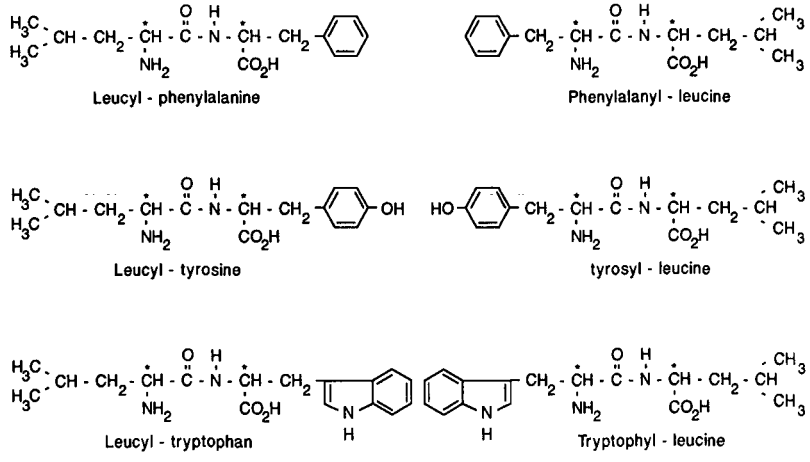

Fig. 1. The structure of the solutes used in this study.

TABLE I

CHROMATOGRAPHIC RETENTION, ENANTIOSELECTIVITY α_1 AND DIASTEREOSELECTIVITY α_2 OF AMINO ACIDS AND DIPEPTIDES ON ACTIVE AND TPCK-DEACTIVATED ACHT-CSP

Column, 100 × 4.6 mm I.D.; stationary phase, α-chymotrypsin-bonded silica, 15 μm; mobile phase, phosphate buffer (0.123 *M*, pH 6.0); flow-rate, 0.30 ml/min; temperature, ambient; detection, UV at various wavelengths.

Solutes	*ACHT-CSP (active)*[a]			*ACHT-CSP (TPCK)*[b]		
	k'	α_1[c]	α_2[d]	k'	α_1[c]	α_2[d]
D,L-Leu	0.10	1.00		0.18	1.00	
L-Leu	0.10			0.19		
D,L-Phe	0.20	1.00		0.39	1.00	
L-Phe	0.23			0.39		
D-Tyr	0.34	1.03		0.36	1.00	
L-Tyr	0.35			0.36		
L-Trp	1.00	1.16		1.02	1.03	
D-Trp	1.16			0.99		
L-Leu–D-Phe	0.39	1.00		0.55	1.07	
D-Leu–L-Phe	0.39		1.08	0.59		1.07
L-Leu–L-Phe	0.41	1.05		0.59	1.05	
D-Leu–D-Phe	0.43			0.62		
L-Phe–D-Leu	0.37	1.06		0.58	1.02	
D-Phe–L-Leu	0.35		1.17	0.59		1.03
D-Phe–D-Leu	0.40	1.10		0.63	1.11	
L-Phe–L-Leu	0.44			0.57		
L-Leu–D-Tyr	0.47	1.00		0.44	1.02	
D-Leu–L-Tyr	0.47		1.47	0.45		1.20
L-Leu–L-Tyr	0.69	1.00		0.53	1.02	
D-Leu–D-Tyr	0.69			0.54		
L-Tyr–D-Leu	0.40	1.03		0.40	1.05	
D-Tyr–L-Leu	0.41		1.74	0.42		1.59
D-Tyr–D-Leu	0.68	1.07		0.60	1.17	
L-Tyr–L-Leu	0.73			0.70		
L-Leu–D-Trp	1.47	1.03		1.49	1.02	
D-Leu–L-Trp	1.51		2.09	1.46		1.32
L-Leu–L-Trp	2.20	1.83		1.85	1.11	
D-Leu–D-Trp	4.03			2.05		
L-Trp–D-Leu	1.05	1.04		1.18	1.02	
D-Trp–L-Leu	1.09		1.80	1.20		1.33
D-Trp–D-Leu	1.91	1.02		1.57	1.01	
L-Trp–L-Leu	1.95			1.59		

[a] Active form of the ACHT.

[b] Inactive form of ACHT after treatment with TPCK.

[c] $\alpha_1 = (t_{Rb} - t_0)/(t_{Ra} - t_0)$ where t_{Ra}, t_{Rb} and t_0 are the retention times of the less retained compound, of the more retained compound, and the dead time, respectively.

[d] $\alpha_2 = [(t_{RD.D} + t_{RL.L})/2 - t_0]/[(t_{RD.L} + t_{RL.D})/2 - t_0]$.

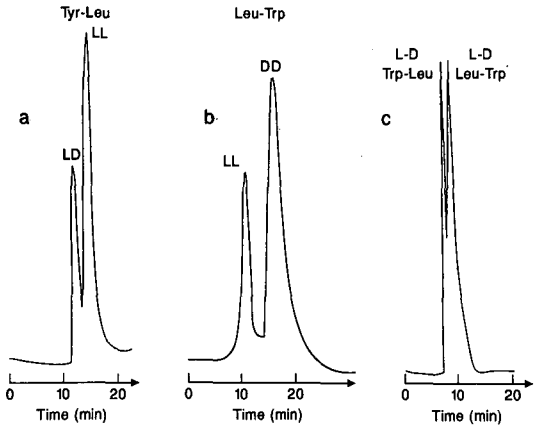

Fig. 2. Representative chromatograms for two of the solutes (a) L,D-/L,L-Tyr–Leu; (b) D,D-/L,L-Leu–Trp; (c) L-Trp–D-Leu/L-Leu–D-Trp. Chromatographic conditions: column, 250 × 4.6 mm I.D.; stationary phase, α-chymotrypsin-bonded silica, 5 μm; mobile phase, phosphate buffer (0.070 *M*, pH 5.5); flow-rate, 0.60 ml/min (optimal); temperature, ambient; detection, UV at 254 nm.

The "active" ACHT-CSP

D,L-/L,D-dipeptides, retention and enantioselectivity. For all the dipeptides studied, the k' values were higher when the aromatic amino acid was at the carboxyl end of the chain. The difference in retention between the two forms increased with increasing hydrophobicity, *i.e.* there was a 5% difference in k' between D-Leu–L-Phe and L-Phe–D-Leu and a 44% difference between D-Leu–L-Trp and L-Trp–D-Leu.

No significant enantioselectivity was achieved for the twelve L,D- and D,L-dipeptides studied. However, when some enantioselectivity was observed, the stereoselectivity (α) was higher when the aromatic amino acid was at the amino end of the chain. In addition, except for Phe–Leu, the L,D-form of the dipeptide was eluted before the D,L-form.

L,L-/D,D-dipeptides, retention and enantioselectivity. For the D,D-forms of the dipeptides composed of Leu and Phe or Tyr, there was little difference in k' between the molecules with the aromatic amino acid at the carboxyl end or at the amino end of the chain. However, the k' values for L-Phe–L-Leu and L-Tyr–L-Leu were about 6% higher than the corresponding dipeptides, L-Leu–L-Phe and L-Leu–L-Tyr. As a result, there was a change in the elution order, *i.e.* L,L- was eluted before D,D- when the aromatic amino acid was at the carboxyl end and D,D- was eluted before L,L- when the position of Phe or Tyr was reversed.

The position of the aromatic amino acid also affected the enantioselectivity between the L,L-/D,D-enantiomers. When the aromatic amino acid was at the carboxyl end of the chain, the stereoselectivity (α) was lower than when that moiety was at the amino end of the dipeptide.

Among the enantiomers of Leu–Trp, L-Leu–L-Trp was eluted before the D,D-isomer while the elution order was reversed for the Trp–Leu enantiomers. This was similar to the results observed with the Phe- and Tyr-containing dipeptides, but the cause of this reversal was different. In this case, the k' values of both the D,D- and

L,L-enantiomers decreased when the aromatic amino acid was shifted from the carboxyl end to the amino end of the chain. However, there was a 53% difference between the retention of D-Leu–D-Trp and D-Trp–D-Leu, and only a 11% difference between the corresponding L,L-isomers.

Unlike the Phe- and Tyr-containing dipeptides, the L,L-/D,D-Leu–Trp enantiomers were better resolved than the Trp–Leu isomers. When Trp was at the carboxyl end of the dipeptide $\alpha = 1.83$, and when it was at the amino terminus the stereoselectivity was almost lost ($\alpha = 1.02$).

D,L-/L,D- and D,D-/L,L-diastereomers, retention and resolution. Among the six sets of diastereomeric dipeptides used in this study, the D,L-/L,D-pairs were eluted before the corresponding D,D-/L,L-pairs. The difference in the k' of the diastereomers, and therefore their stereochemical resolution, increased with the hydrophobicity of the aromatic amino acid. In addition, the stereochemical resolution achieved for the diastereomers with the aromatic amino acid at the amino end of the dipeptide was greater than that observed for the isomers with the aromatic amino acid at the carboxyl terminus.

The "inactive" ACHT-CSP

D,L-/L,D-dipeptides, retention and enantioselectivity. The deactivation of the ACHT-CSP by TPCK had very little effect on the retention and stereoselectivity of the Tyr- and Trp-containing dipeptides used in this study. However, the deactivation resulted in a significant increase in the retention of the Phe-containing solutes. When Phe is at the carboxyl end of the dipeptide, the k' values on the "inactive" ACHT-CSP increased by over 40% relative to the results on the "active" ACHT-CSP, and a stereochemical resolution of the L,D-/D,L-enantiomers was observed ($\alpha = 1.07$).

The k' values for the Phe–Leu enantiomers also increased. In this instance, the k' for the L,D-isomer increased by 57% and the k' for the D,L-isomer increased by 69%. This resulted in a net loss in enantioselectivity, $\alpha = 1.06$ and 1.02, on the "active" and "inactive" CSPs, respectively.

L,L-/D,D-dipeptides, retention and enantioselectivity. As observed with the D,L-/L,D-dipeptides, deactivation of the ACHT-CSP resulted in a significant increase in the k' values of the Phe-containing dipeptides. However, there was no change in the stereoselectivities.

When the Tyr- and Trp-containing dipeptides were chromatographed, there was a significant decrease in the observed k' values for all of the compounds and an increase in α for the Leu–Tyr and Tyr–Leu solutes, $\alpha = 1.02$ and 1.17, respectively. For Leu–Trp there was a decrease in the stereoselectivity relative to the separation observed on the "active" ACHT-CSP ($\alpha = 1.87$ on the "active" CSP and 1.11 on the "inactive" CSP). The chiral resolution of the Trp–Leu enantiomorphs was unchanged.

D,L-/L,D- and D,D-/L,L-diastereomers, retention and resolution. On the "inactive" ACHT-CSP, the relative retention order of the six sets of diastereomeric dipeptides was identical to that found on the "active" form of the CSP, *i.e.* the D,L-/L,D-pairs were eluted before the D,D-/L,L-pairs. All of the diastereomeric pairs were resolved, although the stereochemical resolution was lower on the "inactive" CSP.

DISCUSSION

As stated above, ACHT primarily catalyzes the hydrolysis of amide bonds of proteins and peptides adjacent to the carbonyl group of the aromatic L-amino acid residues of Trp, Tyr and Phe[11]. The catalytic activity takes place at a single site on the enzyme, which is composed of a hydrophobic pocket and a hydrolytically active cavity. In the hydrolytic cavity, the probable contacts are between Ser-195 and His-57 and the carboxylic group of the substrate, Met-192 with C^{α} and the group bonded on it, and the hydrophobic cavity (Met-192, Cys-191, Ser-190, Gly-216, Ser-217, ...) with the aromatic system of the solute[14]. With a D-amino acid, the interactions with Ser-195 may be replaced by interactions with Ser-214[14].

The chromatographic results obtained on the "active" form of the ACHT-CSP can be explained, in part, by binding at the active site of the enzyme. This is particularly clear for the L,L-/D,D-dipeptides, especially the series composed of Trp–Leu and Leu–Trp.

The Trp–Leu dipeptide is in the "normal" configuration for insertion into the active site of the enzyme, *i.e.* the amide bond is formed with the carboxyl group of the aromatic amino acid. In this configuration, the natural L,L-substrate should be more tightly bound than the unnatural D,D-isomer. The enantiomeric elution order (the D,D-enantiomer is eluted before the L,L-) is consistent with this view.

The Leu–Trp dipeptide is not in the "normal" configuration for insertion into the active site of the enzyme, *i.e.* the amide bond is formed with the carboxyl group of the aliphatic amino acid. In this configuration, the best fit between the enzyme and dipeptide would be accomplished by rotating the peptide 180° relative to the position assumed by the Trp–Leu molecule. This should reverse the enantiomeric elution order, since the enzyme now sees the mirror image of the Trp–Leu dipeptide. The observed enantiomeric elution order (the L,L-enantiomer is eluted before the D,D-) is consistent with this interpretation.

However, this mechanism does not explain the results obtained for D,D-/L,L-dipeptides on the TPCK-deactivated ACHT-CSP. If the dipeptides only interact with the enzyme at the active site, there should be a significant loss in retention and stereoselectivity when the active site is blocked with TPCK. Although there were some significant decreases in k' (for example, a 49% decrease in k' for D-Leu–D-Trp), there were also some increases (for example, a 58% increase in k' for both Phe–Leu isomers).

As discussed above, the chromatographic retention on the ACHT-CSP appears to be due to binding at the active site of the enzyme and at one or more additional hydrophobic sites on the molecule. These sites must also possess some enantioselectivity, since there is an increase in the stereochemical resolution of some of the D,D-/L,L-dipeptides on the "inactive" CSP (Tyr–Leu, for example), no change in the resolution of others (Phe–Leu, for example) and a reduced but still significant resolution of Leu–Trp. These results are consistent with the results obtained with amino acid esters on TPCK-deactivated ACHT-CSP[8].

The results for the series of enantiomeric D,L-/L,D-dipeptides are not as easily understood. No significant stereochemical resolutions were obtained on either the "active" or "inactive" forms of the CSP, although the "inactive" ACHT-CSP appeared to be slightly more enantioselective.

TABLE II

NUMBER OF THEORETICAL PLATES (N)[a] FOR EACH CHROMATOGRAPHED DIPEPTIDE ON ACHT-CSP

Chromatographic conditions: see Fig. 2.

Solute	*N*	*Solute*	*N*
D,L-Phe	1035	L,D-Tyr–Leu	1153
L-Tyr	1952	D,L-Tyr–Leu	1221
L-Trp	1591	D,D-Tyr–Leu	323
		L,L-Tyr–Leu	317
L,D-Leu–Phe	1045		
D,L-Leu–Phe	1015	L,D-Leu–Trp	585
L,L-Leu–Phe	519	D,L-Leu–Trp	571
D,D-Leu–Phe	418	L,L-Leu–Trp	265
		D,D-Leu–Trp	139
L,D-Phe–Leu	971		
D,L-Phe–Leu	781	L,D-Trp–Leu	622
D,D-Phe–Leu	362	D,L-Trp–Leu	621
L,L-Phe–Leu	366	D,D-Trp–Leu	94
		L,L-Trp–Leu	141
L,D-Leu–Tyr	1113		
D,L-Leu–Tyr	1085		
L,L-Leu–Tyr	1192		
D,D-Leu–Tyr	389		

[a] $N = 5.54\,(t_R/\delta)^2$ where t_R = retention time and δ = peak width at half-height.

These results suggest that the primary interactions between the D,L-/L,D-dipeptides and the ACHT-CSP do not take place at the active site of the enzyme, but at other hydrophobic sites on the ACHT. This may be due to the existence of molecular conformations of the D,L- and L,D-dipeptides that do not form stable complexes with the active site.

In addition, although the enantiomeric resolutions involving the D,L-/L,D-dipeptides were low, the diastereomeric resolutions of the D,L-/L,D- and D,D-/L,L-dipeptides were significant on both forms of the ACHT-CSP. This may also be a reflection of the fact that the two diastereomeric forms have different primary sites of interaction with the ACHT-CSP.

This possibility may be correlated with the influence of the structure of the dipeptide on the efficiency of its chromatographic peak, as reflected by the calculated theoretical plate number (N) (Table II). The stronger the interactions with the support, the slower the desorption of the solute and the lower the efficiency. As shown in Table II, there are two groups of solutes: (1) the L,D-/D,L-enantiomers with a "high" N; and (2) the D,D-/L,L-enantiomers, with an N which is one-half or less of the corresponding L,D-/D,L-solute. This is consistent with the existence of two types of binding sites with different affinities.

CONCLUSION

The ACHT-CSP is capable of the enantiomeric and diastereomeric resolution of the dipeptides derived from phenylalanine, tyrosine and tryptophan. These resolutions appear to be due to interactions at both the active site of the ACHT and at other hydrophobic sites on the ACHT molecule. The existence of two or more interaction sites is under further investigation through studies of the effect of temperature, mobile-phase composition and solute structure on retention and stereoselectivity.

REFERENCES

1 R. W. Souter, *Chromatographic Separations of Stereoisomers,* CRC Press, Boca Raton, FL, 1985.
2 J. Florance, A. Galdes, Z. Konteatis, Z. Kosarych, K. Langer and C. Martucci, *J. Chromatogr.,* 414 (1987) 313.
3 M. H. Hyun, I.-K. Baik and W. H. Pirkle, *J. Liq. Chromatogr.,* 11 (1988) 1249.
4 W. H. Pirkle, D. M. Alessi, M. H. Hyun and T. C. Pochapsky, *J. Chromatogr.,* 398 (1987) 203.
5 K. Günther, *J. Chromatogr.,* 448 (1988) 11.
6 K. Günther, J. Martens and M. Schickendanz, *Angew. Chem.,* 98 (1986) 284.
7 I. W. Wainer, Ph. Jadaud, G. R. Schonbaum, S. V. Kakodkar and M. P. Henry, *Chromatographia,* 25 (1988) 907.
8 Ph. Jadaud, S. Thelohan, G. R. Schonbaum and I. W. Wainer, *Chirality,* 1 (1989) 38.
9 B. S. Hartley, *Ann. NY Acad. Sci.,* 227 (1974) 438.
10 D. M. Blow, *Acc. Chem. Res.,* 9 (1976) 145.
11 H. R. Mahler and E. H. Cordes, *Biological Chemistry,* Harper & Row, New York, 1966.
12 R. F. Rekker, *The Hydrophobic Fragmental Constant,* Elsevier, Amsterdam, 1977.
13 H. Neurath and G. W. Schwert, *Chem. Rev.,* 46 (1950) 70.
14 T. A. Steitz, R. Henderson and D. M. Blow, *J. Mol. Biol.,* 46 (1969) 337.

Journal of Chromatography, 476 (1989) 175–185
Elsevier Science Publishers B.V., Amsterdam — Printed in The Netherlands

CHROMSYMP. 1570

EFFICIENT ENDOTOXIN REMOVAL WITH A NEW SANITIZABLE AFFINITY COLUMN: AFFI-PREP POLYMYXIN

KENNETH W. TALMADGE* and CHRISTOPHER J. SIEBERT
Bio-Rad Laboratories, 141 Harbour Way, Richmond, CA 94801 (U.S.A.)

SUMMARY

A new affinity column packing for removal of endotoxins has been prepared by coupling USP drug-quality polymyxin B to Affi-Prep, a novel synthetic macroporous polymer. Affi-Prep Polymyxin binds endotoxins from a number of different strains of gram-negative bacteria. Endotoxin binding is not significantly affected by 10 mg/ml of bovine serum albumin or human immunoglobulin G, by 1 mg/ml sodium dodecyl sulphate, or by 1 mg/ml deoxycholate. Affi-Prep Polymyxin is stable to treatment with 1.0 *M* sodium hydroxide, an important property for sanitizing the resin. The resin shows a high ligand stability, since no leakage of polymyxin B from the packing could be detected. Affi-Prep Polymyxin exhibited the highest endotoxin binding efficiency when compared with several commercial agarose affinity packings.

INTRODUCTION

Endotoxins are the pyrogenic lipopolysaccharide (LPS) components of gram-negative bacteria. They can have potent biological effects in man and in many animal species when administered systematically. In addition, endotoxins have been shown to perturb *in vivo* and *in vitro* experiments, even at concentrations of a few ng/ml[1,2]. Thus, the elimination of endotoxins is crucial for many *in vivo* studies and in the purification of drugs intended for injection in man.

As therapeutic and pharmacologically important products are developed in the biotechnology and pharmaceutical industries, the need for efficient chromatographic columns for endotoxin removal has become apparent. Besides removing endotoxins with high efficiency and selectivity, these columns should be able to withstand the treatments necessary for adequate sanitation before use.

Although a number of methods have been used to remove endotoxins[3], the most efficient and practical method utilizes polymyxin B (PMB) affinity chromatography[4]. Polymyxin B is the generic name for a group of chemically related fatty acyl peptide antibiotics produced by *Bacillus polymyxa* and related species. These compounds are generally administered at 2.5 mg/kg/day in the treatment of certain gram-negative bacterial infections, where PMB is thought to disrupt the membrane structure by a high affinity binding to the lipid A moiety of the bacterial lipopolysaccharides[5,6].

This report describes the evaluation of a new affinity packing prepared by

0021-9673/89/$03.50

coupling USP drug-grade polymyxin B to a novel macroporous synthetic polymer. This is the first publication giving a detailed evaluation of a commercial polymyxin B affinity material in terms of specificity, binding conditions, and ligand stability.

MATERIALS AND METHODS

Materials

PMB sulfate from the following sources was utilized: Sigma (St. Louis, MO, U.S.A.), Calbiochem (La Jolla, CA, U.S.A.) and Pharma Tek (Huntington, NY, U.S.A.). Polymyxin E (colistin methanesulfonate), human immunoglobulin G (IgG), and bovine serum albumin (BSA) were obtained from Sigma. The following lipopolysaccharide preparations were obtained from Sigma: *Salmonella abortus equi, S. minnesota, Escherichia coli* 055:B5, *E. coli* 0127:B8, *E. coli* 0111:B4, *E. coli* 0128:B12 and *Serratia marcescens*. Deoxycholic acid (DOC) and *E. coli* 055:B5 were obtained from Calbiochem. Sodium dodecyl sulfate (SDS, electrophoresis grade) was from Bio-Rad Labs. (Richmond, CA, U.S.A.). Sterile, pyrogen-free water (PF-water) was obtained from Cadillac Medical Supplies (Richmond, CA, U.S.A.). Affi-Prep 15 was obtained from Bio-Rad Labs. All buffers used in coupling reactions, wash solutions and endotoxin binding assays were prepared with the PF-water. Phosphate-buffered saline (PBS) consisted of 10 m*M* phosphate buffer (pH 7.2), containing 140 mM sodium chloride. The binding buffer was 10 m*M* phosphate buffer (pH 6.0), containing 100 m*M* sodium chloride. The following affinity packing materials have been tested: polymyxin B-agarose from Sigma; Detoxi-Gel from Pierce (Rockford, IL, U.S.A.); Actigel-polymyxin B from Sterogene Biochemicals (San Gabriel, CA, U.S.A.); and polymyxin B-agarose from Boehringer Mannheim (Indianapolis, IN, U.S.A.).

High-performance liquid chromatographic (HPLC) analysis of PMB

PMB was analyzed on a Bio-Sil ODS 5S column (250 × 4 mm I.D.), connected to a Bio-Rad isocratic HPLC system, equipped with a 100-μl injection loop, a Bio-Rad Model 1330 pump and a Bio-Rad Model 1306 UV monitor, set at 200 nm. Elution was carried out at 1 ml/min with 100 m*M* sodium triphosphate, containing 22% acetonitrile, adjusted to pH 3.0 with orthophosphoric acid.

Coupling of PMB to Affi-Prep

PMB was coupled to the N-hydroxylsuccinimide activated ester of Affi-Prep 15 which contained a spacer arm (succinylmethyliminobispropylaminocarboxymethyl group).

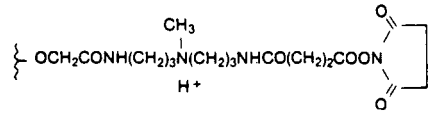

The activated resin was transferred to a coarse-frit sintered glass funnel and the material washed free of 2-propanol with ten bed volumes of ice cold 10 m*M* sodium acetate buffer (pH 4.5). PMB (5 mg/ml), in one bed volume of 0.1 *M* HEPES buffer (pH 8.0) was added immediately to the activated Affi-Prep. The coupling was carried

out at room temperature by allowing this PMB solution to filter through the Affi-Prep material over 10–15 min. The coupled material was washed with one bed volume of 0.1 *M* HEPES buffer (pH 8.0). The effluents from the coupling and the buffer wash were collected and saved for the HPLC analysis of PMB. The Affi-Prep Polymyxin was then washed with two bed volumes of 0.2 *M* ethanolamine (pH 8.5) followed by ten bed volumes each of 0.1 *M* glycine buffer (pH 9.0) containing 1 *M* sodium chloride and 0.1 *M* acetate buffer (pH 4.5) containing 1 *M* sodium chloride. The amount of PMB coupled to Affi-Prep was determined by the HPLC analysis of the initial and effluent PMB solutions. Under these coupling conditions the Affi-Prep Polymyxin contained *ca.* 2.5 mg PMB per ml Affi-Prep.

A control Affi-Prep, lacking PMB, was prepared as described above except PMB was omitted from the coupling reaction.

Endotoxin binding assays

Batch assay. A uniform suspension in water (30–50%, v/v) of the Affi-Prep Polymyxin resin was prepared, from which 30–100 μl of resin was pipetted into a 12 × 75 mm glass test tube, containing 1–10 μg of purified endotoxin in 1.0 ml buffer, usually binding buffer. A control tube was included which contained no resin. The tubes were capped and rotated at room temperature end-over-end for 4–24 h. To determine the amount of endotoxin not bound to the resin, serial 10-fold dilutions in PF-water were made of the supernatant solutions, which were assayed for endotoxin by the limulus ameobocyte lysate (LAL) assay. The total input of endotoxin in each experiment was determined from the total endotoxin units (EU) in the control tube. The results are expressed as the total unbound EU and sometimes as the percent endotoxin removal (bound EU × 100/total EU).

Equilibrium binding capacity. This assay is similar to the batch procedure described above, except that an excess of LPS was added. Approximately 0.5 ml of a 50% suspension of the Affi-Prep Polymyxin was transferred to a test tube. The resin was washed with 5 ml PF-water, and the volume of the solution was adjusted to give an approximately 25–35% suspension. The suspension was stirred and aliquots of 100 μl were added to 12 × 75 mm glass test tubes containing 0.9 ml of binding buffer and 200–800 μg of *E. coli* 055:B5 LPS (Calbiochem). The test tubes were capped, sealed and rotated end-over-end for 14–20 h at room temperature. Serial 10-fold dilutions were made to final dilutions of 10^6–10^7. The amount of LPS bound to the resin was determined by analyzing the supernatant solution and control sample for endotoxin, using the LAL assay. To determine the exact quantity of Affi-Prep Polymyxin added, duplicate 200-μl aliquots of the same 25–35% slurry were added to tared test tubes. These were then dried in an oven for 1 h at 100°C and from the resin dry weight an accurate resin volume was calculated, using a swelling factor of 2.5. The endotoxin bound was calculated from the difference between the total EU added and the unbound EU in the supernatant of the Affi-Prep Polymyxin treated samples.

Column. Poly-Prep columns (10 × 8 mm I.D.) prepared from 0.4–0.6 ml of Affi-Prep Polymyxin were washed with 5 ml of PF-water and two 5-ml aliquots of binding buffer. To each column 2–3 ml of LPS (0.2–1 μg/ml) in binding buffer was applied. The effluent solutions were collected and analyzed for endotoxin.

LAL assay for endotoxin

The amount of endotoxin present in a solution was determined by a modified LAL assay and a synthetic color producing substrate. The assay kits were from Whittaker M.A. Bioproducts (Walkersville, MD, U.S.A.). The assays were performed in microtiter plates according to the instructions supplied with the kits. The LAL assay was linear between 0.1–1.0 EU/ml. 1 EU is approximately equal to 0.1 ng of *E. coli* 055:B5 LPS.

RESULTS

Coupling of PMB to Affi-Prep

PMB was coupled to a new rigid macroporous polymeric resin[8] (Affi-Prep 15) which contains the same spacer arm and N-hydroxysuccinimide ester as previously reported for agarose gels (Affi-Gel® 15). Under the reaction conditions the coupling of PMB to Affi-Prep was rapid, being essentially complete within 10 min. Affi-Prep Polymyxin typically contained 2.5 mg PMB/ml Affi-Prep.

Endotoxin binding

The analysis of multiple samples for endotoxin binding was generally performed using the batch assay described in Materials and methods. This measures equilibrium binding using inputs of 10^3–10^4 EU. This requires 10- to 100-fold dilutions of the supernatant before assaying for endotoxin by a standard LAL test. Table I shows the effect of some incubation conditions, such as buffer strength, salt concentration, and incubation time on the endotoxin binding of Affi-Prep Polymyxin. Comparable binding was observed in water, 10 and 50 m*M* phosphate buffer (pH 7.0) and 10 m*M* phosphate (pH 7.0), containing 100 m*M* sodium chloride. Only in the 250 m*M* phosphate buffer was there a decrease, the binding efficiency dropping from *ca.* 99.5 to 92%. Under most conditions the binding after 48 h was more efficient than after 4 h. As a control for the endotoxin binding experiments, Affi-Prep containing no

TABLE I

EFFECT OF INCUBATION CONDITIONS ON ENDOTOXIN REMOVAL

Affi-Prep Polymyxin (50 μl) was incubated for the indicated times in 1.0 ml of the indicated solutions in the presence of 6500 EU/ml. The supernatants were assayed for unbound endotoxin. The endotoxin removal is expressed as the total EU not bound and as % removal (values in parentheses) (bound EU × 100/total EU).

Binding conditions	*Unbound (EU)*	
	Incubation time	
	4 h	*48 h*
Water	4 (99.9)	2 (99.9)
10 m*M* Phosphate buffer (pH 7.0)	10 (99.8)	6 (99.9)
10 m*M* Phosphate buffer (pH 7.0) 100 m*M* Sodium chloride	20 (99.6)	4 (99.9)
50 m*M* Phosphate buffer (pH 7.0)	32 (99.5)	5 (99.9)
250 m*M* Phosphate buffer (pH 7.0)	500 (92.3)	360 (94.4)
50 m*M* Acetate buffer (pH 5.6)	32 (99.5)	2 (99.9)

TABLE II

EFFECT OF PROTEINS AND DETERGENTS ON ENDOTOXIN REMOVAL

Aliquots of 70 μl of Affi-Prep Polymyxin were rotated at 20°C for 16 h in 1.0 ml of PBS-containing endotoxin and the indicated concentrations of SDS, DOC, BSA and IgG. The supernatants were assayed for endotoxin.

Addition	*Concentration (mg/ml)*	*EU Removal (%)*	*Unbound EU*
None	–	99.9	4.8
SDS	0.06	99.7	15
SDS	0.25	99.8	10
SDS	1.00	99.9	4.1
DOC	0.06	99.8	11
DOC	0.25	99.9	4.8
DOC	1.00	99.9	2.2
		Total added, 6000 EU	
None	–	99.9	2.2
BSA	0.10	99.9	2.0
BSA	1.0	99.9	2.2
BSA	10.0	99.9	2.1
IgG	0.10	99.9	2.4
IgG	1.0	99.9	4.1
IgG	10.0	99.9	6.4
		Total added, 6700 EU	

polymyxin was incubated in binding buffer for 16 h with 10000 EU. This control Affi-Prep left 5600 EU unbound while Affi-Prep Polymyxin was able to bind all but 12 EU.

The addition of up to 10 mg/ml of BSA or human IgG in the binding assay (Table II) had little or no effect on the equilibrium values of endotoxin binding of Affi-Prep Polymyxin. Table II also shows the influence of two different detergents,

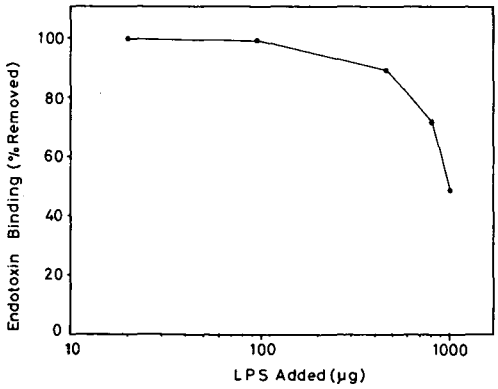

Fig. 1. Endotoxin binding *versus* LPS load. The indicated amounts of LPS (*E. coli* 055:B5) were rotated for 16 h at 20°C with 75 μl of Affi-Prep Polymyxin in 1.0 ml of binding buffer. The percentage removal was calculated from the unbound endotoxin in the supernatant and the total in the respective controls containing no resin.

SDS and DOC. At concentrations of 1 mg/ml there was no inhibition of binding, more than 99.9% of the added endotoxin being bound. However, there was a small but consistent decrease in the unbound endotoxin with dilution.

Fig. 1 shows a curve of endotoxin binding efficiency *versus* added endotoxin. Under conditions of excess endotoxin, theoretical binding capacities of more than 6 mg LPS per ml resin have been obtained in the equilibrium binding assay decribed under Materials and methods.

Binding of different endotoxins by Affi-Prep Polymyxin and Affi-Prep PME

In addition to PMB, a second type of polymyxin is commercially available, colistin or polymyxin E (PME). PMB and PME were coupled separately to Affi-Prep and evaluated for their ability to bind the purified endotoxins isolated from a number of different strains of gram-negative bacteria. The results, presented in Table III, show that both affinity packings were able to bind the LPS molecules from all the strains tested, PMB being superior to PME. In a separate experiment (not shown) the PMB derivative had about twice the endotoxin binding capacity of the PME packing.

Stability

Affi-Prep Polymyxin does not appear to lose endotoxin binding activity after short treatments (5–15 min) with 1% SDS, 1% DOC, 70% aqueous ethanol and 100% 2-propanol. Affi-Prep Polymyxin was examined for its stability toward sodium hydroxide, a standard reagent used to sanitize chromatographic columns. Table IV depicts the binding efficiency of 0.5-ml columns of Affi-Prep Polymyxin, which had been washed with two cycles of sodium hydroxide of different concentrations. No significant loss in binding was observed, even after the two washes with 1 *M* sodium hydroxide, all samples exhibiting binding efficiencies of greater than 99.9%. Time-course experiments (not shown) further indicated little or no loss in endotoxin binding even after 1 h incubation with 1 *M* sodium hydroxide.

TABLE III

BINDING OF ENDOTOXINS FROM DIFFERENT BACTERIAL STRAINS

Approximately 1 μg of the LPS specimens shown were rotated for 16h in 1.0 ml of 10 m*M* phosphate buffer (pH 7.0), containing 70 μl of AP-PMB (Affi-Prep Polymyxin B) or AP-PME (Affi-Prep Polymyxin E). The supernatants were assayed for unbound endotoxin. The endotoxin removal is expressed as the total EU not bound.

Bacterial strain	*Input (EU)*	*Unbound (EU)*	
		AP-PMB	*AP-PME*
E. coli 055:B5	3800	10	60
E. coli 0111:B4	2100	3	5
E. coli 0127:B8	5300	3	16
E. coli 0128:B12	2800	9	20
Salmonella abortus equi	4000	5	35
Salmonella minnesota	1600	17	20
Serratia marcescens	3000	10	35

TABLE IV

EFFECT OF SODIUM HYDROXIDE ON ENDOTOXIN REMOVAL

Poly-Prep columns, containing 0.5 ml of Affi-Prep Polymyxin, were washed over a 5–10 min period with 3.0 ml of sodium hydroxide at the indicated concentrations. The columns were then washed with 4 ml of water, followed by two 4-ml portions of 10 m*M* phosphate buffer (pH 6.0), containing 100 m*M* sodium chloride. Each column was loaded with 3.0 ml of LPS in the above buffer and the eluates were analyzed for unbound endotoxin. The sodium hydroxide wash and assay were repeated on the same columns. The endotoxin removal is expressed as the total EU not bound by the columns.

Sodium hydroxide concentration (M)		*Unbound (EU)*	
		1st Wash	*2nd Wash*
0		1.1	0.6
0.1		0.8	1.2
0.2		1.3	1.2
0.5		1.3	1.5
1.0		1.8	1.5
	Total added	13 500 EU	11 000 EU

Leakage of PMB from Affi-Prep Polymyxin

Commercial preparations of PMB have been separated by HPLC into several major components[7]. The leakage of PMB from the affinity columns was examined by HPLC. Fig. 2A shows the chromatogram of a PMB standard (1 μg/ml), which has two major peaks.

Suspensions of Affi-Prep Polymyxin were rotated overnight at room temperature with one-half volume of 0.1 *M* glycine buffer (pH 10.0). The chromatogram of the resultant supernatant shown in Fig. 2B indicates the absence of any PMB in this 0.1 *M* glycine wash. PMB which had been incubated overnight under these conditions

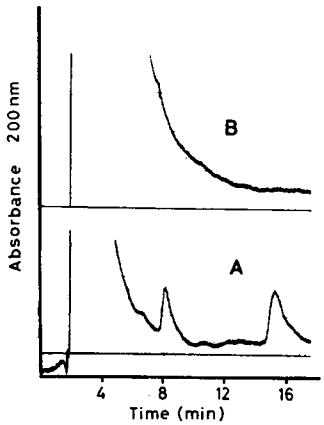

Fig. 2. HPLC analysis of the pH 10 glycine wash of Affi-Prep Polymyxin. PMB was analyzed at an absorbance scale of 0.005 on a Bio-Sil ODS 5S column, as described under Materials and methods. (A) 100 μl of PMB standard (1.0 μg/ml) in 0.1 *M* glycine buffer (pH 10.0). (B) 100 μl of a supernatant, following an overnight incubation at 20°C of Affi-Prep Polymyxin with one-half volume of 0.1 *M* glycine (pH 10.0).

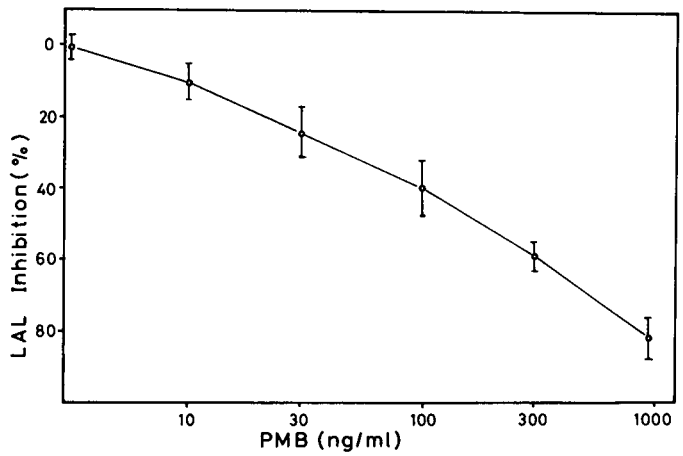

Fig. 3. Inhibition of the LAL assay by PMB. Aliquots of 100 μl of the indicated concentrations of PMB in PBS were incubated for 60 min at 20°C with 75 μl of an endotoxin standard (2 EU/ml in PF-water). Duplicate 50-μl samples were then assayed for endotoxin by the standard assay. The control (0% inhibition), containing only PBS, had an absorbance at 410 nm of 0.4. The values represent the mean of three analyses ± standard deviation.

as a control was fully recoverable by HPLC (data not shown). With a detecton limit of 0.25 μg/ml this would correspond to a leakage of < 125 ppm PMB from the packing. In a similar experiment, no PMB was detected in a supernatant following a 2-h incubation with 0.01 *M* sodium hydroxide at room temperature.

A more sensitive assay for PMB was developed based on an inhibition of the LAL assay for endotoxin. Fig. 3 shows a typical standard inhibition curve where increasing concentrations of PMB were incubated for 60 min with a constant amount of endotoxin (0.4 EU/ml) before the LAL assay. Half of the maximal inhibition typically occurs between 80–150 ng/ml, with a detection limit of *ca.* 20 ng/ml. Affi-Prep Polymyxin, which was endotoxin-free, was incubated for 16 h at 37°C with one volume

TABLE V

COMPARISON OF DIFFERENT AFFINITY PACKINGS

Poly-Prep columns containing *ca.* 0.45 ml of the respective packing were equilibrated in 10 m*M* phosphate buffer (pH 6.0), containing 100 m*M* sodium chloride, and then loaded with 2.0 ml of LPS solutions. The eluates were assayed for endotoxin. In the batch experiments, 30 μl of the resins were incubated overnight in 1.0 ml of the above buffer containing (A) 10 000 EU and (B) $1.2 \cdot 10^6$ EU. The supernatants were assayed for unbound endotoxin. Values in parentheses represent percentage removal.

Packing	*Column*	*Unbound (EU)*	
		Batch A	*Batch B*
Affi-Prep Polymyxin	2 (99.9)	5 (99.9)	$3 \cdot 10^3$ (99.8)
PMB-Agarose (Sigma)	26 (99.8)	90 (99.1)	$4.5 \cdot 10^4$ (96.3)
Detoxi-Gel	34 (99.7)	200 (98.0)	$6.5 \cdot 10^5$ (45.8)
Actigel-PMB	100 (99.2)	60 (99.4)	$6 \cdot 10^5$ (50.0)
PMB-Agarose (BM)	100 (99.2)	1400 (86.1)	$9 \cdot 10^5$ (25.0)
Added (EU)	13 000	10 000	$1.2 \cdot 10^6$

of PBS. Using the inhibition assay, no PMB was detected in the supernatant, which corresponds to a leakage of < 8 ppm of PMB or < 0.5 ppm/h.

Comparison with agarose affinity columns

Several commercially available agarose affinity packings, designed to remove endotoxin, have been compared with Affi-Prep Polymyxin in column and in batch assays at two different endotoxin levels (Table V). Columns (0.45 ml) of all packing materials were able to remove over 99% of the added endotoxin, Affi-Prep Polymyxin showing the most efficient binding (>99.9%). In the batch assay with low endotoxin levels, all except one material exhibited over 98% endotoxin removal. At the high endotoxin load of 1.2 million EU significant differences were noted between some of the packings probably reflecting differences in the binding capacities. Under all test conditions, Affi-Prep Polymyxin was superior to the agarose materials.

Applications of Affi-Prep Polymyxin

In addition to binding purified endotoxins, Affi-Prep Polymyxin can also remove "naturally" occurring endotoxins from various contaminated solutions. Passage of 20 ml of distilled water containing 15 EU/ml through an Affi-Prep Polymyxin column (10 × 8 mm I.D.) yielded a solution containing less than 0.05 EU/ml. The endotoxin level (500 000 EU/ml) of crude culture filtrates from *E. coli* cells could be reduced by >99.5% after incubation with Affi-Prep Polymyxin. HPLC cartridges containing Affi-Prep Polymyxin have also been used to reduce the endotoxin level of HPLC eluates.

Another application is the removal of endotoxin from antibody solutions. As an example, two monoclonal antibodies from ascites fluids have been purified and treated with the affinity material. An anti-human chorionic gonadotropin (HCG) was purified in a Bio-Rad HRLC 800 system by using sequentially, Affi-Prep cation-exchange (ABCM) and Affi-Prep Protein A cartridges. The other antibody against horseradish peroxidase (HRP) was purified on a conventional Affi-Prep Protein A column (1.0 ml). After elution from the Protein A columns with citrate buffer both antibodies were dialyzed against 20 m*M* phosphate buffer (pH 6.5). A 3.0-ml aliquot of the anti-HRP dialyzate, containing 2.1 mg protein/ml and 20 EU/ml was passed through a 0.5-ml column of Affi-Prep Polymyxin. This reduced the endotoxin level 98.5% to 0.3 EU/ml without affecting the protein. The same treatment of the anti-HCG dialyzate, containing 0.5 mg protein/ml and 61 EU/ml, yielded a solution with the same protein content and 6 EU/ml, representing a 90% reduction of endotoxin.

DISCUSSION

Polymyxin B is not a pure compound, but a mixture of closely related chemical substances. Commercial preparations have been separated by HPLC into 10–13 components[7]. The polymyxin B used in the preparation of Affi-Prep Polymyxin is of USP drug-quality, and this could be important in its application for affinity chromatography in purifying products for pharmaceutical applications where leakage of PMB could cause problems. Leakage of nanogram quantities of a substance administered as a drug in milligram quantities may not be objectionable. It should be added here that Affi-Prep Polymyxin appears to have a high ligand stability.

The Affi-Prep matrix has been designed to satisfy the scale-up requirements of industrial production. It is a rigid, macroporous polymer exhibiting excellent pressure/flow characteristics as well as excellent handling properties[8]. In addition, this resin is able to stand the harsh treatments needed for sterilization. The Affi-Prep Polymyxin support is not affected functionally by treatment with 1 *M* sodium hydroxide.

The endotoxin removal by Affi-Prep Polymyxin has been examined under a variety of conditions. Probably the most efficient removal of endotoxins is achieved in the batch mode, where typically 50 μl of resin can bind more than 99.5% of 5000–10 000 EU (0.5–1.0 μg). Efficient binding was also observed in column chromatography (Table V). High salt and buffer concentration appear to inhibit the endotoxin binding somewhat (Table I). However, binding efficiency was not affected by the addition of up to 10 mg/ml of BSA or IgG (Table II).

Endotoxin binding can be carried out in the presence of up to 1 mg/ml SDS or deoxycholate. In several experiments the highest efficiency was observed at concentrations of 1 mg/ml SDS. With dilution, there was a slight but significant decrease in binding efficiency. This may be related to the critical micelle concentrations (CMC) of these detergents. Around the CMC (1–2 mg/ml), the detergents may dissociate the LPS aggregates, making the molecules more accessible to the Affi-Prep Polymyxin resin. The use of a surfactant has recently been reported to reduce contamination by protein-bound endotoxin[9].

In addition to PMB, a second type of polymyxin (PME) is commercially available. If these two polymyxins would exhibit different binding patterns on different endotoxin molecules, it might be advantageous to incorporate a mixture of polymyxin molecules in an affinity support. To test this, PMB and PME were coupled to Affi-Prep and evaluated for their ability to bind the purified endotoxins isolated from a number of different strains of gram-negative bacteria. Both materials were able to bind the molecules from all the strains tested, with Affi-Prep Polymyxin being superior in all cases to the PME support. This result confirms that PMB alone is sufficient and further demonstrates the broad binding specificity of Affi-Prep Polymyxin, suggesting its applicability under a wide variety of conditions.

An important aspect of any affinity packing is the potential leakage of the ligand from the material contaminating the product(s) of interest. We have tested for PMB leakage under several incubation conditions, using two different assays for PMB. Using an HPLC assay with a detection limit of 250 ng/ml, no PMB was found in 0.1 *M* glycine (pH 10) or in 0.01 *M* sodium hydroxide washes. This corresponds to a leakage of <125 ppm PMB from the resin. If these values are calculated on the basis of unit time, they would be <7.5 ppm/h or <0.13 ppm/min. It is difficult to translate these rather long, harsh treatments to more normal chromatographic conditions, such as neutral pH and shorter contact time.

A more sensitive assay for PMB was developed, based on the ability of PMB to inhibit the LAL assay for endotoxin. Using this assay, little or no PMB was detected in the supernatant of a 16-h incubation at 37°C with PBS. This would correspond to a leakage of <20 ng/ml or <8 ppm of PMB from the column material. These results indicate that under these conditions there is little PMB leakage from the packing —a high ligand stability indeed.

Affi-Prep Polymyxin was superior in terms of endotoxin removal when

compared to four commercial agarose materials designed to bind endotoxins. The basis for this better performance is not known. It is probably not due to the PMB, as the source of PMB as well as the amount coupled does not appear to be critical for the binding efficiency of the Affi-Prep Polymyxin material. It is possible that the better performance may be due to the polymer matrix or to a synergism of the Affi-Prep matrix with the PMB.

Although the Affi-Prep Polymyxin has been tested mainly on purified endotoxins, it has been used in several practical applications, such as the efficient removal of endotoxin from water and from purified monoclonal antibodies. Affi-Prep Polymyxin treatment resulted in a 98.5% removal of endotoxin from the anti-HRP and only a 90% removal from the anti-HCG. This suggests that some endotoxin may be more tightly bound to some proteins than to others. It is possible that the use of Affi-Prep Polymyxin in combination with detergents, which may dissociate endotoxin and protein, may aid in the removal of tightly bound endotoxins.

ACKNOWLEDGEMENT

The authors would like to thank Susan Scott for her able assistance in the purification of the monoclonal antibodies.

REFERENCES

1 D. Fumerola, *Cell. Immunol.*, 58 (1981) 216.
2 D. C. Morrison and R. J. Ulevitch, *Am. J. Pathol.*, 93 (1978) 527.
3 M. Weary and F. Pearson III, *Biopharm*, April (1988).
4 A. C. Issekutz, *J. Immunol. Methods*, 61 (1983) 275–281.
5 R. E. W. Hancock, *Annu. Rev. Microbiol.*, 38 (1984) 237–264.
6 D. C. Morrison and D. M. Jacobs, *Immunochemistry*, 13 (1976) 813–818.
7 I. Elverdam, P. Larsen and E. Lund, *J. Chromatogr.*, 218 (1981) 653–661.
8 R. S. Matson and C. J. Siebert, *Prep. Chromatogr.*, 1 (1988) 67–91.
9 T. E. Karplus, R. J. Ulevitch and C. B. Wilson, *J. Immunol. Methods*, 105 (1987) 211–220.

Journal of Chromatography, 476 (1989) 187–194
Elsevier Science Publishers B.V., Amsterdam — Printed in The Netherlands

CHROMSYMP. 1584

ISOLATION OF A SPECIFIC MEMBRANE PROTEIN BY IMMUNOAFFINITY CHROMATOGRAPHY WITH BIOTINYLATED ANTIBODIES IMMOBILIZED ON AVIDIN-COATED GLASS BEADS

JAMES V. BABASHAK[a,*]
Kontes Scientific Glassware, Vineland, NJ (U.S.A.)
and
TERRY M. PHILLIPS
Immunochemistry Laboratory, George Washington University Medical Center, Washington, DC (U.S.A.)

SUMMARY

Avidin-coated, solid glass beads have been used as an immobilization support for attaching biotinylated antibodies. These beads have been packed into analytical, semi-preparative and preparative columns and used to isolate the B27 histocompatibility anigen (HLA) from human lymphocytes. The beads provided a suitable column material for all three chromatographic procedures and, depending on the size of the immunoaffinity column, B27 antigen could be isolated in nanogram to microgram quantities. Polyacrylamide gel electrophoresis demonstrated the presence of only a single band in the immunoaffinity peaks isolated by all three procedures. Enzyme-linked immunosorbent assay analysis of these immunoaffinity-isolated materials revealed that they were biologically active and could be used to determine the levels of anti-B27 antibodies in clinical studies.

INTRODUCTION

The isolation and recovery of membrane proteins can be a tedious and time-consuming job, but recent developments have greatly facilitated this task. Efficient isolation can be achieved by several different techniques, such as lectin affinity chromatography[1,2], immuno-precipitation[3–5] with monoclonal or polyclonal antibodies and immunoaffinity chromatography with antibodies, immobilized on either Protein A or streptavidin-coated glass beads, as the specific ligand[6–8]. The materials recovered by all of these techniques have been shown to be biologically active and, in the latter two techniques, the material was recovered in an immunologically pure form.

Analytical high-performance immunoaffinity separations, on avidin-coated glass beads as the immobilization support for biotinylated antibodies have been reported previously[7–9]. These reports demonstrated that the immobilized avidin–

[a] Present address: Immunochemistry Laboratory, Room 413, Ross Hall, 2300 Eye Street, N.W., Washington, DC 20037, U.S.A.

0021-9673/89/$03.50

biotinylated antibody complex coating of the glass bead was stable up to working pressures of 500 p.s.i.[9]. However, the solid glass bead–avidin complex can also be used as an antibody support for scale-up immunoaffinity isolations. In this paper, we describe the use of avidin-coated glass beads for both semi-preparative and preparative isolation of a lymphocyte membrane protein.

EXPERIMENTAL

Materials

Solid glass beads (diameter, 1 mm) were obtained from Kontes Scientific Glassware (Vineland, NJ, U.S.A.). Purified streptavidin was purchased as a lyophilized, pure product from Bethesda Research Labs. (Gaithersburg, MD, U.S.A.) and reconstituted in 50 m*M* carbonate buffer (pH 9.0). Mouse monoclonal antibodies (MAb), reactive with human leukocyte antigen (HLA) B27, were obtained as a purified immunoglobulin G (IgG) preparation from Chemicon International (El Segundo, CA, U.S.A.). The laboratory chemicals were obtained from Sigma (St. Louis, MO, U.S.A.); 3-aminopropyltriethoxysilane and 1,1′-carbonyldiimidazole from Pierce (Rockford, IL, U.S.A.); stainless-steel columns and column fittings from Alltech (Deerfield, IL, U.S.A.); and preparative glass columns were obtained from Kontes Scientific Glassware. HLA-B27 positive lymphocytes and human anti-HLA antibodies were obtained from normal volunteers.

Derivatization of the glass beads

The glass beads were prepared as previously described by Babashak and Phillips[9]. Briefly, the beads were washed by sedimentation in doubly distilled water to remove manufacturing impurities from the bead surface before peparing them for silanization and derivatization by placing 100 g of the washed beads into 500 ml of 1 *M* hydrochloric acid and gently sonicating for 25 min. This was followed by sedimentation in 1000-ml portions of 1 *M* hydrochloric acid and the process was repeated, using fresh acid solutions, until the acid supernatant became clear. The beads were then removed and air-dried, before refluxing them for 30 min in 500 ml of 1 *M* nitric acid, with constant agitation. The beads were recovered, air-dried, and resuspended in 500 ml of 10% 3-aminopropyltriethoxysilane in toluene. This suspension was gently refluxed for 16 h with constant agitation.

Following silanization, the beads were recovered and washed twice in 500 ml of 95% methanol before being transferred to fresh 95% methanol and refluxed for 20 min to remove the excess silanizing agent. The beads were allowed to settle, washed three times in doubly glass-distilled water, and air-dried prior to derivatization of the reactive side-groups.

The reactive carbonyldiimidazole (CDI) side-groups were attached to the bead surface by suspending the beads in 300 ml of dioxane and slowly adding 6 g of 1,1′-carbonyldiimidazole. The mixture was placed in a 500-ml capped conical flask and incubated for 6 h at room temperature in an oscillating shaker. The beads were then recovered and thoroughly washed in dioxane by sedimentation and decantation before being air-dried and immediately coated with streptavidin.

Bead coating procedure

A 100-g amount of the CDI-derivatized beads was suspended in 200 ml of double distilled water prior to the addition of 200 ml of 50 m*M* carbonate buffer (pH 9.0), containing 5 g of streptavidin. The mixture was placed into a 500-ml capped conical flask and incubated for 18 h at 4°C in an oscillating shaker. Following this incubation, the beads were allowed to settle and washed ten times in 0.01 *M* phosphate buffer by sedimentation and decantation. Attachment of the streptavidin to the beads was checked by incubating a 250-μl drop of the bead suspension, obtained from the last wash, with fluorescein-labelled biotin and examining 100 beads under a fluorescence microscope. Following satisfactory coating of the beads, they were sedimented, recovered and resuspended in 500 ml 0.01 *M* phosphate buffer.

Biotinylation of monoclonal antibodies

The hydrazine biotinylation technique[10] requires modification of the carbohydrate portion of the MAb, which was performed by suspending 100 mg of antibody in 10 ml of 0.1 *M* sodium acetate buffer (pH 5.0) and cooling to 4°C. A 10-ml volume of a 10 m*M* solution of cold sodium metaperiodate was added to the antibody before incubation for 20 min at 4°C in the dark. The reaction was stopped by adding 50 ml of 5% ethylene glycol and dialyzing the solution against 0.01 *M* phosphate buffer for 18 h at 4°C, with five changes of the dialysate. The antibody was then removed from the dialysis tubing and placed in a capped glass tube. To this was added 100 ml of phosphate buffer, containing 15 mg/ml of sodium cyanoborohydride and 25 mg/ml biotin hydrazine and the mixture was placed in a rotating mixer for 1 h at room temperature. The reaction was stopped by dialysis against 0.01 *M* phosphate buffer overnight, in a cold-room.

Column construction

The avidin-coated beads were packed into three different columns. Analytical 100 × 4.6 mm I.D. or semi-preparative 250 × 10 mm I.D. stainless-steel high-performance liquid chromatography (HPLC) columns were slurry-packed at 250 p.s.i., using a conventional pump-driven slurry packing apparatus. Preparative 15 × 1 cm I.D. glass columns were gravity-packed, using a bead–0.1 *M* phosphate buffer (pH 7.0) (1:3) slurry.

Isolation of lymphocyte membranes

Prior to disruption and solubilization of their membranes, human lymphocytes were isolated from whole blood by centrifugation at 400 *g* for 15 min in a Ficoll gradient[11]. The lymphocyte band was recovered, and $1 \cdot 10^8$ cells frozen and thawed until all cells were lysed and then sonicated in a Model 300 sonic dismembrator (Fisher Scientific, Columbia, MD, U.S.A.) for 2 min at 300 W. The sonicated pellet was resuspended in 5 ml of 0.01 *M* phosphate buffer, and the cellular debris sedimented by centrifugation at 10 000 *g* for 30 min. The membrane-containing supernatant was mixed with an equal volume of 1% sodium deoxycholate and incubated for 30 min at room temperature. Finally, the solubilized membrane sample was centrifuged for 1 h at 100 000 *g*, and the supernatant, containing 21–25 μg/ml protein was applied to the immunoaffinity columns.

Chromatography equipment

Analytical system. The avidin-packed analytical column was installed into a Beckman 340 isocratic HPLC system (Beckman, Palo Alto, CA, U.S.A.), equipped with a Model 112 pump, a Model 160 UV detector (set at 280 nm), and a Shimadzu C-R1B recording peak integrator (Shimadzu, Columbia, MD, U.S.A.). The elution profile was automatically controlled by a Model III OPG/S solvent selector/gradient controller (Autochrom, Milford, MA, U.S.A.). Samples were introduced into the system by injection through an Altex 210 injection port, equipped with a 100-μl sample loop.

Semi-preparative system. The semi-preparative column was installed into the same system as described for the analytical column, except that the Model 112 pump was replaced with a Model 110 pump, equipped with a semi-preparative pump head. Samples were injected into the system through an Altex 210 injection port, equipped with a 500-μl sample loop.

Preparative system. The preparative glass column was attached to a peristaltic pump (Pharmacia/LKB Biotechnology, Piscataway, NJ, U.S.A.) and the column effluent was monitored at 280 nm with a UV-2 ultra-violet monitor (Pharmacia/LKB). The peaks were recorded on the Shimadzu recording integrator. Gradient control was performed by the Autochrom Model III OPGS/S, used in both the analytical and semi-preparative studies. Samples of 2 ml were fed into the top of the column by gravity.

Immunoaffinity chromatography

Analytical system. The column was isocratically developed with 0.01 *M* phosphate buffer (pH 7.0) for 15 min at a flow-rate of 0.5 ml/min. Throughout the entire run, the column temperature was maintained at 4°C by a glass column jacket, attached to a recycling ice-bath. Following the initial 15-min run, during which the B27 antigen was bound to the immobilized antibody, an elution recovery phase was started. A chaotropic ion gradient was developed by adding 0 to 2.5 *M* sodium thiocyanate to the running buffer, over a further 15 min, and the upper limit of the gradient was maintained for a further 5 min before recycling the column by returning it to the initial running conditions. Fractions of the eluted material were collected in 500-μl Beckman microfuge tubes, in a modified ISCO Cygnet fraction collector (ISCO, Lincoln, NE, U.S.A.) and dialyzed overnight at 4°C against 0.01 *M* phosphate buffer.

Semi-preparative system. Chromatographic conditions similar to those described above for the analytical system were applied, with the exception that the flow-rate was slowed to 0.3 ml/min and the initial isocratic phase was extended to 60 min. The chaotropic ion gradient was started at 60 min, developed over a further 45 min, and then maintained at the upper limit of the gradient for 15–20 min before recycling the column. Fractions of the eluted material were collected in 1.5-ml Beckman microfuge tubes in the same fraction collector.

Preparative system. The preparative glass column was operated at a flow-rate of 1 ml/min. The initial phase was maintained for 120 min before gently developing the thiocyanate gradient over the following 90 min. The upper limit of the gradient was maintained for 30 min before recycling the column. Fractions of 1 ml of the eluted material were collected in an ISCO fraction collector.

Polyacrylamide gel electrophoresis (PAGE)

Analysis of the isolated materials were preformed by PAGE on a 10–30% linear gradient gel, containing 0.1% sodium dodecyl sulfate (SDS)[12]. Briefly, 25 μl of peak 2, isolated by all three procedures was reduced but not chemically modified by boiling for 5 min at 100°C in an equal volume of sample buffer (1% SDS and 5% β-mercaptoethanol dissolved in 0.01 *M* phosphate buffer, pH 7), and then allowed to cool to room temperature before use. A 10-μl sample of each specimen was placed into the sample wells in the analytical gel and run for 3 h at a constant voltage of 150 V. The gels were fixed in methanol–acetic acid (4:1) and then silver stained[13].

Enzyme-linked immunosorbent assay

The specificity of the immunoaffinity isolated material was tested by an enzyme-linked immunosorbent assay (ELISA)[14], using a battery of standard histocompatibility antisera and the anti-HLA-B27 MAb.

RESULTS AND DISCUSSION

Analysis of 80 batches of streptavidin-coated glass beads has shown that a 1-g batch of beads can be coated with between 0.72 and 1 mg of streptavidin. Once coated, the beads were able to bind between 100 and 124 μg of biotinylated antibody, which gave calculated bound antibody levels of 200 μg per analytical column; 550 μg per semi-preparative column, and 2.2 mg per preparative column. Stability analysis showed that the analytical columns could effectively be recycled between 20 and 30 times before loss of antibody could be detected. The semipreparative columns could be recycled 10–15 times and the peparative columns recycled 8–10 times. All columns remained stable for up to six months when stored in a refrigerator.

Antigen loading experiments showed that the analytical columns could isolate between 28 and 44 ng of B27 antigen, while the semi-preparative columns could isolate between 425 and 475 ng of the same antigen. The preparative columns could isolate

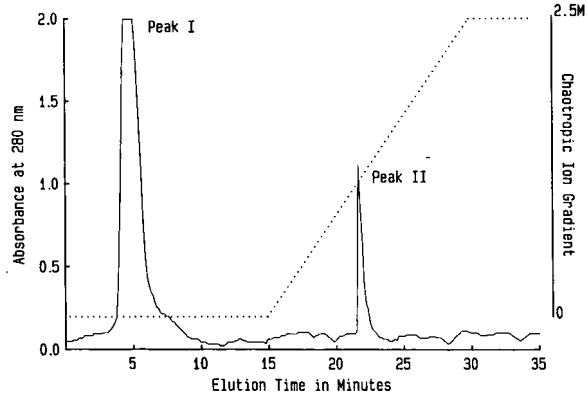

Fig. 1. Immunoaffinity isolation of HLA-B27 antigen from detergent-solubilized lymphocyte membranes. The separation was developed on a 100 × 4.6 mm I.D. analytical column. Flow-rate, 0.5 ml/min; detector, 280 nm, 0.005 a.u.f.s.; sample size, 100 μl. The dotted line represents the chaotropic ion gradient. Peak I represents the unbound material and peak II represents the immunoaffinity isolated material.

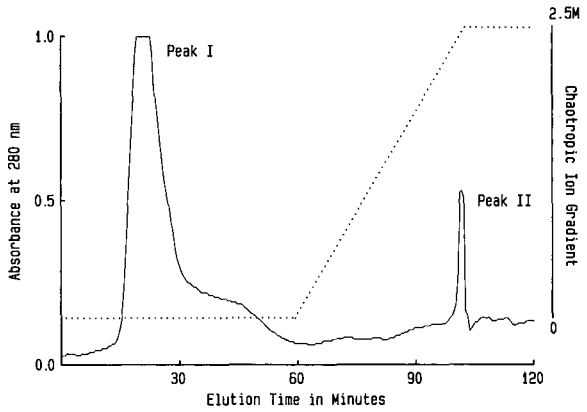

Fig. 2. Semi-preparative immunoaffinity isolation of B27 antigen on a 250 × 10 mm I.D. column. Flow-rate, 0.3 ml/min; detector, 280 nm, 0.08 a.u.f.s.; sample size, 500 μl. The chaotropic elution gradient is shown as a dotted line. Peaks I and II represent the same materials as described in Fig. 1.

between 3 and 8 μg of antigen depending on the protein content of the sample applied to the column and the expression of B27 antigen on the donor lymphocytes.

Fig. 1 demonstrates a typical chromatogram produced by performing an isolation of the B27 antigen on the analytical column. The non-B27 membrane material forms the first peak of the chromatogram, and the immunoaffinity isolated B27 antigen is eluted as the second peak, after 22.5 min.

Fig. 2 illustrates the chromatogram produced by the semi-preparative columns. Although the general profile is similar to that produced by the analytical column, the primary peak extends further into the chromatogram and the second peak is eluted further into the elution phase of the run (100 min). The delay in eluting the second peak is due to the decrease in flow-rate found to be essential when using the larger HPLC columns. Flow-rates of 0.5 ml/min and above caused a sharp decrease in the amount of bound antigen and a poor antigen recovery.

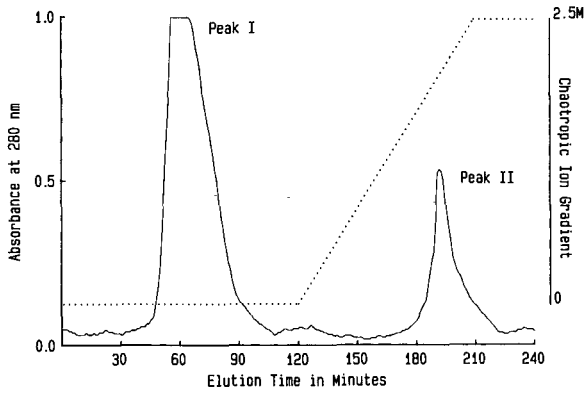

Fig. 3. Preparative immunoaffinity isolation of the same antigen on a 15 × 1 cm I.D. glass column. Flow-rate, 1 ml/min; detector, 280 nm, 0.08 a.u.f.s.; sample size, 2 ml. The elution gradient is indicated by a dotted line. Peaks I and II represent the same materials as described in Fig. 1.

TABLE I
ELISA ANALYSIS OF ISOLATED MATERIALS
All values expressed in absorbance units at 492 nm.

Antisera	*Peak II*		
	Analytical	*Semi-preparative*	*Preparative*
B27	1.389	1.101	0.988
B7-CREG[a]	0.258	0.291	0.300
Bw4[b]	0.206	0.242	0.260
HLA-B Loci (non-polymorphic)	0.816	0.861	0.772

[a] Common reactive group associated with HLA-B27.
[b] Common antigen associated with HLA-B27.

Preparative isolations were long and produced a larger, less well-defined second peak (Fig. 3). This peak was eluted after 190 min, although the immobilized B27 antigen–antibody complex appeared to dissociate earlier in the elution gradient. The antigenic material was also recovered in a large volume, which required concentration before SDS–PAGE and ELISA specificity testing could be performed.

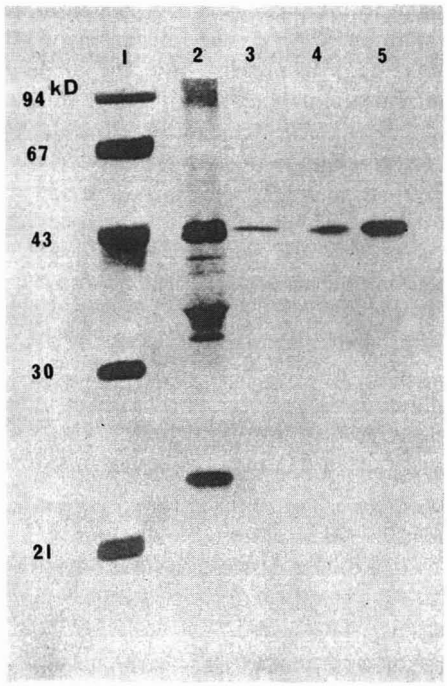

Fig. 4. Silver stained SDS–PAGE gel of the immunoaffinity-isolated material recovered in peak II from all three techniques. Lane 1, molecular weight standards; lane 2, membrane preparation; lane 3, peak II from the analytical column; lane 4, peak II from the semi-preparative column; and lane 5, peak II from the preparative column.

SDS–PAGE analysis of the second (immunoaffinity) peaks, isolated by the three techniques, showed the presence of a single peak at approximately 44 000 kilodalton (kD), which is similar to that described by others for the polymorphic chain of the HLA class I antigens[15,16]. This group includes the products of the HLA-B loci. No other protein bands could be detected in the immunoaffinity-isolated material, even though the gels were silver-stained for extra sensitivity (Fig. 4).

ELISA analysis of the immunoaffinity-isolated material showed strong reactivity with an antiserum directed against the common (non-polymorphic) area of the class I antigen polymorphic chain, associated with HLA-B loci products. This acted to confirm that the isolated material was derived from HLA-B class I antigens. The isolated materials also reacted strongly with the original anti-B27 MAb, which had been used as the immunoaffinity ligand. This reactivity was stronger than that observed with the anti-HLA-B loci antiserum and was strongest in the material isolated on the analytical column. No reactivity was seen with the antisera directed against other HLA-B antigens, even though the Bw4 and B7-CREG antisera have been reported to cross-react with a number of HLA-B antigens and especially B27[17]. The results of the ELISA analysis are shown in Table I.

Immunoaffinity isolation, of HLA, with avidin-immobilized anti-HLA MAb provides a rapid and simple technique for purifying not only these antigens but other membrane proteins[6]. In the HLA system, the molecular size and serological specificity of the immunoaffinity-isolated B27 antigen compared well with other reports on the isolation of class I HLA antigens by biochemical techniques[15,16].

The beads provide a suitable support medium for the immobilization of all classes of biotinylated antibodies and are large enough to provide unrestricted flow when used in semi-preparative and preparative-scale columns. The advantage of this bead system is that analytical procedures can be scaled up to semi-preparative or preparative procedures while still using the same packing material.

REFERENCES

1 J. W. Buckle and G. M. W. Cook, *Anal. Biochem.*, 165 (1986) 463.
2 D. Josić, W. Hofmann, R. Habermann and W. Reutter, *J. Chromatogr.*, 444 (1988) 29.
3 R. A. Roth, B. Maddox, K. Y. Wong, R. L. Styne, G. V. Vliet, R. E. Humble and I. D. Goldfine, *Endocrinology*, 112 (1983) 1865.
4 J. C. Venter, *J. Biol. Chem.*, 258 (1983) 4842.
5 W. C. Greene, J. M. Depper, M. Kronke and W. J. Leonard, *Immunol. Rev.*, 92 (1986) 29.
6 T. M. Phillips, in A. R. Kerlavage (Editor), *Receptor Biochemistry and Methodology*, Alan R. Liss, New York, in press.
7 T. M. Phillips and S. C. Frantz, *J. Chromatogr.*, 444 (1988) 13.
8 T. M. Phillips, S. C. Frantz and J. J. Chmielinska, *Biochromatography*, 3 (1988) 149.
9 J. V. Babashak and T. M. Phillips, *J. Chromatogr.*, 444 (1988) 21.
10 D. J. O'Shannessy and R. H. Quarles, *J. Immunol. Methods*, 99 (1987) 153.
11 H. Wigzell, *Transplant. Rev.*, 5 (1970) 76.
12 A. Chrambach and D. Rodbard, in B. D. Hames and D. Rickwood (Editors), *Gel Electrophoresis of Proteins: A Practical Approach*, IRL Press, Washington, DC, 1981, p. 93.
13 D. W. Sammons, L. D. Adams and E. E. Nishizawa, *Electrophoresis*, 2 (1981) 135.
14 J. E. Butler, *Methods Enzymol.* 73 (1981) 482.
15 H. Kaneoka, E. G. Engleman and F. C. Grumet, *J. Immunol.*, 130 (1983) 1288.
16 E. S. Kimball and J. E. Coligan, *Contemp. Top. Mol. Immunol.*, 9 (1983) 1.
17 B. D. Schwartz, L. K. Luehrman and G. E. Rodey, *J. Clin. Invest.*, 64 (1979) 938.

Journal of Chromatography, 476 (1989) 195–203
Elsevier Science Publishers B.V., Amsterdam — Printed in The Netherlands

CHROMSYMP. 1568

COATED SILICA SUPPORTS FOR HIGH-PERFORMANCE AFFINITY CHROMATOGRAPHY OF PROTEINS

F. L. ZHOU, D. MULLER*, X. SANTARELLI and J. JOZEFONVICZ
L.R.M. CNRS UA502, University Paris-Nord, Avenue J. B. Clément, 93430 Villetaneuse (France)

SUMMARY

Polymer-coated silica supports are potentially good stationary phases for high-performance affinity chromatographic separations of proteins. Silica beads have been coated with a polysaccharide (dextran or agarose), substituted by a calculated amount of positively charged diethylaminoethyl functions in order to neutralize the negatively charged silanol groups of silica and to facilitate the formation of a hydrophilic polymeric layer on the inorganic surface. The silica-based supports were prepared in two steps. First, the silica was impregnated with a solution of diethylaminoethylated polymer, and then the coating polymer was crosslinked in order to avoid leakage of the polymeric layer. The supports present minimal non-specific interactions with proteins, as tested by high-performance size-exclusion chromatography. These coated silica supports were coupled with active ligands, such as protein A, concanavalin A and heparin, by conventional coupling methods. The resulting affinity stationary phases were tested by the elution of proteins in order to study their performance in high-performance affinity chromatography.

INTRODUCTION

Porous silica beads have excellent mechanical proporties and can be prepared easily[1]. However, to be used as support in high-performance liquid chromatography (HPLC) of proteins, they have to be modified to avoid non-specific adsorption by the negatively charged silanol groups[1–6]. Silanol groups on the surface act as weak ion-exchanging groups and are responsible for this interfering adsorption phenomenon. Polysaccharide-based supports, such as Sepharose have excellent chromatographic properties in low-pressure liquid chromatography but, unlike silica, they have bad mechanical properties, leading to slow elution flow-rates[7]. It is interesting to combine the mechanical rigidity of silica with the hydrodynamic behaviour of polysaccharides[8,9]. We have prepared new stationary phases by coating silica beads with dextran or agarose substituted by a calculated amount of diethylaminoethyl (DEAE) functions. These DEAE units neutralize the ion-exchange capacity of native silica and facilitate the formation of a polymeric layer of the hydrophilic polysaccharides on the silica surface. The influence of several characteristics of these silica-based supports (*e.g.*, porosity of the starting silica beads, molecular weight of the

0021-9673/89/$03.50

polymer used, percentage of DEAE units, amount of polymeric coverage) was investigated by determining their performance in high-performance size-exclusion chromatography (HPSEC). These supports were activated by the classical methods used for hydroxyl-rich supports[10]. Ligands (protein A, concanavalin A and heparin) have been immobilized on these activated supports in a good yield. Tests were carried out by eluting samples of human IgG, ovalbumin, human antithrombin III (AT-III) and human α-thrombin from the affinity sorbents in order to investigate their performance in high-performance affinity chromatography (HPAC).

EXPERIMENTAL

The HPLC apparatus consisted of a Merck-Hitachi 655 A-12 gradient system from Labs Merck-Clevenot (LMC, Nogent sur Marne, France) with a Rheodyne 7126 injection valve, connected to an LMC variable-wavelength monitor and to a D2000 integrator. All solutions and buffers were prepared with doubly distilled water, which was degassed and then filtered through a 0.22-μm HA membrane (Millipore, Velizy, France). Molecular weight calibration curves for proteins were obtained as previously described[8]. The standard proteins were purchased from Sigma-Chimie (La Verpilliere, France). All chemical reagents were of analytical grade.

Preparation of silica-based supports

The silica-based supports were prepared in two stages. First, the silica beads (40–100 μm) were impregnated with a concentrated solution of DEAE polymer. Then, the polymer coating the beads was crosslinked in order to avoid leakage of the polymeric layer. The preparation of the dextran-coated support has been described previously[8].

Agarose (Indubiose A37 HAA and A37 NA), kindly provided by IBF Biotechnics (Villeneuve La Garenne, France), were modified by the following procedure. Agarose (10 g) was added to 210 ml of water at 60°C and stirred for 120 min. Then, 20 g of sodium hydroxide in 40 ml of water were added and the mixture was stirred at 55°C for 5 min. Next, 11.5 g of 2-diethylaminoethyl chloride hydrochloride (Janssen Chemica, Pantin, France) was added in several portions and the mixture was stirred at 55°C for 10–30 min. After the reaction had stopped, DEAE-agarose was precipitated with methanol–HCl (49:1, v/v) and the suspension was filtered under gentle suction in a 4-in. coarse sintered funnel. Finally, the filter cake was washed with ethanol, which was drawn off through the filter. The dried product was ground to a powder, and the remaining alcohol was removed under vacuum at 40°C. The characteristics of the DEAE-agarose were determined by acid–base titration of DEAE functions and by elementary analyse.

A batch method, followed by a cross-linking reaction, was used to coat the silica beads (silica X015 and silica X075, from IBF Biotechnics) with the DEAE-agarose. The starting silicas X075 and X015 have mean pore sizes of 300 and 1250 Å and specific surfaces of 100 and 25 m^2/g, respectively. An amount of 10 g of silica was impregnated with 0.46 g of DEAE-agarose in 23 ml of water (adjusted to pH 11.5) for 30 min at 80°C. The material was dried for 15 h at 80°C and the resulting powder was sieved. The impregnated silica was then added to a solution of 71 mg (0.55 mmol) of 1,4-butanediol diglycidyl ether (BDGE) (cross-linking agent) in 20 ml of diethyl ether and the mixture

was stirred for 30 min at 40°C. After evaporation of the solvent, the silica powder was dried for 15 h at 80°C, and the product was sieved. The amount of polymeric coverage, expressed as the weight percentage of impregnating polymer (g of polymer/100 g of support), was determined by elementary analysis for carbon.

Immobilization of active ligands

The supports were activated under the usual conditions for activation of hydroxyl-rich supports with either 1,1'-carbonyl-diimidazole (CDI) or BDGE[10]. Ligands (protein A, concanavalin A and heparin) were immobilized on the activated supports. Protein A and concanavalin A were supplied by IBF Biotechnics, and heparin (101 I.U./mg) was provided by Institut Choay (Paris, France). Immobilization of the ligands was performed by using 2.5 g of activated support suspended with the ligand in 12.5 ml of buffer (100 m*M* sodium carbonate, pH 8.7) at 20°C. The amounts of protein A and concanavalin A immobilized were determined by the Lowry method[11], and the amount of heparin immobilized was determined by the elementary analysis of sulphur on the dry stationary phase.

Performance of the affinity sorbents

The different biospecific affinity sorbents prepared from silica-based supports were used in chromatographic experiments in order to study their HPAC performance. Human IgG (IBF Biotechnics), ovalbumin (Sigma), human antithrombin III (37 I.U./ml, Centre Regional de Transfusion Sanguine, Lille, France) and human thrombin (1000 I.U./mg, Centre National de Transfusion Sanguine, Paris, France) were eluted from these stationary phases under salt gradient conditions. The eluted proteins were detected at 280 nm, and the chromatographic fractions were collected in order to determine the biological activity of the purified proteins and the recovery in the eluates.

RESULTS AND DISCUSSION

The basic principle of preparation of the silica-based supports is to coat inorganic stationary phases with hydrophilic polymer, substituted by a calculated amount of positively charged functional (DEAE) groups. These DEAE units neutralize the ion-exchange capacity of native silica and facilitate the formation of a polymeric layer of the hydrophilic polysaccharides on the silica surface. The hydrophilic layer will improve the chromatographic properties under aqueous eluting conditions. Moreover, these polymers can easily be activated by conventional activation methods, and ligands can be immobilized on the coated silica supports. It was demonstrated previously that the optimal substitution (expressed by the percentage of units bearing DEAE groups) for satisfactory coating is 4–13%[8]. The characteristics of the substituted polysaccharides used for preparation of the silica-based supports are given in Table I.

The amount of polymer covering the silica surface is the most important characteristic of a good coating. It is determined by elementary analysis of carbon, and is expressed as the weight percentage of impregnating polymer (g of polymer/100 g of support).

The effects of several characteristics of these silica-based supports (*e.g.*, the

TABLE I

CHARACTERISTICS OF SUBSTITUTED POLYSACCHARIDES

Modified polysaccharide	*Starting polysaccharide*	*Mw (g/mol)*	*Percentage of DEAE units*
DDT403	Dextran T40	35 600	4.3
DDT705	Dextran T70	68 000	4.5
DDT50011	Dextran T500	488 000	7.2
DHAA1	Indubiose HAA	–	10.0
DNA1	Indubiose NA	–	10.0

porosity of the starting silica beads, percentage of DEAE units and amount of polymeric coverage) have been investigated by studying the performance of the supports in HPSEC. Calibration curves for the standard proteins on the agarose-coated silica[8]. The results demonstrated that a minimum of 4% of polymer units bearing DEAE groups on the hydrophilic polymers covering the silica surface is necessary to minimize the ion-exchange capacity of the starting silica. If the percentage of polymer units bearing DEAE groups exceeds 13%, the cation-exchange capacity of the supports interferes with the steric-exclusion mechanism. A study of calibration curves indicated that silica coated with different polysaccharides exhibited similar chromatographic properties in HPSEC. The 1250-Å silica beads, coated with agarose or dextran, gave better resolution of proteins than the 300-Å silica beads (Fig. 1). Consequently this silica was selected as starting material for the preparation of HPAC supports. The characteristics of the supports used for HPAC are given in Table II.

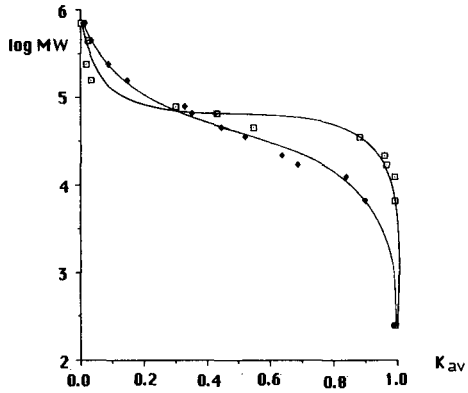

Fig. 1. Molecular weight calibration curves of standard proteins on different agarose-coated silica supports. Column, 25 × 0.7 cm I.D.; eluting buffer, 0.02 *M* Tris–HCl–0.15 *M* NaCl, pH 7.4; flow-rate, 1 ml/min.

Support	*Porosity (Å)*	*DEAE (%)*	*Impregnation (%)*[a]
SIA075HAA1 (□)	300	10.0	4.5
SIA015HAA1 (◆)	1250	10.0	4.7

[a] g of polymer/100 g of support.

TABLE II

CHARACTERISTICS OF SUPPORTS USED FOR HPAC

Support	*Silica porosity (Å)*	*Coating polymer*		*Impregnation (%)*[a]
		Name	*MW (g/mol)*	
SID403	1250	DDT403	35 600	8.1
SID704	1250	DDT704	68 000	10.4
SID5004	1250	DDT5004	488 000	10.1
SID50011	1250	DDT50011	488 000	10.1
SIANA1	1250	DNA1	–	4.5
SIAHAA1	1250	DHAA1	–	4.7

[a] g of polymer/100 g of support.

In order to confirm the passivation of silica, several plasma proteins [human albumin, human immunoglobulin (IgG), human AT-III and cytochrome] were injected into the different coated silica columns. No retention was observed, even at a 0.1 *M* ionic strength of sodium chloride, indicating that non-specific interactions had been minimized.

The immobilization of ligands (protein A, concanavalin A and heparin) on the coated silica supports was performed with CDI and BDGE as activating agents. The amount of immobilized ligand depended on the amount of activating agent used (Fig. 2). Similar coupling yields were obtained on DEAE-dextran- or DEAE-agarose-coated silica supports (Table III). The coupling yields of the coated silica supports were similar to those obtained with commercial polysaccharide-based supports.

In order to study their performance in HPAC, human IgG, ovalbumin, AT-III and thrombin were eluted from these coated silica supports grafted with different ligands. The results of elution experiments are presented in Table IV.

In the initial buffer, the proteins were strongly adsorbed on the coated silica supports grafted with the active ligands. A significant amount of protein was eluted by

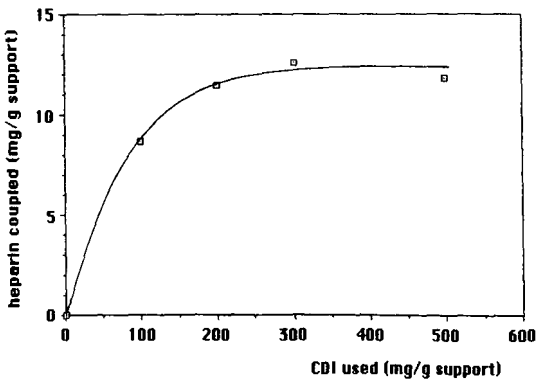

Fig. 2. Variation of the quantity of heparin coupled on SID50011 support with the quantity of 1,1-carbonyldiimidazole (CDI) used (20 mg of heparin/g support).

TABLE III

COUPLING CONDITIONS OF COATED SILICA SUPPORTS

Ql = quantity of ligand used (mg/g support). *Qa* = quantity of CDI used (mmol/g support). Con-A: concanavalin A.

Support	*Ligand*	*Ql*	*Qa*	*Yield (%)*
SID5004	Protein A	2.29	0.615	92
SIAHAA1	Protein A	2.29	0.615	89
SID5004	Con-A	20	1.23	71
SIAHAA1	Con-A	20	1.23	68
SID5004	Heparin	50	1.845	68
SIAHAA1	Heparin	50	1.845	68

a linear gradient. The conditions of desorption and recovery by elution from these affinity stationary phases were similar to those for the corresponding commercial polysaccharide-based affinity stationary phases. The nature of the polysaccharide (agarose or dextran) appears to have only a very slight influence on the chromatographic performance of the affinity stationary phases (conditions of desorption and recovery of eluted protein).

Results of a typical HPAC elution of human IgG on agarose-coated silica grafted with protein A are shown in Fig. 3. The protein was strongly adsorbed at pH 7.4 (0.02 *M* Tris–HCl, 0.15 *M* NaCl) and selectively desorbed by a decreasing pH gradient.

The elution of ovalbumin was carried out on an agarose-coated silica support grafted with concanavalin A. The glycoprotein was strongly adsorbed from the initial buffer (0.02 *M* Tris–HCl, 0.002 *M* $MnCl_2$, 0.002 *M* $CaCl_2$, pH 7.4) and specifically desorbed by competitive elution with glucose (Fig. 4).

Finally, a study was made of the elution of human AT-III (Fig. 5) and human thrombin (Fig. 6) from an agarose-coated support grafted with heparin. Thrombin and AT-III were strongly adsorbed at low ionic strength (0.02 *M* Tris–HCl, 0.1 *M* NaCl, pH 7.4) and selectively desorbed by raising the salt concentration in the eluting buffer. The eluted fractions were collected and then dialyzed against 0.15

TABLE IV

ELUTION CONDITIONS FOR HPAC OF PROTEINS

AT-III = antithrombin III; Pro-A = protein A; Hep = heparin.

Stationary phase	*Protein eluted*	*Conditions of desorption*	*Recovery (%)*	*Figure*
Pro-A SID5004	IgG	pH 3.40	84.5	
Pro-A SIAHAA1	IgG	pH 3.43	84.7	3
Con-A SID5004	Ovalbumin	0.082 *M* glucose	–	
Con-A SIAHAA1	Ovalbumin	0.082 *M* glucose	–	4
Hep-SID5004	AT-III	1.21 *M* NaCl	80	
Hep-SIAHAA1	AT-III	1.22 *M* NaCl	78	5
Hep-SIAHAA1	Thrombin	0.98 *M* NaCl	85	6

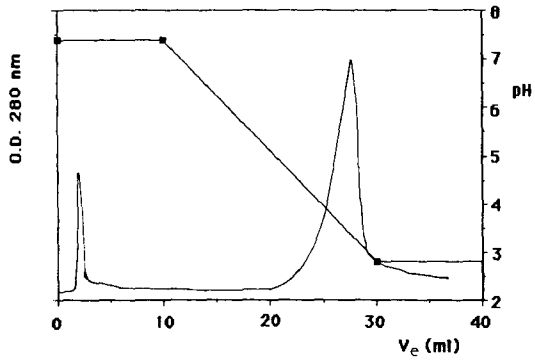

Fig. 3. Elution of human IgG from protein A–SIAHAA1 (gradient from pH 7.4 to 2.8). Column, 5 × 0.7 cm I.D.; sample, 100 µl human IgG (12.5 mg/ml); buffer A, 0.02 *M* Tris–HCl–0.15 *M* NaCl (pH 7.4); buffer B, 0.02 *M* glycine–HCl–0.15 *M* NaCl (pH 2.8); flow-rate, 1 ml/min.

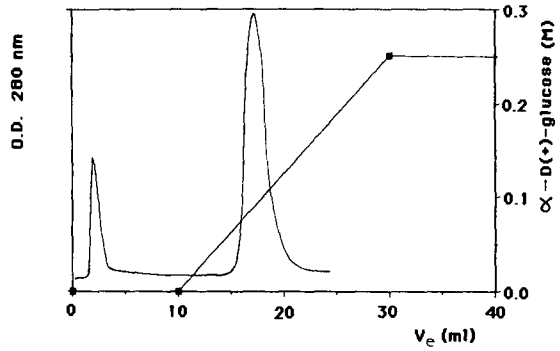

Fig. 4. Elution of ovalbumin from Con A–SIAHAA1 (gradient from 0 to 0.25 *M* α-D(+)-glucose). Column, 5 × 0.7 cm I.D.; sample, 100 µl ovalbumin (2.0 mg/ml); eluent 0.02 *M* Tris–HCl–0.15 *M* NaCl–0.02 *M* $CaCl_2$–0.02 *M* $MnCl_2$ (pH 7.4); flow-rate, 1 ml/min.

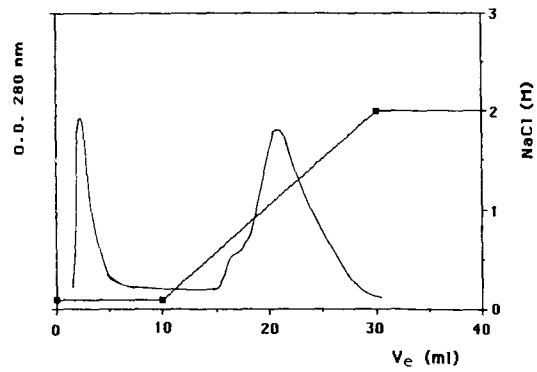

Fig. 5. Elution of human antithrombin III (AT-III) from Hep–SIAHAA1 (gradient from 0.1 to 2.0 *M* sodium chloride). Column, 5 × 0.7 cm I.D.; sample, 100 µl human AT-III (37 I.U./ml); eluent, 0.02 *M* Tris–HCl (pH 7.4); flow-rate 1 ml/min.

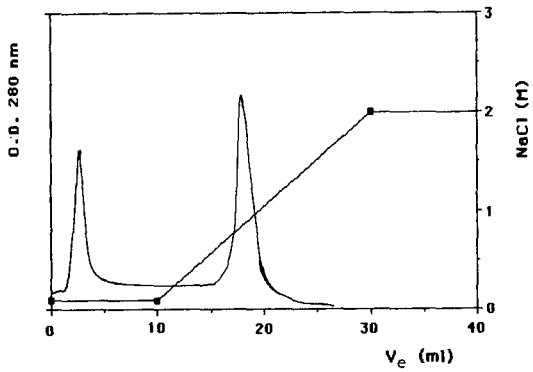

Fig. 6. Elution of human α-thrombin from Hep–SIAHAA1 (gradient from 0.1 to 2.0 *M* sodium chloride). Column, 5 × 0.7 cm I.D.; sample, 100 μl human thrombin (1000 U.NIH/ml); eluent, 0.02 *M* Tris–HCl (pH 7.4); flow-rate, 1 ml/min.

M NaCl aqueous solution for several hours at 4°C. The biological activity of AT-III was assayed for this suitability to inhibit thrombin in the presence of heparin by measuring the hydrolysis of Tos–Gly–Arg–pNa, *i.e.*, Chromo-Thrombin (from Diagnostica Stage, Asniéres-sur-Seine, France). The recovery of the eluted protein was determined by comparing the AT-III activity of human platelet-poor plasma with that of these fractions and of the starting material[12]. The thrombin time of these fractions was measured and compared with that of the starting sample. The recovery of the eluted protein, expressed as a percentage, could be calculated from a calibration curve[13]. Good recovery (>80%) was obtained in these elutions although α-thrombin was slightly inactivated during the separation at 22°C. For all of these separations, similar chromatograms were obtained with a dextran-coated support grafted with the same active ligand[9].

Twenty 100-μl portions of α-thrombin solution were injected successively into an affinity sorbent (Hep-SIAHAA1) under the same elution conditions. Similar chromatograms were obtained, indicating that there was no apparent change in the elution recovery during these elutions. This result demonstrated the excellent chemical stability of the coated silica supports.

CONCLUSION

In order to be used as chromatographic supports for proteins, silica beads must be passivated. This passivation can be carried out by a preliminary impregnation with a hydrophilic polymer having a relatively low percentage of units bearing positively charged DEAE groups. These DEAE units neutralize the ion-exchange capacity of native silica and facilitate the formation of a polymeric layer on the silica surface, so that non-specific adsorption of proteins on the coated silica is minimal. Because these coated silica beads possess the mechanical properties of the starting material and the hydrophilicity of the coating polymers, they can easily be grafted and used in HPAC. The active ligands can be immobilized in good yield by the conventional coupling methods used for polysaccharide-based supports. The chromatographic separations observed with these phases are similar to those obtained with commercial supports,

but can be obtained at high flow-rates. Moreover, because of the mechanical rigidity of the coated silica beads, the separation of proteins can easily be scaled up.

REFERENCES

1 K. K. Unger, *Porous Silica*, Elsevier, New York, 1979.
2 K. K. Unger, *Trends Anal. Chem.*, 2 (1983) 271.
3 F. E. Regnier, *Anal. Chem.*, 55 (1983) 1298A.
4 D. Muller, V. Baudin-Chinch and H. Wacjman, *Biosciences*, 5 (1987) 216.
5 L. Hagel and T. Anderson, presented at the *3rd Int. Symp. HPLC Proteins, Peptides and Polynucleotides, Monte Carlo, 1983.*
6 A. J. Alpert and F. R. Regnier, *J. Chromatogr.*, 185 (1979) 375.
7 J. L. Tayot, M. Tardy, P. Gattel, R. Plan and M. Roumiantzeff, in R. Epton (Editor), *Chromatography of Synthetic and Biological Polymers*, Vol. 2, Ellis Horwood, Chichester, 1978.
8 X. Santarelli, D. Muller and J. Jozefonvicz, *J. Chromatogr.*, 443 (1988) 55.
9 X. Santarelli, F. L. Zhou, D. Muller and J. Jozefonvicz, presented at the *Int. Symp. Biotech. Plasma Proteins, Nancy, 1988.*
10 *Practical Guide for Use in Affinity Chromatography and Related Techniques*, Technical note, IBF Biotechnics, Villeneuve la Garenne, 1983.
11 D. H. Lowry, N. J. Rosenbrough, A. I. Farr and R. J. Randall, *J. Biol. Chem.*, 265 (1951) 193.
12 O. R. Odegard, M. Lie and U. Abildgaard, *Thromb. Res.*, 6 (1975) 287.
13 C. Boisson, D. Gulino, J. Jozefonvicz, A. M. Fischer and J. Tapon-Bretaudiere, *Thromb. Res.*, 34 (1984) 269.

Journal of Chromatography, 476 (1989) 205–225
Elsevier Science Publishers B.V., Amsterdam — Printed in The Netherlands

CHROMSYMP. 1627

HIGH-PERFORMANCE LIQUID CHROMATOGRAPHY OF AMINO ACIDS, PEPTIDES AND PROTEINS

XCII[a]. THERMODYNAMIC AND KINETIC INVESTIGATIONS ON RIGID AND SOFT AFFINITY GELS WITH VARYING PARTICLE AND PORE SIZES

F. B. ANSPACH, A. JOHNSTON and H.-J. WIRTH
Department of Biochemistry and Centre for Bioprocess Technology, Monash University, Clayton, Victoria 3168 (Australia)
K. K. UNGER
Institut für Anorganische Chemie und Analytische Chemie, Johannes Gutenberg-Universität, 6500 Mainz (F.R.G.)
and
M. T. W. HEARN*
Department of Biochemistry and Centre for Bioprocess Technology, Monash University, Clayton, Victoria 3168 (Australia)

SUMMARY

In these investigations Cibacron Blue F3GA was immobilized on soft gels, porous silicas, and non-porous glass beads. Hen egg white lysozyme, human serum albumin and yeast alcohol dehydrogenase were used as adsorbates with the dye-affinity sorbents. Batch experiments with continuous monitoring of protein concentration were employed to evaluate thermodynamic and kinetic behaviour of these proteins in finite bath systems. The observed adsorption kinetic rates of interaction of the above proteins with each of the dye-affinity sorbents were found to decrease with increasing protein molecular weight. Equilibration times, in the batch experimental mode, of the adsorption of lysozyme on the dye-affinity sorbents varied from 20 s for the non-porous glass beads with a size range of 20–40 μm to more than 60 min in the case of a porous sorbent with a particle diameter of 100–300 μm and 60 nm pore size. Furthermore, equilibration times, which represent the overall adsorption rates incorporating all the non-equilibrium effects, increased with all affinity systems when adsorption took place in the non-linear portion of the isotherm. The most dramatic increase was observed when sorbents with relatively high protein size to pore size ratios, λ, were employed.

[a] For Part XCI, see ref. 1.

0021-9673/89/$03.50

INTRODUCTION

Economics, efficiency and practicality are some of the constraints dictating the search for novel chromatographic supports that exhibit high purification performance for proteins of industrial importance. In this regard, protein specific affinity chromatography or ion-exchange and other forms of electrostatic chromatography, which exploit differences in biological specificity or surface charge anisotropy of proteins, have the greatest potential in the isolation of the desired protein[2,3]. The large-scale purification of commercially important proteins to the high degree of purity necessary for pharmaceutical products requires integration of each purification stage. Research-based information is thus essential permit accurate prediction of the mass transport and biological activity behaviour of the solute under various operational conditions.

Development of methods for accurate prediction of the overall mass-transfer resistances associated with the chromatographic separation of proteins, which from practical experience are not comparable to those observed with low-molecular-weight compounds, require the evaluation of a complex family of parameters which describe the large-scale adsorption and elution behaviour of proteins[4–6]. Most mathematical models earlier used for this evaluation do not account for the time course of mass-transfer resistances within and around the stationary phase particles, yet it is established experimentally that the transport of macromolecules in the pores of the sorbent is a slow process[7,8]. Other studies on large-scale ion-exchange chromatography from this and other laboratories have also shown that the near-equilibrium hypothesis is often untenable in the overload mode[9,10].

The work described in the present investigations was aimed at elucidating some aspects associated with dye-affnity chromatography. In this respect, the adsorption and elution of different proteins, *i.e.* hen egg white lysozyme, human serum albumin, and alcohol dehydrogenase (yeast) from Cibacron Blue F3GA, immobilized on different soft and rigid chromatographic supports, was evaluated by using batch adsorption techniques analogous to the experimental set-up described by Chase[5] and Arnold *et al.*[11]. Overall rates of adsorption were determined and the adsorption characteristics compared at approximately 10% and 60% of the saturation of the sorbents.

THEORY

Factors controlling the thermodynamics in batch adsorption

The adsorption of a protein on an affinity sorbent relies on the affinity interaction, often described simply by the equilibrium relationship (eqn. 1), with the assumption that a single-site, homogeneous interaction occurs between the protein, P, and the ligand, L, and that non-specific interactions promoted by the support are absent. This relationship then takes the form

$$P + L \underset{k_2}{\overset{k_1}{\rightleftharpoons}} PL \qquad (1)$$

where k_1 and k_2 are the forward and reverse reaction rate constants. The rate of adsorption, as derived from eqn. 1, is then given by

$$\frac{dq}{dt} = k_1 c (q_m - q) - k_2 q \quad (2)$$

where c is the concentration of the solute in the mobile phase (bulk solution), q the concentration of the solute adsorbed on the affinity sorbent, and q_m the maximum capacity of the sorbent, representing the accessible concentration of immobilized ligands. When equilibrium exists throughout the system, the rate dq/dt is zero and eqn. 2 can be simplified to

$$q^* = \frac{q_m c^*}{K_d + c^*} \quad (3)$$

where K_d represents the dissociation constant. If it is assumed that only one type of interaction takes place, eqn. 3 describes the equilibrium isotherm, which has the same shape as isotherms reported more than 70 years ago by Langmuir for the adsorption of gases on solid phases[12].

These equations represent a simplistic case of protein adsorption. They describe a totally specific affinity of the protein, P, for the ligand, L. The results of the present study highlight the important practical reality that most, if not all, sorbents function as heterogeneous surfaces in terms of their structure and adsorption reactivities. Furthermore, the data are also consistent with the protein solute itself undergoing conformational changes and secondary chemical equilibria upon binding or in solution. This behaviour leads to further changes in sorbent reactivity which deviate from the simple equilibrium balance described above. In designing any process operation, attempts are made to minimize these non-idealities, but as is demonstrated in the present study it is not sufficient to presume that their effects are negligible or that their participation can be disregarded in the adsorption phenomenon.

Factors controlling the kinetics in batch adsorption

Typical analytes in affinity chromatography are large molecules with small diffusion coefficients. Because of their size and mainly globular shape the free diffusivity (intrinsic diffusivity), D_m, of proteins can be described by the modified Stokes-Einstein equation introduced by Young *et al.*[13]. The effective diffusivity, D_p, of a solute in a porous solid is related to its free diffusivity and the porosity of the solid and may be a much smaller value, when the ratio, λ, of the molecular size of the protein to the pore size is not negligible[14]. Additionally, when the ratio λ becomes large ($0.1 < \lambda < 1$), the reaction rate may be limited by rotational masking due to the highly specific adsorption step in affinity chromatography that often requires the appropriate orientation of the solute before adsorption on the affinity sorbent[14]. Similar behaviour has also been described for ion-exchange and hydrophobic interaction sorption of proteins[15,16]. Detailed descriptions of restricted diffusion and rotational masking have also been provided by Smith and Fournier[17,18], and Yau *et al.*[19]. Besides the choice of the protein solute, the selection of the ligand and the sorbent matrix, in terms

of their physical and chemical characteristics, require adequate definitions if data derived from model studies are to be of generic utility.

Selection of model affinity chromatographic systems

In the present studies, the adsorption behaviour of three proteins with 11 different supports to which Cibacron Blue F3GA had been covalently immobilized, has been evaluated. The criteria used for the selection of the model protein, ligand and sorbent systems is indicated below.

Proteins. To investigate the effect of mass transport limitations on the overall adsorption, lysozyme (EC 3.2.1.17), human serum albumin (HSA), and alcohol dehydrogenase (ADH) (EC 1.1.1.1) were chosen as representative of proteins having different molecular weights yet exhibiting different interaction mechanisms with Cibacron Blue F3GA. The protein ADH was chosen as representative of a large protein having a binding rate which should be diffusion controlled. Further, the immobilized triazine dye can behave as a biomimetic ligand capable of mimicking the interactions of the specific cofactor with the reduced nicotinamide-adenine dinucleotide (NADH)-binding site. In contrast, the rate at which lysozyme binds may be not only diffusion but also kinetically controlled whilst the interaction was anticipated to be surface directed. The molecular dimensions of HSA lie between ADH and lysozyme with the interaction again surface directed to each domain. The particular molecular characteristics of these three proteins are summarized in Table I.

Ligand. Biomimetic affinity chromatography based on immobilized triazine dyes is a well-established technique for the purification of proteins. The type of dye ligand employed in the affinity system will determine the nature of the binding to numerous classes of proteins either in a highly specific mode, where the chemical structure of the immobilized dye mimics the cofactor binding to specific allosteric or active sites of various enzymes[20], or in a less specific mode, where oppositely charged ionic groups at the protein surface and within the chemical functionality of the dye as well as hydrophobic binding sites between the two interacting species induce very strong adsorption of several classes of proteins[21,22]. For this study, Cibacron Blue F3GA was selected because it is predominantly used as a reactive dye and because its structure and chemical composition (in terms of impurity composition also) are well

TABLE I

MOLECULAR DIMENSIONS AND PROPERTIES OF PROTEINS

Protein	*Molecular weight* ($\cdot 10^3$ *daltons*)	*Accessible surface area* ($\cdot 10^8$ m^2)[a]	*Diameter (nm)*[b]	*Isoelectric point*
Hen egg white lysozyme	14.4	6.8	2.73	11.0
Human serum albumin	67	18.3	8.35	4.4–4.8
Alcohol dehydrogenase	148	31.1	10.2	8.1–9.3

[a] Taken from Janin[42].

[b] Taken from Travers and Church[43].

known[23]. Furthermore, Cibacron Blue F3GA immobilized on various soft gel and modified silica gel chromatographic supports exhibits similar chromatographic characteristics[24,25] as an affinity sorbent. The similarity shared by these different sorbents in terms of overall selectivity is important if their adsorption characteristics are to be adequately discriminated.

Stationary phases. Cost-effective preparative separation of complex biological mixtures by any chromatographic procedure aims at (i) high mass recovery, (ii) maintenance of biological activity, (iii) high resolution, (iv) high peak productivity and capacity and (v) short separation time. Thus, considerable effort has been devoted by a number of research groups over the past several years to preparing tailor-made sorbents based either on soft gels (*i.e.* new modifications of agarose, dextrans, polyacrylamide, trishydroxymethylpolyacrylamide supports) or on rigid silicas as well as the new polymer-based hybrid-clad inorganic supports. These new sorbents have enlarged pore diameters that freely accommodate proteins with molecular weights of 200 000 and more with average pore diameters of 30–600 nm and particle sizes of 10–150 μm. Typically, such matrices are intended for large-scale purification.

An alternative approach to preparative isolation of proteins is the use of high-performance non-porous packing materials similar to those introduced by us in 1984[26]. These matrices were initially designed as improved biospecific affinity sorbents in the analytical mode, but have been subsequently adapted to all modes of affinity chromatography[25], including dye–ligand affinity[24] and immunoaffinity chromatography[27]. Our investigations have demonstrated much more favorable mass transport and adsorption/desorption kinetic behaviour with these non-porous sorbents.

Finally, a group of stationary phases, based on porous or non-porous fibres, chemically modified to permit their use in biospecific affinity adsorption, can also be considered. Such stationary phases have attracted some attention in recent years (*cf.*, *e.g.*, Wikström and Larsson[28]). In the present study, however, only particulate systems have been examined.

EXPERIMENTAL

System conditions

The equilibration and adsorption buffer was 50 m*M* Tris · HCl, adjusted to pH 7.8, for all systems. With the HSA and lysozyme adsorption studies in finite baths, two experiment protocols were performed, one with the buffer mentioned above and the second with 0.5 *M* NaCl, added to the buffer solution. Because of the effect on the binding characteristics of these two proteins with and without salt present in the buffer with the various affinity sorbents, another set of data was generated to validate the binding characteristics following regeneration. In the regeneration cycle, the gels were suspended 3 times in the buffer described above, containing 2.5 *M* KSCN, and incubated for at least 3 min in order to allow the proteins to diffuse out of the porous matrix. In the case of very low adsorption kinetics, the incubation time was increased up to 15 min. After regeneration, the gels were re-equilibrated in the working buffer by washing the gel 5 times with the 2.5 *M* KSCN solution in a Büchner funnel.

Chromatographic supports

Soft gel chromatographic supports, such as Fractogel HW 55 (S), Fractogel HW

65 (F), and Fractogel HW 75 (F), were obtained from Merck (Darmstadt, F.R.G.), Trisacryl GF 2000 from Reactifs IBF (Villeneuve la Garenne, France), Cellufine GC 200 Medium and Cellufine GC 700 Medium from Amicon (Danvers, MA, U.S.A.), and Sepharose 4B, Sepharose CL6B, and Blue Sepharose CL6B from Pharmacia (Uppsala, Sweden).

The porous silica-based supports which were studied were Spherosil (Type X0B030) from Rhône-Poulenc (Usine de Salindres, France), and Nucleosil 300-2540 from Macherey Nagel (Düren, F.R.G.). Non-porous glass beads were a gift from Polters-Ballotini, Kirchheimbolanden, F.R.G. Characteristic parameters of the chromatographic supports are summarized in Table II.

Chemicals

3-Mercaptopropyltrimethoxysilane (MPS) and 1,6-lutidine were obtained from EGA (Steinheim, F.R.G.). Tris, hen egg white lysozyme (EC 3.2.1.17, dialysed and lyophilized) and ADH (EC 1.1.1.1, crystallised and lyophilized) from baker's yeast were purchased from Sigma (Sydney, Australia). Cibacron Blue F3GA was obtained from Serva (Heidelberg, F.R.G.). HSA (chromatographically isolated, containing 250 mg/ml protein, 85–130 m*M* sodium chloride and 40 m*M* sodium octanoate) was a gift from the Commonwealth Serum Laboratories (Melbourne, Australia).

Dialysis of HSA solution

In order to preclude undesirable absorption of the detergent (sodium octanoate) present in the stock protein solution to the Cibacron Blue F3GA-immobilized affinity sorbents, the HSA solution was diluted to a final concentration of 50 mg/ml protein and dialysed against 50 m*M* Tris · HCl (pH 7.8) at 277 K by changing the buffer 4 times at 8 h intervals.

TABLE II
CHARACTERISTIC PARAMETERS OF CHROMATOGRAPHIC SUPPORTS

Support	*Particle size* d_p *(μm)*	*Operating range of native sorbent (· 10^3 daltons)*	*Pore size* D_{p50} *(nm)*	*Specific surface area* (m^2/ml)
Soft gels				
Fractogel HW 55 (S)	25–40	1–900		
Fractogel HW 65 (F)	32–63	40-4500		
Fractogel HW 75 (F)	32–63	500–45 000		
Trisacryl GF 2000	40–80	120–15 000		
Cellufine GC 700	45–105	10–120		
Cellufine GC 200	45–105	10–400		
Sepharose 4B	45–165	80–20 000		
Sepharose CL6B	40–165	10–5000		
Silica gels and glass beads				
Spherosil X0B030	100–300		60	50
Nucleosil 300-2540	25–40		30	100
Glass beads fraction 4	20–40		–	0.19[a]

[a] Calculated from the geometric surface area, assuming a density for glass of 1.9 g/ml.

Preparation of protein solutions

Solutions of lysozyme and ADH were prepared daily by dissolving the protein of interest in the appropriate buffer to a final concentration between 19 and 21 mg/ml. Except for ADH, which was prone to precipitation during filtration, all protein solutions were filtered through 0.44-μm pore size filters to remove undissolved material.

Preparation of MPS-activated silicas

An amount of 5 g of either Spherosil X0B030 or Nucleosil 300 was suspended in 50 ml water (pH 3.5, adjusted with 0.01 *M* HNO_3). The pH was controlled and readjusted if necessary, and an equimolar quantity of MPS was added to the silica suspension, calculated on the basis of the specific surface area of the total amount of silica present, and an assumed amount of 8 μmol hydroxyl groups per m^2 of surface of the corresponding silica. The reaction vessel was evacuated to 2000 Pa, sonicated in an ultrasonic bath for 10 min, and then heated to 363 K for 3 h with stirring, essentially as described by Regnier and Noel[29]. After it had cooled, the derivatized silica suspension was neutralized by suspending the modified silica in water and filtering several times. Subsequently, the MPS-silica was suspended 3 times in both toluene and chloroform and filtered.

Preparation of MPS-activated non-porous glass beads

In order to obtain particles of narrower particle-size distribution than the original range of 2–40 μm, the glass beads were suspended in water and four fractions (2–5, 5–10, 10–25, and 20–40 μm, determined by microscopic analysis) were separated by sedimentation. Only fraction 4 was used for the bath experiments, whilst fractions 2 (5–10 μm), 3 (10–25 μm) and 4 (20–40 μm) were selected for fundamental chromatographic studies. The glass beads were then suspended in 5 *M* HCl and shaken for 12 h at 323 K in order to remove surface-bound impurities, such as iron, which had been previously shown to be present. In addition, the use of 5 *M* HCl permitted surface-bound aminopropyl groups, covalently attached to the glass (as specified by the manufacturer), to be also removed. The glass beads were washed extensively with water, filtered, and dried in the presence of self-indicating silica gel. Subsequently, 5 g of the glass beads were suspended in 40 ml water (pH 3.5, adjusted with 0.01 *M* HNO_3), 0.3 g MPS (excess) were added, and the suspension was shaken for 2 h at 363 K. The washing procedure was the same as that described above for porous silicas. Due to the relatively high concentration of MPS compared to the surface area of the non-porous glass beads, parts of the surface may have been covered by polymerised silane molecules which had been added in excess. The high silane concentrations were used because very little binding of the silane occurred when a concentration of silane equivalent to surface-located silanol groups was used initially. To avoid polymerization, which can limit the diffusional characteristics of the sorbents, further optimization of this reaction procedure is necessary.

Purity of Cibacron Blue F3GA

According to Hanggi and Carr[30], most of the commercially available triazine dyes are very heterogeneous and often contain only a small percentage of the dye of interest. To survey the purity of triazine dyes which had been previously used for

various purifications, a rapid chromatographic test was performed with a Zorbax ODS column (250 × 4.6 mm I.D.) and a 15-min gradient of acetonitrile (0–80%) at a flow-rate of 1.5 ml/min. A photo diode-array detector, coupled in series with a second detector set at 610 nm, displayed impurities either as single peaks or indicated their presence as part of the peak broadening of the major component of almost all of the Procion dyes. This analysis showed only a single peak for the Cibacron Blue F3GA preparation used in this study. This was in accordance with the product information from Serva, who guaranteed a purity of 85–90%, buffer salts being the major contaminant.

Immobilization of Cibacron Blue F3GA

The modified silicas with immobilized mercapto-group functionalities were suspended in 100 m*M* Na_2CO_3 (pH 8)–0.5 *M* NaCl, containing Cibacron Blue F3GA, according to the procedure decribed by Small *et al.*[31] for agarose-based gels. The reaction was carried out at 333 K by shaking the silica suspension for 12 h. The immobilized dye sorbents were washed by filtration or centrifugation and suspended several times in 50 m*M* Tris · HCl (pH 7.8) until the supernatants were colorless.

The reaction buffer for the soft gels was 100 m*M* Na_2CO_3 (adjusted to pH 9)–0.5*M* NaCl. The soft gels were washed several times with the reaction buffer and filtered in order to remove chemicals added for stabilization of these sorbents. The moist gel (10 g) was suspended in 30 ml of the reaction buffer, and 150 mg Cibacron Blue F3GA were added. The reaction was carried out at 333 K (313 K for the Sepharose 4B support, since a maximum temperature of 313 K had been recommended[32]), and the reaction vessels were shaken for 24 h.

Procedure for bath experiments

Bath experiments were performed by using the experimental set-up illustrated in Fig. 1. When soft affinity sorbents were used, between 0.3 g and 1 g (dried by drawing air through a sintered filter; 2 min for Fractogels, 10 min for other soft gels) of the gel were suspended in 20 ml buffer. When silica-based affinity sorbents were employed, between 0.2 g and 0.5 g of the completely dried gels were suspended in 20 ml buffer. To ensure complete penetration of the buffer solution into the pores of the affinity sorbents, reduced pressure (2000 Pa) was applied to the bath for 5–10 min prior to the experiments in order to remove air from the pore system. Complete mixing was

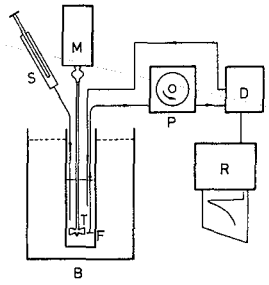

Fig. 1. Schematic diagram of experiment set-up of bath experiments. B = thermostatic bath, D = detector set at 280 nm, F = filter, P = peristaltic pump, R = chart recorder, S = HPLC syringe, T = continuously stirred tank (CSTR).

achieved with a turbine-blade stirrer, accommodating three blades, and operated with a rotary motor at 1100–1200 rpm. The adsorption apparatus was placed in a water bath thermostated at 308.5 K. A peristaltic pump continuously withdrew samples from the adsorption bath at a flow-rate of 1 ml/min, through a detector, set at 280 nm, back into the apparatus to keep the total volume constant. The protein concentration was monitored on a chart recorder connected to the detector. The detector was calibrated for each protein at different concentrations to allow accurate measurement of absolute protein concentrations. The dead volume of the system was kept to a minimum by using a tubing of 0.5 mm I.D. A filter with 12-μm gauze was placed at the end of the inlet (suction) tubing to prevent the particles from passing through the detector cell.

After a steady state had been achieved, a sample of protein solution of known concentration and volume was injected into the apparatus with a high-performance liquid chromatography syringe. The change in free protein concentration (c) in the bulk solution was traced on the chart recorder. When apparent equilibrium was reached, *i.e.* no change in protein concentration in solution, another injection with an increased volume followed, and the differential concentration was recorded. In this manner an adsorption isotherm was constructed over a range of protein concentrations and, simultaneously, the kinetics of adsorption could be followed at each point along the equilibrium isotherm.

By using the stirred tank no problems were encountered with most of the stationary phases as long as particle sizes were above 32 μm. When smaller particles were employed, clogging of the filter occurred, leading to a decrease in the flow-rate. Air bubbles were formed due to cavitation, and this resulted in some experiments being terminated prior to the determination of adsorption data at high concentration ranges. Spherosil and also the Fractogel supports very often gave a similar problem, but the reason was found to be the presence of either very small particles or other contaminants in the gel. In general, most difficulties were encountered with silica-based or non-porous glass beads, where microparticles very quickly accumulated at the filter. These difficulties restricted the use to silicas with diameters >25 μm in the lstirred tank, and kinetic data were obtained only for the Spherosil and non-porous glass bead supports of larger particle diameter.

Procedure for equilibrium experiments

An alternative method of batch adsorption was utilized to circumvent the problems experienced with the stirred-tank system described above and to compare data obtained from the stirred tank. By using 10 tubes with a maximum capacity of 5 ml, 0.1 g of the affinity sorbent, varying protein and buffer solutions, adjusted to a final volume of 2 ml, were added such that the same ratios as in the method above were maintained. The flasks were shaken in a water bath for 2 h to simulate a state of equilibrium. The amount of protein adsorbed on the gel was then determined from the difference in concentration initially added to that found in the supernatant afterwards.

Evaluation of thermodynamic data

The amounts of adsorbed protein (q^*) at equilibrium from either stirred-tank or equilibrium experiments were plotted against the free protein concentration, c^*, in solution (*cf.* Figs. 2 and 3). In the case of HSA, the c^* value was corrected for 6% impurities in the HSA preparation, which were found not to bind to the Cibacron Blue

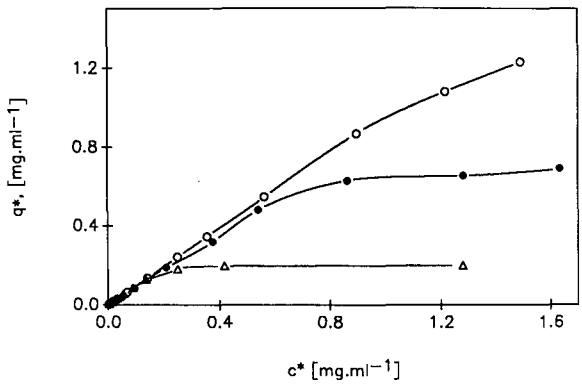

Fig. 2. Equilibrium isotherms for the adsorption of lysozyme onto three different pore size Fractogel TSK HW immobilized Cibacron Blue F3GA. An amount of 1 g of wet gel was suspended in 20 ml of 50 m*M* Tris · HCl pH 7.8, temperature 318.5 K. (○) Fractogel HW 55 (S), (●) Fractogel HW 65 (F). (△) Fractogel HW 75 (F).

F3GA-immobilized sorbents from corresponding frontal analysis experiments. Each experiment was terminated after the system approached saturation (upper part of the isotherm). For the determination of the accessible ligand concentration (q_m) and the dissociation constant (K_d) a double reciprocal plot of $1/q^*$ against $1/c^*$ was chosen. This numerical approach permits q_m to be evaluated from the y-intercept and K_d from the slope of the linear part of the plot, as illustrated in Fig. 4. Additionally, a plot of c^*/q^* against c^* was made to assure that the data selected for the determination of the thermodynamic parameters were appropriate.This could not always be achieved from the double reciprocal plot due to the reciprocal relationship to the concentration. A Scatchard plot analysis[33], *i.e.* plotting q^*/c^* against adsorbed protein q^* (*cf.* Fig. 5) completed this analysis. Due to the sensitivity of the Scatchard plot, different types of interaction could be discerned, mainly non-specific and specific interactions, and protein–protein association, the latter interaction often occurring during protein adsorption.

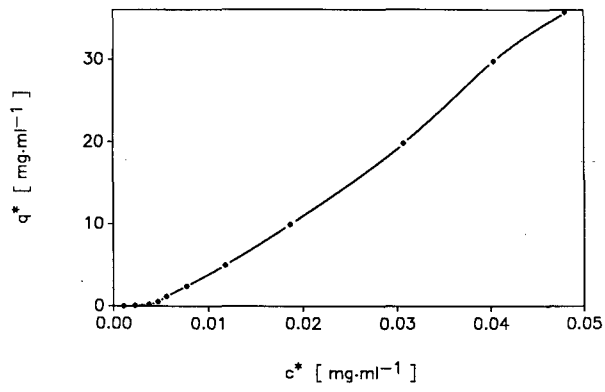

Fig. 3. S-shaped isotherm from adsorption of lysozyme to Cibacron Blue F3GA immobilized to Trisacryl GF 2000. An amount of 1 g of wet gel was suspended in 50 m*M* Tris · HCl pH 7.8, temperature 318.5 K.

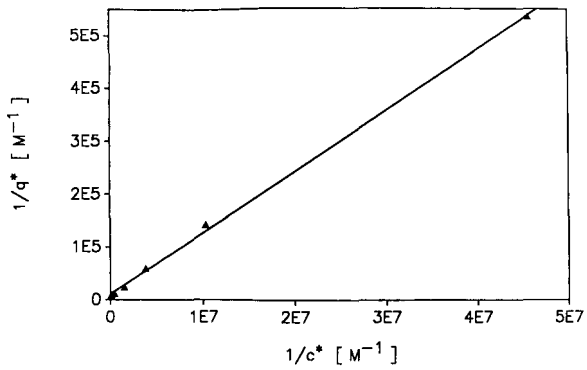

Fig. 4. Double reciprocal plot from the adsorption of HSA to Blue Sepharose CL6B in 50 m*M* Tris · HCl pH 7.8, temperature 318.5 K.

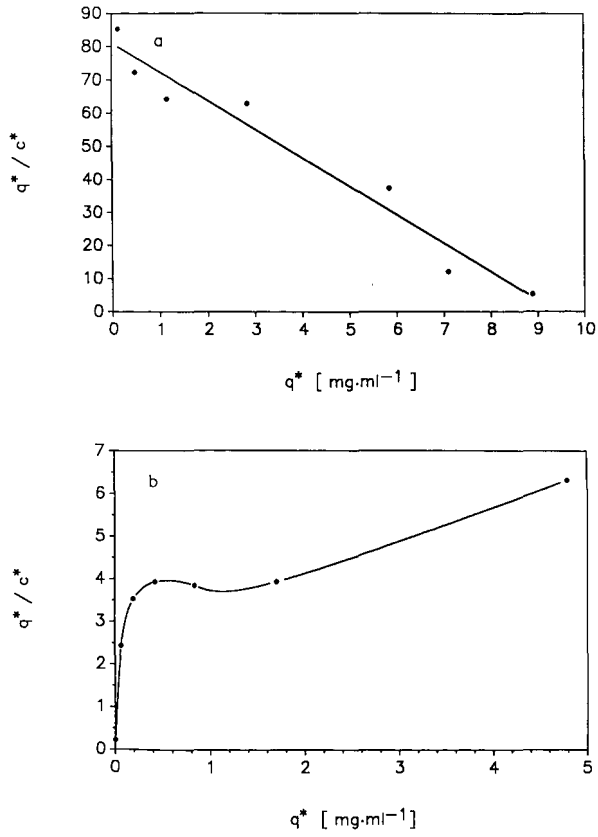

Fig. 5. Scatchard plot analysis derived from adsorption data of the Blue Sepharose CL6B support. (a) HSA adsorption, the observed linearity confirms a specific interaction as expected. (b) Lysozyme adsorption, the increase in protein adsorption at higher protein concentration arises from protein–protein interaction.

Evaluation of equilibrium times

The evaluation of kinetic data was mainly based on comparison of the kinetic uptake of the different proteins by the affinity sorbents. In addition, the periods of time between injection and equilibrium in the stirred-tank experiment at 10 ± 5% and at 60 ± 10% of saturation were measured for each affinity sorbent and protein, as displayed

TABLE III
CHARACTERISTIC PARAMETERS OF AFFINITY SORBENTS

Sorbent	q_m *(mol/ml)*	K_d *(M)*	*Equilibration time (min)*	
			10 ± 5% of saturation	*60 ± 10% of saturation*
Trisacryl GF 2000				
HSA[a]	$2.3 \cdot 10^{-8}$	$2.8 \cdot 10^{-7}$	8	22
HSA[b]	$7.8 \cdot 10^{-8}$	$1.0 \cdot 10^{-6}$	12	40
HSA (+ NaCl)	$6.4 \cdot 10^{-8}$	$2.1 \cdot 10^{-6}$	–	20
Lysozyme[a]	$9.4 \cdot 10^{-6}$	$6.3 \cdot 10^{-6}$	3.4	20
Lysozyme[b]	–	$1.3 \cdot 10^{-5}$	3	20
Lysozyme (+NaCl)	$4.7 \cdot 10^{-6}$	$1.2 \cdot 10^{-3}$	3	> 8
Sepharose CL6B				
HSA	$4.9 \cdot 10^{-8}$	$5.2 \cdot 10^{-7}$	3.6	10
HSA (+ NaCl)	$6.8 \cdot 10^{-8}$	$7.3 \cdot 10^{-7}$	–	12
HSA[c]	$1.3 \cdot 10^{-7}$	$1.4 \cdot 10^{-6}$	4.5	31
ADH[c]	$4.5 \cdot 10^{-8}$	$5.1 \cdot 10^{-7}$	11	46
Sepharose 4B				
HSA	$6.2 \cdot 10^{-8}$	$5.9 \cdot 10^{-7}$	5	16
Cellufine GC 700				
HSA	$5.8 \cdot 10^{-8}$	$2.7 \cdot 10^{-6}$	14	50
Fractogel HW 55 (S)[d]				
HSA	$4.0 \cdot 10^{-8}$	$7.0 \cdot 10^{-5}$	–	–
Lysozyme	$1.9 \cdot 10^{-7}$	$1.9 \cdot 10^{-4}$	–	–
Fractogel HW 65 (F)[d]				
HSA	$3.0 \cdot 10^{-8}$	$3.8 \cdot 10^{-5}$	> 3	> 7
Lysozyme	$1.2 \cdot 10^{-7}$	$1.4 \cdot 10^{-4}$	> 4	> 8
Fractogel HW 75 (F)[d]				
HSA	$1.0 \cdot 10^{-8}$	$2.8 \cdot 10^{-5}$	> 1.3	> 6
Lysozyme	$6.0 \cdot 10^{-8}$	$7.4 \cdot 10^{-5}$	> 0.1	> 8
Nucleosil 300-2540[e]				
HSA	$2.9 \cdot 10^{-7}$	$1.4 \cdot 10^{-6}$	> 5	>40
Glass beads fraction 4				
Lysozyme (+ NaCl)	–	–	~0.5	
Spherosil X0B030				
Lysozyme (+ NaCl)	–	–	>60	

[a] Low density of immobilized Cibacron Blue F3GA.
[b] High density of immobilized Cibacron Blue F3GA.
[c] Commercial available Blue Sepharose CL6B.
[d] Total ligand concentration from differential UV absorbance readings, an overestimate of accessible ligand concentration.
[e] Elution of HSA was impossible.

in Table III. This was found to be the most appropriate way to illustrate adsorption characteristics of the various sorbents used in the present study.

RESULTS

Adsorption of lysozyme

Equilibrium constants of the lysozyme–Cibacron Blue F3GA complex were found to be substantially lower than equilibrium constants for HSA, as indicated in Table III. The adsorptive performance of all Fractogel HW-based sorbents was generally lower than that of to the Trisacryl-based sorbents when no salt was added to the buffer. In Fig. 2 the equilibrium isotherms of the adsorption of lysozyme on three Fractogel-based sorbents HW 55 (S), HW 65 (F) and HW 75 (F) are displayed. The Fractogel HW 55 sorbent demonstrated the greatest capacity. This is consistent with the smaller pore size and corresponding higher surface area of this sorbent compared to the other sorbents. The data obtained with the Fractogel HW 55 dye sorbent from the two methods used, as described in the Experimental section, gave remarkably concordant results, and the calculated isotherms reflected this. However, a crucial point of difference was the leakage characteristics of adsorbed dye molecules which did not bind to the sorbent during the immobilization procedure. With the salt concentration finally chosen for the immobilization conditions (0.5 *M* NaCl), the coupling and washing supernatants contained very little free dye after removal of the dye sorbent by filtration, indicating that either very strong chemical immobilization or physical adsorption of the dye molecules had occurred. When no salt in the washing procedure was employed, most of the physically adsorbed dye was eluted. Nevertheless, when these sorbents were exposed to protein for the first time, more dye molecules were displaced by the adsorbing proteins, as evident from higher UV absorption readings of the effluent than theoretically was possible. The displacement of the dye decreased after incubation of these sorbents with protein solution and subsequent reconditioning prior to the next experiment, but it was never eliminated entirely throughout the experimental series with the Fractogel HW sorbents. In the case of the Trisacryl affinity sorbents no such dye displacement was evident. However, the curve of the equilibrium isotherm for lysozyme with the Trisacryl GF2000 dye sorbent was S-shaped, as indicated in Fig. 3. This result was reproducible with different batches of the Trisacryl GF2000 dye sorbent in subsequent experiments under the same eluent conditions. In other experiments, when 0.5 *M* NaCl was added to the buffer no S-shaped isotherm was observed but rather a linear isotherm, which did not curve downward at higher concentrations. The observed equilibrium constant for lysozyme with the Trisacryl GF2000 dye sorbent in the presence of 0.5 *M* NaCl of 847 M^{-1} was much lower than that obtained from experiments without salt, indicating that added salt decreases the Cibacron Blue–lysozyme interaction dramatically.

At low concentrations, all the transformed isotherm data from different sorbents deviated in the double reciprocal plots from linearity, suggesting that the Langmuir isotherm model is not wholly indicative of the experimental situation. As previously mentioned, the derivation of the simplest form of the Langmuirean equation assumed specific binding and homogeneity of the sorbent. Participation of other phenomena subverting the role of these two important factors may account for this deviation from linearity with the double reciprocal plot. Finally, Scatchard plot analysis indicated that

other mechanisms of interaction are present, as demonstrated by Fig. 5a. For example, at high protein concentrations, lysozyme appeared to have a higher affinity for the dye sorbent, a situation which can only be attributed to protein–protein interaction, exacerbated when lysozyme is dissolved at a pH higher than 8.0[34]. Self association of lysozyme at pH 7.8 might also occur at the surface of the affinity sorbent where locally a higher protein concentration is achieved. The same behaviour in the Scatchard plot was manifested when salt was added to the buffer, although in this case it developed at low protein concentrations. The latter effect confirmed that protein–protein association was an important component of the increased interaction of these proteins at higher salt concentration. The observed equilibrium constant with 0.5 *M* NaCl may be related to the dimerisation equilibrium constant of lysozyme at pH 7.8.

Adsorption of HSA

Compared to lysozyme, HSA displayed a much higher affinity to Cibacron Blue, as illustrated in Table III. Equilibrium isotherms demonstrated normal behaviour, as shown in Fig. 6 for the Trisacryl- and Sepharose-immobilized dye sorbents. In the case of the Cellufine GC 700 sorbent, dye displacement was evident at low protein concentrations, and this leakage behaviour could not be changed by preadsorption of the gel with HSA, as described for lysozyme with the Fractogel affinity sorbents. With the Cellufine GC 200 sorbent the adsorbed dye was readily released in the absence of protein, indicating that significant amounts of dye were physically adsorbed in the pores of the gel. HSA, adsorbed on silica-immobilized Cibacron Blue F3GA, could not be adequately eluted under any elution condition applied. However, the adsorption did not appear to be irreversible, since apparent equilibrium binding was observed after each protein injection. As described for Cellufine GC 700, the silica-based Nucleosil 300-2540 sorbent also displayed dye displacement at low protein concentration.

Despite interference of dye displacement of affinity sorbents with the adsorbate HSA, double reciprocal plots and Scatchard plot analysis of the experimental data suggested the absence of nonspecific interactions, that is, a linear relationship between

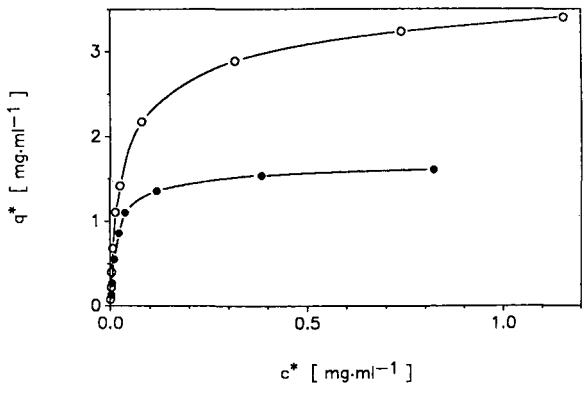

Fig. 6. Langmuirian isotherms for the adsorption of HSA to Cibacron Blue F3GA immobilized supports. An amount of 1 g of wet gel was suspended in 50 m*M* Tris · HCl pH 7.8, temperature 318.5 K. (○) Sepharose CL6B, (●) Trisacryl GF 2000.

the transformed parameters c^* and q^* was observed. Deviations from linearity in the adsorption isotherm at low protein concentrations was always associated with dye displacement, which was evident as high UV absorption readings of the eluent stream. HSA displayed lower affinity for the immobilized dye when 0.5 *M* NaCl was present in the buffer, a result which agrees with those observed for the adsorption of lysozyme in the presence and absence of salt. However, the differences in association affinities were less dramatic (*cf.* Table III). In the case of the Trisacryl GF 2000 dye affinity sorbent, the calculated q_m values are identical for experiments carried out in the presence and absence of 0.5 *M* NaCl. However, when the Sepharose CL6B dye affinity sorbent was employed, a 40% increase in q_m was observed when 0.5 *M* NaCl was added.

The behaviour of the Fractogel sorbent diverged from the other affinity sorbents, displaying only very little adsorption capacity and also low equilibrium constants with HSA. This behaviour may have been a consequence of the shrinkage of the Fractogel sorbent during immobilization or of a change in its microstructure and fractal surface, effects which could be responsible for low protein accessibilities to the immobilized Cibacron Blue F3GA. A change in the microstructure of the Fractogel sorbents was found in our previous experiments, in which carbonyldiimidazole (CDI) activation had been used and where an increase in ligand density on Fractogel HW 65 resulted in only a modest increase in capacity but a significant decrease in the proportion of high-affinity sites accessible to the substrate[35].

Adsorption of ADH

In contrast to results reported in the literature on ADH binding to CibacronBlue F3GA[36], ADH from yeast did not bind to any of the Cibacron Blue F3GA-immobilized soft gels or silica sorbents. This result was unexpected in light of our earlier studies that demonstrated that silica-immobilized Cibacron Blue F3GA binds lactate dehydrogenase (LDH) and malate dehydrogenase in a very specific mode[24]. ADH, like other dehydrogenases, requires NADH as a cofactor, and in a manner analogous to other NADH-dependent enzymes, this enzyme should bind to Cibacron Blue F3GA via the enzyme active site, since the dye is reported to mimic the cofactor NADH[37]. However, the lack of binding of ADH suggests that the adsorption mechanism of this enzyme is different from that of the other dehydrogenases. To verify the binding of LDH to Cibacron Blue F3GA immobilized on soft gels, Trisacryl GF 2000 was chosen as an alternative dye affinity sorbent and LDH was adsorbed on and eluted from this sorbent, confirming the results of our previous work. Commercially available Blue Sepharose CL6B was also chosen for ADH adsorption to examine the influence of dye purity, as detrimental effects due to dye heterogeneity of commercial dyes could influence the experimental outcome. In this case, high affinity of the enzyme for the dye sorbent was demonstrated. Our results, showing no binding of ADH to the other dye sorbents, can be explained if the Cibacron Blue F3GA obtained from Serva contained only the *meta*-substituted isomer at the terminal benzene ring, a compound which is reported not to bind to ADH[38].

The affinity constant of ADH binding to Blue Sepharose CL6B was comparable to the observed affinity constant of HSA for Cibacron Blue F3GA, despite the requirement for ADH to be eluted by using 0.5 *M* NaCl in the buffer. These results suggest that binding of ADH to the dye affinity sorbent is mainly due to ionic interaction and hydrogen-bonding sites, whereas HSA binds also via complementary

hydrophobic binding moieties on the protein and the ligand, where the affinity can only be moderated by addition of salt to the buffer system. To compare the affinity of ADH and HSA for the same affinity sorbent, HSA was also adsorbed on commercially available Blue Sepharose CL6B, by using the same buffer conditions. The results from this experiment showed that the affinity of ADH is twice as high as that of HSA, while the accessibility of protein for the dye affinity ligand is only one-third as large. This behaviour is in accord with the size difference between ADH and HSA which will restrict to a significant extent the diffusion of ADH to the ligand immobilized in narrow pores.

Diffusion properties of the proteins

A dramatic difference in adsorption behaviour is evident when the protein uptake in the bath system for proteins of increasing molecular weights are compared, using the same affinity sorbent. Whilst equilibrium of lysozyme was usually attained with the experimental system between 2 and 5 min, equilibration times for HSA, were 2–3 times longer and for ADH slightly longer than for HSA. Especially at low ADH concentrations, the time required for equilibrium to be accomplished was much longer than for lysozyme and HSA, a result which suggests that ADH binding is mainly diffusion controlled.

Mass-transfer restrictions of affinity sorbents

Equilibration times after injection of protein solution into the stirred tank varied substantially with the extent of saturation of the affinity sorbent. At low adsorption concentration (q^*) the kinetics appeared to be very fast and not controlled by the diffusion of the protein into the porous system of the sorbent (Fig. 7). At this stage, most of the protein is immediately adsorbed on the external surface and the outer shell of the affinity sorbent. Under these conditons, pore diffusion is negligible, if not absent, and has very little influence on the adsorption rate. At higher protein concentrations in the bath experiments, when the affinity sorbent is close to saturation, protein uptake decreased dramatically. This is in concordance with eqn. 2, and dq/dt will reduce as q approaches q_m and also the dissociation of adsorbed protein from the sorbent becomes more noticeable close to saturation. The decrease in protein uptake at these protein concentrations was more noticeable when supports with low permeability ranges were used, like Cellufine GC 700 or Nucleosil 300-2540. This may indicate that steric restrictions at pore entrances and/or inside the porous system of these sorbents may be a major rate-determining step when the protein size to pore size ratio, λ, is greater than 0.2, as suggested by Webster[14]. Upon saturation of the affinity sorbent, only a small amount of protein is adsorbed and the steady state is very quickly attained again. This trend was consistently evident in the results from all sorbents and proteins used in this study.

Protein uptake in the bath experiments decreased with increased particle size due to longer diffusion paths, as expected. For the non-porous glass bead affinity sorbents, equilibration times were in the range of 20–35 s, compared to 10–40 min for the porous gel affinity sorbents. The non-porous glass affinity sorbents also demonstrated a second, slower step, which was probably a consequence of the high degree of polymerization that took place during the activation step when the silane was covalently linked to the glass surface. Surprisingly, the Nucleosil 300-2540 sorbent

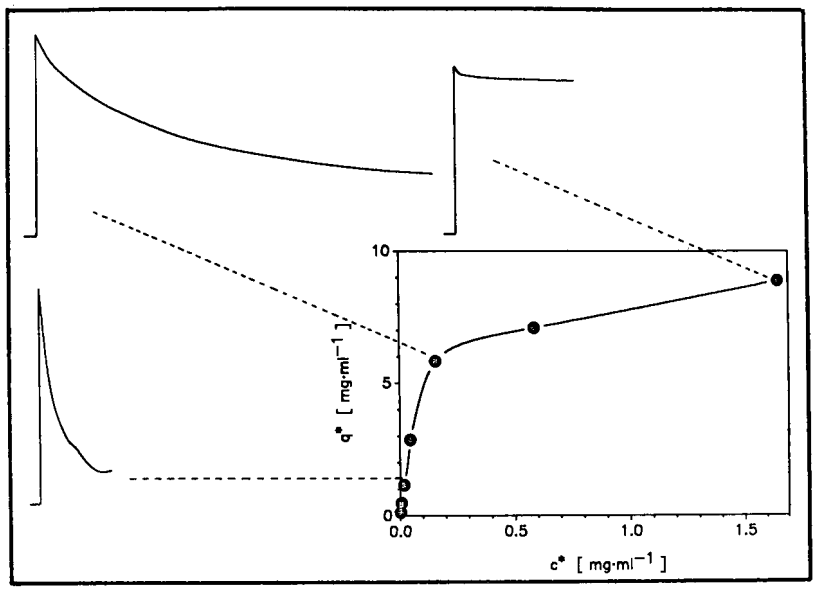

Fig. 7. Experimental kinetic profiles during adsorption of HSA onto Blue Sepharose CL6B for different saturation levels corresponding to data points on the given isotherm.

displayed also slow adsorption kinetics. In this case, pore-size restrictions may influence the adsorption time more dramatically than the particle size. In comparison to the Trisacryl and Sepharose affinity sorbents, which demonstrated the fastest kinetics, the Nucleosil affinity sorbent has a smaller particle size, as shown in Table II. Another explanation for the slow adsorption kinetis of this sorbent could be based on an adsorption mechanism different from that for the soft gel affinity sorbents. The fact that elution of bound HSA from Nucleosil 300 silica-immobilized Cibacron Blue F3GA was not successful points to this possibility. When Spherosil (average particle size of 200 μm) was employed to adsorb lysozyme, equilibrium could not be achieved after more than 40 min. This may indicate that this silica-based sorbent has a relatively high amount of small pore entrances compared to the actual pore size, or that polymerization of the silane used for the modification of this support caused cross-linkage. Both effects would make it difficult for the protein to find its way to the centre of each particle.

DISCUSSION

As demonstrated in this study, the stirred-tank experiments have been found useful to display the characteristics of the affinity system, including information about diffusion restrictions of the affinity sorbents. An alternative way to obtain thermodynamic data is frontal analysis[39], but the experimental set-up is more complicated and the accumulation of data can be a very time-consuming process (*e.g.* low flow-rates need to be used when gels with large particle size are chosen as typically required for large-scale purifications) and processing of thermodynamic data obtained from breakthrough curves is tedious work, requiring high precision when done

manually. Furthermore, no kinetic data can be directly derived from breakthrough curves. Differences in diffusion restrictions can only be detected by comparison of the shape of the curves for different supports. In the finite bath experiment, however, both thermodynamic and kinetic data can be obtained simultaneously. In our experience, two experiments can be conveniently performed per day, yielding most of the data needed to describe the affinity system. Furthermore, systems with relatively low equilibrium constants (K_a = 200) can be investigated, a situation which makes data processing rather difficult when frontal analysis is utilized. In such circumstances the difference between retention volume V_e and V_0 in frontal chromatograms becomes very small and subject to significant errors when small column volumes are employed.

Dye displacement from Fractogels and silica-based affinity sorbents were demonstrated even at very low protein levels due to measured UV absorption readings higher than those achieved when all of the injected protein remained unbound. This situation is often not realized in column experiments, as non-binding contaminants in the protein solution, applied to the column, can result in an increase in UV absorption readings, commencing at V_0. Displacement of dye in column experiments can result in the dye being eluted slowly from the column. In such column experiments, it is not possible to distinguish between adsorption due to contaminants or the dye. However, the detection of even low dye levels that leak from either physically adsorbed sites or weak chemically linked sites within the structure of the gel matrix is important for quantitation before scale-up is performed. The released dye must be removed from the final product if a pharmaceutical product is to be manufactured. Furthermore, the progressive loss of dye from the stationary phase will influence the capacity.

The low capacity and affinity of the Fractogel-based dye sorbents is indicative of a change of the gel structure occurring during the immobilization of Cibacron Blue F3GA, despite the fact that this support is more rigid than the other soft gels used in this study. Structural changes have been previously reported with Fractogel sorbents after using CDI activation[35]. A change in the gel structure may be explained by hydrophobic interaction of the dye with the matrix leading to pore compression. This was indicated by the adsorption of non-bound dye molecules at high salt concentrations. If strong hydrophobic interaction of adsorbed dye molecules with the matrix network takes place, the fractal surface of the matrix will change, trapping also some dye molecules inside the tortuous and cul-de-sac surface pockets that may have formed around the dyes. Hydrophobic interactions may have additionally caused some change in the arrangement of cross-linkage of polymeric chains which could freely move inside the porous system and accommodate proteins before immobilization. The participation of very strongly adsorbed dye in this physical environment would also explain dye displacement during protein adsorption. During adsorption of lysozyme on Fractogel HW 65 at low protein concentration, dye displacement is particularly apparent, equilibrium times before the steady state is reached being at least 3–4 times higher than the equilibration times shown in Table III. The long equilibration times may be a consequence of the movement of lysozyme through the network of polymer chains and the release of adsorbed dye molecules that have formed connections between chains and are trapped inside the pore pockets. This dye displacement phenomenon was less evident in a subsequent experiment and even less apparent after batch incubation with lysozyme for 24 h. When the Fractogel sorbent is used for adsorption of HSA, only a small amount of dye ligands are accessible for protein binding and/or

dye displacement. This observation suggests that the accessibility of the dye ligand is restricted to interaction with either the outer shell or with a limited portion of the geometrical surface of the affinity sorbent. The above observation may be due to the high ligand densities intentionally used and might have been less significant if lower ligand densities had been utilized.

The difficulty of eluting HSA from silica-immobilized dye sorbents is probably due to protein reorientation close to the silica surface. This behaviour consequently leads to irreversible adsorption at either the silica surface itself or at the immobilized ligand, caused by the high immobilization level achieved with the silica sorbent (see Table III). An alternative possibility which must be considered involves the influence of the chaotropic salt potassium thiocyanate used for protein elution. This reagent changes the tertiary structure of proteins, due to alteration of the solvent sphere, and this may expose further sites on the protein for interaction with the dye. These desorption difficulties cannot be explained by irreversible interaction between the protein and the dye during the adsorption step. If irreversible adsorption was always taking place, complete adsorption of HSA would have been achieved until saturation of the affinity sorbent was accomplished, a situation which was not observed experimentally.

Dissociation constants of lysozyme with Trisacryl-immobilized Cibacron Blue F3GA in the absence of salt were in the same range as reported by Chase[5]. The dissociation constant of all Fractogel sorbents was approximately an order of magnitude higher, representing lower affinity interactions. If it is assumed that the same interaction mode occurs between lysozyme and all sorbents used in this study, the dissociation constant should not vary by this magnitude. The observed differences demonstrated that the total capacity, as displayed in Table III for the Fractogel sorbents, does not represent the accessible capacity, q_m, of these sorbents. Because the total capacities were calculated from differential UV absorbance readings before and after coupling of the ligand, they represent an overestimation of the accessible ligand concentration.

Differences in the kinetics between the soft-gel- and silica-based affinity sorbents used in this study demonstrated also distinctive differences in pore diffusion restrictions. Soft-gel supports are considered to be based on an open network system in which the gel is formed and stabilised by cross linkage of this flexible network. Silica-based supports are mainly based on a pore system that cannot be changed by pressure or drag forces. The observed slow kinetics during adsorption of HSA to Nucleosil 300-2540 reflect the high value for λ (0.28). Under these circumstances high diffusion restrictions will occur when saturation of the affinity sorbent is nearly accomplished. The slow kinetics for Cellufine GC 700 are probably also based on a high protein size to pore size ratio, because the unchanged native support accommodates proteins up to a molecular weight of 400 000 daltons. Comparing Trisacryl or Sepharose affinity sorbents with Nucleosil 300, the effective value of λ of the soft gels must be much smaller according to the faster kinetics observed with these sorbents. It appears that among all the sorbents used in this study, Trisacryl and Sepharose had the best characteristics in terms of low non-specific interactions and rapid kinetics.

The observation that equilibration times increase as sorbent saturation is approached and when sorbents with small pore sizes are employed, clearly demonstrate that the assumption of local equilibrium is invalid. Furthermore, mass-transfer

restrictions cannot be ignored and could well be the major adsorption rate-determining factor, particularly when sorbents based on Cellufine GC 700 or Nucleosil 300-2540 for the adsorption of HSA are used, where high protein size to particle size ratios occur. When such sorbents are utilized, mass transfer restrictions change dramatically after the protein has been adsorbed at the outer surface. For example, the value of λ increases from 0.28 to approximately 0.6 based on a diameter of HSA of 8.35 nm and assuming a monolayer of adsorbed proteins in the first stage. Therefore, adsorption kinetics will be controlled much more by diffusion restrictions as well as the reverse reaction rate constant (*cf.* eqn. 2), since protein dissociation from the sorbent at pore constrictions will contribute to the adsorption kinetics throughout the adsorption process. It has been found that equilibration times as presented in Table III for the adsorption of HSA, which are measured from injections at increasing saturation levels, represent a very practical way to compare affinity sorbents of different pore and particle characteristics since they do not require sophisticated computer programs for the calculation of kinetic and diffusion parameters. However, equilibration times are representative for the described affinity systems only because the adsorption depends upon a large number of factors as mentioned above. If information is needed to calculate and predict the behaviour of batch adsorption in large batches for industrial purposes, then discrimination of the pore diffusivity and the film mass-transfer coefficient from the overall reaction rate is recommended[40]. To validate the protocols proposed in these investigations, further detailed analysis of sorbents with different surface characteristics is currently underway in this laboratory, including studies with strong ion exchangers where rectangular equilibrium isotherms may be observed[41].

ACKNOWLEDGEMENT

The support of the Australian Research Grants Committee & Monash University Special Research Grants is gratefully acknowledged. F.B.A. is a recipient of a Monash University Postdoctoral Fellowship.

REFERENCES

1 A. W. Purcell, M. I. Aguilar and M. T. W. Hearn, *J. Chromatogr.*, 476 (1989) 125.
2 R. R. Walters, *Anal. Chem.*, 57 (1985) 1099.
3 E. Boschetti, J. M. Egly and M. Monsigny, *Trends Anal. Chem.*, 5 (1986) 4.
4 F. H. Arnold, H. W. Blanch and C. R. Wilke, *Chem. Eng. J.*, 30 (1985) 25.
5 H. A. Chase, *J. Chromatogr.*, 297 (1984) 179.
6 R. M. Moore and R. R. Walters, *J. Chromatogr.*, 384 (1986) 53.
7 Cs. Horváth and J.-M. Engasser, *Biotechnol. Bioeng.*, 16 (1974) 900.
8 L. Goldstein, *Methods Enzymol.*, 44 (1976) 397.
9 H. Poppe and J. C. Kraak, *J. Chromatogr.*, 255 (1983) 395.
10 M. T. W. Hearn, in S. Asenjo (Editor), *Industrial applications of Biotechnology*, Marcel Dekker, New York, 1989, pp. 140–165.
11 F. H. Arnold, H. W. Blanch and C. R. Wilke, *J. Chromatogr.*, 355 (1986) 1.
12 I. Langmuir, *J. Am. Chem. Soc.*, 38 (1916) 2221.
13 M. E. Young, P. A. Carroad and R. L. Bell, *Biotechnol. Bioeng.*, 22 (1980) 947.
14 I. A. Webster, *Biotechnol. Bioeng.*, 25 (1983) 2479.
15 M. T. W. Hearn, M. Aguilar and A. Hodder, *J. Chromatogr.*, 458 (1988) 45.
16 M. T. W. Hearn, in J. C. Janson (Editor), *High Resolution Purification of Proteins*, VCH Press, FL, 1988 in press.

17 D. M. Smith, *AIChE J.*, 32 (1986) 1039.
18 R. L. Fournier, *AIChE J.*, 32 (1986) 1036.
19 W. W. Yau, J. J. Kirkland and D. D. Bly, *Modern Size Exclusion Chromatography*, Wiley, New York, 1979.
20 D. A. P. Small, T. Atkinson and C. Lowe, *J. Chromatogr.*, 216 (1981) 175.
21 P. G. H. Byfield, S. Copping and R. L. Himsworth, *Mol. Immunol.*, 21 (1984) 647.
22 E. Gianazza and P. Arnaud, *Biochem. J.*, 201 (1982) 129.
23 C. R. Lowe, S. J. Burton, J. C. Pearson and Y. D. Clonis, *J. Chromatogr.*, 376 (1986) 121.
24 F. B. Anspach, K. K. Unger, J. D. Davies and M. T. W. Hearn, *J. Chromatogr.*, 457 (1988) 195.
25 F. B. Anspach, H.-J. Wirth, K. K. Unger, P. Stanton, J. R. Davies and M. T. W. Hearn, *Anal. Biochem.*, (1989) in press.
26 F. B. Anspach, K. K. Unger, H. Giesche and M. T. W. Hearn, *4th International Symposium on HPLC of Proteins, Peptides, and Polynucleotides, Baltimore, MD*, 1984, paper No. 103.
27 A. I. Liapis, F. B. Anspach, M. E. Findley, J. Davies, M. T. W. Hearn and K. K. Unger, *Biotechnol. Bioeng.*, (1989) in press.
28 P. Wikström and P.-O. Larsson, *J. Chromatogr.*, 388 (1987) 123.
29 F. E. Regnier and R. Noel, *J. Chromatogr. Sci.*, 14 (1976) 316.
30 D. Hanggi and P. Carr, *Anal. Biochem.*, 149 (1985) 91.
31 D. A. P. Small, T. Atkinson and C. R. Lowe, *J. Chromatogr.*, 266 (1983) 151.
32 *Gel Filtration Theory and Practice —Laboratory Handbook*, Pharmacia, Uppsala, 1985.
33 J. R. Sportsman and G. S. Wilson, *Anal. Chem.*, 52 (1980) 2013.
34 P. R. Wills, L. W. Nichol and R. J. Siezen, *Biophys. Chem.*, 11 (1980) 71.
35 M. T. W. Hearn, *J. Chromatogr.*, 376 (1986) 245.
36 Y. C. Liu and E. Stellwagen, *J. Chromatogr.*, 376 (1986) 149.
37 D. A. P. Small, T. Atkinson and C. Lowe, *J. Chromatogr.*, 216 (1981) 175.
38 J. F. Biellmann, J. P. Samama, C. I. Brandon and H. Eklund, *Eur. J. Biochem.*, 102 (1979) 107.
39 K.-I. Kasai, Y. Oda, M. Nishikata and S.-I. Ishi, *J. Chromatogr.*, 376 (1986) 33.
40 B. H. Arve and A. T. Liapis, *AIChE J.*, 33 (1987) 179.
41 A. Velayudhan and Cs. Horváth, *J. Chromatogr.*, 443 (1988) 13.
42 J. Janin, *Nature (London)*, 277 (1976) 491.
43 R. C. Travers and F. C. Church, *Int. J. Pept. Protein Res.*, 26 (1985) 539.

Journal of Chromatography, 476 (1989) 227–233
Elsevier Science Publishers B.V., Amsterdam — Printed in The Netherlands

CHROMSYMP. 1601

AFFINITY CHROMATOGRAPHY OF RECOMBINANT *RHIZOMUCOR MIEHEI* ASPARTIC PROTEINASE ON Si-300 BACITRACIN

S. B. MORTENSEN*, L. THIM, T. CHRISTENSEN, H. WOELDIKE, E. BOEL, K. HJORTSHOEJ and M. T. HANSEN
Novo Research Institute, DK-2880 Bagsvaerd (Denmark)

SUMMARY

An high-performance affinity chromatography column was made by activation of coated silica Si-300 polyol with tresyl chloride and coupling it with the antibiotic bacitracin. The column was used to purify recombinant *Rhizomucor miehei* aspartic proteinase.

INTRODUCTION

Isolation of proteinases by affinity chromatography is a rapid and selective chromatographic procedure. The peptide antibiotics bacitracin, bacilliquin and gramicidin S have shown to be suitable for such methods both on soft gels (Sepharose)[1] and on silica-based materials such as "Silochrom"[2]. Especially when working with endoproteinases, which are autoinactivated[3,4], affinity chromatography is of great value. The matrix used most often is agarose[5] in the form of Sepharose or its cross-linked forms, but other forms of entirely synthetic gel materials containing hydroxyl groups are available. We used a coated silica material Si-300 polyol, which is excellent for rapid purification processes. The matrix can be activated with cyanogen bromide or its less harzardous variants[6], the epoxy, aldehyde, vinyl sulphone, carbonylimidazole activation[5], or the recently introduced activation reagents tresyl chloride[7] and fluoro-1-methylpyridinium toluene-4-sulphonate (FMP)[8],

We describe the construction of an high-performance affinity chromatography column coupled with bacitracin by the tresyl chloride method. By use of this column, recombinant *Rhizomucor miehei* aspartic proteinase was purified.

MATERIALS AND METHODS

Reagents

Si-300 (30 μm) polyol was from Serva (Heidelberg, F.R.G.), tresyl chloride (2,2,2-trifluoroethanesulphonyl chloride) from Fluka (Buchs, Switzerland) and bacitracin (zinc free) and Endo H from Sigma (St. Louis, MO, U.S.A.).

0021-9673/89/$03.50

Activation of resin

The Si-300 material was activated by the tresyl chloride method[1]. A 10-g amount of Si-300 polyol was washed three times with 100 ml acetone (dried with molecular sieve 4A, overnight). The moist gel was added to a dry beaker, containing 10 ml of dry acetone and 500 μl dry pyridine. With magnetic stirring, 400 μl tresyl chloride were added to the suspension. After 15 min at 0°C, the gel was washed with 100 ml of each of the following: acetone, 30, 50 and 70% of 5 m*M* HCl in acetone (v/v) and 1 m*M* HCl. The product was stored at +4°C until used.

Coupling with bacitracin

A 2-g amount of bacitracin was dissolved in 100 ml coupling buffer (0.2 *M* sodium phosphate +0.5 *M* NaCl, pH 8.2) and added to the activated Si-300 polyol, which had been briefly washed with cold coupling buffer. Coupling proceeded with gentle rotation on a Celloshaker (Chemetron, Italy) for 20 h at +4°C. The gel was treated with 0.2 *M* Tris (pH 8.5) for 5 h at room temperature and washed with 20 m*M* Tris–1 *M* NaCl–25% *n*-propanol and 20 m*M* Tris (pH 7.0). The slurry was poured into a steel column 12 cm × 1.6 cm (Knauer, Berlin, F.R.G.) and allowed to stand for 30 min. The column was then packed under pressure at a flow-rate of 8 ml/min in 20 m*M* Tris (pH 7.0).

Sodium dodecyl sulphate-polyacrylamide gel electrophoresis (SDS-PAGE)

SDS-PAGE on gradient gels (7.5–20%) was performed essentially as described by Anderson *et al.*[9].

Sequence analysis

N-terminal sequence analysis of purified recombinant *Rhizomucor miehei* aspartic proteinase was carried out by automated Edman degradation, using an Applied Biosystems (Foster City, CA, U.S.A.) Model 470A gas-phase sequencer, and the phenylthiohydantoin (PTH)-amino acids were analysed by high-performance liquid chromatography (HPLC)[10].

Analysis of recombinant Rhizomucor miehei aspartic proteinase enzymatic activity

Clotting activity, determined as kilorennet units (KRU), was measured according to British Standard 3624:1963. One unit of milk-clotting activity is the amount of proteinase that clots 10 ml of reconstituted skim milk in 100 s at 30°C[11].

Clotting activity in column eluates was determined by a microtitre plate assay. An 100-μl volume of a diluted sample from each fraction was pipetted into a microtitre plate well. The diluting buffer (buffer D) was 50 m*M* 2-morpholinoethanesulphonic acid–15 m*M* $CaCl_2$–10 m*M* NaCl (pH 6.1). An 100-μl volume (0.5%) dried skim milk in buffer D was added, and the milk-clotting activity was followed by measuring the change in absorbance at 540 nm in a Perkin-Elmer (Norwalk, CT, U.S.A.) Lambda reader at 1-min intervals.

HPLC

HPLC was performed with a Series 4 Perkin-Elmer HPLC pump, an LC95 detector and a PE7700 data controller. The columns were an Altex Spherogel TSK G3000SWG, 600 mm × 21.5 mm (Beckman Instruments, Berkeley, CA, U.S.A.) and

the bacitracin affinity column described in Materials and Methods. Proteins were detected at 280 nm. Buffers: A, 0.1 *M* sodium acetate (pH 4.5); B, 0.1 *M* sodium acetate–1 *M* NaCl–25% *n*-propanol (pH 4.5); C, 50 m*M* 2-morpholinoethanesulphonic acid (pH 6.1).

RESULTS AND DISCUSSION

Purification and characterization of rRMP

Aspargilus oryzae was transformed with *Rhizomucor miehei* aspartic proteinase and grown as described by Christensen *et al.*[12]. Recombinant *Rhizomucor miehei* aspartic proteinase was recovered from the spent culture medium. The amount of extracellular recombinant *Rhizomucor miehei* aspartic proteinase was measured by clot analysis to be 3.3 g/l. *A. oryzae* culture supernatant was dialysed against distilled water and lyophilized. The recombinant *Rhizomucor miehei* aspartic proteinase enzyme was purified by affinity chromatography on a Si-300 HPLC bacitracin column (Fig. 1). The sample of 317 mg lyophilized culture supernant, dissolved in 30 ml buffer A, was applied to the affinity column (12 cm × 1.6 cm), equilibrated in buffer A at a flow-rate of 5 ml/min. Non-adsorbed material passed through the column with buffer A. Then proteinase was eluted with buffer B. The fractions containing the active enzyme were desalted on a G-25 column (Pharmacia, Uppsala, Sweden) equilibrated in 10 m*M* ammonium bicarbonate and lyophilized. The final purification procedure consisted of size-exclusion chromatography on a TSK G3000SWG column (60 cm × 2.15 cm), equipped with a precolumn TSK-GSWGP (7.5 cm × 2.15 cm) (Fig. 2). Aliqouts of 1.5 ml were loaded on the column equilibrated with buffer C. A flow-rate of 5 ml/min and fraction size of 5 ml were used.

TABLE I

PURIFICATION OF RECOMBINANT *RHIZOMUCOR MIEHEI* ASPARTIC PROTEINASE

Step	*Amount (ml)*	*Specific acitivity (KRU/g)*	*Total activity (KRU)*	*Units/Abs. 280 nm*	*Purification factor*
Supernatant	30	16.5	496	0.54	1.0
Bacitracin affinity chromatography	15	31.0	465	4.35	8.1
Size-exclusion chromatography	50	9.1	452	5.72	10.6

Dialysis and lyophilization of the active fractions from size-exclusion chromatography resulted in a product with a specific activity of 4950 KRU/g. The apparent molecular weight of recombinant *Rhizomucor miehei* aspartic proteinase determined by SDS-PAGE was slightly larger than that obtained for *Rhizomucor miehei* aspartic proteinase[13] (Fig. 3). After treatment of both recombinant *Rhizomucor miehei* aspartic proteinase and *Rhizomucor miehei* aspartic proteinase with Endo H, the apparent molecular weights, determined by SDS-PAGE, were identical (data not shown). *Rhizomucor miehei* aspartic proteinase is reported to be either homogeneous with one N-terminal Ala-Ala-Ala-Asp-Gly-Ser-[14] or heterogeneous, with 3 N-terminals,

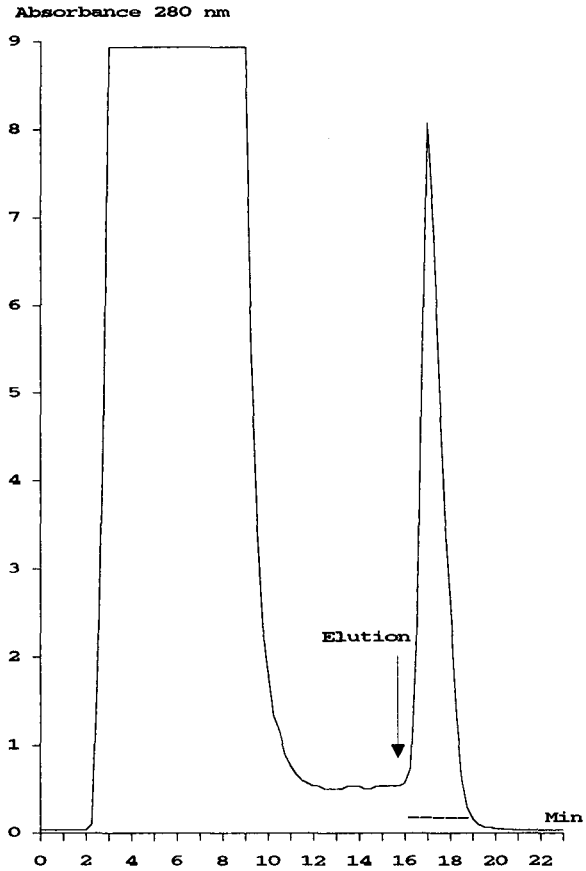

Fig. 1. Bacitracin affinity chromatography of the culture supernatant of *A. oryzae*. The sample (30 ml) was applied to the affinity column (12 cm × 1.6 cm), equilibrated in 0.1 *M* sodium acetate (pH 4.5) at a flow-rate of 5 ml/min. Non-adsorbed material passed through the column with 0.1 *M* sodium acetate (pH 4.5). Then proteinase was eluted with 0.1 *M* sodium acetate–1 *M* NaCl–25% *n*-propanol (pH 4.5). Proteinase-active fractions were packed as indicated by the horizontal bar. Proteins were detected at 280 nm.

Ala-Ala-Ala-Asp-Gly-Ser-, Gly-Ser- or Asp-Gly-Ser-[15]. We found the N-terminal sequence for recombinant *Rhizomucor miehei* aspartic proteinase determined by gas-phase sequencing on an Applied Biosystems gas-phase sequenator to be heterogeneous and consisting of two N-terminals in equal amounts: Ala-Ala-Asp-Gly-Ser- and Gly-Ser-. These differences may represent differently processed forms either during maturation or during purification.

The combination of a rigid column material and an efficient activation method with the proper ligand gives an affinity column that can be used for the rapid isolation of heterologously expressed enzymes, which otherwise would be difficult to separate from host proteins, *e.g.*, similar isoelectric point and molecular weight of a host protein.

The rigid column material is an advantage when working with organism such as

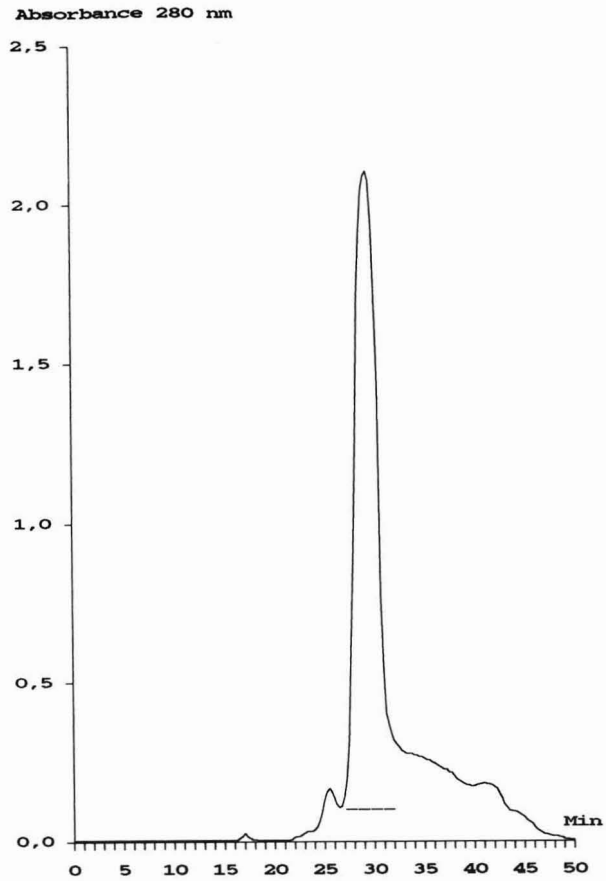

Fig. 2. Separation of recombinant *Rhizomucor miehei* aspartic proteinase from bacitracin affinity chromatography on a TSK G3000SWG size-exclusion column. The lyophilized material from bacitracin affinity chromatography was dissolved in 3 ml 50 m*M* 2-morpholinoethanesulphonic acid (pH 6.1) and the recombinant *Rhizomucor miehei* aspartic proteinase was purified by repeated chromatography on the size-exclusion column (TSK G3000SWG, 600 mm × 21.5 mm). Sample size: 1.5 ml. Proteinase-active fractions were pooled as indicated by the horizontal bar. Proteins were detected at 280 nm.

Aspergillus capable of producing Sepharose-degrading enzymes[1]. The efficiency of the affinity chromatography step is comparable to Sepharose-bacitracin[1] and Silochrom-bacitracin[1]. We did get a purification factor of 8 relative to the starting material (Table I). The binding capacity for the recombinant *Rhizomucor miehei* aspartic proteinase is *ca.* 20 mg/ml gel material.

Of special importance is the very rapid separation obtained. The enzymes are eluted rapidly and with no tailing, which implies that there is no non-specific binding to the column. Elution of enzyme can be performed using 1 *M* NaCl and *n*-propanol (20–30%). The higher the *n*-propanol content, the better is the elution.

Another important ligand for affinity chromatography of aspartic proteinases is pepstatin. This has been used for isolation of both microbial[16] and mammalian[17]

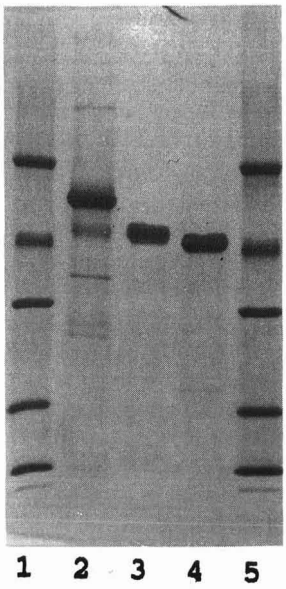

Fig. 3. SDS-PAGE of recombinant *Rhizomucor miehei* aspartic proteinase. Lanes: 1 and 5, standard proteins; MW 67 000, 43 000, 30 000, 20 000 and 14 400; 2, *A. oryzae* culture supernatant; 3, purified recombinant *Rhizomucor miehei* aspartic proteinase; 4, *Rhizomucor miehei* aspartic proteinase.

aspartic proteinases. Pepstatin binds tightly to proteinases and it may be necessary to use up to 6 *M* urea to elute the enzyme[17]. The binding, however, is dependent on the type of pepstatin used, and it seems that N-acetylpepstatin may be used for isolation of microbial milk-clotting enzymes[16], although the elution volume is much larger than when using bacitracin as a ligand.

We find the tresyl chloride method to be easy and safe for activation of silica-based column material. Coupling with bacitracin gives an HPLC affinity column which is superior to conventional soft gel affinity chromatography. The use of bacitracin as a ligand, relative to pepstatin, also makes it possible to use the column to purify proteolytic enzymes other than aspartic proteinases[1].

REFERENCES

1 V. M. Stephanov and G. N. Rudenskaya, *J. Appl. Biochem.*, 5 (1983) 420.
2 V. M. Stephanov, G. N. Rudenskaya, A. V. Garida and A. I. Osterman, *J. Biochem. Biophys.*, 5 (1981) 177.
3 J. S. Fruton, in P. D. Boyer (Editor), *The Enzymes*, Vol. 3, Academic Press, New York, 3rd ed., 1971, p. 119.
4 J. Pohl, M. Zaoral, A. Jindra, Jr. and V. Kostka, *Anal. Biochem.*, 139 (1984) 265.
5 J. Kohn and M. Wilchek, *Appl. Biochem. Biotechol.*, 9 (1984) 285.
6 Y. D. Clonis, *Bio/Technology*, 5 (1987) 1290.
7 K. Nilsson and K. Mosbach, *Methods Enzymol.*, 104 (1984) 56.
8 T. T. Ngo, *Bio/Technology*, 4 (1986) 134.
9 C. W. Anderson, P. R. Baum and R. F. Gesteland, *J. Virol.*, 12 (1973) 241.
10 L. Thim, M. T. Hansen and A. R. Sørensen, *FEBS Lett.*, 212 (1987) 307.
11 N. J. Berridge, *Biochem. J.*, 39 (1945) 179.

12 T. Christensen, H. Woeldike, E. Boel, S. B. Mortensen, K. Hjortshoej, L. Thim and M. T. Hansen, *Bio/Technology*, 6 (1988) 1419.
13 M. Ottesen and W. Rickert, *Compt. Rend. Trav. Lab. Carlsberg*, 37 (1970) 31.
14 A.-M. Bech and B. Foltmann, *Neth.-Milk Dairy J.*, 35 (1981) 275.
15 D. Pâquet, D. Lorient, L. Mejean and C. Alais, *Neth.-Milk Dairy J.*, 35 (1981) 358.
16 H. Kobayashi, I. Kusakabe and K. Murakami, *Anal. Biochem.*, 122 (1982) 308.
17 C. Devaux, J. Ménard, P. Sicard and P. Corvol, *Eur. J. Biochem.*, 64 (1976) 621.

Journal of Chromatography, 476 (1989) 235–244
Elsevier Science Publishers B.V., Amsterdam — Printed in The Netherlands

CHROMSYMP. 1595

IMMUNOLOGICAL-CHROMATOGRAPHIC ANALYSIS OF LYSOZYME VARIANTS

LINDA J. JANIS[a], AMY GROTT and FRED E. REGNIER*
Departments of Chemistry and Biochemistry, Purdue University, West Lafayette, IN 47907 (U.S.A.)
and
SANDRA J. SMITH-GILL
Laboratory of Genetics, National Cancer Institute, Bethesda, MD 20892 (U.S.A.)

SUMMARY

Immunological-chromatographic analysis (ICA) was used to evaluate the cross-reactivities of eight lysozyme variants with five different immobilized monoclonal anti-hen-egg-white lysozyme antibodies. ICA is a dual-column high-performance liquid chromatography-based method in which an immunoaffinity and a conventional analytical column are coupled with a switching valve. Antigens are first captured on the affinity column and then desorbed and concentrated on the second column, where they are separated further. This arrangement permits antigen–antibody interactions occurring on the affinity column to be monitored on-line with the second column. The ICA system was used to perform direct and competitive inhibition binding immunoassays with unlabeled antigens. Seven of the eight lysozymes tested bound to all five immobilized monoclonal antibodies. Competitive inhibition of binding of hen egg white lysozyme to the monoclonal antibody, HyHel-5, was measured by using the variants Japanese quail and bobwhite quail lysozymes as inhibitors. The ratio of the amount of bobwhite quail to Japanese quail lysozyme required to give 50% inhibition of binding of hen egg white determined by ICA compares well with the results obtained by other investigators who used an enzyme-linked immunosorbent assay plate binding assay.

INTRODUCTION

The large-scale production of proteins for pharmaceutical use has resulted in a need for new analytical methods to ensure the safety of the products in medical applications. Biosynthetic fidelity and product purity must be closely monitored. Contaminants of concern in biotechnology may be proteins and nucleic acids derived from the host cells, or product variants resulting from translation errors, improper refolding, incomplete or incorrect post-translational modification, and chemical or proteolytic degradation during purification. The development of methods capable of

[a] Present address: Eli Lilly & Co., Indianapolis, IN 46285, U.S.A.

0021-9673/89/$03.50

distinguishing the contaminating product variants, which are very similar in structure to the protein pharmaceutical product, is a major analytical endeavor.

It has been demonstrated that immunological-chromatographic analysis (ICA) is useful for discrimination of polypeptides of similar three-dimensional structures[1,2]. ICA is a dual-column high-performance liquid chromatography-based method, in which an immunoaffinity and a conventional (*e.g.* reversed-phase) analytical column are coupled with a switching valve. Antigens are captured, then desorbed from the affinity column, and concentrated on the analytical column. They are separated on the second column by a different retention mechanism.

The success of ICA depends on the extent of cross-reactivity of the antisera with the various product variants and on the ability of the second chromatographic system to resolve them. Antibodies often cross-react with similar species that share antigenic groups[1–6]. For example, an antiserum produced by using one immunogen from a family of peptides (such as the endorphin or enkephalin neurotransmitters) often cross-react with other members of the family. Current methods of analysis involve a chromatographic separation step with fraction collection, before an immunoassay on the fractions containing the purified peptides is performed[6].

The ICA system takes advantage of these cross-reactivities by performing an immunoaffinity purification first, followed by chromatographic separation. Often a chromatographic method is able to distinguish between similar species when an immunological method has failed (as was the case with the neurotransmitter peptides[6]). This is because retention in ion-exchange, hydrophobic interaction chromatography (HIC) and reversed-phase chromatography (RPC) is generally determined by a relatively large portion of the surface of the molecule. The immunological contact area, called the epitope, is much smaller. Changes in structure of a molecule outside this small region are undetectable by an immunoassay. Chromatographic methods, which probe a larger portion of molecular surface, may be so sensitive to structural differences that proteins which differ by only one amino acid can be separated. For example, six site-specific subtilisin variants were separated by strong-cation-exchange (CEX) chromatography[7].

The goal of this work was to demonstrate further the utility of ICA is distinguishing proteins with similar structures. Nine lysozyme variants with known amino acid sequences were used as the model system for these studies. The retention mechanisms of most of these lysozymes have been examined previously by HIC[8], CEX and RPC[9]. Five monoclonal anti-hen-egg-white lysozyme (HEL) antibodies were used in the studies. Two of the epitopes of these antibodies (HyHel-5 and HyHel-10) have been defined by X-ray crystallography[10–12]. All of the epitopes of these antibodies have been mapped by comparing their reactivities with lysozyme variants and sugar substrates of lysozyme[3,5].

MATERIALS AND METHODS

Reagents

Bradford reagent for protein assays was purchased from Bio-Rad Labs. (Richmond, CA, U.S.A.); ethanolamine from Aldrich (Milwaukee, WI, U.S.A.); and 3-(N-morpholino)propanesulfonic acid (MOPS) from Sigma (St. Louis, MO, U.S.A.). HPLC-grade solvents were trifluoroacetic acid (TFA) (Pierce, Rockford, IL, U.S.A.)

and acetonitrile (American Burdick & Jackson, Muskegon, MI, U.S.A.). Inorganic reagents were of analytical-reagent grade or comparable quality.

Proteins

Five monoclonal antibodies to HEL (HyHel-5, HyHel-8, HyHel-9, HyHel-10 and HyHel-15), in mouse ascites fluid, were generously supplied by the National Institutes of Health, Bethesda, MD, U.S.A. Hybridomas to HEL were prepared as described[3,5]. The purification of avian lysozyme variants from the egg whites of Peking duck A, B, C, ringed-neck pheasant (RNP), Japanese quail (JEL) and bob-white quail (BEL) was described in a previous paper[9]. Human milk lysozyme (HUL) was purchased from U.S. Biochemicals (Cleveland, OH, U.S.A.). Bovine serum albumin (BSA), mouse immunoglobulin (IgG), HEL and turkey lysozyme (TKY) were obtained in the purest grade available from Sigma.

Preparation of immunoaffinity columns

The monoclonal antibodies to HEL were partially purified from mouse ascites fluid by precipitation in 42% ammonium sulfate. The precipitate was reconstituted in 0.10 *M* phosphate (pH 7.0) and dialyzed against the same buffer until 1 ml each of the dialysate and a 1% (w/w) barium chloride solution showed no barium sulfate precipitate. The protein content of the antibody solutions were determined by a Bradford assay[13].

Monoclonal antibodies and non-immune mouse IgG were coupled to N-hydroxysuccinimide pre-activated gel, Affi-prep 10 (Bio-Rad Labs.) by using the manufacturer's instructions as follows: The antibody solutions containing *ca.* 15 mg of protein (except HyHel-5, which contained 9 mg) were dialyzed overnight against the coupling buffer, 0.10 *M* MOPS–0.15 *M* sodium chloride (pH 7.2) to remove any amino contaminants. Approximately 0.9 ml of the gel was washed with 50 ml of cold 0.01 *M* sodium acetate (pH 4.0), followed by several ml of coupling buffer. The gel was transferred to a 100-ml round-bottom flask containing 1 ml of MOPS coupling buffer. After degassing the solution for 1 min, the antibody solution was added and the volume was adjusted to 3 ml, resulting in a final protein concentration of approximately 5 mg/ml (3 mg/ml for HyHel-5). The reaction mixture was slowly agitated at 4°C for 24 h. Any remaining active groups were blocked by adding 0.10 ml of 1.0 *M* ethanolamine hydrochloride, pH 8.0, and agitating for 1 h at 4°C. After extensive washing with 0.10 *M* phosphate buffer (pH 7.0), the affinity packing material was slurry-packed from this buffer into a stainless-steel column (5 × 0.41 cm I.D.) at 500 p.s.i. by using an Altex pump (Model 110, Altex Scientific, Berkeley, CA, U.S.A.). The amount of protein coupled to the gel was determined by measuring the loss of protein from the supernatant during coupling by the Bradford assay[13]. The lysozyme load capacity of each column was measured by frontal analysis[14]. Duplicate samples of HEL (2 ml, 0.164 mg/ml) were pumped through the column at 0.5 ml/min until a breakthrough occurred. The column was washed twice with 0.10 *M* glycine buffer (pH 2.2) between analyses.

Apparatus

The experimental set-up used for the assays is shown in Fig. 1. The position of the automatic switching valve (Model 7010) attached to a pneumatic actuator (Model

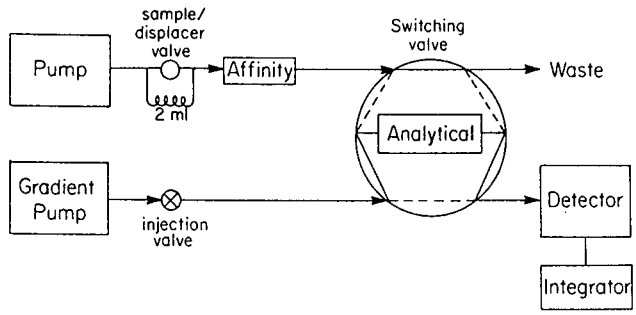

Fig. 1. Column switching apparatus.

5701, both from Rheodyne, Cotati, CA, U.S.A.) determined whether the immunoaffinity column and the analytical column were in series or separate. The timing of the switching valve was controlled by the gradient pump (Model 1090L, Hewlett Packard, Waldbronn, F.R.G.) fitted with a manual injection valve (Model 7125, Rheodyne). The affinity column was equipped with a separate pump (Model 110, Altex) and injection valve (Model C6U, Valco Instruments, Houston, TX, U.S.A.) equipped with a 2-ml injection loop for loading samples and applying desorption buffer. The absorbance was monitored at 280 nm with a variable-wavelength detector (Spectroflow 757, kindly lent by Kratos Division, Applied Biosystems, Ramsey, NJ, U.S.A.) connected to an integrator (Model 740, Waters, Milford, MA, U.S.A.) which calculated peak areas for quantitation.

Binding studies of lysozyme variants

Binding of all the lysozyme variants listed in Fig. 2 (except duck C which was not available in a pure form) on all five monoclonal anti-HEL and non-immune

```
                  -1 5  10  15  20  25  30  35  40  45  50  55  60  65
Chicken           KVFGRCELAAAMKRHGLDNYRGYSLGNWVCAAKFESNFNTQATNRNT DGSTDYGILQINSRWWCN
Bob White quail                                   S               V
Japanese quail      Y               K Q
Ring-necked pheasant G Y            M                             G
Turkey              Y               L                             H
Duck A              YS              L                 NY  S
Duck B              YS              L                 NY  G
Duck C              YS              L                 NY  G
Human Milk           E    RTL  L M G   I  A  M L  W  GY  R   Y AGR   E   F     Y

                  66 70  75  80  85  90  95  100 105 110 115 120 125
Chicken           DGRTPGSRNLCNIPCSALLSSDITASVNCAKKIVSDGDGMNAWVAWRNRCKGTDVQAWIRGCRL
Bob White quail     K                     T
Japanese quail                                    VH              N
Ring-necked pheasant      K   H                                 KH    NV
Turkey                    K                       A G             H
Duck A              K     K A G    V   R   EA R   R                R   SK
Duck B              K  R K A G    V   R   EA R   R                R   SK
Duck C              K  R K A G R  V   R   EA R   R                R   SK
Human milk          K   AV A HLS      QDN ADA A   RVR- PQ IR       QNR  RQYVQ  GV
```

Fig. 2. Primary amino acid sequences of lysozyme variants[8,17].

mouse IgG affinity columns was evaluated, by using each affinity column separately, not in the dual-column mode. The following procedure was used for all six columns. The column was equilibrated with the loading buffer, 0.10 *M* phosphate–0.25 *M* sodium chloride (pH 7.0), at a flow-rate of 1 ml/min. The column was then subjected to four 2-ml step gradients of the desorption buffer, 0.10 *M* glycine hydrochloride (pH 2.2), in order to remove any non-covalently bound proteins. Non-specific binding of BSA and specific binding of the lysozyme variants were measured as follows. Three injections of BSA (20 μl, 10 mg/ml) or five injections of a lysozyme (20 μl, 1 mg/ml), followed by 2 ml of desorption buffer were made into the affinity column. The peak heights of the successive injections and of the desorption buffer step were measured in order to determine qualitatively whether any protein was bound to the column. The column was washed twice with 2-ml portions of glycine buffer between analyses.

ICA of lysozyme variants

Dual-column ICA assay of several lysozyme variants was performed using two types of analytical columns: a cation-exchange and a reversed-phase column. Samples containing RNP, duck A, B and C were analyzed using the monoclonal HyHel-9 anti-HEL immunoaffinity column, coupled to a CEX analytical column (Synchropak S-300, 5 × 0.41 cm I.D., SynChrom, Lafayette, IN, U.S.A.). A mixture of duck B and C lysozymes was available for this analysis. The monoclonal HyHel-5 anti-HEL immunoaffinity column, coupled to a reversed-phase C-4 column (Supelco C-304, 5 × 0.41 cm I.D.), was used to analyze samples of either BEL and HEL or JEL and HEL. The lysozyme mixtures (20 μl, 1 mg/ml) were loaded onto the immunoaffinity column at a flow-rate of 0.5 ml/min in loading buffer [0.05 *M* sodium phosphate (pH 7.0) for CEX; 0.10 *M* phosphate–0.25 *M* sodium chloride (pH 7.0) for RPC]. The automatic switching valve was switched to connect the immunoaffinity and analytical column in series. A 2-ml injection of the desorption buffer (0.05 *M* glycine hydrochloride, pH 3.0 for CEX; 0.10 *M* glycine, pH 2.2 for RPC) eluted the lysozymes from the affinity column into the analytical column at 1 ml/min. (The desorption buffer step is illustrated in the cation-exchange ICA chromatogram as a darkened rectangle.) After 4 or 6 min, the automatic switching valve was changed, connecting the analytical column back to the gradient pump. The lysozymes were separated on the cation-exchange column with a 20-min linear gradient from 0 to 0.5 *M* sodium chloride in 0.01 *M* borate (pH 9.0) at 1 ml/min. The chromatographic conditions for RPC were first a 5-min linear gradient from 0 to 28% acetonitrile in 0.1% TFA, followed by a 9-min linear gradient from 28% to 32% acetonitrile in 0.1% TFA, at 14 min. This condition was maintained until 20 min. The flow-rate was 1 ml/min for RPC.

Competitive inhibition of binding of lysozyme variants

Affinity packing material with monoclonal HyHel-5 anti-HEL was packed into a 3 × 0.2 cm I.D. column. Duplicate samples with increasing amounts of inhibitor lysozyme, BEL and JEL (1-1000 μg) and a constant amount of HEL (4 μg) in 1 ml loading buffer were injected into the immunoaffinity column in 0.10 *M* phosphate–0.25 *M* sodium chloride (pH 7.0) at a flow-rate of 0.3 ml/min. Unbound proteins were routed to waste. The rest of the ICA analysis was carried out as described for HyHel-5, coupled to the RPC column, in the section on *ICA of lysozyme variants*. The

bound fraction of HEL was quantitated from peak area of the RPC analysis. The RPC column was washed with a 5-min linear gradient from 0 to 100% acetonitrile in 0.1% TFA between analyses. B/B_0 was plotted *versus* the log of the dose (μg inhibitor lysozyme), where B is the amount of HEL bound to the antibody in the presence of inhibitor, and B_0 is the amount of HEL bound to the antibody in the absence of inhibitor[15]. This method was used for plotting the data because the data are normalized and not plotted as raw data for free and bound lysozyme in order to facilitate interassay comparisons. Curve fitting and estimation of 50% inhibition points were based on inhibition of binding data linearized by a log–logit transformation[15].

RESULTS AND DISCUSSION

Evaluation of immunoaffinity columns

The immunoaffinity columns were characterized by determining the amount of protein immobilized on the support, antigen-load capacity, the amount of non-specific binding, and the amount of specific binding of each lysozyme variant. The results of this characterization are listed in Table I. The amount of protein immobilized and HEL load capacity of the HyHel-5 column were less than for the other columns because there was less HyHel-5 available for the immobilization. HyHel-9, 10, and 15 had about the same amount of protein immobilized and HEL load capacities. HyHel-9 had about the same amount of protein immobilized as HyHel-9, 10, and 15 but it had only about one-third the antigen load capacity. The reason for this may have been that the amount of specific anti-HEL antibodies in the HyHel-8 ascites fluid (the titer) was less than in the others.

Non-specific binding to the immunoaffinity matrix was investigated with BSA. Constant peak heights of triplicate injections of BSA indicated no non-specific binding on either the monoclonal or non-immune mouse IgG matrix. Nonspecific binding of BSA would have resulted in peak heights slowly increasing with each injection until a constant peak height was reached. The absence of non-specific BSA binding was confirmed when no BSA was eluted during the desorption buffer step.

TABLE I

EVALUATION OF IMMUNOAFFINITY COLUMNS

Affinity column	*Protein immobilized*[a] *(mg/ml gel volume)*	*HEL load capacity*[b] *(μg/ml column volume)*	*Lysozymes bound*
HyHel-5	8.6	31.1	All but HUL
HyHel-8	20.8	97.0	All but HUL
HyHel-9	17.2	287	All but HUL
HyHel-10	21.6	303	All but HUL
HyHel-15	18.3	281	All but HUL
Mouse IgG	15.5		None

[a] Determined by Bradford protein assay.
[b] Determined by frontal analysis[14].

Binding of all the lysozymes used was evaluated for each immunoaffinity column. As shown in Table I, all five monoclonal anti-HEL immunoaffinity columns bound to all of the lysozymes tested, except the human milk. None of these lysozymes bound to the non-immune mouse IgG column, which was used as a control, indicating that the binding was specific. HUL and HEL differ by 53 out of 129 amino acids. Polyclonal anti-HUL antibodies have been observed to cross-react with HEL[2,16]. The HUL structure is sufficiently different from HEL to prevent binding of the monoclonals prepared against HEL. However, the other avian lysozyme variants having amino acid differences from HEL ranging from 4 amino acids for BEL to 20 amino acids for duck B, were still bound. Monoclonal antibodies will frequently cross-react with related antigens. These data demonstrate the ability of antibodies to cross-react with similar species which differ by as much as 20 amino acids from the immunogen. Although there is a great degree of binding cross-reactivity, the affinities of all the variants to the monoclonals are not always equal to that of HEL[3,5].

ICA of lysozyme variants

Conventional chromatographic methods are often more selective than immunoaffinity chromatography. RNP, Duck A, B, and C lysozyme differ from HEL by 10, 19, 20, and 21 amino acids, respectively, but still cross-reacted with the monoclonal HyHel-9 antibody (Fig. 3). JEL and BEL differ from HEL by 6 and 4 amino acids, respectively, but cross-reacted with HyHel-5 (Fig. 4). CEX (Fig. 3) and RPC (Fig. 4) were able to separate lysozymes that were indistinguishable by immunoaffinity analysis alone. These data demonstrate the utility of the ICA system in distinguishing between proteins with similar structural forms. The immunoaffinity column cross-reacts and purifies the species, then the second column separates them.

Mobile phases used in RPC are compatible with most desorption conditions used in immunoaffinity chromatography. CEX chromatography is compatible with

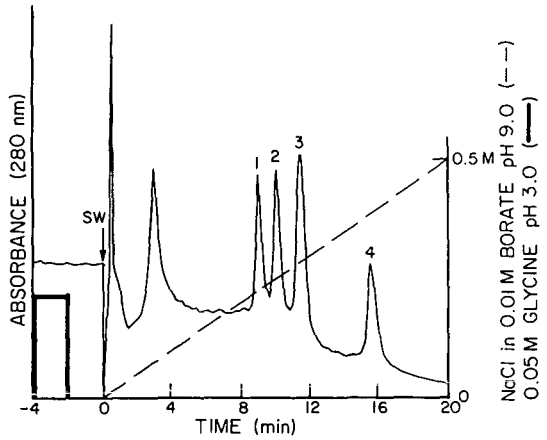

Fig. 3. ICA of lysozyme variants (1 = RNP, 2 = duck A, 3 = duck B, 4 = duck C). Affinity column: monoclonal anti-HEL (HyHel-9) (5 × 0.41 cm I.D.). Analytical column: cation-exchange, Synchropak S300 (5 × 0.41 cm I.D.). Event sequence: −4.0 min, inject 2-ml plug of 0.005 *M* glycine (pH 3.0) (rectangular box); 0 min, analytical column switched (SW) in-line with gradient pump, cation-exchange analysis started with a 20-min linear gradient from 0 to 0.5 *M* sodium chloride in 0.01 *M* sodium borate (pH 9.0) at a flow-rate of 1 ml/min.

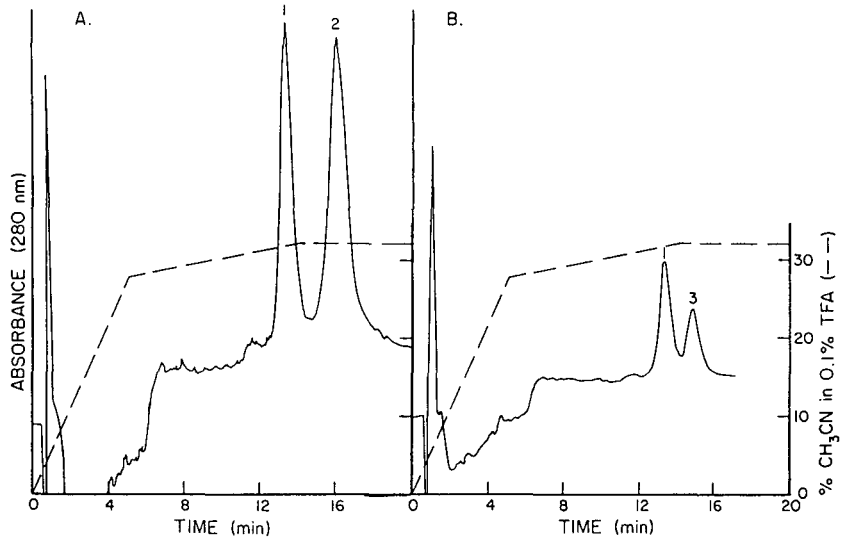

Fig. 4. ICA of lysozyme variants. (A) 1 = HEL, 2 = JEL; (B) 1 = HEL, 3 = BEL. Affinity column: monoclonal anti-HEL (HyHel-5) (5 × 0.41 cm I.D.). Analytical column: reversed-phase, Supelco C-304 (5 × 0.41 cm I.D.). Event sequence: −6.0 min, inject 2-ml plug of 0.10 *M* glycine (pH 2.2); 0 min, analytical column switched (SW) in-line with gradient pump, reversed-phase analysis started with a 5-min linear gradient from 0 to 28% acetonitrile in 0.1% TFA, followed by a 9-min linear gradient from 28 to 32% acetonitrile in 0.1% TFA, at 14 min. These conditions were maintained until 20 min, at a flow-rate of 1 ml/min.

immunoaffinity chromatography when a low pH desorption buffer is used. At a low pH, all proteins will be positively charged and will concentrate on a cation-exchange column before gradient elution is begun. Other desorption conditions are necessary when immunoaffinity chromatography is coupled to anion-exchange and HIC.

Competitive inhibition of binding studies

All of the direct binding studies of a single or mixture of lysozymes were carried out with an antibody excess. Competitive inhibition of binding studies with an antigen excess were also performed by ICA. Immobilized HyHel-5, packed into a 3 × 0.2 cm I.D. column (volume, 0.094 ml), had a HEL load capacity of 2.9 μg HEL, calculated from the HEL load capacity listed in Table I. The lysozymes bound to the immunoaffinity column were desorbed and analyzed by RPC which separated JEL and BEL from HEL, as shown in Fig. 4. The results of the competitive inhibition of binding analyses are shown in Fig. 5. The inhibition data, linearized by the log–logit transformation gave a correlation coefficient of 0.978 and 0.992 for JEL and BEL, respectively. The amount of inhibitor required to give 50% inhibition of HEL binding, obtained from the linearized inhibition data, was 89.77 μg JEL and 1907 μg BEL. This gave a ratio of the concentrations (I) of BEL/JEL of 217.

Each lysozyme variant has been classified according to its relative 50% inhibition of HEL binding ratio (*I*) for each monoclonal by Smith-Gill *et al.*[3,5]. They were placed in broad groups, depending on the order of magnitude of *I* ($I = 1$; $1 < I < 10$; $10 \leqslant I < 100$; $I \geqslant 100$). The relative concentration of BEL:JEL required to obtain a

Fig. 5. Competitive inhibition of binding of hen egg lysozyme to HyHel-5. Inhibitors: (○), Japanese quail; (△), bobwhite quail.

50% inhibition of HyHel–5 binding to HEL was in the same order of magnitude for ICA and enzyme-linked immunosorbent plate binding assay[3], *viz.* 217[a] and 100[b], respectively, placing BEL in the same group ($I \geqslant 100$) by both methods.

These data showed that 217 times more BEL than JEL is necessary to inhibit 50% of the binding of HEL to HyHel-5. JEL competes much more efficiently with HEL for the antibody than BEL. The binding affinity of BEL to HyHel-5 is smaller than that of JEL. This is because the Arg 68 amino acid, which has been identified as a "critical" residue in the epitope of HyHel-5[3,5,10], has been substituted for Lys in BEL, decreasing the binding constant. Differences in affinity were apparent under conditions of antigen excess where there was competition for the available antibody binding sites. In situations of antibody excess, as was the case for the direct binding studies, differences in binding affinities were not apparent.

CONCLUSIONS

Our studies have demonstrated the utility of the ICA system in distinguishing between proteins with similar structures. Monoclonal antibodies frequently cross-react with a variety of closely related antigens. In this case, even antigens which differed by as much as 20 amino acids from the immunogen cross-reacted, presumably because the actual epitopes contain sufficient similarity for binding. For this reason, an immunoaffinity purification step of a recombinant protein is more useful at the beginning rather than at the end of a preparative purification scheme. The ICA system takes advantage of antibody cross-reactivities by performing a purification of all cross-reactive species first, followed by a chromatographic separation. Important applications of this method are monitoring protein fermentation broths or pharmaceutical formulations. A unique feature of the ICA system is that direct and competitive binding immunoassays of single and multiple antigens can be performed on-line,

[a] Value obtained from inhibition data linearized by a log–logit transformation[15].
[b] Data taken from ref. 1.

without fraction collection, by using unlabeled antigens. Previous work has demonstrated the utility of this system for analyzing antigens in crude samples[1,2]. This has applications in many areas, including clinical chemistry[18].

ACKNOWLEDGEMENTS

We thank Dr. G. Thévenon for her work on the cation-exchange chromatographic analysis and M. A. Rounds for assistance in the preparation of this manuscript. This work was supported by NIH Grant GM25431-10. This is Journal Paper No. 11 550 from the Purdue University Agricultural Experiment Station.

REFERENCES

1 L. Rybacek, M. D'Andrea and S. J. Tarnowski, *J. Chromatogr.*, 397 (1987) 355.
2 L. J. Janis and F. E. Regnier, *J. Chromatogr.*, 444 (1988) 1.
3 S. J. Smith-Gill, A. C. Wilson, M. Potter, E. M. Prager, R. J. Feldmann and C. R. Mainhart, *J. Immunol.*, 128 (1982) 314.
4 S. J. Smith-Gill, C. R. Mainhart, T. B. Lavoie, S. Rudikoff and M. Potter, *J. Immunol.*, 132 (1984) 963.
5 S. J. Smith-Gill, T. B. Lavoie and C. R. Mainhart, *J. Immunol.*, 133 (1984) 384.
6 R. F. Venn, *J. Chromatogr.*, 423 (1987) 93.
7 R. M. Chicz and F. E. Regnier, *Anal. Chem.*, submitted for publication.
8 J. L. Fausnaugh and F. E. Regnier, *J. Chromatogr.*, 359 (1986) 131.
9 J. Fausnaugh-Pollitt, G. Thevenon, L. J. Janis and F. E. Regnier, *J. Chromatogr.*, 443 (1988) 221.
10 S. Sheriff, E. W. Silverton, E. A. Padlan, G. H. Cohen, S. J. Smith-Gill, B. C. Finzel and D. R. Davies, *Proc. Natl. Acad. Sci. U.S.A.*, 84 (1987) 8075.
11 D. R. Davies, S. Sheriff, E. A. Padlan, E. W. Silverton, G. H. Cohen and S. J. Smith-Gill, in S. J. Smith-Gill and E. Sercarz, (Editors), *The Immune Response to Structurally Defined Proteins: The Lysozyme Model*, Adenine Press, New York, 1989.
12 E. A. Padlan, E. W. Silverton, S. Sheriff, G. H. Cohen, S. J. Smith-Gill and D. R. Davies, in preparation.
13 M. M. Bradford, *Anal. Biochem.*, 72 (1976) 248.
14 J. Jacobson, J. Frenz and Cs. Horváth, *J. Chromatogr.*, 316 (1984) 53.
15 L. A. Campfield, in W. D. Odell and P. Franchimont (Editors), *Principles of Competitive Protein-Binding Assays*, Wiley, New York, 1983, p. 125.
16 A. Miller, B. Bonavida, J. A. Statton and E. Sercarz, *Biochim. Biophys. Acta*, 243 (1971) 520.
17 R. E. Canfield, S. Kammerman, J. H. Sobel and F. J. Morgan, *Nature (London), New Biol.*, 232 (1971) 16.
18 L. J. Janis and F. E. Regnier, *Anal. Chem.*, in press.

Journal of Chromatography, 476 (1989) 245–255
Elsevier Science Publishers B.V., Amsterdam — Printed in The Netherlands

CHROMSYMP. 1594

ISOLATION OF RECOMBINANT HIRUDIN BY PREPARATIVE HIGH-PERFORMANCE LIQUID CHROMATOGRAPHY

RAINER BISCHOFF*, DANIEL CLESSE, ODILE WHITECHURCH, PIERRE LEPAGE and CAROLYN ROITSCH

Transgene S.A., Analytical and Process Development Division, 11 Rue de Molsheim, F-67000 Strasbourg (France)

SUMMARY

The purification of recombinant hirudin variant 2-Lys^{47} (rHV2-Lys^{47}), produced by a genetically engineered yeast strain, is described. rHV2-Lys^{47} expressed and secreted into the culture medium was the starting material for the purification process of hirudin from the culture broth after cell harvesting by centrifugation. Initial purification of the product by preparative reversed-phase high-performance liquid chromatography (HPLC) using step-gradient elution, followed by precipitation of rHV2-Lys^{47} in the presence of acetone, removed most of the contaminants from the culture medium. The pure product was obtained by successive preparative anion-exchange and reversed-phase HPLC on silica based stationary phases. Characterization of the final product by analytical HPLC, isoelectric focusing gel electrophoresis, quantitative amino acid composition and sequence analysis did not reveal any contaminants. Liquid secondary ion mass spectrometry was used to confirm its primary structure. The isolated product was tested in an inhibition assay of human α-thrombin and proved to be fully active.

INTRODUCTION

Natural hirudin, as first described by Markwardt[1,2], is one of the most potent inhibitors of α-thrombin. It is produced in trace amounts as a mixture of closely related polypeptides of 64–66 amino acids by the leech *Hirudo medicinalis*[3–8]. The rather limited quantities that can be isolated from this natural source and the additional complications caused by its heterogeneity have prevented more extensive and systematic pharmacological evaluations of natural hirudin. However, from various animal studies, evidence has been obtained that natural hirudin functions as a powerful anticoagulant *in vivo*[9]. The first clinical trials have substantiated these results and no adverse side effects have been observed when therapeutic doses were used[10,11].

Only recently has it become possible to produce hirudin in genetically engineered microorganisms, such as *Escherichia coli*[7,12–14] and *Saccharomyces cerevisiae*[15]. This permits the production of recombinant hirudin in quantities sufficient for systematic pharmacological evaluations, provided that the polypeptide can be efficiently purified.

0021-9673/89/$03.50

Recombinant hirudin variant 2 (rHV2) has been expressed and secreted from *Saccharomyces cerevisiae* as previously described[15]. A variant of HV2 in which Asn^{47} has been replaced by a Lys residue (rHV2-Lys^{47}) has been shown to have improved inhibitory properties[16].

In this article we describe the isolation of rHV2-Lys^{47} from the culture medium of a recombinant yeast strain by preparative high-performance liquid chromatography (HPLC). The final product has been characterized by analytical reversed-phase and anion-exchange HPLC, determination of its amino acid sequence and amino acid composition, isoelectric focusing gel electrophoresis, liquid secondary ion mass spectrometry (LSIMS) and its specific inhibitory activity against human α-thrombin.

MATERIALS AND METHODS

Materials

Chromozym PL (tosylglycylprolyllysine-4-nitroanilide acetate) was obtained from Boehringer Mannheim (Mannheim, F.R.G.). Human α-thrombin was obtained from Sigma (St. Louis, MO, U.S.A.). The purity and integrity of α-thrombin was assessed to be higher than 95% by 10% polyacrylamide gel electrophoresis (PAGE) in the presence of sodium dodecyl sulphate (SDS) as previously described[17]. rHV2-Lys^{47} of the described quality is also available from Sigma. Immobiline solutions and protein standards for the range pH 3.8–4.8 were obtained from Pharmacia/LKB (Uppsala, Sweden). Amino acid standards for quantitative amino acid analysis were from Pierce (Rockford, IL, U.S.A.) and sequencing reagents from Applied Biosystems (Foster City, CA, U.S.A.). All solvents used were of HPLC grade from Farmitalia Carlo Erba (Milan, Italy). The HCl used for amino acid composition analysis was of Ultrex grade from Baker Chemical (Phillipsburgh, NJ, U.S.A.). Stationary phases used for analytical HPLC separations were either from Macherey & Nagel (Nucleosil C_8; Düren, F.R.G.) obtained through Société Française Chromato Colonne (SFCC) (Neuilly-Plaisance, France) or from Pharmacia/LKB (Mono Q). Stationary phases used for preparative HPLC were obtained from either SFCC [silica derivatized with an adsorbed and cross-linked coating of poly(vinylimidazole) and poly(vinylpyrrolidone) that was partially quaternized (PVDI-silica) for anion-exchange chromatography] or from Separations Technology (ST/C_8 reversed-phase support; Wakefield, RI, U.S.A.).

Instrumentation

Preparative HPLC was performed on a ST/1200-XP HPLC system controlled by a microcomputer (Separations Technology). Analytical HPLC separations were carried out on an HP-1090 chromatograph equipped with an HP-1040A diode-array detector and a microcomputer (Hewlett-Packard, Waldbronn, F.R.G.). Specific activity determinations were performed with a 8451A diode-array spectrophotometer (Hewlett-Packard). Amino acid composition analysis was performed on a 420A derivatizer, connected to a 130A on-line HPLC analyzer equipped with a 920A microcomputer (Applied Biosystems) after total hydrolysis in a Pico Tag workstation (Waters Assoc., Milford, MA, U.S.A.). For protein sequencing a 477A protein sequencer was employed connected to a 120A on-line phenylthiohydantoin (PTH)-amino acid HPLC analyzer, equipped with a 920A microcomputer (Applied Biosystems).

LSIMS was performed on a VG Analytical ZAB-SE double-focusing mass spectrometer (Manchester, U.K.), using an ionization current of *ca.* 1 μA from 30-keV Cs^+.

Isolation procedure

Recombinant hirudin (rHV2-Lys^{47}) was expressed in yeast and secreted into the culture medium as previously described[15]. After cell harvesting by centrifugation, the supernatant was clarified by microfiltration at 0.1 μm through a hollow-fibre cross-flow filtration system (Amicon, Danvers, MA, U.S.A.). The filtered supernatant was directly loaded onto a reversed-phase C_8 column (50 cm × 4 in.; Separations Technology ST/C_8, 50 μm) and subsequently eluted using water–2-propanol (70:30) at a flow-rate of 300 ml/min. After removing the 2-propanol by rotaevaporation, rHV2-Lys^{47} was precipitated at 4°C with 80% (v/v) aqueous acetone in 20 m*M* sodium phosphate buffer (pH 7.5) in the presence of 150 m*M* NaCl. The precipitated material was pelleted by centrifugation and resolubilized in 20 m*M* sodium phosphate buffer (pH 6.4).

This solution was loaded onto an anion-exchange column (PVDI-silica, 15–20 μm, 25 cm × 2 in.), and rHV2-Lys^{47} subsequently eluted using a gradient from 0–1 *M* NaCl in 20 m*M* sodium phosphate (pH 6.4) in 65 min at a flow-rate of 80 ml/min.

Reversed-phase HPLC on a C_8 stationary phase (Nucleosil, 10 μm, 30 cm × 5 cm) was employed as the final purification step. An 80-min gradient of 0–50% 2-propanol in 10 m*M* sodium acetate (pH 5) at a flow-rate of 70 ml/min was used for elution. rHV2-Lys^{47} was pooled according to the results of analytical reversed-phase and anion-exchange HPLC. Fractions showing homogeneity in both analytical systems were pooled.

Desalting of the final material was achieved by reversed-phase HPLC on a C_8 stationary phase (Nucleosil, 10 μm, 30 cm × 5 cm) with 30% aqueous 2-propanol for elution at a flow-rate of 90 ml/min. After rotaevaporation of 2-propanol under vacuum, the final product was lyophilized from water.

Analytical characterization

Analytical reversed-phase HPLC was performed on Nucleosil-C_8 (3 μm, 10 cm × 0.46 cm) at a flow-rate of 1 ml/min with a gradient from 15% acetonitrile in 0.1% aqueous trifluoroacetic acid (TFA) to 30% acetonitrile in 0.1% aqueous TFA in 15 min. For the analysis of crude samples, a 10-min wash with 15% acetonitrile in 0.1% aqueous TFA preceded the gradient. Detection was performed by UV absorption at 205 nm (for attenuation see individual figures).

Analytical anion-exchange HPLC was done on Mono Q (10 μm, 5 cm × 0.5 cm) at a flow-rate of 1 ml/min with a gradient from 20 m*M* Tris–HCl (pH 7.5) to 0.3 *M* NaCl in 20 m*M* Tris–HCl (pH 7.5) over 20 min (detection by UV absorbance at 280 nm with 0.05 a.u.f.s.).

Protein sequence analysis from the N-terminus was carried out by automated Edman degradation with identification of the individual PTH-amino acids by on-line HPLC analysis.

Complete amino acid composition analysis was performed by acid hydrolysis, followed by derivatization of the amino acids with phenyl isothiocyanate (PITC) and subsequent analysis by HPLC[18].

LSIMS was performed as described[19].

For isoelectric focusing the manufacturer's specifications were followed. An Immobiline system in the range pH 3.8–4.8 was modified as described[20].

The specific activity was determined by inhibition of human α-thrombin as described[16]. Assays were performed in polystyrene cuvettes at 37°C in 5 m*M* 1,4-piperazinediethanesulphonic acid (PIPES)–NaOH (pH 7.9), 0.18 *M* NaCl, 0.1% poly (ethylene glycol) (average molecular weight: 6000 daltons) at a final volume of 1 ml. Increasing amounts of rHV2-Lys^{47} were mixed with 4.3 n*M* α-thrombin [determined by active site titration with *p*-nitrophenyl-*p'*-guanidinobenzoate (NPGB) as previously described[22]] and thermally equilibrated for 3 min. The reaction was started by adding 20 μl of chromozym PL (20 mg in 3 ml water) to a final concentration of 0.2 m*M* and free thrombin was determined by *p*-nitroaniline release at 405 nm. Generally, 9–12 data points were determined and the velocity of substrate hydrolysis was analyzed by non-linear regression[16,21]. The amount of rHV2-Lys^{47} necessary for complete thrombin inhibition was deduced from the x-axis intercept. The concentration of the rHV2-Lys^{47} solution was determined independently by quantitative total amino acid analysis.

RESULTS

Isolation of rHV2-Lys^{47} from the culture medium of a genetically engineered yeast strain was achieved using a series of preparative HPLC steps. After separation of cells from the medium by centrifugation, the supernatant was clarified by cross-flow microfiltration with a 0.1-μm cut-off. The amount of rHV2-Lys^{47} present in this starting material and in the individual pools throughout the purification process was determined by analytical reversed-phase HPLC and integration of the absorbance peak at 205 nm. Purified rHV2-Lys^{47} which had been quantified by total amino acid analysis was used as a standard to calibrate the HPLC system.

The isolation of rHV2-Lys^{47} consisted of a number of individual purification steps, serving two main purposes: (1) the removal of contaminants from the culture medium unrelated to rHV2-Lys^{47} such as nutrients and other additives; (2) the separation of the product from closely similar protein contaminants. The initial purification step which is not listed here was the secretion of the molecule into the culture medium taking place at the level of fermentation. This resulted in a considerable enrichment of rHV2-Lys^{47} and facilitated the subsequent purification process. This is illustrated in Fig. 1 showing the reversed-phase HPLC analysis of the microfiltered culture supernatant. It was found that only the late-eluted peak in the chromatogram corresponds to rHV2-Lys^{47}. However, a closer look at the region of interest in the chromatogram showed that next to the major product peak there were a number of closely similar contaminants which had to be removed during the purification procedure. Analysis of these contaminants after the purification process showed that some of them represented either C-terminal degradation products or partially deamidated forms of rHV2-Lys^{47}.

The initial reversed-phase purification served as a rapid way of concentrating rHV2-Lys^{47} and of removing the bulk of the contaminants (Table I). A pigmented compound that was isolated together with the product as seen by monitoring the analytical reversed-phase HPLC at 450 nm (Fig. 2) was efficiently removed in the

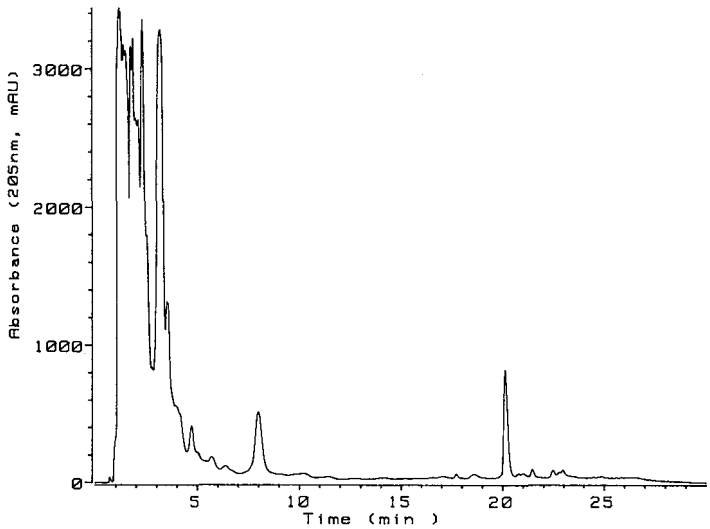

Fig. 1. Reversed-phase HPLC analysis of the culture supernatant after filtration at 0.1-μm cut-off. Experimental conditions: 10 cm × 0.46 cm column (Nucleosil C_8, particle diameter 3 μm); flow-rate, 1 ml/min; gradient, 15% acetonitrile in 0.1% aqueous TFA to 30% acetonitrile in 0.1% aqueous TFA in 15 min after a 10-min wash with 15% acetonitrile in 0.1% aqueous TFA; detection, UV absorption at 205 nm in milliabsorbance units (mAU).

subsequent precipitation of rHV2-Lys[47] with 80% (v/v) aqueous acetone at 4°C (Fig. 3). Precipitation was quantitative after 15 min and did not affect the activity of the molecule.

The pellet was isolated by centrifugation and dissolved readily in the initial buffer for the subsequent anion-exchange purification step. Anion-exchange HPLC was done on a silica matrix of particle diameter 15–20 μm and average pore diameter 30 nm derivatized with an adsorbed and cross-linked coating of poly(vinylimidazole) and poly(vinylpyrrolidone) (PVDI) that was subsequently quaternized[23]. The proteins were adsorbed in 20 m*M* sodium phosphate buffer at pH 6.4 and subsequently eluted with a gradient of increasing sodium chloride concentration. Fractions were pooled according to the results of analytical reversed-phase HPLC, giving a purity of 90% by integration at 205 nm (Fig. 4). The two major contaminants at about 8.5 and 12 min respectively corresponded to C-terminally degraded forms of rHV2-Lys[47]

TABLE I

PURIFICATION YIELDS OF RECOMBINANT HIRUDIN

Purification step	*Concentration (mg/l)*	*Total amount (mg)*	*Yield (%)*
Starting material	90	1930	100
1st Reversed-phase HPLC	677	1460	76
Acetone precipitation	619	1238	64
Anion-exchange HPLC	307	1093	57
2nd Reversed-phase HPLC	1510	801	42
Final product	–	750	39

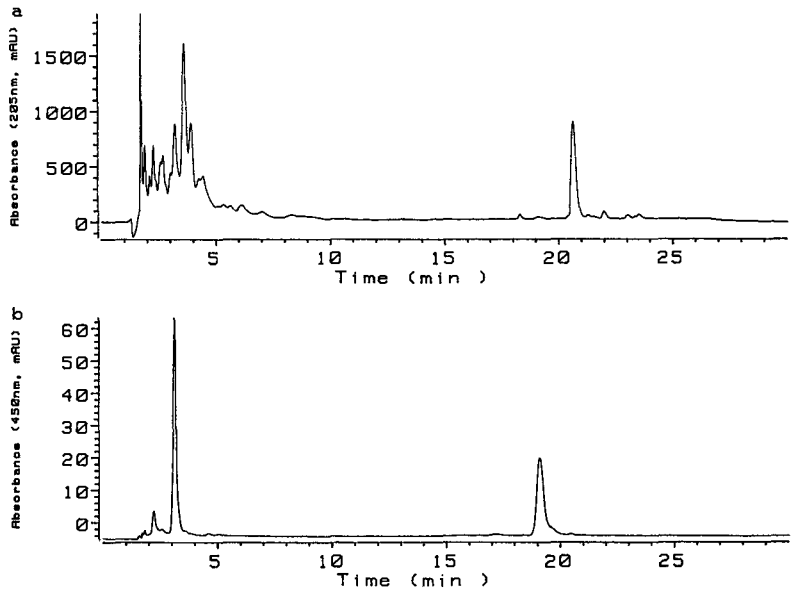

Fig. 2. Reversed-phase HPLC analysis after the first purification step by adsorption to a C_8 reversed-phase stationary phase. Experimental conditions as in Fig. 1 with detection at (a) 205 and (b) 450 nm.

with 63 and 64 amino acids as determined by quantitative total amino acid analysis and LSIMS (results not shown).

Final purification was achieved by reversed-phase HPLC on a silica-based C_8

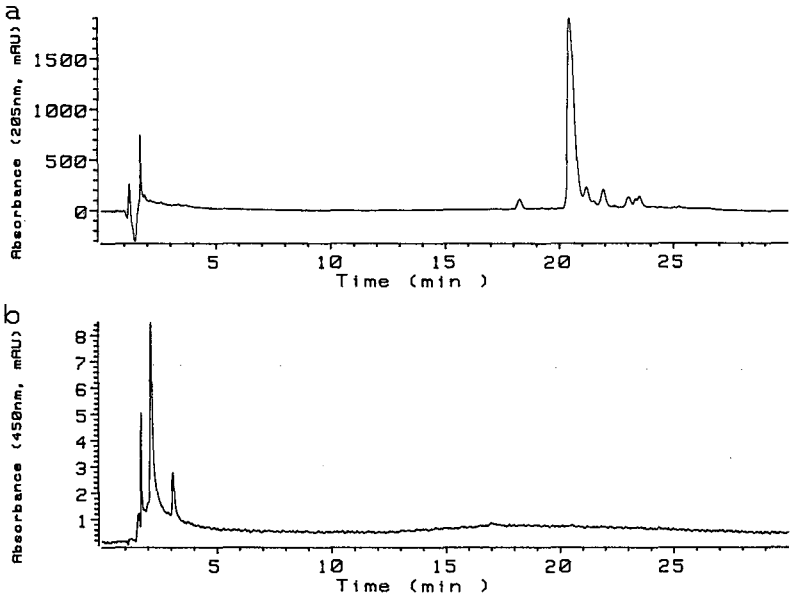

Fig. 3. Reversed-phase HPLC analysis after acetone precipitation of rHV2-Lys[47]. Experimental conditions as in Fig. 1 with detection at (a) 205 and (b) 450 nm.

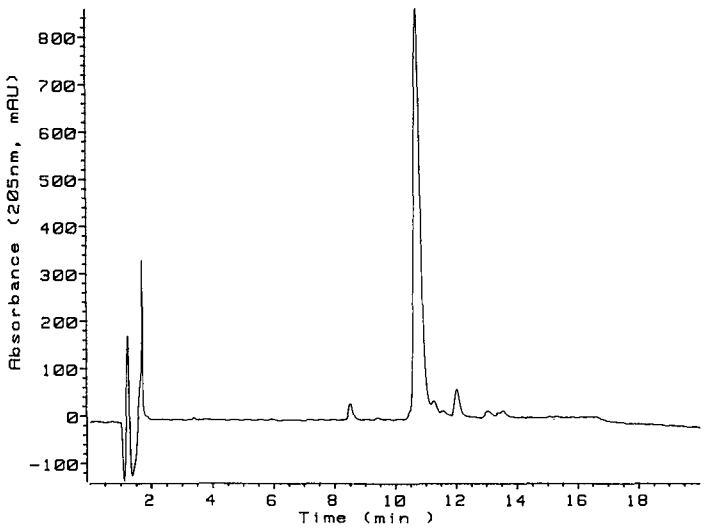

Fig. 4. Reversed-phase HPLC analysis of the pool obtained after preparative anion-exchange HPLC. Experimental conditions as in Fig. 1 but without the 10-min wash.

stationary phase with particle diameter 10 μm and average pore diameter 12 nm. rHV2-Lys^{47} was eluted using a gradient of increasing 2-propanol concentration in 10 m*M* sodium acetate at pH 5. Fractions which did not show any contaminating peaks by either analytical reversed-phase HPLC at pH 2 or by anion-exchange HPLC at pH 7.5 were pooled. After rotaevaporation of 2-propanol and desalting by reversed-phase HPLC, the final product was lyophilized from water and stored at -20°C. Analysis of the material after several months of storage, by reversed-phase or anion-exchange HPLC, did not reveal any degradation (Figs. 5 and 6).

rHV2-Lys^{47} isolated by the procedure described was further characterized by the following analytical methods (results not shown): (1) quantitative amino acid analysis after total acid hydrolysis; (2) complete amino acid sequence determination by automated Edman degradation; (3) assignment of disulphide bridges between residues 6–14, 16–28 and 22–39 as in the natural molecule by sequence analysis of peptides obtained after digestion with thermolysin. These criteria confirmed the primary structure and purity of the isolated molecule.

Isoelectric focusing gel electrophoresis on Immobiline gels was subsequently employed in the range pH 3.8–4.8 to verify the homogeneity of the purified rHV2-Lys^{47} with respect to its isoelectric point (p*I*) (Fig. 7). No contaminating bands were detected even when overloading the gel with 50 μg rHV2-Lys^{47} and the measured p*I* of 4.30 corresponded exactly with the calculated value (DNASTAR, Madison, WI, U.S.A.). The resolution of the gel system was determined to be ± 0.01 pH units. In an independent experiment it was shown that forms of rHV2-Lys^{47} which were deamidated at individual amino acid residues were easily discriminated from the correct molecule in this gel system.

Further structural information on the isolated molecule was obtained by LSIMS as described[19]. A wide scan gave an average mass of 6907.0 $\pm$ 1 dalton for

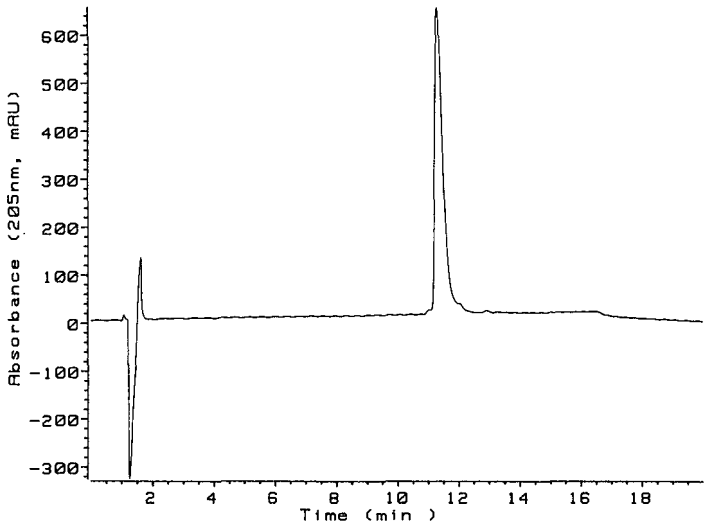

Fig. 5. Reversed-phase HPLC analysis of the product obtained after the final preparative reversed-phase purification step. Experimental conditions as in Fig. 1 but without the 10-min wash.

the protonated molecular ion (Fig. 8). Better accuracy of the measured average mass was obtained by using voltage scanning over only 300 mass units (narrow scan). This resulted in an average mass of 6907.5 daltons for the protonated molecular ion with an accuracy of ±0.5 dalton (data not shown). This value is identical to the calculated value of 6907.5 daltons.

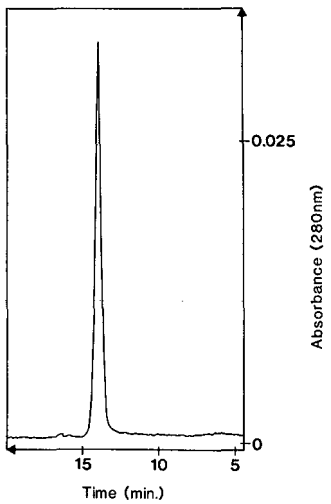

Fig. 6. Analysis of the final product by anion-exchange HPLC on Mono Q. Experimental conditions: 5 cm × 0.5 cm column (Mono Q, particle diameter 10 μm); flow-rate, 1 ml/min; gradient, 20 m*M* Tris–HCl pH 7.5 to 20 m*M* Tris–HCl pH 7.5 + 0.3 *M* NaCl in 20 min; detection, UV absorbance at 280 m.

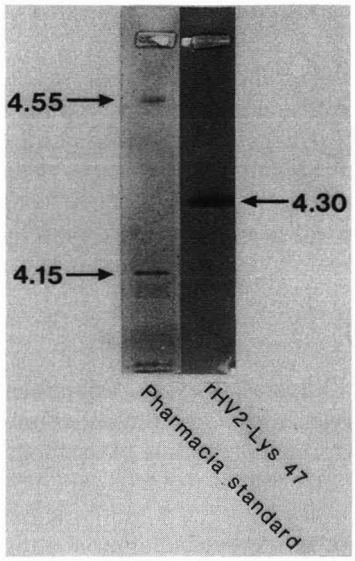

Fig. 7. Isoelectric focusing gel electrophoresis of the final product with an Immobiline system in the range pH 3.8–4.8. Left lane: p*I* standards (Pharmacia). Right lane: rHV2-Lys^{47} (purified).

The biological activity of rHV2-Lys^{47}, as prepared by the purification procedure described, was evaluated by determining its specific inhibitory activity against human α-thrombin, as described[16]. Briefly, increasing quantities of rHV2-Lys^{47} were added to a fixed amount of human α-thrombin, and the residual proteolytic activity of free thrombin was determined in a spectrophotometric assay, using a chromogenic substrate. This result verified that the rHV2-Lys^{47} preparation obtained was fully active as an α-thrombin inhibitor.

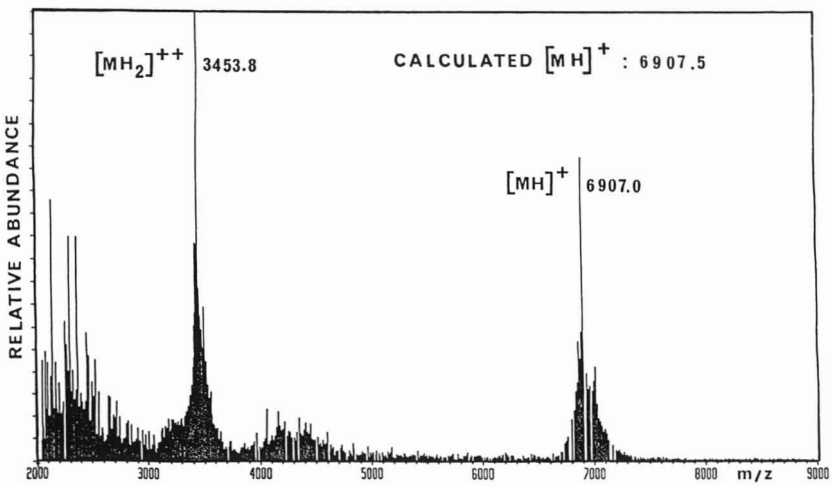

Fig. 8. Determination of the average molecular mass of rHV2-Lys^{47} by wide scan LSIMS. The spectrum shows the mono- and the diprotonated molecular ion.

DISCUSSION

The purification process described allowed the isolation of rHV2-Lys^{47}, a naturally occurring hirudin variant, starting from the culture medium of a recombinant yeast strain. The overall process yield ranged from 35 to 40% giving 750 mg of final product from *ca.* 2 g of starting material in the culture supernatant.

The purification process consisted of two major parts. In the initial stages it was necessary to remove the bulk of the contaminants present in the culture medium by adsorption of rHV2-Lys^{47} to a reversed-phase support followed by precipitation of the protein with aqueous acetone. In the second part, preparative anion-exchange and reversed-phase HPLC were used to separate the product from other proteins, in particular from some degraded forms.

Characterization of the isolated rHV2-Lys^{47} by different analytical techniques did not reveal any contaminants or structural heterogeneities. Quantitative amino acid analysis and amino acid sequencing confirmed the primary structure of the molecule. However, contaminants which are not proteins or peptides would escape this kind of analysis. In addition, these analyses, although very powerful in verifying the primary structure of the molecule, are not sensitive enough to detect contaminating proteins below the level of *ca.* 5%. They were therefore complemented by reversed-phase and anion-exchange HPLC analyses which had been optimized to separate either C-terminal degradation products or deamidated forms of rHV2-Lys^{47} which had been identified as possible contaminants. The sensitivity of these analytical methods was better than 1% with regard to these contaminants. All these techniques did not reveal any contaminants and the isolated rHV2-Lys^{47} had a minimum purity of 99% based on these criteria. Isoelectric focusing gel electrophoresis was subsequently used to measure the p*I* of rHV2-Lys^{47} which corresponded exactly to the calculated value.

LSIMS was employed as an additional criterion for assessing the structural integrity of the isolated rHV2-Lys^{47}. While this method is not able to detect contaminants below a level of *ca.* 10%, it has a high mass resolution and is thus able to detect structural changes in the molecule which result in a difference of 1 or 2 daltons, such ad deamidations of individual amino acids or reduced disulphide bridges.The isolated rHV2-Lys^{47} was homogeneous based on this criterion.

In conclusion it was shown that rHV2-Lys^{47} isolated by the procedure described was homogeneous with regard to its primary structure and pure to at least 99%. It was fully active as an inhibitor of human α-thrombin *in vitro*.

ACKNOWLEDGEMENTS

The pharmaceutical development of recombinant hirudin is being pursued within a partnership agreement between Transgene, 16 Rue Henri Regnault, 92411 Courbevoie Cedex, France and Sanofi, 40 Avenue Georges V, 75008 Paris, France. The authors would like to thank Professors P. Chambon and P. Kourilsky as well as Drs. J. P. Lecocq and M. Courtney for their continued interest in the work and for helpful discussions. We are indebted to our colleagues from the departments of Fermentation Development and Molecular Genetics, since without their research and development work this publication would not have been possible. The authors would

like to thank Drs. A. van Dorsselaer (Strasbourg, France) and B. Green (Manchester, U.K.) for performing the LSIMS measurements.

REFERENCES

1 F. Markwardt, *Arch. Exp. Pharm.*, 229 (1956) 389.
2 F. Markwardt, *Methods Enzymol.*, 19 (1970) 924.
3 F. Markwardt, *Biomed. Biochim. Acta*, 44 (1985) 1007.
4 J. Y. Chang, *FEBS Lett.*, 164 (1983) 307.
5 J. Dodt, H. P. Müller, U. Seemüller and J. Y. Chang, *FEBS Lett.*, 165 (1984) 180.
6 J. Dodt, W. Machleidt, U. Seemüller, R. Maschler and H. Fritz, *Biol. Chem. Hoppe-Seyler*, 367 (1986) 803.
7 R. P. Harvey, E. Degryse, L. Stefani, F. Schamber, J. P. Cazenave, M. Courtney, P. Tolstoshev and J. P. Lecocq, *Proc. Natl. Acad. Sci. U.S.A.*, 83 (1986) 1084.
8 D. Tripier, *Folia Haematol. (Leipzig)*, 115 (1988) 30.
9 F. Markwardt, J. Hauptmann, G. Nowak, Ch. Klessen and P. Walsmann, *Thromb. Haemostasis. (Stuttgart)*, 47 (1982) 226.
10 J. Bichler, B. Fichtl, M. Siebeck and H. Fritz, *Arzneim.-Forsch./Drug. Res.*, I (1988) 704.
11 F. Markwardt, G. Fink, B. Kaiser, H.-P. Klöcking, G. Nowak, M. Richter and J. Stürzebecher, *Pharmazie*, 43 (1988) 202.
12 C. Bergmann, J. Dodt, S. Köhler, E. Fink and H. G. Gassen, *Biol. Chem. Hoppe-Seyler*, 367 (1986) 731.
13 J. Dodt, T. Schmitz, T. Schäfer and C. Bergmann, *FEBS Lett.*, 202 (1986) 373.
14 E. Fortkamp, M. Rieger, G. Heisterberg-Moutses, S. Schweitzer and R. Sommer, *DNA*, 5 (1986) 511.
15 G. Loison, A. Findeli, S. Bernard, M. Nguyen-Juilleret, M. Marquet, N. Riehl-Bellon, D. Carvallo, L. Guerra-Santos, S. W. Brown, M. Courtney, C. Roitsch and Y. Lemoine, *Bio/Technology*, 6 (1988) 72.
16 E. Degryse, M. Acker, J. P. Maffrand, C. Roitsch and M. Courtney, *Protein Eng.*, 2 (1989) 459.
17 U. K. Laemmli, *Nature (London)*, 227 (1970) 680.
18 B. A. Bidlingmeyer, S. A. Cohen and T. L. Tarvin, *J. Chromatogr.*, 336 (1984) 93.
19 A. van Dorsselaer, P. Lepage, F. Bitsch, O. Whitechurch, N. Riehl-Bellon, D. Fraisse, B. Green and C. Roitsch, *Biochemistry*, 28 (1989) 2949.
20 N. Riehl-Bellon, D. Carvallo, M. Acker, A. van Dorsselaer, M. Marquet, G. Loison, Y. Lemoine, S. W. Brown, M. Courtney and C. Roitsch, *Biochemistry*, 28 (1989) 2941.
21 J. W. Williams and J. F. Morrison, *Methods Enzymol.*, 63 (1979) 437.
22 T. Chase, Jr. and E. Shaw, *Methods Enzymol.*, 19 (1970) 20.
23 B. Sebille, B. Boussouira and J. Piquiom, *Eur. Pat. Appl.*, 86,402,633 (1987).

Journal of Chromatography, 476 (1989) 257–268
Elsevier Science Publishers B.V., Amsterdam — Printed in The Netherlands

CHROMSYMP. 1624

COMPARISON OF PROTEIN A, PROTEIN G AND COPOLYMERIZED HYDROXYAPATITE FOR THE PURIFICATION OF HUMAN MONOCLONAL ANTIBODIES

ALOIS JUNGBAUER*, CHRISTA TAUER, MANFRED REITER, MARTIN PURTSCHER, ELISABETH WENISCH, FRANZ STEINDL, ANDREA BUCHACHER and HERMANN KATINGER

University of Agriculture and Forestry, Institute of Applied Microbiology, Peter Jordanstr. 82, A-1190 Vienna (Austria)

SUMMARY

Protein A Superose, protein G Sepharose fast flow and copolymerized hydroxyapatite were used for the purification of human monoclonal antibodies against HIV 1. Both desalted culture supernatant and a prepurified protein solution were used as starting materials. The different runs were compared with respect to yield and recovery of biological activity. The biological activity (specific reactivity) was checked by antigen enzyme-linked immunosorbent assay with recombinant antigen. The human monoclonal antibodies could not be selectively eluted from the hydroxyapatite but elution could be effected from the protein A Superose at pH 4.0 and from protein G at pH 3.0. The eluted immunoglobulin G was distributed over a broad pH range when protein G Superose was used. Biologically active material could be obtained from protein A Superose and protein G Sepharose fast flow.

INTRODUCTION

Various methods have been described for the purification of monoclonal antibodies of murine origin. In general, the methods involve two major steps. First, a prepurification step, *i.e.*, a precipitation step, can be carried out (ammonium sulphate, caprylic acid, polyethylene glycol or isoelectric precipitation) or a concentration step can be performed by ultrafiltration[1–6]. Second, various chromatographic methods are used, such as ion-exchange chromatography or affinity chromatography on protein A, immunoligands or synthetic antigen analogues[7,8]. For murine monoclonal antibodies (G and M isotypes), Pavlu *et al.*[9] and Chen *et al.*[10] compared different purification methods.

The pretreatment steps depend on the starting material if ascites or culture supernatant is used. Clezardin and co-workers[11,12] used Mono Q and gel chromatography on Superose 6. Methods have been described for immunoglobulins M (IgM) and G (IgG) from ascites fluid or culture supernatant. Nearly all workers apply the purification mode to accomplish the purification of the monoclonal antibody. How-

0021-9673/89/$03.50

ever, for preparative purposes, especially starting from the diluted culture supernatant, the concentration mode[13] is to be preferred. In this mode, the advantage is in the reduction of the column size, resulting in a high product concentration in the eluate.

Few papers have described purification methods for human monoclonal antibodies. In this paper, different purification strategies for human monoclonal antibodies are compared. In all experiments the concentration mode was applied. Human and murine monoclonal antibodies differ in many ways. The most important difference with respect to purification is the binding behaviour on protein A and protein G[14,15]. The affinity purification of human monoclonal antibodies is the method of choice.

Three different methods were investigated in these comparative experiments. Starting from the desalted culture supernatant or a concentrated eluate from a CM-Sepharose fast flow step, the purification power of protein A Superose, protein G Sepharose fast flow and hydroxyapatite Ultrogel were tested. The following criteria were investigated in this comparative study: purity [checked by sodium dodecyl sulphate-polyacrylamide gel electrophoresis (SDS-PAGE)], capacity and recovery (yield and avidity). Using protein A or protein G, a highly pure and biologically active protein could be obtained.

EXPERIMENTAL

Human hybridoma cells producing humAb against HIV 1, as described by Grunow *et al.*[16], were mass cultivated in an airlift fermenter, using RPMI[a] 1640 cell culture medium (Gibco, Paisley, U.K.) supplemented with 5% foetal calf serum as substrate. The culture broth was clarified by means of microfiltration on Pellicon cross-flow membranes (Millipore, Bedford, MA, U.S.A.). The clear supernatant was used for the chromatographic experiments.

The starting material was either a desalted culture supernatant or a highly concentrated material, as described in detail elsewhere[17]. Briefly, the culture supernatant was desalted and applied to a CM-Sepharose fast-flow column. The column was equilibrated with 100 m*M* histidine–hydrochloric acid buffer (pH 6.5) and elution was effected by a step gradient with 50 m*M* sodium chloride. The fractions containing the human monoclonal antibody were concentrated 10-fold on a 30 000-dalton cut-off polysulphone membrane (PTTK; Millipore).

The chromatography on protein A, protein G and hydroxyapatite Ultrogel (IBF, Paris, France) was performed on an fast protein liquid chromatography apparatus (Pharmacia, Uppsala, Sweden). The column effluent was monitored continuously with a UV monitor and a pH/ion monitor (2195 pH/ion monitor, Pharmacia-LKB). The ion monitor was calibrated with 1 *M* hydrochloric acid (highest value) and distilled water (lowest value).

Protein A Superose (Pharmacia) was used in this experiment. Similar conditions were used to those described in detail by Martin[18] for Rhesus monkey IgG. Briefly, the protein solution was desalted on Sephadex G-25 (coarse) to increase the pH to 9.0 as the protein A Superose was equilibrated with 0.1 *M* citric acid–0.2 *M*

[a] RPMI = Rosevelt Park Memorial Institute.

sodium phosphate buffer (pH 9.0). Then a step gradient from pH 6.0 to 3.0 was applied to elute the human monoclonal antibody. Immediately after elution, the humAb solution was desalted.

Protein G Sepharose fast-flow (Pharmacia) was used. The recombinant protein G without the albumin-binding region was immobilized. Similar conditions to those described for protein A were used. The culture supernatant or the concentrated material was desalted. The equilibration buffer was 0.1 *M* glycine–sodium hydroxide (pH 9.0). Elution was performed by a step gradient from pH 5.0 to 2.5, and a step gradient with two steps, pH 3.0 and 2.5. Immediately after elution, the samples were desalted.

The capacity was determined by a dynamic method. At least twice the amount of IgG was percolated over the gel. The difference between the amount in the original sample and the flow through was defined as the capacity.

SDS-PAGE was carried out in a Phast System (Pharmacia). According to the manufacturer's recommendations, the desalted samples were applied to a gradient gel (from 8 to 25%T). The gels were silver-stained and both reduced and non-reduced samples were applied.

IgG determination

The human monoclonal antibody was determined by enzyme-linked immusorbent assay (ELISA) as described by Grunow *et al.*[16]. Human monoclonal IgG (Sigma, St. Louis, MO, U.S.A.) was used as a standard protein. As the first antibody, goat anti-human gamma-chain was coated on microtitre plates. After coating and washing, samples and the calibration proteins were applied to the wells. The standard proteins were diluted (eight 2^n dilutions from 250 ng/ml to 1.953 ng/ml). Eight equal dilutions (2^n dilutions) were made from each sample. As the second antibody, goat anti-human gamma-chain conjugated with horseradish peroxidase was used. After staining, the absorption at 455 nm was measured. The results were evaluated with a fourth-degree polynomial.

Specific reactivity

The same sample dilutions as used for the determination of IgG content were tested for specific reaction to recombinant gp 160 (recombinant envelope glycoprotein from HIV 1 was a gift from Immuno, Orth, Austria). Instead of the first antibody, recombinant gp 160 was coated on microtitre plates. The subsequent steps were performed in the same manner as described for the IgG determination. The different chromatographic fractions were related to the main fraction or the culture supernatant.

RESULTS

A 1-ml volume of gel (protein G Sepharose fast flow) was packed into a column of 0.6-cm^2 cross-sectional area. A desalted culture supernatant was loaded on the column. To minimize loss of biological activity caused by denaturation at low pH during elution, a step gradient was used. The antibody was eluted over a broad pH range, as indicated in Fig. 1. The purity of the recovered antibody was shown by SDS-PAGE (Fig. 2).

Prepurified material (eluate from CM-Sepharose fast flow) was also loaded on

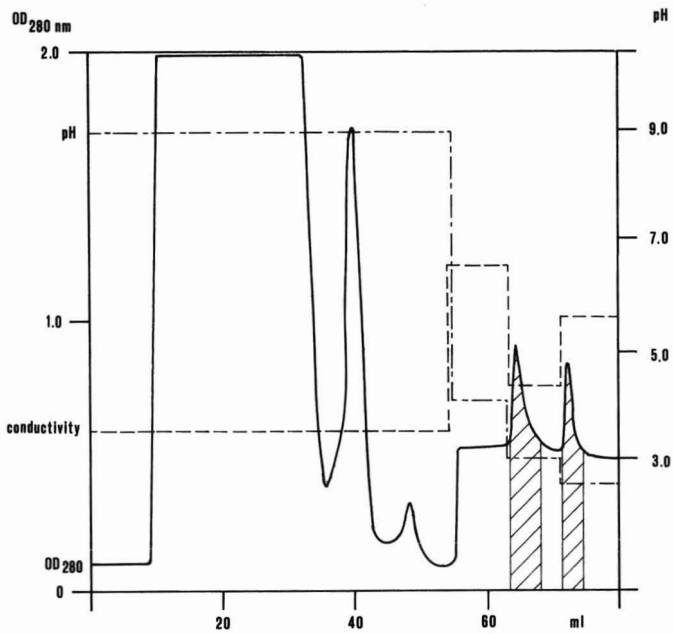

Fig. 1. Chromatography of desalted culture supernatant on protein G Sepharose fast flow. Sample, 30 ml of a concentrated (5-fold, by ultrafiltration) and desalted (on Sephadex G-25 coarse) culture supernatant; column, 1.3 ml; linear velocity, 150 cm/h. The column was loaded at pH 9.0 and a step gradient from pH 4.0 to 2.5 was used. The hatched area indicates the eluted antibody.

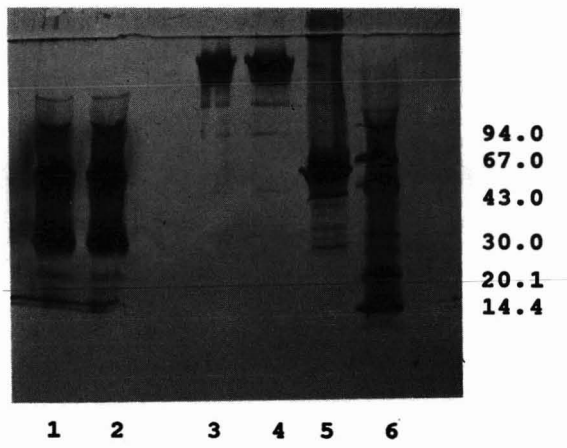

Fig. 2. SDS-PAGE from the chromatogram in Fig. 1. The samples were separated on a 8–25% polyacrylamide gradient gel. Samples: lane 1, eluate pH 2.5 (reduced); lane 2, eluate pH 3.0 (reduced); lane 3, eluate pH 2.5; lane 4, eluate pH 3.0; lane 5, culture supernatant, 5-fold concentrated; lane 6, molecular weight marker.

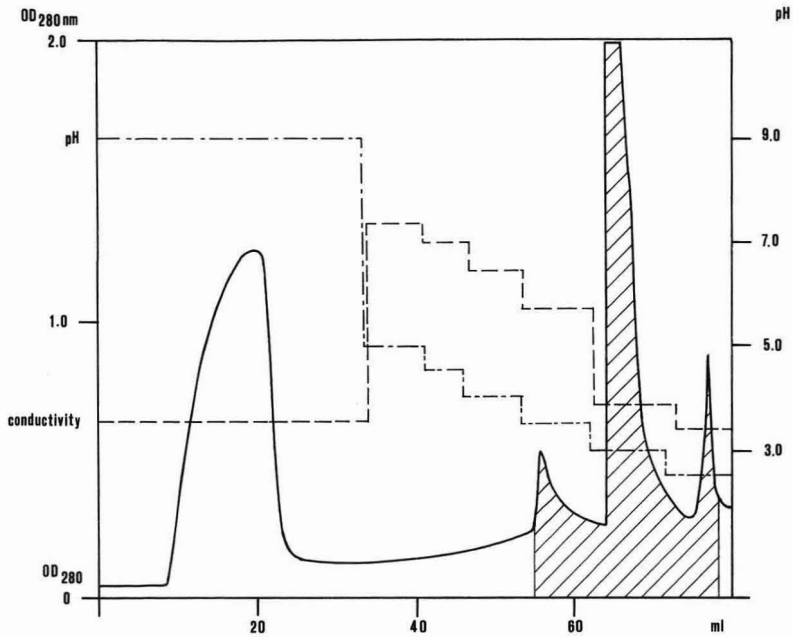

Fig. 3. Chromatogram of protein G Sepharose fast flow. Sample, 14 ml of desalted eluate from CM-Sepharose fast flow was loaded at pH 9.0; column, 1.3 ml; linear velocity, 150 cm/h. Elution was effected by a step gradient from pH 5.0 to 2.5 in 0.5 pH intervals. The hatched area indicates the eluted antibody.

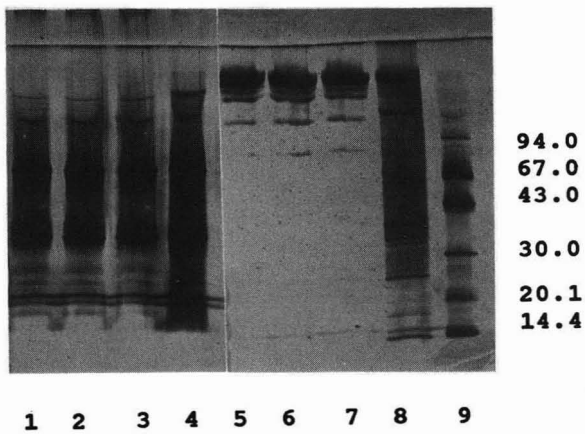

Fig. 4. Electropherograms referring to Fig. 3. Samples: lane 1, eluate pH 2.5 (reduced); lane 2, eluate pH 3.0 (reduced); lane 3, eluate pH 3.5 (reduced); lane 4, concentrated ion-exchange eluate (reduced); lane 5, eluate pH 2.5; lane 6, eluate pH 3.0; lane 7, eluate pH 3.5; lane 8, concentrated ion-exchange eluate; lane 9, molecular weight marker.

TABLE I

SPECIFIC REACTIVITY TO gp 160 OF THE DIFFERENT CHROMATOGRAPHIC STEPS AND PEAKS

The specific reactivity of the culture supernatant was set arbitrarily at 100%.

Gel	*Concentrated culture supernatant*	*CM-Sepharose eluate*	*Peak 1*	*Peak 2*	*Peak 3*
Protein G Sepharose (Fig. 1)	98.4	–	92.0	95.3	–
Protein G Sepharose (Fig. 3)	–	95.3	97.6	95.4	98.1
Protein G Sepharose (Fig. 5)	–	95.3	93.6	97.2	–
Protein A Superose (Fig. 6)	–	95.3	98.7	–	–
Protein A Superose (Fig. 7)	98.4	–	95.3	–	–

the column. To investigate the elution conditions, a step gradient with smaller pH intervals (0.5 pH unit from pH 5.0 to 2.5) was applied. The antibody was eluted in three fractions at pH 3.5, 3.0 and 2.5. The main fraction was eluted at pH 3.0. On applying more concentrated material (eluate from the CM-Sepharose fast flow) to the column (Fig. 3), the same purity (Fig. 4) and biological reactivity (Table I) were obtained. Moreover, a higher concentration of the final purified material could be achieved (Table II). To avoid incomplete elution from the protein G Sepharose fast flow, the step gradient was reduced to one step (Fig. 5). Again, the biological activity was checked by antigen ELISA (Table I). It is important that the eluted antibody is immediately transferred into phosphate-buffered saline (PBS), glycine buffer or equivalent buffer, because a low pH destroys the antibody completely within 24 h (results not shown).

A prepacked 1-ml protein A Superose column was used at half the linear flow-rate used for protein G; chromatograms are shown in Figs. 6 and 7. The purity of the

TABLE II

SUMMARY OF ALL CHROMATOGRAPHIC EXPERIMENTS WITH THE HUMAN MONOCLONAL ANTIBODY

Gel	*Starting material*	*Capacity (mg/ml gel)*		*Recovery (%)*	*Concentration factor*
		Manufacturer's declaration	*Experimental results*		
Protein A	Culture supernatant	12	12	70	5.0
	Ion-exchange eluate	12	12	76	5.9
Protein G	Culture supernatant	17	n.d.[a]	50[b]	5.0
	Ion-exchange eluate	17	n.d.	60[b]	1.2
	Ion-exchange eluate[c]	17	n.d.	70	n.d.
Hydroxyapatite	Culture supernatant	–	n.d.	n.d.	n.d.

[a] Not determined.
[b] Poor recovery owing to the broad elution zone.
[c] Elution at pH 2.5 instead of a step gradient.

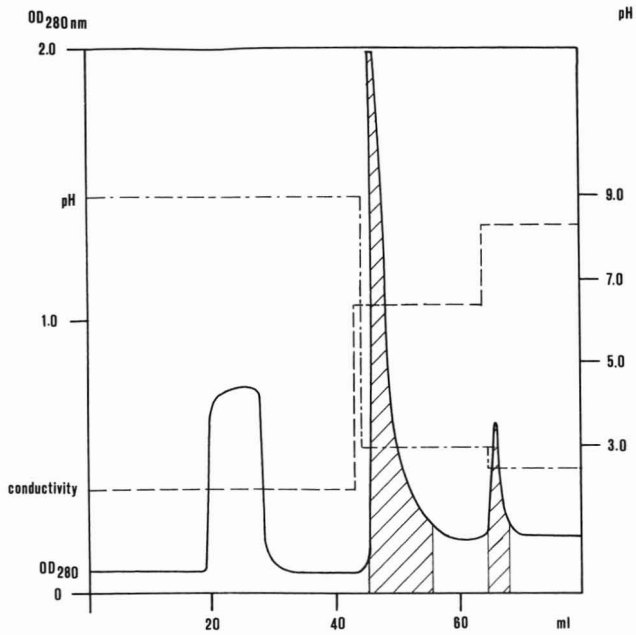

Fig. 5. Chromatogram of protein G Sepharose fast flow. Conditions as in Fig. 3; the step at pH 3.5 was neglected to reduce the broad elution. The hatched area indicates the eluted antibody.

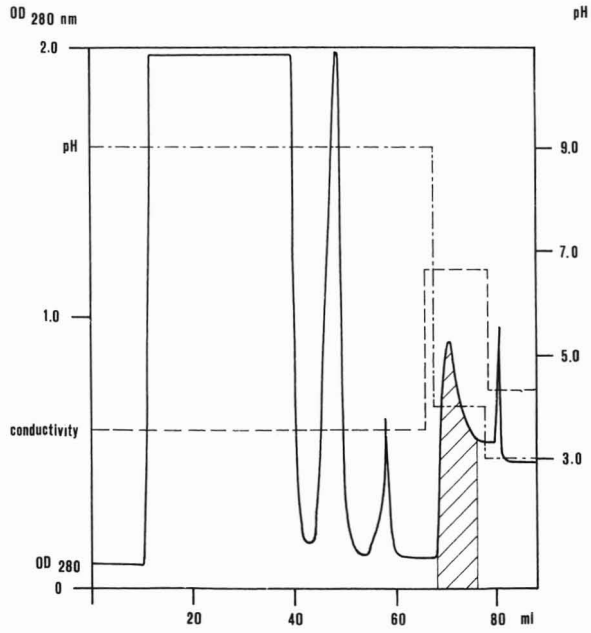

Fig. 6. Chromatogram of desalted culture supernatant on protein A Superose. Sample, 30 ml of concentrated (5-fold by ultrafiltration) and desalted culture supernatant (on Sephadex G-25 coarse); column, 1 ml; linear velocity, 75 cm/h. Elution was effected by a step gradient. The sample was loaded at pH 9.0, eluted at pH 4.0 and regenerated at pH 3.0. The hatched area indicates the eluted antibody.

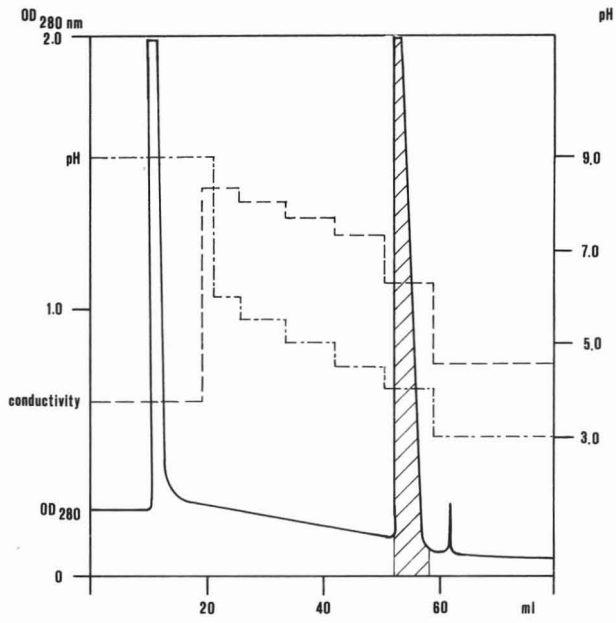

Fig. 7. Chromatogram of protein A Superose. Sample, eluate from CM-Sepharose fast flow; 1 ml of desalted (Sephadex G-25 coarse) ion-exchange eluate was loaded on a 1-ml column. Linear velocity, 75 cm/h. The sample was loaded at pH 9.0, a step gradient was used; elution was effected at pH 4.0; regeneration at pH 3.0. The hatched area indicates the eluted antibody.

eluted material was checked by SDS-PAGE (Figs. 8 and 9). The results were similar to those with protein G and the same purity was obtained. However, the human monoclonal antibody was eluted sharply at higher pH (4.0) and was not distributed over a broad pH range. The yield in the main fraction was twice that with protein G

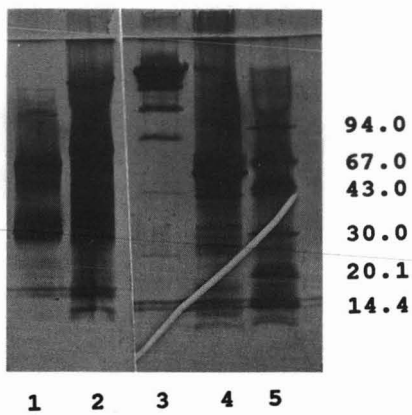

Fig. 8. Electropherograms referring to Fig. 6. The eluates at pH 3.0 contained undetectable amounts of protein. Samples: lane 1, eluate pH 4.0 (reduced); lane 2, culture supernatant, 5-fold concentrated (reduced); lane 3, eluate pH 4.0; lane 4, culture supernatant, 5-fold concentrated; lane 5, molecular weight marker.

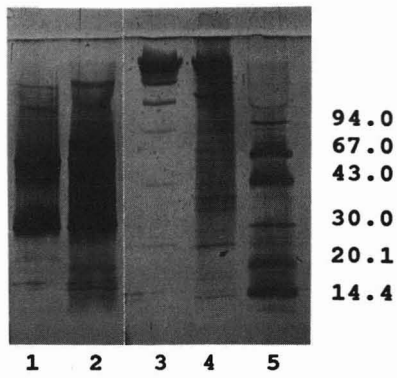

Fig. 9. Electropherograms referring to Fig. 7. Samples: lane 1, eluate pH 4.0 (reduced); lane 2, concentrated ion-exchange eluate (reduced); lane 3, eluate pH 4.0; lane 4, concentrated ion-exchange eluate; lane 5, molecular weight marker.

(Table II). The biological activity was checked by an antigen ELISA with recombinant gp 160 as antigen (Table I).

A 5-ml volume of hydroxyapatite Ultrogel was packed into a column of 5.3-cm^2 cross-sectional area. The desalted concentrated ion-exchange eluate was pumped over the column and equilibrated with 10 m*M* sodium phosphate (pH 6.8). The

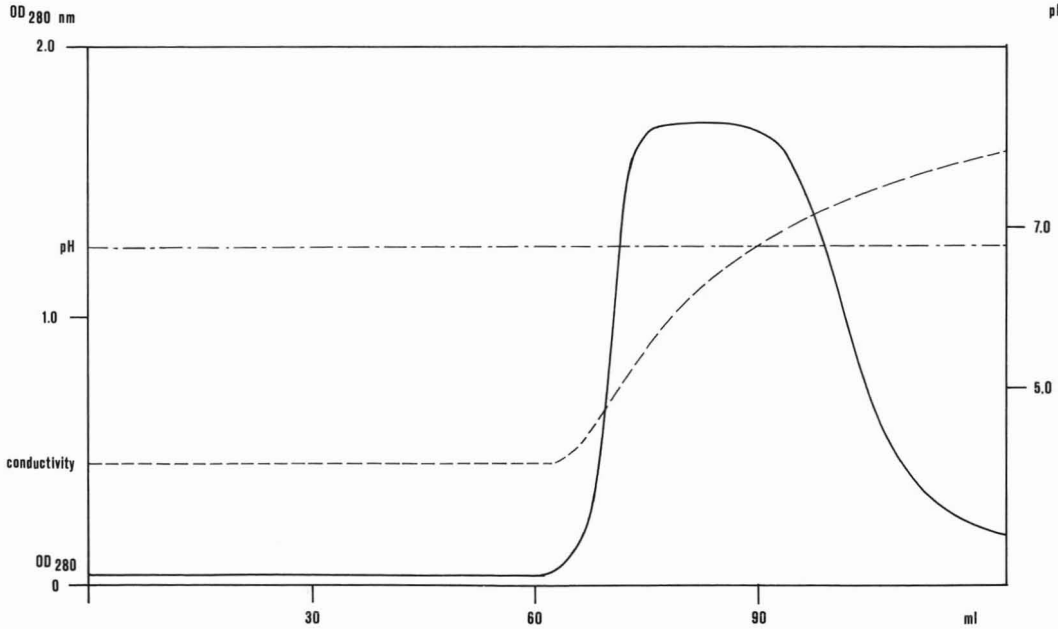

Fig. 10. Chromatogram of hydroxyapatite Ultrogel. Sample, eluate from CM-Sepharose fast flow; 20 ml of desalted (Sephadex G-25 coarse) concentrated (by ultrafiltration) ion-exchange eluate was loaded on a 14-ml column; linear velocity, 11 cm/h. The sample was transferred into the equilibration buffer (10 m*M* phosphate buffer, pH 6.8) and elution was effected by a linear gradient from 10 to 500 m*M* phosphate (gradient volume = 8.5 × the total column volume).

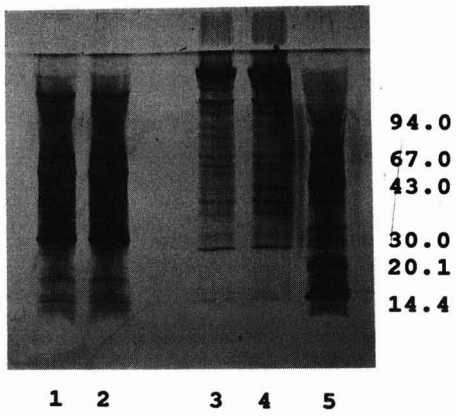

Fig. 11. Electropherograms referring to Fig. 10. Samples: lane 1, eluate (reduced); lane 2, concentrated ion-exchange eluate (reduced); lane 3, eluate; lane 4, concentrated ion-exchange eluate; lane 5, molecular weight marker.

elution was effected by a linear gradient. As shown in Fig. 10, nearly 100% of the total protein was bound to the hydroxyapatite, and could not be selectively eluted from the gel. Varying the gradient did not change this behaviour (results not shown). SDS-PAGE applied to the eluted proteins is shown in Fig. 11.

DISCUSSION

The aim of these experiments was to compare different methods of purification for human monoclonal antibodies with respect to purity and recovery. The biological activity has often been neglected by other workers describing methods for the purification of monoclonal antibodies[9,19–23]. In many instances, the use of affinity chromatography for the isolation of monoclonal antibodies requires rigid elution conditions to break the tight binding of the protein to the affinity matrix. It often happens that such conditions can destroy the biological activity (in general measured as avidity by ELISA or similar immunological assays). Many workers consider only the purity and recovery (yield) and not the biological activity.

Protein A Superose is preferred to protein G Sepharose because elution can be effected at pH 4.0 instead of 3.0, although the biological activity could be preserved in all experiments. A step gradient with narrow pH steps (Fig. 3) was tried in order to optimize the elution conditions. The elution profile from protein G Sepharose fast flow was similar to that from protein A Superose if monoclonal antibody was eluted at pH 3.0 instead of with a step gradient. The broad elution (Fig. 3) observed when using a step gradient with narrow pH steps is not caused by the human monoclonal antibody itself, because in all three fractions the antibody displays similar specific reactivity to the antigen gp 160 (Table I). This incomplete elution might be effected by the elution buffers. As already reported, protein G binds polyclonal IgG more tightly than does protein A.

As already pointed out, the low pH denatures the antibody, which therefore must be transferred immediately after elution to an appropriate buffer. The addition

of solid Tris to increase the pH in the eluate has the disadvantage that local overconcentrations can occur and the antibody can be denatured. Desalting by gel filtration instead of addition of solid Tris preserves the biological activity.

SDS-PAGE and an immunochemical technique such as antigen ELISA with the appropriate antigen are suitable methods for checking the biological activity of monoclonal antibodies. The use of SDS-PAGE alone is not sufficient as it shows only if the antibody molecule is complete, and provides no information on the biological activity. The antigen ELISA shows the biological activity, also called specific reactivity. Recombinant gp 160 was used only for safety reasons to avoid handling complete HIV 1 virus. When the antibody is used in a broad diagnostic or research programme, such as the presently described antibody, it must be proved that the isolation and purification procedure does not influence the properties of the antibody[24].

In this instance, binding of the monoclonal antibody to hydroxyapatite is very tight and the antibody could not be separated from other impurities. Albumin was present in the protein solution. The separation of IgG and albumin was not investigated because, in general, the removal of albumin from the monoclonal antibody solution causes no problems.

Therefore, we conclude that both protein A Superose and protein G Sepharose fast flow are suitable for the purification of human monoclonal antibodies. It is possible to start with either the desalted culture supernatant or a prepurified material. Both techniques lead to satisfactory results. The purified antibody was pyrogen-free and could be used for *in vitro* cell culture assays (results not shown). The techniques used with protein A and protein G are simple compared with methods described by Clezardin and co-workers[11,12], who used Mono Q and Superose 6. They are also easier to perform than either precipitation or ion-exchange methods described by other investigators.

ACKNOWLEDGEMENTS

Parts of this work were supported by a grant from the Innovations- und Technologiefond from the Federal Ministry of Science and Research of the Austrian Government (Project No. 7/62). We thank CL-Pharma, Linz, Austria, for supporting this work.

REFERENCES

1 F. Steindl, A. Jungbauer, E. Wenisch, G. Himmler and H. Katinger, *Enzyme Microb. Technol.*, 9 (1987) 361–364.
2 J. R. Ogden and K. Leung, *J. Immunol. Methods*, 111 (1988) 283–284.
3 S. Neoh, C. Gordon, A. Potter and H. Zola, *J. Immunol. Methods*, 91 (1986) 231–235.
4 A. Jungbauer, F. Unterluggauer, F. Steindl, F. Rücker and H. Katinger, *J. Chromatogr.*, 397 (1987) 313–320.
5 A. Jungbauer, F. Unterluggauer, K. Uhl and A. Buchacher, *Biotechnol. Bioeng.*, 32 (1988) 326–333.
6 M. Grazia-Gonzales, S. Bettinger, S. Ott, P. Diver, J. Kadauche and P. Pauletty, *J. Immunol. Methods*, 111 (1988) 17–23.
7 S. Lee, M. Gustafson, D. V. Pickle, M. Flickinger, G. Musehik and A. Morgan, *J. Biotechnol.*, 4 (1986) 189–204.
8 P. Englebienne and G. Doyen, *J. Immunol. Methods*, 62 (1983) 197–204.

9 B. Pavlu, V. Johanson, C. Nyghlen and A. Wichman, *J. Chromatogr.*, 359 (1986) 449–460.
10 F. Chen, G. Naeve and A. Epstein, *J. Chromatogr.*, 444 (1988) 153–164.
11 P. Clezardin, N. R. Hunter, I. R. McGregor, J. L. MacGroger, D. Pepper and J. Davis, *J. Chromatogr.*, 358 (1986) 209–218.
12 P. Clezardin, G. Bougro and J. L. MacGroger, *J. Chromatogr.*, 354 (1986) 425–433.
13 A. Jungbauer and E. Wenisch, in A. Mizrahi (Editor), *Advances in Biotechnology*, Vol. 11, Alan R. Liss, New York, 1989, pp. 161–192.
14 B. Akerström, T. Brondin, K. Reis and L. Bjorck, *J. Immunol.*, 135 (1985) 2589–2592.
15 D. Richman, D. Cleveland, M. N. Oxman and K. Jonson, *J. Immunol.*, 128 (1982) 2300–2305.
16 R. Grunow, S. Jahn, T. Porstmann, S. Kiessing, H. Steinkellner, F. Steindl, D. Mattanovich, L. Gürtler, F. Deinhardt, H. Katinger and R. von Baehr, *J. Immunol. Methods*, 106 (1988) 257–265.
17 A. Jungbauer, C. Tauer, E. Wenisch, F. Steindl, M. Reiter and H. Katinger, *J. Biochem. Biophys. Methods*, in press.
18 L. Martin, *J. Immunol. Methods*, 50 (1982) 319–329.
19 Y. Yamakawa and J. Chiba, *J. Liq. Chromatogr.*, 11 (1988) 665–681.
20 P. Clezardin, J. L. MacGroger, M. Manach, H. Boukerche and M. Dechavanne, *J. Chromatogr.*, 319 (1985) 67–77.
21 D. R. Nau, *Biochromatography*, 1 (1986) 82–94.
22 C. Östlund, P. Borwell and B. Malm, *Dev. Biol. Stand.*, 66 (1987) 367–375.
23 M. P. Strickler and M. J. Gemski, *J. Liq. Chromatogr.*, 9 (1986) 1655–1677.
24 S. Döpel, T. Porstmann, R. Grunow, A. Jungbauer and R. von Baehr, *J. Immunol. Methods*, 116 (1989) 229–233.

Journal of Chromatography, 476 (1989) 269–290
Elsevier Science Publishers B.V., Amsterdam — Printed in The Netherlands

CHROMSYMP. 1629

HIGH-PERFORMANCE LIQUID CHROMATOGRAPHY OF AMINO ACIDS, PEPTIDES AND PROTEINS

XCIII[a]. COMPARISON OF METHODS FOR THE PURIFICATION OF MOUSE MONOCLONAL IMMUNOGLOBULIN M AUTOANTIBODIES

G. COPPOLA, J. UNDERWOOD*, G. CARTWRIGHT and M. T. W. HEARN
Department of Biochemistry, Monash University, Wellington Road, Clayton, Victoria 3168 (Australia).

SUMMARY

A comparison of methods for the purification of naturally occurring mouse monoclonal autoantibodies, of the immunoglobulin M (IgM) isotype, has been performed to determine the optimal strategies for the isolation of IgM from ascites fluid and *in vitro* tissue culture hybridoma supernatants. In order to quantify each purification procedure, the concentration of IgM in eluted fractions was determined by using a double-sandwich μ-chain-specific anti-IgM enzyme-linked immunosorbent assay, and the purity of the IgM was determined by a bicinchoninic acid-based protein assay and sodium dodecyl sulphate-polyacrylamide gel electrophoresis (SDS-PAGE). The most efficient single-step purification was based on size-exclusion chromatography on high-resolution Superose 6 HR 10/30 fast protein liquid chromatography (FPLC) columns. This procedure resulted in recoveries of monoclonal IgMs of *ca.* 71–86% with purities between 68 and 86%. Single-step chromatography of monoclonal IgM, on Superose 6 FPLC columns resulted in a 21-fold purification of IgM, prepared by the *in vitro* culture of hybridoma cells in dialysis membrane. Size-exclusion chromatography, performed with Sephacryl S-300 columns, resulted in reduced resolution of monoclonal IgM, with yields of *ca.* 57–80% and purity of *ca.* 42–58% compared with the high-resolution Superose 6 FPLC columns. "Non-ideal" size-exclusion chromatography on Superose 6 FPLC columns resulted in selective retention of monoclonal IgMs and elution of IgM with high-ionic-strength buffers in the trailing peak. Recovery of IgM with this strategy was high (*ca.* 82–92%) but the purity was not comparable to the single-step fractionation of IgM on Superose 6 FPLC columns. Single-step anion- and cation-exchange and mixed-mode hydroxyapatite chromatography resulted in only partial purification of monoclonal IgM with the applied procedures. With these latter separation techniques, monoclonal IgM was eluted with a variety of other ascites fluid or supernatant proteins, including those with apparent molecular weights identical to those of mouse IgG and albumin. Sequential purification of monoclonal IgMs by Mono Q anion exchange, followed by Superose 6 FPLC columns, resulted in a 2- to 3-fold purification of IgM but did not

[a] For Part XCII, see ref. 36.

0021-9673/89/$03.50

separate IgM from high-molecular-weight contaminants with apparent molecular weights similar to those of α_2-macroglobulin and IgG.

Enrichment of monoclonal IgM from ascites fluid by ammonium sulphate precipitation revealed increasing IgM recovery with increasing ammonium sulphate final concentrations up to 60%. Isolation of IgM, based on euglobulin properties, following dialysis in either 2% (w/v) boric acid (pH 6.0), 5 m*M* Tris–HCl (pH 7.8), or distilled water, resulted in low IgM yields ($\leqslant$ 10%) and purity (*ca.* 10–20%). Precipitation of monoclonal IgM from ascites fluid with polyethylene glycol 6000 (PEG 6000) resulted in *ca.* 63% recovery and purification of 4- to 5-fold, indicating that this procedure may be advantageous for enrichment or concentration of IgM. Antibody reactivity with intracellular and cell surface murine autoantigens, as determined by indirect immunofluorescence, was maintained following all purification procedures. The results indicate that optimal purification of monoclonal IgMs, on the laboratory scale, was performed in a single step by size-exclusion chromatography on Superose 6 HR 10/30 FPLC columns. This procedure will allow the isolation of naturally occurring mouse monoclonal IgM autoantibodies for the characterization of their autoreactive specificities.

INTRODUCTION

Fusion of B lymphocytes from the spleens of healthy mice with myeloma cells has revealed that a high proportion of the resulting hybridomas produce autoantibodies[1–3]. These autoantibodies, which react with a variety of intracellular, extracellular and cell surface autoantigens, demonstrate highly polyspecific properties and are almost exclusively of the Immunoglobulin M (IgM) class[4]. In order to understand the significance of these autoantibodies in apparently healthy animals and their relationship to immunological self tolerance and autoimmunity, characterization of the autoantigenic specificities of these autoantibodies is required. Such analyses are most easily undertaken by using purified forms of the monoclonal autoantibodies.

Many methods for the purification of monoclonal IgM from ascites fluid and tissue culture supernatant have been described[5]. Purification of IgM, based on its molecular weight (900 000 daltons) has been successfully undertaken with size-exclusion chromatography (SEC)[6–8]. Variations in purity and yield depend on the chromatographic matrices used for size-based separations. In the purification of IgMs advantage can also be taken of "non-ideal" SEC and the propensity of IgM to precipitate in low-ionic-strength buffers[9]. In these latter procedures, IgM is eluted from the size-exclusion matrix as the last peak, being selectively detained and eluted with high-ionic strength buffers.

Alternatively, IgM has been purified by anion- and cation-exchange chromatography[8,10,11], mixed mode chromatography[8,12] and combinations of these chromatographic techniques[8,11,13,14]. Affinity chromatography has also been used to purify IgM from sera, ascites fluids, or tissue culture supernatants. Using anti-IgM antibodies or specific antigen coupled to a solid phase, IgM has been highly purified[15–17]. Affinity chromatography based on protein A[18,19] or concanavalin A[20] has not resulted in isolation of IgM in a highly purified form. Isolation of IgM from hybridoma ascites fluid and supernatant has also been undertaken by utilizing the euglobulin

properties of IgM[21], polyethylene glycol (PEG)[22,23] and ammonium sulphate precipitation[24].

Few of the procedures described above have been quantitatively analysed in relation to the yield and purity of the recovered IgM, often relying on estimates obtained by scanning of Coomassie Blue-stained sodium dodecyl sulphate-polyacrylamide gels. In order to identify the optimal procedures for isolation of naturally occurring autoreactive IgM monoclonal antibodies in the functional state, a quantitative comparison of purification methods was undertaken. Here we describe the results of purification of monoclonal IgM autoantibodies derived from three hybridoma lines by means of ammonium sulphate precipitation, low-ionic-strength precipitation, and PEG enrichment procedures. Separation of monoclonal IgMs, based on size-exclusion, anion- and cation-exchange and hydroxyapatite chromatography, and combinations of anion-exchange and size-exclusion chromatography have also been examined.

MATERIALS AND METHODS

Materials

Chemicals used in this study were of the analytical reagent grade. All buffers were prepared with distilled deionized water (Milli Q purified, Millipore, Bedford, MA, U.S.A.). Buffers were filtered through 0.22 μm filters (Millipore).

All chromatographic procedures were performed at room temperature. Chromatography in open columns was performed by using an ISCO UA-5 absorbance monitor with an ISCO Type 6 optical unit reading at 280 nm, coupled to an ISCO 328 fraction collector (ISCO, Lincoln, NB, U.S.A.). Constant flow-rate was maintained by means of a P-3 peristaltic pump (Pharmacia, Uppsala, Sweden).

All fast protein liquid chromatography (FPLC) experiments were performed on a Pharmacia FPLC system, consisting of an LCC-500 gradient programmer, two P-500 syringe pumps, an MV-7 injector, a UV-1 280 nm fixed-wavelength UV detector, coupled to an REC-482 two-channel pen recorder and a Perkin-Elmer LCI-100 integrator (Perkin-Elmer, Norwalk, CT, U.S.A.). Column eluates were generally collected in 1-ml fractions by using a FRAC-100 fraction collector (Pharmacia).

Hybridomas producing naturally occurring IgM autoantibodies for this study were produced by fusion of myeloma cells and splenocytes from either unimmunized healthy 8 day old neonatal Balb/c mice or germ-free adult Balb/c mice, as previously described[3]. Indirect immunofluorescence characterization revealed that the germ-free mouse-derived autoantibodies GFM-5 1B12 reacted with nuclei of acetone-fixed mouse cells, while GFM-4 1G8 reacted with the Golgi complex of these cells. The hybridoma antibodies derived from neonatal mice (NNS-10 2D5) reacted with membrane antigens of Balb/c mouse thymocytes. IgM-containing ascites fluids or supernatants were produced from the three hybridoma cell lines.

Ascites fluids were generated for two hybridoma cell lines GFM-5 1B12 and NNS-10 2D5. Ascites fluids containing IgM autoantibodies were produced by injection of $5 \cdot 10^6$ hybridoma cells intraperitoneally into 4 week old Balb/c mice primed 10 days earlier with 0.5 ml 2,6,10,14-tetramethylpentadecane (pristane)[25]. Ascites fluids were collected 14–23 days after injection of cells, clarified by centrifugation at

2000 *g* for 10 min, and stored at −20°C with 0.02% sodium azide as preservative.

Tissue culture supernatants containing increased concentrations of IgM were prepared by culturing $5 \cdot 10^7$ hybridoma cells ($5 \cdot 10^6$ cells/ml) in dialysis membrane (Spectropor 4, Spectrum Medical Industries, Los Angeles, CA, U.S.A.) in 200-ml tissue culture flasks on a roller bottle apparatus (Wheaton Instruments, U.S.A.) at 1 rotation per 4.5 min[26].

All supernatants and ascites fluids were ultracentrifuged (100 000 *g*, 1 h at 4°C) after collection, followed by dialysis into the appropriate chromatography buffers prior to loading onto chromatography columns.

Methods for purification of hybridoma IgM

Enrichment methods

Salting-out precipitation procedures with saturated ammonium sulphate. Appropriate volumes of saturated ammonium sulphate (pH 7.4) were added dropwise at 4°C, at a constant rate (200 μl/min, P3 peristaltic pump, Pharmacia) to 2-ml aliquots of ascites fluid to achieve final concentrations of 40, 45, 50, 55 and 60%. The ammonium sulphate–ascites fluid slurry was stirred for 2 h at 4°C, and the precipitate was collected by centrifugation (12 000 *g*, 30 min, 4°C). The precipitate was resuspended in phosphate-buffered saline (PBS, pH 7.2) and dialysed against at least 100 volumes at 4°C with three buffer changes.

Precipitation of IgM with low-ionic-strength buffers. Aliquots of 2 ml of ascites fluids were dialysed against either 5 m*M* Tris–HCl (pH 7.5), 2% (w/v) boric acid (pH 6.0), or doubly distilled water. Dialysis was carried out against 3 × 100 ml of buffer for 16 h at 4°C. The resulting precipitate was collected by centrifugation at 12 000 *g* for 30 min and redissolved in PBS containing 0.5 *M* NaCl. Both the redissolved precipitate and supernatant from dialysis were stored at −20°C prior to analysis.

Precipitation of IgM with PEG 6000. The procedures used for partial purification of mouse IgM from ascites fluid using PEG 6000 precipitation were based on the methods described by Neoh *et al.*[23]. Monoclonal antibody-containing ascites fluids were delipidated either by centrifugation (10 000 *g*, 30 min, 4°C) or by incubation with silicon dioxide[23]. The optimal PEG 6000 concentration for IgM precipitation was determined by adding appropriate volumes of a 50% (w/v) PEG solution to 100 μl aliquots of ascites fluid to give final PEG concentrations of 0–25%. After incubation on ice for 15 min, the precipitated protein was removed by centrifugation (12 000 *g*, 20 min, 4°C), and the supernatants were analysed by agarose electrophoresis (Corning, Palo Alto, CA, U.S.A.). The lowest concentration of PEG 6000 that precipitated the IgM with the least contaminating protein was selected for preparative analysis. Preparative PEG precipitation was performed by addition of appropriate volumes of 50% PEG 6000 in veronal-buffered saline (pH 7.2) to 2-ml samples of clarified, delipidated ascites fluids. Samples were incubated on ice for 30 min with occasional mixing, and precipitated protein was collected by centrifugation (12 000 *g*, 20 min, 4°C). The precipitate containing IgM was redissolved in PBS and stored at −20°C prior to analysis.

Chromatographic procedures

SEC. Open-column SEC was performed by using Sephacryl S-300 columns (100 × 1 cm I.D., Pharmacia). For single-buffer determinations, isocratic elution with 100 m*M* Tris–HCl (pH 8.0), containing 50 m*M* NaCl was employed at a flow-rate of 30 ml/h. Prior to analyses, the S-300 columns were calibrated by chromatography of Blue dextran (M_r $2 \cdot 10^6$, Pharmacia), ferritin (M_r 475 000, Sigma), myosin (M_r 200 000, Sigma), phosphorylase B (M_r 94 000, Sigma), bovine serum albumin (BSA) (M_r 66 200, Sigma) and carbonic anhydrase (M_r 30 000, Sigma). For analyses of IgM purification, 1-ml aliquots of ascites fluids were dialysed into appropriate buffers, ultracentrifuged (100 000 *g*, 1 h, 4°C) and applied to the S-300 columns.

FPLC purifications of mouse monoclonal IgM were performed on Superose 6 HR 10/30 columns with single- and dual-buffer systems. For the single-buffer determinations the Superose 6 columns were equilibrated and eluted with 100 m*M* Tris–HCl (pH 7.8), containing 50 m*M* NaCl, at a flow-rate of 0.5 ml/min. For dual-buffer determinations, performed essentially as described by Bouvet *et al.*[9], the Superose 6 columns were equilibrated with 5 m*M* L-histidine (pH 6.0) and eluted with 50 m*M* L-histidine (pH 6.0), containing 1.7 *M* NaCl at a flow-rate of 0.5 ml/min. Loadings of 200 μl of IgM-containing supernatants or ascites fluids, dialysed into appropriate buffers and ultracentrifuged, were applied to the Superose 6 HR 10/30 columns.

Anion-exchange chromatography. Anion-exchange chromatography was performed with Mono Q HR 5/5 pre-packed columns (5 × 50 mm I.D., Pharmacia). Samples of ascites fluids were dialysed, applied (200 μl) in 20 m*M* L-histidine (pH 6.0), and eluted with a gradient of 20 m*M* L-histidine (pH 6.0), containing 500 m*M* NaCl essentially as described by Clerzardin *et al.*[13] A gradient of 0–100% NaCl was generated in two steps over 25 min at a flow-rate of 1 ml/ml. A 0–50% gradient was generated over 20 min with a 50–100% gradient generated over 5 min.

Cation-exchange chromatography. Cation-exchange chromatography was performed on Mono S HR 5/5 pre-packed columns (5 × 50 mm I.D., Pharmacia) essentially as described by Boonekamp and Pomp[10]. The 200 μl samples of supernatants or ascites fluids, containing monoclonal IgM antibodies, were dialysed and applied in 50 m*M* sodium acetate (pH 5.5), and eluted with 50 m*M* sodium acetate (pH 5.5), containing 1.0 *M* NaCl. The elution conditions for cation-exchange chromatography were as follows. The sample was applied and the column was washed for 10 min with starting buffer. Retained material was eluted with a 0–100% gradient of eluting buffer over 10 min, at a flow-rate of 1.0 ml/min.

Hydroxyapatite chromatography. Hydroxyapatite chromatography was performed on a Bio-Gel high-performance hydroxyapatite (HPHT) column (100 × 7.8 mm I.D., Bio-Rad Labs., Richmond, CA, U.S.A.), essentially as described by Stevens and Brooks[27]. The column was equilibrated with 10 m*M* sodium phosphate butter (pH 6.8), containing 0.3 m*M* calcium chloride, and eluted with 300 m*M* sodium phosphate buffer (pH 6.8), containing 0.01 m*M* calcium chloride. Elution of bound protein was performed with a 0–100% linear gradient generated over 15 min at a flow-rate of 0.5 ml/min.

Combinations of chromatographic procedures. The IgM-rich fractions from Mono Q-purified ascites fluid were pooled and concentrated to 400 μl. Samples of 200 μl were then applied to Superose 6 HR 10/30 size-exclusion columns equilibrated in 100 m*M* Tris–HCl (pH 8.0), containing 50 m*M* NaCl, and chromatographed at 0.5 ml/min as described above.

Analysis of the purity of isolated mouse IgM

The purity of the isolated IgM was analysed by SDS-PAGE, and double-sandwich anti-IgM capture enzyme-linked immunosorbent assay (ELISA).

Polyacrylamide gel electrophoresis

Fractions from all procedures used to purify IgM, were analysed by SDS-PAGE as described by Laemmli[28]. Analysis for purity of IgM was performed on 12.5% polyacrylamide resolving gels under reducing conditions or on 3–12.5% polyacrylamide gradient resolving gels under non-reducing conditions. Electrophoresis was performed at 200 V, 25 mA, per gel until the Bromophenol blue tracking dye had reached the lower edge of the resolving gel. Following silver staining of the electrophoresed proteins according to methods described by Morrissey[29], the purity of the IgM was determined by estimation of detectable contaminants. Highly purified IgM and IgG monoclonal antibodies were used for comparison on all gels (see next section).

Measurement of IgM concentrations by ELISA

To determine the concentrations of IgM in all purified fractions a double-sandwich capture anti-IgM ELISA was performed. ELISA plates (Nunc-Immunoplate, Maxisorp F96, Nunc, Roskilde, Denmark) were coated with 25 ng per well anti-IgM μ-chain-specific antibodies (KPL, Gaithersburg, MD, U.S.A.) in 0.05 *M* bicarbonate buffer (pH 9.6). After 4 h at room temperature, the plates were washed in PBS containing 0.05% Tween 20 (PBS-T) and blocked overnight at 4°C with 100 μl of 1% (w/v) BSA in PBS per well. Duplicate samples of the fractions for which the concentration of IgM was to be determined and highly purified IgM standards were applied to appropriate wells. After 30 min at room temperature, the plates were washed 9 times with PBS-T, and bound IgM was identified by sequential incubations of sheep anti-mouse-biotin, streptavidin horseradish peroxidase (Amersham, Sydney, Australia) and H_2O_2–*o*-phenylenediamine-containing substrate solution. Absorbance values were determined at 492 nm, by using an MCC-340 Multiscan ELISA reader (Flow, Stanmore, Australia). Concentrations of IgM in chromatographic fractions were determined from a standard plot of the concentrations of the IgM standard *versus* absorbance values.

The IgM standard used for all ELISA and SDS-PAGE analyses was derived from ascites fluid of the GFM-5 1B12 hybridoma. Highly purified IgM was produced following 40% ammonium sulphate precipitation, Superose 6 HR 10/30 SEC and absorption on an anti-mouse IgG affinity column. Double-sandwich capture ELISA analysis with anti-IgG γ-chain-specific antibodies (KPL) as well as SDS-PAGE revealed a highly purified IgM preparation containing no contaminating IgG. Monoclonal mouse IgG_1 purified from hybridoma ascites fluid by DEAE-cellulose ion-exchange chromatography was also used as a standard for comparison with IgM in SDS-PAGE.

Estimation of protein concentration of IgM-containing samples

In order to determine the efficiency of the IgM purification procedures compared in this study, protein concentrations of all samples were determined by the use

of the bicinchoninic acid (BCA) protein assay kit (Pierce, Rockford, IL, U.S.A.). Serial dilutions, in duplicate, of protein standards (BSA) and unknown IgM-containing samples were prepared in PBS. Aliquots of 50 μl of standards or unknown protein solutions were diluted in 1000 μl of BCA diluent buffer. Samples were then incubated at 37°C for 60 min. From the absorbance values, measured at 562 nm, protein concentrations were determined for unknown samples from the standard curve. The assay performed as described could detect protein in the range 5–250 μg/ml.

Determination of the immunoreactivity of isolated IgM autoantibodies

Immunoreactivity of IgM-containing fractions from the various purification procedures was assessed by indirect immunofluorescence. Fractions containing monoclonal IgMs, derived from GFM-5 1B12 or GFM-4 1G8 hybridomas, were incubated for 20 min in a humidified chamber with acetone-fixed Balb/c mouse 3T3 cells, which had been grown on multiwell slides (Flow Labs., Stanmore, Australia) overnight ($2 \cdot 10^4$ cells per well). Following three washes with PBS, the cells were incubated with affinity-purified anti-mouse immunoglobulins, coupled to fluorescein isothiocyanate (FITC) (Silenus, Melbourne, Australia) for 20 min and washed three times. Bound monoclonal IgM was identified by narrow-band blue illumination under a Leitz Dialux epi-illumination fluorescence microscope.

Fractions containing IgM, isolated from NNS-10 2D5 ascites fluid, were allowed to react with $1 \cdot 10^6$ viable intact Balb/c mouse thymocytes for 20 min at 4°C. Following three washes with PBS, containing 10% FCS and 0.1% NaN_3 (PBS–FCS), the cells were incubated with affinity-purified anti-mouse immunoglobulins, coupled to FITC (Silenus) for 20 min at 4°C. Following a further three washes in PBS–FCS, the thymocytes were resuspended in 100 μl PBS–fetal bovine serum (FCS) and examined, after being mounted on slides, by narrow-band blue illumination under a Leitz Dialux epi-illumination fluorescence microscope.

RESULTS

Examination of three procedures routinely used in laboratories for the isolation or enrichment of IgM demonstrated that PEG 6000 precipitation, based on the method of Neoh *et al.*[23], led to the recovery of *ca.* 60% of the IgM from GFM-5 1B12 ascites fluid and a purification factor of between 4- to 5-fold (Table I). SDS-PAGE of PEG 6000-precipitated samples revealed contamination of the IgM-containing fractions with proteins of high and low apparent molecular weights, including those similar to α_2-macroglobulin, IgG, and albumin (Fig. 1). Delipidation of GFM-5 1B12 ascites fluid by using silicon dioxide or centrifugation did not effect levels of monoclonal IgM in the samples prior to PEG 6000 precipitation (data not shown). Analysis of ammonium sulphate enrichment procedures revealed that, with GFM-5 1B12 antibodies, increasing ammonium sulphate concentrations precipitated increasing amounts of IgM. For example, 40% ammonium sulphate precipitated *ca.* 31% of IgM, and 60% ammonium sulphate precipitated *ca.* 83% of the IgM from ascites fluid but with increasing amounts of other protein contaminants (Table I, Fig. 2). For GFM-5 1B12 ascites fluid-derived IgM antibodies, the optimal purification of *ca.* 3-fold was achieved with 45% (v/v) final ammonium sulphate concentration. SDS-

TABLE I

COMPARISON OF METHODS FOR ENRICHMENT OF MONOCLONAL IgM ANTIBODIES FROM ASCITES FLUIDS

Purification procedure	*Antibody*	*Fraction(s) analysed*	*Protein applied (μg)*	*IgM applied (μg)*	*Protein recovered (μg)*	*IgM recovered (μg)*	*Yield of IgM (%)*	*Purification factor*
Ammonium sulphate precipitation	GFM-5 1B12	Ascites fluid	16 850.0	2520.0[a]	–	–	100.0	1.0
		40% (v/v) ammonium sulphate			2620.0	780.0	31.0	2.0
		45% (v/v) ammonium sulphate			3340.0	1350.0	53.5	2.7
		50% (v/v) ammonium sulphate			3720.0	1440.0	57.0	2.5
		55% (v/v) ammonium sulphate			5600.0	1610.0	63.0	1.9
		60% (v/v) ammonium sulphate			6500.0	2080.0	82.5	2.1
Euglobulin precipitation	GFM-5 1B12	Ascites fluid	16 850.0	2520.0[a]	–	–	100.0	1.0
		2% (w/v) boric acid (pH 6.0)			1250.0	237.0	9.4	1.3
		5 m*M* Tris–HCl (pH 7.5)			700.0	136.0	5.3	1.3
		Double distilled H_2O			950.0	100.0	4.0	0.7
Polyethylene glycol precipitation	GFM-5 1B12	Ascites fluid	16 850.0	2520.0[a]	–	–	100.0	1.0
		PEG 6000/SiO_2 clarified			2060.0	1600.0	63.5	5.2
		PEG 6000/centrifuge-clarified			2600.0	1660.0	66.0	4.3

[a] Amount of monoclonal IgM in 1.0 ml of GFM-5 1B12 ascites fluid.

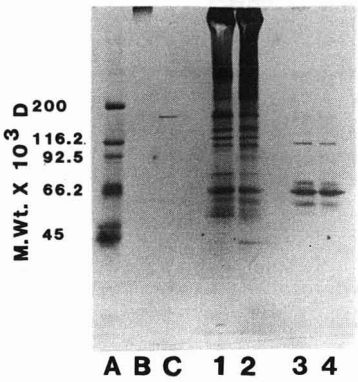

Fig. 1. Fractions from PEG 6000 precipitation of GFM-5 1B12 ascites fluid analysed on a 3–12.5% SDS–polyacrylamide gradient gel under non-reducing conditions. Lanes A, B and C represent molecular weight, IgM, and IgG standards respectively. Lanes 1 and 2 contain redissolved samples from the centrifuge- and SiO_2-clarified PEG 6000 precipitates of GFM-5 1B12 ascites fluid, respectively. Lanes 3 and 4 contain supernatants from the precipitates of centrifuge- and SiO_2-clarified GFM-5 1B12 ascites fluid, respectively.

PAGE revealed considerable contamination of the precipitated IgM with lower-molecular-weight species, particularly IgG and albumin (Fig. 2). The euglobulin properties of IgM have often been used for IgM purification[30]. However, the results with 2% (w/v) boric acid (pH 6.0) and 5 m*M* Tris–HCl (pH 7.5) indicated little purification and poor yields of GFM-5 1B12 ascites fluid IgM (*ca.* 9 and 5% respectively, Table I). Dialysis of GFM-5 1B12 ascites fluid against distilled water was least successful, with 100 μg of IgM present in 950 μg of total protein (Table I). Similarly, analysis of samples derived from euglobulin precipitations by SDS-PAGE also demonstrated poor purity (Fig. 3). Another consideration in the use of the euglobulin properties of hybridoma IgMs for purification or enrichment was the observed in-

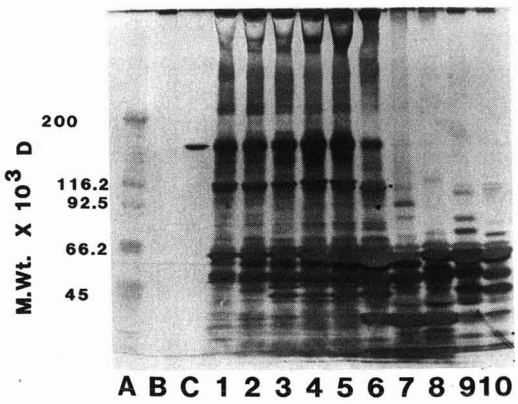

Fig. 2. Analysis of samples of ammonium sulphate precipitates and supernatants from GFM-5 1B12 ascites fluid on a 3–12.5% SDS–polyacrylamide gradient gel under non-reducing conditions. Lanes A–C contain molecular weight, IgM and IgG standards, respectively. Lanes 1–5 contain samples of redissolved ammonium sulphate precipitates in the order of 40, 45, 50, 55 and 60%, respectively. Lanes 6–10 contain samples of supernatants from the ammonium sulphate precipitates in the order of 40, 45, 50, 55 and 60%, respectively.

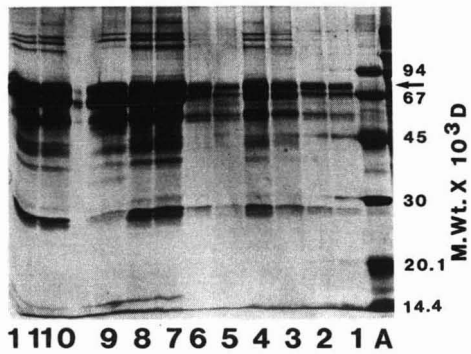

Fig. 3. SDS–PAGE (12.5%), under reducing conditions, of precipitate and supernatant fractions, following dialysis of GFM-5 1B12 ascites fluid in low-ionic-strength buffers. Lane A contains molecular-weight standards. Lanes 1 and 2 contain samples of redissolved precipitate following dialysis into 5 m*M* Tris–HCl (pH 7.8). Lanes 3 and 4 contain samples of redissolved precipitate, following dialysis into 2% (w/v) boric acid. Lanes 5 and 6 contain redissolved samples of precipitates following dialysis against distilled water. Lanes 7–11 contain samples from supernatants of precipitates following dialysis against 5 m*M* Tris–HCl pH 7.8 (lanes 7 and 8) 2% boric acid (lane 9), and distilled water (lanes 10 and 11). The arrow indicates heavy chain of IgM (M_r 80 000; ref. 24).

ability of the IgM-containing precipitates to redissolve completely, indicating denaturation.

Resolution of hybridoma IgMs based on SEC resulted in purification of all the monoclonal antibodies examined. Sephacryl S-300 purification resulted in *ca.* 2- to 4-fold purification of IgM, derived from ascites fluid of GFM-5 1B12 and NNS-10 2D5 hybridomas, with yields of *ca.* 57–80% (Table II, Fig. 4). The fractions initially eluted from S-300 contained IgM in a purity of *ca.* 80–86% but in low yield (Table II). These fractions were contaminated with other high-molecular-weight species, having apparent molecular weights similar to α_2-macroglobulin and its subunits. Subsequent fractions were contaminated with a variety of lower-molecular-weight species (data not shown). Purification of IgM from crude ascites fluids and supernatant on the Superose 6 HR 10/30 columns resulted in separation of IgM from other proteins and recoveries of IgM of *ca.* 71–86% (Table II, Fig. 5). Purity, as assessed by SDS-PAGE (Fig. 6) was very high, with *ca.* 68–86% of the total protein being actually IgM (Table II). Interestingly, analysis of silver-stained SDS–polyacrylamide gels alone, in the absence of actual measurements of amounts of IgM and protein in IgM-containing fractions, would indicate an IgM purity of $\geqslant 90\%$ from Superose 6 chromatography (Fig. 6). This observation demonstrates that caution must be exercised when estimating IgM purity solely from polyacrylamide gels. Both the NNS-10 2D5 and GFM-5 1B12 ascites fluid-derived IgM antibodies were also separated by 'non-ideal' SEC, similar to that described by Bouvet *et al.*[9]. The Superose 6 HR columns were equilibrated with 5 m*M* L-histidine, pH 6.0, and eluted with 50 m*M* L-histidine (pH 6.0), containing 1.7 *M* NaCl. This procedure is based on the euglobulin properties of IgM. Under the equilibration conditions of this chromatographic procedure, IgM is selectively slowed as it approaches the limits of solubility in the low-ionic-strength buffer and is eluted with the high-ionic-strength buffer in the trailing peak (Fig. 7). Recoveries of hybridoma IgM under these conditions was *ca.* 82–92% (Table III). However

TABLE II

PURIFICATION OF MOUSE MONOCLONAL IgM ANTIBODIES FROM HYBRIDOMA CULTURE SUPERNATANT AND ASCITES FLUIDS BY SINGLE-STEP SEC

Purification procedure	*Antibody*	*Fraction(s) analysed*	*Protein applied (μg)*	*IgM applied (μg)*	*Protein recovered (μg)*	*IgM recovered (μg)*	*Yield of IgM (%)*	*Purification factor*
Sephacryl S-300	NNS-10 2D5	Ascites fluid	18 500.0	4693.5[a]	–	–	100.0	1.0
		8			24.0	20.7	0.44	2.3
		9–12			6630.0	3812.5	57.2	
	GFM-5 1B12	Ascites fluid	13 750.0	1501.9[a]	–	–	100.0	1.0
		8			3.2	2.7	0.18	3.9
		9–12			2845.0	1195.0	79.5	
Superose 6 HR 10/30	NNS-10 2D5	Ascites fluid	7510.0	1877.4[b]	–	–	100.0	1.0
		10–13			1880.0	1613.8	86.0	3.4
	GFM-5 1B12	Ascites fluid	5100.0	619.0[b]	–	–	100.0	1.0
		10–12			630.0	503.0	80.0	6.6
	GFM-4 1G8	Dialysis bag supernatant	2850.0	90.0[b]	–	–	100.0	1.0
		10–13			94.3	64.3	71.0	21.5

[a] Amount of IgM present in 1.0 ml of ascites fluid following dialysis into 100 m*M* Tris–HCl (pH 7.8)–50 m*M* NaCl.

[b] Amount of IgM present in 200 μl of ascites fluids or supernatants following dialysis into 100 m*M* Tris–HCl (pH 7.8)–50 m*M* NaCl.

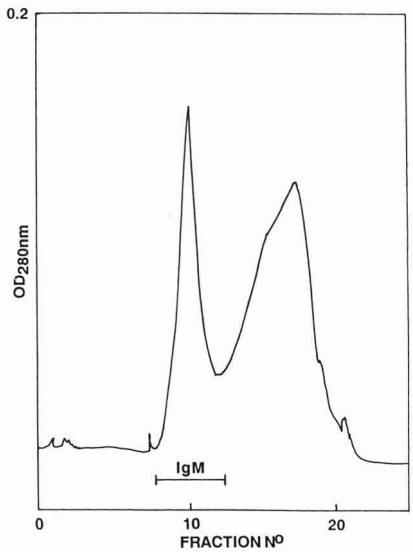

Fig. 4. Chromatography of monoclonal IgM from NNS-10 2D5 hybridoma on a Sephacryl S-300 column (100 × 1 cm I.D.), equilibrated in 100 m*M* Tris–HCl (pH 8.0), containing 50 m*M* NaCl. Sample applied, 1 ml ascites fluid; flow-rate, 0.5 ml/min; 0.2 a.u.f.s.

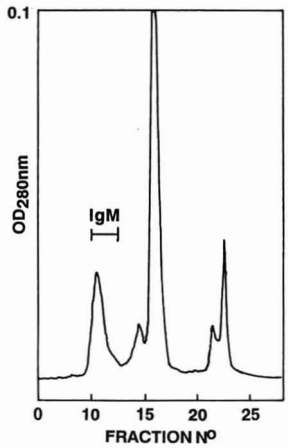

Fig. 5. Purification of IgM from GFM-5 1B12 ascites fluid by SEC on a Superose 6 HR 10/30 FPLC column equilibrated in 100 m*M* Tris–HCl (pH 8.0), containing 50 m*M* NaCl. Volume of ascites fluid applied, 200 μl; flow-rate, 0.5 ml/min; 0.1 a.u.f.s.

SDS-PAGE, IgM, and protein determinations demonstrated that low-molecular-weight protein contaminants, including those with apparent molecular weights similar to mouse IgG and albumin are not separated from IgM. (Table III, Fig. 8). Using this procedure, purification of IgM in the range 3.5- to 4.2-fold was achieved.

Purification of IgM from ascites fluids and supernatants by anion- and cation-exchange chromatography did not result in highly purified IgM. Anion-exchange chromatography on Mono Q FPLC columns produced only *ca.* 1.5-fold purification of GFM-5 1B12 and NNS-10 2D5 IgMs (Table IV). These hybridoma IgMs were eluted with *ca.* 160 m*M* NaCl in the trailing shoulder of the second-eluted peak through Fractions 25–38 and 27–38, for GFM-5 1B12 and NNS-10 2D5 antibodies,

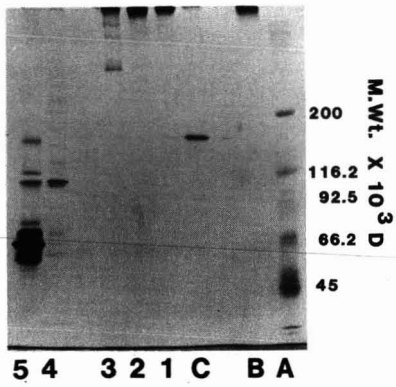

Fig. 6. SDS-PAGE of fractions eluted from a Superose 6 HR FPLC column following application of GFM-5 1B12 ascites fluid (3–12.5% gradient gel, non-reducing conditions). Lanes A, B, and C represent molecular-weight, IgM, and IgG standards, respectively. Lanes 1–5 represent samples from fractions 10, 11, 12, 14, and 15 eluted from the Superose 6 column.

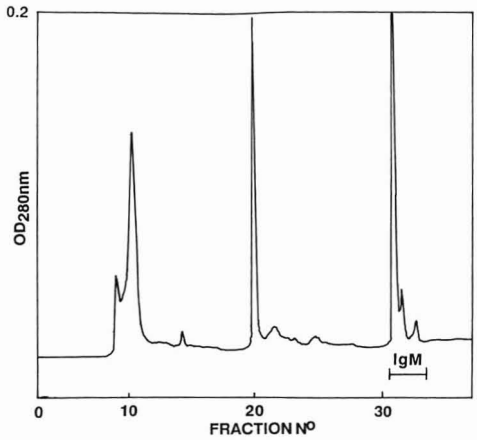

Fig. 7. "Non-ideal" SEC of GFM-5 1B12 ascites fluid on a Superose 6 HR 10/30 FPLC column, equilibrated in 5 m*M* L-histidine (pH 6.0) and eluted with 50 m*M* L-histidine (pH 6.0), containing 1.7 *M* NaCl. Volume applied, 200 ml; flow-rate, 0.5 ml/min; 0.2 a.u.f.s.

respectively (Fig. 9). Recovered IgM consisted of *ca.* 50–80% of the amount loaded and was significantly contaminated with co-eluting species (Table IV, Fig. 10). For NNS-10 2D5 ascites, only *ca.* 2.0% of the protein recovered from the Mono Q column was IgM, whilst for the GFM-5 1B12 antibody this value was *ca.* 5.0% (Table IV). Cation-exchange chromatography on Mono S FPLC columns lead to IgM recoveries of 52–94% (Table IV). The IgMs were eluted, commencing at *ca.* 150 m*M* NaCl, in a broad band through fractions 15–22, 15–27 or 18–28 depending on the specific antibodies (Table IV, Fig. 11). The eluted IgM-containing fractions also contained species with apparent molecular weights similar to α_2-macroglobulin, IgG and albumin (Fig. 12). The IgM represented less than *ca.* 12% of the total protein in the IgM-containing fractions for the three hybridoma antibodies eluted from the Mono S column (Table IV).

Mixed-mode chromatography on hydroxyapatite (HPHT) resulted in lower resolution of IgM than did SEC or mixed-mode chromatography on Abx col-

TABLE III

FRACTIONATION OF MOUSE MONOCLONAL IgM FROM ASCITES FLUIDS BY "NON-IDEAL" SEC ON SUPEROSE 6 HR COLUMNS

Antibody	*Fraction(s) analysed*	*Protein applied (μg)*	*IgM applied (μg)*	*Protein recovered (μg)*	*IgM recovered (μg)*	*Yield of IgM (%)*	*Purification factor*
NNS-10 2D5	Ascites fluid	4600.0	44.7[a]	–	–	100.0	1.0
	31–34			1000.0	41.2	92.3	4.2
GFM-5 1B12	Ascites fluid	3750.0	130.0[a]	–	–	100.0	1.0
	31–34			876.8	106.8	82.2	3.5

[a] Amount of IgM present in 200 μl of ascites fluids following dialysis into 5 m*M* L-histidine (pH 6.0).

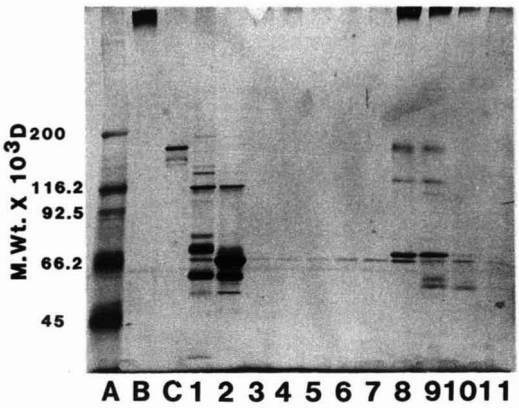

Fig. 8. Analysis of fractions of GFM-5 1B12 ascites fluid with SDS–PAGE (3–12.5% gradient gel, non-reducing conditions), following chromatography on a Superose 6 HR 10/30 FPLC column under "non-ideal" size-exclusion conditions. Lanes A–C represent molecular weight, IgM, and IgG standards, respectively. Lanes 1, 2, 8–11 contain samples from eluted fractions 9, 10, 31–34, respectively.

umns[8,31]. The IgMs derived from NNS-10 2D5 and GFM-5 1B12 ascites fluids were eluted in the second-elution peak from HPHT (Fig. 13). The recovery of IgM was *ca.* 40% with significant contamination from a variety of lower-molecular-weight species, including several of apparent molecular weights similar to α_2-macroglobulin, IgG, and albumin (Table V, Fig. 14).

TABLE IV

ANION- AND CATION-EXCHANGE CHROMATOGRAPHY OF MOUSE MONOCLONAL IgM ANTIBODIES FROM HYBRIDOMA SUPERNATANT AND ASCITES FLUIDS

Purification procedure	*Antibody*	*Fraction(s) analysed*	*Protein applied (μg)*	*IgM applied (μg)*	*Protein recovered (μg)*	*IgM recovered (μg)*	*Yield of IgM (%)*	*Purification factor*
Mono Q anion exchange	NNS-10 2D5	Ascites fluid 27–38	4500.0	62.6[a]	–	–	100.0	1.0
					1532.0	31.6	50.6	1.5
	GFM-5 1B12	Ascites fluid 25–38	4480.0	176.0[a]	–	–	100.0	1.0
					2696.8	142.8	81.1	1.3
Mono S cation exchange	NNS-10 2D5	Ascites fluid 18–28	4675.0	75.0[b]	–	–	100.0	1.0
					1165.6	70.3	93.7	3.8
	GFM-5 1B12	Ascites fluid 15–28	4300.0	476.8[b]	–	–	100.0	1.0
					3662.0	441.3	92.5	1.1
	GFM-4 1G8	Dialysis bag supernatant 15–27	504.0	2.0[b]	–	–	100.0	1.0
					137.0	1.0	50.0	1.9

[a] Amount of IgM present in 200 μl of ascites fluids following dialysis into 20 m*M* L-histidine (pH 6.0).
[b] Amount of IgM present in 200 μl of ascites fluids following dialysis into 50 m*M* sodium acetate (pH 5.5).

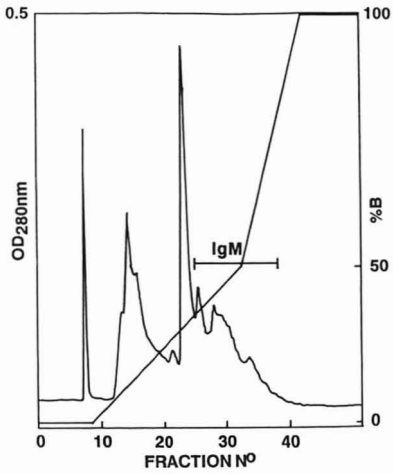

Fig. 9. Mono Q anion-exchange chromatography of GFM-5 1B12 ascites fluid. Volume applied, 200 μl; flow-rate, 1.0 ml/min; 0.5 a.u.f.s. Column equilibrated in 20 m*M* L-histidine (pH 6.0) (buffer A) and eluted with 20 m*M* L-histidine (pH 6.0), containing 500 m*M* NaCl (buffer B). Linear gradient, 0–50% B generated over 20 min and 50–100% B over 5 min.

Combinations of anion-exchange chromatography and SEC have been used to purify hybridoma IgM from supernatants and ascites fluids[8,11,13]. In our study, ascites fluid-derived hybridoma IgMs were initially separated with Mono Q FPLC, the IgM-containing fractions were pooled, concentrated and applied to Superose 6 HR 10/30 columns. Recovery of the IgMs, initially eluted from Mono Q columns following SEC, was *ca.* 60% (Table VI). However, their purity was less than 6%. The proportional changes in the molecular mass of IgM in relation to lower-molecular-

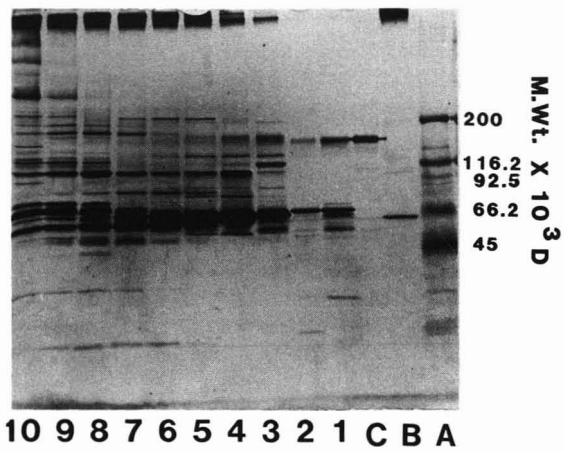

Fig. 10. Analysis with SDS-PAGE of fractions eluted from a Mono Q FPLC column, following the application of 200 μl of GFM-5 1B12 ascites fluid (3–12.5% gradient gel, non-reducing conditions). Lanes A–C represent molecular weight, IgM, and IgG standards, respectively. Lanes 1–10 correspond to aliquots from fractions 8 and 15, and 25–32, respectively.

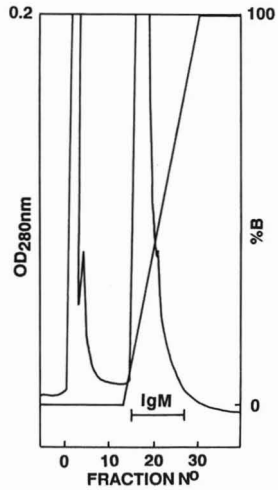

Fig. 11. Cation-exchange chromatography of GFM-5 1B12 ascites fluid. Volume applied, 200 μl; flow-rate, 1.0 ml/min; 0.2 a.u.f.s. Columns equilibrated in 50 m*M* sodium acetate (pH 5.5) (buffer A) and eluted with 50 m*M* sodium acetate (pH 5.5), containing 1.0 *M* NaCl (buffer B). Linear gradient, 0–100% B over 10 min.

weight contaminants following elution from Mono Q columns resulted in poor resolution of IgM by SEC (Fig. 15) in comparison with ascites fluid or supernatant IgM chromatographed in a single step on Superose 6 columns (Fig. 5).

The immunoreactivity of hybridoma IgMs was determined, following fractionations, by indirect immunofluorescence. In all cases, fractions containing IgM from GMF-5 1B12 produced anti-nuclear immunofluorescence and from GFM-4 1G8, anti-Golgi complex reactivity, when tested on acetone-fixed mouse 3T3 cells. Similarly, with the NNS-10 2D5 hybridoma, anti-Balb/c mouse thymocyte cell surface

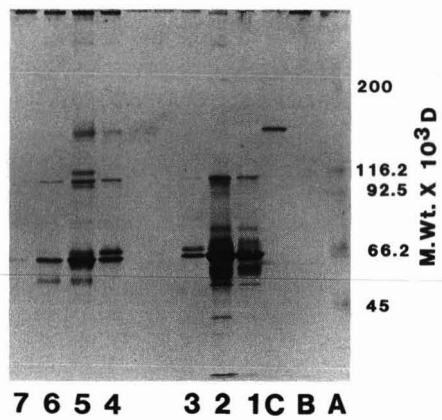

Fig. 12. SDS-PAGE of fractions of GFM-5 1B12 ascites fluid eluted from a Mono S FPLC column (3–12.5% gradient gel, non-reducing conditions). Lanes A–C contain molecular weight, IgM and IgG standards, respectively. Lanes 1–3 contain aliquots from eluted fractions 2–4, respectively. Lanes 4–7 contain aliquots from eluted fractions, 15, 17, 19, and 21, respectively.

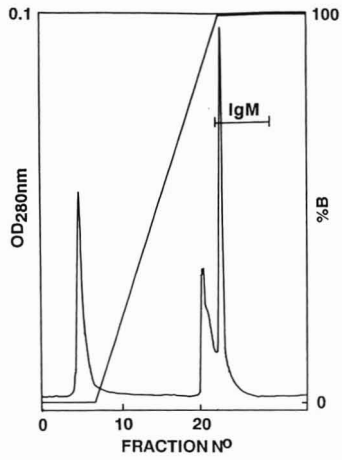

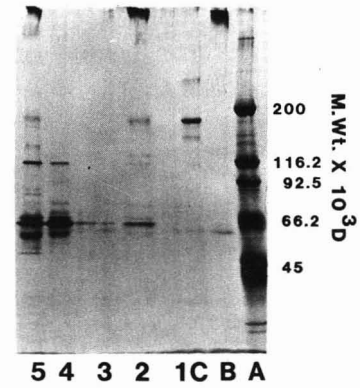

Fig. 13. Mixed-mode chromatography of NNS-10 2D5 ascites fluid on hydroxyapatite. Volume applied, 200 μl; flow-rate, 0.5 ml/min; 0.1 a.u.f.s. Column equilibrated in 10 m*M* sodium phosphate buffer (pH 6.8)–0.3 m*M* calcium chloride (buffer A) and eluted with 300 m*M* sodium phosphate buffer (pH 6.8)–0.01 m*M* calcium chloride (buffer B). Linear gradient 0–100% B generated over 15 min.

Fig. 14. Analysis of fractions with SDS-PAGE (3–12.5% non-reducing gradient gel) of NNS-10 2D5 ascites fluid, following HPHT chromatography. Lanes A–C represent molecular weight, IgM, and IgG standards, respectively. Lanes 4 and 5 contain aliquots from fractions 21 and 23, respectively. Lane 2 contains an aliquot from fraction 23, following HPHT chromatography of a 45% ammonium sulphate-precipitated sample of NNS-10 2D5 ascites fluid.

immunofluorescence could be detected in all isolated fractions containing NNS-10 2D5 hybridoma IgM following the various purification strategies. These results indicate the maintenance of immunoreactivity of each of the hybridoma IgMs following purification by all procedures.

TABLE V

ISOLATION OF MOUSE MONOCLONAL IgMs FROM ASCITES FLUID BY HYDROXYAPATITE CHROMATOGRAPHY

Antibody	*Fraction(s) analysed*	*Protein applied (μg)*	*IgM applied (μg)*	*Protein recovered (μg)*	*IgM recovered (μg)*	*Yield of IgM (%)*	*Purification factor*
NNS-10 2D5	Ascites fluid	4900.0	330.0[a]	–	–	100.0	1.0
	22–28			2362.5	128.8	40.0	0.8
GFM-5 1B12	Ascites fluid	4440.0	342.1[a]	–	–	100.0	1.0
	20–30			3159.0	135.3	39.5	0.6

[a] Amount of IgM present in 200 μl of ascites fluids following dialysis into 10 m*M* sodium phosphate (pH 6.8) – 0.3 m*M* calcium chloride.

TABLE VI

SEQUENTIONAL PURIFICATION OF MOUSE MONOCLONAL IgM ANTIBODIES BY MONO Q ANION-EXCHANGE CHROMATOGRAPHY AND SUPEROSE 6 SEC

Antibody	*Fraction(s) analysed*	*Protein applied (μg)*	*IgM applied (μg)*	*Protein recovered (μg)*	*IgM recovered (μg)*	*Yield of IgM (%)*	*Purification factor*
NNS-10 2D5	Mono Q eluate	610[a]	5.8	–	–	100.0	1.0
	8–12			132.6	3.6	62.0	2.8
GFM-5 1B12	Mono Q eluate	848[b]	41.5	–	–	100.0	1.0
	8–12			260.0	26.8	64.5	2.1

[a] Pooled fractions 27–38 from Mono Q FPLC column.
[b] Pooled fractions 25–38 from Mono Q FPLC column.

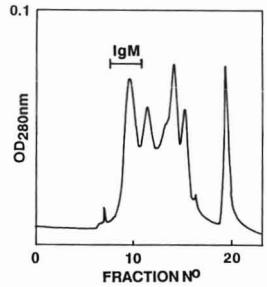

Fig. 15. Separation of IgM-containing fractions eluted from a Mono Q column of NNS-10 2D5 ascites fluid, following chromatography on a Superose 6 HR 10/30 FPLC column. Volume of sample, 200 μl; flow-rate, 0.5 ml/min; 0.1 a.u.f.s.

DISCUSSION

The above comparison of methods for the purification of monoclonal IgM autoantibodies was undertaken in order to ascertain an efficient procedure for the recovery and isolation of IgM. Data in the literature indicate that assessment of purity of isolated IgM has usually been undertaken by SDS-PAGE relying on either densitometric or manual estimation for quantification of IgM purity[8,13,30,31]. We have compared the methods for IgM purification by a double-sandwich anti-IgM ELISA for the measurement of IgM concentrations in ascites fluids, supernatant, and fractions from purification procedures. With ELISA we were able to detect as little as 2.0 ng of IgM per ml. In conjunction with this ELISA, IgM purity was further assessed in two ways. First, IgM-containing fractions were subjected to SDS-PAGE under either reducing (12.5% gels) or non-reducing (3–12.5% gel) conditions, and protein was detected by silver-staining[29], a method claimed to be at least 100-fold more sensitive than Coomassie Blue R250 staining[24]. Secondly, protein concentrations of IgM-containing fractions were determined by a BCA-based protein assay

with a detection sensitivity of 5–250 μg protein per ml[32]. These assay procedures enabled the definition of the relative purity of IgM in any given fraction following chromatography and visualization of the apparent molecular weights of protein species contaminating the IgM.

The IgM separation techniques tested in this study included routinely used procedures, such as ammonium sulphate[24], euglobulin precipitation[24,31,33], PEG-induced precipitation[23], and more advanced techniques such as size-exclusion, anion- and cation-exchange and mixed-mode chromatographic methods. Combinations of separation strategies were also tested.

Ammonium sulphate precipitation of immunoglobulins has been used as an initial enrichment and concentration method[24]. This study demonstrates that complete recovery of murine monoclonal IgMs does not occur at the commonly used 40–45% (v/v) final concentration of ammonium sulphate. The highest recovery of IgM (*ca.* 83%) occurred at 60% (v/v) final concentration of ammonium sulphate, suggesting that care should be taken in selecting ammonium sulphate concentrations if recovery of monoclonal IgM is of importance. In contrast, precipitation of monoclonal IgM based on euglobulin properties in low-ionic-strength solutions resulted in low IgM recovery ($\leqslant$ 10%) under conditions known to precipitate serum IgM[21]. Dialysis of ascites fluid against 2% boric acid (pH 6.0) produced the greatest recovery of monoclonal IgM consistent with reports that euglobulins precipitate more readily in boric acid, and boric acid protein complexes are more readily redissolved than other precipitates[33]. Of significance, however, with the low-ionic-strength buffer precipitation of IgM was the observed inability of precipitated material to redissolve completely indicating some protein denaturation.

PEG 6000 precipitation produced *ca.* 4- to 5-fold purification of IgM with *ca.* 65% recovery. Purity of PEG-precipitated hybridoma IgM was *ca.* 64–70%, as assessed by protein estimations contrasting with >90%, reported by Neoh *et al.*[23] who used Coomassie Blue-stained agarose gels. Consequently, the use of PEG 6000 may provide a useful enrichment and concentration procedure for hybridoma IgM antibodies.

The results demonstrate that in a single step, SEC on Superose 6 HR 10/30 FPLC columns produced a purification of 3- to 22-fold for IgMs derived from ascites fluids and supernatants. With a single-buffer system, IgM was recovered in *ca.* 70–80% purity and *ca.* 68–80% yield from Superose 6 columns. These values are slightly less than the estimates from Coomassie Blue-stained SDS-PAGE reported by Chen *et al.*[8] although the resolution in our system was apparently greater (Fig. 6). The differences in IgM resolution following Superose 6 chromatography demonstrated in this study compared to that reported by Chen *et al.*[8] may be due to differences in buffer systems [100 m*M* Tris–HCl, (pH 7.8)–50 m*M* NaCl *versus* 100 m*M* PBS (pH 8.0)] or subtle differences in the monoclonal IgM, allowing hydrophobic or ionic interactions with the chromatographic matrix. Further studies in our laboratory have revealed that resolution of IgM can be achieved with 50 m*M* L-histidine (pH 6.0) buffers, containing 1.7 *M* NaCl on Superose 6 HR 10/30 FPLC columns.

Separation of IgM based on "non-ideal" SEC resulted in high recoveries of IgM (*ca.* 82–92%) but with comparatively low purity ($\leqslant$ 12%). This is in contrast with the results reported by Bouvet *et al.*[9] and Chen *et al.*[8] for isolation of IgMs from ascites fluid. Both authors reportedly purified IgM from ascites fluids using "non-

ideal" SEC to $\geqslant$ 90% purity, as assessed by Coomassie Blue-stained SDS-PAGE. Differences in purities reported here from those reported by others may again be related to either subtle differences in the monoclonal IgM autoantibodies such that poor resolution from other selectively slowed proteins occurred under the conditions applied. Alternatively, variations may be explained by differences between the buffers used for the analyses, or differences in methods for estimating sample purity. However, the results presented here, demonstrate the retention of monoclonal IgMs on Superose 6 columns under low-ionic-strength conditions, possibly due to euglobulin properties of IgM and/or the potential for hydrophobic behaviour of the chromatographic matrix, and their elution in the final peak with high-ionic-strength buffers. The behaviour of the hybridoma IgMs examined in this study with respect to this latter point is similar to that reported by others[8,9]. The contaminating lower-molecular-weight species, including mouse IgG and albumin, found to be eluted with IgM under "non-ideal" SEC conditions may not have been unexpected, as similar contaminants were found in IgM-containing precipitates from the low-ionic-strength analyses (Fig. 3).

Under the conditions investigated, anion- or cation-exchange chromatography and Mono Q and Mono S FPLC columns, was unable to separate the specific monoclonal IgMs from other proteins present in ascites fluids or concentrated tissue culture supernatants in a single step. In contrast to the purity of *ca.* 50% estimated for single-step Mono Q-purified IgM by Chen *et al.*[8], the purity of IgM eluted from the Mono Q column in this study was $\leqslant$ 5%, albumin constituting a major contaminant. In order to achieve high recovery of IgMs in this study, IgM eluted in the broad, trailing shoulder of the second-eluted peak was pooled. Thus, recovered IgMs were of significantly lower purity, as these fractions also contained many other proteins (Fig. 10). The buffers used in this study were those reported by Clerzardin *et al.*[13] for monoclonal IgM purification on Mono Q columns. Chen *et al.*[8] used 20 m*M* Tris–HCl (pH 8.0) for equilibration of the Mono Q column and this buffer, containing 1.0 *M* NaCl, for elution. Variations in the purity of the monoclonal IgMs eluted from Mono Q columns may be related to the different net-charge characteristics and surface distribution of these charges on the IgM molecules at the two different buffer pH values used in these studies.

Results from this study indicate that cation-exchange chromatography on Mono S columns cannot be used to isolate monoclonal IgM in a highly purified form from ascites fluids or tissue culture supernatants. Similarly, mixed-mode chromatography on hydroxyapatite did not result in the purification of IgM reported by others[27,34].

Combinations of anion-exchange chromatography and SEC have been reported to result in the purification of monoclonal IgMs free from α_2-macroglobulin and other supernatant and ascites fluid proteins[8,11,13]. In this study, separation of IgMs eluted from Mono Q columns from other proteins did not occur following passage through Superose 6 HR 10/30 FPLC columns. In this dual-step procedure, recovery of monoclonal IgM was high (*ca.* 65%) whilst the purification factor was 2- to 3-fold. These results were attributable to proportional increases in the amounts of contaminant proteins in relation to IgM, following Mono Q chromatography. This resulted in poor separation of IgM from high-molecular-weight contaminants (Fig. 15). Thus, the purification factor of monoclonal IgMs for this dual-step procedure was lower

than for single-step SEC on Superose 6 columns. Other authors reported significant purification of IgM by "non-ideal" SEC following anion-exchange chromatography[8,9,11].

A notable observation in this study was that of variable recovery of hybridoma IgMs following dialysis of ascites fluids and supernatants into the appropriate buffers for the different chromatographic procedures (see Tables II–VI).

The results of this study indicate that monoclonal IgMs can be readily purified in a single step from hybridoma ascites fluid or dialysis culture supernatants to reasonable purity and yield by SEC on Superose 6 HR 10/30 FPLC columns. This system, rather than "non-ideal" SEC, produced significantly enhanced purification of monoclonal IgMs. Other single-step chromatographic procedures based on anion- and cation-exchange and hydroxyapatite columns could not separate monoclonal IgMs from contaminant proteins under the conditions applied. Similarly, sequential use of anion-exchange chromatography and SEC did not resolve the monoclonal IgMs. Comparison of the procedures tested in this study demonstrates that monoclonal IgMs can be rapidly purified on laboratory scale by size-exclusion FPLC, based on their molecular weight. This finding will enable the isolation of naturally occurring monoclonal IgM autoantibodies from concentrated supernatants and ascites fluids for the characterization of their autoantigenic specificities and further understanding of their relationship to autoimmune diseases.

REFERENCES

1 G. Dighiero, P. Lymberi, J. C. Mazie, S. Rouyre, G. S. Butler-Browne, R. G. Whalan and S. Avrameas, *J. Immunol.*, 131 (1983) 2267.
2 G. Dighiero, P. Lymberi, D. Holmberg, I. Lyndguist, A. Coutinho and S. Avrameas, *J. Immunol.*, 134 (1985) 765.
3 J. R. Underwood, J. Pedersen, P. J. Chalmers and B. H. Toh, *Clin. Exp. Immunol.*, 60 (1985) 417.
4 S. Avrameas, *Ann. Inst. Pasteur (Paris)*, 137D (1986) 150.
5 S. Seaver (Editor), *Commercial Production of Monoclonal Antibodies*, Marcel Dekker, New York, 1987.
6 P. Flodin and J. Killander, *Biochim. Biophys. Acta*, 63 (1962) 403.
7 G. Sann, G. Schneider, S. Loeke and H. W. Doerr, *J. Immunol. Methods*, 59 (1983) 121.
8 F. M. Chen, G. S. Naeve and A. L. Epstein, *J. Chromatogr.*, 444 (1988) 153.
9 J. P. Bouvet, R. Pires and J. Pillet, *J. Immunol. Methods*, 66 (1983) 229.
10 F. M. Boonekamp and R. Pomp, *Sci. Tools*, 33 (1986) 5.
11 H. H. Hwang, M. C. Healey and A. V. Johnston, *J. Chromatogr.*, 430 (1988) 329.
12 D. R. Nau, *Biochromatography*, 1 (1986) 82.
13 P. Clerzardin, G. Bourgo and J. L. McGregor, *J. Chromatogr.*, 354 (1986) 425.
14 J. M. Bidlack and P. C. Mabie, *J. Immunol. Methods*, 91 (1986) 157.
15 W. Romer and E. W. Rauterburg, *J. Immunol. Methods*, 38 (1980) 239.
16 F. Cormont, P. Mancouriez, L. DeCleroq and H. Bazin, *Methods Enzymol.*, 121 (1986) 622.
17 P. K. Lim, *Mol. Immunol.*, 24 (1987) 11.
18 J. P. Balint, Y. Ikeda, T. Nagai and D. S. Terman, *Immunol. Commun.*, 10 (1981) 533.
19 M. Harboe and I. Folling, *Scand. J. Immunol.*, 3 (1974) 471.
20 R. Klein, M. Klapperstuck, A. I. Chukhrova and Y. A. Lapik, *Mol. Immunol.*, 16 (1979) 421.
21 D. J. Hayzer and J. O. Jaton, *Methods Enzymol.*, 112 (1984) 26.
22 M. D. Bubb and J. D. Conradie, *Immunol. Commun.*, 6 (1977) 33.
23 S. H. Neoh, G. Gordon, A. Potter and H. Zola, *J. Immunol. Methods*, 91 (1986) 231.
24 J. W. Goding, *Monoclonal Antibodies: Principles and Practice*, Academic Press, London, 1986.
25 N. H. Hoogenraad and C. J. Wraight, *Methods Enzymol.*, 121 (1986) 375.
26 E. Sjorgren-Jansson and S. Jeansson, *J. Immunol. Methods*, 84 (1985) 359.
27 A. Stevens and T. L. Brooks, *Am. Biotech Lab.*, September (1985) 22.

28 U. Laemmli, *Nature (London)*, 227 (1970) 680.
29 H. J. Morrissey, *Anal. Biochem.*, 117 (1981) 307.
30 M. Garcia-Gonzalez, S. Bettinger, S. Oh, P. Oliver, J. Kadouche and P. Pouletty, *J. Immunol. Methods*, 111 (1988) 17.
31 A. H. Ross, D. Herlyn and H. Koprowski, *J. Immunol.*, 102 (1987) 227.
32 P.K. Smith, R.I. Krohn, G. T. Hermanson, A. K. Mallia, F. H. Gartner, M. D. Provenzano, E. K. Fujimoto, N.M. Goeke, B. J. Olsen and D. C. Klenk, *Anal. Biochem.*, 150 (1985) 76.
33 J. S. Garvey, N. E. Cremer and D. H. Sussdorf, *Methods in Immunol.*, WA Benjamin, Reading, MA, 3rd ed., 1977.
34 T. L. Brooks and A. Stevens, *Am. Lab.*, October (1985) 54.
35 A. W. Purcell, M. I. Aguilar and M. T. W. Hearn, *J. Chromatogr.*, 476 (1989) 125.

Journal of Chromatography, 476 (1989) 291–297
Elsevier Science Publishers B.V., Amsterdam — Printed in The Netherlands

CHROMSYMP. 1592

IMPROVED SEPARATION OF HUMAN PEPSINS FROM GASTRIC JUICE BY HIGH-PERFORMANCE ION-EXCHANGE CHROMATOGRAPHY

K. PEEK, N. B. ROBERTS* and W. H. TAYLOR
Department of Chemical Pathology, Royal Liverpool Hospital, Liverpool L7 8XW (U.K.)

SUMMARY

A simple and precise separative procedure can now be used to isolate individual pepsins from gastric juice, and by measurement of the protein absorbance at 280 nm enable their direct quantitation. This will facilitate the study of pepsin secretion, particularly in patients with peptic ulcer disease.

INTRODUCTION

Newton *et al.*[1] recently reported the development of a high-performance ion-exchange chromatography (HPIEC) method for the separation of human pepsins 3 and 5 from gastric juice. However, the pepsin 1 component was not identified. In view of the marked mucolytic activity of human pepsin 1 (ref. 2) and the evidence that this enzyme may be involved in the pathogenesis of peptic ulcer disease[3] it is important to develop an analytical procedure that will identify and quantitate this enzyme in addition to the other pepsins.

Hutton *et al.*[4] quantified pepsin 1 after agar gel electrophoresis at pH 5.0 by eluting the enzyme from the gel and then measuring the resultant proteolytic activity. Thus, they confirmed the conclusion of Walker and Taylor[5], who used a semi-quantitative electrophoretic procedure, that pepsin 1 is increased in the gastric juice of patients with peptic ulcer disease. Such electrophoretic procedures are laborious, time consuming and relatively imprecise and restrict the processing of large numbers of samples required in investigative gastroenterology.

We now report a modified HPIEC procedure, in which a ternary pump with low pressure mixing is used to resolve the human pepsins, including pepsin 1. The procedure is rapid and relatively easy, thus enabling the direct quantitation of all the human pepsins present in gastric juice.

EXPERIMENTAL

Chemicals

All chemicals used were of AnalaR grade (British Drug Houses, Poole, U.K.). Naphthalene black, bovine haemoglobin, bovine globin, and swine pepsin were obtained from Sigma (Poole, U.K.). Agar was purchased from Oxoid (London, U.K.),

0021-9673/89/$03.50

and the polyacrylamide gradient gels (PAA 4/30) and low-molecular-weight markers from Pharmacia (Milton Keynes, U.K.).

Apparatus

The ion-exchange column used was a 7.5 × 0.75 cm, TSK DEAE 5PW, 10 μm (Toyo Soda Manufacturing, Tokyo, Japan) column, connected with a guard column packed with TSK guard gel DEAE 5PW. The high-performance liquid chromatography (HPLC) system included a CM4000 low-pressure mixing ternary pump (Milton Roy, Stone, U.K.). The eluent was monitored at 280 nm with a SM4000 variable-wavelength detector (Milton Roy). Samples were injected automatically, using a Gilson 231 autosampler (Anachem, Bedford, U.K.), through a 500-μl loop.

Sample preparation

Human gastric juice was obtained from patients undergoing routine gastric function tests with pentagastrin as the stimulant. For the analysis of individual samples of gastric juice, 1–3 ml aliquots were dialysed against 1 l of 50 m*M* sodium acetate (pH 4.1) for 16 h, and filtered through a 0.45-μm Gelman Acro LC 13 filter before injection in to the HPIEC system.

For the preparation of large quantities of pepsins 3 and 1, a modification of the column technique reported by Roberts and Taylor[6] was used. Pooled gastric juices (up to 4 l) were filtered through a Whatman 113V filter paper to remove large particulate matter and then concentrated to 800 ml by ultrafiltration, using a Sartorius tangential flow ultrafiltration apparatus (V. A. Howe, London, U.K.). The concentrated juice (up to 1 l) was dialysed against 10 l of 50 m*M* sodium acetate (pH 4.1) for 16 h, and then mixed with 100 g of DEAE cellulose previously equilibrated with 50 m*M* sodium acetate (pH 4.1). The slurry was stirred for 1 h, allowed to settle, and the supernatant was discarded. Pepsins 3 and 5 were eluted with 750 ml of 50 m*M* sodium acetate buffer (pH 4.1), containing 0.25 *M* NaCl. The pepsin 3 and 1 fraction was eluted with 750 ml of 50 m*M* sodium acetate buffer (pH 4.1) containing 1 *M* NaCl. The pepsin-rich supernatants were concentrated in 200-ml aliquots to 10 ml by ultrafiltration, using stirred cells (Amicon, Stonehouse, U.K.), then dialysed for 16 h against 1 l of 50 m*M* sodium acetate (pH 4.1) containing 50 m*M* NaCl, and filtered through a 0.45-μm filter before injection in to the HPIEC system.

The procedure for obtaining pure pepsin 5 was modified to improve the poor recovery obtained in the above method. Pooled or individual samples of gastric juice were filtered through a Whatman 113V filter paper, dialysed for 16 h against 1 l of 50 m*M* sodium acetate (pH 4.1), and concentrated by ultrafiltration in stirred cells. All preparative and dialysis procedures were performed at +4°C.

The concentrates (10 ml) were filtered through a 0.45-μm filter and pumped directly into the TSK DEAE 5PW column. Individual pepsin fractions were collected into 10-ml plastic tubes on ice, and dialysed against 50 m*M* sodium acetate (pH 4.1) before use in the chromatographic and analytical studies outlined.

High-performance ion-exchange chromatography

The elution of human pepsins was performed with a linear binary gradient profile (Table I). The flow-rate was 1 ml/min (pressure < 10 bar). All solvents were filtered through a 0.45-μm filter under vacuum and purged with helium for 10 min

TABLE I

ELUTION PROFILE FOR SEPARATION OF HUMAN PEPSINS

Solvent A = 50 m*M* sodium acetate (pH 4.1). Solvent B = A + 1 *M* NaCl.

Time (min)	*Solvent composition (%)*	
	A	*B*
0	100	0
5	100	0
30	70	30
30.1	0	100
40	0	100
42	100	0

before use. At the end of each day, the system was flushed with methanol for 10 min and then with deionised water for 10 min.

Chromatographic fractions were collected into 5-ml plastic tubes on ice, and analysed for protein[7], and for proteolytic activity using bovine haemoglobin as a substrate at pH 2.0 (ref. 8) (calibrated with a swine pepsin standard). Specific activity was expressed as the proteolytic activity in swine pepsin equivalents per mg of protein.

Agar gel electrophoresis

Agar gel electrophoresis was performed at pH 5.0, using a Panagel electrophoresis unit (Millipore, London, U.K.) for 1.5 h at 150 V and 40 mA on 1.5% (w/v) agar gels at +4°C, containing 25 m*M* sodium acetate pH 5.0, as described by Newton *et al.*[1]. The pepsins were visualised after incubation with bovine globin at pH 2.0[8].

Sodium dodecyl sulphate-polyacrylamide gel electrophoresis

Polyacrylamide gel electrophoresis (PAGE) was performed using the Pharmacia gel electrophoresis apparatus GE-2/4. Individual pepsins (100 μl) were prepared by the addition of an equal volume of 20 m*M* Tris buffer (pH 8.0), containing 2 m*M* EDTA, 5% sodium dodecyl sulphate (SDS) and 10% mercaptoethanol and heated to 100°C for 2–3 min. When cooled, a small amount 5% glycerol, containing 0.5% bromophenol blue, was added to the mixture. Gradient gels were pre-equilibrated in 40 m*M* Tris–20 m*M* sodium acetate (pH 7.4), containing 2 m*M* EDTA and 0.2% (w/v) SDS, by electrophoresis for 1 h at 70 V. Samples were then applied to the gel and electrophoresed at 125 V for 1 h after the tracking dye had migrated out of the gel.

RESULTS

Fig. 1 shows the resolution of pepsins 5, 3 and 1 by means of low-pressure mixing and the modified linear chloride gradient in Table I. Pepsins 5 and 3 were eluted between 0.15 and 0.3 *M* sodium chloride, and pepsin 1 after a rapid, stepwise increase to 1.0 *M* NaCl. Pepsin 1 was still separated from pepsin 3 when 15 mg of protein, from a pepsin 3 and 1 concentrate, was loaded onto the TSK column. Fig. 1 also shows the variable secretion of pepsins in separate gastric juices. In particular, pepsin 1 varied

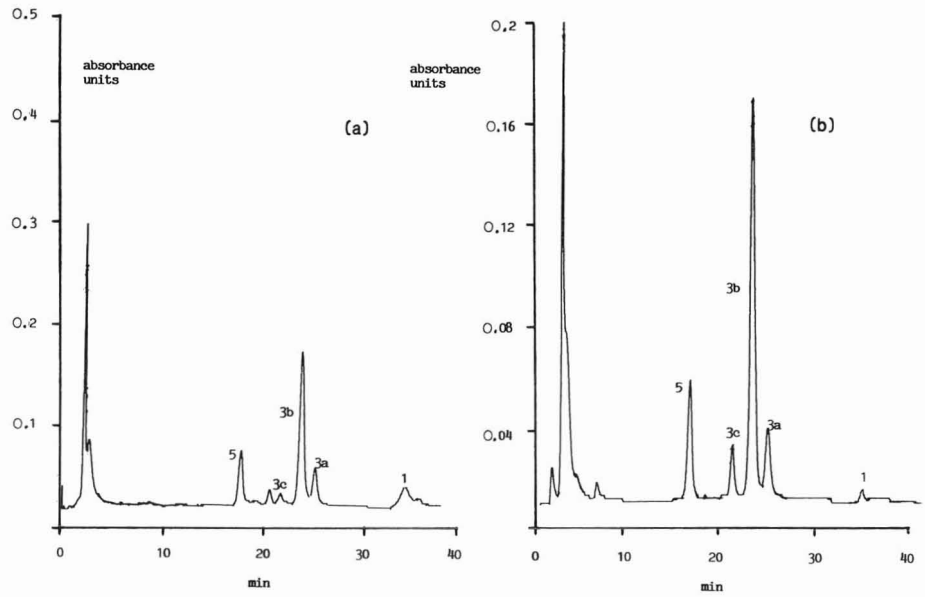

Fig. 1. The separation of human pepsins from gastric juice. The composition is expressed as the percentage of each pepsin peak area compared to the total pepsin peak area. Injection volume 500 μl. ——, UV 280 nm. (a) Patient 1: % composition for pepsin 5, 3c, 3b, 3a, and 1 was 16.5, 4.1, 56.8, 9.2 and 9.4, respectively. (b) Patient 2: % composition for pepsin 5, 3c, 3b, 3a, and 1 was 16.7, 6.9, 66.3, 9.5 and 0.6, respectively.

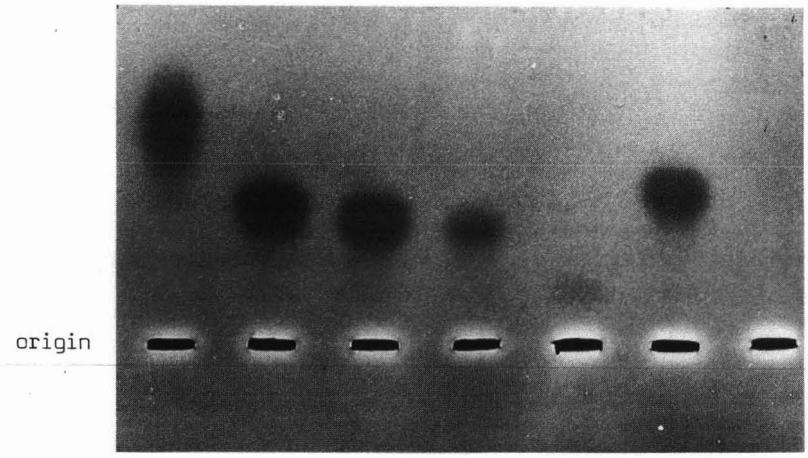

Fig. 2. Agar gel electrophoresis of individual human pepsins obtained by HPIEC. Enzymic activity is shown as zones of unstained areas (dark in the photograph) as a result of depletion of the substrate (bovine globin) contained in the gel.

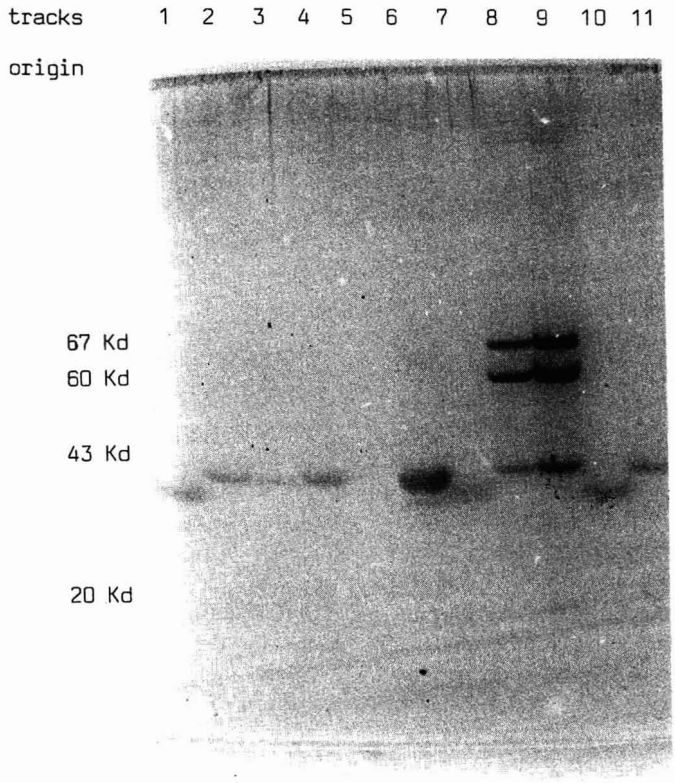

Fig. 3. SDS-PAGE of the individual human pepsins obtained by HPIEC. Tracks: 1 = pepsin 5; 2 = pepsin 3c; 3 = pepsin 3b; 4 = pepsin 3a; 5 = pepsin 1; 6 = gastric juice; 7 = swine pepsin; 8 = molecular weight markers; 9 = molecular weight markers; 10 = pepsin 5; 11 = pepsin 3c. Kd = Kilodaltons.

TABLE II

RETENTION TIMES, ANALYTICAL PRECISION AND RECOVERY OF PROTEOLYTIC ACTIVITY FOR HUMAN PEPSINS

Data from replicate injections (n = 6) of individual pepsins prepared by HPIEC. C.V. = coefficient of variation.

Pepsin	*Retention time (min)*		*Peak areas (arbitrary units)*		*Proteolytic recovery (%)*	
	Mean	*C.V.*	*Mean*	*C.V.*	*Mean*	*C.V.*
5	17.5	1.3	52.8	1.6	99.0	8.0
3c	22.6	0.7	30.0	3.6	82.0	8.0
3b	25.2	0.7	109.0	2.5	101.0	10.0
3a	27.4	0.7	44.5	1.5	69	3.4
1	35.7	0.2	11.2	3.2	101	3.6

TABLE III

SPECIFIC ACTIVITIES OF PURIFIED HUMAN PEPSINS

Values are the mean ± 1 S.D. for six measurements.

Pepsin	*Mean specific activity ± S.D. (μg swine pepsin equiv./μg protein)*
5	0.87 ± 0.05
3c	0.42 ± 0.01
3b	0.86 ± 0.09
3a	0.42 ± 0.01
1	0.20 ± 0.01

from 9.4 to 0.6% of the total secretion. Pepsin 3 clearly consist of three peaks, 3a, 3b and 3c, labelled such that 3a is the same as pepsin 3a found on electrophoresis[9].

Agar gel electrophoresis at pH 5.0 showed that pepsins isolated by HPIEC were present as single zones of proteolytic activity (Fig. 2). Pepsins 3c, 3b and 3a had slightly increasing rates of migration towards the anode, in agreement with their increased retention on the ion-exchange column. SDS–PAGE of pepsin 5, 3c, 3b and 3a also showed single protein bands (Fig. 3), but pepsin 1, was not visualized. Rechromatography of the individual pepsins further confirmed the presence of single components. However, with extended gradients, pepsin 1 was eluted as a broad band of unresolved peaks.

To assess the analytical performance of the procedure purified pepsins were reinjected into the HPIEC system. Table II shows good precision of retention time, mean peak area, and recovery of proteolytic activity. The recovery of proteolytic

TABLE IV

THE RELATIVE AMOUNTS OF HUMAN PEPSINS IN GASTRIC JUICE COLLECTED DURING A PENTAGASTRIN STIMULATION TEST

The relative percentage was calculated from peak areas.

Gastric juice	*pH*	*Vol. (ml)*	*Pepsin (relative %)*				
			5	*3c*	*3b*	*3a*	*1*
Basal							
0–15[a]	1.7	12.0	23.0	7.5	63.5	4.2	1.7
15–30	1.3	34.0	14.3	4.3	74.0	5.9	1.4
30–45	2.0	19.0	15.1	4.2	73.0	5.6	2.0
After Pentagastrin							
0	0.9	45.0	12.4	5.0	77.1	5.1	0.4
0–15	1.0	16.0	13.2	4.2	76.6	4.9	1.1
15–30	0.9	82.0	13.7	4.1	77.0	4.8	0.4
30–45	0.9	92.0	13.8	4.2	77.3	4.6	0.2
45–60	0.9	41.0	13.5	4.2	76.7	5.3	0.2
60–75	0.9	31.0	13.3	4.3	77.0	5.2	0.1

[a] Minutes.

activity of 3a and 3c was less than the *ca.* 100% obtained for pepsins 5, 3b and 1. However, there was no loss of protein for any of the pepsins after repeated chromatography.

The specific activities of purified pepsins are shown in Table III. Pepsin 1 has approximately one quarter the activity of pepsin 3b and pepsin 5. The lower specific activities of pepsins 3a and 3c compared with 3b may indicate some loss of activity during purification or different activities towards bovine haemoglobin.

The relative percentages of the individual pepsins secreted in a series of gastric juices, obtained from a patient undergoing a pentagastrin test, are given in Table IV. The percentage of pepsin 1 was maximal during the prestimulation period, with variable secretion of pepsin 5 and 3. However, after pentagastrin stimulation, the relative percentage of the different pepsins was remarkably consistent, the only change being the volume of juice secreted.

DISCUSSION

The chromatographic separation which we have developed allows the resolution of all the major human pepsins present in gastric juice, as confirmed by agar gel electrophoresis. We have previously shown the separation of pepsin 5 from pepsin 3b and 3c, but pepsins 3a and 1 were not identified. The successful resolution of pepsin 1 was achieved by a rapid stepwise change in gradient to 1.0 *M* NaCl, which resulted in the elution of this enzyme as a single peak. The improved separation of pepsin 5 and the three components of pepsin 3 was achieved with a modified chloride gradient formed by low-pressure mixing.

The specific activities reported are in agreement with those reported by Roberts[10]. The low specific activity observed for pepsin 1 would suggest the presence of non-pepsin protein *e.g.*, a proteoglycan[11], inactive enzyme, or activity towards haemoglobin different from that of swine pepsin.

The analysis of a pentagastrin test showed that there was little change in the percentage composition of pepsins following pentagastrin stimulation. However, during the prestimulation period, the composition was more variable. In particular, pepsin 1 was increased. Chromatograms of the basal secretion showed this to be a true increase in the amount of pepsin 1 compared with post stimulatory juices. In addition, pepsin 5 was present in all samples of gastric juice, unlike the earlier observation of Newton *et al.*[1] when this enzyme decreased after pentagastrin stimulation.

REFERENCES

1 C. J. Newton, N. B. Roberts and W. H. Taylor, *J. Chromatogr.*, 417 (1987) 391.
2 J. P. Pearson, R. Ward, A. Allen, N. B. Roberts and W. H. Taylor, *Gut*, 27 (1986) 243.
3 W. H. Taylor, *Adv. Clin. Enzymol.*, 2 (1982) 79.
4 D. A. Hutton, A. Allen, J. P. Pearson, R. Ward and C. W. Venables, *Biochem. Soc. Trans.*, 14 (1986) 735.
5 V. Walker and W. H. Taylor, *Gut*, 21 (1980) 766.
6 N. B. Roberts and W. H. Taylor, *Biochem. J.*, 169 (1978) 607.
7 O. H. Lowry, N. J. Rosenbrough, N. J. Farr and R. J. Randall, *J. Biol. Chem.*, 193 (1937) 265.
8 D. J. Etherington and W. H. Taylor, *Biochem. J.*, 113 (1969) 663.
9 D. J. Etherington and W. H. Taylor, *Nature (London)*, 216 (1967) 279.
10 N. B. Roberts, *Ph.D. Thesis*, University of Liverpool, Liverpool, 1975.
11 J. P. Pearson, A. Allen, N. B. Roberts and W. H. Taylor, *Clin. Sci.*, 72 (1987) 33p.

Journal of Chromatography, 476 (1989) 299–308
Elsevier Science Publishers B.V., Amsterdam — Printed in The Netherlands

CHROMSYMP. 1599

SEPARATION AND PURIFICATION OF COMPONENT PROTEINS OF THE CYTOCHROME P-450-DEPENDENT MICROSOMAL MONOOXYGENASE SYSTEM BY HIGH-PERFORMANCE LIQUID CHROMATOGRAPHY

HISAAKI TANIGUCHI* and WALTER PYERIN
Institute of Experimental Pathology, German Cancer Research Center, Im Neuenheimer Feld 280, D-6900 Heidelberg (F.R.G.)

SUMMARY

The component proteins of the hepatic microsomal monooxygenase system, including various cytochrome P-450 isozymes, were separated and isolated from liver microsomes of untreated rabbits by Aminohexyl Sepharose and high-performance liquid chromatography (TSK preparative DEAE 5-PW, Bio-Rad HPHT). In addition to the known cytochrome P-450 isozymes, two new isozymes and one variant of the major isozyme were isolated. The monooxygenase activity was reconstituted by incorporating the purified proteins into liposomal membranes.

INTRODUCTION

The hepatic microsomal cytochrome P-450 (P-450)-dependent monooxygenase system is a key enzyme system in chemical carcinogenesis and metabolism of foreign substances, such as drugs[1]. This system is unique, since all component proteins are membrane-bound, and the interaction between them takes place in the plane of the endoplasmic reticulum membrane[2–4]. Although the best way to study such a complex system is to separate and purify each component and then to reconstitute the system, this is rather difficult due to the complexity of the system, including more than 20 different P-450 isozymes, in addition to several other component proteins, and also due to the membrane-bound nature of these proteins[5,6].

The high resolution obtained by high-performance liquid chromatography (HPLC) is very useful in the separation and purification of various component proteins of the monooxygenase system, and the application of this technique to the purification of various P-450 isozymes has recently been reported[7–9]. It led not only to the rapid purification of various isozymes, but also to the purification of various isozymes which have not yet been described[9]. In the present study, we have utilized HPLC for the separation and purification of the component proteins of the monooxygenase system as well as for various P-450 isozymes.

The combination of hydrophobic interaction chromatography with ion-exchange chromatography (TSK DEAE 5-PW) and hydroxyapatite (Bio-Rad HPHT) enabled the isolation of the three proteins which supply electrons to P-450, namely

0021-9673/89/$03.50

NADPH-cytochrome P-450 reductase (fp2), NADH-cytochrome b_5 reductase (fp1) and cytochrome b_5 (b5), as well as that of various P-450 isozymes, some of which are reported for the first time, and of epoxide hydrolase. Monooxygenase activity was restored upon incorporation of the purified proteins into liposomal membrane, demonstrating the usefulness of the purification procedure in reconstitution studies.

EXPERIMENTAL

Materials

NADPH, NADH, cytochrome *c* (Type VI), 7-ethoxycoumarin, 7-hydroxycoumarin and Tergitol NP-10 were obtained from Sigma (München, F.R.G.), acrylamide, bis-acrylamide and sodium dodecyl sulphate (SDS) from Bio-Rad (München, F.R.G.), and acetonitrile (gradient grade), sodium deoxycholate and cholic acid from Merck (Darmstadt, F.R.G.). Egg yolk phospatidylcholine was obtained from Lipid Products (South Nutfield, U.K.) while trypsin (N-tosylphenylalanine chloromethyl ketone-treated) was from Interchem (München, F.R.G.). 2',5'-ADP-Sepharose, 5'-ADP-agarose, Sephadex G-100 and Sepharose 4B were from Pharmacia (Freiburg, F.R.G.). Aminohexyl Sepharose was synthesized according to the published method[10]. TSK DEAE-HPLC columns (Toyo Soda; semipreparative, 150 mm × 21.5 mm; analytical, 75 mm × 7.5 mm) were obtained through LKB (München, F.R.G.). Mono Q columns were obtained from Pharmacia, while the Bio-Gel HPHT column (100 mm × 7.8 mm) was from Bio-Rad. A Vydac 218-TP54 reversed-phase column (250 mm × 4.6 mm) was obtained from The Separations Group (Hesperia, CA, U.S.A.). All other chemicals and biochemicals used were of the highest grade available commercially.

HPLC apparatus

An LKB HPLC system, consisting of two 2150 HPLC pumps with a high-pressure mixing chamber (LKB), was used together with a Kratos SF 575 UV–VIS detector (Kratos, Karlsruhe, F.R.G.). The conductivities of the eluates were measured continuously with a WTW LF 42 conductivity monitor with a micro-flow cell (WTW, Wilhelm, F.R.G.). All buffers used were continuously degassed using an ERC 3320 degasser (ERC, Regensburg, F.R.G.).

Preparation of microsomes

Male New Zealand white rabbits, weighing 3–4 kg, were starved overnight and killed by decapitation. Liver microsomes were prepared by differential centrifugation, as described[10]. The microsomes were washed once with 0.15 *M* KCl, containing 10 m*M* EDTA (pH 7.4), and stored at −70°C.

Solubilization of microsomes and Aminohexyl Sepharose chromatography

Microsomes were solubilized with cholate and applied directly to an Aminohexyl Sepharose column in order to lower the load for the HPLC column as well as to achieve partial separation of several enzymes[10,11]. All manipulations up to the HPLC separations were conducted at 0–4°C. The microsomes (about 3 g protein) were thawed and resuspended in 1 l of 0.1 *M* potassium phosphate buffer (pH 7.3), containing 0.6% cholic acid, 20% glycerol, 1 m*M* dithiothreitol and 1 m*M* EDTA. The

slightly turbid solution was subjected to ultra centrifugation at 150 000 *g* for 1 h. The clear supernatant was applied directly to an Aminohexyl Sepharose column (30 cm × 2.6 cm), equilibrated with the same buffer as that used for the solubilization. The column was washed with 500 ml of the solubilization buffer, containing 0.4% cholic acid, and eluted with the solubilization buffer, containing 0.4% cholic acid and 0.08% Tergitol NP-10.

The column was further eluted with the same buffer, containing 0.4% cholic acid and 0.2% Tergitol NP-10 (second elution, as indicated with an arrow in Fig. 1), and with 50 m*M* potassium phosphate buffer (pH 7.3), containing 20% glycerol, 0.15% cholic acid, 0.35% sodium deoxycholate and 1 m*M* EDTA (third elution, as indicated with an arrow in Fig. 1).

Preparative anion-exchange HPLC

The fractions obtained from the Aminohexyl Sepharose column were collected in two pools as indicated in Fig. 1, and dialyzed overnight against 10 m*M* Tris–acetate buffer (pH 7.5), containing 20% glycerol, 1 m*M* dithiothreitol and 1 m*M* EDTA. The dialysates (150–200 mg protein) were diluted three-fold with 20% glycerol, containing 1 m*M* dithiothreitol and 1 mM EDTA, and applied to a semi preparative TSK DEAE 5-PW column, which had been equilibrated with 10 m*M* Tris–acetate buffer (pH 7.5), containing 0.4% Tergitol NP-10, 20% glycerol, 1 m*M* dithiotreitol and 1 m*M* EDTA (buffer A). The column was washed with 40 ml of buffer A, and eluted with a linear gradient of 0–15% buffer B (20 mM Tris–acetate buffer pH 7.5, containing 20% glycerol, 0.4% Tergitol NP-10, 1 m*M* dithiothreitol and 1 m*M* EDTA) in buffer A in 240 min at a flow-rate of 2 ml/min.

Analytical anion-exchange HPLC

The fractions obtained from the preparative DEAE-HPLC column were re-chromatographed in an analytical TSK DEAE 5-PW column or in two Mono Q columns connected in series. The column was eluted with a linear gradient of 0–10% buffer B, incorporated into buffer A in 40 min at a flow-rate of 1 ml/min.

Hydroxyapatite HPLC

The fractions from the analytical DEAE-HPLC column were pooled and dialyzed overnight against 10 m*M* potassium phosphate buffer (pH 7.3), containing 20% glycerol and 0.1 m*M* dithiothreitol. The dialyzed fractions were applied directly to an hydroxyapatite HPLC column which had been equilibrated with buffer C (10 m*M* potassium phosphate buffer pH 7.3, containing 15% glycerol, 0.2% Tergitol NP-10, and 0.1 m*M* dithiothreitol). The column was eluted with a linear gradient of 0–100% buffer D (350m*M* potassium phosphate buffer pH 7.3, containing 15% glycerol, 0.2% Tergitol NP-10 and 0.1 m*M* dithiothreitol), incorporated into buffer C in 60 min at a flow-rate of 0.7 ml/min.

Trypsin hydrolyzate analysis

The purified proteins were diluted in 50 m*M* Tris–HCl buffer (pH 8.0) to a concentration of 0.5 mg protein/ml. To 100 μl of the sample solution, 5 μg of trypsin, dissolved in 5 μl of 1 m*M* HCl, were added, and the mixture was incubated at 37°C for 15 h. The reaction was stopped by adding 10 μl of 10% trifluoroacetic acid, and the

sample was directly injected into a Vydac 218-TP54 reversed-phase column. The column was eluted with a linear gradient of 0–70% acetonitrile in 0.1% trifluoroacetic acid for 60 min at a flow-rate of 0.7 ml/min. The elution of peptides was monitored at 210 nm.

Affinity chromatography of fp1 and fp2

The fp1-containing fractions from the preparative DEAE-HPLC column were pooled and purified to homogeneity, using a 5′-ADP-agarose column (5 cm × 1 cm), as described previously[3]. The fp2-containing fractions from the aminohexyl Sepharose column were pooled and directly applied to a 2′,5′-ADP-Sepharose column (5 cm × 1.6 cm). fp2 was purified to homogeneity as described earlier[3].

Purification of b5

Cytochrome b_5 was isolated from the third eluate from the aminohexyl Sepharose column by gel filtration chromatography on Sephadex G-100, as described previously[3].

Analytical methods

P-450 was determined from its CO-difference spectrum in microsomes and from its absorbance at 417 nm in purified, soluble form[3]. The concentration of b5 was determined from its absorbance at 413 nm (ref. 3). fp1 was determined by measuring the NADH-dependent ferricyanide reductase activity[12] or flavin absorption[13], and fp2 was determined from its flavin absorption[14]. The reconstituted monooxygenase activity was measured in 50 m*M* potassium phosphate buffer (pH 7.3) containing 300 μM ethoxycoumarin as the substrate. The reaction was started by adding 1 m*M* NADPH, and the increase in the fluorescence of the product, 7-hydroxycoumarin, was measured in a Perkin-Elmer LS-3 fluorescence spectrophotometer. The excitation wavelength was 380 nm, and the emission wavelength was set at 455 nm. Reconstitution of the monooxygenase was achieved by incorporating the purified proteins into liposomes by the cholate dialysis method as described previously[2–5]. Sodium dodecyl sulphate (SDS) gel electrophoresis was carried out according to Laemmli[15]. The protein concentration was determined by the method of Lowry *et al.*[16].

RESULTS AND DISCUSSION

Aminohexyl Sepharose chromatography

Aminohexyl Sepharose chromatography, which was first developed for the purification of the phenobarbital-inducible form of P-450 from rabbit liver[10,17] and later adapted to the purification of P-450 isozymes from various sources[18,19], was used as the first step in order to achieve the partial separation and purification of various proteins as well as to lower the load for the HPLC columns. As has been described by Imai[11], the combination of various detergents enabled the separation of fp2 and b5 from the two P-450-containing fractions (Fig. 1). Under the conditions employed, fp2 was eluted from the column as a broad peak, just after the first P-450 peak. No NADPH-cytochrome *c* reductase activity, which is catalyzed by fp2, was detected in the third eluate, as described[11]. The first P-450 peak was divided into two fractions (pools 1 and 2 in Fig. 1), dialyzed and further purified on a DEAE-HPLC

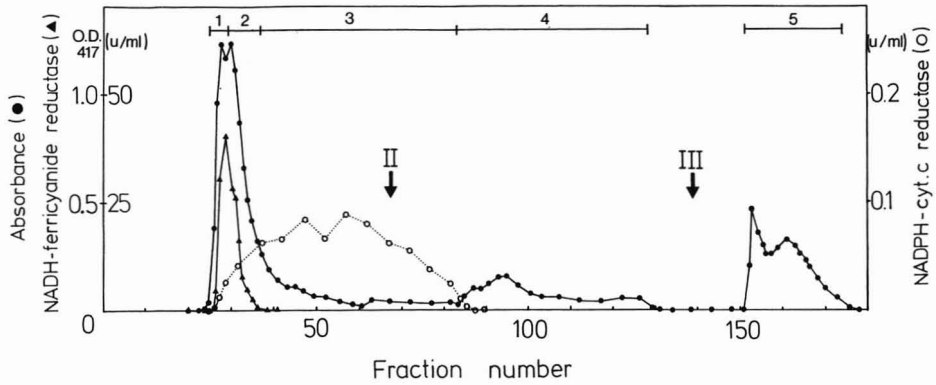

Fig. 1. Chromatography of solubilized microsomes on an aminohexyl Sepharose 4B column. The microsomes obtained from untreated rabbit liver were solubilized with cholic acid, and applied to the column. The elution buffers were changed at the times indicated by arrows. Absorption was monitored at 417 nm, and the activities of the two reductases (fp1 and fp2) were measured as described in Experimental. The fractions obtained were pooled as indicated. The column dimensions and eluent composition are described in Experimental.

column. The third pool, which contained most of the fp2, was further purified on a 2′,5′-ADP-Sepharose affinity column, as described in Experimental. The peak eluted by the combination of cholate and deoxycholate contained most of the b5. Cytochrome b_5 was isolated from the pool by gel filtration chromatography as described in Experimental. The two component proteins of the monooxygenase system, fp2 and b5, were thus separated from the majority of the P-450 by Aminohexyl Sepharose chromatography, and purified to homogeneity.

Preparative DEAE-HPLC of pool 1

The first half of the main peak eluted from the Aminohexyl Sepharose column (pool 1 in Fig. 1) was further resolved on a semipreparative TSK DEAE 5-PW column, as described in Experimental. The column eluate was monitored at 417 nm, where the two haemoproteins, P-450 and b5, can be detected specifically (Fig. 2a). The collected fractions were subjected to SDS gel electrophoresis, and several proteins were immediately identified by their apparent molecular weights (Fig. 2b).

The first peak, which was only weakly bound to the column and was eluted immediately with buffer A, contained one of the two major P-450 isozymes in the uninduced rabbit liver microsomes, isozyme 3c, as well as isozyme 2, which is inducible with drugs, such as phenobarbital (Fig. 2). The last large peak which was eluted at around 6–7% buffer B (elution volume 240 ml) contained another major P-450 isozyme in the control rabbit liver microsomes, namely isozyme 3b. The identity of these isozymes was established from their chromatographic behaviour, mobility in SDS gel electrophoresis and activity. In addition to these two major forms, at least two peaks contained P-450 isozymes. One peak, eluted at the beginning of the gradient (at around 100 ml elution volume), and a small peak eluted just before the 3b peak (elution volume around 220 ml), contained proteins which migrated between isozymes 2 and 3b in SDS gel electrophoresis (marked a and b in Fig. 2b). The only

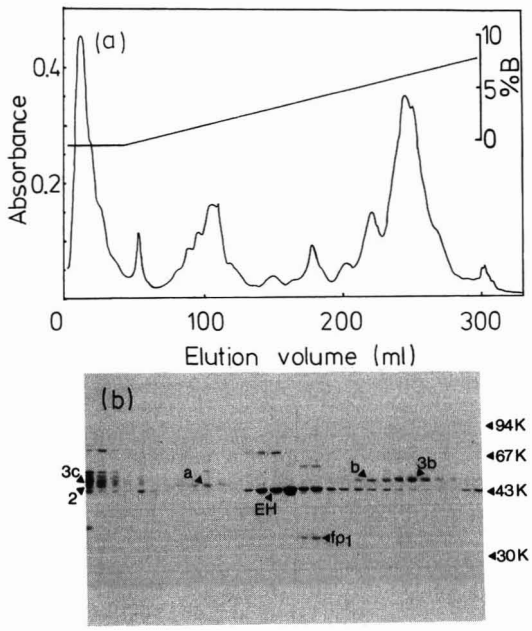

Fig. 2. (a) HPLC separation of Aminohexyl Sepharose pool 1 on a TSK preparative DEAE 5-PW column. The pooled fractions were dialyzed and applied to the column as described in Experimental. The column eluate was monitored at 417 nm. The buffer concentration in the eluate was determined from the conductivity measured continuously in a micro-flow cell. (b) SDS gel electrophoresis of the fractions obtained from the DEAE 5-PW column: 2, 3b and 3c are known P-450 isozymes, a and b are unknown isozymes. Cytochrome b_5 reductase is marked fp1, while epoxide hydrolase is marked EH.

P-450 which has been purified from rabbit liver microsomes and which migrates between isozymes 2 and 3b is isozyme 3a[20]. Since isozyme 3a shows an absorption maximum at around 390 nm, while the two isozymes separated in the present study show absorption maxima at around 416 nm, these two P-450 peaks appear to represent two as yet unidentified P-450 isozymes.

In addition to P-450 isozymes, two other proteins were identified by their activities and apparent molecular weights. Epoxide hydrolase was eluted as a rather broad peak (the peak fraction was eluted around 160 ml between a and b and is marked as EH in Fig. 2b), and showed an apparent molecular weight of 46 000, corresponding well to the published value[21]. Slightly after epoxide hydrolase, fp1 was eluted as a sharp peak at around 200 ml, and was seen in the SDS gel (Fig. 2b). The small peak around 200 ml is due to the flavin absorption of fp1. The latter was easily purified to homogeneity by affinity chromatography on 5′-ADP-agarose[3]. Epoxide hydrolase represents the major protein, and is almost pure in the peak fraction. The peak fractions were pooled and further purified by rechromatography on an analytical DEAE 5-PW column.

Preparative DEAE-HPLC of pool 2

The second half of the first main peak from the Aminohexyl Sepharose column was separately collected as pool 2, and applied on the preparative DEAE 5-PW

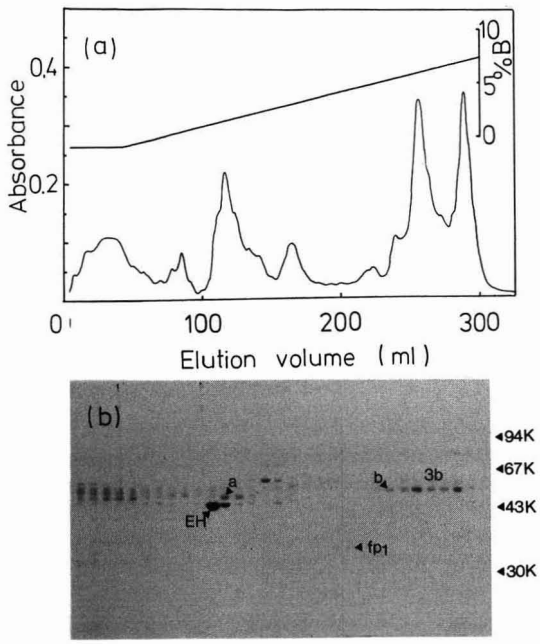

Fig. 3. (a) HPLC separation of Aminohexyl Sepharose pool 2 on a TSK preparative DEAE 5-PW column, The pooled fractions from Aminohexyl Sepharose were applied to the column and eluted as described in Experimental. (b) SDS gel electrophoresis of the fractions obtained from the DEAE 5-PW column. Several protein bands are marked as in Fig. 2. Note that the two protein bands corresponding to the last two large peaks showed similar electrophoretic mobility, while the band marked b migrated slightly more rapidly than the other two bands.

column (Fig. 3) partly because of the capacity of the HPLC column. Although there are similarities between the two chromatograms (Figs. 2 and 3), two significant differences are noted. First, the last large peak is now split into two peaks of similar size, and the two corresponding protein bands migrated together in SDS gel (Fig. 3b). These two proteins migrated at the same rate as 3b, obtained from pool 1, and were further purified separately in order to establish their identity, as will be described below. Secondly, a protein corresponding to epoxide hydrolase was eluted earlier than the P-450 isozyme marked as a, suggesting the separation of the two epoxide hydrolase isozymes in the Aminohexyl Sepharose column[22]. In contrast, other proteins, such as fp1 and P-450 isozymes 2, 3c and the two new isozymes marked as a and b, were eluted as in the resolution of pool 1, although the first peak, containing P-450 2 and 3c, was smaller, and correspondingly, less 3c was seen in the SDS gel. There is some partial resolution of various proteins in the first peak of the Aminohexyl Sepharose chromatogram.

Comparative trypsin peptide mapping of P-450s

In order to establish the identity of the two P-450 isozymes which migrated with isozyme 3b in SDS gel electrophoresis but were resolved by preparative DEAE-HPLC (Fig. 3), each peak was separately purified to homogeneity by analytical

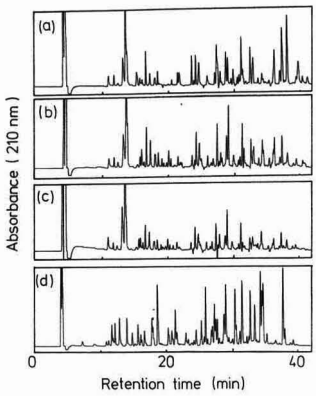

Fig. 4. Comparative HPLC trypsin peptide mapping of P-450 isozymes. (a) P-450 isozyme 3b, isolated from pool 1 of the aminohexyl Sepharose column, (b) the two isozymes migrating with 3b, isolated from pool 2 of the aminohexyl Sepharose column (first peak) and (c) preparation obtained from the second peak were treated with trypsin, and the resulting tryptic peptides were separated on a Vydac C_{18} reversed-phase column, as described in Experimental. For comparison, P-450 isozyme 4, purified from β-naphthoflavone-induced rabbit liver microsomes, which has little sequence similarity with isozyme 3b[6] was treated with trypsin, and the peptides obtained were separated (d). The baseline, obtained from a trypsin control, was subtracted by using a Shimadzu C-R3A integrator.

DEAE-HPLC and HPLC on hydroxyapatite columns. The purified P-450 isozymes were treated with trypsin, and the resulting tryptic peptides were separated on a Vydac C_{18} reversed-phase column, as described in Experimental. As shown in Fig. 4, the two isozymes isolated from pool 2 showed almost the same peptide pattern as isozyme 3b isolated from pool 1, although some differences were noted. These results suggest that the three preparations are at least very similar in primary structure. Several lines of evidence, which suggest the presence of variants of isozyme 3b in rabbit liver microsomes, have recently been reported[23], although the isolation of these variants has not yet been achieved. The preparations obtained in the present study, therefore, may represent these isozyme 3b variants. Studies are now in progress to clear up the relationship between these preparations.

Reconstitution of monooxygenase activity

Three proteins isolated from rabbit liver microsomes as described above were then incorporated into liposomal membranes by the cholate dialysis method[2–5] in order to examine the intactness of the purified proteins. Proteins fp2 and P-450 isozyme 2, from the first peak of the preparative DEAE-HPLC column, which has been further purified by HPLC on hydroxyapatite, and various amounts of cytochrome b_5 were reconstituted into liposomes of egg yolk phosphatidylcholine. As shown in Fig. 5, the inclusion of b5 in the system stimulates the monooxygenase activity. This confirms the previous observations that the second of the two electrons needed for the monooxygenase reaction is preferentially supplied by b5[3] and shows clearly that the enzyme preparations obtained in the present study by HPLC keep their structure intact, and are able to interact properly with each other in the liposomal membranes as in intact microsomes.

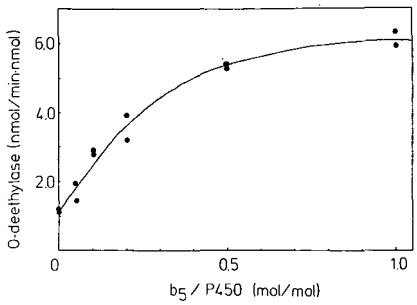

Fig. 5. Effect of b5 on the reconstituted monooxygenase activity. Purified cytochrome P-450 isozyme 2, fp2, and various amounts of b5 in a molar ratio of fp2–P-450–lipid = 1:1:400 were incorporated into liposomes of egg yolk phosphatidylcholine, and the NADPH-dependent monooxygenase was measured with ethoxycoumarin as a substrate as described in Experimental.

CONCLUSION

The combination of conventional hydrophobic interaction chromatography (Aminohexyl Sepharose column) with HPLC on resin-based ion-exchange columns and hydroxapatite columns, developed for protein purification, enabled a rapid simultaneous resolution and isolation of various component proteins of the hepatic microsomal monooxygenase system. In addition to the three proteins which supply electrons to P-450 (fp1, fp2, b5), various P-450 isozymes, including two unknown isozymes, were easily purified. At least two variants of P-450 isozyme 3b were separated by anion-exchange HPLC. The purified proteins conserved their ability to bind to liposomal membranes, and monooxygenase activity was restored when these proteins were incorporated into membranes. The HPLC techniques are, therefore, very useful in the study of complex membrane-bound enzyme systems.

REFERENCES

1 R. Sato and T. Omura (Editors), *Cytochrome P-450*, Kodansha-Academic Press, Tokyo, New York, 1979.
2 H. Taniguchi, Y. Imai, T. Iyanagi and R. Sato, *Biochim. Biophys. Acta*, 550 (1979) 341.
3 H. Taniguchi, Y. Imai and R. Sato, *Arch. Biochem. Biophys.*, 232 (1984) 585.
4 H. Taniguchi, Y. Imai and R. Sato, *Biochemistry*, 26 (1987) 7084.
5 H. Taniguchi and W. Pyerin, *J. Cancer Res. Clin. Oncol.*, 114 (1988) 335.
6 P. R. Ortiz de Montellano (Editor), *Cytochrome P-450, Structure, Mechanism and Biochemistry*, Plenum, London, 1986.
7 S. K. Bansal, J. H. Love and H. L. Gurtoo, *J. Chromatogr.*, 297 (1984) 119.
8 A. N. Kotake and Y. Funae, *Proc. Natl. Acad. Sci. U.S.A.*, 77 (1980) 6473.
9 Y. Funae and S. Imaoka, *Biochim. Biophys. Acta*, 842 (1985) 119.
10 Y. Imai and R. Sato, *J. Biochem. (Tokyo)*, 75 (1974) 689.
11 Y. Imai, *J. Biochem. (Tokyo)*, 80 (1976) 267.
12 K. Mihara and R. Sato, *J. Biochem. (Tokyo)*, 71 (1972) 725.
13 K. Mihara and R. Sato, *J. Biochem. (Tokyo)*, 78 (1975) 1057.
14 T. Iyanagi and H. S. Mason, *Biochemistry*, 12 (1973) 2297.
15 U. K. Laemmli, *Nature (London)*, 227 (1970) 680.
16 O. H. Lowry, A. J. Rosebrough, A. L. Farr and R. J. Randall, *J. Biol. Chem.*, 193 (1951) 265.

17 Y. Imai and R. Sato, *Biochem. Biophys. Res. Commun.*, 60 (1974) 8.
18 Y. Imai, C. Hashimoto-Yutsudo, H. Satake, A. Girardin and R. Sato, *J. Biochem. (Tokyo)*, 88 (1980) 489.
19 F. P. Guengerich, *Pharmacol. Ther.*, 6 (1979) 99.
20 D. R. Koop, E. T. Morgan, G. E. Tarr and M. J. Coon, *J. Biol. Chem.*, 257 (1982) 8472.
21 J. Halpert, H. Glaumann and M. Ingelman-Sundberg, *J. Biol. Chem.*, 254 (1979) 7434.
22 F. P. Guengerich, P. Wang, M. B. Mitchel and P. S. Mason, *J. Biol. Chem.*, 254 (1979) 12248.
23 H. Dieter and E. F. Johnson, *J. Biol. Chem.*, 257 (1982) 9315.

Journal of Chromatography, 476 (1989) 309–318
Elsevier Science Publishers B.V., Amsterdam — Printed in The Netherlands

CHROMSYMP. 1585

CROWN ETHERS AS LIGANDS FOR HIGH-PERFORMANCE LIQUID CHROMATOGRAPHY OF PROTEINS AND NUCLEIC ACIDS

DJURO JOSIĆ* and WERNER REUTTER
Institut für Molekularbiologie und Biochemie, Freie Universität Berlin, Arnimallee 22, D-1000 Berlin 33 (Dahlem) (F.R.G.)
and
JOACHIM REUSCH
Säulentechnik Dr. Knauer GmbH, Hegauer Weg 38, D-1000 Berlin 37 (F.R.G.)

SUMMARY

By immobilization of the crown ether 1,10-diaza-18-crown-6 to different porous and non-porous, epoxy-activated supports, a chromatographic sorbent was prepared, which, mediated by potassium ions, can be used for the separation of both nucleic acids and proteins. Model experiments have been carried out with ribonucleic and deoxyribonucleic acids. In experiments with standard proteins the influence of pH and the role of loading of the column with potassium ions were demonstrated. The column was used for separating complex protein mixtures, such as serum and plasma membrane extracts, in the presence of detergents.

INTRODUCTION

Crown ethers are neutral, macrocyclic polymers. In 1967 Pedersen[1] demonstrated for the first time that the cyclically arranged ethylene glycol units can form stable and stoichiometrically defined complexes with alkali-metal cations. In the presence of such cations, all C–O–C structure elements point inwards, thus coordinating them by means of ion–dipole interaction. As a consequence of this orientation, all CH_2 groups point outwards and, in a way, the cation is coated by a lipophilic environment. Therefore, alkali-metal salts can be dissolved in lipophilic media[2] or channeled in complex form through lipophilic membranes, *e.g.*, into a cell[3]. The formation of complexes takes place in an highly selective manner. A potassium ion with an ionic radius of 2.66 Å, for example, will fit well into the inner cavity of an 18-crown-6 molecule, which has an diameter of 2.70 Å. However, a sodium ion, with its smaller diameter, will not take up all the space, and consequently will form less stable complexes.

As crown ethers not only coordinate metal ions, but also ammonium, diazonium and guanidinium ions, corresponding asymmetric ligands should allow chiral separations as well. A kind of made-to-measure cavity architecture provides a close adaption to the structural characteristics of the target molecule[4,5]. Specific interac-

0021-9673/89/$03.50

tions of crown ethers and nucleic acids was first observed by Pitka and Smid[6]. They found that, in the presence of potassium ions, polyadenylate formed a water-insoluble complex with the water-soluble poly-vinylbenzo-18-crown-6). In turn, polyadenylate immobilized on Sepharose can bind poly(vinylbenzo-18-crown-6). The highest concentration of two crown ether molecules per nucleotide is reached at a concentration of 0.1 *M* potassium ions.

The crown ether 1,10-diaza-18-crown-6 contains two secondary amino groups in its molecule and can therefore be immobilized on activated rigid supports, such as silica gel or organic polymers. In order to provide better interaction between the immobilized crown ether and the ligate, sufficient space between the ligand and matrix is necessary. This is achieved through a spacer[7,8]. Fig. 1 shows the course of such reaction.

In this paper, the synthesis of chromatographic sorbents with immobilized crown ethers is described, together with their use in high-performance liquid chromatography (HPLC) of nucleic acids and proteins.

EXPERIMENTAL

Chemicals

All chemicals were of analytical reagent grade from Merck (Darmstadt, F.R.G.) or Sigma (München, F.R.G.). Bacterial RNA and DNA samples were a gift from Dr. B. Wittig (Institut für Molekularbiologie und Biochemie, Freie Universität, Berlin, F.R.G.). Liver plasma membranes were isolated and fractionated by stepwise extraction, as described elsewhere[9].

Immobilization of ligands

The 1,10-diaza-18-crown-6 was immobilized on epoxy-activated silica gel (Eu-

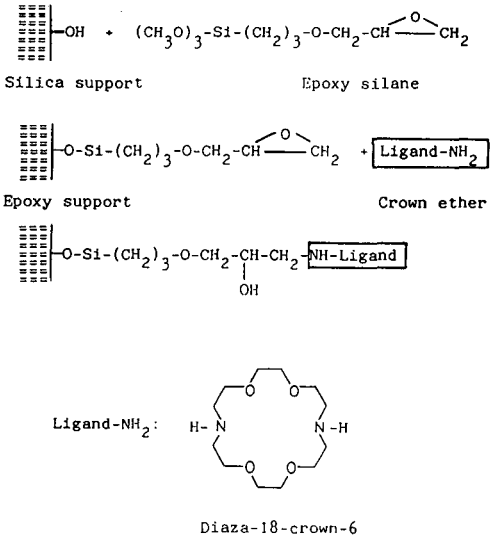

Fig. 1. Route for the preparation of ligand-substituted silica or polymer support.

rochrom; Säulentechnick Knauer, Berlin, F.R.G.) or polymethacrylamide (Eupergit, Röhm Pharma, Weiterstadt, F.R.G.), as described elsewhere[7,8]. The characteristics of the silica gel support were: particle size 7 μm and pore size 300 Å. The synthetic support, Eupergit C 30N had 30-μm particles and 450-Å pores, the non-porous Eupergit C 1Z had 1-μm particles.

HPLC

The HPLC system consisted of two pumps, a programmer, a spectrophotometer with a deuterium lamp, a loop injection valve (all from Knauer, Berlin, F.R.G.) and a Frac-100 fraction collector (Pharmacia-LKB, Freiburg, F.R.G.). The chromatographic conditions are given in the Figure legends.

Protein recovery was determined by measuring the protein concentration before and after separation according to the procedure of Lowry *et al.*[10]. The recovery of dipeptidylpeptidase IV (DPP IV) was determined by measuring its enzymatic activity[11].

Columns

All analytical columns, with dimensions of 60 mm × 4.0 mm, and all semipreparative columns, with dimensions of 120 mm × 8.0 mm, were produced and packed by Säulentechnik Knauer.

Buffers

The following buffers were used: eluent A was 5 m*M* Tris–HCl (pH 6.8), containing 20 or 50 m*M* KCl. The elution buffer (eluent B) was eluent A with 1 *M* NaCl added. In some experiments 0.1% (w/v) detergent was added to both buffers.

Sodium dodecyl sulphate–polyacrylamide gel electrophoresis (SDS-PAGE)

Dialysed and freeze-dried samples were dissolved in 62.5 m*M* Tris–HCl buffer (pH 6.8), containing 3% (w/v) SDS, 5% (v/v) mercaptoethanol, 10% (v/v) glycerol and 0.001% (w/v) bromophenol blue and boiled for 3 min. SDS-PAGE was performed by the Laemmli method[12]. An amount of 100–150 μg of protein was applied to each track when standard equipment was used (Pharmacia-LKB). Between 5 and 15 μg of protein were applied to each track when working with a mini-system (Bio-Rad, München, F.R.G.).

RESULTS AND DISCUSSION

Production of chromatographic supports with immobilized crown ethers

To the epoxy-activated silica gel or the synthetic support, Eupergit, 1,10-diaza-18-crown-6 is added to excess. It is assumed that one ligand has bound to each epoxy group (see Fig. 1). The activated silica gel contains between 250 and 300 μmol epoxy groups per 1 g of dry gel while Eupergit C 30N contains about twice as much. Non-reacted epoxy groups are blocked with mercaptoethanol by shaking for 2 h, a procedure which is routinely used for the binding of ligands. The capacity of the silica-based support with crown ether ligands is about 25 mg of 5S RNA per g (ref. 1), and about 40 mg of 5S RNA per 1 g of Eupergit C 30N support. The capacity of non-porous Eupergit C1Z crown ether support is 5–10% of the capacity of Eupergit

C 30N crown ether. This is explained by the fact that the specific surface area of this support is smaller, and the amount of available ligand therefore lower.

Separation of nucleic acids

The interaction between nucleic acids and crown ethers, as observed by Pitka and Smid[6], is the basis of their chromatographic separation. The separation is reproducible, the retention time depending on the size of the nucleic acid. As is seen in Fig. 2, the smaller 5S rRNA is eluted before the larger 23S rRNA. Fig. 3 shows the separation of denatured and coiled DNA from a plasmid of *Escherichia coli*. The only difference between the two components is that the denaturated DNA is unfolded; it is exposing more phosphate groups for interaction with the potassium ions, immobilized in crown ether, than the non-denaturated coiled DNA. Consequently, the retention time for denaturated DNA is longer. The smaller by-products, which have resulted from cleavage of the DNA during the isolation process, have a shorter retention time, or are even excluded in the dead-volume (see smaller peaks in the front in Fig. 3). Nucleotides are not bound, which suggests that several free phosphate groups are necessary for strong binding to the support (Fig. 4). This is confirmed by the experiment shown in Fig. 5. A thymus DNA sample was separated before and after digestion with DNAse on an Eupergit C1Z crown ether column with 1-μm non-porous particles. In this way, the progress of digestion can easily be controlled since the chromatographic analysis takes only 10 min.

Fig. 4 shows a model representing the interaction between the nucleic acids and the potassium ions, immobilized on the crown ethers. It is shown that the interaction

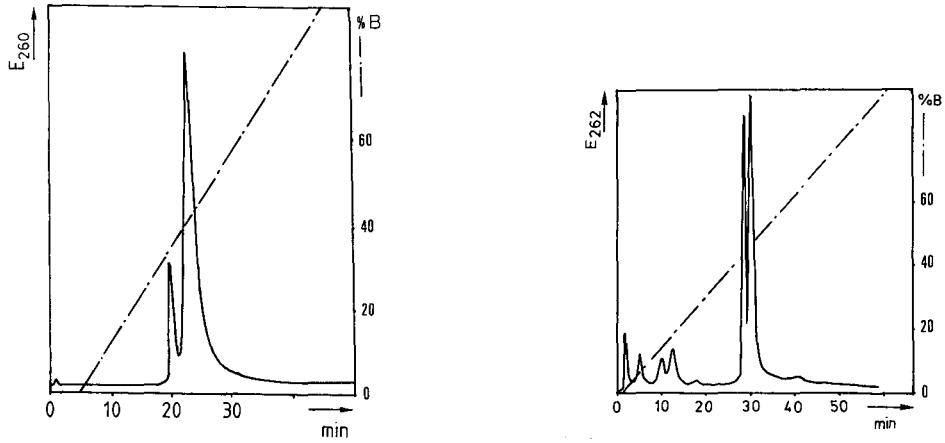

Fig. 2. Separation of 5S and 23S rRNA from *Bacillus stearothermophilus*. An 0.5-mg sample was applied to a 60 mm × 4.0 mm silica-based crown ether column. The content of KCl in the loading buffer (A) was 50 m*M*; the pH of both buffers was 7.6. Other chromatographic conditions: flow-rate, 1 ml/min; pressure, 6.0 MPa; room temperature. The gradient is shown in the chromatogram. For other conditions see Experimental.

Fig. 3. Separation of denaturated and coiled DNA of a plasmid from *Escherichia coli*. A 25-μg sample in 20 μl of eluent A was loaded on the column. The first peak is denatured DNA, the second is non-denatured, coiled DNA. Products resulting from the cleavage are either excluded or appear at the beginning of the gradient. Chromatographic conditions as in Fig. 2.

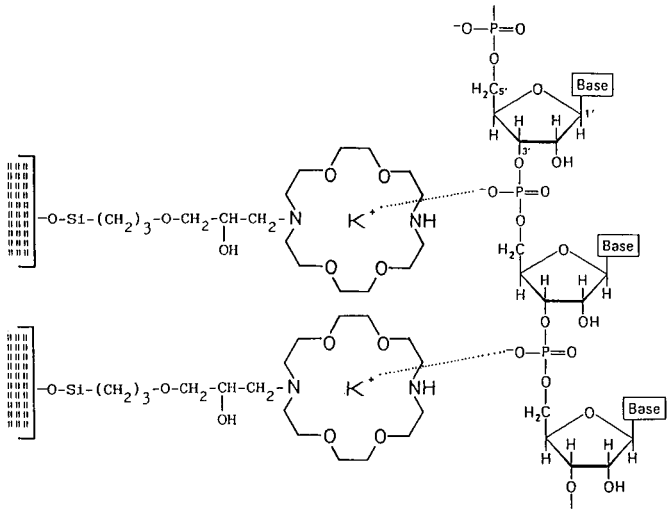

Fig. 4. Interaction between the nucleic acids and the potassium ions immobilized on crown ethers.

with the ligate and, consequently, its retention time increases with the number of free phosphate groups available on the molecule surface.

Separation of proteins

Some proteins also interact with immobilized ethers. This interaction is mediated by potassium ions and is pH-dependent (see Fig. 6 a–c for the pH dependency of such separations). Of the standard proteins, transferrin and ovalbumin are hardly retarded at all at pH 4.2. If, however, the column is previously saturated with potassium ions by injecting 1 ml of 0.5 *M* KCl, a fundamental change is observed. The retention time of all three standard proteins, transferrin, ovalbumin and ferritin, is extended (*cf.*, the dashed line in Fig. 6a). A similar, though less distinct effect is seen

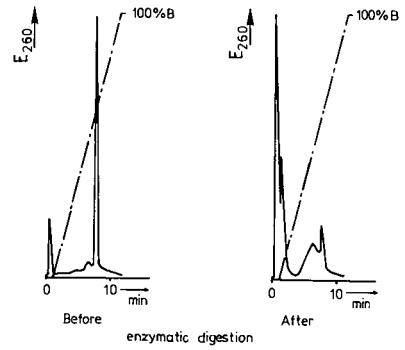

Fig. 5. Separation of a thymus DNA sample before and after DNAse digestion. For each experiment, 25 μg of sample were applied to the column. DNA is retarded on the column; the short-chain products after digestion are excluded. Chromatographic conditions: column, 60 mm × 4.0 mm; packed with the non-porous support Eupergit C 1Z crown ether (particle size 1 μm); flow-rate, 0.5 ml/min; pressure, 8.0–12.0 MPa; room temperature. The gradient is shown in the chromatogram. For other conditions see Fig. 2.

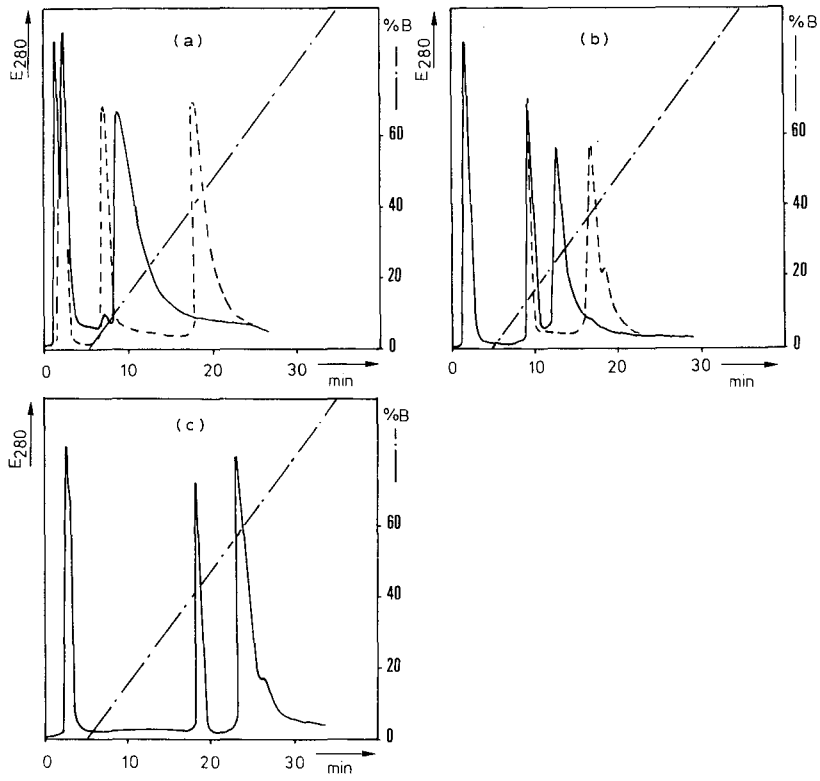

Fig. 6. Influence of pH on the separation of the standard proteins transferrin, ovalbumin and ferritin: pH 4.2 (a); 5.8 (b) and 6.8 (c). (———) Without loading of the column with 1 ml of 0.5 *M* KCl; (– – –) after loading the column with 1 ml of 0.5 *M* KCl. For chromatographic conditions see Fig. 2.

during the separation at pH 5.8 (see Fig. 6b). Here, the retention of ferritin is prolonged considerably. If the separation is carried out at pH 6.8, the previous saturation with potassium ions has no effect at all on the retention time of the standard proteins used (see Fig. 6c). This suggests that the pH dependency affects the loading of the crown ethers with potassium ions rather then the interaction between the ligates and the already immobilized potassium ions. At pH 6.8 a concentration of 50 m*M* potassium in the equilibration buffer (eluent A) is sufficient to saturate the immobilized crown ethers. Such a saturation is not provided by 50 m*M* potassium at lower pH.

The columns with synthetic supports (Eupergit C 30N and C 1Z) show a slightly different behaviour in this respect. Retention times are similarly pH dependent; the column loading with potassium ions has to be carried out in all cases, regardless of the pH investigated. This is shown in Fig. 7 in the case of the Eupergit C 1Z column. If the column is not saturated with KCl, all three standard proteins are excluded, even at pH 6.8 (*cf.*, the chromatogram on the left in Fig. 7). Retention of standard proteins and their separation is achieved only after saturation of the column with 1 ml of 0.5 *M* KCl (chromatogram on the right of Fig. 7).

The model for the interaction between nucleic acids and potassium ions immobilized on crown ether, as shown in Fig. 4, cannot be applied to proteins without some

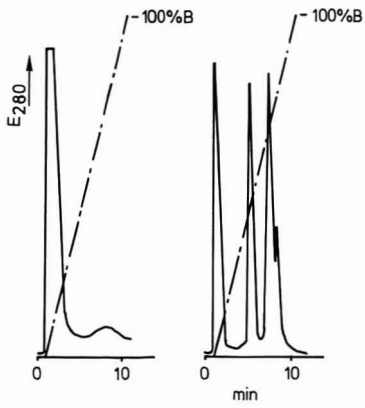

Fig. 7. Separation of the standard proteins transferrin, ovalbumin and ferritin on the Eupergit C 1Z crown ether column with 1-μm non-porous particles. Buffer pH, 6.8. On the left, no loading of the column with an injection of 0.5 *M* KCl; on the right, the column was loaded with 200 μl 0.5 *M* KCl. Other conditions as in Fig. 5.

modification. Here, the non-phosphorylated proteins, such as serum albumin, are also retarded (not shown). The basic proteins such as trypsin inhibitor, lysozyme and cytochrome *c* do not bind to the crown ether column, and neither does immunoglobulin G (IgG). A comparison between crown ether sorbents and anion exchangers shows that the crown ether columns behave completely different in protein separation. Both trypsin inhibitor and IgG are bound by most anion exchangers at low salt concentrations[13], but not by crown ether sorbents under identical conditions. For the interaction of crown ethers with nucleic acids as well as with proteins, the immobilized potassium ion has an important function. Without loading with KCl, none of the listed substances can be bound (*cf.*, Fig. 7).

Further investigations were carried out with complex protein mixtures, such as serum samples and plasma membrane extracts. The object of these experiments was to find out whether the columns can also be used under complex conditions, *e.g.*, with the application of detergents and with samples that contain less water-soluble components.

Fig. 8 shows the separation of a sample containing rat serum on a crown ether column with silica gel as the support. Under the conditions used for the separation of standard proteins (see above, Fig. 6c), most sample components do not bind to the column. Even serum albumin is excluded, although it was retarded in other experiments, when a salt gradient had to be used for elution (see Fig. 8b, left). However, when 0.1% (w/v) detergent is added, *e.g.*, octyl glucoside or decanol-N-methylglucamide (MEGA-10), the separation is markedly improved (Fig. 8b, centre and right). In the presence of 0.1% MEGA-10, transferrin (peak 1), serum albumin (2) and a protein with an apparent molecular weight in SDS-PAGE of 200 000 daltons (probably fibronectin, 3) were isolated.

As serum albumin tends to aggregate with itself and other proteins, the improved separation in the presence of a detergent can be explained by the prevention of this kind of interaction. The non-ionic and zwitterionic detergents, *e.g.*, CHAPS, do not adversely affect column life and column performance.

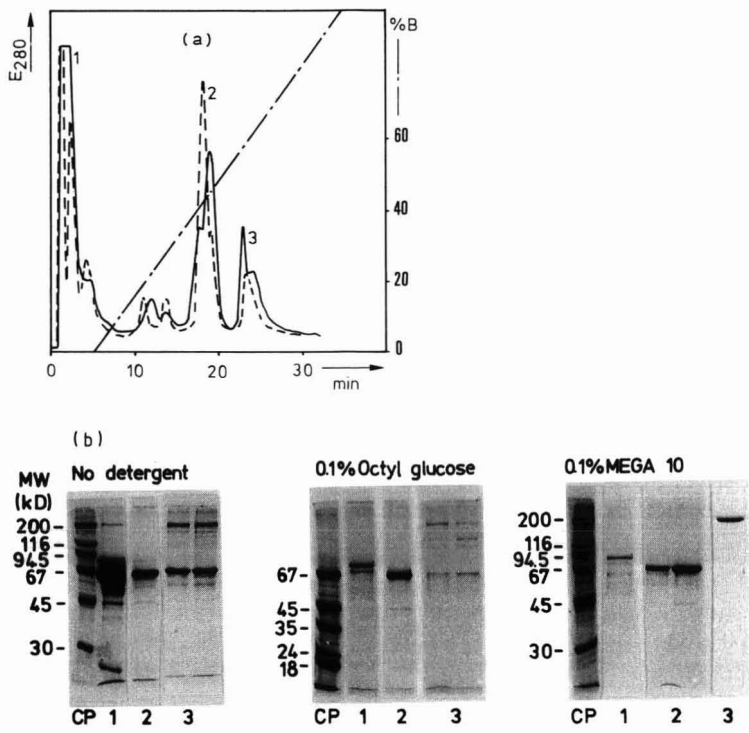

Fig. 8. Influence of detergents on the separation of serum proteins on a silica-based crown ether column. (a) The chromatogram, conditions as in Fig. 6c; (———) without detergent; (– – –) with 0.1% MEGA-10 in both buffers. (b) SDS-PAGE, showing the peaks in (a), with and without two different detergents. CP = Complex protein mixture.

In Fig. 9 another experiment is shown, involving the separation of a complex protein mixture. From a liver plasma membrane extract, 60 mg of protein were applied to an 120 mm × 8.0 mm crown ether column with silica gel as the support, leading to an enrichment of the enzyme dipeptidylpeptidase IV. The separation was carried out in the presence of 0.1% Triton X-100 (reduced). The recovery of the enzymatic activity was 80–95%; the enrichment in one step was 20- to 30-fold. During separation with a gradient of 0–1 *M* NaCl in the presence of Triton X-100, 80% of the proteins were recovered, and another 18% were obtained by elution with a 1% aqueous Triton X-100 solution (arrow in Fig. 9).

The following results, which are shown in this report, suggest that interactions other than ion-exchange mechanisms are also involved:

Mono- and short oligonucleotides are not bound by the crown ether sorbent, see Fig. 5. Apparently several phosphate groups are required for retention, see the model in Fig. 4

Without potassium ion loading, none of the investigated substances was bound to the column

Comparisons carried out between crown ether sorbents and anion exchangers have shown a clearly different behaviour in the separation of standard proteins as well as serum proteins, *cf.*, ref. 13.

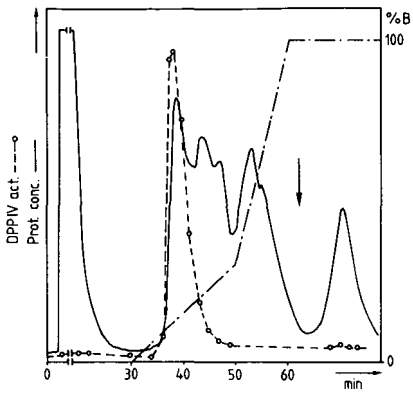

Fig. 9. Separation of membrane proteins on a 120 mm × 8.0 mm silica-based crown ether column. A protein (60 mg), dissolved in 20 ml of eluent A, was applied to the column. Separation was carried out in the presence of 0.1% Triton X-100 (reduced). The protein content (———) and dipeptidyl peptidase (DPP) IV enzymatic activity (– – –) were determined. In the non-bound fraction and up to 100% eluent B, 47.6 mg of protein (80%) were recovered. The remaining 10.8 mg of protein (18%) were recovered by an injection of 5 ml of 1% Triton X-100 in eluent B (arrow in the chromatogram). Chromatographic conditions: flow-rate, 1 ml/min; pressure, 1.0 MPa; room temperature. The gradient is shown. For other conditions see Fig. 6c and Experimental.

These results also show a similarity between crown ether sorbents and other sorbents used for the separation of biopolymers, such as hydroxyapatite and triazine dyes. All these substances are regarded as pseudo-affinity ligands, which can bind a variety of biopolymers. The nature of the underlying separation mechanism, however, is not yet fully understood[14].

Both a silica-based and a synthetic support column have shown no impairment in performance after being used for 150 separations. The application of non-ionic and zwitterionic detergents has not affected the column life. However, the use of the denaturing agents urea and guanidine hydrochloride (guanidinium) must be avoided, as they impair columns performance considerably and irreversibly, even after only two to three separations. This is probably due to the blocking of crown ethers by the formation of complexes with these substances[4]. This, in turn, prevents the loading of the column with potassium ions. SDS can form an insoluble precipitate with sodium, and cannot be used for separation for this reason.

ACKNOWLEDGEMENTS

This research was supported by the Deutsche Forschungsgemeinschaft (Re 523/3-i), the Fonds der Chemischen Industrie, Maria Sonnenfeld-Stiftung and Trude-Goerke-Stiftung.

REFERENCES

1 C. J. Pedersen, *Angew. Chem.*, 84 (1972) 16.
2 J. Berger, A. J. Rachlin, W. E. Scott, L. H. Sternbach and W. M. Goldberg, *J. Am. Chem. Soc.*, 73 (1951) 287.
3 P. O. Chock and E. O. Titus, *Prog. Inorg. Chem.*, 18 (1973) 287.

4 D. J. Cram and J. M. Cram, *Science (Washington, D.C.)*, 183 (1974) 803.
5 G. Manecke and H. J. Winter, *Makromol. Chem. Rep. Commun.*, 2 (1981) 569.
6 J. Pitka and J. Smid, *Biochim. Biophys. Acta*, 425 (1976) 287.
7 J. Reusch, *Labo (German)*, No. 153/1988, 38.
8 Dj. Josić, W. Reutter and D. Krämer, *Angew. Makromol. Chem.*, in press.
9 Dj. Josić, W. Schütt. R. Neumeier and W. Reutter, *FEBS Lett.*, 185 (1985) 182.
10 D. H. Lowry, N. J. Rosenbrough, A. L. Farr and R. J. Randall, *J. Biol. Chem.*, 195 (1951) 265.
11 S. Hartel, Ch. Hanski, W. Kreisel, C. Hoffmann, J. Mauck and W. Reutter, *Biochim. Biophys. Acta*, 924 (1987) 543.
12 U. K. Laemmli, *Nature (London)*, 227 (1970) 680.
13 Dj. Josić, W. Hofmann and W. Reutter, *J. Chromatogr.*, 371 (1986) 43.
14 Dj. Josić, A. Becker and W. Reutter, in M. T. W. Hearn (Editor), *HPLC of Peptides, Proteins and Polynucleotides*, Verlag Chemie, Weinheim, New York, in press.

Journal of Chromatography, 476 (1989) 319–327
Elsevier Science Publishers B.V., Amsterdam — Printed in The Netherlands

CHROMSYMP. 1604

COMPARISON OF NON-IONIC DETERGENTS FOR EXTRACTION AND ION-EXCHANGE HIGH-PERFORMANCE LIQUID CHROMATOGRAPHY OF SENDAI VIRUS INTEGRAL MEMBRANE PROTEINS

J. VAN EDE*, J. R. J. NIJMEIJER and S. WELLING-WESTER
Laboratorium voor Medische Microbiologie, Oostersingel 59, 9713 EZ Groningen (The Netherlands)
C. ÖRVELL
Department of Virology, Karolinska Institute, School of Medicine and Department of Virology, National Bacteriological Laboratory, S-10521 Stockholm 1 (Sweden)
and
G. W. WELLING
Laboratorium voor Medische Microbiologie, Oostersingel 59, 9713 EZ Groningen (The Netherlands)

SUMMARY

The integral membrane proteins of Sendai virus haemagglutinin–neuraminidase (HN) and fusion protein (F) were extracted from purified virions with 2% of a non-ionic detergent, *i.e.*, polyoxyethylene alkyl ethers varying by 8–14 hydrocarbon units in the alkyl chain and by 4–8 ethylene glycol units in the oxyethylene chain. Triton X-100 and octyl glucoside were included as reference detergents. The hydrophile–lipophile balance (HLB) and the critical micelle concentration (CMC) of the detergents were determined. A decrease in length of the oxyethylate by 8–5 ethylene glycol units and an increase in the alkylate by 8–12 hydrocarbon units resulted in higher yields of extracted proteins. The highest yields were obtained for $C_{12}E_5$ with an HLB of 11.7. Yields of extracted protein could be correlated with the HLB values of the polyoxyethylene alkyl ethers. The structural integrity of HN and F was not affected during extraction by either detergent as measured by their reactivity with monoclonal antibodies directed against native HN and F. Extracts were subjected to anion-exchange high-performance liquid chromatography (HPLC) on a Mono Q column in the presence of 0.1% of the detergent used for extraction. Eluate fractions were analysed by sodium dodecyl polyacrylamide gel electrophoresis and recoveries of HN and F protein were determined by size-exclusion HPLC. The immunological activity of HN and F was tested in an enzyme-linked immunosorbent assay. The highest recoveries of HN and F (80%) were obtained with $C_{10}E_5$ in the elution buffer. HN and F were partially purified and the immunological activity was well preserved.

INTRODUCTION

Polyoxyethylene alkyl ethers are widely used as non-ionic detergents (surfactants)[1]. In biological research, they are employed for the solubilization of membrane

0021-9673/89/$03.50

proteins[2] and as additives in eluents for various modes of high-performance liquid chromatography (HPLC)[3–5]. Organic solvents which have been used for solubilization often cause denaturation of membrane proteins, whereas non-ionic detergents effective in solubilizing the protein allow their isolation in a biologically active form[2,6]. To study the enzymic, immunological as well as physico-chemical properties of hydrophobic proteins and for detergent removal or exchange in the preparation of membrane proteins, chemically pure and homogeneous non-ionic detergents are required[7]. Early studies were made with commercial products that best embodied the desired properties, but these products are often chemically impure and heterogeneous and hence may vary from one preparation to another. In ionic detergents the solubilizing power of the ionic group is fixed, and the hydrophobic group must be modified to alter the detergent properties. However, in non-ionic detergents the hydrophilic characteristic of the oxyethylate increases with increasing chain length and hence there is the possibility in oxyethylene-based compounds of modifying both the hydrophilic and the hydrophobic portions. Nowadays, many systematic changes in their structure have been made in order to produce pure and homogeneous detergents with extremely low toxicity, for a wide range of applications in biochemical research.

This paper reports a comparative study of a number of non-ionic detergents, *i.e.*, the polyoxyethylene (E_y) alkyl (C_x) ethers C_8E_5, C_8E_6, C_8E_7, $C_{10}E_5$, $C_{10}E_6$, $C_{10}E_7$, $C_{10}E_8$, $C_{12}E_4$, $C_{12}E_5$, $C_{12}E_6$, $C_{12}E_7$, $C_{12}E_8$, $C_{14}E_5$, Triton X-100 and octyl glucoside with Sendai virus envelope proteins as a model. Sendai virus is a paramyxovirus of mice. The viral envelope is composed of a lipid bilayer in which two integral membrane proteins are embedded, the fusion protein F (Mr = 65 000) and the haemagglutinin–neuraminidase protein HN (Mr = 68 000). Detergent extracts contain the F protein in a monomeric form and the HN protein in a tetrameric (HN_4), dimeric (HN_2) and occasionally a truncated form of the dimer without the anchoring region of the polypeptide chain (HN_2–)[8]. Both are hydrophobic proteins. The detergents were compared with respect to their ability to solubilize these proteins and the preservation of their immunological activity after extraction. In addition, a possible relationship between extraction properties and either the critical micelle concentration (CMC), *i.e.*, the concentration at which micelles begin to form, or the hydrophile–lipophile balance (HLB), *i.e.*, the ratio between the hydrophilic oxyethylene part and the hydrophobic alkyl part, was investigated.

The suitability of some of the detergents as additives in ion-exchange (IE) HPLC eluents was investigated with respect to separation, recovery and immunological activity of the proteins after IE-HPLC.

EXPERIMENTAL

Detergent extraction of Sendai virus

Sendai virus was cultured in 10-day-old embryonated chicken eggs. Allantoic fluid was collected after incubation for 72 h at 37°C. Debris was removed by low-speed centrifugation (10 min at 2000 *g*) and virus was pelleted by ultracentrifugation (90 min at 70 000 *g*). Virus pellets were resuspended in 10 m*M* Tris–HCl (pH 7.2) containing 10% (w/v) sucrose and stored at −80°C. The amount of protein was determined[9]. Sendai virus suspensions containing 40 mg of protein were pelleted (90 min at 100 000 *g*) and resuspended in 1 ml of 10 m*M* Tris–HCl (pH 7.2). Detergent

extraction of F and HN proteins was performed by the addition of 1 ml of the same buffer, containing 4% (w/w) detergent [detergent to protein ratio = 1 (w/w)]. After 20 min at room temperature, extraction was terminated by ultracentrifugation (90 min at 100 000 *g*), and the supernatant, which contained the virus proteins HN and F, was stored in aliquots of 200 μl at −80°C. In some cases, detergent was removed by treatment with Amberlite XAD-2[8].

Detergents

Extraction and chromatography of the Sendai membrane proteins were performed with non-ionic detergents, *i.e.*, different polyoxyethylene alkyl ethers, Triton X-100 (BDH, Poole, U.K.) and 1-O-*n*-octyl β-D-glucopyranoside (octyl glucoside) (Boehringer, Mannheim, F.R.G.). The polyoxyethylene alkyl ethers C_8E_5, C_8E_6, C_8E_7, $C_{10}E_5$, $C_{12}E_5$ and $C_{12}E_8$ were a gift from Kwant-Hoog Vacolie Recycling and Synthesis (Bedum, The Netherlands). The polyoxyethylene alkyl ethers $C_{10}E_6$, $C_{10}E_7$, $C_{10}E_8$, $C_{12}E_4$, $C_{12}E_6$, $C_{12}E_7$ and $C_{14}E_5$ were obtained from Fluka (Buchs, Switzerland).

Determination of critical micelle concentration and hydrophile–lipophile balance

The CMC of each detergent was determined with magnesium 8-anilinonaphthalene-1-sulphonate (ANS)[10] (Fluka). The fluorescence of serially diluted detergent solutions in demineralized water was measured with ANS using a Perkin-Elmer LS-2 filter fluorimeter. The excitation wavelength was 375 nm and the emission wavelength was 490 nm.

The HLB of polyoxyethylene alkyl ethers was calculated as the weight percentage of the oxyethylene content divided by 5, as described by Becher[11].

Size-exclusion and ion-exchange HPLC

Chromatography was performed with an LKB 2150 pump (LKB, Zoetermeer, The Netherlands), a Rheodyne 7125 injector (Inacom, Veenendaal, The Netherlands), a Waters 441 detector (Waters, Etten Leur, The Netherlands) or an LKB 2151 detector connected with a Kipp BD 40 recorder (Kipp & Zonen, Delft, The Netherlands) and an LDC/Milton Roy Cl-10B integrator (Interscience, Breda, The Netherlands). Gradients were generated with an LKB 2152 LC controller and a LKB Ultrograd mixer driver.

Size-exclusion (SE) HPLC was performed on two tandem-linked Zorbax Bioseries GF 450 columns (250 × 9.2 mm I.D.) (DuPont, Wilmington, DE, U.S.A.) or on a TSK G4000SW column (600 × 7.5 mm I.D.) (LKB, Bromma, Sweden). Aliquots of 200 μl of virus envelope extracts were heated for 3 min in a boiling waterbath in the presence of 4% (w/w) sodium dodecyl sulphate (SDS) (electrophoresis grade, Bio-Rad Labs., Richmond, CA, U.S.A.) and injected into the HPLC system. The mobile phase was 50 m*M* sodium phosphate (pH 6.5) containing 0.1% SDS. The flow-rate was 1.0 ml/min and the absorbance was monitored at 280 nm. Yields of HN and F proteins were determined, using bovine serum albumin (BSA), ovalbumin (OVA) and trypsin inhibitor as a reference mixture with a concentration of 50 μg of each protein per 100 μl.

Anion-exchange (IE) HPLC was carried out on a Mono Q HR 5/5 column (50 × 5 mm I.D.) (Pharmacia, Uppsala, Sweden), which was eluted with 20 m*M*

Tris–HCl (pH 7.8) containing 0.1% (w/w) of the same detergent as used for extraction. A 24-min gradient from 0 to 0.5 *M* sodium chloride was started after 10 min of isocratic elution. The flow-rate was 1.0 ml/min and the absorbance was monitored at 280 nm. The total amount of protein injected was between 0.95 and 1.05 mg for each detergent extract. Fractions of 2–3 ml were collected in 70 × 11 mm Minisorp tubes (Nunc, Roskilde, Denmark), and aliquots of 50 μl of each fraction were analysed by SDS-polyacrylamide gel electrophoresis (PAGE). The remaining part of the fractions was dialysed against demineralized water and freeze-dried. Each freeze-dried fraction was dissolved in 560 μl of water. Samples of 140 μl were made 5% with respect to SDS, heated for 3 min in a boiling water-bath and analysed by SE-HPLC to determine the amount of HN and F protein present in the fractions. The remaining part (420 μl) was analysed in an enzyme-linked immunosorbent assay (ELISA).

SDS-PAGE

The eluate fractions were analysed on 8% SDS-polyacrylamide gels[12], and polypeptide bands were revealed by silver staining[13], using phosphorylase b (M_r = 92 500), bovine serum albumin (M_r = 68 000), the heavy chain of immunoglobulin G (IgG) (M_r = 50 000) and chymotrypsin (M_r = 23 500) as reference proteins.

Enzyme-linked immunosorbent assay with monoclonal antibodies (Mabs) against Sendai virus HN and F protein

The immunological activities of HN and F protein (i) in the extract and (ii) in the fraction after IE-HPLC were determined in an ELISA[8] with a panel of six Mabs against Sendai virus HN protein (97, 135, 851, 852, 1.182 and 820) and two Mabs against Sendai virus F protein (1.017 and 1.216)[14]. Plates were coated with a serial dilution of the extracts and of the IE-HPLC fractions, starting at a protein concentration of 1–5 μg per well, and the ELISA was performed as described earlier[8]. The absorbance was monitored at 492 nm and reactions were considered to be positive at $A_{492} \geqslant 0.2$. An absorbance of 1.2 at 492 nm was used as an arbitrary measure of immunological activity. The immunological activity is inversely related to the amount of protein needed to obtain an absorbance of 1.2 at 492 nm.

RESULTS AND DISCUSSION

Extraction of Sendai virus membrane proteins with different detergents: yields of HN and F protein by SE-HPLC

Characteristics of the non-ionic detergents that have been used in this study are listed in Table I. The suitability of these detergent for extraction of the Sendai virus integral membrane proteins HN and F was investigated, and the amount of HN and F protein in the extracts was determined by SE-HPLC. It has been calculated by others[15,16] that the amount of HN and F protein accounts for *ca.* 39% of the total amount of protein present in Sendai virus particles. Extraction of Sendai virus with $C_{12}E_5$ gave the highest yields, which was about one quarter of the total amount of HN and F protein. For different virus preparations the amount of HN and F extracted per milligram of virus by $C_{12}E_5$ was slightly different. A second and third successive extraction can enhance the yield, but may cause partial disruption of the virus particles, resulting in a mixture of membrane and internal proteins. To allow compar-

TABLE I

CHARACTERISTICS OF NON-IONIC DETERGENTS; RELATIVE YIELDS OF HN AND F PROTEIN AFTER EXTRACTION OF SENDAI VIRUS

Detergent	*MW*[a] *(average)*	*HLB*[b]	*CMC*[c] *(mg/ml)*	*Micellar wt.*[d] *(aggregation number)*	*Relative yield*[e] *(%)*
C_8E_5	350	13.5	3.2		65
C_8E_6	394	14.3	3.4	15.5 (39)	64
C_8E_7	438	14.8	3.7		62
$C_{10}E_5$	378	12.5	0.26		82
$C_{10}E_6$	422	13.3	0.35	32 (76)	77
$C_{10}E_7$	466	14.0	0.41		74
$C_{10}E_8$	510	14.5	0.47		71
$C_{12}E_4$	362	10.7	0.017		14
$C_{12}E_5$	406	11.7	0.020		100
$C_{12}E_6$	450	12.5	0.029	47 (105)	90
$C_{12}E_7$	494	13.2	0.033		78
$C_{12}E_8$	538	13.7	0.036	65 (120)	74
$C_{14}E_5$	434	10.9	0.004		14
Triton X-100	628	13.5	0.15	90 (140)	63
Octyl glucoside	292	12.6	7.1	8 (27)	43

[a] Molecular weights in daltons.

[b] Hydrophile–lipophile balance, calculated according to Becher[11].

[c] Critical micelle concentration, determined according to De Vendittis *et al.*[10].

[d] Micellar weights in kilodaltons, from refs 2, 3 and 19.

[e] The yield obtained with $C_{12}E_5$, which was *ca.* one quarter of the total amount of HN and F protein, was taken as 100%.

ison between different detergents, the highest yield obtained with extractions performed with $C_{12}E_5$ was taken as 100%. The relative yields of HN and F protein calculated for the different detergent extracts are shown in Table I. An increase in the number of ethylene glycol units in the oxyethylene chain from 5 to 8 (at a fixed alkyl chain length) and a decrease in the number of hydrocarbon units in the alkyl chain from 12 to 8 (at a fixed oxyethylene chain length) decreases the yields of HN and F protein in the extracts. An increase in the alkyl chain length to C_{14} or a decrease in the oxyethylene chain to E_4 resulted in very low yields (14%), and these detergents ($C_{14}E_5$ and $C_{12}E_4$) dissolved poorly in aqueous solutions and therefore were not suitable for IE-HPLC. Extracts of Sendai virus obtained with Triton X-100 and with octyl glucoside (included as reference detergents) gave protein yields of 63% and 43%, respectively.

In Fig. 1, the yields of protein after extraction are related to the HLB values of the detergents. The highest yields were obtained with polyoxyethylene alkyl ethers with HLB values ranging from 11.5 to 12.5. Detergents with HLB values below 11.5 are probably not suitable because of their insolubility in aqueous solutions. Umbreit and Strominger[6] reported optimum HLB values of detergents ranging from 12 to 14. They investigated other types of non-ionic detergents for the extraction of D-alanine carboxypeptidase from *Bacillus subtilis* and phosphoacetylmuramylpentapeptide translocase and succinate dehydrogenase from *Micrococcus luteus*. Presumably, opti-

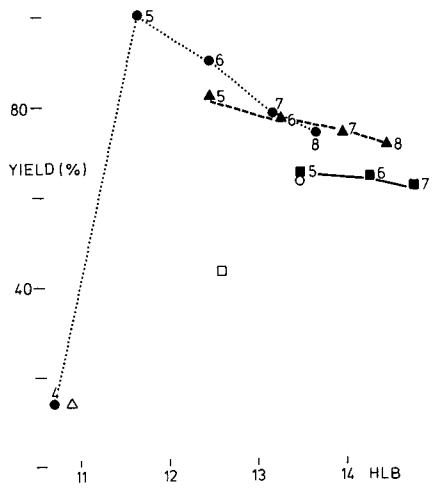

Fig. 1. Relative yields of Sendai virus membrane proteins after extraction with 2% of a non-ionic detergent. The highest yield was obtained with $C_{12}E_5$ and this was taken as 100%. Yields were estimated from SE-HPLC elution patterns. Either a TSK 4000SW or two tandem-linked Zorbax GF 450 columns were used. The mobile phase was 50 m*M* sodium phosphate (pH 6.5) containing 0.1% SDS. Yields are plotted against the HLB values of the detergents investigated: (■—■) C_8E_{5-7}; (▲- - -▲) $C_{10}E_{5-8}$; (●· · ·●) $C_{12}E_{4-8}$; (△) $C_{14}E_5$; (○) Triton X-100; (□) octylglucoside. The numbers indicate the number of ethylene glycol units in the oxyethylene chain.

mum HLB values depend on the hydrophobicity of the protein to be solubilized, although different types of non-ionic detergents may also differ in their solubilizing properties. In the study reported by Umbreit and Strominger[6], the yield could be correlated with the length of the oxyethylene chain but did not correlate with the chemical nature of the hydrophobic portion of the detergent. In other studies, an increase in the solubilizing ability of the detergent with an increase in the hydrophobic moiety of the detergent has been described[17,18]. In our study, solubilization of HN and F protein depends on the length of the oxyethylene chain and, to a larger extent, on the length of the hydrocarbon chain. It may be possible that this correlation only applies to non-ionic detergents within the group of polyoxyethylene alkyl ethers.

The CMC values may be an important parameter for detergent removal or detergent exchange[2,7,19], and they may serve as an indication of the degree of homogeneity of a detergent[1,2], but CMC values do not correlate with the solubilizing properties of the detergent, and nor do other physical parameters such as micellar weight, size, shape and aggregation number.

IE-HPLC of detergent extracts of Sendai virus membrane proteins

As detergent extracts of Sendai virus obtained with C_8E_5 $C_{10}E_5$ and $C_{12}E_5$, gave a relatively high yield of HN and F protein, they were selected for further studies, together with the more commonly used detergents octyl glucoside and $C_{12}E_8$. IE-HPLC was performed with 0.1% of the detergent used for extraction, added to the elution buffer. The amount of HN and F protein injected was between 0.95 and 1.05 mg for each chromatographic run. Fig. 2 shows the IE-HPLC elution pattern of a $C_{10}E_5$ extract of Sendai virus and 0.1% $C_{10}E_5$ in the elution buffer.

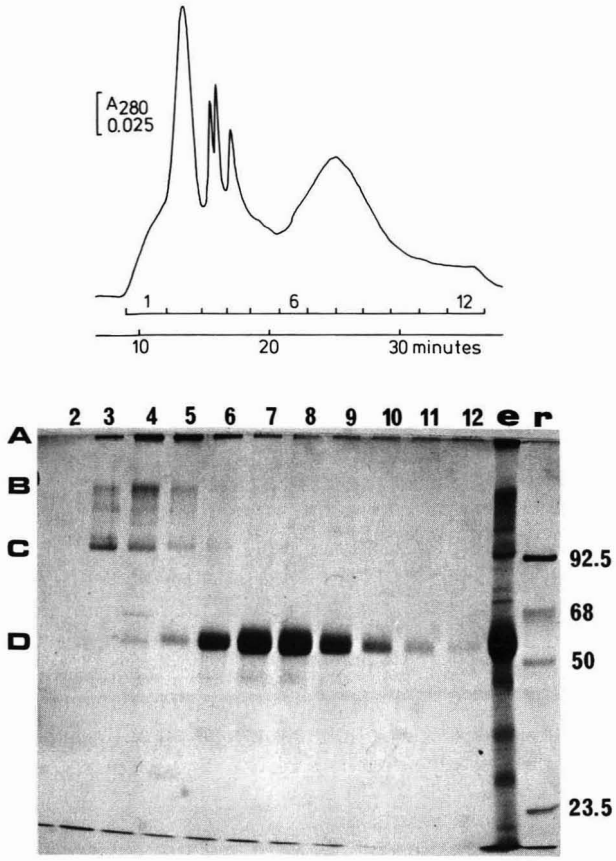

Fig. 2. IE-HPLC of a $C_{10}E_5$ extract of Sendai virus membrane proteins on a Mono Q column. Elution was performed with a 40-min gradient from 20 m*M* Tris–HCl (pH 7.8), containing 0.1% $C_{10}E_5$, to 0.5 *M* NaCl in the same buffer. The flow-rate was 1 ml/min and the absorbance was monitored at 280 nm. Fractions were collected as indicated, and samples were analysed by SDS-PAGE (8% gel) under non-reducing conditions. Polypeptides were revealed by silver staining. Lane numbers of the gel refer to IE-HPLC fractions. A, B, C and D are the tetrameric, dimeric and truncated form of HN protein and F protein, respectively. r, reference proteins; molecular weights are given in kilodaltons. e, the $C_{10}E_5$ extract prior to chromatography.

Recoveries of HN and F protein after IE-HPLC were determined by SE-HPLC of the fractions collected, as indicated in Fig. 2, and are listed in Table II. The highest recovery for both HN (83%) and F (80%) was obtained with $C_{10}E_5$ in the eluent. IE-HPLC in the presence of other detergents resulted in lower yields: 61% and 44% (C_8E_5), 64% and 46% ($C_{12}E_5$), 64% and 48% ($C_{12}E_8$) and 31% and 4% (octyl glucoside) for HN and F protein, respectively (see Table II). All detergents were used at a concentration of 0.1%. For some of them (C_8E_5 and octyl glucoside), this is below the CMC, and it could be argued that for these detergents higher concentrations should be used[5,17]. However, the recoveries of the HN and F protein after IE-HPLC with 0.1% C_8E_5 and 0.1% $C_{12}E_5$ were similar and ranged from 44 to 46% for the F protein and from 61 to 64% for the HN protein (Table II), despite the

TABLE II

RECOVERIES OF HN AND F PROTEIN AFTER IE-HPLC

Detergent[a]	*Recovery (%)*	
	HN	*F*
C_8E_5	61	44
$C_{10}E_5$	83	80
$C_{12}E_5$	64	48
$C_{12}E_8$	64	46
Octyl glucoside	31	4

[a] Sendai virus C_8E_5 extracts were subjected to IE-HPLC with the same detergent in the mobile phase as used for extraction.

100-fold difference in CMC (Table I). Fractions of the elution patterns after IE-HPLC, as indicated in Fig. 2, were collected and analysed by SDS-PAGE on 8% gels. The gel pattern of the fractions after IE-HPLC with $C_{10}E_5$ in the elution buffer of a $C_{10}E_5$ extract is shown in Fig. 2. Fractions 3–6 contained most of the various multimeric forms of the HN protein, and fractions 6–10 contained most of the F protein. Similar patterns were found for the other extracts, each time with the detergent used for extraction at a concentration of 0.1% in the eluent. The only difference was the relative amount of the various multimeric forms of HN. For example, the amount of HN_2– was higher after IE-HPLC of a C_8E_5 extract (not shown). The HN and F protein were only partially purified by IE-HPLC. Optimum purification of the Sendai virus proteins HN and F possibly requires repeated IE-HPLC.

Immunological activity in ELISA of Sendai virus membrane proteins

As a measure of the intact conformation of HN and F protein, the immunological activity of these proteins was determined in an ELISA with conformation-dependent Mabs against Sendai virus HN and F protein[8,14]. ELISA was performed with (i) Sendai virus HN and F proteins extracted with C_8E_5, $C_{10}E_5$, $C_{12}E_5$, $C_{12}E_8$, Triton X-100 and octyl glucoside and (ii) fractions after IE-HPLC with 0.1% of C_8E_5, $C_{10}E_5$, $C_{12}E_5$ and $C_{12}E_8$ in the eluent. ELISA of the extracts was performed with and without detergent removal. The amount of protein necessary to obtain an absorbance of 1.2 at 492 nm (A_{492}) was measured for each extract. These amounts ranged from 4 to 11 ng for HN and from 2 to 7 ng for F (Table III). When detergent was not removed, only $C_{12}E_5$ and $C_{12}E_8$ interfered with protein coating at a concentration of 0.004% detergent. Lower concentrations of the detergents did not affect protein coating and, for this reason, ELISA of the IE-HPLC fractions could be performed without removing the detergent. ELISA of the IE-HPLC fractions was performed with the same panels of Mabs against Sendai virus HN and F protein. In all fractions (with exception of the first fractions which did not contain protein), HN and F protein could be detected ($A_{492} \geqslant 0.200$). The amounts of HN and F necessary to obtain an A_{492} of 1.2 were estimated, and varied from 16 to 39 ng for HN and from 4 to 9 ng for F protein (Table III). For instance, 4 ng of the HN protein in the $C_{12}E_5$ extract (the starting material for IE-HPLC) was required to obtain an A_{492} of 1.2. A larger amount (39 ng) of HN protein was necessary to obtain the same absorbance

TABLE III

IMMUNOLOGICAL ACTIVITY OF HN AND F PROTEIN IN THE DETERGENT EXTRACTS AND AFTER IE-HPLC

Detergent	*HN Protein*[a]		*F Protein*[a]	
	Extract	*IE-HPLC*	*Extract*	*IE-HPLC*
C_8E_5	10	16	2	9
$C_{10}E_5$	11	36	6	6
$C_{12}E_5$	4	39	5	3
$C_{12}E_8$	4	30	7	4

[a] Immunological activity, amount of protein in ng needed to obtain an absorbance of 1.2 at 492 nm.

after it had been subjected to IE-HPLC. However, after denaturation of the HN protein by boiling in 4% SDS, more than 1000 ng of protein was necessary to measure an A_{492} of 1.2. This means that there is less than a 3.5% loss of immunological activity of the HN protein after it had been subjected to IE-HPLC, which indicates that the conformation of the protein is still largely intact.

The results in Table III show that the immunological activity of F protein is not affected by IE-HPLC in the presence of the various detergents. The results show that polyoxyethylene alkyl ethers can be used for adequate solubilization of integral membrane proteins of Sendai virus and that the conformation of the proteins remains intact during extraction and after IE-HPLC in the presence of the detergent used for extraction.

ACKNOWLEDGEMENT

We thank Berend Kwant for providing a number of polyoxyethylene alkyl ethers.

REFERENCES

1 M. J. Schick (Editor), *Nonionic Surfactants*, Marcel Dekker, New York, 1967.
2 A. Helenius and K. Simons, *Biochim. Biophys. Acta*, 415 (1975) 29.
3 G. W. Welling, R. van der Zee and S. Welling-Wester, *J. Chromatogr.*, 418 (1987) 223.
4 G. W. Welling, K. Slopsema and S. Welling-Wester, *J. Chromatogr.*, 397 (1987) 165.
5 Y. Kato, T. Kitamura, K. Nakamura, A. Mitsui, Y. Yamasaki and T. Hashimoto, *J. Chromatogr.*, 391 (1987) 395.
6 J. N. Umbreit and J. L. Strominger, *Proc. Natl. Acad. Sci. USA*, 70 (1973) 2997.
7 A. J. Furth, *Anal. Biochem.*, 109 (1980) 207.
8 S. Welling-Wester, B. Kazemier, C. Örvell and G. W. Welling, *J. Chromatogr.*, 443 (1988) 255.
9 O. H. Lowry, N. J. Rosebrough, A. L. Farr and R. J. Randall, *J. Biol. Chem.*, 193 (1951) 265.
10 E. De Vendittis, G. Palumbo, G. Parlato and V. Bocchini, *Anal. Biochem.*, 115 (1981) 278.
11 P. Becher, in M. J. Schick (Editor), *Nonionic Surfactants*, Marcel Dekker, New York, 1967.
12 U. K. Laemmli, *Nature (London)*, 227 (1970) 680.
13 W. Wray, T. Boulikas, V. P. Wray and R. Hancock, *Anal. Biochem.*, 118 (1981) 197.
14 C. Örvell and M. Grandien, *J. Immunol.*, 129 (1982) 2779.
15 M. A. K. Markwell and C. F. Fox, *Biochemistry*, 17 (1978) 4807.
16 Y. Hosaka and K. Shimizu, in G. Poste and G. L. Nicholson (Editors), *Virus Infection and Cell Surface*, Elsevier North-Holland, Amsterdam, 1977, p. 129.
17 H. Ikigai, T. Nakae and Y. Kato, *J. Chromatogr.*, 322 (1985) 212.
18 D. Lichtenberg, R. J. Robson and E. A. Dennis, *Biochim. Biophys. Acta*, 737 (1983) 285.
19 C. Tanford and J. A. Reynolds, *Biochim. Biophys. Acta*, 457 (1976) 133.

Journal of Chromatography, 476 (1989) 329–344
Elsevier Science Publishers B.V., Amsterdam — Printed in The Netherlands

CHROMSYMP. 1618

PROPERTIES, IN THEORY AND PRACTICE, OF NOVEL GEL FILTRATION MEDIA FOR STANDARD LIQUID CHROMATOGRAPHY

LARS HAGEL*, HÅKAN LUNDSTRÖM, TORVALD ANDERSSON and HANS LINDBLOM
Pharmacia LKB Biotechnology, S-751 82 Uppsala (Sweden)

SUMMARY

The influence of experimental parameters on the separation result in gel filtration may readily be predicted from a few basic equations, as demonstrated with the aid of experimental observations on Sephacryl® HR. Excellent agreement between the predicted resolution and that determined experimentally was found for parameters such as temperature, particle size, column length, flow velocity, sample volume and gel porosity. The theoretical prediction of an optimum sample volume for a constant processing rate was also experimentally verified. An exhaustive investigation of the physical, chemical and functional properties of Sephacryl HR was undertaken to facilitate the interpretation of experimental observations.

INTRODUCTION

During the last decade several new media designed for aqueous size-exclusion chromatography (gel filtration) have been introduced[1–10]. The majority of products has been developed to meet demands for high resolution at short separation times, *e.g.*, pre-packed columns of micro-particulate gels at the expense of cost and system flexibility.

Recently, a new family of chromatography packings, Sephacryl® High Resolution, claimed to offer a rational compromise between chromatographic performance, system flexibility and economy for standard liquid chromatography, was introduced by Pharmacia[11]. Information on the physico-chemical and functional properties of new matrices facilitates interpretation of experimental observations and is thus of vital importance to the researcher. We therefore wish to communicate an exhaustive examination of the characteristics of the new packing materials.

Predictability of separation results is important in order to facilitate the development of chromatographic separation schemes. This know-how is sometimes commercialized into expert or knowledge-based systems[12,13]. This study illustrates the application of some fundamental theoretical relationships of size-exclusion parameters to produce simple guidelines for work with standard gel filtration chromatography.

0021-9673/89/$03.50

THEORETICAL

Size-exclusion chromatography (SEC) is, in the ideal mode, based on a relatively uncomplicated separation principle, *i.e.*, elution is solely governed by the differences between the solute and pore dimensions[14–16]. Thus, estimates of the separation result are readily inferred from some basic equations[17–20]. The resolution, R_s, between two solutes of molecular weights M_1 and M_2 may conceptually be described by

$$R_s = \frac{1}{4} \log M_1/M_2 \left(\frac{b}{V_0/V_p + \bar{K}_D} \right) \sqrt{\frac{L}{\bar{H}}} \tag{1}$$

where b is the slope of the selectivity curve, *i.e.*, $\mathrm{d}\log M/\mathrm{d}K_D$, $\bar{K}_D$ is the mean value of the distribution coefficients, *i.e.*, $\frac{1}{2}(K_{D1} + K_{D2})$, V_0 is the void volume of the column, V_p the pore volume of the packing material, L the length of the column and $\bar{H}$ the packing efficiency of the column, expressed as the mean value of the plate heights for the two solutes[20]. For very precise calculations the expression $(V_0/V_p + \bar{K}_D)\sqrt{\bar{H}}$ in eqn. 1 must be replaced by:

$$\frac{1}{2}(V_0/V_p + K_{D1})\sqrt{H_1} + \frac{1}{2}(V_0/V_p + K_{D2})\sqrt{H_2}$$

The equation for the plate height may, for macromolecules, be reduced to

$$H = 2\lambda d_p + R(1 - R)d_p^2 u/30\gamma_s D_m \tag{2}$$

i.e., the B term is in most cases negligible compared to the C term of the Van Deemter equation[20]. In eqn. 2, λ is a geometrical factor close to 1 for many gel filtration columns[20], R is the ratio of the zone velocity to the mobile phase velocity, *i.e.*, V_0/V_R, d_p is the particle size, u is the interstitial linear flow velocity, D_m is the diffusion coefficient in the mobile phase and γ_s is the obstruction factor to diffusion in the pores[20].

The diffusion coefficient (cm^2/s) of globular proteins may be estimated from[20,21]:

$$D_{25,H_2O} \approx 2.6 \cdot 10^{-5} M^{-1/3} \tag{3}$$

The diffusivity is affected by the temperature according to[22]

$$D_{t1}/D_{t2} = T_1/T_2 \cdot \eta_{t2}/\eta_{t1} \tag{4}$$

where T is the absolute temperature (K) and η the viscosity of the solution at t°C. The viscosity of water (in cP) is fairly accurately given by[23]

$$\eta_t = \exp\{1301/[998.333 + 8.1855\,(t - 20) + 0.00585\,(t - 20)^2]\} - 1.30233 \tag{5}$$

where t is the temperature in °C between 0 and 30°C.

The extra-column peak broadening is, with well designed systems, mainly a function of the sample volume and the total zone broadening may then be calculated from[24,25]

$$\sigma_{tot}^2 = \sigma_{inj}^2 + \sigma_{column}^2 \approx V_{inj}^2 K_{inj}^{-1} + V_R^2 N^{-1} \quad (6)$$

where V_{inj} is the sample injection volume, K_{inj} an injector-dependent constant (empirically close to 5 for our injection device[25]) and N the plate number of the column. The plate number was calculated, assuming a Gaussian distribution of solute molecules, from

$$N = 5.54\left(\frac{V_R}{W_h}\right)^2 \quad (7)$$

where W_h is the peak width at half peak-height.

For maximum process economy it is of interest to find an optimum combination of cycle time, *i.e.*, flow velocity and cycle number, *i.e.*, processed sample volume per cycle. This may be inferred by combining eqns. 1, 2 and 6. The result is illustrated in Fig. 1 indicating that an optimum combination exists for each feed. The relative feed, F_{rel}, expresses the sample volume, in terms of column bed volume, V_c, that is processed per hour.

Approximations of the optimum sample volume and flow-rate for processing totally F ml sample per hour may be found by combining eqns. 2 and 6 and differentiation of H_{tot} with respect to V_{inj} which yields:

$$V_{inj,opt} \approx (FK_{inj}V_cV_pd_p^2/15D_m)^{1/3} \quad (8)$$

and

$$F_{opt} = FL/V_{inj,opt} \quad (9)$$

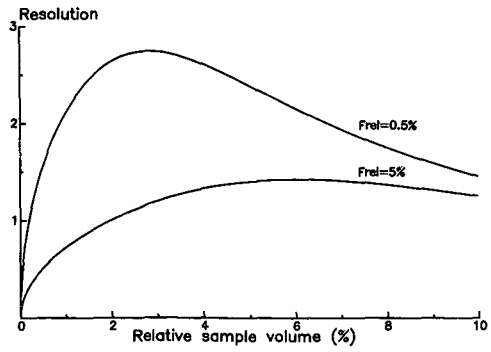

Fig. 1. Resolution as a function of sample volume at constant processing rate. Relative sample volume, $V_{rel} = V_{inj}/V_c$, and relative feed, $F_{rel} = V_{rel}$ per hour. Calculated from eqns. 1, 2 and 6 for bovine serum albumin and myoglobin on Sephacryl S-200 HR.

EXPERIMENTAL

Pore and surface structure

The surface topology of Sephacryl HR was studied by scanning-electron microscopy (SEM), using a Philips (Eindhoven, Holland) 400, FEG at 60 kV, with a spot size of 2 nm, providing a magnification factor of 100 000 times. Before SEM, the beads were freeze-dried by first immersing the fixed beads in liquid nitrogen and then allowing the eutectic ice thus formed to sublime for 48 h at $-78°C$ and 10^{-5} mmHg. The beads were then vapour phase impregnated with osmium to yield a very small extra surface layer and still a sufficiently large emission of scattered electrons[26].

Bead size distribution

The particle-size distribution of Sephacryl HR was routinely analysed on a Coulter Counter. The instrument was calibrated with the aid of absolute data, obtained by microscopy and image analysis with the aid of an IBAS 2000 (Kontron, Eching/Munich, F.R.G.)[27]. The particle size, d_p, in this context is the mean of the volume-size distribution. This estimate is, for this size distribution of beads, useful for the calculation of the reduced plate height, *i.e.*, $h = H/d_p$ and the pressure drops over gel beds[3].

Matrix rigidity

The effect on bead rigidity of the improved cross-linking procedure was tested by running a flow gradient through a packed column and monitoring the pressure drop generated over the column. The data were compared with the results expected on the basis of the pressure-drop equation. The procedure has been described in detail elsewhere[3].

Packing procedure

A new packing procedure was developed in order to pack this new media efficiently. The principle is to form an homogeneous gel bed by first packing the bed at a medium flow velocity to avoid a compressed zone of beads at the end piece and then stabilizing the bed at an higher flow velocity.

We found that typical flow velocities for the steps were 30 cm/h for 2 h and 60 cm/h for 1 h, respectively, when packing a 70-cm column. Optimum flow velocities are due to the column length (increasing flow with decreasing length) as well as the rigidity of the gel. Detailed packing instructions for various column dimensions and gel types are now available from the manufacturer[28]. The columns were packed according to the two-step procedure in the reverse order of elution, *i.e.*, towards the inlet adaptor, thus providing a undisturbed, dense and homogeneous bed at the sample application zone.

The efficiency of the packing procedure was evaluated by passing 200 μl of acetone (5 μl/ml water) through the column at 30 cm/h. A leading peak indicates channeling and the column had to be repacked at a reduced flow velocity, *e.g.*, 10% less in step 2. A tailing peak may be caused by too loose a packing, but this can be adjusted by increasing the flow velocity in step 2 by 5–20%. This packing procedure should yield columns with high efficiencies, expressed by a reduced plate height of approximately 2 (corresponding to more than 10 000 plates per metre), and a peak symmetry of 1.0 ± 0.2.

Chromatographic performance

All equipment and gels were obtained from Pharmacia (Uppsala, Sweden). The efficiency of the columns was checked by evaluating the plate number and symmetry for acetone, as outlined above. The selectivity and the separation range were evaluated by chromatographing mixtures of model proteins, listed in Table I. The chromatographic system typically was comprised of an high precision pump (P-500), injection valve (MV-7), UV monitor (UV-M, 280 nm), recorder (REC-482) and a controller unit (LCC-500 Plus).

TABLE I

PROTEINS USED FOR CHARACTERIZATION OF SEPHACRYL® HR

Sources: A = Pharmacia LKB Biotechnology; B = Sigma; C = Boehringer Mannheim.

Substance	*Source*	*Lot. No.*	*Molecular weight (kilodaltons)*	*Yield determined on Sephacryl S-100 HR (%)*
Blue Dextran 2000	A	C 619	2 000	97
Ferritin	A	C 620	440	99
Catalase	A	C 621	232	96
Aldolase	A	C 627	158	100
Bovine serum albumin	A	C 623	67	100
Ovalbumin	A	C 626	43	99
β-Lactoglobulin A + B	B	106F-8120	35	101
Chymotrypsinogen A	A	C 624	25	99
Myoglobin	B	34F-7180	17.6	99
Lysozyme	C	10321922-61	14.4	96
Ribonuclease A	A	C 625	13.7	104
Cytochrome *c*	B	56F-7020	12.4	99
Immunoglobulin G	B	54F-9390	160	
Human serum albumin	A		67	
Transferrin	B	14F-9425	81	

The columns XK 16/70 (70 cm × 1.6 cm I.D.), XK 26/70 and XK 50/100 were packed with Sephacryl S-100 HR, S-200 HR, S-300 HR, S-400 HR and S-500 HR according to the new packing procedure. The eluent was 0.05 *M* phosphate buffer in 0.15 *M* sodium chloride, adjusted to pH 7.0 and containing 0.04% sodium azide as a preservative.

Adsorption of model proteins on Sephacryl under recommended chromatographic conditions was determined by applying 1 mg of protein to 24 ml of fresh gel, packed into an HR 10/30 column, and calculating the decrease in absorption of the collected peak as compared to a reference sample. Sephacryl S-100 HR, being the packing material of largest matrix volume, was chosen for this test.

The influence of temperature was studied in a cold room (3°C) and at room temperature (22°C). The impact of particle size on the resolution was elucidated by comparing the performance of columns packed with Sephacryl S-200 HR (47 μm) and S-200 SF (70 μm). The sample volume was varied with the aid of a Superloop. The effects of the column length and dead-volume were studied by connecting columns in

series. The influence of all these parameters as well as that of the flow velocity and solute molecular weight was compared to results predicted by the theoretical relationships.

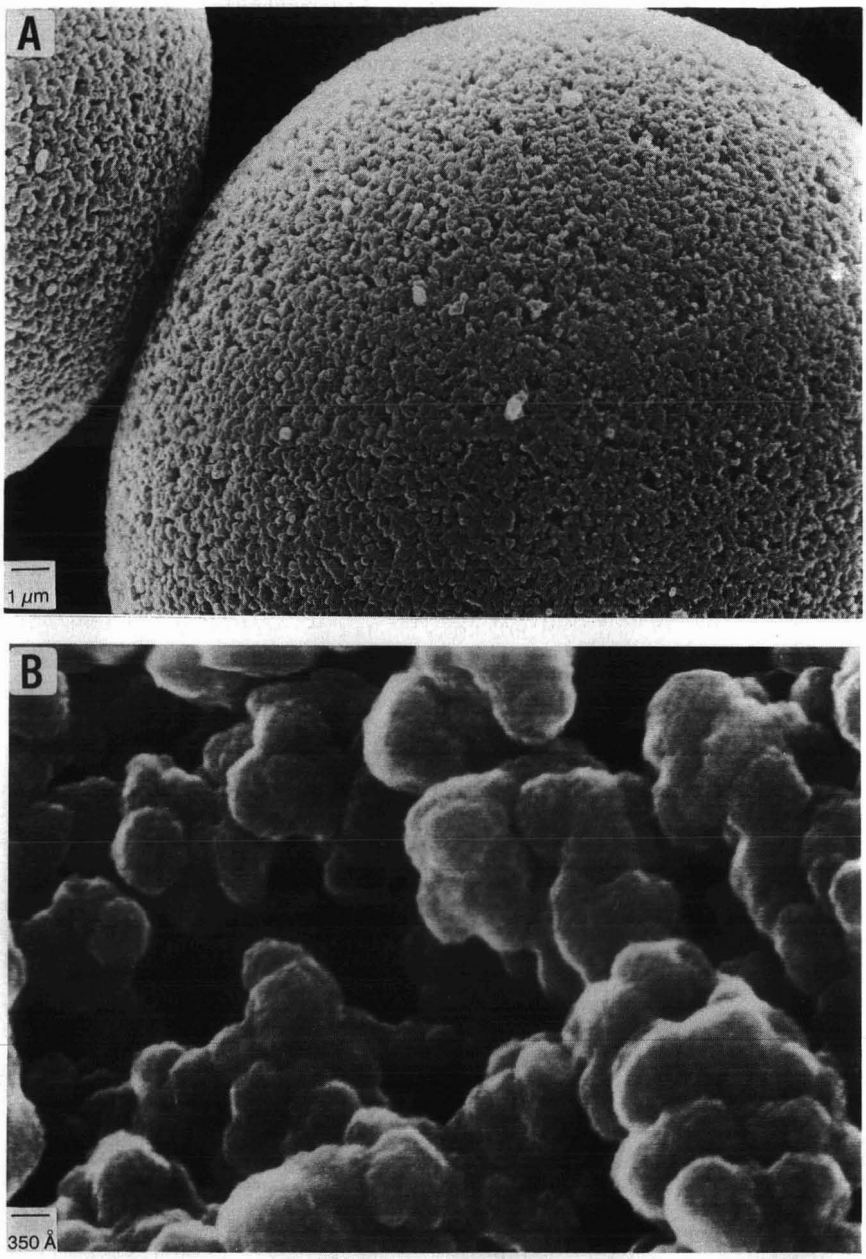

Fig. 2. Scanning electron micrographs of Sephacryl S-500 HR at different magnification factors (courtesy of B. Medin, Institute of Biochemistry, Uppsala University).

RESULTS AND DISCUSSION

Pore and surface structure

The structure of Sephacryl HR, as observed by SEM, is shown in Fig. 2. The topology of the surface is not identical to that shown for agarose-based media[29].

From the micrograph in Fig. 2B it can be concluded that Sephacryl S-500 HR contains cavities of widths in the range of 750–2000 Å. The granular structures of polymerized bis(acrylamide), assumed to form the macroreticular structure, are clearly visualized in Fig. 2B. Allyldextran is believed to be co-polymerized with or in some cases trapped in the polymerized granular structures[30]. We have noticed affinity of lentil lectin to Sephacryl which indicates that sugar structures, *i.e.*, dextran are exposed to solutes[31]. Other workers have found that treatment of Sephacryl with dextranase yields an increase in porosity but no substantial decrease in rigidity[32]. These observations provide support for the tentative structure of Sephacryl given here.

Bead size distribution

The particle-size distribution of Sephacryl is fairly narrow, *i.e.*, $s = 20\%$ of the mean as shown in Table II. The optimum particle size of a chromatographic material is a compromise between considerations such as the allowable column zone broadening and tolerable column pressure drop at the flow velocities required and the extra column contribution, *e.g.*, introduced by large injection volumes[25]. Whereas efficient column packing techniques for standard media, *e.g.*, $20 \leqslant d_p \leqslant 200$ μm are well established, the packing of micro-particulate materials, *e.g.*, $d_p \leqslant 5$ μm is still considered to be very difficult[33]. The particle size range of 30–50 μm is often claimed to be optimal for preparative liquid chromatography[34,35]. It may be noted that overload conditions, *i.e.*, an experimental situation where the sample volume and/or concentration is the major cause of the total peak width, is for gel filtration achieved at smaller sample volumes for smaller bead sizes[25].

TABLE II

PROPERTIES OF SEPHACRYL® HR USED IN THIS STUDY

Parameter	*Gel type*				
	S-100	*S-200*	*S-300*	*S-400*	*S-500*
Particle size (μm)					
mean of volume distribution	48	48	43	44	46
width (5–95%)	31–68	31–67	29–63	31–63	32–66
Separation range, $K_D = 0.1$–0.8					
proteins	$(1–75) \cdot 10^3$	$(3–160) \cdot 10^3$	$(5–1000) \cdot 10^3$	$(2–2000) \cdot 10^4$	$2 \cdot 10^4–3 \cdot 10^9$
dextrans[a]				$3 \cdot 10^3–1.6 \cdot 10^6$	$10^4–2 \cdot 10^7$
Matrix volume (%)	15	12	10	10	8
Permeability, V_p/V_0	1.5	1.7	1.6	1.5	1.6
Void fraction, V_0/V_c	0.36	0.34	0.36	0.37	0.37
Packing efficiency, h	1.9	2.1	2.1	2.1	2.1

[a] In-house preparations and substances from Pharmacosmos, Denmark.

Matrix rigidity

The enhanced flow properties due to an increase in matrix rigidity of the different types of Sephacryl is illustrated in Fig. 3. As can be noted, the flow pressure characteristics are in accordance with the pressure-drop equation, and this indicates that the column bed is very homogenous, *i.e.*, the void fraction is constant over the entire column length. An abnormal drop in the pressure curve at very high flow velocities may be noted with Sephacryl. This is probably caused by cracking of the bed, leading to void channels. Maximal flow resistance of semi-rigid media is due not only to the bead strength but also to the column internal diameter and length. The flow velocities obtained with Sephacryl HR are sufficient for most standard gel filtration chromatography separations.

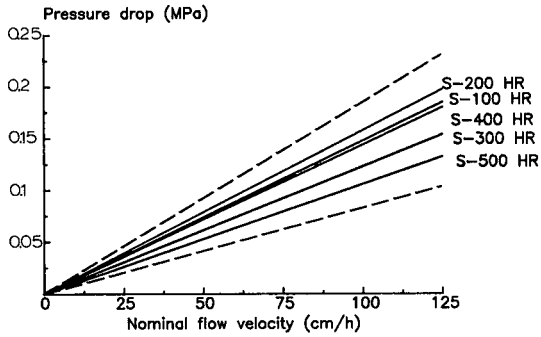

Fig. 3. Pressure–flow relationships for Sephacryl HR. Bed dimensions, void fractions as listed in Table II. Dotted curves illustrate theoretical limits for homogeneous beds, calculated for the actual particle size and void fractions[3].

Column packing

The optimum packing procedure of a certain material is related to a large number of parameters, and one may therefore assume that each type of material must be treated on an individual basis[33]. With the proposed method we routinely achieved columns with a reduced plate height of better than 2.1, *i.e.*, 10 000 theoretical plates per metre and a symmetry in the range 0.9–1.1 for acetone.

Chromatographic performance

The adsorption of model proteins on Sephacryl is very low, when a buffer of intermediate ionic strength is used, as indicated by the data in Table I. The yield is very similar to that reported for agarose gels[3,5]. It should be noted that elution of lysozyme is delayed, indicating a non-ideal behaviour of this protein. The behaviour is probably not due to the shape of the protein, *i.e.*, other more asymmetric proteins are eluted as expected, but is caused by a "salting-out" effect. Reduction of the ionic strength of the buffer was accompanied by a reduction in the elution volume of lysozyme. Lysozyme is claimed to undergo strong hydrophobic interactions[36].

The chemical stability of Sephacryl HR allows the continuous use of eluents of pH between 2 and 11 (ref. 37). Anionic interactions at low ionic strengths have been

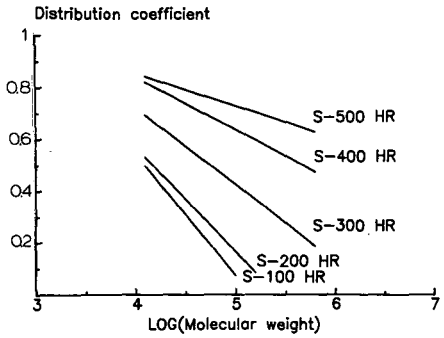

Fig. 4. Selectivity curves of Sephacryl HR for globular proteins.

noted, and the effect was eliminated by the use of neutral buffers at intermediate ionic strength, *e.g.*, the buffer used in this study[37].

The selectivity of Sephacryl HR for globular proteins is illustrated in Fig. 4. By comparison with published data for Sephacryl SF it can be concluded that the separation ranges for the two types of supports are very similar (see also Fig. 11)[38]. The separation range given by the molecular weight of globular proteins at K_D = 0.1 and 0.8 is given in Table II.

The influence of the porosity on the resolution, *e.g.*, eqns. 1 and 2 indicates that optimum resolution is achieved for a medium from which the substances are eluted at *ca.* K_D = 0.2, provided the selectivity is constant[20]. This is illustrated in Fig. 5, showing the elution pattern of protein mixtures for Sephacryl HR of different porosities. Immunoglobulin G–human serum albumin is best resolved on S-200 HR and ferritin–aldolase on S-300 HR. Even though the effect is not dramatic, *i.e.*, a maximum gain in resolution of 20% may be expected[20], selection of a gel from which the substances are eluted at K_D = 0.2 is favourable for the resolution. This is illustrated in Figs. 6–8, for which different porosities of Sephacryl HR have been selected for the final purification of important proteins.

The effect of the flow velocity on the resolution may be estimated with the aid of eqns. 1 and 2. The effect on the peak zone broadening for various types of Sephacryl HR is shown Fig. 9, which also illustrates the effect of porosity on the obstruction factor.

A change in temperature will influence the diffusion coefficient, predominantly through the change in solvent viscosity. The largest effect is obtained in situations where the C term dominates over the A term and H becomes proportional to $1/D_m$. Changing the temperature from 22 to 3°C will, in this situation, reduce the resolution by 26%, *i.e.*, $R_{s,3}/R_{s,22} \approx \sqrt{D_3/D_{22}} = 0.74$.

The result in Fig. 10 shows that the reduction due to temperature was *ca.* 20% (the A term was not negligible compared to the C term). The increase in peak width due to decreased temperature may be compensated for by a decrease in flow velocity (see eqn. 2). This is also illustrated in Fig. 10. However, it should be noted that an increase in viscosity is accompanied by an equally large increase in column pressure drop. Transfer of columns between extreme temperatures must therefore be made with great care, *e.g.*, at a reduced flow-rate.

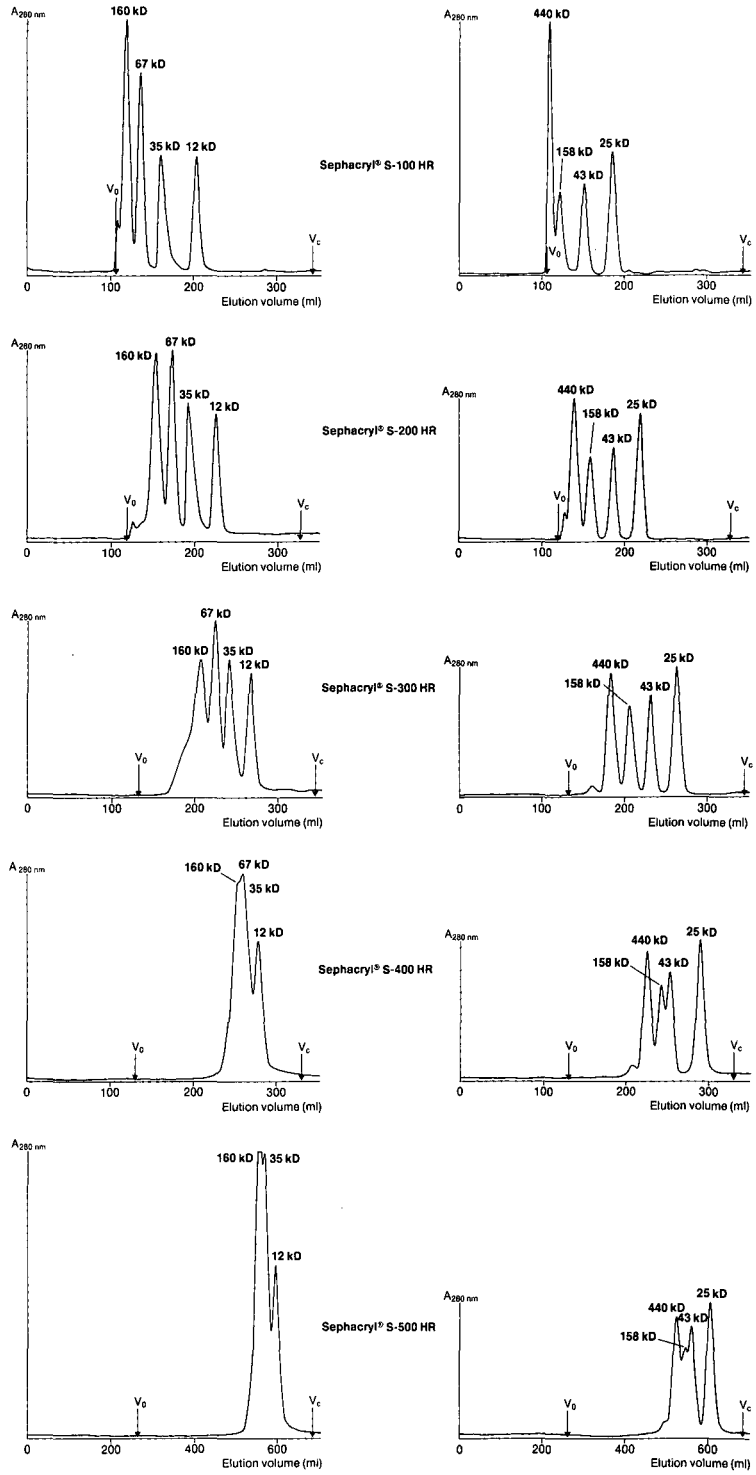

Fig. 5. Separation characteristics of Sephacryl HR of different pore sizes. Solutes: (left) immunoglobulin G, human serum albumin, β-lactoglobulin and cytochrome *c*; (right) ferritin, aldolase, ovalbumin and chymotrypsinogen A. Sample volume: 500 μl. Bed dimensions: 62–65 cm × 2.6 cm (column XK 26/70). Eluent: 0.05 *M* phosphate in 0.15 *M* NaCl (pH 7.0).

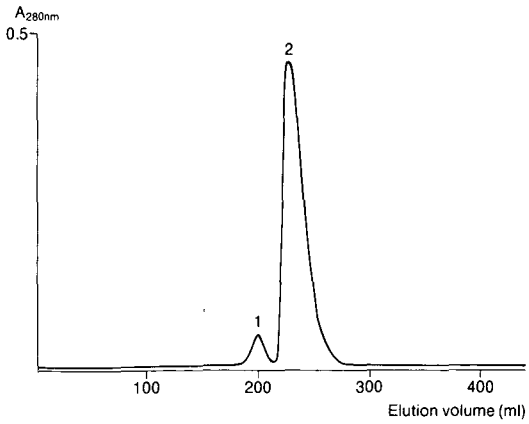

Fig. 6. Separation of human growth hormone (hGH) on Sephacryl S-100 HR. Sample: 14 ml hGH solution. Bed dimensions: 90 cm × 2.6 cm (K 26/100). Eluent: glycine phosphate (pH 7.0); flow-rate 21 ml/h (courtesy of KabiVitrum, Peptide Hormones, R&D). Peaks: 1 = hGH dimers; 2 = hGH monomers.

The influence of particle size on resolution is readily predicted from eqns. 1 and 2. A reduction of the particle size from 65.5 to 46.5 μm would theoretically increase the resolution by 20–30%. This was experimentally confirmed for a protein mixture eluted from Sephacryl S-200 SF and S-200 HR (see Fig. 11). The gain in peak sharpness from

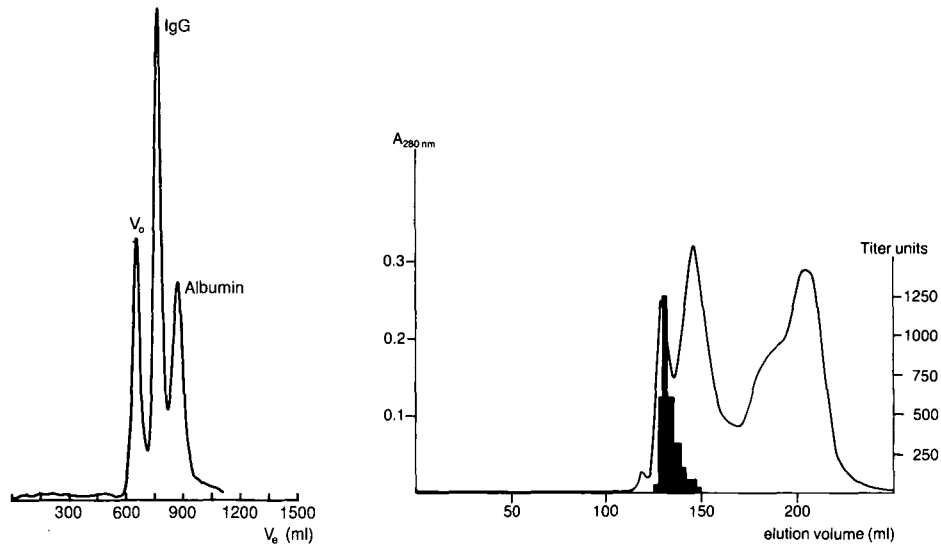

Fig. 7. Final purification of monoclonal immunoglobulin G on Sephacryl S-200 HR. Sample: 30 ml pre-purified solution from cell culture; bed dimensions 90 cm × 5 cm (K 50/100). Eluent: 0.05 *M* phosphate in 0.15 *M* NaCl (pH 7.4); flow-rate, 126 ml/h (courtesy of G. Vestin, Pharmacia Diagnostics).

Fig. 8. Purification of immunoglobulin M monoclonal antibodies on Sephacryl S-300 HR. Sample: 2 ml pre-concentrated solution from hybridoma cell culture. Bed dimensions: 63 cm × 2.6 cm (K 26/70). Eluent: 0.02 *M* phosphate in 0.5 *M* NaCl (pH 6.5); flow-rate 60 ml/h. Antibody titre determined by haemolytic test (courtesy of A. Domicelj, Pharmacia LKB Biotechnology).

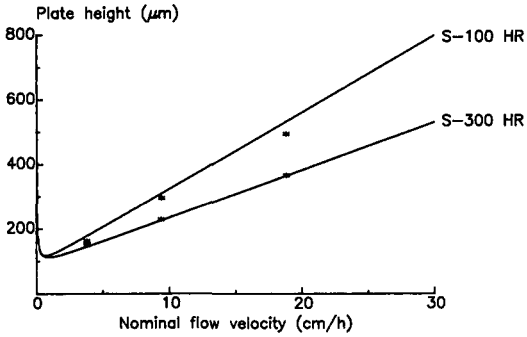

Fig. 9. Zone broadening of macromolecules as a function of flow velocity. Solid lines are theoretical curves, calculated for bovine serum albumin. Dots represent experimentally found peak widths of bovine serum albumin on Sephacryl HR.

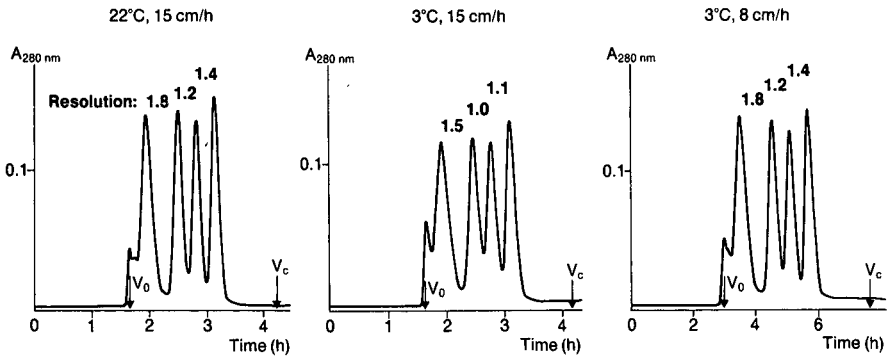

Fig. 10. Influence of temperature and flow-rate on the resolution on Sephacryl S-300 HR. Sample: 3.3 ml of a protein mixture, consisting of thyroglobulin, aldolase, ovalbumin and myoglobin. Bed dimensions: 63.2 cm × 2.6 cm (XK 26/70). Eluent: 0.05 *M* phosphate in 0.15 *M* NaCl (pH 7.0).

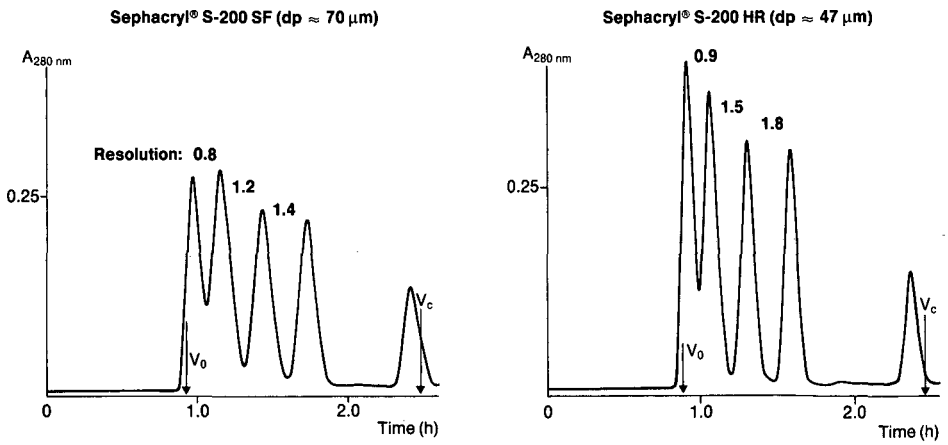

Fig. 11. Influence of particle size on the peak width and resolution of Sephacryl S-200. Sample: 3.3 ml of a mixture consisting of ferritin, aldolase, ovalbumin, myoglobin and glycyltyrosine. Bed dimensions: Sephacryl S-200 SF, 62.1 cm × 2.6 cm; Sephacryl S-200 HR, 61.3 cm × 2.6 cm. Eluent as in Fig. 10.

the use of a smaller particle size may be utilized either to improve the separation and/or to decrease the separation time (in this case by a factor of 2) with retained resolution.

Another way to increase the resolution is to use long columns (see eqn. 1). Since it is generally more difficult to produce optimum packing of very long columns, the desired length may be achieved by connecting several medium-length columns in series, provided that the proper design of connectors is used to minimize extra-column zone broadening. However, the use of very long columns is only meaningful for very difficult separations. For many separations of macromolecules, approximately equal

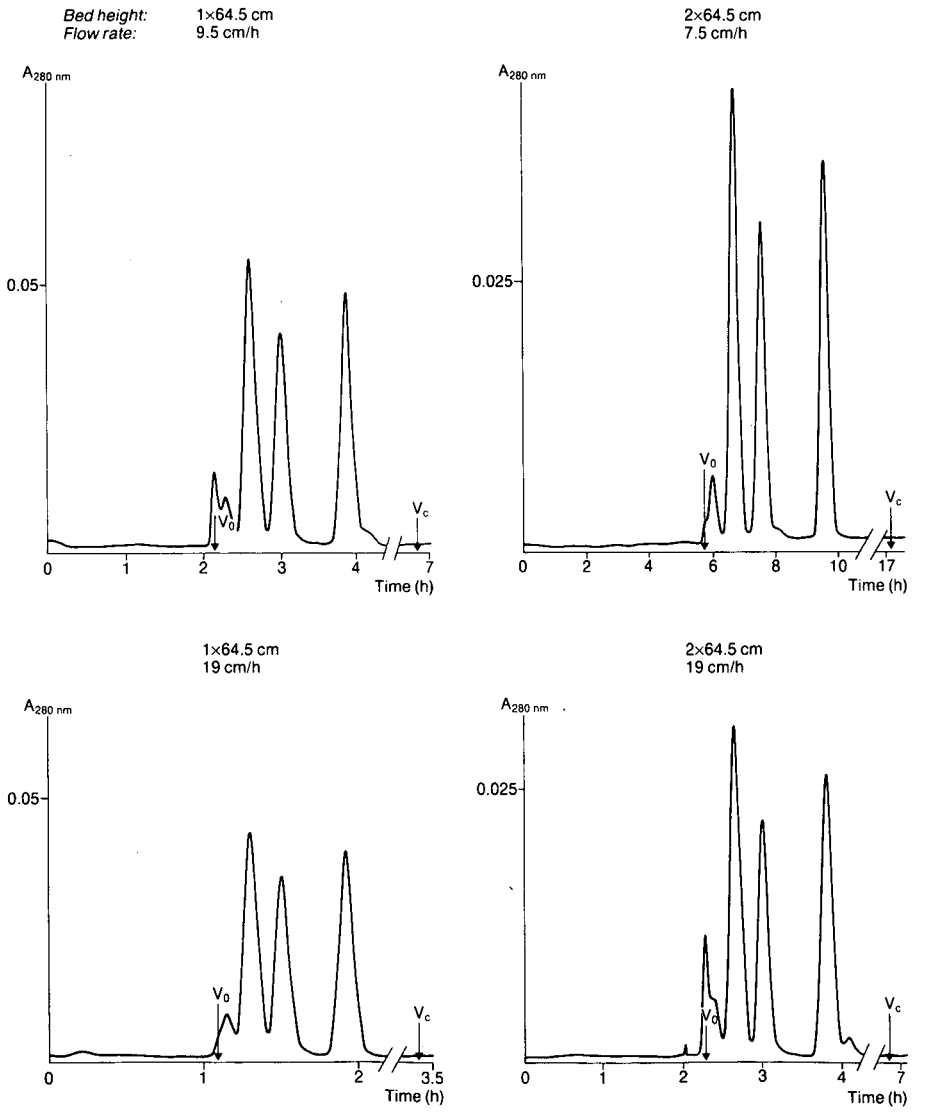

Fig. 12. Resolution at various column lengths and flow velocities on Sephacryl S-100 HR. Sample: 500 μl of transferrin, ovalbumin and myoglobin. Eluent as in Fig. 10.

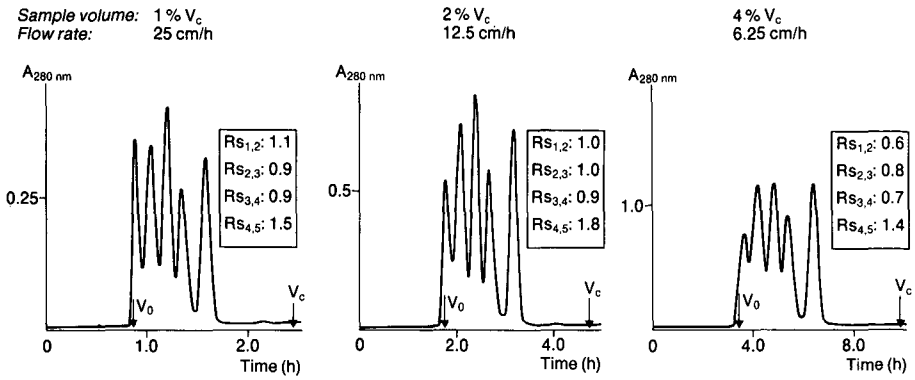

Fig. 13. Resolution for various sample volumes at a constant processing rate (ml sample/hour). Peaks in order of elution: aggregates; immunoglobulin G; bovine serum albumin; β-lactoglobulin; myoglobin. Processing rate: 1.33 ml/h (0.004 V_c/h). Bed dimensions: 61.3 cm × 2.6 cm (XK 26/70, V_c = 325 ml). Eluent as in Fig. 10.

resolution per unit time will be achieved through rapid elution of a long column or slow elution of a short column, *i.e.*, keeping L/H constant. These theoretically based rules-of-thumb are illustrated experimentally with a protein mixture in Fig. 12.

The optimum sample volume is directly related to the application of the chromatography step. For analytical purposes, the extra-column zone broadening is to be mininized, and the sample volume is therefore kept very small, typically less than 0.2% of the column bed volume[25]. The approach is drastically different for processing larger sample volumes, and an optimum of column zone broadening, *i.e.*, flow velocity and extra-column zone broadening, *i.e.*, sample volume is sought. Theory, as illustrated by Fig. 1, predicts an optimum sample volume of 2–3% of the column bed volume when 0.5% of the column volume is processed per hour. This is confirmed by the chromatograms shown in Fig. 13.

For purification of very large sample volumes it is of interest to prepare columns of larger diameters. We found that the packing method proposed for Sephacryl HR was applicable to columns even as large as 50 mm I.D. As illustrated in Fig. 14, the separation efficiencies of these columns were as good as those of the analytical columns.

TABLE III

INFLUENCE OF EXPERIMENTAL PARAMETERS ON RESOLUTION

Parameter	*Variation*	*Change in resolution (%)*	
		Predicted	*Experimental (Figure; peaks)*
Particle size (μm)	65.5–46.5	35	33 (11; 3, 4)
Flow velocity (cm/h)	19–9.5	25	27 (12; 2, 3)
Column length (cm)	64.5–129	40	33 (12; 2, 3)
Temperature (°C)	3–22	26	25 (10; 1, 2, 3)
Sample volume (%) at constant feed	2–1	23	13 (13; 3, 5)

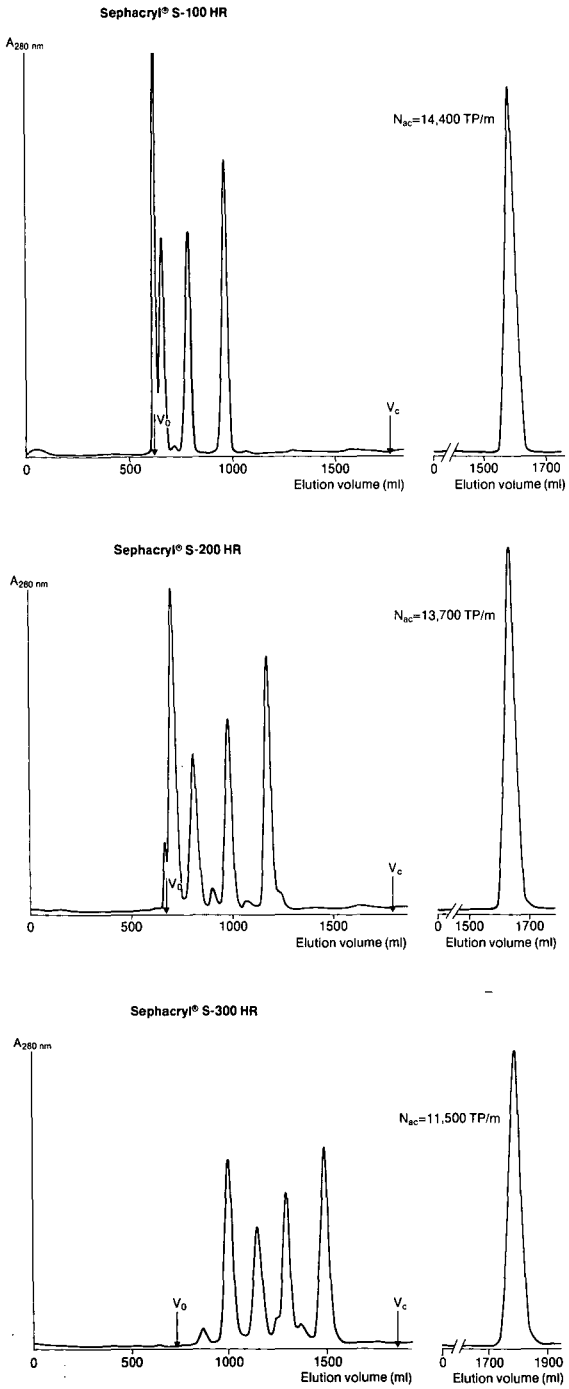

Fig. 14. Separation efficiencies (TP = theoretical plates) of Sephacryl on a small production scale. Sample: 10 ml of ferritin (4 mg), aldolase (30 mg), ovalbumin (25 mg) and chymotrypsinogen A (15 mg). Bed dimensions: 91–94 cm × 5 cm (XK 50/100). Eluent as in Fig. 10.

In conclusion, with the aid of some basic equations, the resolution obtainable in SEC of proteins may readily be predicted, and furthermore, the detrimental impact of one parameter, *e.g.*, a decrease in temperature, may be compensated for by proper adjustment of another parameter, as illustrated in Table III.

REFERENCES

1 Y. Kato, K. Komiya, H. Sasaki and T. Hashimoto, *J. Chromatogr.*, 190 (1980) 297.
2 R. A. Jenik and J. W. Porter, *Anal. Biochem.*, 111 (1981) 184.
3 L. Hagel and T. Andersson, *J. Chromatogr.*, 285 (1984) 295.
4 Y. Kato, K. Komiya and T. Hashimoto, *J. Chromatogr.*, 247 (1982) 184.
5 T. Andersson, M. Carlsson, L. Hagel, P.-Å. Pernemalm and J.-C. Janson, *J. Chromatogr.*, 326 (1985) 33.
6 R. W. Stout and J. J. De Stefano, *J. Chromatogr.*, 326 (1985) 63.
7 R. V. Vivilecchia, B. G. Lightbody, N. Z. Thimot and H. M. Quinn, *J. Chromatogr. Sci.*, 15 (1977) 424.
8 H. G. Barth, *J. Chromatogr. Sci.*, 18 (1980) 409.
9 E. Pfannkoch, K. C. Lu, F. E. Regnier and H. G. Barth, *J. Chromatogr. Sci.*, 18 (1980) 430.
10 Y. Kato, Y. Yamasaki, H. Moriyama, K. Tokunaga and T. Hashimoto, *J. Chromatogr.*, 404 (1987) 33.
11 *Sephacryl® High Resolution Gel Filtration Media*, Pharmacia, Uppsala, 1987.
12 L. R. Snyder, M. A. Stadalius and M. A. Quarry, *Anal. Chem.*, 55 (1983) 1413.
13 J. W. Dolan and L. R. Snyder, presented at the *12th International Symposium on Column Liquid Chromatography, Washington, DC, June 19–24, 1988.*
14 G. H. Lathe and C. R. J. Ruthven, *Biochem. J.*, 62 (1956) 665.
15 J. Porath, *J. Pure Appl. Chem.*, 6 (1963) 233.
16 T. C. Laurent and J. Killander, *J. Chromatogr.*, 14 (1964) 317.
17 J. C. Giddings and K. L. Mallik, *Anal. Chem.*, 38 (1966) 997.
18 F. E. Regnier and K. M. Gooding, *Anal. Biochem.*, 103 (1980) 1.
19 B. F. D. Ghrist, M. A. Stadalius and L. R. Snyder, *J. Chromatogr.*, 387 (1987) 1.
20 L. Hagel, in J.-C. Janson and L. Rydén (Editors), *Protein Purification, Methods for High Resolution Protein Separation and Analysis*, VCH, Deerfield Beach, FL, 1989, Ch. 3.
21 C. Tanford, *Physical Chemistry of Macromolecules*, Wiley, New York, 1961, Ch. 6.
22 C. R. Cantor and P. R. Schimmel, *Biophysical Chemistry Part II, Techniques For The Study of Biological Structure And Function*, Freeman, San Francisco, CA, 1980, p. 584.
23 *Handbook of Chemistry and Physics*, R. C. Weast (Editor), CRC Press, Palm Beach, FL, 59th ed., 1978, p. F-51.
24 J. J. Kirkland, W. W. Jau, H. J. Stoklosa and C. H. Dilks, Jr., *J. Chromatogr. Sci.*, 15 (1977) 303.
25 L. Hagel, *J. Chromatogr.*, 324 (1985) 422.
26 A. Medin, Institute of Biochemistry, Uppsala University, Personal communication, 1988.
27 B. Göransson and E. Dagerus, in P. J. Lloyd (Editor), *Particle Size Analysis 1988*, Wiley, London, 1988, p. 159.
28 *Packing Instructions, Sephacryl S-100, S-200, S-300, S-400, S-500 High Resolution*, Pharmacia-LKB Biotechnology, Uppsala, 1987.
29 L. Hagel, in P. L. Dubin (Editor), *Aqueous Size-Exclusion Chromatography*, Elsevier, Amsterdam, 1988, p. 127.
30 I. Johansson, Pharmacia-LKB Biotechnology, personal communication, 1988.
31 L. Hagel and G. Johansson, Pharmacia-LKB Biotechnology, unpublished results, 1987.
32 A. Medin, Institute of Biochemistry, Uppsala University, personal communication, 1983.
33 M. Verzele, C. Dewaele and D. Duquet, *J. Chromatogr.*, 391 (1987) 111.
34 J. H. Knox and H. M. Pyper, *J. Chromatogr.*, 363 (1986) 1.
35 K. Jones, *Chromatographia*, 25 (1988) 437.
36 D. E. Schmidt, R. W. Giese, D. Conron and B. L. Karger, *Anal. Chem.*, 52 (1980) 177.
37 B.-L. Johansson, Pharmacia-LKB Biotechnology, personal communication, 1988.
38 *Gel Filtration Theory and Practice*, Pharmacia, Uppsala, 1979, p. 15.

Journal of Chromatography, 476 (1989) 345–361
Elsevier Science Publishers B.V., Amsterdam — Printed in The Netherlands

CHROMSYMP. 1628

PEPTIDE MAPPING AND INTERNAL SEQUENCING OF PROTEINS ELECTROBLOTTED FROM TWO-DIMENSIONAL GELS ONTO POLYVINYLIDENE DIFLUORIDE MEMBRANES

A CHROMATOGRAPHIC PROCEDURE FOR SEPARATING PROTEINS FROM DETERGENTS

RICHARD J. SIMPSON*, LARRY D. WARD, GAVIN E. REID, MICHAEL P. BATTERHAM and ROBERT L. MORITZ

Joint Protein Structure Laboratory, Ludwig Institute for Cancer Research (Melbourne Branch) and the Walter and Eliza Hall Institute of Medical Research, P.O. Royal Melbourne Hospital, Melbourne, Victoria 3050 (Australia)

SUMMARY

Direct sequence analysis of proteins electroblotted from two-dimensional polyacrylamide gels onto immobilizing matrices provides an efficient technique for obtaining N-terminal sequence data for proteins not amenable to purification by reversed-phase high-performance liquid chromatography (RP-HPLC). We present in this paper a procedure for obtaining peptide fragments from electroblotted proteins for internal amino acid sequence analysis. First, Coomassie Blue-stained proteins are extracted from polydivinylidene difluoride membranes, using a detergent mixture of sodium dodecylsulfate and Triton X-100. Proteins are then separated from the detergent mixture by a chromatographic procedure which relies on the ability of proteins to interact with certain reversed-phase sorbents at high organic solvent concentrations. Under these conditions, detergents and Coomassie Blue are not retained and pass through the column. Proteins are recovered by simultaneously: (i) introducing trifluoroacetic acid into the mobile phase and (ii) decreasing the organic solvent concentration. After proteolytic fragmentation, peptides are purified by microbore-column (1–2 mm I.D.) RP-HPLC for microsequence analysis.

INTRODUCTION

It is now well-recognized that sample preparation is one of the major limitations to obtaining amino acid sequence information from peptides and proteins isolated in subnanomole quantities from their biological source material[1–3]. Although reversed-phase high-performance liquid chromatography (HPLC) is an established tool for purifying a large range of peptides and proteins, it does have limitations with certain classes of proteins (*e.g.*, membrane proteins and large molecular weight, M_r, hydrophobic proteins). For this category of proteins, electrophoretic separation

0021-9673/89/$03.50

provides an important alternative high-resolution technique. Indeed, two-dimensional (2D) polyacrylamide gel electrophoresis (PAGE), pioneered in 1975 by O'Farrell[4], is a high-resolution technique capable of separating thousands of proteins from various biological sources (*e.g.*, tissue extracts and cell lines)[5].

One of the drawbacks in the past with PAGE-purified proteins has been the difficulty in isolating these proteins from the gel in sufficient quantities and in a form suitable for sequence analysis. The most widely used procedures for recovering proteins from sodium dodecylsulfate (SDS)-PAGE include electroelution[6–8], passive elution[9] and electrotransfer (electroblotting) onto an immobilizing matrix[10–20] (see ref. 1 for review). The latter technique has received considerable attention in recent times due to its simplicity (no expensive equipment required), speed, and potential for handling proteins not suited to RP-HPLC technology. Direct N-terminal sequence analysis of proteins electroblotted onto immobilizing matrices [chemically activated glass, polybase-treated glass, polyvinylidene difluoride (PVDF) membrane] from SDS-polyacrylamide gels is now an important strategy for obtaining amino acid sequence information from subnanomole quantities of protein.

Although direct N-terminal analysis of proteins immobilized on PVDF membranes is an important first step in establishing the identity of proteins resolved by gel electrophoresis, for further characterization it is important that immobilized proteins can be efficiently recovered from the PVDF membrane. For instance, protein recovered from the membrane can be used for immunological studies (*e.g.*, raising antisera) as well as high-sensitivity peptide mapping. Internal protein sequence information, obtained by peptide mapping and sequence analysis is of considerable importance for the following reasons: (i) many proteins are N-terminally blocked and are not amenable to the Edman degradation procedure; (ii) the construction of oligonucleotide probes for molecular cloning; (iii) providing confirmatory evidence for cDNA-derived protein sequences; (iv) "fingerprinting" recombinant proteins; (v) complete protein structure determinations; (vi) identifying post-translational modification sites; (vii) epitope mapping; (viii) disulfide bond assignments and; (ix) ligand binding sites.

During sequence analysis, if the N-terminus of a protein is found to be blocked, then useful internal sequence can be obtained by *in situ* cyanogen bromide treatment of the immobilized protein in the sequencer[21]. This approach was recently used to obtain internal sequence for the N-terminally blocked T-cell growth factor P40[22,23]. However, the most widely used procedure for obtaining internal sequence data is by first fragmenting the molecule (either enzymically or chemically), followed by sequence analysis of the RP-HPLC-purified peptide fragments.

In this report we describe a method for obtaining internal sequence information from proteins electroblotted onto PVDF membrane from SDS-polyacrylamide gels. First, Coomassie Blue-stained proteins are passively eluted from the PVDF membrane, employing a mixture of detergents[24]. Eluted proteins are then separated from the Coomassie Blue and detergents by an inverse-gradient RP-HPLC procedure[25,26] which involves retention of the protein on a reversed-phase sorbent at high organic solvent concentrations. The method is based upon earlier reports in the literature[27–29] that at very high organic solvent concentrations (> 50%) proteins can interact strongly with certain silica-based reversed-phase packings. Interestingly, those packings which best exhibit this behaviour (*i.e.*, U-shaped or bimodal dependency) are characterized

by small pore sizes (6–12 nm), large surface areas (200–400 m^2/g), and high carbon content (7–15%). Using such sorbents, SDS, Coomassie Blue, and gel-related artifacts are not retained at high organic solvent concentrations (*e.g.*, 90% aq. propanol or acetonitrile) and pass through the column: proteins, which strongly interact with the packing under these conditions can be recovered in high yield (>90%) by the simultaneous addition of: (i) an ion-pairing agent (*e.g.*, trifluoroacetic) to the mobile phase and (ii) the introduction of a gradient of decreasing organic solvent (*i.e.*, an "inverse gradient"). Proteins recovered from eluates from SDS-PAGE by this means are free of high concentrations of SDS and acrylamide-related contaminants, and suitable for proteolytic digestion. After enzymatic cleavage, peptide fragments are separated by microbore column (1–2 mm I.D.) HPLC[1–3,30] and subjected to sequence analysis. The general utility of this technique is illustrated for a number of proteins, isolated by either one-dimensional (SDS-PAGE) or by 2D gel electrophoresis.

EXPERIMENTAL

HPLC apparatus

The chromatographic equipment consisted of a Hewlett-Packard (Waldbronn, F.R.G.) liquid chromatograph (HP 1090A), equipped with an autosampler and diode-array detector (HP 1040A). Spectral and chromatographic data were stored on disc, using a Hewlett-Packard Model 85B computer and a Model 9153B disc drive. Spectral analysis (*e.g.*, derivative spectroscopy) were performed with the EVALU 1 and 2 software packages obtained from Hewlett-Packard. Manual injections were performed with a Rheodyne Model 7125 injector, equipped with a 2-ml injection loop, installed in the column oven compartment.

Column supports

The following packing materials were used in this study: (a) Brownlee VeloSep [either, 3 μm octylsilica (C_8) or octadecylsilica (C_{18}), 10 nm pore size, packed into a 40 × 3.2 mm I.D. cartridge], obtained from Applied Biosystems (Foster City, CA, U.S.A.). (b) Hypersil C_{18} (5 μm octadecylsilica, 12 nm pore size, packed into either a 20 × 2.1 mm I.D. cartridge or 100 × 2.1 mm I.D. column or 3 μm octadecylsilica, packed into a 60 × 4.6 mm I.D. column), obtained from Hewlett-Packard. Hypersil C_{18} microbore columns (50 × 2.1 mm I.D. or 50 × 1.0 mm I.D.) containing 3 μm octadecylsilica (12 nm pore size) were packed as previously described[25]. (c) Brownlee RP-300 C_8 (7 μm dimethyloctyl silica, 30 nm pore size, packed into a 100 × 2.1 mm I.D. cartridge), obtained from Applied Biosystems.

Chemicals and reagents

Cytochrome *c*, bovine serum albumin, α-lactalbumin, ribonuclease, insulin, ovalbumin, α-amylase, carbonic anhydrase, transferrin, trypsin inhibitor, 3-(cyclohexylamino)-1-propane sulfonic acid (CAPS), thioglycolic acid, tris(hydroxymethyl)-aminomethane (Tris) base and 2-mercaptoethanol were purchased from Sigma (St. Louis, MO, U.S.A.). SDS was obtained from British Drug Houses (Poole, U.K.). Chymotrypsin and pepsin were purchased from Worthington (NJ, U.S.A.). Proteins were ^{125}I radioiodinated by the chloramine-T procedure[31]. Iodoacetic acid (puriss. grade) from Fluka (Buchs, Switzerland) was recrystallized prior to use. Dithiothreitol

was obtained from Calbiochem (San Diego, CA, U.S.A.). HPLC-grade organic solvents were purchased from Mallinckrodt (Melbourne, Australia). Trifluoroacetic acid (99+% grade), Tween 20, Brij-35, Triton X-100, and Lubrol-PX were obtained from Pierce (Rockford, IL, U.S.A.). Deionised water, obtained from a tandem Milli-RO and Milli-Q system (Millipore, Bedford, MA, U.S.A.) was used for all buffers. Nonidet P40, Coomassie Blue R250 and ampholines (pH 3.5–10) were purchased from LKB (Bromma, Sweden). PVDF membrane (Immobilon) was purchased from Millipore. Styles of defined S-genotype from the tobacco plant *Nicotinia alata* were obtained as described previously[32].

Preparation of Nicotiana alata style extracts

Protein extracts were prepared from 40 styles from various homozygous clones of *N. alata*, using procedures described elsewhere[32].

Electrophoretic techniques

Style extract proteins were fractionated by 2D gel electrophoresis, using the non-equilibrium pH gradient (NEPHGE) procedure[33]. First-dimension isoelectric focusing gels [4% acrylamide–8.0 *M* urea–2% ampholytes (pH 3.5–10)–2% non-ionic detergent NP-40] were polymerized for 1.5 h. Typically, 100 μg protein was applied to the NEPHGE gels, and electrophoresis was performed at 500 V for 4 h. After NEPHGE, the gels were extruded into 5 ml of SDS-equilibration buffer[4] and stored at −20°C. SDS-PAGE gels (12.5% acrylamide, 1.5 mm thick and 16 cm in length) for the second dimension were prepared the previous day and pre-electrophoresed for 16 h (60 V, 80 mA) with running buffer [0.38 *M* Tris–HCl buffer (pH 8.8), containing 0.1 m*M* thioglycolic acid)]. Equilibrated NEPHGE gels were positioned on top of the second-dimension SDS-PAGE gels using 1.0% (w/v) aqueous agarose. Electrophoresis (240 V, 25 mA) was performed, using the Laemmli SDS-running buffer[34] until the dye-front (bromophenol blue) had migrated 15 cm into the resolving gel.

Electroblotting

After 2D gel electrophoresis, gels were equilibrated for 15 min in transfer buffer (10 m*M* CAPS–10% methanol (pH 11.0)[13]. Prior to use, PVDF membranes were rinsed with 100% methanol, soaked in water for 5 min, and then stored in transfer buffer for at least 15 min. Electrotransfer of proteins from 2D gels onto PVDF membranes was conducted at 4°C in a standard blotting apparatus, the Bio-Rad "Trans-Blot" cell, employing a Model 250/2.5 constant voltage power supply. Electrophoretic conditions: 90 V (300 mA) for 2 h.

Visualisation of blotted proteins

Immediately after electroblotting, blotted proteins were detected by soaking the PVDF membrane in methanol–acetic acid–water (50:10:40, v/v/v), containing 2% (w/v) Coomassie Blue R250, for 10 min. Destaining was performed by soaking the membrane in methanol–acetic acid–water (50:10:40, v/v/v) for 10 min, following by rinsing in water for 10 min. The PVDF sheets were air-dried for 20 min and then stored at −20°C. Alternatively, selected spots for sequence analysis were cut out as disks and stored at −20°C under nitrogen in polypropylene (Eppendorf) tubes.

Amino acid sequence analysis

Automated Edman degradation of electroblotted proteins was performed in an Applied Biosystems sequencer (Model 470A), equipped with an on-line phenylthiohydantoin (PTH) amino acid analyzer (Model 120A) with an improved sample transfer device[35]. Typically, PVDF strips containing the protein were partially sliced and positioned upon a Polybrene[36]-treated glass filter in such a way as to achieve optimal reagent/solvent flow.

Amino acid analysis

Amino acid analysis was performed on a Beckman amino acid analyser (Model 6300), equipped with a Model 7000 integrator. Samples were hydrolysed, *in vacuo*, in 6 *M* HCl containing 0.1% (w/v) phenol for 18 h at 110°C.

Elution of proteins from PVDF

Coomassie Blue-stained proteins were eluted from PVDF membranes with an aqueous detergent mixture [2% (w/v) SDS–1% (w/v) Triton X-100–0.1% (w/v) dithiothreitol]. Briefly, the PVDF strip containing the blotted protein was excised, placed in a polypropylene (Eppendorf) tube and soaked with 100 μl detergent mixture at 25°C for 30 min. The eluent was removed by centrifugation at 20 000 *g*, the procedure was repeated, and the eluates were combined.

Preparation of S-carboxymethyl (CM) S_7-glycoprotein

Dithiothreitol was added to the combined S_7-glycoprotein eluents (*ca.* 15 μg in 200 μl) to achieve a final concentration of 10 m*M*, and the mixture was heated for 5 min at 95°C. After reduction, the S_7-glycoprotein was alkylated by the addition of iodoacetic acid (final concentration, 50 m*M*) for 30 min at 25°C in the absence of light. The reaction was halted by the addition of 5 μl of 2-mercaptoethanol.

Chromatographic recovery of proteins from detergent eluent

PVDF-eluted proteins were recovered from the detergent mixture by a chromatographic procedure previously described[25], with minor modifications. Briefly, the aqueous detergent eluate (200 μl) containing *ca.* 6–15 μg of Coomassie Blue-stained protein was diluted in the sample-loading syringe to 1.5 ml with 1-propanol. The sample was applied at 1 ml/min to a VeloSep C_8 cartridge (40 × 3.2 mm I.D.), previously equilibrated (40 ml) with 90% 1-propanol. The column was developed at 200 μl/min with a linear 10-min gradient from 0 to 100% B where eluent A was 90% aq. 1-propanol and eluent B was 50% aq. 1-propanol, containing 0.4% (v/v) trifluoroacetic acid. The column temperature was 40°C. Peaks were collected manually after correction for post-detector dead volume.

Peptide mapping

Prior to proteolytic digestion, protein samples [*ca.* 6–15 μg in 300 μl 70% aq. 1-propanol 0.2% (v/v) trifluoroacetic acid] were adjusted to 0.02% (w/v) with respect to Tween 20, concentrated three-fold in a centrifugal vacuum concentrator (Savant, Hicksville, NY, U.S.A.) and then diluted to 1 ml with 1% (w/v) ammonium bicarbonate, (pH 7.8), containing 0.02% (w/v) Tween 20 (for chymotrypsin digestion); or 5% formic acid, containing 0.02% (w/v) Tween 20 (for pepsin digestion). Proteins

were digested at an enzyme/substrate mass ratio of 1:20 at 37°C for either 1 h (pepsin) or 4 h (chymotrypsin). Resultant peptide mixtures were fractionated by microbore RP-HPLC, using procedures previously described[1,37].

RESULTS AND DISCUSSION

Two-dimensional gel electrophoresis of Nicotinia alata style extract proteins

Fig. 1 shows a 2D gel of proteins extracted from the styles of a homozygous clone (S_6S_6) of the tobacco plant (*N. alata*). Since the S-allele self-incompatibility glycoproteins located in the style are highly basic[38], NEPHGE was employed in the first electrophoretic dimension to achieve optimal resolution, followed by size fractionation (SDS-PAGE) in the second dimension. Visualization of the proteins on the 2D gel by silver-staining revealed at least 100 clearly resolved spots (Fig. 1). For the purpose of sequence analysis, proteins from identical gels were electrotransferred onto PVDF membranes and visualised with Coomassie Blue R250 (see Experimental section). The major self-incompatibility S-allele glycoproteins from three homozygous clones, (S_2S_2, S_3S_3, and S_6S_6) were chosen for sequence analysis (Table I) along with a number of minor protein spots (P1–P5 from Fig. 1), standards which were selected for the purpose of comparing gels run on different days. In total, 8 proteins were subjected to Edman degradation (Table I) for 15–25 cycles, yielding a total of 82

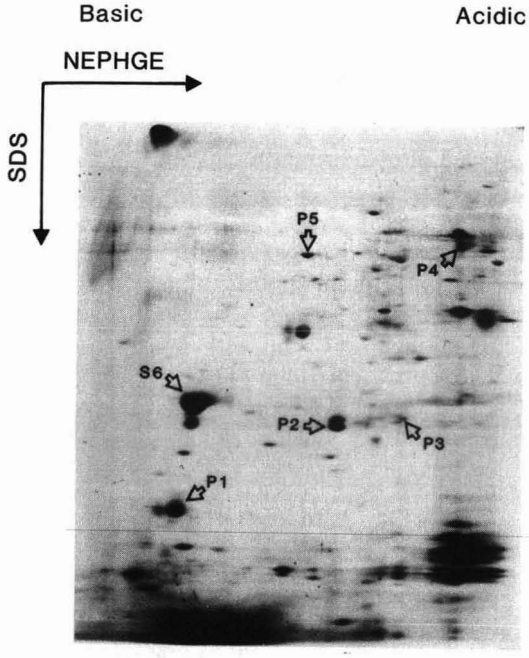

Fig. 1. Two-dimensional gel electrophoresis of *N. alata* style proteins. Total protein extract of 40 styles (*ca.* 100 μg) from homozygous S_6S_6 clones were resolved by non-equilibrium pH gel electrophoresis (horizontal direction) and SDS-PAGE (vertical direction). Proteins were detected by silver-staining. For sequence analysis, proteins from identical gels were electroblotted onto PVDF membranes and then visualised with Coomassie Blue R250. The numbered proteins indicate those selected for sequence analysis (Table I).

TABLE I

N-TERMINAL SEQUENCES OF *NICOTINIA ALATA* STYLE PROTEINS, RESOLVED ON 2D GELS AND ELECTROBLOTTED ONTO PVDF MEMBRANES

Proteins are denoted as shown in Fig. 1 with the exception of S_2 and S_3, which were obtained from analogous 2D gels (not shown). The amino acid sequence is given in the one-letter notation. ?, positions where an unambiguous PTH amino acid assignment could not be made; X, a modified PTH amino acid residue in P1 with a retention time previously not seen in our PTH-amino acid analysis system. Blocked proteins did not yield any amino acid sequence.

Protein	$M_r \cdot 10^{-3}$	*Sequence*																			
		1				5					10					15					20
S_2	31	A	F	E	Y	M	Q	L	V	L	T	W	P	I	T	F	?	R	I	K	
S_3	33	A	F	E	Y	M	Q	L	V	L	Q	W	P	A	A	F	?	H	T	T	P
S_6	32	A	F	E	Y	M	Q	L	V	L	Q	W	P	T	A	F	?	H	X		
			X																		
P1	25	A	P	I	S	K	P	N	?	N	?	N	A	?	Q						
P2	30	?	F	D	?	L	?	L	V	L	T	?	P								
P3	31	D	L	P	V	L	S	E	V	L											
P4	57	Blocked																			
P5	54	Blocked																			

residues. The sequencing efficiencies of this procedure are summarized in Table II. The average repetitive sequencing yields for these proteins, 94–95%, were obtained with an initial coupling yield in the first cycle of 15–22 pmol.

In this study, care was taken to minimize possible chemical modification of proteins (*e.g.* N-terminal blockage and oxidation of tryptophan and methionine residues) during electrophoresis by: (i) introducing an antioxidant (*e.g.*, 0.1 m*M* thioglycollate) in the electrophoresis buffer and (ii) conducting pre-electrophoresis (approximately 12 h) of the gel prior to sample loading. Previously, we[1] and others[11,14,19] had shown that significant improvements in the overall sequencing yields can be obtained by these measures. For instance, the levels for PTH-methionine and -tryptophan in proteins S_2, S_3, and S_6 (residues 5 and 11, respectively) indicate no significant destruction of these labile amino acids (data not shown). If this

TABLE II

REPETITIVE YIELDS (RY) FOR S-GLYCOPROTEINS FROM *NICOTINIA ALATA*

Repetitive yields were calculated using Residues Leu-7 and Ile-13 (S_2). Quantitation of PTH amino acids in each Edman degradation cycle was determined by measuring the peak areas of the PTH signals in each cycle and in a 12.5-pmol standard mixture. Initial yield is the extrapolated value (pmol) of PTH amino acid in cycle 1, determined from a least-squares plot of the data from the sequence run. S_3 was electrophoresed under the neutral conditions described by Moos *et al.*[14].

Protein	$M_r \cdot 10^{-3}$	*Initial yield (pmole)*	*No. of residues identified*	*RY (%)*
S_2	31	22	18/19	94.0
S_6	32	12	16/17	94.7
S_3	33	98	19/20	95.8

TABLE III

ELUTION OF ELECTROBLOTTED PROTEINS FROM PVDF MEMBRANES BY VARIOUS ELUENTS

Proteins were radiolabelled with ^{125}I, electrophoresed on SDS-PAGE, and electrotransferred to PVDF membranes (*cf.* Experimental). After visualization with Coomassie Blue R250, protein spots were excised, placed in an Eppendorf tube and passively eluted with 2 × 100 μl eluent (30 min, 25°C). All detergent elutions were carried out with 50 m*M* Tris–HCl buffer (pH 9.0). Amount of protein loaded onto SDS-PAGE: S_6-glycoprotein, 4 μg; all other proteins, 2 μg. Protein recoveries, determined by measurement of radioactivity, are the amounts of protein eluted, expressed as a percentage of total protein electroblotted onto the PVDF membrane. Values are the average of two experiments performed in triplicate.

Eluent	*Bovine serum albumin, recovery (%)*	*S_6-glyco protein*	*Ovalbumin*	*Carbonic anhydrase*	*Trypsin inhibitor*
2% SDS–1% Triton X-100	64.6	46.0	69.2	74.5	61.4
2% SDS–1% Triton X-100–0.1% DTT	73.1	56.8	74.1	78.0	61.0
2% SDS–1% Nonidet P40	64.7	45.1	67.7	77.3	60.9
2% SDS–1% Nonidet P40–0.1% DTT	66.3	69.0	70.1	70.1	58.7
2% SDS–1% Tween 20	60.9	46.8	59.7	71.3	59.0
2% SDS–1% Tween 20–0.1% DTT	61.6	43.6	60.6	72.6	56.4
2% SDS–1% Lubrol	55.7	27.8	57.6	72.8	55.9
2% SDS–1% Brij-35	56.6	29.7	56.0	73.4	57.2
70% 1-propanol–5% TFA	44.0	41.9	23.2	45.1	38.3
70% 1-propanol–5% TFA–0.1% DTT	47.1	32.5	29.7	37.8	38.5
20% acetonitrile–2% SDS	15.3	5.1	12.5	11.8	29.3

pre-electrophoresis step with an antioxidizing agent is omitted, significant destruction of tryptophan in PVDF-immobilized proteins can result[13].

In contrast to other reports[12], we do not find abnormally low yields of PTH-Asp and PTH-Glu when sequencing PVDF-immobilized proteins (data not shown). It should be noted that for optimal sequencer performance we routinely position the PVDF-immobilized protein strips on top of a Polybrene (3 mg)-conditioned filter disc[1]. This is particularly important when handling peptides or very hydrophilic proteins[1].

Elution of electroblotted proteins from PVDF membranes

We have examined a number of different regimens for eluting proteins from PVDF after their transfer from SDS-polyacrylamide gels. Inspection of Table III reveals that electroblotted proteins of varying molecular weight can be efficiently eluted from PVDF membranes by various regimens of detergents and, to a lesser extent, mixtures of organic solvent and trifluoroacetic acid.

For high-molecular-weight proteins, a small but significant increase in yield was obtained with the addition of 0.1% dithiothreitol (DTT) to the eluent (2% SDS–1% Triton X-100).

HPLC procedure for recovering proteins from detergent eluates

In our earlier studies[25] with inverse-gradient HPLC we employed ODS-Hypersil (3 μm or 5 μm, 12 nm pore size), a sorbent commonly utilized for the RP-HPLC of low-M_r substances (*e.g.*, peptides). We have recently extended these studies to examine

TABLE IV

DATA FOR SPHERICAL POROUS SILICA PACKINGS

Data obtained directly from the manufacturers.

Support	*Particle size (μm)*	*Pore size (nm)*	*Surface area (m^2/g)*	*Surface coverage ($\mu mol/m^2$)*	*Pore volume (ml/g)*	*Carbon content (%)*
Hypersil C_{18}	3–5	12	170	2.06	0.7	9.5–10.0
Brownlee VeloSep C_8	3	10	200	2.2	0.8	7.4–8
Brownlee VeloSep C_{18}	3	10	200	1.9	0.8	12–13.2
Brownlee RP-300	7	30	80–110	8.7	0.5–0.6	7

the applicability of other commercially available silica-based reversed-phase sorbents for this purpose; details of these packings are given in Table IV.

Of the four sorbents examined in this study, the small-pore-size, large-surface-area sorbents (*e.g.* ODS-Hypersil and Brownlee C_8 VeloSep) exhibited comparable efficiencies for the panel of proteins chromatographed in the inverse-gradient mode; the large-pore-size (30 nm) packing (Brownlee RP-300) was not considered useful in the inverse-gradient mode, since proteins exhibited very large peak bandwidths and, consequently, were recovered in unacceptably large volumes (600–1500 μl) (Fig. 2). As previously reported[25], the ion-pairing agent trifluoroacetic acid modulates protein retention behaviour in the inverse-gradient chromatographic mode, as well as chromatographic efficiencies and protein recoveries. For practical purposes, we routinely use 0.4% (v/v) trifluoroacetic acid in the mobile phase in order to minimize peak bandwidth; under these conditions, proteins were typically recovered in 100–300 μl when using 2.1 or 3.2 mm I.D. columns.

The effect of protein load on peak width for a representative small-pore-size packing (ODS-Hypersil), operated in reversed-phase or inverse-gradient elution

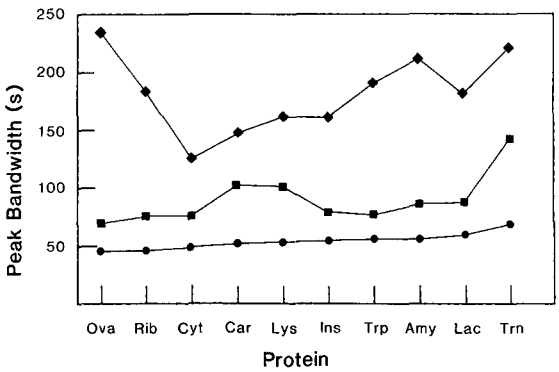

Fig. 2. Plot of the peakwidth (seconds) of eluted proteins from various columns, operated in the inverse-gradient elution mode. Chromatographic conditions are given in Table V. Columns: (◆) Brownlee RP-300 (100 × 2.1 mm I.D.) (●) Brownlee VeloSep C_8 (40 × 3.2 mm I.D.); (■) ODS-Hypersil (100 × 2.1 mm I.D.). Proteins: Ova, ovalbumin; Rib, ribonuclease; Cyt, cytochrome *c*; Car, carbonic anhydrase; Lys, lysozyme; Ins, insulin; Trp, trypsin inhibitor; Amy, α-amylase; Lac, α-lactalbumin; Trn, transferrin.

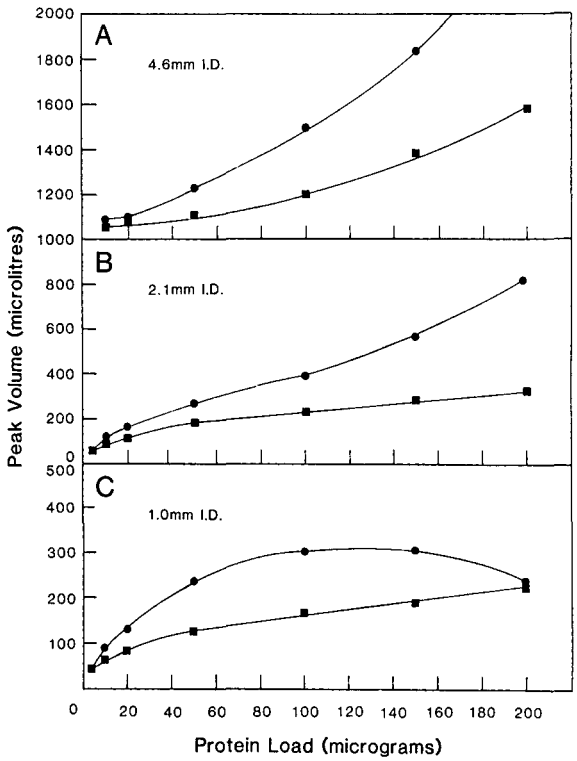

Fig. 3. Effect of protein load on peakwidth of eluted protein for columns of varying internal diameter. Column: ODS-Hypersil (3 μm particle size, octadecyl silica) of varying column dimensions: (A) 60 × 4.6 mm I.D.; (B) 50 × 2.1 mm I.D.; (C) 50 × 1.0 mm I.D. Values are the average of two experiments. Chromatographic conditions: reversed-phase elution mode; linear 50-min gradient from 0–100% B where eluent A is 0.1% (v/v) aq. trifluoroacetic acid and eluent B is 50% aq. 1-propanol, containing 0.1% trifluoroacetic acid. Inverse-gradient elution mode: linear 50-min gradient from 0–100% B, where eluent A is 100% 1-propanol and eluent B is 50% aq. 1-propanol, containing 0.4% (v/v) trifluoroacetic acid. Column temperature 40°C, detection, 280 nm, flow-rates, 1 ml/min, 100 μl/min, and 40 μl/min for 4.6 mm I.D., 2.1 mm I.D., and 1.0 mm I.D. columns, respectively. Sample, α-lactalbumin (varying concentrations in 20 μl water). ●, Inverse-gradient elution mode; ■, reversed-phase elution mode.

mode, is shown in Fig. 3. For sample loads of 1–10 μg, proteins are typically recovered in peak volumes of 70–130 μl from 1–2 mm I.D. columns operated in the inverse-gradient elution mode. These volumes are acceptable for subnanomole structural analysis (*e.g.*, sequence determination in gas-phase/pulsed-liquid sequencers or peptide mapping strategies) where minimization of protein volumes is an important consideration[1]. It is now well established that attempts to concentrate solutions containing subnanomole quantities of protein by classical procedures (*e.g.*, lyophilization or organic solvent precipitation) can result in severe sample loss.

Thus, proteins recovered from detergent mixtures by this means are in an acceptable form for further structural analysis (*e.g.*, mass spectrometry, NMR and peptide mapping). The chromatographic efficiency of proteins in the inverse-gradient mode, *ca.* 90% of that achieved in the reversed-phase mode, is sufficient to facilitate

TABLE V

EFFECT OF PROTEIN LOAD ON PEAK BANDWIDTH

Column: Brownlee C_8 VeloSep (40 × 3.2 mm I.D.). Chromatographic conditions. Reversed-phase elution mode: column was developed with a linear 50-min gradient from 0–100% B where eluent A is 0.1% (v/v) aq. trifluoroacetic acid and eluent B is 50% aq. 1-propanol, containing 0.1% (v/v) trifluoroacetic acid. Inverse-gradient elution mode: column was developed with a linear 50-min gradient from 0–100% B where eluent A is 100% 1-propanol and eluent B is 50% aq. 1-propanol, containing 0.4% (v/v) trifluoroacetic acid. Flow-rate, 400 μl/min, detection, UV at 280 nm, column temperature, 40°C. Peak volumes were determined by measurement of peak width at the peak base. Sample: cytochrome *c* in 20 μl water. Values are peak volume in μl, the values in parenthesis were for samples loaded in the presence of 0.5% SDS.

Amount of protein (μg)	*Chromatographic mode*	
	Reversed-phase	*Inverse-gradient*
0.5	72 (182)	86 (106)
1.0	100 (204)	84 (106)
2.0	97 (224)	93 (112)
4.0	104 (230)	106 (129)
6.0	122 (262)	114 (150)
10.0	111 (297)	129 (165)
15.0	136 (333)	146 (182)
20.0	154 (391)	164 (212)
40.0	200 (450)	218 (288)

their separation (Table V). However, it should be noted that a significant decrease in efficiency (reflected by increased peak volumes) occurs when SDS-containing samples are chromatographed in the reversed-phase elution mode (Table V). This is in marked contrast to chromatography in the inverse-gradient elution mode, where the presence of SDS in the sample does not significantly influence the peak volume of eluted proteins. Thus, the inverse-gradient elution procedure described here offers the potential for resolving proteins at high organic solvent concentrations from detergent mixtures.

Peptide mapping of PVDF-eluted proteins

As mentioned earlier, Coomassie Blue-stained proteins can be efficiently eluted from PVDF membranes with 2% SDS–1% Triton X-100–0.1% dithiothreitol. However, for proteolytic digestion of detergent-eluted proteins, it is necessary to reduce the concentration of detergent, since most proteases used in peptide mapping strategies are inactive in the presence of detergents above concentrations of 0.1–0.2%. Also, it is often necessary to buffer-exchange the eluate to achieve the desired pH (and in some cases, buffer ion) conditions for proteolysis. Although proteins can be separated from detergents by organic solvent precipitation[8,39,40] or by the recently reported[41] size-exclusion chromatography on Sephacryl S-200 with 80% aq. formic acid–methanol (3:1), there are drawbacks with these procedures, the most notable being recoveries, and in the latter case, cleavage of acid-labile peptide bonds (particularly aspartyl–prolyl bonds). In our experience, attempts to achieve acceptable detergent levels (*e.g.*, 0.1–0.2% SDS) for peptide mapping by diluting the eluate were unacceptable, since Coomassie Blue and the ultraviolet-absorbing detergents (*e.g.*,

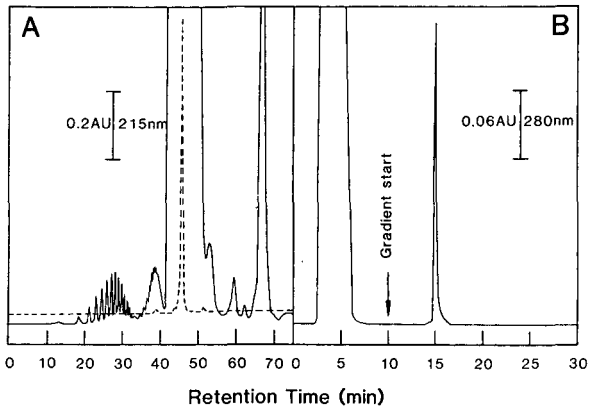

Fig. 4. Chromatography of protein–Triton X-100 mixtures in inverse-gradient and reversed-phase elution modes. Chromatographic conditions: column, Brownlee C_8 VeloSep, 5 μm particle size, 40 × 3.2 mm I.D. (A) Reversed-phase elution mode. The elution position of S_7, determined in the absence of detergent is denoted by the broken line (– – –); (B) inverse-gradient elution mode (see Table IV for chromatographic details). Sample: 200 μl of aq. 1% Triton X-100, containing 10 μg of S_7.

Triton X-100) were enriched on the reversed-phase column and subsequently interfered with interpretation of the peptide map (Fig. 4). Our approach to this problem is to elute the Coomassie Blue-stained proteins from the PVDF membrane (see Experimental) and to recover the protein from the eluate (free of Coomassie Blue and detergents) by the inverse-gradient HPLC procedure mentioned above (Fig. 4).

As reported earlier[25], SDS concentrations up to 1.2% do not influence the load capacity of small-pore packings, used in the inverse-gradient mode. Beyond this SDS concentration, the amount of protein retained on the column during loading diminishes; this may be due to the reversed-phase packing becoming a dynamic ion exchanger[42]. For example, only 50–60% of a sample protein is retained on a column loaded in the presence of 5% SDS. For samples containing SDS in concentrations greater than 1.2% this problem is circumvented by diluting the sample (in the sample-loading syringe) with up to 1.5 ml of 1-propanol (to reduce the overall SDS concentration) and loaded directly onto the column.

Proteins recovered from detergent eluates by inverse-gradient HPLC (Fig. 5) are then subjected to proteolytic digestion in the polypropylene (Eppendorf) collecting tube. Prior to digestion, the sample is diluted with an appropriate buffer (see Experimental) in order to affect buffer-exchange and to lower the organic solvent concentration (for most proteases, typically, to less than 15%). The resultant peptides were purified by microbore-column (1–2 mm I.D.) RP-HPLC, at a low pH [trifluoroacetic acid (pH 2.1)–acetonitrile system] (Fig. 5). As we have reported elsewhere[1–26,30–34,37], in many cases a second and sometimes a third chromatographic step was required to obtain homogenous peptides. In this application, short columns (< 10 cm) are preferred, since they permit the use of high flow-rates (typically, 0.4–1 ml/min for a 1 mm I.D. column and 0.5–2 ml/min for a 2.1 mm I.D. column). The major advantages of high flow-rates are: (i) rapid trace enrichment of sample onto an interactive sorbent and (ii) rapid column re-equilibration. Previously

we have shown[1–3,37] that short microbore columns do not seriously compromise the chromatographic separation of peptides and proteins on reversed-phase columns.

A summary of sequence data, obtained for selected peptides in this study, is given in Table VI. Fig. 6 shows the HPLC analysis of PTH amino acid derivatives from the Edman degradation of peptic peptide T1, derived from electroblotted β-lactoglobulin (Fig. 5A and B). The good yield of PTH-tryptophan in cycle 7 illustrates that no significant destruction of tryptophan occurs during the electrophoresis/electroblotting/peptide mapping procedure.

It is noteworthy that real-time spectral analysis of eluted peptides was a useful adjunct to this peptide mapping strategy. For instance, the use of derivative ultraviolet absorbance spectra[43,44] allowed the rapid identification of peptides containing

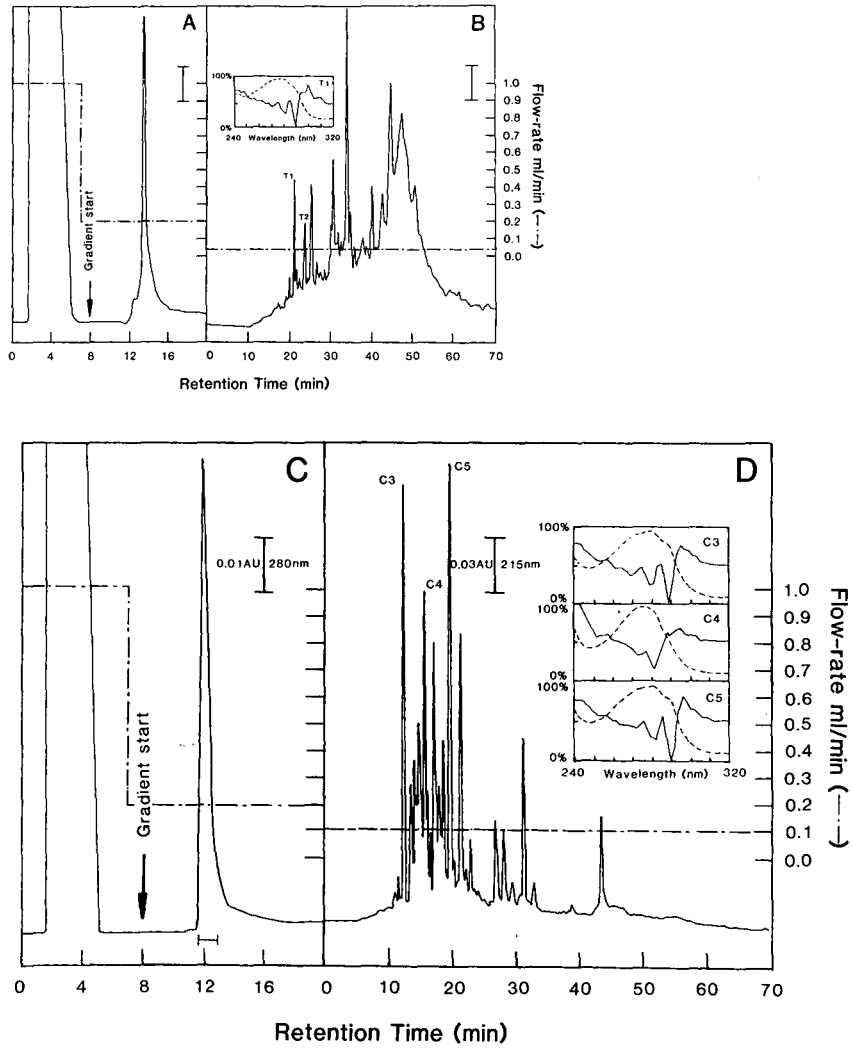

Fig. 5

(*Continued on p. 358*)

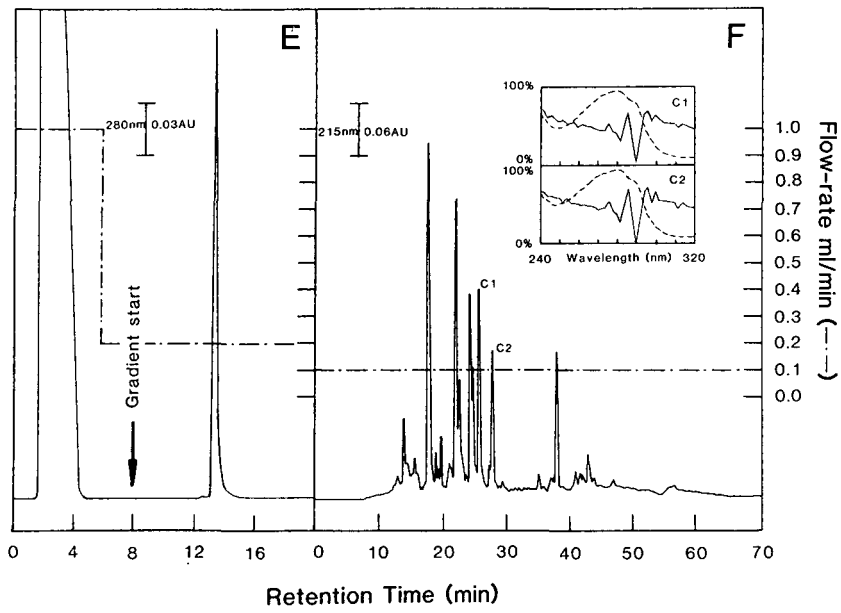

Fig. 5. Peptide mapping of proteins, recovered from detergent mixtures by inverse-gradient HPLC. Conditions for SDS-PAGE electrophoresis, electroblotting onto PVDF membrane, and visualisation with Coomassie Blue are described in Experimental. Coomassie Blue-stained proteins were eluted with 200 μl of 2% SDS–1% Triton X-100–0.1% dithiothreitol in 50 m*M* Tris–HCl buffer, (pH 9.0). Inverse-gradient HPLC conditions are given in Fig. 3. (A) Inverse-gradient HPLC of Coomassie Blue-stained β-lactoglobulin (6 μg) in 200 μl of 2% SDS–1% Triton X-100 elution buffer. Chromatographic conditions: column, Brownlee C_8 VeloSep (40 × 3.2 mm I.D.); the sample was loaded at 1 ml/min; the column was developed at 200 μl/min with a 5-min linear gradient from 0–100% B where eluent A = 90% aq. 1-propanol and eluent B = 50% aq. 1-propanol, containing 0.4% (v/v) trifluoroacetic acid. (B) Separation of a peptic digest of β-lactoglobulin, recovered from (A). For conditions of digestion see Experimental. Chromatographic conditions: column, Brownlee RP-300 (50 × 1.0 mm I.D.); the column was developed with a linear 60-min gradient from 0–100% B, where eluent A = 0.1% (v/v) aq. trifluoroacetic acid and eluent B = 60% aq. acetonitrile, containing 0.085% (v/v) trifluoroacetic acid. Peptides selected for sequence analysis are indicated. (C) Inverse-gradient HPLC of Coomassie Blue-stained S-carboxymethyl-lysozyme (g-type) (7 μg) from the Black Swan[45]. Conditions were the same as in (A). (D) Separation of peptic peptides of S-carboxymethyl-lysozyme (g-type) on a Brownlee RP-300 column (30 × 2.1 mm I.D.). Conditions were the same as in (B). (E) Inverse-gradient HPLC of Coomassie Blue-stained S-carboxymethyl S_7-glycoprotein (15 μg). Conditions were the same as in (A). (F) Separation of chymotrypsin peptides of S-carboxymethyl-S_7 glycoprotein on a Brownlee RP-300 column (30 × 2.1 mm I.D.). Conditions were the same as in (B). Selected peptides (identified by capital letters) were subjected to sequence analysis (Table VI). Spectral analysis of these peptides, obtained using a diode-array detector during elution, are illustrated in the insets. The absorption spectra have been normalized to relative absorbance on a scale of 0–100%. Zero-order-derivative spectra (– – –); second-order-derivative spectra (——).

aromatic amino acids. This is particularly useful if amino acid sequence data are required for the purpose of designing DNA probes, since tryptophan, with its unique codon, is readily identifiable by this means. An inspection of the spectra obtained in this study (Fig. 5, insets) reveals that all of the selected peptides contain aromatic amino acids, as judged by their absorption peaks in the range 270–300 nm. Enhancement of resolution by second-order-derivative spectroscopy reveals an

TABLE VI

SEQUENCE ANALYSIS OF PEPTIDES, ISOLATED BY SDS-PAGE ELECTROBLOTTING/ INVERSE-GRADIENT HPLC/RP-HPLC

Proteins (15 μg) were electrophoresed on SDS-PAGE and then electroblotted onto PVDF membranes (*cf.* Experimental). After visualisation with Coomassie Blue R250, protein spots were excised, placed in an Eppendorf tube and passively eluted for 30 min at 25°C with 2 × 100 μl 2% SDS–1% Tritons X-100–0.1% dithiothreitol–50 m*M* Tris–HCl buffer (pH 9.0). Protein recoveries, determined by amino acid analysis, were *ca.* 6 μg. Proteins were recovered from the detergent eluent by inverse-gradient reversed-phase HPLC, digested with either pepsin or chymotrypsin and the resultant peptides fractioned by microbore column HPLC (see Fig. 5). Selected peptides were subjected to sequence analysis.

Sample	*Initial yield in 1st cycle (pmol)*	*Sequence*	*Sequence matched*
β-Lactoglobulin:			
Peptide T1	14	Q K V A G T W	Residues 13–19
Peptide T2	13	Y V E E L K P T P E	Residues 42–51
S_7-Glycoprotein:			
Peptide C1	150	T I H G L W P D D V S T	Residues 29–40
Peptide C2	113	V L Q W P T A F	Residues 8–15
Lysozyme (g-type):			
Peptide C3	75	Q V D K R S H K P Q G T W	Residues 95–107
Peptide C5	104	K K F P S W T K D Q W	Residues 129–139

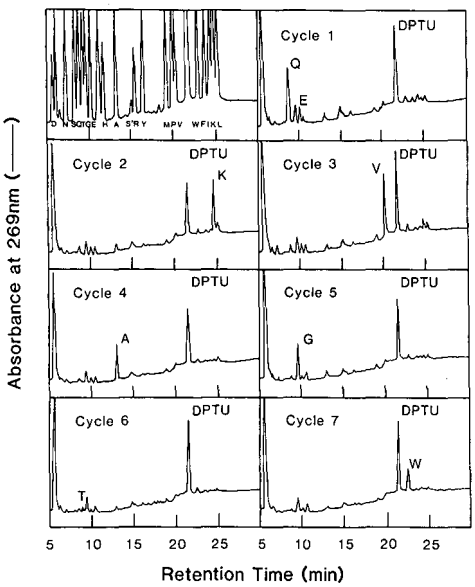

Fig. 6. Sequence analysis of peptic digest Peptide T1 from electroblotted β-lactoglobulin. β-lactoglobulin (*ca.* 20 μg) was electrophoresed by SDS-PAGE, electrotransferred onto PVDF, visualized with Coomassie Blue, and then eluted from PVDF with 200 μl of 2% SDS–1% Triton X-100 in 50 m*M* Tris–HCl buffer (pH 9.0), containing 0.1% dithiothreitol. The recovery of β-lactoglobulin, determined by amino acid analysis, was 6 μg. The remaining portion of β-lactoglobulin (*ca.* 4.5 μg) was recovered from the detergent mixture by inverse-gradient HPLC (Fig. 5A), digested with pepsin, and the peptide digest was fractionated by microbore HPLC (Fig. 5B). Peptide T1 (Fig. 5B) was subjected to sequence analysis. The HPLC elution patterns are shown. The positions of the PTH amino acids, assigned in the chromatograms from cycles 1–7, are indicated by the one-letter notation. The elution profile of a calibration mixture of PTH amino acids (25 pmol) is shown in the top left panel. DPTU denotes the byproduct, diphenyl thiourea.

extremum at 290 ± 2 nm for peptides C1, C2, C3, C5, and T1 (Fig. 5) and an extremum at 280 ± 2 nm for peptides C1–C5, T1 and T2 (Fig. 5); these are characteristic of tryptophan[43]. A maximum at 280 ± 2 nm only (*e.g.*, peptide C4) is characteristic of tyrosine residues[43]. The presence of tryptophan residues in peptides C1–C3, C5, and T1 and a tyrosine residue in peptide T2 was confirmed by amino acid sequence analysis (Table VI).

In summary, we present here a novel procedure for obtaining internal amino acid sequence information for proteins resolved by either SDS-PAGE or 2D gel electrophoresis. By combining gel electrophoresis, electroblotting, and HPLC (in both reversed-phase and inverse-gradient elution modes) we can obtain internal sequence data for electroblotted proteins, isolated in the low-microgram range. In the absence of detergents, the inverse-gradient HPLC reported in this study should be applicable to the separation of proteins under conditions of high organic solvent concentrations.

REFERENCES

1 R. J. Simpson, R. L. Moritz, G. S. Begg, M. R. Rubira and E. C. Nice, *Anal. Biochem.*, 177 (1989) 221.
2 R. J. Simpson and E. C. Nice, in O. L. Kon (Editor), *Integration Control of Metabolic Processes: Pure and Applied Aspects: 4th FAOB Conference, 1986, Singapore*, ICSU Press, 1987, pp. 473–487.
3 R. J. Simpson and E. C. Nice, in K. A. Walsh (Editor), *Methods in Protein Sequence Analysis, 1986*, Humana Press, Clifton, NJ, 1987, pp. 213–228.
4 P. H. O'Farrell, *J. Biol. Chem.*, 250 (1975) 4007.
5 J. E. Celis and R. Bravo (Editors) *Two-Dimensional Gel Electrophoresis of Proteins: Methods and Applications*, Academic Press, 1984.
6 M. W. Hunkapiller, E. Lujan, F. Ostranger and L. E. Hood, *Methods Enzymol.*, 91 (1983) 227.
7 P. A. Stearne, I. R. Van Driel, B. Grego, R. J. Simpson and J. W. Goding, *J. Immunol.*, 134 (1985) 443.
8 G. S. Baldwin, R. Chandler, K. L. Seet, J. Weinstock, B. Grego, M. R. Rubira, R. L. Moritz and R. J. Simpson, *Protein Seq. Data Anal.*, 1 (1987) 7.
9 A. Tsugita, T. Ataka and T. Uchida, *J. Protein Chem.*, 6 (1987) 121.
10 J. Vandekerckhove, G. Bauw, M. Puype, J. Van Damme and M. Van Montagu, *Eur. J. Biochem.*, 152 (1985) 9.
11 R. H. Aebersold, D. B. Teplow, L. E. Hood and S. B. Kent, *J. Biol. Chem.*, 261 (1986) 4229.
12 G. Bauw, M. De Loose, D. Inze, M. Van Montagu and J. Vandekerckhove, *Proc. Natl. Acad. Sci. U.S.A.*, 84 (1987) 4806.
13 P. Matsudaira, *J. Biol. Chem.*, 262 (1987) 10035.
14 M. Moos, N. Y. Nguyen and T.-Y. Liu, *J. Biol. Chem.*, 263 (1988) 6005.
15 S. Yuen, M. N. Hunkapiller, K. J. Wilson and P. M. Yuan, *Anal. Biochem.*, 168 (1988) 5.
16 D. B. Smith, M. R. Rubira, R. J. Simpson, K. M. Davern, W. U. Tiu, P. G. Board and G. F. Mitchell, *Molec. Biochem. Parasitol.*, 27 (1988) 249.
17 R. H. Aebersold, J. Leavitt, L. E. Hood and S. B. H. Kent, *Proc. Natl. Acad. Sci. U.S.A.*, 184 (1987) 6970.
18 R. H. Aebersold, G. D. Pipes, H. Nika, L. E. Hood and S. B. H. Kent, *Biochemistry*, 27 (1988) 6860.
19 M. J. Walsh, J. McDougall and B. Wittmann-Liebold, *Biochemistry*, 27 (1988) 6867.
20 C. Eckerskorn, W. Mewes, H. Goretzki and F. Lottspeich, *Eur. J. Biochem.*, 176 (1988) 509.
21 R. J. Simpson and E. C. Nice, *Biochem. Int.*, 8 (1984) 787.
22 C. Uyttenhove, R. J. Simpson and J. Van Snick, *Proc. Natl. Acad. Sci. U.S.A.*, 85 (1988) 6934.
23 R. J. Simpson, R. L. Moritz, J. J. Gorman and J. Van Snick, *Eur. J. Biochem.*, in press.
24 B. Szewczyk and D. F. Summers, *Anal. Biochem.*, 168 (1988) 48.
25 R. J. Simpson, R. L. Moritz, E. C. Nice and B. Grego, *Eur. J. Biochem.*, 165 (1987) 21.
26 R. J. Simpson, G. E. Reid, M. R. Rubira, L. D. Ward, G. S. Begg and R. L. Moritz, in B. Wittman-Liebold (Editor), *Methods in Protein Sequence Analysis*, Springer-Verlag, Berlin, in press.
27 K. E. Bij, Cs. Horváth, W. R. Melander and A. Nahum, *J. Chromatogr.*, 203 (1981) 65.
28 M. T. W. Hearn and B. Grego, *J. Chromatogr.*, 218 (1981) 497.
29 D. N. Armstrong and R. E. Boehm, *J. Chromatogr. Sci.*, 22 (1984) 378.

30 E. C. Nice and R. J. Simpson, *Biochem. Int.*, 8 (1984) 787.
31 W. M. Hunter and F. C. Greenwood, *Nature*, 194 (1962) 495.
32 C. Des Francs, H. Thiellmeut and D. De Vienne, *Plant Physiol.*, 78 (1985) 178.
33 P. Z. O'Farrell, H. M. Goodman and P. H. O'Farrell, *Cell*, 12 (1977) 1133.
34 U. K. Laemmli, *Nature*, 227 (1970) 680.
35 G. S. Begg and R. J. Simpson, in T. E. Hugli (Editor), *Techniques in Protein Chemistry*, Academic Press, New York, in press.
36 D. K. Klapper, C. E. Wilde and J. D. Capra, *Anal. Biochem.*, 85 (1978) 126.
37 R. J. Simpson, R. L. Moritz, M. R. Rubira and J. Van Snick, *Eur. J. Biochem.*, 176 (1988) 187.
38 W. Jahnen, M. P. Batterham, A. C. Clarke, R. L. Moritz and R. J. Simpson, *The Plant Cell*, 1 (1989) 5.
39 T. Ratajczak, M. Comber, R. Moir, R. Hahnel, B. Grego, M. R. Rubira and R. J. Simpson, *Biochem. Biophys. Res. Commun.*, 143 (1987) 218.
40 T. Ratajczak, M. J. Brockway, R. Hahnel, R. L. Moritz and R. J. Simpson, *Biochem. Biophys. Res. Commun.*, 151 (1988) 1156.
41 H. Schagger, H. Aquila and S. Von Jagow, *Anal. Biochem.*, 173 (1988) 201.
42 J. Knox and J. Jurand, *J. Chromatogr.*, 125 (1975) 89.
43 A. F. Fell, *Trends Anal. Chem.*, 2 (1983) 63.
44 B. Grego, I. R. Van Driel, J. W. Goding, E. C. Nice and R. J. Simpson, *Int. J. Pept. Protein Res.*, 27 (1986) 201.
45 R. J. Simpson, G. S. Begg, D. S. Dorow and F. J. Morgan, *Biochemistry*, 19 (1980) 1814.

Journal of Chromatography, 476 (1989) 363–375
Elsevier Science Publishers B.V., Amsterdam — Printed in The Netherlands

CHROMSYMP. 1630

CORRELATION OF PROTEIN RETENTION TIMES IN REVERSED-PHASE CHROMATOGRAPHY WITH POLYPEPTIDE CHAIN LENGTH AND HYDROPHOBICITY

COLIN T. MANT*, NIAN E. ZHOU and ROBERT S. HODGES
Department of Biochemistry and the Medical Research Council of Canada Group in Protein Structure and Function, University of Alberta, Edmonton, Alberta T6G 2H7 (Canada)

SUMMARY

The use of amino acid retention or hydrophobicity coefficients for the prediction of peptide retention time behaviour on hydrophobic stationary phases is based on the premise that amino acid composition is the major factor affecting peptide retention in reversed-phase chromatography. Although this assumption holds up well enough for small peptides (up to *ca.* 15 residues), it is now recognized that polypeptide chain length must be taken into account when attempting to equate retention time behaviour of larger peptides and proteins with their overall hydrophobicity. In the present study, we have examined the reversed-phase retention behaviour of 19 proteins of known sequence on stationary phases of varying hydrophobicity and ligand density. From the observed protein retention behaviour on C_4, C_8 and C_{18} stationary phases under gradient elution conditions, we have been able to correlate the observed retention times of proteins ranging in molecular weight from 3500 to 32 000 dalton and in chain length from 30 to 300 residues with their overall hydrophobicity (based on retention parameters derived from small peptides) and the number of residues in the polypeptide chain. The retention behaviour of the proteins on the C_4, C_8 and C_{18} columns was also compared to that obtained on supports containing lower ligand densities (phenyl ligands). The maintenance of native or partially folded protein conformation on the phenyl columns, resulting in lower retention times than would be expected for fully denatured proteins, underlined the importance of efficient protein denaturation for satisfactory correlation of protein retention times with protein hydrophobicity. In addition, the effectiveness of increasing temperature and/or ligand density of the stationary phase in denaturing proteins was also demonstrated.

INTRODUCTION

The most widely-used mode of high-performance liquid chromatography (HPLC) for peptide separations is, by far, reversed-phase chromatography (RPC)[1]. Although RPC has, for the most part, been used for the separation of relatively small molecules (< 50 residues), its application to the separation of larger polypeptides and proteins has seen a significant increase in recent years.

0021-9673/89/$03.50

A major factor governing the retention behaviour of peptides and proteins during RPC is the relative hydrophilic/hydrophobic contribution that the side-chains of individual amino acid residues make to the overall hydrophobicity of the molecule. In fact, several research groups[2–13] have determined sets of coefficients for predicting peptide retention times during RPC on the assumption that the contribution of each residue to peptide retention is additive and that retention time is linearly related to the sum of the contribution of each residue. This assumption, that the chromatographic behaviour of a peptide is mainly or solely dependent on amino acid composition, holds up well enough for small peptides (up to *ca.* 15 residues), but several researchers have noted that peptides larger than 15–20 residues tended to be eluted more rapidly than predicted from hydrophobic considerations alone[1,4,5,7,14–17]. Attempts by various researchers[14,15,18] to correlate protein retention times with protein hydrophobicity, as expressed by the sum of Recker fragmental constants[14,15] or the sum of HPLC-derived retention parameters[18], have been largely unsuccessful.

In the present study, we have subjected 23 proteins of known sequence to RPC on five stationary phases of varying hydrophobicity and ligand density. From the observed protein retention behaviour, we have been able to correlate the observed retention times of proteins ranging in molecular weight from 3500 to 32 000 dalton and in chain length from 30 to 300 residues with their overall hydrophobicity (expressed as the sum of amino acid side-chain hydrophobicity coefficients) and the number of residues in the polypeptide chain.

EXPERIMENTAL

Materials

HPLC-grade water and acetonitrile were obtained from J. T. Baker (Phillipsburg, NJ, U.S.A.). HPLC-grade trifluoroacetic acid (TFA) was obtained from Pierce (Rockford, IL, U.S.A.. A synthetic decapeptide reversed-phase peptide standard, S4, and a mixture of five synthetic peptide polymers [Ac-(G-L-G-A-K-G-A-G-V-G)$_n$-amide, where n = 1, 2, 3, 4 and 5] (referred to as the "X" series of peptide polymers in the text) were obtained from Synthetic Peptides Inc. (Department of Biochemistry, University of Alberta, Edmonton, Canada). Bovine insulin, bovine insulin (chain B), equine cytochrome *c*, bovine α-lactalbumin, bovine ribonuclease A, chicken avidin, chicken lysozyme, sperm whale myoglobin, sheep prolactin, papain, jack bean concanavalin A, porcine elastase, bovine α-chymotrypsinogen A, equine alcohol dehydrogenase, chicken ovalbumin, bakers yeast enolase and bovine serum albumin (BSA) were obtained from Sigma (St. Louis, MO, U.S.A.). Rabbit skeletal troponin C (RsTnC), turkey skeletal TnC, rabbit skeletal troponin I (RsTnI), rabbit skeletal troponin T (RsTnT), rabbit cardiac troponin T (RcTnT), and rabbit cardiac tropomyosin (RcTM) were prepared from tissue extracts in this laboratory.

Peptide synthesis

Three series of peptide polymers were synthesized on an Applied Biosystems (Foster City, CA, U.S.A.) peptide synthesizer Model 430A, using the general procedure for solid phase synthesis described by Parker and Hodges[19] and Hodges *et al.*[20]. The sequences of the peptides were ("G" series) Ac-(G-K-G-L-G)$_n$-amide, where n = 1, 2, 4, 6, 8, 10 (5–50 residues); ("A" series) Ac-(L-G-L-K-A)$_n$-amide, were n = 1,

2, 4, 6, 8, 10 (5–50 residues); ("L" series) Ac-(L-G-L-K-L)$_n$-amide, where n = 1, 2, 4 (5–20 residues).

Apparatus

The HPLC instrument consisted of a Hewlett-Packard (Avondale, PA, U.S.A.) HP 1090 liquid chromatograph coupled to an HP 1040A detection system, HP 9000 Series 300 computer, HP 9133 disc drive, HP 2225A Thinkjet printer and HP 7440A plotter.

Columns

Proteins were separated on five columns: (1) SynChropak RP-4 (C_4), 250 × 4.1 mm I.D., 6.5 μm particle size, 300 Å pore size, *ca.* 7.5% carbon loading (SynChrom, Linden, IN, U.S.A.); (2) Aquapore RP-300 (C_8), 220 × 4.6 mm I.D., 7 μm, 300 Å (Brownlee Labs., CA, U.S.A.); (3) SynChropak RP-P (C_{18}), 250 × 4.6 mm I.D., 6.5 μm, 300 Å, *ca.* 10% carbon loading (SynChrom); (4) Bio-Gel TSK Phenyl-5PW, 75 × 7.5 mm I.D., 10 μm, 1000 Å (Bio-Rad Labs., Richmond, CA, U.S.A.); (5) Bio-Gel TSK Phenyl RP+, 75 × 4.6 mm I.D., 10 μm, 1000 Å (Bio-Rad Labs.).

RESULTS AND DISCUSSION

In order to correlate overall hydrophobicity of a polypeptide or protein with its retention behaviour in RPC, it is important to have an accurate means of expressing this hydrophobicity. Most attempts to determine the effective contribution of each amino acid side chain and end group to the retention process in RPC from HPLC-derived data have involved computer-calculated regression analyses of the retention times of a wide range of peptides of varied composition[2–8,11,12]. Comparison of the various sets of retention indices or coefficients derived in this manner showed numerous discrepancies both in the relative order of hydrophobicities of the amino acid side chains, and in the magnitude of the contributions of specific residues[9]. A possible explanation for these discrepancies is that certain residues did not appear often enough in the various peptide mixtures used to enable an accurate determination of their contributions. In addition, possible polypeptide chain-length-dependence effects are not being taken into account since the peptides used to determine the coefficients were of a wide range of size, composition and sequence[13]. The most precise set of retention coefficients yet determined was reported by Guo and co-workers[9,10] who examined the contribution of individual amino acid residues to retention of a model synthetic peptide: Ac-G-X-X(L)$_3$-(K)$_2$-amide, where X was substituted by the 20 naturally occurring amino acids found in proteins. This method overcame the problems associated with the computer-calculated regression analysis approach, and the retention parameters derived from this work were applied to the present study.

Guo *et al.*[9] obtained their retention coefficients by subjecting their peptide analogues to linear 0.1% aqueous TFA to 0.1% TFA in acetonitrile gradients at pH 2.0, and these conditions were also used in the present study. The acidic nature (pH 2.0) of the TFA-containing mobile phase suppresses the ionization of surface silanols on silica-based columns, thereby overcoming undesirable ionic interactions between basic solutes and the column packing. In addition, TFA not only provides an acidic medium, but is an excellent protein solubilizing agent[21,22], which is used routinely in solid phase peptide synthesis to extract peptides and proteins from the resin support after cleavage.

Complete denaturation of a protein is required for full expression of its overall hydrophobicity. The hydrophobicity of a protein in its native conformation is dramatically different from its unfolded state, since the hydrophobic side-chains are buried during the folding process. The hydrophobic interactions stabilizing the three-dimensional structure of a protein must be disrupted to maximize interaction of the polypeptide chain with the reversed-phase sorbent. Lau *et al.*[22] demonstrated that the primary cause of protein denaturation during RPC is the hydrophobicity of the stationary phase which disrupts the hydrophobic interactions stabilizing the native conformation. These workers showed that even an ultra-short (C_3) sorbent with low carbon loading was able to denature very stable synthetic model proteins. These model proteins consisted of two-stranded α-helical coiled coils in which the quaternary structure was stabilized by hydrophobic interactions between the two α-helics. These proteins are probably the most stable proteins yet reported as indicated by temperature and denaturation studies in 0.1% aqueous. TFA which is a starting solvent for RPC. For example, the coiled coil consisting of two 35-residue chains was only 30% denatured at temperatures greater than 70°C[23,24]. Yet, interaction with the hydrophobic matrix during RPC caused disruption of the hydrophobic interactions that

TABLE I
PROTEINS USED IN THIS STUDY

Protein	*Molecular weight*	*N*[a]	*Relative hydrophobicity*[b]
1 Insulin (chain B)[c]	3500	30	0.49
2 Insulin	6030	51	0.79
3 Cytochrome *c*	11 700	104	1.00
4 α-Lactalbumin	14 180	123	1.76
5 Ribonuclease A	13 690	124	1.10
6 Avidin	14 330	128	1.55
7 Lysozyme	14 310	129	1.62
8 Myoglobin	17 200	153	1.71
9 RsTnC	17 960	159	2.25
10 Turkey TnC	18 000	162	2.17
11 RsTnI	20 700	178	1.89
12 Prolactin	22 550	198	2.89
13 Papain	23 430	212	2.83
14 Concanavalin A	25 570	237	3.25
15 Elastase	25 900	240	3.33
16 α-Chymotrypsinogen A	25 670	245	3.35
17 RsTnT	30 520	259	2.39
18 RcTnT	32 880	276	2.57
19 RcTM	32 000	284	3.20
20 Alcohol dehydrogenase	39 800	374	5.46
21 Ovalbumin	45 000	386	6.50
22 Enolase	46 700	436	5.97
23 BSA	66 300	582	7.82

[a] Number of amino acid residues.

[b] Expressed as ΣR_c of the protein/ΣR_c of cytochrome *c*, where ΣR_c is the sum of the retention coefficients of the amino acid residues as reported by Guo *et al.*[9].

[c] Although only polypeptides of more than 50 residues are classed as proteins, insulin (chain B) was included as a protein for the purposes of the present study.

stabilized these proteins, suggesting that this denaturation during RPC would be representative of the situation for most proteins. Thus, the 23 proteins listed in Table I were subjected to linear gradient elution (1% B/min), at a flow-rate of 1 ml/min, on analytical C_4, C_8 and C_{18} columns, where eluent A was 0.1% aqueous TFA and eluent B was 0.1% TFA in acetonitrile. Considering the work of Lau *et al.*[22], it was assumed that the extremely hydrophobic nature of these sorbents would denature these proteins. In addition, the 300-Å pore size of the three columns is very suitable for separating both peptides and proteins[1,22,25]. To standardize retention behaviour, each protein was run separately with an internal peptide standard, S4, and cytochrome *c* as a protein standard. A representative separation of a mixture of eight proteins, including cytochrome *c* (protein 3), and peptide S4 on the C_8 column is shown in Fig. 1. Elution profiles obtained on the C_4 and C_{18} columns were very similar.

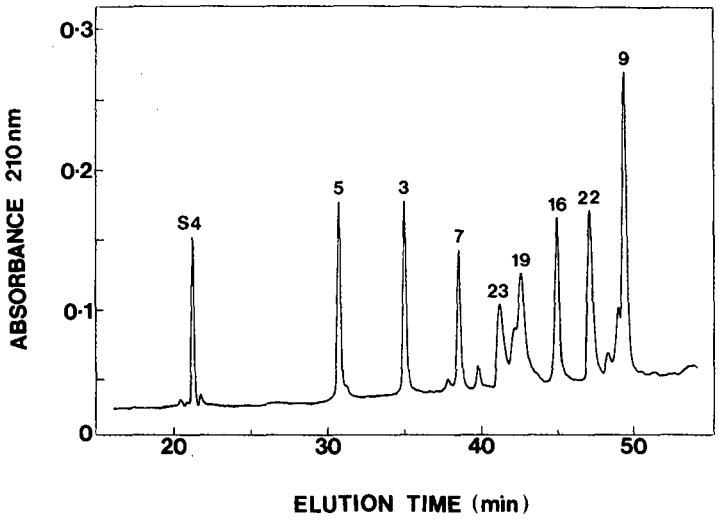

Fig. 1. RPC of a mixture of proteins. Column, Aquapore RP-300 C_8 (220 × 4.6 mm I.D.); mobile phase, linear A–B gradient (1% B/min), where eluent A is 0.1% aqueous TFA and eluent B is 0.1% TFA in acetonitrile (pH 2.0), flow-rate, 1 ml/min; temperature, 26°C. Numbers denote proteins listed in Table I. S4 is a synthetic reversed-phase decapeptide standard.

Effect of polypeptide chain length on retention time

There is a peptide chain length effect on retention behaviour of polypeptides, independent of any conformational considerations[26]. Thus, Lau *et al.*[22] reported a linear relationship between log molecular weight and peptide retention time during RPC for a series of five peptide polymers of 8–36 residues. Mant and Hodges[1] demonstrated a similar exponential relationship for a series of five peptide polymers of 10–50 residues. The effect on peptide retention of increasing peptide length decreased progressively with each ten-residue addition.

Fig. 2 compares the results of plotting observed retention times on the C_{18} column *versus* the logarithm of the number of residues (ln N) for four series of peptide polymers (Fig. 2A) and the 23 proteins listed in Table I (Fig. 2B). The peptide polymers

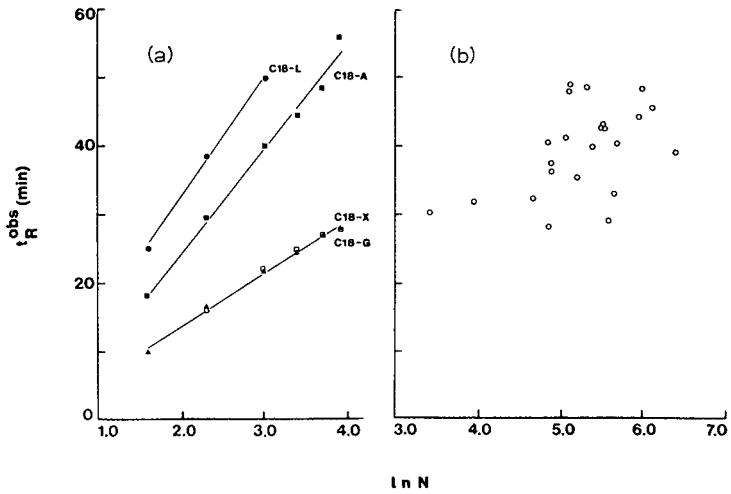

Fig. 2. Effect of polypeptide chain length on observed peptide and protein retention times in RPC. Observed retention time (t_R^{obs}) *versus* ln N (where N = number of residues) for four series of peptide polymers (a) or 23 proteins (b). Column, SynChropak RP-P C_{18} (250 × 4.6mm I.D.); mobile phase, linear A–B gradient (1% B/min), where eluent A is 0.1% aqueous TFA and eluent B is 0.1% TFA in acetonitrile (pH 2.0); flow-rate, 1 ml/min; temperature, 26°C; absorbance, 210 nm. C18-X, C18-G, C18-A, C18-L denote results for the "X", "G", "A" and "L" series of peptide polymers, respectively. Sequences of the polymers are shown in the Experimental section. The proteins are listed in Table I.

(described in the Experimental section) were run under the same conditions as described above for the proteins. The plots for the polymers resulted in straight-line plots with different slopes, depending on the hydrophobicity of a particular peptide polymer series. The "G" and "X" series of polymers are very similar in hydrophobicity, resulting in overlapping profiles (Fig. 2A). The slopes of the plots in Fig. 2A increased with increasing hydrophobicity of the peptide polymers, *i.e.*, "G" ≈ "X" < "A" < "L" series. By comparison, the plot for the proteins (Fig. 2B) did not show any linear relationship. This was not surprising since, unlike the peptide polymers which increase in length and hydrophobicity in a well-defined manner, the proteins differ widely in size, composition and hydrophobicity. The results shown in Fig. 2 suggested that a clearer understanding of protein retention behaviour during RPC required clarification of the effects of polypeptide hydrophobicity, as well as chain length, on observed retention times.

Correlation of protein retention behaviour with polypeptide chain length and hydrophobicity

Predicted protein retention times were determined by use of the rules for prediction of peptide retention times developed by Guo *et al.*[9],

$$\tau = \Sigma R_c + t_s$$

where the predicted retention time (τ) equals the sum of the retention coefficients (ΣR_c) for the amino acid residues, plus the time correction for the internal peptide standard

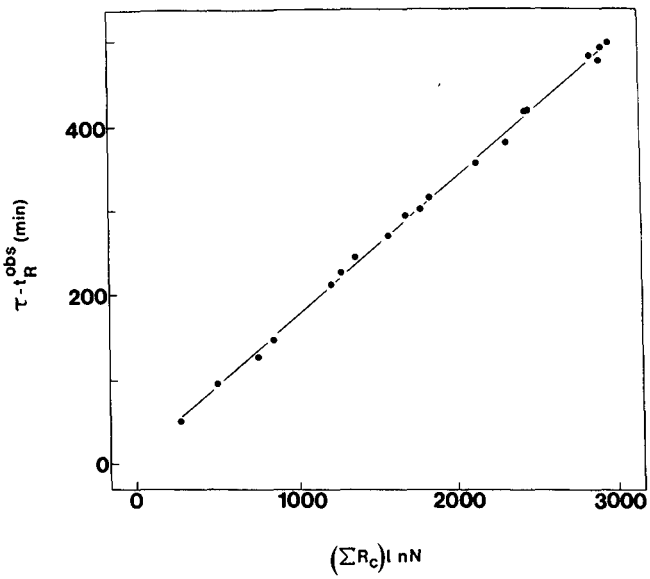

Fig. 3. Correlation of protein retention time with polypeptide chain length and hydrophobicity. Predicted minus observed protein retention time ($\tau - t_R^{obs}$) *versus* ΣR_c ln N, where ΣR_c is the sum of the retention coefficients of Guo *et al.*[9] for the amino acid residues in a protein, and N is the number of residues in the protein. Results are for an Aquapore RP-300 C_8 column (220 × 4.6 mm I.D.). Mobile phase conditions as described in Fig. 2. Absorbance at 210 nm. Results shown are for proteins 1–19 (Table I).

(t_s). The value t_s is obtained by subtracting the sum of the retention coefficients for the peptide standard S4 (ΣR_c^{std}), from the observed retention time of the same peptide (t_R^{std})

$$t_s = t_R^{std} - \Sigma R_c^{std}$$

This intimate relationship between protein hydrophobicity and chain length and their combined effect on protein retention behaviour in RPC is clearly shown in Fig. 3. Plotting predicted (τ) minus observed (t_R^{obs}) protein retention time *versus* the product of protein hydrophobicity (expressed as ΣR_c, the sum of the coefficients of Guo *et al.*[9]) and the logarithm of the number of residues (ln N)[26], resulted in a single, straight-line plot (correlation, $r = 1.00$) for 19 proteins (proteins 1–19 in Table I), *i.e.*, a range of 30–284 residues in polypeptide chain length and 3500–32 000 dalton in molecular weight. Thus, the discrepancy between predicted and observed protein retention times is linearly related to ΣR_c ln N. Fig. 3 shows the plot for the C_8 column. Interestingly, the results on the C_4 and C_{18} columns (different *n*-alkyl chain lengths and ligand densities) gave very similar results. When ln molecular weight replaced ln N in the above relationship, the correlation of the resulting plot was not as high.

When the expression denoting polypeptide hydrophobicity (ΣR_c) was removed from the relationship producing the straight-line plot shown in Fig. 3, *i.e.*, plotting ($\tau - t_R^{obs}$) *versus* ln N, the profiles shown in Fig. 4 were obtained. Results are shown for both the four series of peptide polymers (Fig. 4A) and for proteins 1–19 (Table I) (Fig. 4B) on the C_8 column. When the peptide polymers were plotted in identical fashion to

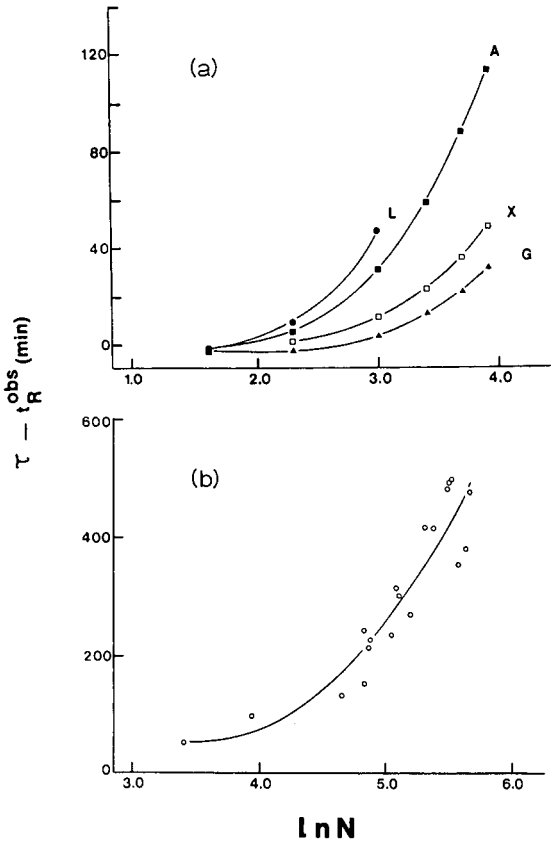

Fig. 4. Plot of predicted minus observed peptide (a) and protein (b) retention time ($\tau - t_R^{obs}$) *versus* ln N. Column, Aquapore RP-300 C_8 (220 × 4.6 mm I.D.). Mobile phase conditions as described in Fig. 2. Absorbance at 210 nm. Sequences of the peptide polymer series "G", "X", "A" and "L" are shown in the Experimental section. Results shown are for proteins 1–19 (Table I).

that shown for the proteins in Fig. 3, the result was a single, straight-line plot[26]. Removing the expression denoting hydrophobicity, ΣR_c, from the abscissa resulted in the profiles for the four peptide series becoming non-linear and diverging (Fig. 4A). The proteins showed a similar relationship (Fig. 4B), with a scattering of data points around a single, non-linear line. Fig. 4 again stresses the importance of taking the hydrophobicity of a peptide or protein into account when attempting to correlate retention time with polypeptide chain length.

Prediction of protein retention time in RPC

From Fig. 3

$$\tau - t_R^{obs} \propto \Sigma R_c \ln N$$
$$\tau - t_R^{obs} = \Sigma R_c \ln N + b$$
$$t_R^{obs} = \tau - (m\Sigma R_c \ln N + b) \quad (1)$$

As described above

$$\tau = \Sigma R_c + t_s \tag{2}$$

where t_s is the time correction for the peptide standard S4. Substituting eqn. 2 into eqn. 1 produces the expression

$$t_R^{obs} = \Sigma R_c + t_s - (m\Sigma R_c \ ln \ N + b) \tag{3}$$

When predicting the retention time of proteins, taking into account polypeptide chain length, t_R^{obs} in eqn. 3 becomes τ_c (predicted protein retention time):

$$\tau_c = \Sigma R_c + t_s - (m\Sigma R_c \ln N + b), \tag{4}$$

where $(m\Sigma R_c \ln N + b)$ is the correction factor for polypeptide chain length[22].

Eqn. 4 was applied to retention time prediction of proteins 1–19 (Table I) and the results are shown in Fig. 5. The closed symbols denote observed *versus* predicted (τ) protein retention times when polypeptide chain length is not taken into account, *i.e.*, following application of the equation, $\tau = \Sigma R_c + t_s$ (see above); open symbols denote observed *versus* predicted (τ_c) retention times when chain length has been taken into account, *i.e.*, following application of eqn. 4. The solid line represents a perfect correlation between predicted and observed protein retention times. The contrast between the two sets of results is striking. It is clear that there is no correlation between predicted and observed protein retention times unless a polypeptide chain length

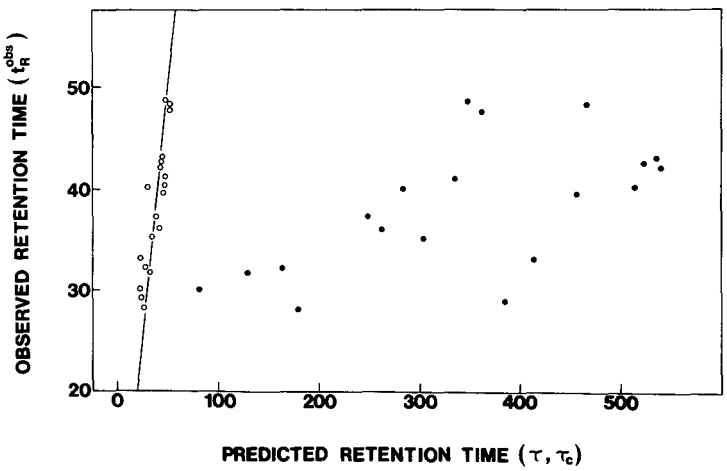

Fig. 5. Correlation of predicted and observed protein retention times in RPC. Results shown are for proteins 1–19 (Table I) on an Aquapore RP-300 C_8 column (220 × 4.6 mm I.D.). The predicted retention times either with (τ_c) or without (τ) taking polypeptide chain length into account were calculated as described in the text. Closed symbols denote observed *versus* predicted protein retention times without taking polypeptide chain length into account (τ); open symbols denote correlation when chain length has been taken into account (τ_c). The solid line represents perfect correlation between predicted and observed protein retention times. Mobile phase conditions as described in Fig. 2. Absorbance at 210 nm.

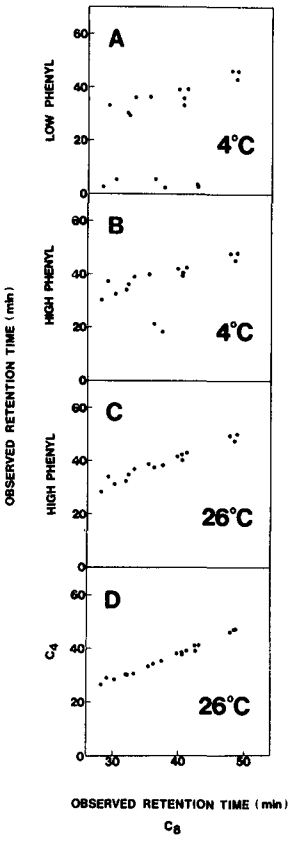

Fig. 6. Effect of hydrophobicity and ligand density of the stationary phase on the retention times of proteins in RPC. Columns, Bio-Gel TSK Phenyl-5PW (75 × 7.5 mm I.D.) (A); Bio-Gel TSK Phenyl RP+ (75 × 4.6 mm I.D.) (B and C), SynChropak RP-4 C_4 (250 × 4.1 mm I.D.) (D), and Aquapore RP-300 C_8 (220 × 4.6 mm I.D.); mobile phase, linear A–B gradient (1% B/min), where eluent A is 0.1% aqueous TFA and eluent B is 0.1% TFA in acetonitrile; flow-rate, 1 ml/min; temperatures as shown; absorbance at 210 nm. Proteins 1–19 (Table I) were chromatographed on all four columns. Where the occasional protein produced a badly skewed peak, thereby preventing accurate retention time measurement, this data point was not used.

correction is applied. Once this correction was applied, the improvement in prediction of protein retention time was quite dramatic (an error of only ± 5 min for the majority of the proteins). This improvement was especially gratifying considering the potential causes for deviations, including (1) incomplete denaturation of the protein on interaction with the hydrophobic sorbent, although this is unlikely for the proteins used in this study for the reasons given above[22], (2) formation of secondary structure on interaction with the reversed-phase sorbent[1,22], (3) preferential interaction of hydrophobic domains in the protein with the reversed-phase sorbent although this is unlikely for the proteins used in the study for the reasons given above[22] and (4) maintenance of tertiary structure in the protein by disulfide bonds, preventing accessibility of all regions of the amino acid sequence to interact with the reversed-phase sorbent.

Effect of hydrophobicity and ligand density of the bonded phase on the retention time behavour of proteins

The results shown in Figs. 3 and 5 justified the original assumption that the hydrophobic C_4, C_8 and C_{18} sorbents would effectively denature proteins. If this had not been the case, the correlation of the plot shown in these figures would not have been as good. To underline this point, the effect of less hydrophobic reversed-phase sorbents on the retention time behaviour of proteins was examined.

Proteins 1–19 in Table I were subjected to RPC on two polymer-based columns containing phenyl groups as hydrophobic ligands. One column (Bio-Gel TSK Phenyl-5PW) was developed for the related HPLC technique of hydrophobic interaction chromatography (HIC), with the phenyl groups only sparsely distributed across the support ("low phenyl"). The second column (Bio-Gel TSK Phenyl RP+) was based on the above HIC packing, but contained a much greater density of phenyl groups ("high phenyl") and was intended to function as a reversed-phase column. The proteins were chromatographed on both columns using a linear gradient (1% B/min) at a flow-rate of 1 ml/min, where eluent A was 0.1% aqueous TFA and eluent B was 0.1% TFA in acetonitrile. Fig. 6 compares the results of plotting observed protein retention time on the C_8 column at 26°C against the observed retention times on the low phenyl column at 4°C (Fig. 6A), the high phenyl column at 4°C (Fig. 6B) and 26°C (Fig. 6C), and the C_4 column at 26°C.

It would be expected that, if two hydrophobic sorbents denatured proteins to the same extent, and allowing for slight selectivity differences between the packings, then a plot of observed protein retention times on one column against observed retention times on the other would produce a linear plot with little scatter of data points. This linear relationship is clearly lacking for the low phenyl column at 4°C (Fig. 6A), where there is a wide scatter of data points. In fact, several proteins [insulin (chain B), ribonuclease A, avidin, lysozyme, concanavalin A, α-chymotrypsinogen A] were barely, if at all, retained by the column suggesting that these proteins are being separated in their native or only partially unfolded states. This result for lysozyme reflected similar results reported by Ingraham *et al.*[27]. In addition, these results showed that the acidic nature of the starting solvent, 0.1% aqueous TFA, does not necessarily denature all proteins. The low temperature (4°C) used for these runs also favoured maintenance of native protein conformation.

The effect of the more hydrophobic nature of the high phenyl column on the retention times of the proteins is clearly apparent in Fig. 6B, where the scatter of data points has lessened considerably. All proteins were now retained by the column, with just lysozyme and avidin still showing only partial unfolding. The temperature for the low phenyl and high phenyl runs shown in Fig. 6A and B, respectively, remained constant (4°C); thus, the increase in hydrophobicity of the column packing was solely responsible for the improvement in correlation of the data points shown in Fig. 6B. The results shown in Fig. 6A and B suggested that changes in reversed-phase sorbent hydrophobicity could be a useful aid to improving the resolution of protein mixtures in RPC.

The effect on protein retention time behaviour on the high phenyl column as the temperature was raised from 4°C (Fig. 6B) to 26°C is shown in Fig. 6C. Although in standard RPC the primary cause of denaturation is the hydrophobicity of the sorbent[27], an increase in temperature also has a denaturing effect; hence, the further

improvement in correlation between observed protein retention times on the high phenyl and C_8 columns seen in Fig. 6C. As noted by several researchers[27–29], such differences in protein retention times at different temperatures could also be used to improve the resolution of proteins with similar retention times.

The effect of increased sorbent hydrophobicity on the retention time behaviour of proteins at constant temperature (26°C) is again shown in Fig. 6D. The correlation of the observed protein retention times on the C_4 and C_8 columns has again improved, this time compared to the high phenyl column (Fig. 6C). In fact, the linearity of the plot shown in Fig. 6D indicated that the C_4 and C_8 sorbents denatured the proteins to the same extent. It should be noted that attempts to generate linear plots for the low and high phenyl columns similar to that shown in Fig. 3 for the C_8 column (and also representative of the C_4 and C_8 columns) met with little success, reflecting again the importance of efficient protein denaturation for satisfactory correlation of protein retention times with their overall hydrophobicity.

The polypeptide chain length effect demonstrated by the retention behaviour of peptide polymers of repeating units[26] or protein retention behaviour (this study) in RPC suggests that only a relatively small proportion of the amino acid residues are interacting with the stationary phase at any one time even when the polypeptide chain is fully unfolded. The excellent correlations shown in Figs. 3 and 5 (open circles) suggest that when the protein is completely unfolded, there is full expression of its overall hydrophobicity. Thus, there is not one specific portion of the unfolded polypeptide chain interacting with the stationary phase. Instead, all of the amino acid residues in an unfolded polypeptide chain can interact, in small portions, at any one time. Because of this polypeptide chain length effect, retention coefficients must be determined at a fixed peptide chain length and will vary depending on the length of the peptide used. If one is predicting retention times of polypeptides using coefficients derived at the same chain length as these polypeptides, then the predicted retention is simply equal to the sum of the coefficients. On the other hand, if you use coefficients derived from one chain length to predict retention times of peptides with different chain lengths, then a polypeptide chain length correction must be introduced.

CONCLUSIONS

The present study has shown that retention parameters derived from small peptides can be applied to the correlation of the overall hydrophobicity of proteins with their retention time behaviour during RPC. A clearer understanding of the three-dimensional structures of proteins on interacting with a hydrophobic sorbent will likely be required to improve further the accuracy of protein retention time prediction.

ACKNOWLEDGEMENTS

This work was supported by the Medical Research Council of Canada and equipment grants from the Alberta Heritage Foundation for Medical Research.

REFERENCES

1 C. T. Mant and R. S. Hodges, in K. Gooding and F. Regnier (Editors), *High Performance Liquid Chromatography of Biological Macromolecules: Methods and Applications*, Marcel Decker, New York 1989, p. 1101.
2 J. L. Meek, *Proc. Natl. Acad. Sci. U.S.A.*, 77 (1980) 1632.
3 J. L. Meek and Z. L. Rossetti, *J. Chromatogr.*, 211 (1981) 15.
4 S. J. Su, B. Grego, B. Niven and M. T. W. Hearn, *J. Liq. Chromatogr.*, 4 (1981) 1745.
5 K. J. Wilson, A. Honegger, R. P. Stötzel and G. J. Hughes, *Biochem. J.*, 199 (1981) 31.
6 C. A. Browne, H. P. J. Bennett and S. Solomon, *Anal. Biochem.*, 124 (1982) 201.
7 T. Sasagawa, T. Okuyama and D. C. Teller, *J. Chromatogr.*, 240 (1982) 329.
8 T. Sasagawa, L. H. Ericsson, D. C. Teller, K. Titani and K. A. Walsh, *J. Chromatogr.*, 307 (1984) 29.
9 D. Guo, C. T. Mant, A. K. Taneja, J. M. R. Parker and R. S. Hodges, *J. Chromatogr.*, 359 (1986) 499.
10 D. Guo, C. T. Mant, A. K. Taneja and R. S. Hodges, *J. Chromatogr.*, 359 (1986) 519.
11 Y. Sakamoto, N. Kawakami and T. Sasagawa, *J. Chromatogr.*, 442 (1988) 69.
12 K. Jinno and E. Tanigawa, *Chromatographia*, 25 (1988) 613.
13 C. T. Mant and R. S. Hodges, in M. T. W. Hearn (Editor), *HPLC of Proteins, Peptides and Polynucleotides*, VCH Publishers, Weinheim, in press.
14 M. J. O'Hare and E. C. Nice, *J. Chromatogr.*, 171 (1979) 209.
15 E. C. Nice, M. W. Capp, N. Cooke and M. J. O'Hare, *J. Chromatogr.*, 218 (1981) 569.
16 K. J. Wilson, A. Honegger and G. J. Hughes, *Biochem. J.*, 199 (1981) 43.
17 C. T. Wehr, L. Correia and S. R. Abbott, *J. Chromatogr. Sci.*, 20 (1982) 114.
18 J. Heukeshoven and R. Dernick, *J. Chromatogr.*, 252 (1982) 241.
19 J. M. R. Parker and R. S. Hodges, *J. Protein Chem.*, 3 (1985) 465.
20 R. S. Hodges, R. J. Heaton, J. M. R. Parker, L. Molday and R. S. Molday, *J. Biol. Chem.*, 263 (1988) 11 768.
21 F. E. Regnier, *Methods Enzymol.*, 91 (1983) 137.
22 S. Y. M. Lau, A. K. Taneja and R. S. Hodges, *J. Chromatogr.*, 317 (1984) 129.
23 S. Y. M. Lau, A. K. Taneja and R. S. Hodges, *J. Biol. Chem.*, 259 (1984) 13 253.
24 R. S. Hodges, P. D. Semchuk, A. K. Taneja, C. M. Kay, J. M. R. Parker and C. T. Mant, *Peptide Res.*, 1 (1988) 19.
25 M. Hermodson and W. C. Mahoney, *Methods Enzymol.*, 91 (1983) 352.
26 C. T. Mant, T. W. L. Burke, J. A. Black and R. S. Hodges, *J. Chromatogr.*, 458 (1988) 193.
27 R. I. Ingraham, S. Y. M. Lau, A. K. Taneja and R. S. Hodges, *J. Chromatogr.*, 327 (1985) 77.
28 L. R. Snyder, *J. Chromatogr.*, 179 (1979) 167.
29 R. A. Barford, B. J. Sliwinski, A. C. Breyer and H. L. Rothbart, *J. Chromatogr.*, 235 (1982) 281.

Journal of Chromatography, 476 (1989) 377–389
Elsevier Science Publishers B.V., Amsterdam — Printed in The Netherlands

CHROMSYMP. 1631

STRONG CATION-EXCHANGE HIGH-PERFORMANCE LIQUID CHROMATOGRAPHY OF PEPTIDES

EFFECT OF NON-SPECIFIC HYDROPHOBIC INTERACTIONS AND LINEARIZATION OF PEPTIDE RETENTION BEHAVIOUR

T. W. LORNE BURKE*, COLIN T. MANT, JAMES A. BLACK and ROBERT S. HODGES
Department of Biochemistry and the Medical Research Council of Canada Group in Protein Structure and Function, University of Alberta, Edmonton, Alberta T6G 2H7 (Canada)

SUMMARY

Strong cation-exchange chromatography (strong CEX) is probably the most useful mode of high-performance ion-exchange chromatography (IEC) for peptide separations. Although the hydrophobic character of high-performance ion-exchange packings, often giving rise to mixed-mode contributions to solute separations, has long been recognized, a systematic approach to examining the effect and magnitude of the hydrophobicity of these packings during IEC of peptides has so far been lacking.

In the present study, we report the synthesis of three series of positively charged peptide polymers which vary significantly in overall hydrophobicity and polypeptide chain length (5–50 amino acid residues): Ac-(Gly-Lys-Gly-Leu-Gly)$_n$-amide, Ac-(Leu-Gly-Leu-Lys-Ala)$_n$-amide and Ac-(Leu-Gly-Leu-Lys-Leu)$_n$-amide (n = 1, 2, 4, 6, 8, 10). We have examined non-specific hydrophobic interactions of these peptides with both silica- and polymer-based ion-exchange packings, demonstrating how these interactions are overcome by the addition of acetonitrile to the mobile phase. It was also shown that removal of non-specific hydrophobic interactions may be necessary just to elute peptides from the ion-exchange matrix. In addition, from the observed retention times of these three peptide polymer series and other peptides which vary substantially in charge density, net charge, polypeptide chain length and hydrophobicity, we have established a simple approach to linearization and, thus, prediction of peptide retention behaviour in CEX.

INTRODUCTION

High-performance ion-exchange chromatography (IEC) has become increasingly popular for the analysis of both peptides and proteins in recent years[1]. Although, as the name implies, the major separation mechanism of this mode of high-performance liquid chromatography (HPLC) is electrostatic in nature, ion-exchange packings may also often exhibit significant hydrophobic characteristics, giving rise to

0021-9673/89/$03.50

mixed-mode contributions to solute separations[2,3]. As pointed out by Rounds *et al.*[4], a small amount of hydrophobic character in an ion exchanger is not necessarily detrimental to the separation of proteins, and may even enhance resolution by mixed-mode effects. Several researchers have exploited these mixed-mode effects to aid in peptide and protein separations on anion-exchange (AEX)[3–8] and cation-exchange (CEX) columns[9,10]. However, when only the predominant, *i.e.*, ionic, stationary phase–solute interaction is required, the mobile phase must be manipulated so as to minimize non-specific interactions, *e.g.*, by the addition of a non-polar organic solvent such as acetonitrile to the mobile phase buffers to suppress hydrophobic interactions between the solute and the ion-exchange packing. Although the hydrophobic character of high-performance ion-exchange packings has long been recognized, a systematic approach to examining the effect and magnitude of the hydrophobicity of these packings during IEC of peptides has so far been lacking.

Strong cation-exchange chromatography (strong CEX) is probably the most useful mode of IEC for peptide separations[1,9–13]. The utility of strong CEX packings, generally containing sulphonate functionalities, lies in their ability to retain their negatively charged character in the acidic to neutral pH range. At low pH, the side-chain carboxyl groups of acidic amino acid residues are protonated, emphasizing any positively charged character of the peptides. Thus, by manipulating the pH of the mobile phase, the net charge of a peptide may be varied. In addition to overall net charge, other factors which may affect the retention behaviour of peptides during IEC include peptide conformation, polypeptide chain length, charge distribution, and charge density. To understand peptide retention behaviour during IEC completely, it is not sufficient merely to demonstrate that these various factors have an effect on peptide retention, it is also necessary to quantitate the relative contribution each factor makes to retention behaviour.

In the present study, we have synthesized three series of basic peptide polymers (5–50 residues) of varying hydrophobicity and subjected them to strong CEX. From the observed retention behaviour of the polymer sets, we have clearly demonstrated the effects on peptide elution profiles of hydrophobic interactions of peptides with ion-exchange packings. In addition, from the observed retention times of these three peptide polymer series and other peptide mixtures, we have gained a clearer understanding of the effect of both polypeptide chain length and charge density on peptide retention behaviour during strong CEX.

EXPERIMENTAL

Materials

Water (HPLC-grade), acetonitrile (HPLC-grade), and sodium chloride (ACS-grade) were obtained from J. T. Baker (Phillipsburg, NJ, U.S.A.). Four synthetic undecapeptide cation-exchange standards (1–4) were obtained from Synthetic Peptides Inc. (Department of Biochemistry, University of Alberta, Edmonton, Canada). Peptides 1 and 2 were based on the sequence, X^1-X^2-Gly-Leu-Gly-Gly-Ala-Gly-Gly-Leu-Lys, where X^1-X^2 were substituted with Gly^1-Gly^2- (peptide 1) or Lys^1-Tyr^2- (peptide 2); peptides 3 and 4 were based on the sequence, X^1-X^2-Ala-Leu-Lys-Ala-Leu-Lys-Gly-Leu-Lys, where X^1-X^2- were substituted with Gly^1-Gly^2- (peptide 3) or Lys^1-Tyr^2- (peptide 4). Each peptide contained an N^{α}-acetylated N-terminal and a C-terminal amide.

A mixture of five synthetic size-exclusion peptide standards was also obtained from Synthetic Peptides Inc. The sequence of the standards was Ac-(Gly-Leu-Gly-Ala-Lys-Gly-Ala-Gly-Val-Gly)$_n$-amide, where n = 1–5, *i.e.*, 10–50 residues in length.

Peptide synthesis

The peptide polymers described were synthesized on an Applied Biosystems peptide synthesizer Model 430A (Foster City, CA, U.S.A.), using the general procedure for solid-phase synthesis described by Parker and Hodges[14] and Hodges *et al.*[15].

Apparatus

The HPLC instrument consisted of a Varian Vista Series 5000 liquid chromatograph (Varian, Walnut Creek, CA, U.S.A.), coupled to a Hewlett-Packard (Avondale, PA, U.S.A.) HP 1040A detection system, HP 9000 Series 300 computer, HP 9133 disc drive, HP 2225A Thinkjet printer and HP 7440A plotter. Samples were injected with a Model 7125 200-μl injection loop (Rheodyne, Cotati, CA, U.S.A.).

Columns

Peptide mixtures were separated on three strong cation-exchange columns: (1) SynChropak S300, 250 × 4.1 mm I.D. 6.5 μm particle size, 300-Å pore size (SynChrom, Linden, IN, U.S.A.); (2) PolySulfoethyl Aspartamide, 250 × 4.6 mm I.D. 5 μm, 300 Å (PolyLC, Columbia, MD, U.S.A.); (3) Mono S HR 5/5, 50 × 5 mm I.D., 10 μm (Pharmacia, Dorval, Canada).

RESULTS AND DISCUSSION

Design of peptide polymers

In order to examine the effect of peptide chain length on peptide retention behaviour during strong CEX, as well as monitoring any non-specific hydrophobic interactions between solute and column packing, it was necessary to design series of positively charged peptide polymers covering a similar range of chain length, but differing in overall hydrophobicity. Three series of peptide polymers were subsequently synthesized: (a) Ac-(Gly-Lys-Gly-Leu-Gly)$_n$-amide, where n = 1, 2, 4, 6, 8, 10 (5–50) residues, +1 to +10 net charge); (b) Ac-(Leu-Gly-Leu-Lys-Ala)$_n$-amide, where n = 1, 2, 4, 6, 8, 10 (5–50 residues, +1 to +10 net charge); (c) Ac-(Leu-Gly-Leu-Lys-Leu)$_n$-amide, where n = 1, 2, 4, 6, 8, 10 (5–50 residues, +1 to +10 net charge). The hydrophobicity of the polymer series increased in the order, Ac-(Gly-Lys-Gly-Leu-Gly)$_n$-amide ("G" series) < Ac-(Leu-Gly-Leu-Lys-Ala)$_n$-amide ("A" series) < Ac-(Leu-Gly-Leu-Lys-Leu)$_n$-amide ("L" series). In addition, the single lysine residue in each repeating unit of five residues ensured that the overall charge density of every peptide was identical. For the purposes of this study, each peptide is referred to by a number and letter which denote, respectively, the number of residues it contains and to which polymer series it belongs. Thus, 5G refers to the five-residue "G" series peptide; 30A refers to the 30-residue "A" series peptide, etc.

Effect of hydrophobic interactions in strong CEX

The peptide polymers were chromatographed on three different strong cation-exchange columns: (1) the SynChropak S300 was a silica-based column containing

sulphonate groups as the negatively charged functionalities[12,13]; (2) the PolySulfoethyl Aspartamide column also contained a silica-based packing with sulphonate functionalities, but the chemistry of sulphonate attachment to the silica support was different compared to that of the S300[9,10]; (3) the Mono S column contained sulphonate groups attached to a polyether support.

Fig. 1 shows elution profiles of the mixture of the "A" series of peptide polymers on the S300 column. Similar results were obtained on the other two columns. The peptides were chromatographed using a linear sodium chloride gradient (20 m*M* sodium chloride per min, following 10 min elution with starting buffer, at a flow-rate of 1 ml/min) in 5 m*M* KH_2PO_4 buffer at pH 6.5. The mobile phase buffers also contained 0, 10, 20, 30 or 40% acetonitrile (v/v). In the absence of acetonitrile (results not shown), only peptides 5A (+1 net charge) and 10A (+2 net charge) were eluted, with reasonable peak shape, by a sodium chloride gradient up to a concentration of 0.5 *M*. Peptide 20A (+4 net charge) appeared as a late-eluted very broad, badly skewed peak. The more hydrophobic 30A, 40A and 50A peptides (+6, +8 and +10 net charge, respectively) were not eluted by 0.5 *M* sodium chloride. It had previously been shown by Mant and Hodges[13] that a mixture of peptides of average hydrophobicity and a range of net charge from +2 to +8 at pH 6.5 was easily removed from the S300, in the absence of an organic solvent, by a salt gradient up to a concentration of only 0.4 *M*. In fact, in the present study, the "G" series of polymers of the same polypeptide chain length and net charge as the "A" series was easily eluted from the column in the absence of acetonitrile, including the highly charged (+10) 50-residue peptide (50G). Thus, in the present study, it was apparent that, in addition to ionic interactions between the "A" series of peptides and the column packing, non-specific hydrophobic interactions were also affecting the retention behaviour of the polymer series. With the addition of 10% acetonitrile to the mobile phase buffers, designed to help overcome any hydrophobic, as opposed to ionic, interactions, peptides 5A, 10A and 20A (+1, +2 and +4 net charge, respectively) were all now eluted with good peak shape within a concentration range of 0–0.3 *M* sodium chloride. As the concentration of acetonitrile was increased further to 20, 30 and 40%, the more hydrophobic peptides [30A, 40A and 50A (+6, +8 and +10 net charge, respectively)] were also eluted from the column (Fig. 1). In addition, the retention times of all peptides decreased with increasing levels of acetonitrile. At a level of 40% acetonitrile in the mobile phase buffers, the most hydrophobic peptide, 50A (+10 net charge), was eluted at a salt concentration of only *ca.* 0.2 *M*. Raising the level of acetonitrile above 40% in the mobile phase was found to be impractical due to problems associated with salt insolubility at high concentrations of the non-polar solvent. It should be noted that the peptide with a net charge of only +1 (5A) was eluted from the S300 during the initial 10-min isocratic elution with the starting buffer and not by the subsequent gradient. However, the elution time of this peptide also decreased with increasing levels of acetonitrile.

Fig. 2 shows a graphical representation of the results shown in Fig. 1, demonstrating decreasing retention times of peptides 10A–50A with increasing levels of acetonitrile in the mobile phase buffers. The absence of data points for a particular peptide below a certain percentage of acetonitrile means that this peptide was either not eluted by a salt gradient up to 0.5 *M* sodium chloride, or was eluted very late as an extremely broad, poorly defined peak. Although the plots for each peptide are curv-

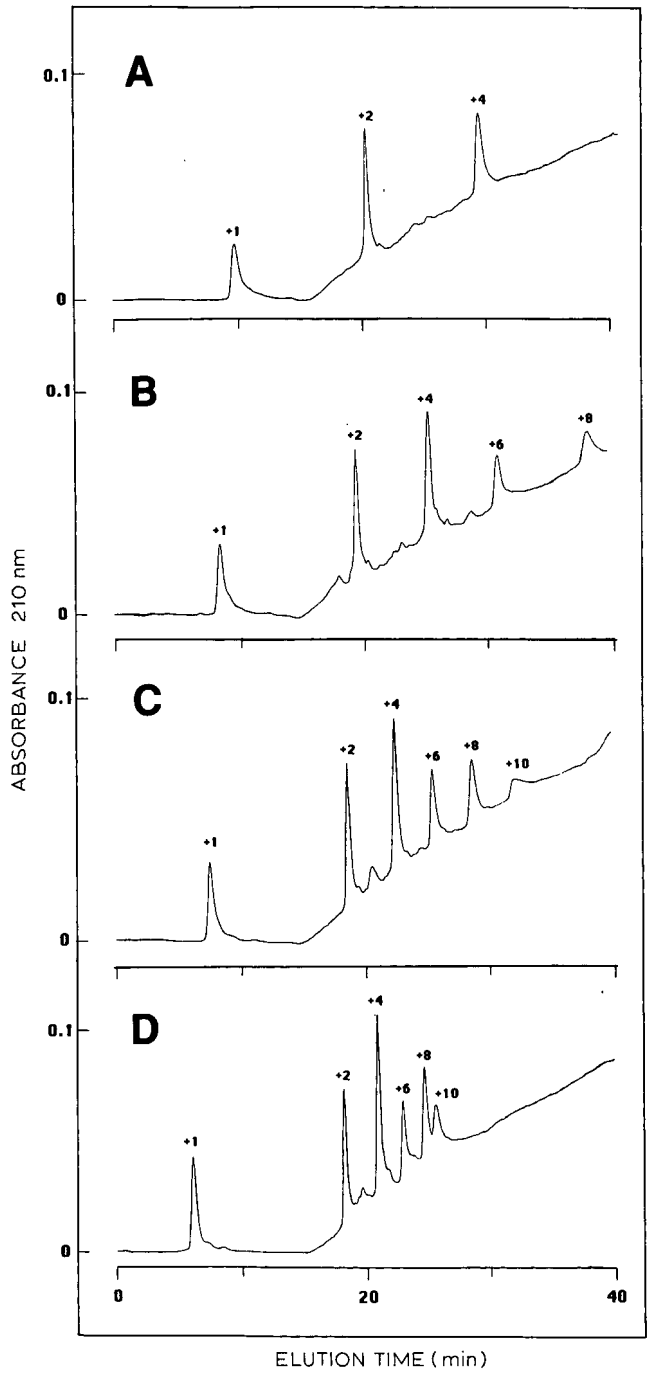

Fig. 1. Strong cation-exchange chromatography of synthetic peptide polymers. Conditions: column, SynChropak S300 (250 × 4.1 mm I.D.); mobile phase, linear A–B gradient (20 m*M* salt per min following 10-min isocratic elution with buffer A), where buffer A is 5 m*M* KH_2PO_4 (pH 6.5) and buffer B is buffer A plus 0.5 *M* NaCl, both buffers containing 10 (A), 20 (B), 30 (C) or 40% (D) acetonitrile (v/v); flow-rate, 1 ml/min; temperature, 26°C. The sequence of the peptides was Ac-(Leu-Gly-Leu-Lys-Ala)$_n$-amide, where n = 1, 2, 4, 6, 8, 10 (+1, +2, +4, +6, +8, +10 net charge, respectively).

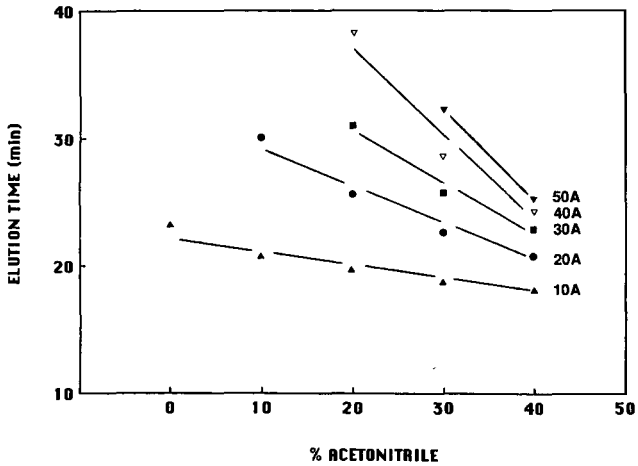

Fig. 2. Plot of peptide elution time *versus* percentage of acetonitrile in mobile phase buffers during strong cation-exchange chromatography of synthetic peptide polymers. Column and conditions as described in Fig. 1. 10A, 20A, 30A, 40A, 50A denote, respectively, 10-, 20-, 30-, 40- and 50-residue peptides of "A" series of peptide polymers (sequences shown in Fig. 1).

ing, they are drawn as best-fit straight lines to highlight the effect of acetonitrile concentration on peptide retention times. From the different slopes of the plots for peptides 10A–50A, it is clear that the effect of increasing acetonitrile concentration on the retention time of a particular peptide is dependent on its hydrophobicity. For instance, in raising the level of acetonitrile from 30 to 40% in the mobile phase, the retention times for 10A, 20A, 30A, 40A and 50A were reduced by 0.7, 1.8, 2.8, 4.2 and 6.8 min, respectively. Thus, the more hydrophobic the peptide (50A > 40A > 30A > 20A > 10A), the greater the comparative effect of increasing acetonitrile concentration in reducing peptide retention time. Similar results were obtained for the less hydrophobic "G" series and more hydrophobic "L" series of peptide polymers.

The relationship between peptide hydrophobicity and mobile phase acetonitrile concentration in strong CEX of peptides is again shown in Fig. 3, which compares the effect of increasing acetonitrile concentration on the retention times of all three series of peptide polymers ("G", "A" and "L"). The plots shown in Fig. 3 were all obtained on the S300 column under the same chromatographic conditions as described in Fig. 1. In Fig. 2, the peptides increased in length (50A > 40A >, etc.) as well as hydrophobicity. In contrast, each panel of Fig. 3 compares the retention times of peptides with varying hydrophobicity but the same chain length, *e.g.*, 50G + 50A + 50L (50-res), 40G + 40A + 40L (40-res), etc. In ideal ion-exchange chromatography, peptides of the same length and net charge should have similar retention times. From Fig. 3, it can be seen that for peptides of the same length and net positive charge, the more hydrophobic the peptide, the greater the retention time due to hydrophobic interactions with the cation-exchange matrix. When these hydrophobic interactions are suppressed (40% acetonitrile in the mobile phase), peptides of the same length and net charge are eluted from the column at similar times. From the varying steepness of the plots, it is again clear that, for each trio of peptides, the more hydrophobic the

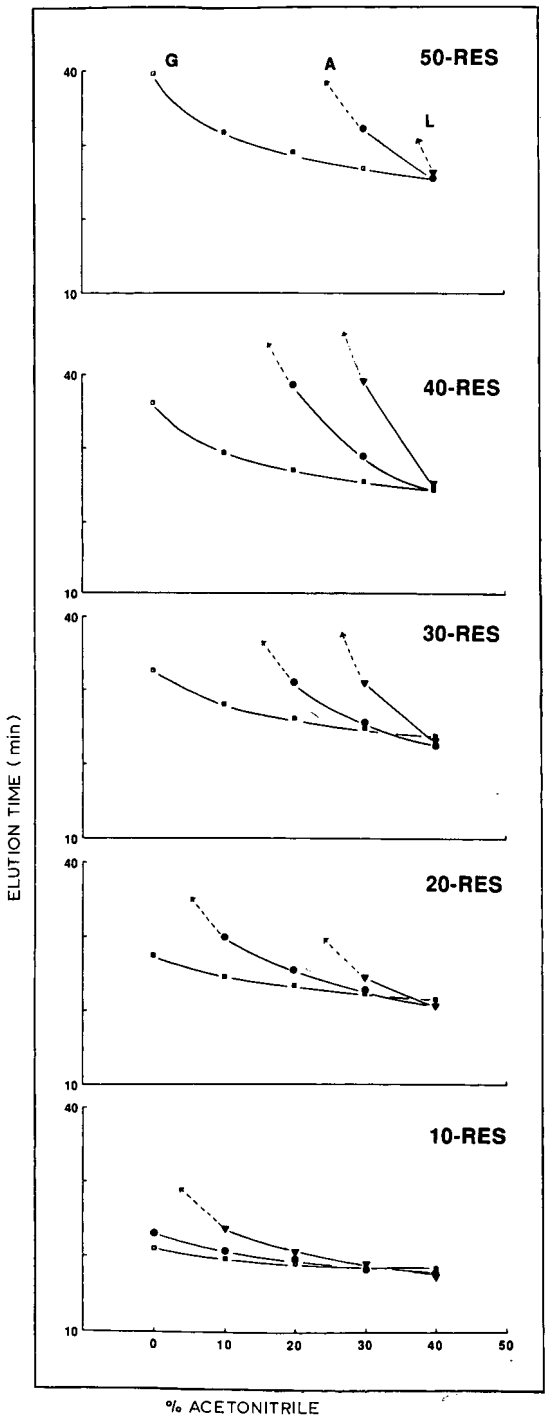

Fig. 3. Plot of peptide elution time *versus* percentage of acetonitrile in mobile phase buffers during strong cation-exchange chromatography of synthetic peptide polymers. Column and conditions as described in Fig. 1. Sequence of the "G", "A" and "L" series of peptide polymers are described in the text. 10-res, 20-res, 30-res, 40-res, 50-res denote 10–50 residues, respectively. A dotted line denotes that a peptide was not eluted, or was eluted as a very broad and/or skewed peak, below a certain level of acetonitrile in the mobile phase.

peptide, the greater the effect of increasing acetonitrile concentration in reducing peptide retention time. For instance, in raising the level of acetonitrile from 30 to 40% in the mobile phase, the retention times for 40G, 40A and 40L were reduced by 1.1, 4.2 and 14.2 min, respectively; the retention times for 30G, 30A and 30L were reduced by 0.9, 2.8 and 8.1 min, respectively, etc.

The differences in hydrophobicity of the three series of peptide polymers and, hence, differences in the intensity of their non-ionic interactions with the ion-exchange packing are also well demonstrated in Fig. 3. All five peptides of the least hydrophobic series (10G–50G) were eluted, with good peak shape, over the entire range of acetonitrile concentrations examined (0–40%). In contrast, only the 10-residue peptide (10A) of the more hydrophobic "A" series of peptide polymers was eluted in the absence of acetonitrile; 20A, 30A, 40A and 50A required at least, respectively, 10, 20, 20 and 30% acetonitrile in the mobile phase to be eluted from the column. In the case of the most hydrophobic "L" series, peptides 10L, 20L, 30L, 40L and 50L required at least, respectively, 10, 30, 30, 30 and 40% acetonitrile in the mobile phase to overcome hydrophobic interactions with the column packing. It should be noted that the five-residue peptides (5G, 5A, 5L) were not included in Figs. 2 and 3, since they were eluted from the S300 column during the initial 10-min isocratic elution with starting buffer and not by the salt gradient.

Effect of polypeptide chain length and charge density on peptide retention times

Fig. 4 shows elution profiles of a mixture of five synthetic peptide size-exclusion standards[1,16]. (Fig. 4A) and a mixture of four synthetic peptide cation-exchange standards (Fig. 4B) on the Mono S strong cation-exchange column. The peptides were eluted with a linear sodium chloride gradient (20 m*M* sodium chloride per min, following 10 min elution with starting buffer) at a flow-rate of 1 ml/min. Since only the effects of polypeptide chain length and/or charge density were being examined, it was important to minimize any non-specific, hydrophobic interactions of peptides with the ion-exchange packing. Thus, both the starting buffer (5 m*M* KH_2PO_4, pH 6.5) and the gradient buffer (5 m*M* KH_2PO_4 + 0.5 *M* NaCl, pH 6.5) contained 40% acetonitrile (v/v). For the purposes of the present study, the five size-exclusion standards (10, 20, 30, 40 and 50 residues; +1, +2, +3, +4 and +5 net charge, respectively) were denoted as the "X" series of peptide polymers; *i.e.*, 10X, 20X, etc.; the four cation-exchange standards were denoted C1–C4 (11 residues in length with +1, +2, +3 and +4 net charge, respectively). The sequences of the two sets of standards are described under Experimental.

From Fig. 4, it can be seen that similarly charged species were not necessarily eluted at similar times. For instance, peptide 50X (+5 net charge) (Fig. 4A) was not retained as long as C3 (+3 net charge) or C4 (+4 net charge) (Fig. 4B). Similarly, peptide 40X (+4 net charge) (Fig. 4A) was eluted prior to C3 (+3 net charge) (Fig. 4B). The two series of peptide standards differed significantly in their range of both peptide chain length (10–50 residues for peptides 10X–50X, respectively; eleven residues each for peptides C1–C4 and charge density (+1 net charge per 10 residues for 10X–50X; +1 to +4 net charge per 11 residues for C1–C4). In order to rationalize the elution profiles shown in Fig. 4, it was necessary to determine the relative contribution that polypeptide chain length and charge density individually make to peptide retention behaviour during strong CEX.

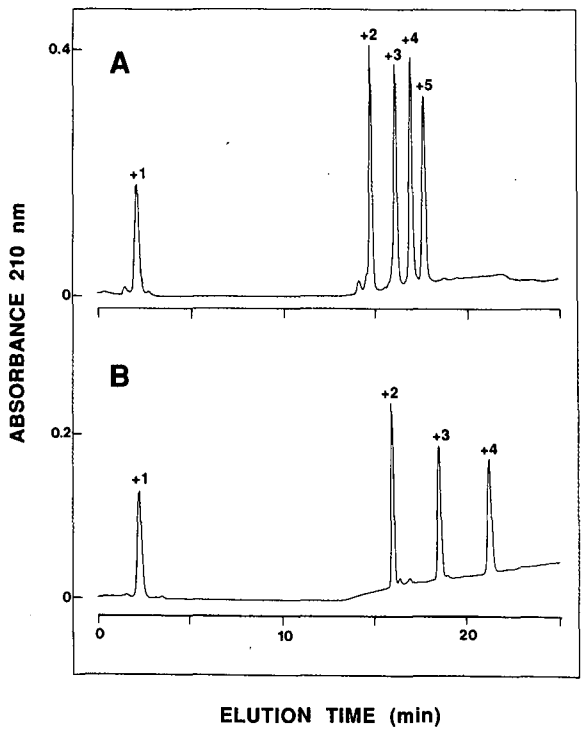

Fig. 4. Strong cation-exchange chromatography of synthetic peptides. Conditions: column, Mono S (50 × 5 mm I.D.); mobile phase, linear A–B gradient (20 m*M* salt per min following 10 min isocratic elution with buffer A), where buffer A is 5 m*M* KH_2PO_4 (pH 6.5) and buffer B is buffer A plus 0.5 *M* NaCl, both buffers containing 40% acetonitrile (v/v); flow-rate, 1 ml/min; temperature, 26°C. (A) Mixture of five synthetic peptide size-exclusion standards (10–50 residues; +1 to +5 net charge). (B) Mixture of four synthetic undecapeptide cation-exchange standards (+1 to +4 net charge). Sequences of the peptides are described under Experimental.

Fig. 5, top panel, demonstrates the relationship between elution time on the S300 column and net charge for the "A" and "X" series of peptide polymers and the cation-exchange peptide standards ("C"). The chromatographic conditions were the same as those described for Fig. 4. The peptides containing a single net positive charge (5A, 10X, C1) were eluted during the initial 10-min isocratic elution with starting buffer and are not included in the plots. The plot for the remaining three cation-exchange standards, C2–C4 (+2 to +4 net charge) demonstrated a linear relationship between peptide elution time and net charge. However, the plots for the two peptide polymer series, "X" and "A", showed a non-linear relationship, with the peptides being eluted earlier than expected with increasing net charge and chain length. Plotting the elution times of the "X" and "A" series of peptides against the logarithm of the number of residues they contained (ln *N*) resulted in the straight-line relationships shown in Fig. 5, middle panel. This exponential relationship between peptide retention time and peptide chain length reflected a similar relationship reported for reversed-phase chromatography of peptides[1,17]. A plot of elution time *versus* ln *N* for C2–C4 (all 11 residues in length) naturally produced a straight, vertical line.

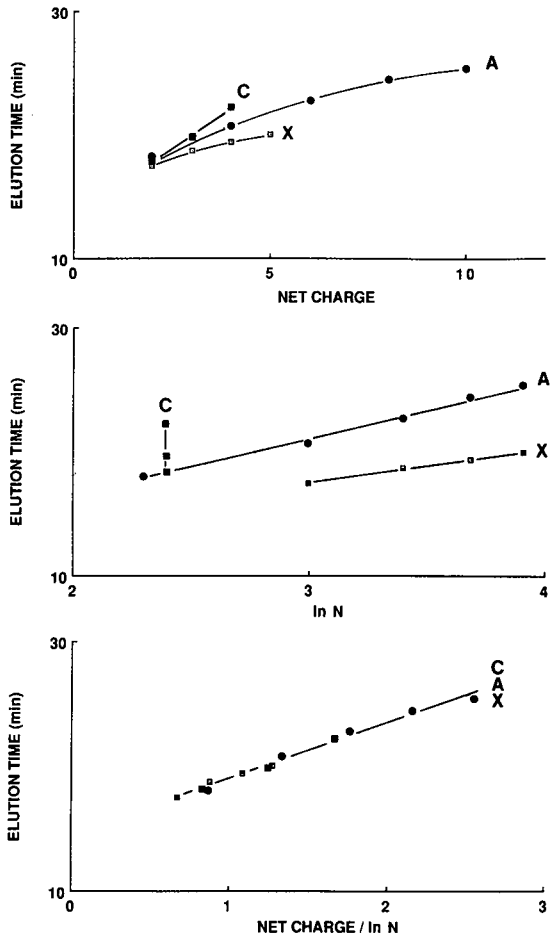

Fig. 5. Relationship of peptide elution time with polypeptide chain length and charge density during strong cation-exchange chromatography of synthetic peptides. Conditions: column, SynChropak S300 (250 × 4.1 mm I.D.; mobile phase, as described in Fig. 4. Top panel: peptide elution time *versus* peptide net charge. Middle panel: peptide elution time *versus* logarithm of the number of residues (ln *N*). Bottom panel: peptide elution time *versus* peptide net charge divided by the logarithm of the number of residues (net charge/ln *N*). The letters C, A and X denote the cation-exchange standards (sequences shown under Experimental), the "A" series of peptide polymers (sequence shown in Fig. 1), and the "X" series of size-exclusion standards (sequence shown under Experimental), respectively.

The divergence of the plots in Fig. 5, top panel, and the difference in slopes in Fig. 5, middle panel, appeared to reflect a difference in the charge densities of the peptides (+1 net charge per 10 residues for the "X" series; +2 net charge per 10 residues for the "A" series; +1 to +4 net charge per 11 residues for C2–C4).

From Fig. 5, bottom panel, it can be seen that dividing the net charge of the peptides from the two polymers series ("X" and "A") and the mixture of cation-exchange standards (C2–C4) by the logarithm of the number of residues they contain (net charge/ln *N*), and plotting this value against the observed elution time resulted in

a single, straight-line plot with a correlation of 0.99 (determined by linear least-squares fitting)[18]. The elution time *versus* net charge/ln *N* relationship held true for all three columns tested. This simple linearization approach is important for the prediction of retention behaviour of peptides where the net charge is known. The validity of this approach is supported by the diversity of the peptides used in this study. These peptides varied substantially in charge density (+0.1 to +0.4 per residue), net charge (+2 to +10), polypeptide chain length (10–50 residues) and overall hydrophobicity.

Fig. 6 underlines the importance of minimizing non-specific, hydrophobic interactions between peptides and the ion-exchange packing for the elution time *versus* net charge/ln *N* relationship to remain valid. The "G", "A" and "L" series of peptide polymers were eluted from the S300 column with a linear sodium chloride gradient (20 m*M* sodium chloride per min, following 10 min elution with starting buffer) at a

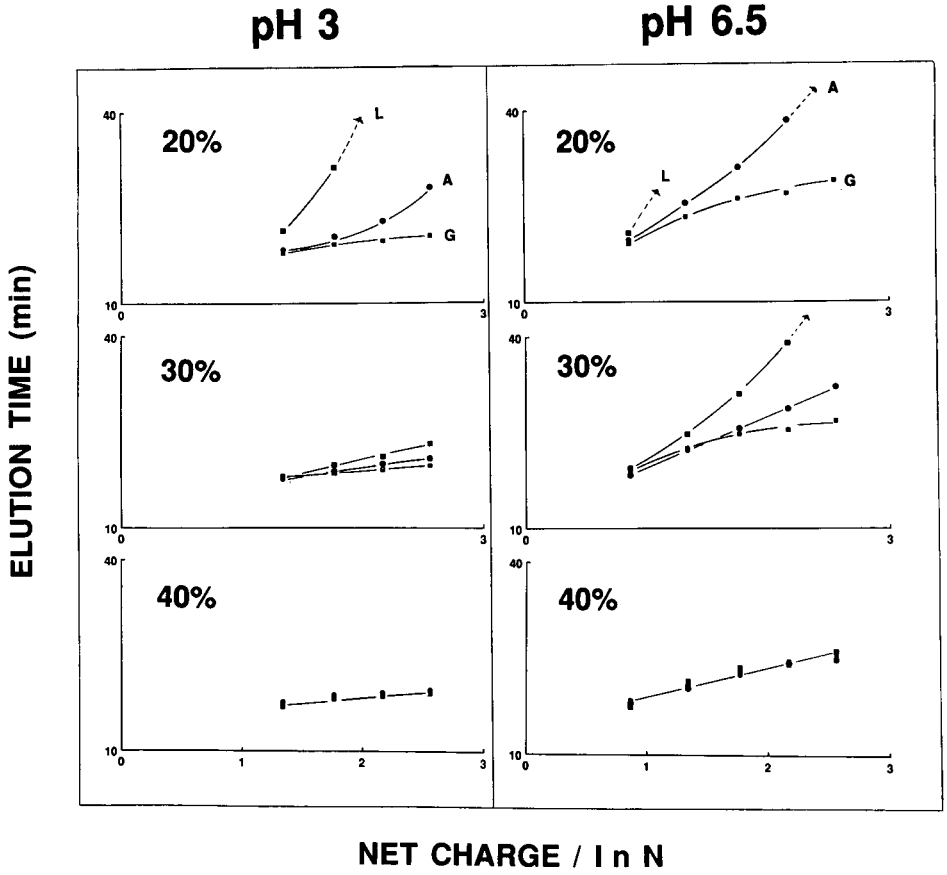

Fig. 6. Plot of peptide elution time *versus* peptide net charge/ln *N* following strong cation-exchange chromatography of synthetic peptide polymers. Conditions: column, SynChropak S300 (250 × 4.1 mm I.D.); mobile phase, linear A–B gradient (20 m*M* salt per min following 10 min isocratic elution with buffer A), where buffer A is 5 m*M* KH_2PO_4 (pH 3.0 or 6.5) and buffer B is buffer A plus 0.5 *M* NaCl, both buffers containing 20, 30 or 40% acetonitrile (v/v); flow-rate, 1 ml/min; temperature, 26°C. Sequences of the "G", "A" and "L" series of peptide polymers are described in the text.

flow-rate of 1 ml/min. The starting buffer (5 m*M* KH_2PO_4, pH 3.0 or 6.5) and the gradient buffer (5 m*M* KH_2PO_4 + 0.5 *M* NaCl, pH 3.0 or 6.5) contained 20, 30 or 40% acetonitrile (v/v). At either pH, the effect of incompletely suppressed hydrophobic interactions between the peptides and the column packing served to disrupt the linearity of the elution time *versus* net charge/ln *N* relationship. This disruption decreased as hydrophobic interactions were progressively suppressed with increasing levels of acetonitrile in the mobile phase until, at a concentration of 40% acetonitrile, the expected linearity was obtained with correlations of 0.95 and 0.98 at pH 3.0 and pH 6.5, respectively. Similar results were again obtained on both the other columns. As previously reported[13], the S300 column exhibits a pH effect in that peptides with a net positive charge of +2 are retained at pH 6.5, but not at pH 3.0. Hence, while five peptides from each of the polymer series were retained at pH 6.5 (+2, +4, +6, +8 and +10 net charge), only four peptides were retained at pH 3.0 (+4, +6, +8 and +10). In addition, all the retained peptides were eluted by a lower sodium chloride concentration at pH 3.0 than at pH 6.5.

A simple relationship between peptide elution time and net positive charge during strong CEX was reported by Mant and Hodges[13] and later by Crimmins *et al.*[9], *i.e.*, a satisfactory linear relationship was obtained without any correction for peptide chain length. The results shown in Fig. 5 (top panel) suggested that the polypeptide chain length effect on peptide retention times becomes significant only beyond a length of *ca.* 20 residues. The peptides utilized by the previous workers ranged in chain length from only 12–21 residues[13] or 7–13 residues[9]. Thus, for these particular mixtures of peptides, any effect on peptide retention behaviour due to chain length differences was probably fairly small. However, as shown in the present study, it is important to take polypeptide chain length into account for prediction of peptide retention behaviour of peptides >20 residues in length. Interestingly, conformational effects cannot explain the observed divergencies with polypeptide chain length. The peptide polymers used in this study do not have any unique tertiary structure, since the mobile phase conditions used to ensure ideal ion-exchange behaviour (buffers containing 40% acetonitrile) are denaturing to tertiary structures, favouring the exposure of all charged residues. In addition, their secondary structure ranges from random coil to substantial α-helical content (as measured by circular dichroism), yet they still exhibit a similar polypeptide chain length effect.

The importance of overcoming hydrophobic interactions with cation-exchange columns in order to ensure their elution from the column matrix and/or to ensure a linear relationship between peptide elution time and net charge/ln *N* was clearly shown in Fig. 6. The peptides used in this study covered an extreme range of peptide hydrophobicities to values far exceeding those of most peptides encountered and it is not very likely, or desirable, that organic solvent concentrations of as high as 40% (v/v) in the mobile phase buffers will be regularly necessary for strong CEX of average peptide mixtures. However, the results of this study do suggest that, if predictable peptide elution profiles are required, the addition on a regular basis of a low level of acetonitrile [*e.g.*, 10% (v/v)] to the mobile phase buffers would be worthwhile during strong CEX of peptides to suppress any hydrophobic interactions with the ion-exchange packing and, hence, ensure the linearity of the retention *versus* net charge/ln *N* relationship.

Our observations in this study also suggested that the hydrophobic character of

ion-exchange packings has a greater impact on the separation of peptides than those previously reported for proteins[2–4,7,8]. This is probably due to the fact that, under non-denaturating conditions, proteins are folded molecules (tertiary structure) with most of the hydrophobic residues situated in the interior of the molecule and, hence, not available to interact with the column matrix[19]. In contrast, peptides containing less than 50 residues usually exhibit little tertiary structure and all or most of the molecule is available to interact with ion-exchange packings.

ACKNOWLEDGEMENTS

This work was supported by the Medical Research Council of Canada and equipment grants from the Alberta Heritage Foundation for Medical Research.

REFERENCES

1 C. T. Mant and R. S. Hodges, in K. Gooding and F. Regnier (Editors), *High Performance Liquid Chromatography of Biological Macromolecules: Methods and Applications*, Marcel Dekker, New York, 1989, p. 1101.
2 W. Kopaciewicz, M. A. Rounds, J. Fausnaugh and F. E. Regnier, *J. Chromatogr.*, 266 (1983) 3.
3 L. A. Kennedy, W. Kopaciewicz and F. E. Regnier, *J. Chromatogr.*, 359 (1986) 73.
4 M. A. Rounds, W. D. Rounds and F. E. Regnier, *J. Chromatogr.*, 397 (1987) 25.
5 M. Dizdaroglu, H. C. Krutzsch and M. G. Simic, *J. Chromatogr.*, 237 (1982) 417.
6 M. Dizdaroglu, *J. Chromatogr.*, 334 (1985) 49.
7 W. Kopaciewicz, M. A. Rounds and F. E. Regnier, *J. Chromatogr.*, 318 (1985) 157.
8 M. L. Heinitz, L. Kennedy, W. Kopaciewicz and F. E. Regnier, *J. Chromatogr.*, 443 (1988) 173.
9 D. L. Crimmins, J. Gorka, R. S. Thoma and B. D. Schwartz, *J. Chromatogr.*, 443 (1988) 63.
10 A. J. Alpert and P. C. Andrews, *J. Chromatogr.*, 443 (1988) 85.
11 P. Mychack and J. R. Benson, *LC·GC Mag. Liq. Gas Chromatogr.*, 4 (1986) 462.
12 C. T. Mant and R. S. Hodges, *J. Chromatogr.*, 326 (1985) 349.
13 C. T. Mant and R. S. Hodges, *J. Chromatogr.*, 327 (1985) 147.
14 J. M. R. Parker and R. S. Hodges, *J. Protein Chem.*, 3 (1985) 465.
15 R. S. Hodges, R. J. Heaton, J. M. R. Parker, L. Molday and R. S. Molday, *J. Biol. Chem.*, 263 (1988) 11 768.
16 C. T. Mant, J. M. R. Parker and R. S. Hodges, *J. Chromatogr.*, 397 (1987) 99.
17 C. T. Mant, T. W. L. Burke, J. A. Black and R. S. Hodges, *J. Chromatogr.*, 458 (1988) 193.
18 R. S. Hodges, J. M. R. Parker, C. T. Mant and R. R. Sharma, *J. Chromatogr.*, 458 (1988) 147.
19 R. R. Drager and F. E. Regnier, *J. Chromatogr.*, 359 (1986) 147.

Journal of Chromatography, 476 (1989) 391–411
Elsevier Science Publishers B.V., Amsterdam — Printed in The Netherlands

CHROMSYMP. 1606

HIGH-PERFORMANCE LIQUID CHROMATOGRAPHY OF AMINO ACIDS, PEPTIDES AND PROTEINS

LXXXIX[a]. THE INFLUENCE OF DIFFERENT DISPLACER SALTS ON THE RETENTION PROPERTIES OF PROTEINS SEPARATED BY GRADIENT ANION-EXCHANGE CHROMATOGRAPHY

A. N. HODDER, M. I. AGUILAR and M. T. W. HEARN*
Department of Biochemistry, Monash University, Clayton, Victoria 3168 (Australia)

SUMMARY

The influence of eight different displacer salts on the retention properties of four globular proteins, ranging in molecular weight from 14 000 to 43 000, was investigated by using the Mono-Q strong-anion-exchange resin as the stationary phase. Proteins were eluted under gradient conditions with a range of alkali metal halides to vary systematically the anion and cation species in the series F^-, Cl^-, and Br^- and Li^+, Na^+ and K^+. Protein Z_c values (*i.e.* slopes of the ion-exchange retention plots, as derived from the dependency of the logarithmic capacity factor log k' on the concentration of the ionic displacer) generally increased when both the anion and cation were either chaotropic, *e.g.* KBr, or kosmotropic, *e.g.* NaF, in nature. Conversely, Z_c values decreased when the displacer salt contained an anion–cation combination of a chaotropic and a kosmotropic ion, *e.g.* KF. These results indicate that the lyotropic properties of salts are additive in their effect on the interactive properties of proteins in anion-exchange chromatography. The Z_c values were also found to depend on the manner in which the ionic strength was manipulated to affect elution, *i.e.* isocratic or gradient change in concentration of the displacing salt. Thus, isocratic experiments and gradient experiments with varied gradient time or varied flow-rate were observed to result in log k' *versus* log $1/c$ dependencies with non-coincident Z_c values. The relationship between protein Z_c values, the electrostatic contact area or ionotope, A_c, and the electrostatic potential of the protein surface, ψ_s, is discussed.

INTRODUCTION

Several recent studies[1–6] on the theoretical and experimental aspects of protein retention behaviour in high-performance ion-exchange chromatography (HPIEC) have placed increasing emphasis on the mechanistic details of the electrostatic

[a] For Part LXXXVIII, see ref. 20.

0021-9673/89/$03.50

interaction between the solute and the sorbent surface. These investigations have demonstrated that composite contributions from the protein surface structure, protein–ion interactions and the properties of the double layer all have an important bearing on the retention mechanism. Thus, protein retention in HPIEC is dependent on both the number, *i.e.* the ionisation state, and distribution, *i.e.* the ionisation asymmetry, of charged sites on the protein surface. Protein selectivity in HPIEC can therefore be manipulated through changes in mobile phase pH and ionic strength, by altering the electrostatic surface potential (ψ_s) of the protein surface.

The nature of the displacer ion and co-ion have also been shown to influence significantly the ion-exchange retention properties of proteins, through their effects on protein solubility and aggregation. Furthermore, it is well known that elution methods also influence protein retention behaviour. For example, in a previous paper[3] we reported that deviations occurred between the value of the protein Z_c[4] as derived from isocratic and gradient experiments with varied gradient time or varied flow-rate. These results indicated that, while empirical treatments, such as the linear-solvent-strength (LSS) model of gradient elution may, in some selected situations, be equated with isocratic models to evaluate retention dependencies of proteins in HPIEC, these approaches do not yet adequately account for changes in protein surface interactive potential induced by specific solvent effects or elution mode effects. The present paper describes the results of our further investigations into the effect of various monovalent alkali halide salts on the gradient elution behaviour of several proteins, further tests the validity of the LSS model in the HPIEC of proteins, and examines the physicochemical relationship between Z_c, ψ_s, and the ionotopic contact area, A_c, of a protein.

MATERIALS AND METHODS

Apparatus

All chromatographic experiments were performed with a Pharmacia (Uppsala, Sweden) fast protein liquid chromatography (FPLC) system, as previously described[3].

Chemicals and reagents

Bovine erythrocyte carbonic anhydrase, sperm whale skeletal muscle myoglobin (Type iii), hen egg ovalbumin (Grade V), hen egg white lysozyme (Grade I) and piperazine were purchased from Sigma (St. Louis, MO, U.S.A.). Sodium fluoride (Univar grade), sodium bromide (Unilab grade), lithium fluoride (Unilab grade), lithium chloride (Unilab grade) and potassium bromide (Univar grade) were obtained from Ajax (Sydney, Australia). Lithium bromide (LR grade), sodium chloride (AnalaR grade), potassium fluoride (AnalaR grade) and potassium chloride (AnalaR grade) were obtained from BDH (Port Fairy, Australia). Quartz-distilled water was further purified on a Milli-Q system (Millipore, Bedford, MA, U.S.A.). Buffers were adjusted to pH 9.60 by either hydrofluoric acid (48%, AnalaR grade), hydrochloric acid (specific gravity 1.16, AnalaR grade) or hydrobromic acid (specific gravity 1.46–1.49, AnalaR grade), all of which were purchased from BDH.

Chromatographic procedures

Eluent A was 0.02 *M* piperazine solution, adjusted to pH 9.60. Eluent B consisted of 0.02 *M* piperazine and 0.3 *M* displacer salt at pH 9.60. Eluents A and

B were filtered (0.45-μm cellulose acetate HAWP 04700, from Millipore) and degassed under vacuum. Protein solutions were prepared by dissolving purified protein in eluent A at a concentration of 5 mg/ml, unless otherwise specified. Before use, protein solutions were filtered through 0.22-μm ACRO LC13 filters (Gelman Sciences, Sydney, Australia). Protein sample sizes ranged from 5 to 1000 μg in injection volumes between 10 and 200 μl.

Gradient elution was performed from 0 to 100% eluent B under conditions of either constant flow-rate (F) and varied gradient time t_G or constant t_G and varied F. Varied-flow gradient experiments were conducted at flow-rates between 0.1 and 2.0 ml/min, while varied-gradient-time experiments were run with t_G varying between 17.1 and 171.1 min. The column dead-time, t_0, was obtained from the retention time of a salt breakthrough peak, following a 50-μl injection of 1 M sodium chloride in 100% eluent B (0.3 M sodium chloride). The gradient elapse time, t_e, required for eluent B to reach the column inlet, was determined from plots of conductivity *versus* time. Protein samples were eluted isocratically, starting at 100% eluent B, and elution was repeated at decreasing concentrations of B until the elution volume was greater than 30 column volumes. All data points represent the average of at least duplicate measurements.

In each type of elution experiment log k' or log $\bar{k}$ and log $1/c$ or log $1/\bar{c}$ data were collected for each protein and subjected to an iterative regression analysis to determine the y intercept (log K), slope (Z_c), and correlation coefficient (r^2). The iterative regression analyses were performed by statistical packages on a Monash University Computer Centre VAX11780 mini-computer system. The various chromatographic parameters were calculated by using the ChromoCalc programme series, developed in this laboratory and written in BASIC language for an IBM XT or AT computer.

RESULTS AND DISCUSSION

Influence of salt type on Z_c values

Protein retention on ion-exchange surfaces arises from electrostatic interactions between the protein surface and the charged stationary phase. Various theoretical models which describe protein retention behaviour have been developed from retention models for small organic molecules by the incorporation of an interactive charge term to account for multivalent attachment[7]. Thus, a non-mechanistic, stoichiometric equation, which is often written to describe the mass distribution in IEC of a polyelectrolyte solute molecule, $P^{\pm a}$, of net charge $\pm a$, is as follows

$$(P^{\pm a})_m + (a/b)(D^{\pm b})_s \rightleftarrows (P^{\pm a})_s + (a/b)(D^{\pm b})_m \quad (1)$$

where $D^{\pm b}$ is the displacer counter-ion and the subscripts m and s represent the mobile phase and stationary phase, respectively. Over a limited range of solvent composition, the relationship between the capacity factor, k', and the concentration, c, of the displacer ion is often approximated to a linear dependency of the form

$$\log k' = \log K + Z_c \log 1/c \quad (2)$$

where K is the distribution coefficient which incorporates several terms, including the binding constant, K_b, for the equilibrium process shown in eqn. 1, the phase ratio, φ, and the stationary phase ligand concentration D_b such that

$$K = \frac{K_b \varphi [D_b]^{Z_t}}{(z_a)(z_b)} \tag{3}$$

with the constants z_a and z_b adjusted for solute and salt valency. Under isocratic elution conditions, values for Z_c and log K can be determined over a narrow range of ionic strengths by linear regression analyses of plots of log k' *versus* log $1/c$. Alternatively, if gradient elution conditions are employed, application of the LSS theory[3,8] allows the determination of the median capacity factor, $\bar{k}$, and the corresponding salt concentration, $\bar{c}$, according to the relationships

$$\bar{k} = 1/1.15\, b \tag{4}$$

$$\bar{c} = c_0 + [t_g - t_0 - t_e - 0.30(t_0/b)]\Delta c/t_G \tag{5}$$

where b is the gradient steepness parameter, t_G is the gradient time and $\Delta c = c_f - c_0$, c_0 and c_f being the initial and final salt concentrations, respectively, for the gradient. Values of Z_c and log K can then be obtained from eqn. 2 by regression analysis of plots of log $\bar{k}$ *versus* log $1/\bar{c}$.

The central hypothesis of the stoichiometric relationship given by eqn. 1 assumes that the displacement of a protein solute from the charged surface is accompanied by the adsorption of a stoichiometric amount of displacing counter-ion. The value of Z_t is then defined as the ratio of the interactive charge on the solute to that on the counter-ion. For monovalent salt systems, the Z_t value is then equivalent to the average number of point charge interactions occurring between the protein solute and the charged sorbent support surface. The relative selectivity of protein solutes separated under anion-exchange conditions is thus anticipated to be directly related to the number of interacting charges and the displacing power of the counter-ion. According to the stoichiometric model (eqn. 1) values of Z_t, and as a consequence values of Z_c, should be independent of the chemical nature of the displacer ion and the type of elution conditions. However, previous studies[2] on the influence of different displacer salts on the retention and bandwidth properties of proteins separated by isocratic anion-exchange chromatography indicated that protein Z_c values vary with the type of anion used, and that the cationic co-ion also influences solute retention properties. In addition, deviations have been observed[3] between the Z_c values obtained from isocratic experiments and from gradient experiments with varied gradient time and varied flow-rate. These studies indicate that the chaotropic and kosmotropic properties of various salts, coupled with the degree of solute exposure to the mobile phase associated with varying elution conditions, could significantly alter the interactive properties of protein solutes in ion-exchange systems. Acquisition of experimental support for this concept formed the basis of the following investigations.

Based on these considerations, the present paper extends the results of our earlier investigations on both the influence of various monovalent alkali metal halides and the validation of the LSS model for gradient elution in HPIEC. The influence of the

TABLE I

PHYSICAL PARAMETERS OF PROTEINS

No.	*Protein (source)*	*pI*	*MW*
1	Ovalbumin (egg white)	4.70	43 500
2	Carbonic anhydrase (bovine erythrocytes)	5.89	30 000
3	Myoglobin (sperm whale muscle)	7.68 8.18	17 500
4	Lysozyme (hen egg white)	11.00	14 300

counter-ion and the co-ion on solute retention and bandwidth behaviour was studied by using LiCl, LiBr, NaF, NaCl, NaBr, KF, KCl and KBr. LiF was not used, due to limited solubility. Gradient retention data were obtained for four globular proteins, listed in Table I, by using a Mono-Q strong-anion-exchange stationary phase. All proteins were chromatographed by using a piperazine (20 m*M*) buffer at pH 9.60. Gradient data were obtained by either a constant flow-rate of 1 ml/min, with t_G

TABLE II

Z_c VALUES OBTAINED BY LINEAR REGRESSION FOR VARIED GRADIENT TIME

Correlation coefficient given in parentheses.

Salt	*Protein*			
	Carbonic anhydrase	*Ovalbumin*	*Myoglobin*	*Lysozyme*
LiF	Not done	Not done	Not done	Not done
LiCl	5.60 ± 2.12(0.78)	9.92 ± 2.90(0.80)	17.75 ± 3.23(0.97)	2.50 ± 0.26(0.98)
LiBr	3.14 ± 0.71(0.80)	7.30 ± 0.46(0.98)	1.96 ± 0.66(0.69)	4.21 ± 0.66(0.93)
NaF	3.55 ± 0.45(0.91)	6.56 ± 0.71(0.95)	5.49 ± 1.71(0.78)	2.99 ± 0.31(0.96)
NaCl	3.07 ± 0.21(0.99)	9.40 ± 0.50(0.99)	4.61 ± 1.57(0.90)	1.48 ± 0.17(0.97)
NaBr	2.92 ± 0.17(0.99)	7.83 ± 0.47(0.99)	1.43 ± 0.02(1.00)	2.41 ± 0.44(0.94)
KF	2.37 ± 0.25(0.95)	6.37 ± 0.57(0.97)	1.98 ± 0.27(0.93)	3.58 ± 0.14(1.00)
KCl	3.84 ± 0.05(1.00)	8.40 ± 0.76(0.98)	4.54 ± 0.51(0.99)	1.16 ± 0.15(0.95)
KBr	5.60 ± 0.75(0.92)	9.48 ± 0.69(0.97)	4.84 ± 0.75(0.89)	3.28 ± 0.24(0.98)[a] 0.98 ± 0.14(1.00)[b]
LiF	Not done	Not done	Not done	Not done
NaF	3.55 ± 0.45(0.91)	6.56 ± 0.71(0.95)	5.49 ± 1.71(0.78)	2.99 ± 0.31(0.96)
KF	2.37 ± 0.25(0.95)	6.37 ± 0.57(0.97)	1.98 ± 0.27(0.93)	3.58 ± 0.14(1.00)
LiCl	5.60 ± 2.12(0.78)	9.92 ± 2.90(0.80)	17.75 ± 3.23(0.96)	2.50 ± 0.26(0.98)
NaCl	3.07 ± 0.21 (0.99)	9.40 ± 0.50(0.99)	4.61 ± 1.57(0.90)	1.48 ± 0.17(0.97)
KCl	3.84 ± 0.05(1.00)	8.40 ± 0.76(0.98)	4.54 ± 0.51(0.99)	1.16 ± 0.15(0.95)
LiBr	3.14 ± 0.71(0.80)	7.30 ± 0.46(0.98)	1.96 ± 0.66(0.69)	4.21 ± 0.66(0.93)
NaBr	2.92 ± 0.17(0.99)	7.83 ± 0.48(0.99)	1.43 ± 0.02(1.00)	2.41 ± 0.44(0.94)
KBr	5.60 ± 0.75(0.92)	9.48 ± 0.69(0.97)	4.84 ± 0.75(0.89)	3.28 ± 0.24(0.98)[a] 0.98 + 0.14(1.00)[b]

[a] Z_c determined at low log $1/\bar{c}$ values.
[b] Z_c determined at high log $1/\bar{c}$ values.

ranging between 17.1 and 171 min, or setting the gradient time to 17.1 min and varying the flow-rate between 0.1 and 2.0 ml/min. Table II shows the Z_c values obtained for carbonic anhydrase, ovalbumin, myoglobin and lysozyme, eluted at gradient times ranging from 8.6 to 171.1 min at a constant flow-rate of 1 ml/min. Z_c values were determined by regression analysis of the linear portions of the log $\bar{k}$ *versus* log $1/\bar{c}$ curves. Values of Z_c are tabulated with an error range of one standard deviation; the correlation coefficient, r^2, is listed in parentheses. The ions used in this study were classified either as chaotropes (*e.g.*, Br^- and K^+), kosmotropes (*e.g.*, F^- and Li^+) or neutral (*e.g.*, Cl^- and Na^+). This relates to their relative position in the lyotropic series. Chaotropic ions exhibit properties which disrupt water structure and are known to destabilise protein structure while kosmotropic species stabilise water structure and have a stabilising effect on protein structure. When combinations of the above ions were used to elute proteins from the anion-exchange columns, several general trends concerning the change in the Z_c values were apparent:

(1) Z_c increased as the anion and cation of the displacer salt became more chaotropic in nature (*e.g.*, potassium or bromide salt series).

(2) Z_c increased as the anion and cation of the displacer salt became more kosmotropic in nature (*e.g.*, lithium or fluoride salt series).

(3) Z_c decreased when the displacer salt contained a combination of a chaotropic and kosmotropic ion (*e.g.*, LiBr in the bromide series and KF in the potassium series).

(4) Sodium and chloride ions generally resulted in intermediate values of Z_c in an anion or cation series (*e.g.* potassium and bromide salts).

More specifically, the anion effect on Z_c values for carbonic anhydrase, ovalbumin and myoglobin, was $Br^- < Cl^-$ for lithium, and $Br^- > Cl^- > F^-$ for potassium. For the sodium salt, the anion effect was $Br^- \approx Cl^- \approx F^-$ for carbonic anhydrase, $Br^- < Cl^- > F^-$ for ovalbumin, and $Br^- < Cl^- < F^-$ for myoglobin. Overall, there is a reversal in the effect that anion species exert on Z_c, as the cation is changed from potassium through to sodium and lithium. In anion-exchange chromatography, the elution process is often assumed to be independent of the cationic co-ion. However, the changes in Z_c observed with different cations in solution, as shown in Table II, indicate that cation selection can significantly influence solute retention behaviour. The effects of the cation on experimental Z_c values for all proteins, except lysozyme, were $K^+ > Na^+ \approx Li^+$ for bromide, $K^+ \approx Na^+ < Li^+$ for chloride, and $K^+ < Na^+$ for fluoride. These results indicate that the influence of the cationic species on Z_c can also be reversed as the anion is systematically changed from bromide to chloride to fluoride.

Recent studies[9] on the characterisation of ionic species that affect protein stability indicated that relative to bulk water chaotropic species, which destabilise protein structure, interact less strongly with the first layer of adjacent water molecules. In contrast, polar kosmotropes, which are known to stabilise protein tertiary structure, interact with the first layer of adjacent water molecules more strongly than bulk water itself. Furthermore, chaotropes increase the solubility and hydrodynamic radii of other solutes, while kosmotropes decrease their solubility and hydrodynamic radii. These findings suggested that the lyotropic properties of ions from neutral salts arise from their influence on water structure and are additive over all ions in solution. The observed changes in Z_c values suggest that the contact area or ionotopic region of the protein is altered in the presence of the different ions. Furthermore, the variation in Z_c

values with different combinations of chaotropic and kosmotropic ions result in both synergistic and antagonistic effects between the anions and cations selected as displacer salts. Thus, the influence of different salts on protein interactive behaviour, which is experimentally manifested as changes in Z_c values, is additive in the presence of salts comprised of only chaotropes (KBr) or kosmotropes (LiCl). However, a combination of chaotropic and kosmotropic ions (*i.e.* KF, LiBr) results in opposing effects on the magnitude of Z_c. Minor perturbations in protein tertiary structure or even small shifts in protein–ion interactions would result in changes in the ionotopic contact area, A_c, thereby altering the experimentally observed Z_c values. The question then immediately arises whether any fundamental physicochemical relationship exists between Z_c and A_c and the distribution coefficient, K.

The stoichiometric displacement model (SDM) also defines Z_t as arising solely from solute–sorbent surface electrostatic interactions. However, in a highly charged and polar environment, additional types of dipolar interactions may also contribute to the retention mechanism, as the solute molecule interacts with the support surface. Table III lists the ranges in which various types of dipolar interactions significantly occur and their relative magnitudes. One can see that most of these dipole interactions are significant as the protein approaches, interacts with, and departs from the stationary-phase surface. These dipolar forces are also known to be important in other forms of macromolecular association/dissociation in biologocal systems, *e.g.* antigen–antibody complexes. If all these dipolar interactions contribute to the retention process and are reflected in the experimentally derived Z_c value, then the definition of Z_c becomes far more complex than that delineated by the SDM.

TABLE III

MAGNITUDE AND EFFECTIVE RANGE OF VARIOUS DIPOLE INTERACTIONS

Interaction	*Magnitude*[10] *(kJ mol^{-1})*	*Effective range*[11] *(Å)*
Ion–ion	40–400	100
Ion–dipole	4–40	
Dipole–dipole	0.4–4	
Dipole–induced-dipole	0.4–4	100[a]
Ion–induced-dipole	0.4–4	
Dispersion	4–40	
Hydrogen bond	4–40	1.5–5

[a] Some long-range Van der Waals forces may be operative at distances greater than 1000 Å.

Influence of elution conditions on Z_c values

If the desorption process in HPIEC were solely dependent on the concentration of displacer salt in the mobile phase, it would be anticipated that similar Z_c values should be observed for isocratic and gradient experiments, and that no difference should exist between gradient elution data obtained under conditions of varying gradient time and varying flow-rate. However, previous studies[3] on the comparison of retention properties of proteins, eluted by gradient and isocratic HPIEC with NaCl as the eluting salt, indicated that deviations existed between the Z_c values obtained under these different elution conditions. In light of the effects of various displacer salts on the

TABLE IV

Z_c VALUES OBTAINED BY LINEAR REGRESSION FOR VARIED FLOW-RATE

Correlation coefficient given in parentheses.

Salt	*Protein*			
	Carbonic anhydrase	*Ovalbumin*	*Myoglobin*	*Lysozyme*
LiF	Not done	Not done	Not done	Not done
LiCl	6.76 ± 0.80(0.95)	20.40 ± 3.57(0.92)	6.72 ± 3.11(0.82)	4.46 ± 0.25(0.99)
LiBr	4.16 ± 0.40(0.96)	7.45 ± 0.68(0.96)	4.11 ± 0.44(0.95)	3.96 ± 0.77(0.93)[a] 1.96 ± 0.09(1.00)[b]
NaF	1.57 ± 0.07(0.99)	4.09 ± 0.36(0.99)	1.46 ± 0.14(0.96)	2.91 ± 0.12(0.99)
NaCl	3.31 ± 0.16(0.99)	7.42 ± 0.79(0.95)	5.09 ± 0.80(0.95)	1.88 ± 0.23(0.96)
NaBr	4.53 ± 0.53(0.94)	8.05 ± 0.36(0.99)	3.48 ± 0.59(0.92)	3.30 ± 0.33(0.99)[a] 0.56 ± 0.00(1.00)[b]
KF	2.01 ± 0.22(0.95)	4.43 ± 0.21(1.00)	1.32 ± 0.12(0.97)	3.23 ± 0.50(0.89)
KCl	2.17 ± 0.24(0.97)	5.65 ± 0.63(0.95)	1.47 ± 0.15(0.97)	1.73 ± 0.11(0.99)
KBr	5.95 ± 1.19(0.83)	10.92 ± 0.88(0.97)	6.03 ± 2.26(0.70)	4.52 ± 0.75(0.95)[a] 2.53 ± 0.28(0.97)[b]
LiF	Not done	Not done	Not done	Not done
NaF	1.57 ± 0.07(0.99)	4.09 ± 0.36(0.99)	1.46 ± 0.14(0.96)	2.91 ± 0.12(0.99)
KF	2.01 ± 0.22(0.95)	4.43 ± 0.21(1.00)	1.32 ± 0.12(0.97)	3.23 ± 0.50(0.89)
LiCl	6.76 ± 0.80(0.95)	20.40 ± 3.57(0.92)	6.72 ± 3.11(0.82)	4.46 ± 0.25(0.99)
NaCl	3.31 ± 0.16(0.99)	7.42 ± 0.79(0.95)	5.09 ± 0.80(0.95)	1.88 ± 0.23(0.96)
KCl	2.17 ± 0.24(0.97)	5.65 ± 0.63(0.95)	1.47 ± 0.15(0.97)	1.73 ± 0.11(0.99)
LiBr	4.16 ± 0.40(0.96)	7.45 ± 0.68(0.96)	4.11 ± 0.44(0.95)	3.96 ± 0.77(0.93)[a] 1.96 ± 0.09(1.00)[b]
NaBr	4.53 ± 0.53(0.95)	8.05 ± 0.36(0.99)	3.48 ± 0.59(0.92)	3.30 ± 0.33(0.99)[a] 0.56 ± 0.00(1.00)[b]
KBr	5.95 ± 1.19(0.83)	10.92 ± 0.88(0.97)	6.03 ± 2.26(0.70)	4.52 ± 0.75(0.95)[a] 2.53 ± 0.28(0.97)[b]

[a] Z_c determined at low log $1/\bar{c}$ values.
[b] Z_c determined at high log $1/\bar{c}$ values.

retention properties of proteins in HPIEC, these investigations were extended to study the influence of flow-rate and gradient time conditions on the effects of anions and cations on protein Z_c values. Table IV lists the Z_c values for the four model proteins, eluted with a gradient time of 17.1 min and flow-rates ranging from 0.1 to 2 ml/min. Consider first the effect of varying the displacer anion on the value of Z_c. For these studies, fluoride, chloride, and bromide salts of sodium and potassium, and the chloride and bromide salts of lithium were investigated. The value of Z_c for the potassium salts was found to increase under both sets of gradient conditions in the order $F^- < Cl^- < Br^-$ for all proteins, except lysozyme, where other phenomena complicated the observed trend (see below). The varied gradient time and isocratically derived Z_c values obtained for the sodium salts generally decreased in the order $F^- > Cl^- > Br^-$ whereas the order was reversed for the varied flow experiments, such that Z_c increased as $F^- < Cl^- \approx Br^-$. The influence of the cationic co-ion was also found to be dependent on the elution conditions. The value of Z_c for the bromide salts was

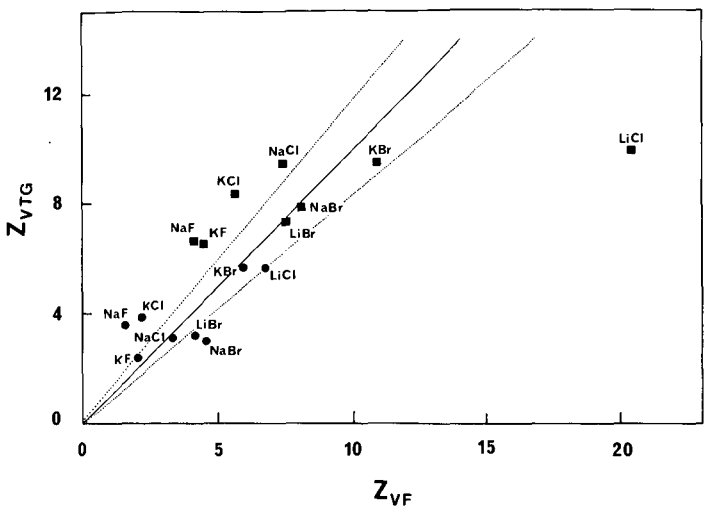

Fig. 1. Plot of Z_c values derived from varied gradient time experiments (Z_{VTG}) versus Z_c values for varied flow-rate experiments (Z_{VF}) for ovalbumin (■) and carbonic anhydrase (●) eluted with different salts as indicated. Gradient data were obtained with t_G varying between 17.1 and 171.1 min at a flow-rate of 1 ml/min or a constant t_G of 17.1 min and the flow-rate varying between 0.1 and 2.0 ml/min. The straight lines shown correspond to the theoretical relationship $Z_{VTG} = Z_{VF}$, with a ± 20% error margin.

found to decrease under both sets of gradient data in the order $K^+ > Na^+ \approx Li^+$ for all proteins, except lysozyme. Both sets of gradient data for the chloride salts have Z_c values increasing with the series $K^+ \approx Na^+ < Li^+$. For the fluoride salts, the order of cations leading to increased Z_c values was also dependent on the gradient elution mode. The Z_c value was found to increase with $K^+ < Na^+$ for the varied gradient time data while $K^+ \approx Na^+$ for the varied flow experiments. Thus for the fluoride salt series, a change in elution mode, from varied gradient time and constant flow-rate to constant gradient time and varied flow-rate conditions caused a decrease in Z_c values while for the sodium salt series there was a reversal of the effect of ions on Z_c. In Fig. 1 the Z_c values derived from varied gradient time (fixed flow-rate) experiments (Z_{VTG}) with ovalbumin and carbonic anhydrase are plotted against the Z_c values derived from varied flow-rate (fixed gradient time) experiments (Z_{VF}). According to the stoichiometric retention model and LSS theory, Z_{VTG} and Z_{VF} values should all fall on a common line (slope = 1). As is evident from the number of data points which fall outside the error margin of ± 20%, divergencies from this ideal behaviour predicted by these theoretical relationships occur. These results suggest that changes in the physicochemical basis of the adsorption/desorption process, (*e.g.* the results for the sodium and fluoride salts investigated) can be induced by experimental factors controlling the elution mode. In this instance, the rate of change of displacer salt concentration is the primary difference between the two gradient elution modes. The difference between a variable and a constant rate of change could influence the number and type of solute species interacting with the sorbent surface and ultimately the thermodynamics involved with the adsorption/desorption process.

Comparison of gradient and isocratic retention data

The linear solvent strength (LSS) model is a non-mechanistic theoretical treatment, designed to relate solute retention in gradient and isocratic elution. An assumption inherent in the development of this model is that identical physicochemical phenomena control the migration of a solute in both isocratic and gradient elution modes, giving rise (in principle) to superimposable retention plots. Hence, from a minimum of two different gradient experiments, sufficient data can be obtained to predict solute retention behaviour in a corresponding isocratic system and *vice versa*. The advantage of using models such as the LSS is immediately evident, since these approaches represent quick, cost-saving methods for optimising sample retention and provide alternative, more systematic procedures than the trial-and-error techniques usually employed. In particular, the LSS model has been used successfully in reversed-phase HPLC to optimise purifications of both small and large molecules[12–14] and has recently been extended to assess protein retention in hydrophobic interaction chromatography (HIC)[15] and ion-exchange HPLC systems[3,8].

However, recent studies[3] indicate that in the case of HPIEC, the physicochemical phenomena controlling gradient and isocratic elution may not be totally synonomous, and the differences could ultimately affect the accuracy and general utility of the LSS model in HPIEC systems. In order to investigate further the relevance of LSS methods to the physicochemical basis of the elution process in HPIEC, solute retention data from isocratic and gradient elution were compared for a variety of monovalent alkali metal halide salts.

Gradient retention data were obtained by varying the gradient time, t_G, between 8.6 and 171.1 min at a flow-rate of 1 ml/min or by varying the flow-rate from 0.1 to 2.0 ml/min with t_G = 17.1 min. Values of log $\bar{k}$ and log $1/\bar{c}$ for retention mapping were obtained by using eqns. 4 and 5 from the LSS model. Isocratic retention data were collected by systematically decreasing the concentration of the displacer salt in the eluent at a constant flow-rate of 1 ml/min. Values of log k' and log $1/c$ for the isocratic elutions were obtained directly from experimental data. Both gradient and isocratic experiments were conducted with a mobile phase pH equal to 9.6.

Table V lists the Z_c values obtained from linear regression of the combined isocratic and varied gradient time and varied flow conditions. The correlation coefficient was also used to assess the superimposability of the combined data, *i.e.* the

TABLE V

Z_c VALUES OBTAINED BY LINEAR REGRESSION DATA FOR COMBINED DATA

Salt	*Protein*			
	Carbonic anhydrase	*Ovalbumin*	*Myoglobin*	*Lysozyme*
NaF	2.24 ± 0.27(0.78)	4.52 ± 0.46(0.88)	1.84 ± 0.36(0.62)	−0.81 ± 0.63(0.09)
NaCl	2.41 ± 0.35(0.77)	7.37 ± 0.47(0.95)	1.70 ± 0.32(0.74)	0.37 ± 0.21(0.11)
NaBr	2.72 ± 0.25(0.90)	5.85 ± 0.44(0.92)	1.93 ± 0.23(0.85)	1.26 ± 0.31(0.55)
LiCl	3.63 ± 0.48(0.80)	9.97 ± 1.80(0.74)	0.92 ± 0.50(0.26)	0.66 ± 0.14(0.58)
NaCl	2.41 ± 0.35(0.77)	7.37 ± 0.47(0.95)	1.70 ± 0.32(0.74)	0.37 ± 0.21(0.11)
KCl	2.14 ± 0.19(0.90)	5.61 ± 0.38(0.94)	0.85 ± 0.25(0.39)	−0.14 ± 0.86(0.00)

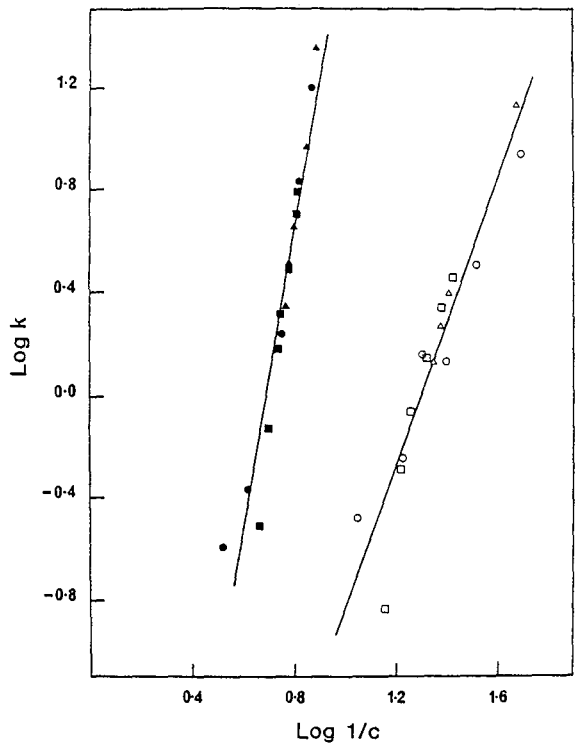

Fig. 2. Retention plots for isocratic (log k' *versus* log $1/c$) and gradient experiments (log $\bar{k}$ *versus* log $1/\bar{c}$) for ovalbumin and carbonic anhydrase, eluted with sodium bromide (isocratic data were derived from experiments with varied salt concentrations at pH 9.60 and a flow-rate of 1 ml/min). Other chromatographic conditions are given in the Materials and Methods section and legend to Fig. 1. See Tables II, IV, and V for the derived Z_c values. For ovalbumin: (●), Isocratic; (▲), VTG; (■), VF. For carbonic anhydrase: (○), Isocratic; (△), VTG; (□), VF.

level of correlation, as predicted by the LSS theory. Fig. 2 and 3 show plots of log k versus log $1/c$ for the four proteins eluted with NaBr. These data illustrate the variation in the degree of correlation between isocratic and gradient data for different experimental conditions. The extent of divergency in the correlation between theoretically and exprimentally derived dependencies of log $\bar{k}$ on log $1/\bar{c}$ generally followed the order ovalbumin < carbonic anhydrase < myoglobin < lysozyme for correlation of the superimpossibility of isocratic to gradient data. These results suggest that gradient and isocratic elution do not have an identical physicochemical basis for controlling solute retention. In particular, an assumption inherent in the derivation of equations that relate isocratic and gradient retention data is that each k' value is measured under equilibrium or near-equilibrium conditions. However, if the interactive properties of the protein solute are dependent on, for example, the mobile phase composition or the dwell-time of the system, then time-dependent changes in salt concentration associated with varied gradient time will result in protein–ligand interactions that are not at the identical point in the equilibrium trajectory. In particular, it was observed that r^2 for superimposability of retention data approached

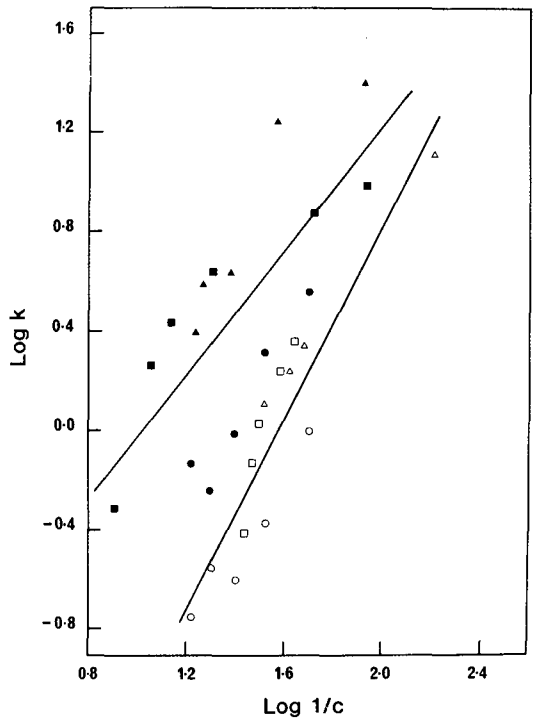

Fig. 3. Retention plots for isocratic and gradient experiments with myoglobin and lysozyme eluted with sodium bromide. See legend to Fig. 2 for experimental details. For myoglobin: (○), Isocratic; (△), VTG; (□), VF. For lysozyme: (●), Isocratic; (▲), VTG; (■), VF.

zero for myoglobin eluted with KCl or for lysozyme eluted with NaF. In such an event, isocratic, varied gradient time and varied flow-rate retention data were observed to form three distinct and separate plots, corresponding to each elution mode. In the example of lysozyme, eluted with NaF, an additional complication arises. Gradient-derived Z_c and log K values are used to obtain the isocratic k' and c values by substitution into eqn. 5. Lysozyme in this instance has similar Z_c values for both varied gradient time and varied flow-rate modes, but different log K values. Hence, the theoretical isocratic k' and c values obtained, which are derived from the gradient retention data used in the calculation, will not correspond to the true experimental isocratic values.

In evaluating the LSS model for use in HPIEC, Stout *et al.*[8] observed small, consistent differences between the theoretical and experimentally derived gradient Z_c values. They postulated that by using a simple correction factor, the experimentally derived Z_c value could be corrected for non-LSS behaviour. This factor was to ensure improved accuracy in calculating the corresponding isocratic k' and c values. This approach assumed that all displacer salts have a similar effect on this correction factor. In light of the data shown in Tables II and IV, where substantial differences were found to exist between solute Z_c values obtained with different displacer salts, this assumption requires modification. Furthermore, for a particular salt system, it is

evident from the data that significant differences in Z_c for a solute can arise from the use of different elution modes, *i.e.* varied gradient time, varied flow-rate or isocratic elution. These results therefore indicate that an accurate correction factor cannot yet be substantiated for use in all HPIEC systems.

Finally, for the displacer salts used in this study, it was found that r^2 values for the correlation of data from isocratic and gradient experiments generally improved as the hydrated-ion size decreased within a particular salt series. A reason for such an occurrence is not apparent at the present time, but the existence of such a trend may be a useful criterion for selecting alkali metal halide displacer salts that improve LSS behaviour in solute retention.

Influence of displacer salt and elution conditions on anion-exchange retention properties of proteins, where eluent pH < protein pI

According to the net charge concept[7], proteins chromatographed on a strong-anion-exchange column at mobile phase pH values below their known p*I* will not be retained due to the existence of a net positive surface charge. However, various examples of proteins have been reported where significant deviations occur[1,14] from the retention behaviour, expected on the basis of this assumption. For example, lysozyme, with a p*I* equal to 11.0, will exhibit a net positive charge under the mobile phase conditions of pH 9.6 used in the present study. However, in most cases, this protein exhibits a significant degree of retention on the anion-exchange column *e.g.* $\bar{k}$ values ≥ 10. Furthermore, in some solvent systems, the decreased solubility and the tendency of lysozyme to aggregate results in retention behaviour which does not conform to the simple dependency between k' and c, as expressed by eqn. 2. However such divergencies can give valuable insight into IEC retention mechanism(s) that are not always evident with the relatively well-behaved proteins. Examination of Tables II and IV and Figs. 4 and 5 reveals that the elution mode can not only modulate the effect of various ions on Z_c but can also influence the elution mechanism. For example, when lysozyme is isocratically eluted with KCl as the displacer salt, a downward curving retention plot (with a negative Z_c value) is obtained (Fig. 4) on adsorption which is indicative of a "salting out" phenomenon. However, under gradient elution conditions, again with KCl as the displacer salt, lysozyme exhibits "normal" ion-exchange retention, giving rise to positive Z_c values with increasing retention plots.

Plots of $\log \bar{k}$ versus $\log 1/\bar{c}$, which are used to map solute retention behaviour of proteins, are generally presented as linear dependencies with a slope corresponding to Z_c. In situations where the IEC retention process ceases to dominate the retention mechanism, *i.e.* when hydrophobic or salt-bridge interactions occur, then curvilinear dependencies of $\log \bar{k}$ on $\log 1/\bar{c}$ will be observed. Under these conditions, multiphasic retention plots will exhibit individual slope components, which are characteristic of the protein, the displacing salt system, the pH, and the chemical nature and concentration of the buffer salt. Recently, HPIEC retention maps for subtilisins[6] were also found to be curvilinear, consisting of two distinct lines with independent slopes and intercepts. These observations were believed to result from a change in the coulombic interactive area or ionotope, which was dependent upon mobile phase ionic strength. In the current study, the elution of lysozyme with a series of bromide salts resulted in similar biphasic retention plots. Fig. 5 shows retention plots for lysozyme, eluted by potassium salts under conditions of varied gradient time and constant flow-rate. Examination of

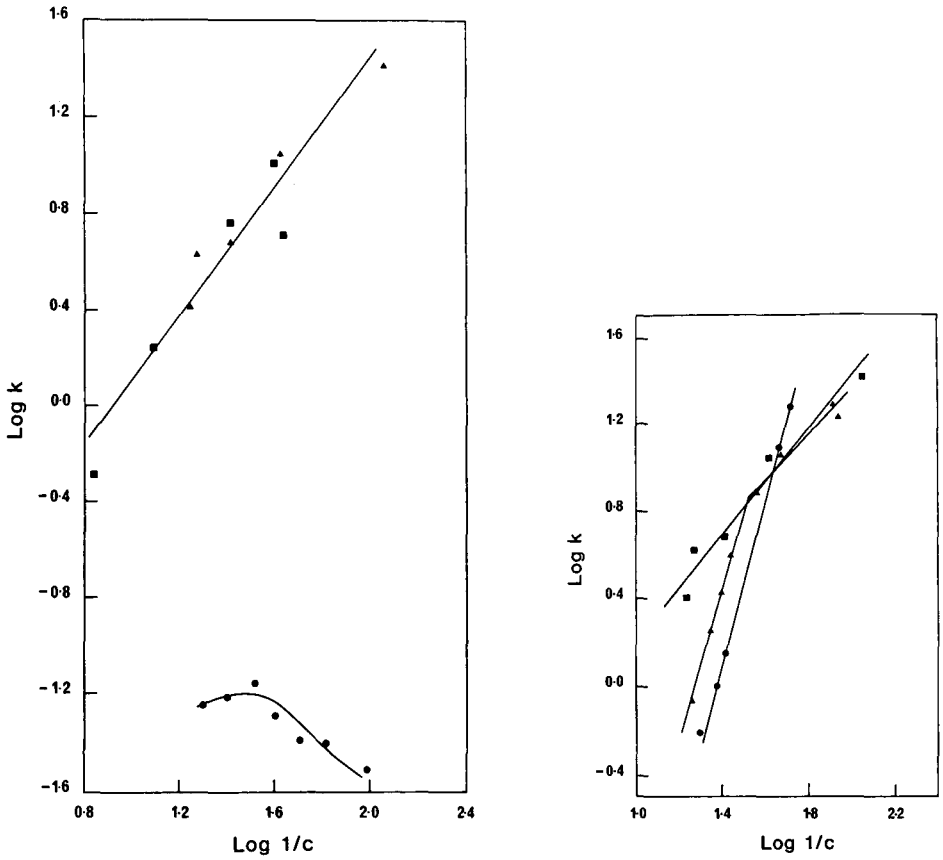

Fig. 4. Retention plots for isocratic and gradient experiments with lysozyme, eluted with potassium chloride. See legend to Fig. 2 for experimental details. (●), Isocratic; (▲), VTG; (■), VF.

Fig. 5. Retention plots for lysozyme eluted under gradient conditions, with t_G varying between 17.1 and 171.1 min at a flow-rate of 1 ml/min. The displacer salts used were: (●), KF; (■), KCl and (▲), KBr.

Table II reveals that the slope of the retention plot for lysozyme, eluted with KBr, at longer column residence times is similar to that for KCl and at shorter column residence times approximates the slope for KF. These observations clearly reflect the existence of several potentially interactive binding sites (*i.e.* different ionotopes) at the surface of the lysozyme molecule. The selection of these binding sites may thus not only depend upon column residence time but also the ionic species present in the eluent. For short column residence times, the ionotope for lysozyme, eluted with KBr, recognises the sorbent surface in a manner similar to that for KF, whilst at longer residence times the ionotope is similar to that for the KCl salt system. The sharp transition at intermediate ionic strength suggests a two-state surface-mediated phenomenon, in which the transition between the two ionotopic forms is very fast, because no unusual curve deformity is noted in the bandwidth data[17]. Similar results are also observed for lysozyme eluted with the potassium salt series under conditions of constant gradient time and varied flow-rate (Table IV). However, the biphasic phenomenon was not as

pronounced, and the ionic strength of KBr at the break point corresponded to a higher value, *i.e.* 30 m*M*, for varied gradient time and 65 m*M* for varied flow-rate conditions.

The retention plots for lysozyme, eluted with all bromide salts under conditions of constant gradient time and varied flow-rate were also found to be biphasic. At lower flow-rates (lower log $1/\bar{c}$ values) and at higher flow-rates (higher log $1/\bar{c}$ values) beyond the break points, significant differences between Z_c values for each salt system were observed with $K^+ > Li^+ > Na^+$. This indicates that the magnitude of the area of the lysozyme ionotope in each of the two-state systems was significantly different for each bromide salt. The break points in the retention plot for the bromide salts was found to vary, depending upon the cation, *i.e.* LiBr = 102 m*M*, NaBr = 69 m*M* and KBr = 65 m*M*. The data for the potassium salt indicated that the transition between each of the lysozyme ionotopic states is also fast, as there was no anomalous bandbroadening observed for this cation series[17].

The choice of gradient elution mode can also influence the expression of these bi-linear retention dependencies. For example, comparison of the retention plots of lysozyme eluted with LiBr (Fig. 6) under conditions of either varied flow-rate and constant gradient time or varied gradient time and constant flow-rate, indicates that the results of the varied gradient time experiments more closely approximate a first-order model of retention.

The nature of the displacer ion clearly has a significant influence on the ability of lysozyme, a protein with a net positive surface charge, to interact with a positive anion-exchange surface. In a previous study[2], it was found that under isocratic elution conditions lysozyme exhibited significant retention with eluents containing NaF, NaBr, and LiCl, yet no retention was observed with NaCl or KCl as the displacer salt. However, in the present study, involving the gradient elution mode, the elution of lysozyme with LiCl or NaCl consistently resulted in breakthrough elution profiles as shown in Fig. 7. In these instances, Z_c values were calculated from retention data

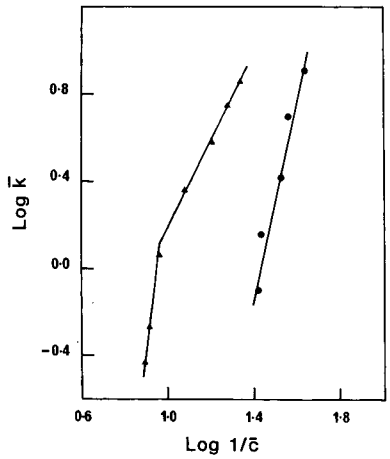

Fig. 6. Retention plots for lysozyme eluted under gradient conditions with LiBr as the displacer salt. Gradient data were derived with varied gradient time or varied flow-rate, as described in Fig. 1. (●), VTG; (▲), VF.

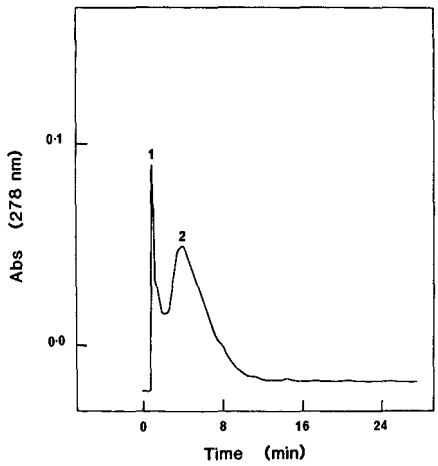

Fig. 7. Chromatogram illustrating pseudo-overload conditions with LiCl as displacer salt. t_G = 17.1 min; flow-rate = 0.7 ml/min; 100 μg of lysozyme.

associated with peak 2. It appears therefore that the time-dependent changes in the salt concentration have resulted in retention behaviour which is typical of column-overload conditions. However, only analytical loads (10–100 μg) were employed, and this indicates that the ionic capacity of the column has not been exceeded. In these cases, it appears that the delay in the exposure of lysozyme to the displacer salt, which occurs in gradient modes, results in a interactive process different from the mechanism of isocratic elution, in which the protein is loaded in the presence of varying salt concentrations. In particular, the elution of two different protein zones suggests that there is either a mobile-phase-dependent equilibrium between two alternate forms of lysozyme with different interactive properties or, alternatively, kinetic competition between diffusion and adsorption. This is evidenced by comparison of Z_c values, obtained, *e.g.*, for LiCl and LiBr. The value of Z_c in LiBr remains essentially constant ($\approx$ 4) in both gradient elution modes, and the absence of a breakthrough peak indicates the presence of a single interactive species. With LiCl, however, the Z_c values almost doubles from 2.5 with varied gradient time to 4.5 under varied flow-rate conditions. These results, therefore, graphically demonstrate the influence of both the mobile phase composition and the rate of change of displacer salt concentration on the retention properties of proteins in HPIEC.

The ion-exchange distribution constant

The K term, as defined in eqn. 2, is related to the overall distribution coefficient and incorporates several factors including the equilibrium binding constant, K_b, the phase ratio, φ, the stationary-phase ligand concentration, D_b, and the fractional occupancy of the ligands. According to eqn. 2, graphic extrapolation of the linear dependency between log k' and log $1/c$ yields log K as the intercept in the limit case of log $1/c \rightarrow 0$, *i.e.* when the displacer salt concentration is equal to 1 mol/l. However, this extrapolation assumes that the retention dependencies remain linear at high salt concentrations. Several examples have been reported[1,2] where curvilinear dependen-

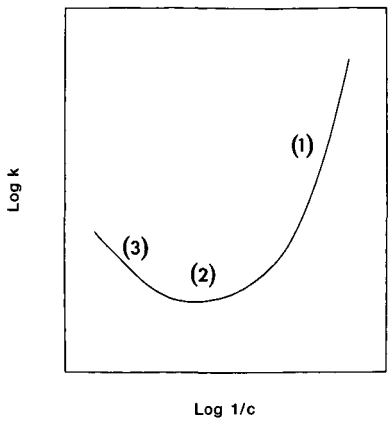

Fig. 8. General dependence of retention on salt concentration for proteins separated by HPIEC, illustrating (1) electrostatic, (2) size exclusion and (3) hydrophobic-interaction phenomena.

cies between log k' and log $1/c$ have been observed, such as that depicted by the hypothetical curve in Fig. 8. As is evident from this diagram, section 1 of the curve corresponds to retention behaviour dominated by ion-exchange interactions, while hydrophobic interactions govern the retention mechanism in section 3 leading to increasing k' values with increasing salt concentration. In section 2 of the curve size-exclusion phenomena dominate under conditions of displacing-ion concentrations where minimal interaction occurs between the solute and the sorbent surface. Thus, the K value obtained by linear extrapolation of section 1 to the y intercept will not represent the distribution coefficient at this particular salt concentration. Furthermore, numerical evaluation of this parameter bears no physicochemical relationship to an interactive distribution constant, which must be derived under conditions of infinite dilution of buffer constituents.

Analogous circumstances have been discussed for HIC and protein solubility[18,19]. In a subsequent paper the involvement of hydrophobic interaction effects and salting-out effects in the HPIEC of these proteins will be evaluated. These additional studies also have permitted the dependency of surface tension on log k' to be assessed. In the absence of displacer salt, the chromatographic capacity factor, K_0, will be related to the interactive affinity of the protein solute for the charged stationary-phase surface. This, in turn, is related to the area and charge density of the interactive region, *i.e.* the ionotope. According to the Debey-Hückel theory of electrostatics, the electrostatic free energy, W_e, of a spherical ion of radius r_p is given by

$$W_e = \int_0^{Z_t} \psi_s \, de \tag{6}$$

where Z_t is the full charge of the ion, and ψ_s is the potential at its surface. Because of the spherical symmetry, the electrical intensity, E, will be constant over this surface, and according to Gauss' law is given by

$$E = \frac{Z_t \varepsilon}{Dr^2} = \frac{4\pi Z_t \varepsilon}{DA_t} = \frac{-d\psi_s}{dr} \tag{7}$$

where ε is the protonic charge, D is the dielectric constant of the medium, and A_t is the total surface area of the charged sphere. For a protein solute with a single ionotopic region that dominates the coulombic interaction with an ion-exchange surface, the electrical intensity of the ionotopic surface may be given by

$$E_c = \frac{Z_c \varepsilon}{D \Sigma r_i r_j} = \frac{C_c Z_c \varepsilon}{DA_c} \tag{8}$$

where $\Sigma\ r_i r_j$ accounts for the ionotopic surface area, A_c, of three-dimensional coordinates, r_i, r_j, r_z, whilst C is a constant.

If it is assumed[20] that the distance, a, between the ionotope and the charged ligand corresponds to the distance of closest approach between the vector centres of the protein ion of radius r_p and the charged ligand, then integration of eqn. 6 with respect to r yields

$$\psi = \frac{CZ_c \varepsilon r_z}{D} \frac{1}{A_c} + F \tag{9}$$

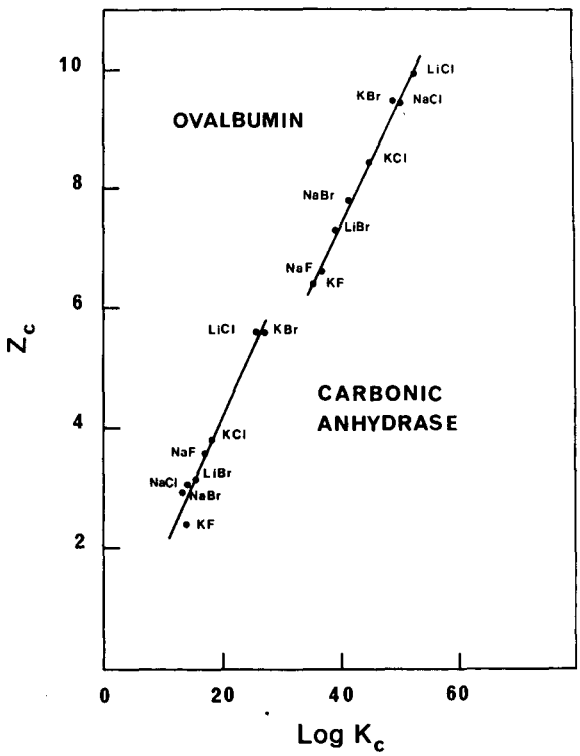

Fig. 9. Plots of Z_c *versus* log K_c for ovalbumin and carbonic anhydrase, separated under conditions of varied gradient time.

for $r_p \leqslant r \leqslant a$, and where F is given by

$$F = \frac{-Z_c\varepsilon}{D} \frac{\kappa}{1 + \kappa a} \tag{10}$$

and

$$\kappa^2 = \frac{4\pi\varepsilon^2}{DkT} \Sigma c_i Z_i^2 \tag{11}$$

The term κ depends only on the composition of the solution, and the $\Sigma\ cZ^2$ term represents the summation of all charged species of concentration c and charge Z. The term F of eqn. 9 corresponds to the potential due to the ion atmosphere surrounding the ionotope and is proportional to the charge of the ionotope. For a particular ligand type and mobile phase composition, F will be constant for a defined protein in the ionisation state Z_i. Furthermore, if solute elution is carried out under conditions that maximise electrostatic interactions, the electrostatic free energy term, ΔG_e, for ion-exchange solute retention is equivalent to W_c. Thus, integration of ψ with respect to an incremental charge increase, de, yields

$$W_c = \frac{Z_c Z_i \varepsilon^2}{2D} \frac{r_p}{A_c} - \frac{\kappa}{1 + \kappa a} = \frac{-RT}{2.303} \log K_0 \tag{12}$$

Hence, if the above assumptions apply, it follows that log K_0 is proportional to the ionotopic constant area, A, and, from eqn. 12, a linear dependency of log K_0 on Z_c is anticipated.

Fig. 9 shows plots of Z_c *versus* log K_c for ovalbumin and carbonic anhydrase. For these calculations, values of log K_c were determined by extrapolation of the log $\bar{k}$ *versus* log $1/\bar{c}$ plots to the limit case of $c \rightarrow 10^{-6}$ mol/l. While these values are not equivalent to the true log K_0 value, which by definition is a constant for a particular protein solute, log K_c values will provide some indication of the relative influence of different displacer salts on protein retention behaviour. The high correlation of the data shown in Fig. 9. ($r^2 = 0.99$ and 0.98, respectively) provide support for the conclusions summarised in the relationship shown in eqn. 12.

CONCLUSION

The current investigation provides a detailed experimental and theoretical basis for the quantitative characterisation of the electrostatic contact area and the electrostatic potential of the protein surface in HPIEC systems. In particular, the present data clearly demonstrate the influence on protein interactive behaviour of different cations and anions with known chaotropic or kosmotropic properties. Changes in the ionotopic surface of a protein under different environmental conditions can now be rapidly assessed by chromatographic analysis. If it is assumed that NaCl has little influence on protein structure, different displacer salts can be categorised on the basis of their effects on Z_c and log K_c. Correlation of these effects with

spectroscopic analysis of the eluted protein zone will then enable full optimisation of HPIEC separations to maximise chromatographic performance in both analytical and preparative HPIEC.

SYMBOLS

a	Closest approach distance between protein and charged ligand
A_c	Ionotopic surface area
A_t	Total surface area of a charged sphere
b	Gradient steepness parameter
$\bar{c}$	Median salt concentration during gradient elution
C	Constant of integration in eqn. 8
c_i	Concentration of a charged species in solution (eqn. 1)
c_0	Initial salt concentration for the gradient
c_f	Final salt concentration for the gradient
Δc	Change in concentration equivalent to $c_f - c_0$
D	Dielectric constant of medium
D_b	Stationary phase ligand concentration
E	Electrical intensity for a spherical ion
E_c	Electrical intensity for a spherical protein in an ion-exchange system
ε	Protonic charge
F	Potential due to the ion atmosphere surrounding the ionotope, *i.e.* proportional to the charge on the ionotope
k	Boltzmann constant
K	Distribution coefficient, as defined by eqn. 3
K_c	Capacity factor at $C = 10^{-6}$ mol/l, *i.e.* an estimate of K_0
K_b	Binding constant for the equilibrium shown in eqn. 1
K_0	Capacity factor in the absence of displacer salt
k'	Isocratic capacity factor
$\bar{k}$	Gradient capacity factor
κ	Debye length
LSS	Linear solvent strength model
R	Gas constant
r_i, r_j, r_z	Three-dimentional coordinates of protein ionotope
r_p	Radius of the protein
SDM	Stoichometric displacement model
T	Temperature
t_e	Gradient elapse time
t_G	Gradient time
t_g	Solute gradient retention time
t_0	Column dead-time
VF	Varied flow-rate conditions
VT_G	Varied gradient time conditions
W_e	Electrostatic free energy
z_a	Constant, adjusting for solute valency in eqn. 3
z_b	Constant, adjusting for salt valency in eqn. 3
Z_i	Valency of a charged species in solution (see eqn. 11)

Z_c Number of charges on a protein associated with adsorption, obtained from the slope of log k' *versus* log $1/c$ plots
Z_t Ratio of the interactive charge on the protein to that on the displacer ion
ψ_s Electrostatic potential of the protein
φ Phase ratio

REFERENCES

1 M. T. W. Hearn, A. N. Hodder, P. G. Stanton and M. I. Aguilar, *Chromatographia*, 24 (1987) 769.
2 M. T. W. Hearn, A. N. Hodder and M. I. Aguilar, *J. Chromatogr.*, 443 (1988) 97.
3 M. T. W. Hearn, A. N. Hodder and M. I. Aguilar, *J. Chromatogr.*, 458 (1988) 27.
4 R. R. Drager and F. E. Regnier, *J. Chromatogr.*, 406 (1987) 237.
5 M. L. Heinitz, L. Kennedy, W. Kopaciewicz and F. E. Regnier, *J. Chromatogr.*, 443 (1988) 173.
6 R. M. Chicz and F. E. Regnier, *J. Chromatogr.*, 443 (1988) 193.
7 W. Kopaciewicz, M. R. Rounds, J. Fausnaugh and F. E. Regnier, *J. Chromatogr.*, 266 (1983) 3.
8 R. W. Stout, S. I. Sivakoff, R. D. Ricker and L. R. Snyder, *J. Chromatogr.*, 353 (1986) 439.
9 M. W. Washabaugh and K. D. Collins, *J. Biol. Chem.*, 261 (1986) 12477.
10 R. Chang, *Physical Chemistry with Applications to Biological Systems*, MacMillan, New York, 2nd ed., 1981, p. 487.
11 C. J. Van Oss, R. J. Good and M. K. Chaudhury, *J. Chromatogr.*, 376 (1986) 111.
12 M. A. Stadalius, M. A. Quarry and L. R. Snyder, *J. Chromatogr.*, 327 (1985) 93.
13 M. A. Quarry, R. L. Grob and L. R. Snyder, *Anal. Chem.*, 58 (1986) 907.
14 M.-I. Aguilar, A. N. Hodder and M. T. W. Hearn, *J. Chromatogr.*, 327 (1984) 115.
15 N. T. Miller and B. L. Karger, *J. Chromatogr.*, 326 (1985) 45.
16 W. Kopaciewicz and F. E. Regnier, *Anal. Biochem.*, 13 (1983) 251.
17 A. N. Hodder, M. I. Aguilar and M. T. W. Hearn, in preparation.
18 W. R. Melander and Cs. Horváth, *Arch. Biochem. Biophys.*, 183 (1977) 200.
19 W. R. Melander, D. Corradini and Cs. Horváth, *J. Chromatogr.*, 317 (1984) 67.
20 M. T. W. Hearn, A. N. Hodder and M. I. Aguilar, *J. Chromatogr.*, 458 (1988) 45.

Journal of Chromatography, 476 (1989) 413–421
Elsevier Science Publishers B.V., Amsterdam — Printed in The Netherlands

CHROMSYMP. 1591

IMPROVED SEPARATION SPEED AND EFFICIENCY FOR PROTEINS, NUCLEIC ACIDS AND VIRUSES IN ASYMMETRICAL FLOW FIELD FLOW FRACTIONATION

A. LITZÉN and K.-G. WAHLUND*
Department of Analytical Pharmaceutical Chemistry, University of Uppsala Biomedical Center, Box 574, S-751 23 Uppsala (Sweden)

SUMMARY

The performance of the asymmetrical flow field-flow fractionation channel has been improved by the use of a much thinner (0.12-mm) channel than before and by flow programming (stepwise gradient elution). The thinner channel contributes to a decreased zone broadening which enables complete resolution in a shorter time. Three protein peaks, representing molecular weights from 12 000 to 136 000, were completely resolved within 3 min. Flow programming speeds up the elution of the high-molecular-weight materials which occur late in a fractogram. This enabled separation of a small plasmid fragment (700 base pairs) from the large amounts of a big fragment (4600 base pairs) in 30 min and improved detection of a presumed trimer of albumin. Two viruses ($1.8 \cdot 10^6$ and $50 \cdot 10^6$ daltons) were eluted as narrow peaks within 5 min.

INTRODUCTION

Field flow fractionation (FFF) comprises a group of analytical and micro-preparative separation methods especially suited for macromolecular and particle separations. The basic idea originated with Giddings in 1966[1]. Many different modes of FFF have since been described[2]. The flow FFF method used in this work is universal in the sense that it can separate material having a very broad range of molecular weights and particle sizes in one single separation unit. Adjustment of conditions for the actual molecular or particle size is simply made by changing the flow-rates of the cross- and channel-flows. The almost general applicability makes it especially important to develop the performance of flow FFF further. The separation is based on differences in the diffusion coefficients, and the factors which influence separation are thus the molecular and the particle mass and shape. For a more complete list of references to earlier work and a detailed description of the principle the reader is referred to a previous article[3].

The type of separations that can be obtained by flow FFF is perhaps best described as a size fractionation, and the results are therefore in a way similar to those of size-exclusion chromatography (SEC). One important aspect in a comparison of flow FFF with SEC is that the former may lack some of the problems observed in the

0021-9673/89/$03.50

latter for ultra-high-molecular-weight materials[4]. For example, there is no upper "exclusion limit" in flow FFF (except when the particle size approaches that of the channel thickness) and, if properly designed, elution times in flow FFF may become much smaller than in SEC for a certain resolution level. Theoretical calculations show that the selectivity of flow FFF is superior to that of SEC[2]. This means that there is a potential in flow FFF for better resolution than in SEC if the zone broadening in the flow FFF channel can be kept low enough. A further advantage of flow FFF is that gradient elution can be obtained by programming the flow-rate.

In the previous study[3] we obtained much improved resolution and separation speed for proteins by using a thinner channel (0.3 mm). The application of flow FFF was also expanded to new types of compounds, such as the separation of plasmids and plasmid fragments. In the present study we have obtained a further improvement in resolution and speed by using an even thinner channel (0.12 mm). Stepwise flow programming was used to optimize the separation speed. The examples given show rapid separations of proteins and their dimers and trimers, a small plasmid fragment from large amounts of a big fragment, three small plasmid fragments and two plasmids and the isolation of two virus particles.

Very recently, a flow FFF separation system was described in which circular hollow fibres are used as the separation channel instead of the flat, rectangular channel used in our work[5,6]. The separation appears to be slower in the hollow fibre system.

EXPERIMENTAL

The reader is referred to the authors' previous papers[3,7] for a detailed description of the construction of the asymmetrical flow FFF channel and its operation. Here, we will note those parts which differ in size or material from those in the previous paper[3].

Two channels (I and II) were used, of length 28.5 cm and breadth 1.0 cm. The semipermeable membrane serving as the accumulation wall was a Millipore Type PLGC ultrafiltration membrane (Millipore, Bedford, MA, U.S.A.) with a nominal molecular weight cut-off of 10 000. It consists of a regenerated cellulose membrane on a polypropylene substrate. The two channels differed in their thicknesses, which are determined by the thickness of the spacer material that was clamped between the ultrafiltration membrane and the glass plate serving as the upper wall for the channel. Channel I had a poly(tetrafluoroethylene) (PTFE) spacer with a measured thickness of 0.032 cm. The resulting geometrical volume (void volume) of the channel was 0.87 ml. Channel II had a fluorinated ethylene propylene (FEP) spacer with a measured thickness of 0.012 cm, giving a geometrical volume of 0.35 ml. Calculation of the void time was based on the geometrical volume. The real void volume of a channel may be somewhat smaller than that calculated from the thickness of the spacer. This depends on the compression of that part of the membrane which is covered by the spacer. The values of the void time reported may therefore be somewhat overestimated.

Sample loops were 10 or 98 μl in volume. The carrier inlet flow was delivered by a Gynkotek constant-flow pump, Model 600/200, Version 600 (Gynkotek, Munich, F.R.G.). The eluate composition was monitored by a Spectromonitor III spectrophotometric detector (Laboratory Data Control, Riviera Beach, FL, U.S.A.) set at 280 nm for proteins and 260 nm for DNA (plasmids, plasmid fragments) and viruses.

Flow programming was performed by manually stepping the needle valve N2 or N3 (see ref. 3), which causes the ratio $\dot{V}_c/\dot{V}_{out}$ to change.

Human serum albumin fraction V, fatty acid-free, and cytochrome *c* from horse heart Type III were obtained from Sigma (St. Louis, MO, U.S.A.). Ferritin and thyroglobulin were from a gel filtration calibration kit (Pharmacia, Uppsala, Sweden). The plasmids were gifts from the Department of Pharmaceutical Microbiology, University of Uppsala (Uppsala, Sweden) and Pharmacia Biotechnology (Uppsala, Sweden). Purified samples of Satellite tobacco necrosis virus (STNV) and Semliki forest virus (SFV) were gifts from the Department of Molecular Biology, University of Uppsala.

The carrier was a Tris–HNO_3 buffer (pH 7.4), ionic strength 0.1, containing 0.02% sodium azide and 1 m*M* EDTA.

RESULTS AND DISCUSSION

The experimental procedures were as described in previous papers[3,7] for an asymmetrical flow FFF channel. The same symbols, describing the operating conditions, have been used here: z' = focusing point (distance from channel inlet end); $\dot{V}_c$ = cross-flow-rate during relaxation; $\dot{V}_c$ = cross-flow-rate during elution; $\dot{V}_{out}$ = flow-rate at channel outlet end; $\dot{V}_{in}$ = flow-rate at channel inlet end; t_0 = void time; t_R = retention time; $R = t_0/t_R$ = retention ratio.

Sample injection, channel thickness, retention time and zone broadening

Sample injections were made by the so-called "downstream central sample injection" method, presented in our previous paper[3]. Thus, the elution of a compound starts from the focusing point, z', at which the sample was loaded, relaxed and concentrated.

Experiments were performed in two channels, one having a nominal thickness of 0.032 cm, the other 0.012 cm.

The cross-flow-rate during elution determines the retention level of the sample. The higher the cross-flow-rate used, the higher will be the degree of retention, *i.e.*, the lower will be the retention ratio, *R*. The retention time is a complex function of both the retention ratio and the flow-rates, $\dot{V}_c$, $\dot{V}_{out}$ and $\dot{V}_{in}$ (ref. 7). At high retention degrees (low retention ratios) the retention time is constant for constant $\dot{V}_c/\dot{V}_{out}$ or $\dot{V}_{in}/\dot{V}_{out}$ (ref. 7).

The relative zone broadening in flow FFF, *e.g.*, expressed as the observed average plate height, $\bar{H}$, or the plate number, *N*, should decrease as the retention ratio decreases if the non-equilibrium processes are the dominating zone broadening effects[8]. Zone broadening is also strongly dependent on the channel thickness, *i.e.*, it decreases as the channel is made thinner[8], provided the retention ratio is constant. However, results published so far show that the observed plate height is much higher than expected, indicating that some "instrumental" zone broadening processes occur that have not been included in the zone broadening theory. Nevertheless, it should be worthwhile to decrease the channel thickness so as to produce more efficient separations.

In a normal, symmetrical flow FFF channel the resolution between two compounds will steadily increase when the cross-flow-rate is increased[8], *i.e.*, when

retention increases. The separation can then be optimized by keeping the ratio of the cross-flow-rate to the channel flow-rate constant, while increasing the values of both[8]. This approach keeps the retention time constant while increasing the resolution. For rapid separations, a flow-rate ratio is chosen that gives a suitable retention time.

In the asymmetrical flow FFF channel a similar situation exists: the retention time is a function of the ratio $\dot{V}_c/\dot{V}_{out}$ (ref. 7). When this ratio is kept constant the retention time remains constant. In the absence of a complete theory for the plate height and resolution in the asymmetrical channel, we optimized the separation speed and resolution empirically. A similar approach to that for a symmetrical channel was used, *i.e.*, the ratio $\dot{V}_c/\dot{V}_{out}$ was chosen to give the desired retention times, while the value of $\dot{V}_{in} = \dot{V}_c + \dot{V}_{out}$ was increased to improve resolution.

It should be pointed out that the present asymmetrical flow FFF channel creates a linearly decreasing longitudinal velocity gradient down the channel[7]. The local non-equilibrium plate height, H, will therefore decrease along the channel's longitudinal axis, and the resulting average (or observed) plate height, $\bar{H} = L\sigma_t^2/t_R^2$ (where σ_t is the standard deviation of the peak in time units) will be a complex function of the flow-rates $\dot{V}_c$ and $\dot{V}_{out}$. This effect will be dealt with in subsequent papers. The plate numbers presented below have been calculated from the observed average plate height, $\bar{H}$.

Proteins and aggregates

Figs. 1 and 2 show the separation of the monomer and the presumed dimer of the two proteins ferritin and thyroglobulin. These separations are of the same kind as already reported for albumin[3] and were performed in the thicker channel (0.032 cm). The flow-rates were adjusted to give an elution time of 7 min for both monomers. Under these conditions they are highly retained, corresponding to about 40 and 50

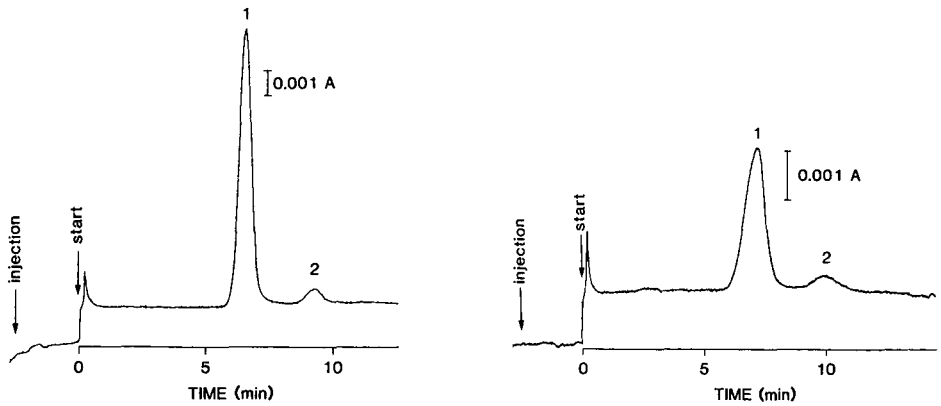

Fig. 1. Fractionation of ferritin (MW = 440 000) in channel I. Peaks: 1 = monomer; 2 = dimer. Sample: ferritin, 2 mg/ml, 10 µl. Relaxation/focusing; $\dot{V}_c$ = 4 ml/min. z' = 4.3 cm. Injection: flow-rate = 0,05 ml/min during 0.25 min and 0.02 ml/min during 1.75 min; loop volume = 10 µl. Elution; $\dot{V}_c$ = 4.7 ml/min, $\dot{V}_{out}$ = 2.4 ml/min, t_0 = 0.18 min.

Fig. 2. Fractionation of thyroglobulin (MW = 669 000) in channel I. Peaks: 1 = monomer; 2 = dimer. Sample: thyroglobulin, 2 mg/ml, 10 µl. Relaxation/focusing: $\dot{V}_c$ = 5 ml/min, z' = 4.2 cm. Injection, as in Fig. 1. Elution; $\dot{V}_c$ = 3.7 ml/min, $\dot{V}_{out}$ = 3.4 ml/min, t_0 = 0.15 min.

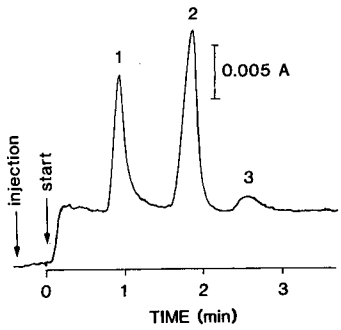

Fig. 3. Rapid separation of a protein mixture in channel II. Peaks: 1 = cytochrome *c*; 2 = albumin monomer; 3 = albumin dimer. Sample: cytochrome *c*, 10 mg/ml, 1 μl; human serum albumin, 1.25 mg/ml, 9 μl. Relaxation/focusing: $\dot{V}_c' = 5$ ml/min during 1 min, and 9.9 ml/min during 15 s, $z' = 5$ cm. Injection: flow-rate = 0.1 ml/min, loop volume = 10 μl, time = 1 min. Elution; $\dot{V}_c = 8.9$ ml/min, $\dot{V}_{out} = 0.8$ ml/min, $t_0 = 0.09$ min.

void times ($t_R/t_0 = 1/R$), respectively. The presumed dimers occur at about 50 and 70 void times, respectively. The high retention levels lead to the high resolution observed. The plate numbers for the monomer peaks are 840 and 340, respectively. When lower values for $\dot{V}_c/\dot{V}_{out}$ were used, elution times were shorter at the cost of lower resolution.

Fig. 3 shows the separation of two proteins and a presumed dimer in the thin (0.012 cm) channel. Here, the ratio $\dot{V}_c/\dot{V}_{out}$ was adjusted to give very rapid elution, and $\dot{V}_{in}$ was raised to an high value to improve resolution. The plate numbers are 172 and 455, respectively, for peaks 1 and 2, while the retention levels correspond to about 10, 20 and 28 void times. When the same sample was studied in the thicker channel with the same short elution times, the resolution was much lower. These results appear very promising for rapid protein separations.

The identity of the presumed dimer peaks was not confirmed by other techniques but is supported by several observations. The proteins used are known to show aggregate peaks in SEC. Further, the ratio of the dimer peak retention time to the monomer peak retention time is constant, 1.40, for all three proteins, albumin, ferritin and thyroglobulin. For well retained components the retention time in asymmetrical flow FFF is inversely dependent on the component's diffusion coefficient[7], D, which in turn depends on the component's molecular weight according to a simple power law[8], $D = A/M^b$ (A is a constant, M is the molecular weight). The exponent b is 0.33 for a spherical particle and increases as the particle becomes more elongated[8]. The ratio 1.40 then corresponds to a value of $b = 0.49$ which does not seem unreasonable for a protein dimer.

One obvious application for flow FFF would be the detection of higher aggregates of proteins. Isocratic experiments like those represented by Figs. 1–3 would then result in very long retention times and considerable dilution of aggregates, making detection difficult. In such cases, the use of flow programming[8] to decrease the ratio $\dot{V}_c/\dot{V}_{out}$ would speed up the elution of the aggregates. Fig. 4 demonstrates such an experiment in the thicker channel. The ratio $\dot{V}_c/\dot{V}_{out}$ was initially set very high to retain the low-molecular-weight end of the sample spectrum sufficiently long for the first peak to become relatively narrow. The ratio $\dot{V}_c/\dot{V}_{out}$ was then decreased rapidly to a low value so that the presumed dimer and trimer were eluted relatively rapidly. In

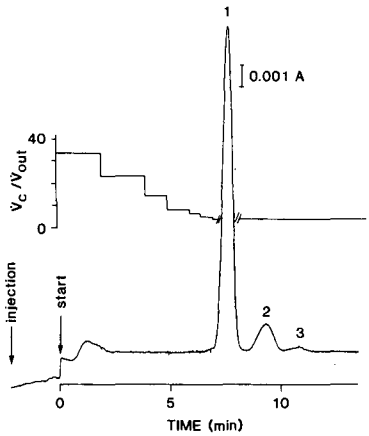

Fig. 4. Stepwise gradient elution of human serum albumin (HSA, MW = 67 000) in channel I. Peaks: 1 = monomer; 2 = dimer; 3 = trimer. Sample: HSA, 3 mg/ml, 10 μl. Relaxation/focusing; $\dot{V}_c$ = 5 ml/min, z' = 4.2 cm. Injection as in Fig. 1. Elution; $\dot{V}_c + \dot{V}_{out}$ = 7 ml/min, decreasing $\dot{V}_c/\dot{V}_{out}$ in six steps.

isocratic experiments the trimer was undetected due to the dilution. The fractogram in Fig. 4 should be compared with the isocratic experiment in Fig. 3 in our previous work[3]. By proper adjustment of the ratio $\dot{V}_c/\dot{V}_{out}$ it should be possible to detect much larger aggregates.

Plasmids

Fig. 5 illustrates a model separation of two plasmids, differing in the number of base pairs by a factor of 1.8. The separation time is short and the resolution is more than adequate for many applications. The fractogram was obtained by using the thin channel: the plate numbers for both peaks are about 450. When the same separation was carried out in the thicker channel the resolution was incomplete (see also similar experiments in ref. 3). Optimization of the flow-rates with the thin channel resulted in much improved resolution and decreased separation time.

The small interfering responses close to peak 2 in Fig. 5 appear to be due to an heterogeneous composition of the plasmid pGL101 (peak 1). When this plasmid was

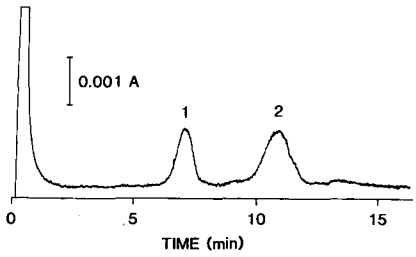

Fig. 5. Separation of the plasmids pGL101 (2390 base pairs) and pBR322 (4320 base pairs) in channel II. Peaks: 1 = pGL101, 0.1 μg/μl, 1 μl; 2 = pBR322, 0.1 μg/μl, 1 μl. Relaxation/focusing: $\dot{V}_c$ = 2 ml/min, z' = 4.2 cm, time = 3 min. Injection: flow-rate = 0.1 ml/min, loop volume = 98 μl, time = 2 min. Elution: $\dot{V}_c$ = 1.9 ml/min, $\dot{V}_{out}$ = 0.6 ml/min, t_0 = 0.24 min.

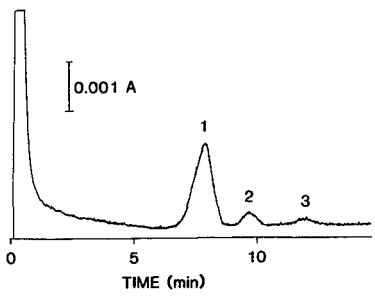

Fig. 6. Fractionation of the plasmid pGL101 (2390 base pairs) in channel II. Peaks: 1 = plasmid; 2 and 3 = possibly aggregates or conformational variants of the plasmid. Sample: pGL101, 0.1 μg/μl, 5 μl. Relaxation/focusing: $\dot{V}_c$ = 2 ml/min, z' = 4.3 cm, time = 2 min. Injection: flow-rate = 0.05 ml/min, loop volume = 10 μl, time = 1 min. Elution: $\dot{V}_c$ = 1.6 ml/min, $\dot{V}_{out}$ = 0.42 ml/min, t_0 = 0.32 min.

fractionated separately (see Fig. 6) two extra responses occurred. They may be due to aggregates or conformation variants of the plasmid pGL101 sample.

In the course of this study, we noted changes in the retention characteristics with sample load. These effects increased with the size of the plasmid, and were more pronounced in the thinner channel. The result of these effects was a tendency for peak fronting, and elution of a portion of the sample close to the void time. The effect is demonstrated by the differences between the two fractograms in Figs. 5 and 6. A possible explanation is that the highly concentrated sample zone formed during sample focusing creates an intermolecular repulsion which prevents the entire sample from relaxing to the correct equilibrium level above the accumulation wall. Thus, part of the sample would be relaxed too far away from the wall, resulting in early elution. The maximum sample size may be increased by allowing the sample to focus over a larger area of the ultrafiltration membrane.

Plasmid fragments

Separation of the fragments, obtained from plasmids after treatment with restriction enzymes, can be carried out rapidly with asymmetrical flow FFF[3]. Those cases where relatively few fragments occur seem best suited for the technique. In our previous study[3] with a thick channel (0.03 cm), the separation of two fragments, one relatively small, the other big, was easily achieved. However the separation time was rather long (about 40 min) and the late-eluted big fragment gave a very broad band.

Stepwise flow programming can be used to speed up the elution of the large fragments in such work. This is demonstrated in Fig. 7, where the small fragment is eluted isocratically at a relatively high retention level, corresponding to about 22 void times. This contributes to an improved resolution for the small fragment. Then, the cross-flow-rate is reduced to zero in one step, resulting in immediate elution of the big fragment. The total separation time was 30 min, compared to 60 min in the previous work[3]. The sample applied was 16 μg.

Fig. 8 shows a rapid high-resolution separation of three "small" plasmid fragments (200, 700 and 1200 base pairs), performed in the thinner channel. The plate numbers for the three peaks are, respectively, 330, 580 and 1350, and the retention degree corresponds to *ca.* 13, 27 and 59 void times, respectively. All three fragments were eluted in about 0.5 ml of carrier. The thin channel has the advantage of giving

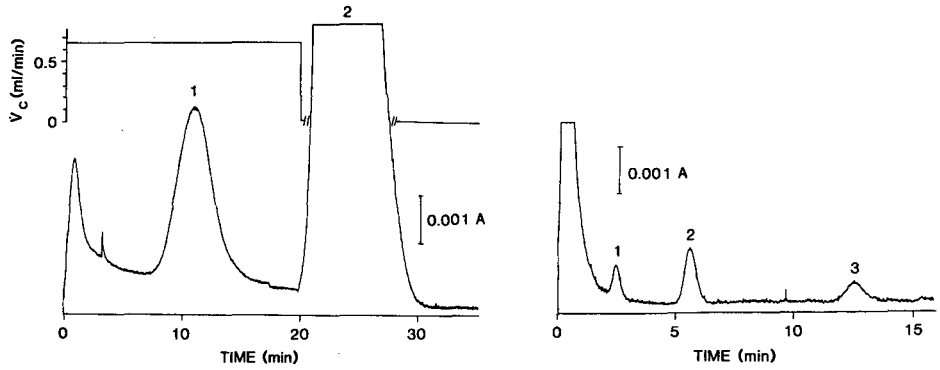

Fig. 7. Micropreparative separation of plasmid fragments with flow programming in channel I. Peaks: 1 = 700 base pairs (bp); 2 = 4600 bp. Sample: fragments from the plasmid pTL830 cleaved with PstI and BglII, 0.4 μg/μl, 40 μl. Relaxation/focusing, $\dot{V}_c$ = 4 ml/min, z' = 4.7 cm, time = 8 min. Injection: flow-rate = 0.05 ml/min, loop volume = 10 μl, four loop volume were injected during 7 min. Elution: time = 0–20 min, $\dot{V}_c$ = 0.66 ml/min, $\dot{V}_{out}$ = 1.2 ml/min, t_0 = 0.49 min; time > 20 min, $\dot{V}_c$ = 0 ml/min, $\dot{V}_{out}$ = 1.2 ml/min.

Fig. 8. Separation of three plasmid fragments in channel II. Peaks: 1 = 200 bp, 0.01 μg; 2 = 700 bp, 0.05 μg; 3 = 1200 bp, 0.04 μg. The fragments were obtained from three different digests of the plasmid pTL830, each giving one big and one small fragment. The small fragments had previously been isolated in channel I. Sample volume = 700 μl. Relaxation/focusing: $\dot{V}_c$ = 4 ml/min, z' = 4.7 cm, time = 7.5 min. Injection: flow-rate = 0.2 ml/min, loop volume = 98 μl, seven loop volumes were injected during 6.5 min. Elution: $\dot{V}_c$ = 2.8 ml/min, $\dot{V}_{out}$ = 0.5 ml/min, t_0 = 0.22 min.

greater separation speed, resolution and smaller peak elution volumes. A disadvantage is the concentration effect noted for large fragments, similar to the large plasmids discussed above. This effect limits the sample sizes in preparative separations.

Viruses

The retention, separation and characterization of virus particles by flow FFF has already been studied[9]. However, the conditions used led to very long elution times, often several hours. In line with on-going efforts to develop rapid flow FFF separations[3,8], we now demonstrate such separations for viruses. Two viruses were studied, with molecular weights of *ca.* $1.8 \cdot 10^6$ and $50 \cdot 10^6$. Results are shown in Figs. 9 and 10. The cross-flow-rate in each case was chosen to give high retention levels (18 and 22 void times, respectively) which increases the resolution; the ratio $\dot{V}_c/\dot{V}_{out}$ was adjusted to give short elution times. The smaller virus (Fig. 9) was given an elution time of only 2.5 min while the larger virus was eluted at 5 min (Fig. 10). It should be pointed out that by proper change of the ratio $\dot{V}_c/\dot{V}_{out}$ any elution time can be chosen for a given component.

The virus peaks appear well shaped, but the smaller virus in Fig. 9 has a tendency to give a skewed peak, which may be caused by an heterogeneous composition of the sample (perhaps due to some aggregation). The peak from the larger virus shows a slight tail which may be caused by instrumental factors. The peak efficiency, as expressed by the plate number, N, is 242 and 590, respectively.

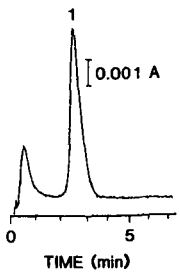

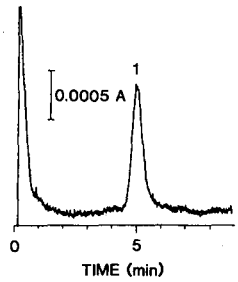

Fig. 9. Isolation of Satellite tobacco necrosis virus (MW = $1.8 \cdot 10^6$) in channel II. Peaks: 1 = virus, 3 μg/μl, 2 μl. Relaxation/focusing: $\dot{V}_c$ = 3 ml/min, z' = 4.3 cm, time = 2 min. Injection: flow-rate = 0.05 ml/min, loop volume = 10 μl, time = 1 min. Elution; $\dot{V}_c$ = 4.35 ml/min, $\dot{V}_{out}$ = 0.67 ml/min, t_0 = 0.15 min.

Fig. 10. Isolation of Semliki forest virus (MW = $50 \cdot 10^6$) in channel II. Peaks: 1 = virus, 0.1 μg/μl, 5 μl. Relaxation/focussing: $\dot{V}_c$ = 2 ml/min, z' = 3.8 cm, time = 2 min. Injection: flow-rate = 0.1 ml/min, loop volume = 10 μl, time = 0.5 min. Elution: $\dot{V}_c$ = 1.65 ml/min, $\dot{V}_{out}$ = 0.74 ml/min, t_0 = 0.23 min.

ACKNOWLEDGEMENTS

Drs. L. Liljas and T. Unge (Department of Molecular Biology, University of Uppsala, Uppsala, Sweden) generously gave the samples of SFV and STNV, respectively. We are grateful for discussions with Professor B. Strandberg of the same Department. Dr. G. Swedberg (Department of Pharmaceutical Microbiology, University of Uppsala) generously supplied samples of plasmids and cleaved plasmids. Pharmacia Biotechnology generously gave plasmids, protein samples and instrument parts. This work was financially supported by the Swedish Natural Science Research Council.

REFERENCES

1 J. C. Giddings, *Sep. Sci.*, 1 (1966) 123.
2 J. C. Giddings, *Sep. Sci. Technol.*, 19 (1984–85) 831.
3 K.-G. Wahlund and A. Litzén, *J. Chromatogr.*, 461 (1989) 73.
4 J. C. Giddings, in J. C. Giddings, E. Grushka, *Adv. Chromatogr. (N.Y.)*, 20 (1982) 217.
5 J. Å. Jönsson and A. Carlshaf, *Anal. Chem.*, 61 (1988) 11.
6 A. Carlshaf and J. Å. Jönsson, *J. Chromatogr.*, 461 (1989) 89.
7 K.-G. Wahlund and J. C. Giddings, *Anal. Chem.*, 59 (1987) 1332.
8 K.-G. Wahlund, H. S. Winegarner, K. D. Caldwell and J. C. Giddings, *Anal. Chem.*, 58 (1986) 573.
9 J. C. Giddings, F. J. Yang and M. N. Myers, *J. Virol.*, 21 (1977) 131.

Journal of Chromatography, 476 (1989) 423–438
Elsevier Science Publishers B.V., Amsterdam — Printed in The Netherlands

CHROMSYMP. 1587

ESTER AND RELATED DERIVATIVES OF RING N-PENTAFLUOROBENZYLATED 5-HYDROXYMETHYLURACIL

HYDROLYTIC STABILITY, MASS SPECTRAL PROPERTIES, AND TRACE DETECTION BY GAS CHROMATOGRAPHY–ELECTRON-CAPTURE DETECTION, GAS CHROMATOGRAPHY–ELECTRON-CAPTURE NEGATIVE ION MASS SPECTROMETRY, AND MOVING-BELT LIQUID CHROMATOGRAPHY–ELECTRON-CAPTURE NEGATIVE ION MASS SPECTROMETRY

GERHARD M. KRESBACH, MOHAMED ITANI, MANASI SAHA and EUGENE J. ROGERS[a]
Barnett Institute of Chemical Analysis and Materials Science, Northeastern University, Boston, MA 02115 (U.S.A.)
PAUL VOUROS
Department of Chemistry, Northeastern University, Boston, MA 02115 (U.S.A.)
and
ROGER W. GIESE*
Department of Medicinal Chemistry, Northeastern University, Boston, MA 02115 (U.S.A.)

SUMMARY

One consequence of radiation damage to DNA is the conversion of thymine to 5-hydroxymethyluracil (HMU). In order to sensitively detect this DNA adduct by gas chromatography (GC) or high-performance liquid chromatography (HPLC) with electron-capture detection techniques, it is necessary to derivatize it. This study was designed to select an optimum ester derivative of the aliphatic hydroxyl group on HMU. N^1,N^3-Bis(pentafluorobenzyl)-HMU was formed as a parent derivative, and from this a series of esters. Also O-pentafluorobenzyl and O-tetrafluorobenzyl ether derivatives were prepared. Of the esters the pivalyl derivative was the best choice because it formed easily, was relatively stable to aqueous hydrolysis ($t_{1/2}$ = 9.8 days at pH 11.5, 24°C) and gave a response at fmol levels by GC and LC comparable to that of the ethers. Unanticipated was a good response as well for the parent derivative, a free hydroxyl compound, by GC and LC at this level. The work also demonstrates a high performance by LC–electron-capture negative ion mass spectrometry with a belt interface for the trace detection of derivatives of this type.

INTRODUCTION

We are developing mass spectrometric (MS) techniques for the determination of chemically and otherwise induced damage to human DNA, commonly called "DNA

[a] Present address: University of Lowell, Lowell, MA, U.S.A.

0021-9673/89/$03.50

adducts". Such trace level determinations are intended to help define the risks associated with human exposure to chemicals and radiation.

Some of these DNA adducts, especially those with alkyl and related modifications, can be obtained as free bases by acid hydrolysis[1] or oxidation[2] of DNA nucleosides. We have shown that it is attractive to derivatize alkyl nucleobases on their acidic ring NH sites with pentafluorobenzyl bromide (PFBBr) prior to the determination of such adducts by gas chromatography–electron-capture negative ion mass spectrometry (GC–ECNI-MS)[3], GC with electron-capture detection (GC–ECD)[4], or high-performance liquid chromatography (HPLC) with electron-capture negative ion mass spectrometry (LC–ECNI-MS) via a moving-belt interface[5].

In some cases a hydroxyalkyl group is present in a modified nucleobase, *e.g.* 5-hydroxymethyluracil (HMU), a consequence of damage to DNA by ionizing radiation. One strategy that we have employed to derivatize this hydroxy group is to conduct an alkylation reaction with PFBBr under phase transfer conditions[6]. While to date this latter reaction has been useful, we wanted to explore whether ester derivatives offer advantages in terms of reaction yield, ease of subsequent post-derivatization clean-up, or improved MS properties. In this paper we report the first stage of this work, in which several ester derivatives are evaluated.

MATERIALS AND METHODS

Reagents

5-Hydroxymethyluracil (Sigma grade) and Tris (Trizma, reagent grade) were purchased from Sigma (St. Louis, MO, U.S.A.). 2,3,5,6-Tetrafluorobenzyl bromide was from Lancaster Synthesis (Windham, NH, U.S.A.). α-Phenylcyclopentaneacetic acid, α-phenylcyclohexaneacetic acid, 4-dimethylaminopyridine (DMAP), acetic anhydride, benzoic anhydride, pivalic anhydride, butyric anhydride, thionyl chloride, pentafluorobenzyl bromide, tetrabutylammonium hydrogensulfate, and light petroleum (b.p. 35–60°C) (A.C.S. reagent) were from Aldrich (Milwaukee, WI, U.S.A.). Potassium carbonate, sodium bicarbonate, sodium sulfate, hydrochloric acid, and benzene were of Baker analytical reagent grade from J. T. Baker (Phillipsburg, NJ, U.S.A.). 1,1,1-Trichloro-3,3,3-trifluoroacetone was from Crescent (Hauppauge, NY, U.S.A.). Potassium di-hydrogenphosphate (HPLC grade), sodium borate (HPLC grade), and solvents (Burdick and Jackson) were from Fisher Scientific (Fair Lawn, NJ, U.S.A.). Cinnamic anhydride was obtained as described[6].

Chromatography

Thin-layer chromatography (TLC) with silica gel GF was performed on Uniplates (Analtech, Newark, DE, U.S.A.) containing fluorescent indicator: 250-μm plates were used for monitoring reactions, and 1000-μm plates were used for preparative TLC. Flash chromatography, in which a moderate air pressure (*e.g.*, 10–20 p.s.i.) was used to establish a flow-rate of 1–2 ml/min, was performed with silica gel 60, 230–400 mesh (E. Merck, Darmstadt, F.R.G.) in a column 15 × 2.5 cm I.D. For off-line HPLC an Econosil C_8 silica reversed-phase column, 250 × 4.6 mm, 10-μm particle size (Alltech, Deerfield, IL, U.S.A.) was used. The mobile phase was acetonitrile–water, 80:20 (v/v) at 1 ml/min. Typically 20-μl injections were made containing 100 ng of compound. Detection of the derivative was performed at the

absorption maximum (264 nm) using a Spectromonitor III variable-wavelength detector (LDC-Milton Roy, Riviera Beach, FL, U.S.A.), and integration was done using an SP 4270 integrator (Spectra-Physics, San Jose, CA, U.S.A.). For the on-line HPLC–MS experiments, a Supelcosil LC-18 DB column, 150 × 4.6 mm, 3-μm particles (Supelco, Bellefonte, PA, U.S.A.) was used with 1.2 ml/min acetonitrile–water (70:30, v/v) as eluent.

GC–ECD experiments were performed on a Varian Model 3700 gas chromatograph (Varian, Palo Alto, CA, U.S.A.), equipped with a Varian on-column capillary injector (Model 03-908719-00) and a ^{63}Ni electron-capture detector. The GC was interfaced to an SP 4270 integrator with a memory module. GC conditions were: column, 25 m × 0.32 mm I.D. HP Ultra 2, coated with 5% phenylmethylsilicone, 0.17 μm film thickness (Hewlett-Packard, Avondale, PA, U.S.A.), 1.3 ml He/min (determined at 250°C), and a temperature gradient from 50 to 320°C with 25°C/min (oven and on-column injector). N_2 at a flow-rate of 29 ml/min was used as make-up gas for the electron-capture detector.

Mass spectrometry

Electron impact, positive chemical ionization, and electron-capture negative ion mass spectra were obtained by using a Finnigan 4021B quadrupole mass spectrometer with pulsed positive ion negative ion chemical ionization option, coupled to an HP 5890 gas chromatograph (Hewlett Packard, Waldbronn, F.R.G.). Data were acquired with an INCOS data system (Finnigan, San Jose, CA, U.S.A.).

GC conditions were: column, 10 m and 25 m × 0.32 mm I.D. HP Ultra 2, coated with 5% phenylmethylsilicone, 0.17 μm film thickness (Hewlett Packard), 15 p.s.i. head pressure, and a temperature gradient from 50 to 320° with 25°C/min, then 20 min isothermal. For the LC–MS experiments, a Finnigan moving-belt interface with Kapton (R) belts was used. Belt speed was adjusted to 2 cm/s. The HPLC eluent was deposited without split onto the belt, by using a direct electrically heated spray device[7].

Standard MS conditions were: ionizing energy 70 eV, filament current 0.5 mA, and source temperature 220°C. Methane chemical ionization (CI) gas pressure was maintained at an indicated range of between 0.22 and 0.25 Torr. Scan range was usually from 50 to 750 a.m.u. in 1 s unless indicated otherwise.

Glassware used for the trace GC–MS, GC–ECD and LC–MS detection steps was acid washed and gas phase silanized[4].

Synthesis

α-Phenylcyclohexaneacetyl chloride. α-Phenylcyclohexaneacetic acid (0.50 g, 2.4 mmol) was combined with 2 ml (24 mmol) of thionyl chloride and 15 ml of benzene. The resulting solution was refluxed with stirring under nitrogen for 2 h. The reaction mixture was evaporated four times with intermediate additions of benzene to fully remove the thionyl chloride. The resultant oily product was diluted with 10 ml of toluene and used as described below without further purification.

α-Phenylcyclohexaneacetic anhydride. Following a general procedure for synthesizing anhydrides[8], to 0.16 ml (1.2 mmol) of trichlorotrifluoroacetone in a 100-ml round bottom flask were added 0.022 ml (1.2 mmol) of water in a nitrogen atmosphere at room temperature. After 15 min, first 5 ml of toluene, then the above mentioned solution of acid chloride in toluene were added dropwise, followed by 0.1 ml of

TABLE I

^{1}H-NMR AND SELECTED IR DATA OF COMPOUNDS **1–10**

s = Singlet; d = doublet; t = triplet; m = multiplet; ch = cyclohexyl; cp = cyclopentyl; ph = phenyl.

Compound	*^{1}H-NMR chemical shift (ppm)*	*IR frequency (cm^{-1})*
1	7.36 (C^6-*H*, 1H, s), 5.23 (N^3-CH_2, 2H, s), 5.03 (N^1-CH_2, 2H, s), 4.40 (CH_2-OH, 2H, broad s)[a]	3000–3400[c]
2	7.50 (C^6-*H*, 1H, s), 5.12 (N^3-CH_2, 2H, s), 5.00 (N^1-CH_2, 2H, s), 4.83 (CH_2-OCO, 2H, s), 2.07 ($COCH_3$, 3H, s)[a]	1230[d]
3	7.47 (C^6-*H*, 1H, s), 5.18 (N^3-CH_2, 2H, s), 4.97 (N^1-CH_2, 2H, s), 4.83 (CH_2-OCO, 2H, s), 2.27 (OCO-CH_2-CH_2-CH_3, 2H, t), 1.95 (OCO-CH_2-CH_2-CH_3, 2H, m), 0.90 (OCO-CH_2-CH_3, 3H, t)[a]	1175[d]
4	7.42 (C^6-*H*, 1H, s), 5.17 (N^3-CH_2, 2H, s), 5.01 (N^1-CH_2, 2H, s), 4.83 (CH_2-OCO, 2H, s), 1.17 [$C(CH_3)_3$, 9H, s][a]	1140[d]
5	8.01 (CO-ph *ortho*, 2H, d), 7.68 (C^6-*H*, 1H, s), 7.63–7.40 (CO-ph *meta* and *para*, 3H, m), 5.23 (N^3-CH_2, 2H, s), 5.16 (N^1-CH_2, 2H, s), 5.04 (CH_2-OCO, 2H, s)[b]	1170[d]
6	7.82 (CH=CH-ph *ortho*, 2H, d), 7.63–7.13 (CH=CH-ph *meta*, *para* and C^6-*H*, 4H, m), 6.53 (CH=C*H*-ph, 1H, s), 6.27 (C*H*=CH-ph, 1H, s), 5.17 (N^3-CH_2, 2H, s), 5.10 (N^1-CH_2, 2H, s), 5.00 (CH_2-OCO, s)[a]	1170[d]
7	7.34 (C^6-*H*, 1H, s), 7.17 (CH_2-C_6F_4H, 1H, m), 5.22 (N^3-CH_2, 2H, s), 4.98 (N^1-CH_2, 2H, s), 4.67 (O-CH_2-C_6F_4H, 2H, s), 4.30 (CH_2-O, 2H, s)[a]	1120[e]
8	7.38 (C^6-*H*, 1H, s), 5.25 (N^3-CH_2, 2H, s), 5.02 (N^1-CH_2, 2H, s), 4.71 (O-CH_2-ph, 2H, s), 4.35 (CH_2-O, 2H, s)[b]	1125[e]
9	7.26 [C^6-*H* and CO-CH-(cp)ph 6H, m], 5.17 (N^3-CH_2, 2H, s), 4.84 (N^1-CH_2, 2H, s), 3.26 [CO-C*H*-(cp)ph, 1H, d], 2.6–0.8 (cp, 11H, m)	—[f]
10	7.39 (C^6-*H*, 1H, s), 7.20 [CO-CH-(ch)ph, 5H, s], 5.15 (N^3-CH_2, 2H, s), 4.86 (N^1-CH_2 and O-CH_2, 4H, s), 3.28 [CO-C*H*-(ch)ph, 1H, d], 2.2–0.3 (ch, 11H, m)[a]	—[f]

[a] 60 MH_2 spectrum.
[b] 300 MH_2 spectrum.
[c] O-H-O hydrogen bonding.
[d] C-O stretching vibration of the ester.
[e] C-O stretching vibration of the ether bridge in position 5.
[f] Broad and weak signals.

pyridine. After stirring for 8 h at room temperature, 10 ml of ethyl acetate were added followed by an extraction with 10% hydrochloric acid, saturated sodium hydrogencarbonate, and saturated sodium chloride. The separated organic layer was filtered and dried over anhydrous sodium sulfate. Evaporation gave a white solid which was recrystallized from hexane to yield white crystals (67%). IR: 1820 and 1750 cm^{-1}.

α-Phenylcyclopentaneacetic anhydride. This compound was prepared in the same way as the preceding anhydride.

5-[(α-Phenylcyclohexane)acetoxymethyl]-N^1,N^3-bis(pentafluorobenzyl)uracil. To a stirred solution of 60 mg (0.12 mmol) of N^1,N^3-bis(pentafluorobenzyl)-5-hydroxymethyluracil in 0.1 ml of pyridine under nitrogen were added 15 mg of dimethylaminopyridine and 2 ml of dry (distilled and stored over molecular sieves) acetonitrile. After 10 min, 0.145 g (0.36 mmol) of α-phenylcyclohexaneacetic anhydride were added, and refluxing was done for 8 h (no starting material was detected at this point by silica TLC). Ethyl acetate (15 ml) was added and the solution was washed with 5% hydrochloric acid and saturated sodium hydrogencarbonate, then dried over anhydrous sodium sulfate. Evaporation gave an oil that was purified by flash chromatography (70% yield) using methylene chloride–ethyl acetate (1:1, v/v) and gave a single peak by HPLC.

Other esters. The corresponding product derived from α-phenylcyclopentaneacetic anhydride was prepared in the same way. The other esters were similarly prepared and characterized except that the acylation reaction was performed at room temperature and was complete after 6–12 h, depending on the anhydride. ^1H NMR and selected IR data are shown in Table I.

5-Hydroxymethyl-N^1,N^3-bis(pentafluorobenzyl)uracil. To a stirred suspension at room temperature of 485 mg (3.50 mmol) of potassium carbonate in acetone (10 ml) were added 100 mg (0.70 mmol) of 5-hydroxymethyluracil. Ten min later 485 mg (3.51 mmol) of PFBBr in 5 ml of acetone were added, followed by continued stirring for 24 h. Silica TLC using light petroleum–ethyl acetate (1:1, v/v) showed the product at R_F = 0.43. The potassium carbonate was removed by filtration and washed with acetone. The acetone solution was evaporated to a small volume and purified by flash chromatography using light petroleum–ethyl acetate (1:1, v/v) and 20-ml fractions were collected. Fractions 19–24 upon evaporation gave a clear colorless oil that turned white when light petroleum (10 ml) was added. After storage overnight at 4°C, the precipitate was collected on a filter, washed with light petroleum, and dried by suction and then in a vacuum desiccator over anhydrous calcium chloride giving 247 mg (70%) of white crystal (m.p. = 146–147°C).

5-Pentafluorobenzyloxymethyl-N^1,N^3-bis(pentafluorobenzyl)uracil. To a stirred solution of 170 mg (0.57 mmol) of tetrabutylammonium hydrogensulfate in 5 ml of 1 *M* potassium hydroxide were added 50 mg (0.10 mmol) of the above compound in a 50-ml round bottom flask. After stirring at room temperature for 20 min, PFBBr (0.15 ml, 1.1 mmol) in 3 ml of methylene chloride was added, and vigorous stirring was continued for 3 h. Silica TLC of the methylene chloride layer by using ethyl acetate–light petroleum (1:4, v/v) showed the product at R_F = 0.65. The separated aqueous layer was extracted with 2 × 10 ml of methylene chloride, and the combined organic fractions were washed with water, dried (sodium sulfate), filtered and concentrated to a yellow oil by rotary evaporation. Purification by preparative TLC on silica (half of the yield on each of two plates), by using ethyl acetate–light petroleum

(1:4, v/v), and extracting the product from the scraped silica in hot ethyl acetate gave a light yellow oil after rotary evaporation. Light petroleum was used to obtain, after vacuum drying, 42 mg (60%) of white crystals, m.p. 100–102°C.

5-(2,3,5,6-Tetrafluorobenzyloxymethyl)-N^1,N^3-bis(pentafluorobenzyl)uracil. The procedure for the preparation of the above product was used, except the product was purified by flash column chromatography using ethyl acetate–light petroleum (1:4, v/v) yielding 154 mg (56%) of white crystals, m.p. 109–111°C.

Hydrolysis

The compound was dissolved in the HPLC mobile phase and diluted with a 0.25 volume of buffer at time zero. (This buffer was 0.01 *M* borate pH 10; 0.381 g of $Na_2B_4O_7 \cdot 10H_2O$ were dissolved in 100 ml of water, and the pH was adjusted to 10.0 with 1.5 *M* KOH.) The initial apparent pH was 11.6, and the final pH ranged from 11.4 to 11.5 at the end of the experiment. The solutions were stored together at room temperature (24°C), and aliquots were analyzed by HPLC as a function of time up to two or more half-lives. A plot of $\ln(A_t/A_0 \times 100)$ *vs.* time was linear for each compound and used to calculate the half-life for ester hydrolysis, where A_0 = initial peak area for the ester, and A_t = area at the corresponding reaction time.

RESULTS AND DISCUSSION

A modified nucleobase containing a hydroxyalkyl group can potentially be derivatized by alkylation of its acidic ring NH site(s) with pentafluorobenzyl bromide (PFBBr), followed by acylation of its hydroxyalkyl site(s) with an esterifying reagent such as acetyl chloride. In principle this approach is attractive because these types of reactions can proceed under mild conditions in good yields. Adequate sensitivity for ECNI-MS detection should be provided by the first step, which replaces each acidic hydrogen with a PFB group. Nevertheless, one concern is the susceptibility of an ester to aqueous hydrolysis, which could limit the usefulness of such a derivative for trace analysis. Accordingly, we evaluated a series of ester derivatives in terms of their relative ease of preparation, hydrolytic stability, and GC–MS as well as LC–MS properties.

For these studies we chose to esterify N^1,N^3-bis(pentafluorobenzyl)-5-hydroxymethyluracil (**1**, Fig. 1). The ester derivatives that we formed from this parent compound were compared relative to each other, and, as, appropriate, to the parent compound and its O-PFB and O-tetrafluorobenzyl (O-TFB) derivatives.

Synthesis

Based on TLC, each of the acylation reactions gave an essentially complete conversion of **1** to its corresponding ester. Consistent with this the preparative yields of the esters, working on a mg scale, were all above 65% with no effort to optimize this micropreparative yield. In this respect, these ester derivatives are more attractive than the ether derivative **8** since TLC shows some minor side products when **1** is converted to **8** by phase transfer alkylation. Within the acyl series of derivatives, products **2–6** could be formed at room temperature, whereas the formation of **9** and **10**, no doubt due to steric effects, required refluxing. Thus, derivatives **2–6** are most attractive from a synthetic standpoint, aside from parent compound **1**, which of course avoids the acylation reaction.

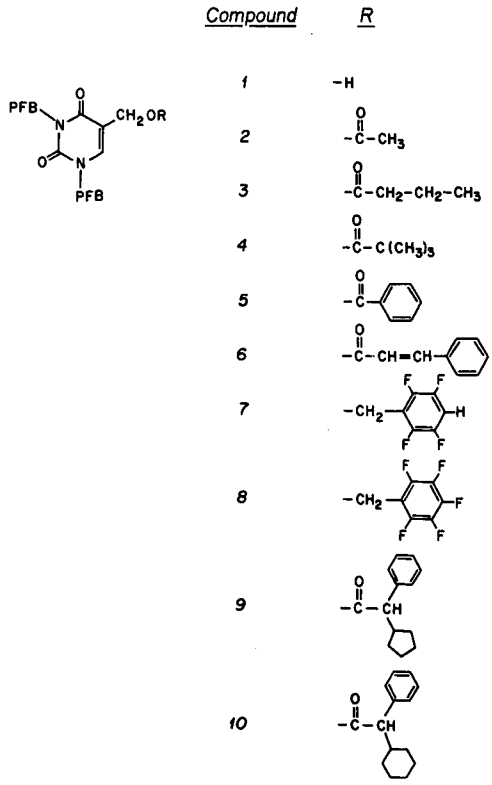

Fig. 1. Electrophoric derivatives of 5-hydroxymethyluracil (HMU).

Hydrolytic stability

The relative hydrolytic stabilities of the ester derivatives of **1** are shown in Table II. These data were obtained by dissolving each ester in 80% acetonitrile, and then diluting this solution at time zero with a 0.25 volume of 0.01 *M* borate, pH 10, giving an apparent pH of 11.6. The hydrolysis of each ester was then followed by HPLC. As seen in this table, the hydrolysis half-lives range from 1.4 to 11.6 days. Apparently the relative hydrolytic stabilities of the esters are largely determined by the steric properties of the acyl moiety. The most stable esters, **4**, **9**, and **10**, are those with the bulkiest side chains. Overall the best derivative up to this point, also taking into account the prior synthetic results, is the pivalyl derivative **4** since it forms easily and yet has a high hydrolytic stability ($t_{\frac{1}{2}}$ = 9.8 days under the conditions used).

An artifact was encountered early in our hydrolysis studies of the ester derivatives. When pivalyl ester **4**, the first compound that we studied, was dissolved in methanol–0.01 *M* phosphate, pH 7.8 (80:20, v/v), and subjected to reversed-phase silica HPLC, a second, earlier eluted peak formed slowly. It became equal in area to that of **4** after 12 d. This earlier eluted peak was not the anticipated hydrolysis product **1**. If **4** was dissolved instead in a corresponding buffer containing acetonitrile instead of methanol, this unknown product did not appear. The peak was collected and found by ECNI-MS to give an intense ion at *m/z* 451. Assuming that this corresponds to

TABLE II

HPLC AND HYDROLYSIS PROPERTIES OF ESTER DERIVATIVES OF RING-PENTAFLUOROBENZYLATED 5-HYDROXYMETHYLURACIL

Apparent pH of hydrolysis solution was 11.6. See Materials and Methods for details.

Compound	*Substituent*	*Retention time (min) reversed-phase HPLC*	*Half-life (days) for hydrolysis*
1	H	2.9	–
2	Acetyl	3.2	1.4
3	Butyl	3.6	4.5
4	Pivalyl	4.0	9.8
5	Benzoyl	3.7	6.8
6	Cinnamoyl	3.9	5.8
7	Tetrafluorobenzyl		–
8	Pentafluorobenzyl		–
9	Phenyl-cyclopentaneacetyl	5.5	10.2
10	Phenyl-cyclohexaneacetyl	6.5	11.6

$[M-181]^-$ (see below), and taking into account the formation of the compound in aqueous methanol but not in aqueous acetonitrile, we concluded that it is a dimethylketal derivative of **4**, either at C2 or C4. The structure of the second option is as follows:

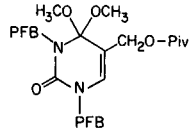

Mass spectrometry

The following issues were considered to be important in our evaluation of the utility of the derivatives **1–10** for trace analysis by GC–MS and LC–MS: (1) The presence of intense, structurally characteristic ions in the ECNI spectra for high sensitivity and reliable identification; (2) the influence of the side chain on the abundance of diagnostic ion(s); (3) the influence of the side chain on the GC and LC behavior; and (4) the amount of structural information which could be obtained from electron impact and positive chemical ionization mass spectra as a function of the moiety in position 5.

ECNI spectra. Fig. 2 shows the reconstructed ion chromatogram of 100 pmol each of compounds **1** and **3–10**, separated by GC and detected by ECNI-MS. Since compound **2** is not separated from **1**, the spectral data of the latter compound were obtained in a separate experiment. Symmetrical peaks are observed for all of the compounds, even for **1** containing a free hydroxyl group. The relative responses will be discussed later.

The ECNI mass spectra obtained from the peaks in Fig. 2 are summarized in Table III. Notable are the extremely low relative intensities of the molecular ion peaks. Consistent with previous observations made with other PFB derivatives of even less

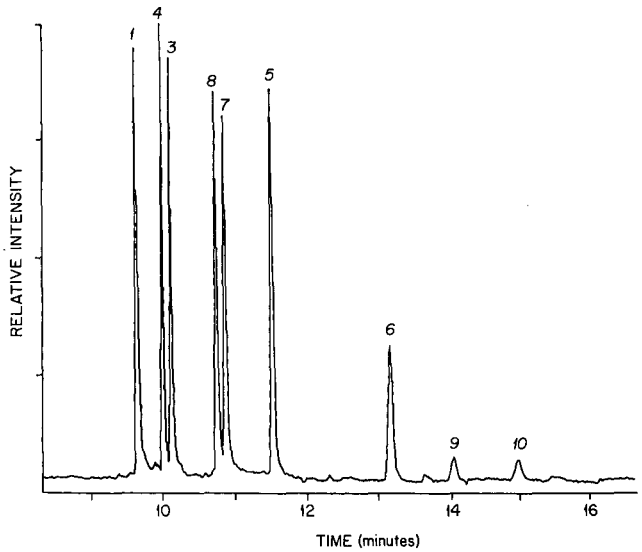

Fig. 2. GC–ECNI-MS reconstructed ion chromatogram of 100 pmol each of compounds **1**, **3–10**. Source temperature: 220°C; methane pressure: 0.25 Torr; scan mode: 10–750 a.m.u. in 1 s; column: 10 m HP Ultra 5% phenylmethylsilicone.

stable compounds[9–12], the base peak is a $[M-181]^-$ ion, produced in a dissociative reaction from loss of a pentafluorobenzyl radical. Typical of this type of ionization, the formation of the pentafluorobenzyl ion is energetically less favored and thus only of minor abundance[9,13].

Fig. 3 summarizes the fraction of the total ion current (TIC) carried by $[M-PFB]^-$ ion for the different derivatives determined by GC–ECNI-MS in the pmol range. As much as 60% of the TIC from an extreme scan range of 10 to 750 a.m.u. is concentrated in this ion. Most of the remaining intensity is concentrated in the intense

TABLE III

ECNI SPECTRA OF ELECTROPHORIC HMU DERIVATIVES

Source temperature: 220°C; 0.25 Torr methane, electron energy: 70 eV. Data in parentheses refer to % relative intensity. n.r. = Not recorded.

Compound	M^-	$[M-PFB]^-$	*RO–*	PFB^-	b_1	b_2	b_3	*Other*
1	502(–)	321(100)	n.r.	181(4)	305(16)	304(4)	125(4)	
2	544(1)	363(100)	n.r.	181(4)	305(20)	304(9)	125(4)	
3	572(1)	391(100)	87(2)	181(1)	305(4)	304(–)	125(2)	
4	586(2)	405(100)	101(6)	181(3)	305(19)	304(11)	125(4)	
5	606(4)	425(100)	121(56)	181(6)	305(47)	304(25)	125(10)	
6	632(–)	451(100)	147(25)	181(5)	305(37)	304(16)	125(5)	407(22)
7	664(–)	483(100)	179(–)	181(2)	305(9)	304(4)	125(2)	
8	682(–)	501(100)	197(1)	181(5)	305(15)	304(5)	125(4)	
9	688(1)	507(100)	203(50)	181(6)	305(45)	304(22)	125(5)	
10	702(–)	521(100)	217(58)	181(8)	305(48)	304(27)	125(6)	

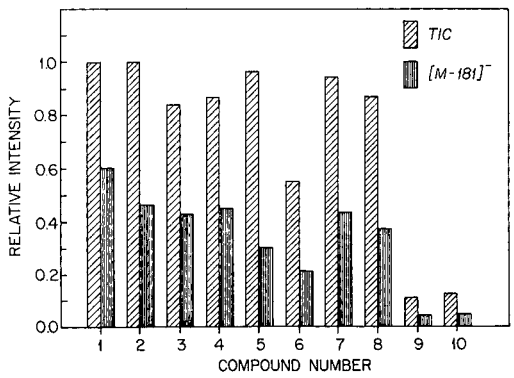

Fig. 3. Relative molar responses of 100 pmol each of electrophoric derivatives of HMU by GC–ECNI-MS; data obtained from the experiment of Fig. 2.

isotope cluster ion. The high absolute response of the $[M-PFB]^-$ ion makes it ideally suited for trace level determinations as well as for characterization purposes of this group of compounds by ECNI-MS.

It is apparent that optimal electron capturing properties are attained by the two pentafluorobenzyl groups as incorporated in compound **1**. Additional electrophoric or other types of groups do not enhance the sensitivity in terms of total ion current any further and, in some cases, are detrimental (see below) for GC–ECNI-MS analysis.

The structures of the most significant fragment ions in the GC–ECNI mass spectra of the derivatives are given in Fig. 4. In addition to the $[M-PFB]^-$ ion, this includes the ions m/z 304 (loss of PFB and RO groups) and m/z 305 (same as m/z 304, plus back-transfer of a hydrogen radical). Relative to these latter ions, the RO^- ion is

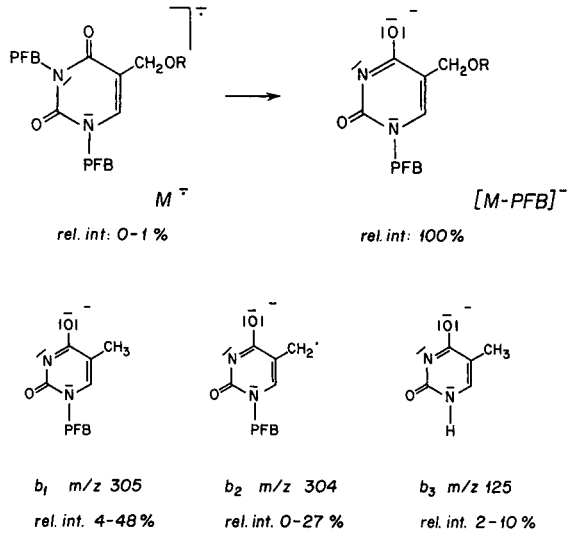

Fig. 4. Principal ions in the GC–ECNI mass spectra (see Table III) of electrophoric derivatives of HMU.

similarly abundant, indicating there is similar charge retention by the core and side chain for loss of RO. As expected, due to the higher strength of ether bonds, these ions are very weak for compounds **7** and **8**. Complete cleavage of PFB groups from the core leads to *m/z* 125. No further influence of the side chain on the extent of the formation of this ion is apparent.

Unique in the series of the derivatives of the ester type, the cinnamoyl ester **6** loses CO_2 via an intramolecular rearrangement as postulated in Fig. 5. According to the proposed mechanism, the information necessary for this transition state seems to be induced by the formation of a six-membered ring comprising positions 5 and 6 of the core, and further promoted by the loss of a neutral molecule. Upon loss of a styrene radical, the intermediate finally fragments to form the ion *m/z* 304. The importance of the ethylene group is further apparent when considering the mass spectrum of compound **5**. While the benzyl group is similarly capable of forming the complex, the shortened distance between base and aromatic center does not permit an overlap of the two aromatic rings, or introduces steric effects, so no similar fragment resulting from loss of CO_2 is observed.

Positive chemical ionization mass spectra. For these spectra (data not shown), obtained on GC peaks of the compounds, well defined protonated molecular ions were observed for compounds **1–8** and, in most cases, further confirmed by the occurrence of $[M + C_2H_5]^+$ adduct ions. A significant ion in every spectrum was *m/z* 485, resulting from cleavage of the side chain (loss of OR; see Fig. 1). Further loss of a PFB group and reprotonation yielded the fragments *m/z* 305 and *m/z* 307.

Favorable protonation of the PFB group was apparent judging from the intensity of the peaks at *m/z* 182 and 183, which far exceeded the intensity from calculated isotopic contribution. Loss of F˙ (or HF) from these ions led to a prominent *m/z* 163 ion for all of the compounds.

In contrast to the results of the ECNI-MS experiments, direct structural information about the acyl substituents at the 5-hydroxymethyl group were obtained in the positive chemical ionization mode. Ions of the composition $[ROH + H]^+$ (protonated acids) were observed as base peaks in the spectra of the aliphatic and benzoic esters and were still very abundant in the spectra of the cinnamoyl and phenylcycloalkaneacetyl derivatives. In addition, the spectra of compounds **3**, **4**, and **5** showed significant R^+ ions.

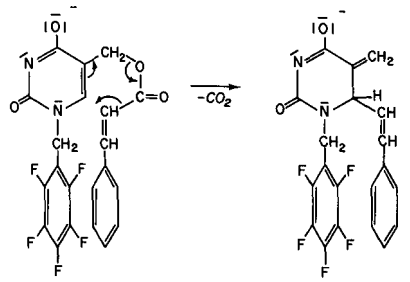

Fig. 5. Proposed fragmentation of the ion $[M-181]^-$ from compound **6**.

Electron impact mass spectra. For these spectra (data not shown), obtained on GC peaks of the compounds, most of the ion current was carried by the ion $[PFB]^-$ at *m/z* 181. Loss of HF from this ion yielded *m/z* 161. With the exception of the ethers **7** and **8**, ions derived from the core structure of the nucleobase were weak. Unique to the electron impact mass spectra was the ion *m/z* 262, which corresponded to $[C_6F_5N{=}CH{-}C(=CH_2){-}C{=}O]^+$. A loss of the RO side chain, followed by loss of pentafluorobenzylisocyanate, apparently led to this ion. A weak complementary ion at *m/z* 222 for $[C_6F_5CH{-}N{=}C{=}O]^+$ was also found. In compound **1**, which lacks a side chain, the same general pattern was observed with the additional presence of an ion *m/z* 278 due to retention of the hydroxyl oxygen atom. The formation of *m/z* 501 and a cluster 484 to 486 was very sensitive to the substitution at position 5 and was mirrored by the occurrence of the corresponding ions R^+ and $[R - CO]^+$.

Comparison of derivatives and detection techniques

In addition to hydrolytic stability and structural information by MS, another important criterion that we applied to the selection of a most suitable ester derivative of 5-hydroxymethyluracil was the chromatographic performance of the compounds, with special emphasis on sensitivity by GC–ECD, GC–ECNI-MS and LC–ECNI-MS.

Fig. 6 shows a GC–ECD chromatogram for a mixture containing 4 fmol each of compounds **1** and **3–10**. Compound **2**, which co-elutes with **1** under these conditions, is not included. The relative molar responses (peak areas) of compounds **1**, **3–5**, **7** and **8** are comparable (Table IV) whereas that for **6** is somewhat lower. Compounds **9** and **10**, which are also the least volatile, give only 1/10 of the response of the most sensitive compound, **8**. Since their lower response is independent of the absolute amounts determined, we suspect that **9** and **10** are inherently less sensitive in the ECD. However, it is difficult to rule out the alternate possibility that they undergo a low recovery in the chromatographic system. Although compounds **9** and **10** are the most hydrolytically stable of the ester derivatives, their more difficult synthesis and, as shown here,

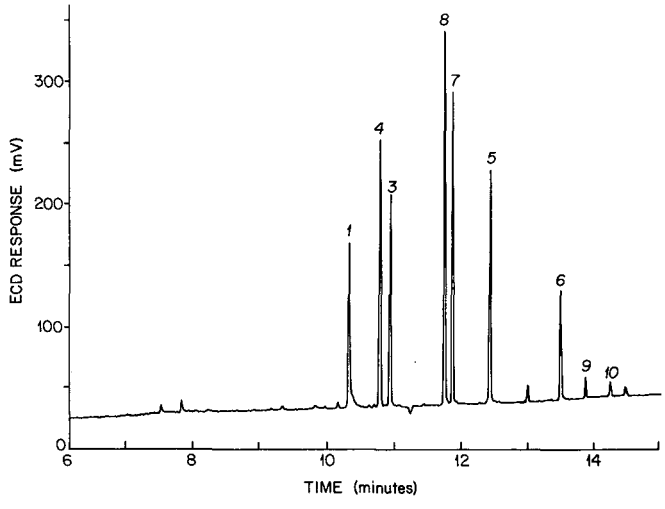

Fig. 6. GC–ECD chromatogram of 4 fmol each of derivatives **1**, **3–10**. 25 m HP Ultra 2, 5% phenylmethylsilicone column. See Materials and Methods for conditions.

TABLE IV

COMPARISON OF THE RELATIVE MOLAR RESPONSE (PEAK AREA) UNDER DIFFERENT SEPARATION AND DETECTION CONDITIONS

FS = Full scan detection. SIM = Selected ion monitoring of ions $[M-181]^-$. RIC = Reconstructed ion chromatogram, ion traces $[M-181]^-$ extracted from the FS experiment. All areas are normalized relative to compound **8**. Relative standard deviation: usually smaller than 10%.

Method	*Compound*								
	1	*3*	*4*	*5*	*6*	*7*	*8*	*9*	*10*
GC–ECNI-MS									
FS, n = 3, range: 4–20 pmol	1.0	1.1	1.1	1.0	0.7	1.0	1	0.2	0.2
RIC	1.0	1.0	0.9	0.6	0.4	1.0	1	0.1	0.1
GC–ECNI-MS									
SIM, n = 3, range: 10–40 fmol	0.5	0.5	0.6	0.4	0.2	0.9	1	–	–
GC–ECD, n = 6, range: 4 fmol	0.6	0.6	0.7	0.6	0.3	0.8	1	0.1	0.1
LC–ECNI-MS									
SIM, n = 1, range: 2 pmol	0.4	0.4	0.5	0.3	0.2	1.0	1	–	–
LC–ECNI-MS									
SIM, n = 3, range: 20–40 fmol	0.5	0.5	0.6	0.3	0.2	0.9	1	–	–

reduced response by GC–ECD, makes them unattractive as derivatives for the trace analysis of HMU. Compound **6** cannot be considered as a particularly useful derivative either. Not only is its response somewhat low, but also we previously encountered reproducibility problems when we similarly determined a cinnamoyl derivative of a nucleoside[14].

The chromatogram of a ten-fold concentrated sample (40 fmol each) of the above mentioned mixture, analyzed by GC–ECNI-MS in a selected ion mode, is shown in Fig. 7. In order to obtain a direct comparison of this and the prior GC–ECD data, the identical column as well as similar GC conditions were used. As seen in this figure, the relative responses of the compounds by GC–ECNI-MS are quite similar to those seen by GC–ECD, reflecting the similar nature of these two detection techniques. Consistent with their low response by GC–ECD, compounds **9** and **10** fail to give peaks at this fmol level by GC–ECNI-MS, although they were previously observed at the 100 pmol level by this technique (Fig. 2).

It is interesting to note the high relative response and relative symmetric shape for compound **1**, which contains a free hydroxyl group, both by GC–ECD (Fig. 6) and GC–ECNI-MS (Fig. 7) even at the fmol level. While bonded fused silica columns are well known to handle more polar solutes, the GC behavior of polar solutes can degrade when trace amounts are determined. (This is examined in more detail for this compound, and the esters, below.)

Taking into account the signal-to-noise ratios, the sensitivity was about 50-fold lower by GC–ECNI-MS than by GC–ECD (compare Figs. 6 and 7). It is likely that this simply reflects the conditions of the GC–ECNI-MS system when the experiment was

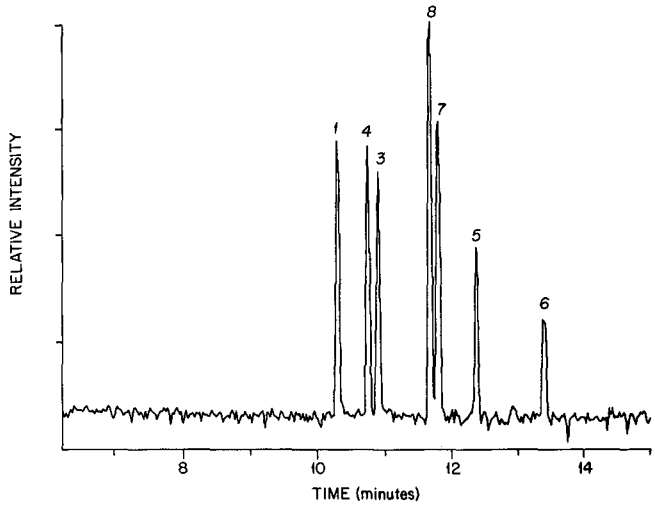

Fig. 7. GC–ECNI-MS reconstructed ion chromatogram of 40 fmol each of the derivatives **1**, **3–10**. Source temperature: 220°C; methane pressure: 0.25 Torr; selected ions: $[M-PFB]^-$, 0.1 s/ion. 25 m HP Ultra 2, 5% phenylmethylsilicone column.

conducted. In a number of cases we have observed that these two techniques give comparable responses for standards of strong electrophores, while GC–ECNI-MS is more useful for the analysis of "real" samples because of its greater discriminating power.

Table IV shows a comparison of the relative molar responses for the compounds as a function of their concentration and the mode of detection, summarizing data from two of the prior experiments (data from Figs. 6 and 7) and also additional studies especially by LC–ECNI-MS. The general pattern of relative responses is similar throughout all of these experiments, with the appearance of somewhat higher relative responses for compounds **1** and **3–6** at the 4–20 pmol level by GC–ECNI-MS. To investigate this latter variation in response in more detail, we measured the responses of representative compounds **1**, **4** and **8** as a function of concentration by GC–ECNI-MS as shown in Fig. 8a and b. As seen, there is a saturation of the response at levels $\geq$ 250 fmol, explaining the change in response for **1** and **4**, and therefore the other compounds, at lower levels relative to that of **8** when comparing fmol with pmol levels. In fact, this figure shows that the responses for **1**, **4** and **8** are all linear with concentration below 250 fmol. Fig. 8a shows this most clearly, in which the 1–100 fmol responses of Fig. 8b are plotted against linear axes. For this region of concentration, correlation coefficients greater than 0.9990 were obtained. Similarly, the same responses, within experimental error, are seen for these compounds and for the others by LC–ECNI-MS at 2 pmol and 20–40 fmol levels (Table IV; a representative chromatogram is presented in Fig. 9). It is interesting that, overall, the four compounds possessing an aromatic moiety in their ester group (**5**, **6**, **9**, and **10**) give the lowest responses.

In all of the experiments shown in Table IV which were conducted at fmol levels, the response of pivalyl ester **4** is at least slightly higher than that for any of the other

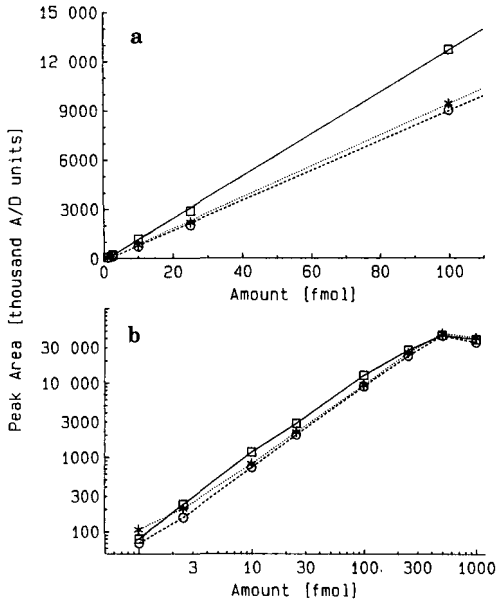

Fig. 8. Response by GC–ECNI-MS for compounds **1** (*), **4** (○) and **8** (□) as a function of concentration; conditions the same as in Fig. 7. In (a), the 1–100-fmol data of (b) are plotted against linear axes.

esters, and the free hydroxyl compound **1** consistently gives a high relative response as well. Thus, taking into account this information plus earlier considerations about the various esters, the pivalyl derivative emerges overall as the best one, but the free hydroxyl compound needs to be considered as well.

The GC–ECNI-MS (Fig. 7) and LC–ECNI-MS (Fig. 9) chromatograms can be

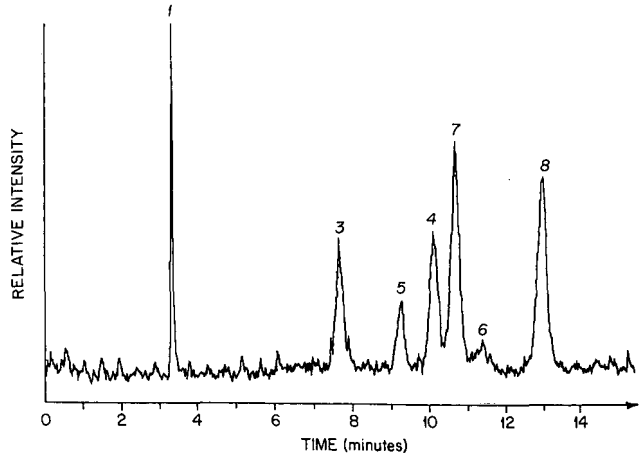

Fig. 9. Moving-belt LC–ECNI-MS reconstructed ion chromatogram of 40 fmol each of the derivatives **1**, **3**–**10**. Source temperature: 250°C; methane pressure: 0.20 Torr; selected ions: $[M-PFB]^-$, 0.1 s/ion. HPLC column: Supelcosil LC-18DB, 150 × 4.6 mm, 3 μm particles, 1.2 ml/min, 70% acetonitrile; belt speed: 2 cm/s; vaporizer temperature: 330°C.

compared directly as they were determined in the same mass spectrometer. The relative molar responses of the compounds at the 40 fmol level are essentially the same, and nearly identical detection limits are achieved both by GC–ECNI-MS and LC–ECNI-MS. This indicates that no significant loss of material occurs during the eluent deposition and solvent evaporation steps on the Kapton (R) belt, an issue that we have addressed previously[7]. Analogous to the results in the GC–MS experiment, compounds **9** and **10** were also not detected by LC–MS. Even under LC–MS conditions, compound **1** behaves favorably. It is important to point out this result, since LC–ECNI-MS has the important advantage over GC–ECNI-MS that larger sample volumes are more easily introduced into the MS system.

CONCLUSIONS

The goal of selecting an optimum ester derivative for the aliphatic hydroxyl moiety on ring-pentafluorobenzylated HMU was reached: pivalyl is the best choice. Unanticipated was a good performance at trace levels of the parent derivative, in which the hydroxyl group is left underivatized. Thus, four derivatives of HMU now deserve further study for its trace analysis by GC or LC with electron capture detection techniques; namely, the aforementioned two compounds and the two others (pentafluorobenzyl and tetrafluorobenzyl).

For electrophoric derivatives of HMU, LC–ECNI-MS with a belt interface produces similar sensitivity and identical spectral data as GC–ECNI-MS using the same MS equipment.

The structural information that can be obtained about the various derivatives by MS is comparable.

ACKNOWLEDGEMENTS

Financial support for this work was provided by Grant CA 35843 from the National Cancer Institute, and Grant CR 812740 from the Reproductive Effects Assessment Group of the United States Environmental Protection Agency (EPA). G.M.K. acknowledges additional support by a Gustel Giessen Award from the Barnett Institute. This is contribution Number 367 from the Barnett Institute for Chemical Analysis and Materials Science.

REFERENCES

1 O. Minnetian, M. Saha and R. W. Giese, *J. Chromatogr.*, 410 (1987) 453.
2 B. Singer and D. Grunberger, *Molecular Biology of Mutagens and Carcinogens*, Plenum Press, New York, 1983.
3 G. B. Mohamed, A. Nazareth, M. J. Hayes, R. W. Giese and P. Vouros, *J. Chromatogr.*, 314 (1984) 211.
4 J. Adams, M. David and R. W. Giese, *Anal. Chem.*, 58 (1986) 345.
5 R. S. Annan, G. M. Kresbach, R. W. Giese and P. Vouros, *J. Chromatogr.*, in press.
6 J. Adams and R. W. Giese, *J. Chromatogr.*, 347 (1985) 99.
7 G. M. Kresbach, T. R. Baker, R. J. Nelson, A. Wronka, B. L. Karger and P. Vouros, *J. Chromatogr.*, 394 (1987) 89.
8 S. Abdel-Baky and R. W. Giese, *J. Org. Chem.*, 51 (1986) 3390.
9 T. M. Trainor and P. Vouros, *Anal. Chem.*, 59 (1987) 601.
10 A. Martineau and P. Falardeau, *J. Chromatogr.*, 417 (1987) 1.
11 J. S. Hadley, A. Fradin and R. C. Murphy, *Biomed. Mass Spectrom.*, 15 (1988) 175.
12 H. Schweer, H. W. Seyberth, C. O. Meese and O. Furst, *Biomed. Mass Spectrom.*, 15 (1988) 143.
13 R. J. Strife and R. C. Murphy, *J. Chromatogr.*, 305 (1984) 3.
14 T. M. Trainor, R. W. Giese and P. Vouros, *J. Chromatogr.*, 452 (1988) 369.

Journal of Chromatography, 476 (1989) 439–443
Elsevier Science Publishers B.V., Amsterdam — Printed in The Netherlands

CHROMSYMP. 1575

PURIFICATION OF SYNTHETIC OLIGONUCLEOTIDES ON A WEAK ION-EXCHANGE COLUMN

J. LIAUTARD, C. FERRAZ, J. SRI WIDADA, J. P. CAPONY and J. P. LIAUTARD*
CRBM du CNRS, U-249 INSERM et Université de Montpellier I, B.P. 5051, 34033 Montpellier Cedex (France)

SUMMARY

A weak ion-exchange column (PVDI 4000-5) was used to purify oligonucleotides of relatively large size. The purification of polynucleotides was very rapid, they were separated according to size and retained all their properties relevant to genetic engineering experiments.

INTRODUCTION

Molecular biology is developing very rapidly and synthetic oligonucleotides are required for numerous types of experiments. The synthesis of oligonucleotides can now be performed rapidly, owing to automatic apparatus, but although the yield of each reaction is quite good it never approaches 100%. This means that synthetic polynucleotides are generally contaminated by undesired species. In some cases, purification is performed on protected nucleotides, and separation based on hydrophobicity is carried out on reversed-phase columns[1]. However, in other cases the purification must be performed on deprotected polynucleotides, and reversed-phase separation is then difficult for two reasons: first it can be achieved only for small oligonucleotides; secondly, since it proceeds according to the composition as well as the number of bases, the resulting chromatogram is difficult to interpret[2].

It has been shown that ion-exchange chromatography allows the separation of oligonucleotides according to their sizes. However, this method gives poor resolution for oligonucleotides containing more than fifteen nucleotides. On the other hand, it is possible to separate rapidly relatively large oligonucleotides according to size by using a weakly basic ion-exchange column. This property has been exploited successfully by different authors[4–6], using different columns. We have chosen to use a new packing material, designed for protein separation, and developed a procedure that allows the separation of synthetic oligonucleotides according to their sizes. The purification is more rapid than by electrophoresis, the yield is quite good and the biological activity is totally retained.

0021-9673/89/$03.50

EXPERIMENTAL

Materials

All experiments were performed with a Gilson apparatus equipped with two high performance liquid chromatography (HPLC) pumps (Model 302) and an UV detector set at 254 nm (Model 111B). The PVDI 4000-5 columns (100 mm × 4.6 mm; Société Française de Chromato Colonne, Neuilly-Plaisance, France) are weak silica-based ion exchangers, with a large pore size of 4000 Å. The packing was made by the polymerization of poly(vinylimidazole). Oligonucleotides were synthesized on a Model 380B apparatus (Applied Biosystem, Roissy C. de Gaule, France). Ultra pure urea was obtained from Bethesda Research Labs. (Cergy Pontoise, France).

Methods

The columns were eluted with a gradient of salt (ammonium acetate pH 6.5), starting with 0.2 *M* ammonium acetate in 5 *M* urea (eluent A) and increasing to 2 *M* ammonium acetate in 5 *M* urea (eluent B). The gradient slope and time dependency is described in the figure legends. The flow-rate was 1 ml/min, except where stated otherwise.

Analysis of oligonucleotides by polyacrylamide gel electrophoresis was performed on 20% acrylamide in 8 *M* urea[7].

RESULTS

We have studied the efficiency of PVDI 4000 for the separation of oligonucleotides. For this purpose we used poly(A) (A = adenosine), hydrolysed by boiling in water, to obtain a range of oligonucleotides. Elution was performed by increasing the salt concentration linearly from 0 to 40% of eluent B. Under these conditions, sep-

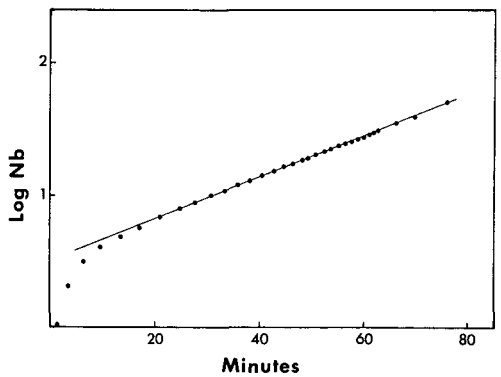

Fig. 1. Relationship between the retention time and the number of nucleotides in an oligonucleotide. Oligonucleotides of different sizes, varying by one nucleotide, were generated by hydrolysis of poly(A). A 150-μg amount of this mixture was analyzed on the PVDI 4000 column (100 mm × 4.6 mm). After equilibration in eluent A (0.2 *M* ammonium acetate in 5 *M* urea), elution was performed by increasing the amount of eluent B (2 *M* ammonium acetate in 5 *M* urea) from 0 to 40% in 90 min at a flow-rate of 1 ml/min. The logarithm of the number of nucleotides is plotted against the elution time. Each individual point represents the top of an elution peak.

aration was obtained for molecules up to the 50-mer. The separation is quite good in the degree of polymerization range 20–35, *i.e.*, the degree of polymerization of the majority of synthetic oligonucleotides. Fig. 1 shows the relationship between the retention time and the number of nucleotides, which is logarithmic within the range of 5–50 nucleotides.

We have used this column to purify synthetic oligonucleotides. Each oligonucleotide was purified in less than 15 min (not shown). Although the desired nucleotide represents *ca.* 85% of the starting mixture, purification is necessary if it is to be used for sequencing. It is noteworthy that electrophoresis, the method generally employed in molecular biology, requires at least 24 h for migration and elution. The preparation presented here was completed in 1 h, including ethanol precipitation, giving a purified oligonucleotide suitable for further applications. For example, these oligonucleotides were successfully used for sequence determinations.

In order to perform library screening, we have synthesized oligonucleotides containing 6-methyladenine and inosine. These rare bases decreased the yield of the reaction, resulting in a very small amount of the desired oligonucleotides. Under these conditions the desired oligonucleotides represent less than 5% of the total nucleic acids. Fig. 2 shows their separation obtained in a few minutes. Because the separation is achieved according to the sizes of the molecules, identification of each nucleotide is very easy. The desired oligonucleotide is always the longest species. The purified oligonucleotides were used for library screening.

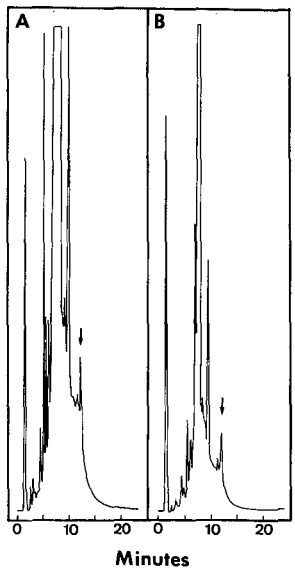

Fig. 2. Purification of a complex mixture of oligonucleotides. Two oligonucleotides were synthesized containing the rare bases 6-methyladenine and inosine (TCIGGIGCIAmGITAmGTCIGGIGTICC and TCIGGIGCIAmGITAmATCIGGIGTICC). Purification was performed on the weak ion-exchanger PVDI 4000 (100 mm × 4.6 mm, pore size 400 Å) by gradient elution, increasing the amount of eluent B (see Fig. 1) from 0 to 50% in 20 min at a flow-rate of 1 ml/min. A 50-μg amount of oligonucleotides was chromatographed. After separation the different components were analysed by acrylamide gel electrophoresis. The expected oligonucleotide was the longest (arrow) and is purified in one step.

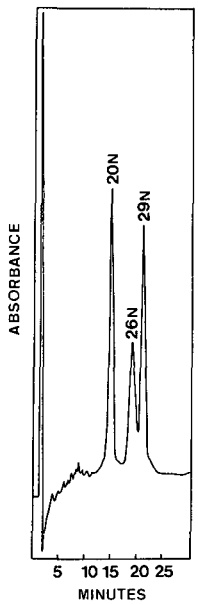

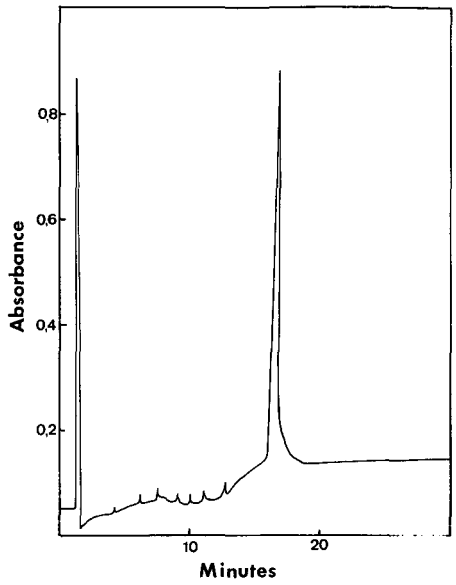

Fig. 3. Separation of three oligonucleotides having chain lengths of 20, 26 and 29 nucleotides. A 2-μg amount of each oligonucleotide was mixed and analysed on a PVDI 4000 column. Gradient elution was performed by increasing the amount of eluent B (see Fig. 1) from 0 to 25% in 35 min at a flow-rate of 1 ml/min.

Fig. 4. Analysis of a self-associating 12-mer oligonucleotide (CCCGAATTCGGG). Gradient elution was performed by increasing the amount of eluent B to 50% in 30 min. For other conditions see Fig. 1 and the Experimental section.

The resolution can be further improved by changing the elution gradient. Fig. 3 shows an example of a total separation of three different oligonucleotides ranging in size from 20 to 29 residues. The recovery of oligonucleotides is excellent, *ca.* 90%, in each case. They precipitate readily after the addition of two volumes of ethanol and can be used for sequence determination, library screening, linker addition, radioactive labelling or site-directed mutagenesis.

In the course of analysis and purification of the oligonucleotides we have used self-complementary oligonucleotides containing the recognition sequence of EcoRI restriction enzyme: GAATTC. The behaviour of this molecule is depicted in Fig. 4. This oligonucleotide having twelve residues exhibits the retention time observed for a 24-mer. This result implies that, in spite of the presence of 5 *M* urea, the two strands of the DNA were still hybridized and the number of phosphates was therefore twice as high.

CONCLUSIONS

A poly(vinylimidazole)-based column (PVDI 4000) originally designed for protein separation is very useful for the purification of oligonucleotides used in genetic engineering. Although other materials achieve approximately the same degree of

separation[4–6] they are generally more expensive. The biological activity of the purified products was also tested. The use of high pH[4] may result in the degradation of oligoribonucleotides, although oligodeoxynucleotides are not affected. Conversely, the use of low pH may result in a partial depurination of the nucleic acids. We have employed a nearly neutral solution (pH between 6.5 and 7.0) containing urea. These conditions are generally used for the preparation of large cellular nucleic acids[7].

ACKNOWLEDGEMENTS

We are indebted to R. Ordonnez for making available the PVDI column and to C. Gouyette for a generous gift of methyladenine phosphoramidite. This work was supported by CNRS and INSERM.

REFERENCES

1 F. Chow, T. Kempe and G. Palm, *Nucleic Acids Res.*, 9 (1981) 2807–2816.
2 J. Crowther, in P. Brown (Editor), *HPLC in Nucleic Acid Research*, Marcel Dekker; New York, Basel, 1984.
3 C. Newton, A. Greene, G. Heathcliffe, T. Atkinson, D. Holland, A. Markham and M. Edge, *Anal. Biochem.*, 129 (1983) 22–30.
4 Y. Kato, T. Kitamura, A. Mitsui, Y. Yamasaki, T. Hashimoto, T. Murotsu, S. Fukushige and K. Matsubara, *J. Chromatogr.*, 447 (1988) 212–220.
5 D. Drager and F. Regnier, *Anal. Biochem.*, 45 (1985) 47–56.
6 M. Colpan, J. Schumacher, W. Bruggemann, H. Sanger and D. Riesner, *Anal. Biochem.*, 131 (1983) 257–263.
7 T. Maniatis, E. Fritsch and J. Sambrook, *Molecular Cloning a Laboratory Manual*, Cold Spring Harbor Laboratory, Cold Spring Harbor, New York, 1982.

Journal of Chromatography, 476 (1989) 445–453
Elsevier Science Publishers B.V., Amsterdam — Printed in The Netherlands

CHROMSYMP. 1607

HIGH-PERFORMANCE LIQUID CHROMATOGRAPHY OF AMINO ACIDS, PEPTIDES, PROTEINS AND POLYNUCLEOTIDES

XCIV[a]. SOLID-PHASE HYBRIDIZATION OF COMPLEMENTARY OLIGONUCLEOTIDES

M. GUTHRIDGE, J. BERTOLINI and M. T. W. HEARN*
Department of Biochemistry, Monash University, Clayton, Victoria 3168 (Australia)

SUMMARY

The ability of synthetic oligonucleotides to specifically hybridize to a complementary oligonucleotide immobilized on an anionic stationary phase has been investigated. A sigmoidal melting curve was obtained when oligonucleotide duplex formation on the column was plotted against hybridization stringency over the ionic strength range 0.2–0.42 *M*. These studies confirm a rapid method for determining the relative melting temperature of hybridized oligonucleotide complexes and provide a basis for the selection of stringency conditions optimal for various synthetic oligonucleotide probes.

INTRODUCTION

Synthetic oligonucleotide probes complementary to specific regions of DNA and RNA have found wide application in molecular biology, including Northern and Southern blot analysis[1,2], screening of gene libraries[3], *in vitro* mutagenesis[4] and as primers for template-directed polymerization enzymes, such as DNA polymerases and reverse transcriptase[5,6]. The ease of preparing oligonucleotides as compared to cloning a cDNA fragment has resulted in their increased use. Successful application of such probes requires the establishment of appropriate hybridization conditions that preclude non-specific annealing. At present, criteria for hybridization stringency are established by calculating theoretical melting temperatures, using published formulae[7]. However, due to the inherent limitations of mathematically derived melting temperatures, these estimations can significantly differ from experimentally observed values and their use can account for ambiguous or misleading results obtained in Northern and Southern blots, *in situ* hybridization to RNA and DNA and the screening of transfected plaques[8,9].

During investigation on the high-performance ion-exchange (HPIEX) chromatographic purification of oligonucleotides, we observed that some oligonucleotides were eluted as a broad or asymmetrical peak, while others produced a second, highly

[a] For Part XCIII see ref. 14.

0021-9673/89/$03.50

retained peak. Closer examination of the sequences revealed partially complementary regions, suggesting that self-hybridization may have occurred, producing complexes with altered retention characteristics. It was therefore decided to investigate in detail the hybridization of complementary oligonucleotides in a solid-phase system. Two oligonucleotides were loaded sequentially onto an anion-exchange column, so that the first was immobilized on the solid support and was available to form a complex with the second during its passage through the column. The amount of duplex formed was found to be related to the ionic strength of the loading buffer, and the data derived from these experiments enabled the construction of a melting curve. We propose that this model of solid-phase oligonucleotide hybridization can be used to study the interaction of various matched and slightly mismatched probes in order to obtain relative hybridization stringency. Furthermore, it is envisaged that the procedure can be adapted to approximate closely the situation found in Northern, Southern and plaque blot experiments and establish quickly and conveniently the appropriate hybridization conditions.

EXPERIMENTAL

Oligonucleotide synthesis

Oligonucleotides complementary to unique sections of the acidic and basic form of bovine fibroblast growth factor (FGF-β[10] and FGF-α[11], respectively) gene and of the *int-2* gene[12] were synthesized on an Applied Biosystems (Foster City, CA, U.S.A.) Model 380A DNA synthesizer using phosphoramidite chemistry. The synthesized sequences were: 5′GA CAC AAC CCC TCT CTC TTC TGC TTG 3′ (probe 01, FGF-β), 3′CT GTG TTG GGG AGA GAG AAG ACG AAC 5′ (probe 02, complement of probe 01), 5′CAC CTC CCC CAC GCT TTC CGC ACT G 3′ (probe 03, FGF-α), 5′G CCG TTG AGC TCC TGG CCC 3′ (probe 04, *int-2*).

Chromatographic methods

Chromatographic separations were performed by HPIEX liquid chromatography, using a Waters Assoc. (Milford, MA, U.S.A.) system, incorporating a U6K injector, two M600A pumps and an M660 gradient programmer with a Zorbax Bio Series Oligo column (DuPont) (80 mm × 6.2 mm I.D.). Eluent A consisted of 0.02 *M* phosphate buffer (pH 7.0)–20% acetonitrile, while eluent B contained 0.02 *M* phosphate buffer (pH 7.0)–20% acetonitrile–1 *M* NaCl. Oligonucleotides were routinely purified and analysed on the column with a 0–100% eluent B linear gradient over 1 h at 1.0 ml/min.

The elution of oligonucleotides was monitored at 260 nm with a Lambda Max (Waters) M481 LC spectrophotometer.

Hybridization experiments

Solution hybridization was performed with a mixture of probe 01 and probe 02 at a molar ratio of 1:2. The probes, in eluent A, were boiled for 3 min, and the solution was allowed to cool slowly over 1 h to allow hybridization. The mixture was then loaded onto the column and oligonucleotides were eluted with a 1-h 0–100% eluent B linear gradient at a flow-rate of 1 ml/min.

Solid-phase hybridization was accomplished by loading probe 01 in eluent A at

a flow-rate of 1.0 ml/min, followed by a two-fold molar excess of probe 02 in either 0, 10, 2, 30, 35, 40 or 43% eluent B at a flow-rate of 0.1 ml/min for 30 min. Immediately prior to each run probe 01 and probe 02 were denatured in boiling water for 3 min and quenched on ice. Following the loading of probe 02, the flow-rate was increased to 1.0 ml/min and the column was subjected to a linear gradient, commencing with the loading elution conditions for probe 02 to 100% eluent B at a rate of 1.67% eluent B per min, thus ensuring that the slope of the gradients was identical in all experiments.

RESULTS AND DISCUSSION

In the course of investigations on the regulation of expression of mRNAs coding for growth factors and putative oncogene products[13], we utilised HPIEX chromatography to purify oligonucleotide probes 01, 02, 03 and 04. The chromatographic profile associated with the purification of probe 01 exhibited a highly resolved symmetrical peak (results not shown). A single peak with identical retention was observed on rechromatography, demonstrating the homogeneous composition of the eluted oligonucleotide (Fig. 1). Other oligonucleotides (*e.g.*, probes 03 and 04) exhibited anomalous retention and band-broadening behaviour. Similar profiles were obtained on rechromatography of the major peaks (Fig. 2a and b). Thus, it is probable that under ideal HPIEX conditions some synthetic oligonucleotides are resolved according to charge differences in a sequential fashion with little evidence of effects arising from secondary or higher-order hierarchical structures. However, in other cases, such simple retention versus net charge dependencies do not prevail. Thus, chromatographic behaviour can be characterized as 'regular' when the elution is mediated by net charge and the capacity factor is relatively constant over a range of

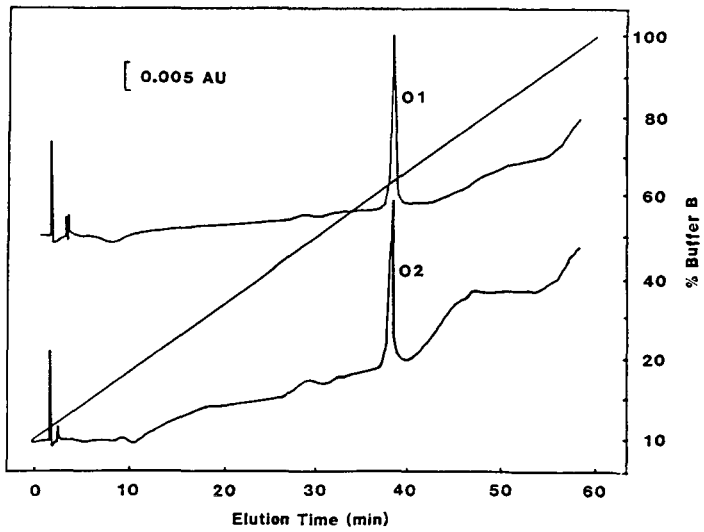

Fig. 1. Elution profiles of purified probe 01 and probe 02. Each oligonucleotide was fractionated on a Zorbax Bio Series Oligocolumn. Eluent A consisted of 0.02 *M* phosphate buffer (pH 7.0)–20% acetonitrile, while eluent B contained 0.02 *M* phosphate buffer (pH 7.0)–20% acetonitrile–1 *M* NaCl. A linear gradient of 0–100% eluent B was developed over 1 h at a flow-rate of 1.0 ml/min.

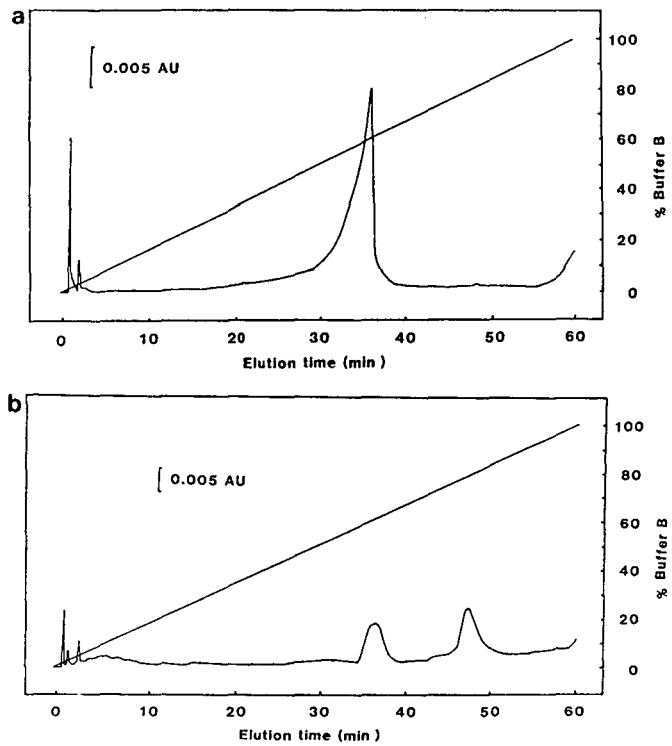

Fig. 2. Elution profiles of purified probe 03 (a) and probe 04 (b). Chromatographic conditions as described in Fig. 1.

mass loading conditions. Alternatively, chromatographic behaviour can be characterised as 'non-regular' when the elution is not mediated solely by net charge and the capacity factor, and the peak shape exhibits very complex dependencies on mass loading and concentration conditions. The latter behaviour may reflect aggregation or other slow, secondary chemical equilibrium processes involving the stationary phase surface. In the case of oligonucleotides, this behaviour could reflect internal autohybridization or inter-chain hybridization. This consideration led us to examine the possibility that chromatographic methods could be used to optimise hybridization conditions.

Two purified complementary 26-base oligonucleotide probes, probe 01 and probe 02, were used in the HPIEX chromatography hybridization experiments. The chromatogram of each probe exhibited a single sharp peak at 65% eluent B (Fig. 1). These oligonucleotides were also labelled at the 5'-end with [γ-^{32}P] dATP and found to migrate as a single band on polyacrylamide gel (data not shown).

Solution hybridization of a mixture of probe 01 and probe 02 was performed at a molar ratio of 1:2. The probes were boiled for 3 min in eluent A and allowed to cool slowly to ambient temperature. Fractionation of the sample by HPIEX chromatography on the Zorbax Bio Series Oligo column resulted in the elution of peaks A and B, as shown in Fig. 3a. While the monomeric forms of probes 01 and 02 are eluted

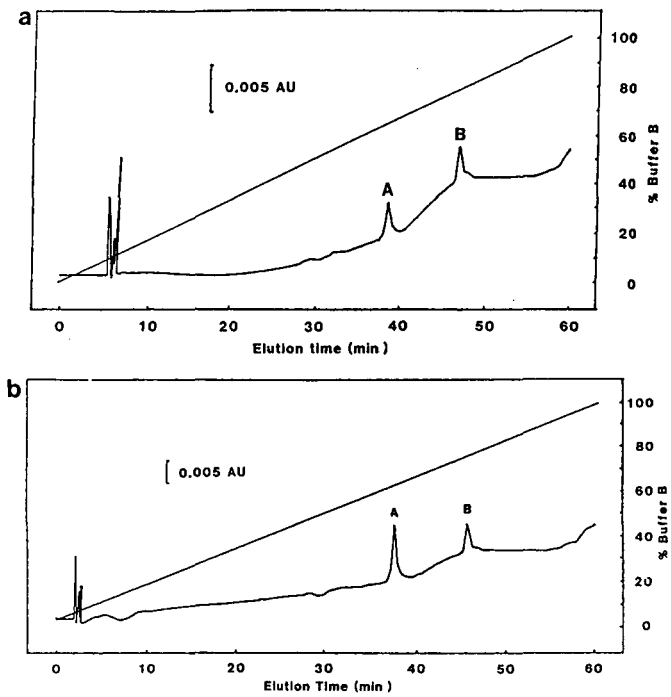

Fig. 3. Elution profiles of probe 01 and probe 02, hybridized in solution prior to loading (a). Peak B was collected, boiled in eluent B containing 50% deionized formamide and reloaded (b). Chromatographic conditions are as described in Fig. 1.

together as peak A at an eluent composition of 65% eluent B, an additional peak (B), containing duplex DNA, was eluted with 75% eluent B. Peak B was collected, boiled in eluent A containing 50% deionized formamide and reloaded. In addition to the expected elution of peak B an additional peak with a retention time identical to that of the individual oligonucleotide probes 01 and 02 was observed (Fig. 3b). Denaturation of the collected material and the subsequent appearance of monomeric probes 01 and 02, when rechromatographed, confirmed the duplex nature of peak B.

For solid-phase hybridization, probe 01 was immobilized on the ion exchanger prior to the loading a two-fold molar excess of probe 02. The salt gradient resulted in the elution of two peaks, 1 and 2 (Fig. 4a) from the column with retention times identical to those observed for peaks A and B, respectively, in Fig. 3. This suggests that the probing oligonucleotide, probe 02, hybridized to the immobilized target sequence, probe 01, in a manner indistinguishable from to that observed for solution hybridization when Fig. 3a is compared to Fig. 4a.

The ability of increasing salt concentrations to stabilize base pairing further and to facilitate more favourable hybridization stringency was investigated, using the same approach. Following loading of probe 01 onto the column, probe 02 was loaded in salt concentrations ranging from 0.0 to 0.43 *M* NaCl (Fig. 4a–g), and the magnitude of duplex formation at a particular ionic strength was calculated from the height/area of peak 2. In the absence of NaCl or at low NaCl concentrations, *e.g.* over the range

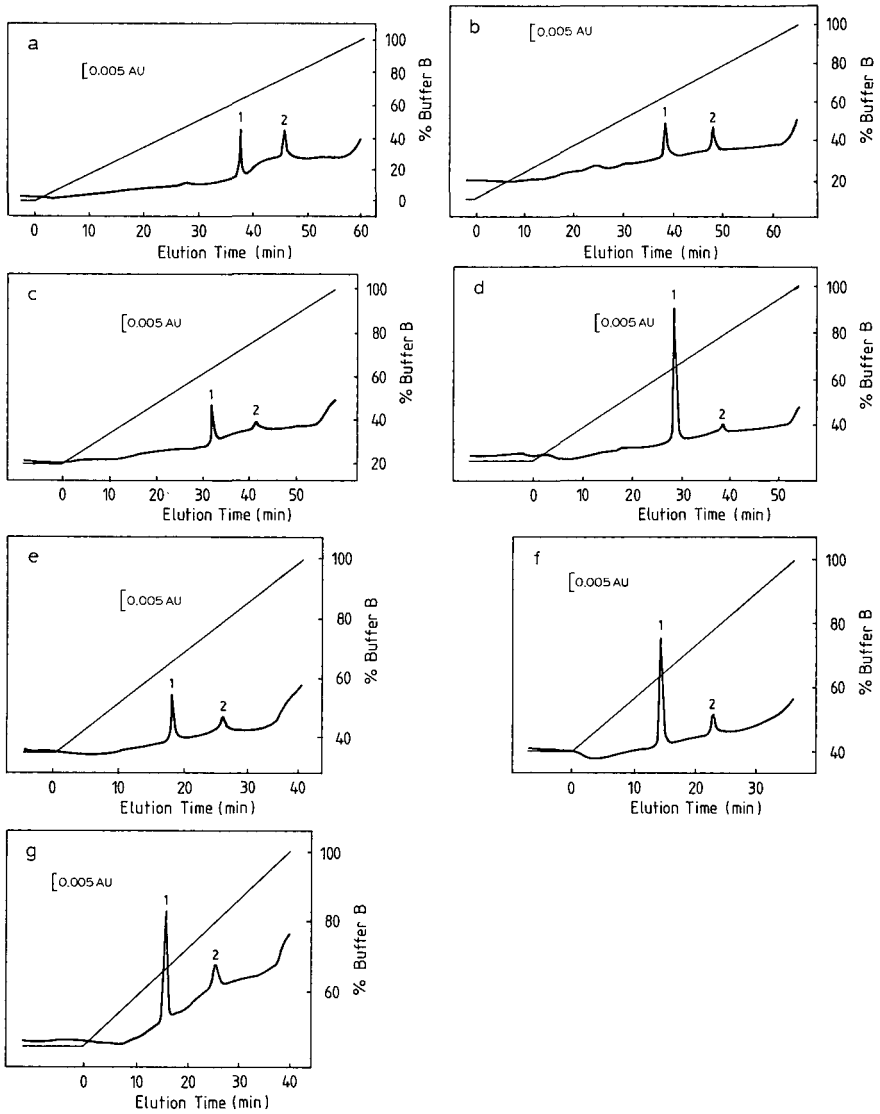

Fig. 4. Elution profiles of probes 01 and 02, allowed to hybridize on the column. After loading probe 01 in eluent A, a two-fold excess of probe 02 was loaded in (a) 0% eluent B, (b) 10% eluent B, (c) 20% eluent B, (d) 30% eluent B, (e) 35% eluent B, (f) 40% eluent B and (g) 43% eluent B at a flow-rate of 0.1 ml/min. The flow-rate was returned to 1.0 ml/min after loading probe 02, the oligonucleotides were eluted with a linear gradient from the loading conditions (a–g) of probe 02 and the gradient was developed to 100% eluent B at a rate of 1.67% eluent B per min. This elution protocol ensured that the slopes of the gradients were identical in all experiments.

0.0–0.1 *M* NaCl (Fig. 4a and b), significant hybridization occurred. With further increases of NaCl concentration up to 0.35 *M* (Fig. 4c–e) lower levels of complex formation were observed, but with high salt concentrations of 0.40 and 0.43 *M* (Fig. 4f and g) hybridization was facilitated, as indicated by the increased height of peak 2.

Data on the efficacy of hybridization above 0.43 *M* NaCl could not be obtained, due to the low retention of probe 01 on the column.

The significant degree of hybridization that was observed at low ionic strength (0.0–0.1 *M* NaCl) may, in part, be due to the high affinity of probe 01 for the column matrix under these conditions. The strength of this binding serves to retard the mobility of probe 01 and, therefore, to enhance the stability of the probe 01–probe 02 complex. Evidence for similar enhancement of duplex stability by solid phases is already available[8,9] from comparative data on the estimates of melting temperature, obtained by solution hybridization procedures and by probing of sequences immobilised on membranes.

In Fig. 5 is shown the derived melting curve for the probe 01–probe 02 hybrid, calculated by plotting the amount of duplex formation against the NaCl concentration. As is evident from Fig. 5, a number of interactive events occur at the different ionic conditions. Hybridization of the probing oligonucleotide to an immobilized oligonucleotide becomes energetically favourable, even at low salt concentrations, if the flexibility of the target oligonucleotide is constrained by the strength of its bonding to the solid phase. This matrix-mediated effect allows the weak interaction between complementary nucleotides to maintain the complex at low ionic strength. At intermediate ionic conditions, the target probe, although still interacting with the column materials exhibits considerable flexibility, and this behaviour tends to disrupt the bonds mediating hybridization.

At high ionic strength, hybridization is favoured, due to preferential bonding associated with the specific recognition. Although the target probe under these conditions would have considerable mobility and structural flexibility, the strength of the hybridization interaction nevertheless ensures the formation of a hybridized complex. A sigmoidal melting curve (comparable to other solid-phase melting curves generated when probing RNA and DNA on nitrocellulose, Zeta Probe and Gene Screen[13]) was obtained when oligonucleotide duplex formation on the column was

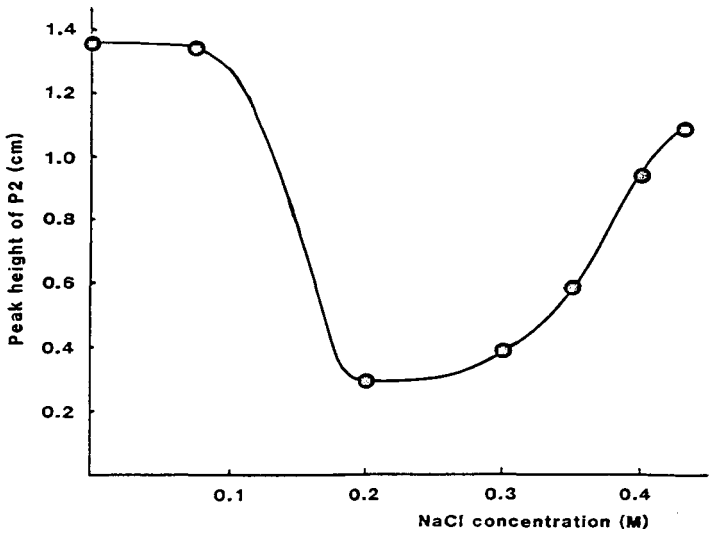

Fig. 5. Calculated melting point curve for the hybridization of probes 01 and 02.

plotted against hybridization stringency over the ionic strength range 0.2–0.42 *M*. While maximum hybridization could not be obtained due to the low retention of the oligonucleotides in high salt conditions the estimated melting temperature was considerably less than the theoretical value[7], *e.g.* up to *ca.* 20°C difference in melting temperature. Similar divergencies between the theoretical and experimental values of the 'melting temperature' are commonly found when dimethyl formamide is added to the buffer solutions with other solid-phase hybridization systems. This discrepancy could be due to the presence of acetonitrile added to the eluent to prevent hydrophobic interactions between the oligonucleotides and the column. Investigations currently underway will examine the ability of acetonitrile and other organic solvents to interface with the stacking of nucleotide bases. Nevertheless, the present results indicate that the described procedure is readily adaptable to examine the effects of one or more mismatches on the stability of the duplex derived from oligonucleotide probes. Results of these studies with additional oligonucleotides specifically designed to evaluate this question will be reported subsequently.

This paper shows that hybridization of oligonucleotide probes can be studied rapidly by the use of anion-exchange chromatography. With appropriate modification of instrumentation, including data handling standardisation, this procedure should be adaptable into a quantitative and predictive technique which will allow the investigation of hybridization of probes under a wide range of solvent/buffer conditions. Existing mathematical formulaes can predict optimum hybridization under a limited range of standard conditions (*e.g.* when performed with solutions containing NaCl, formamide and of pH 7.0–7.5). However, when probes are used as primers for template-directed polymerase enzymes, such as reverse transcriptase and DNA polymerases, conditions that ensure specific hybridization must be determined empirically, due to the unknown effects of such variables as pH or the salt type and its concentration. The technique described in this paper should enable the rapid assessment of the relative hybridization stringency over a range of such unique experimental conditions.

ACKNOWLEDGEMENTS

The support of the National Health and Medical Research Council of Australia, the Tobacco Research Foundation and Monash University Special Research Grants (to M.T.W.H.) is gratefully acknowledged. M.G. is a Monash University Postgraduate Scholar.

REFERENCES

1 M. E. Lewis, T. G. Sherman, S. Burke, H. Akil, L. G. Davis, R. Arentzen and S. J. Watson, *Proc. Natl. Acad. Sci. U.S.A.*, 83 (1986) 5419.
2 M. L. Collins and W. R. Hunksaker, *Anal. Biochem.*, 151 (1985) 211.
3 S. V. Suggs, R. B. Wallace, T. Hirose, E. H. Kawashima and K. Itakura, *Proc. Natl. Acad. Sci. U.S.A.*, 78 (1981) 6613.
4 I. T. Nisbet and M. W. Beilharz, *Gene Anal. Tech.*, 2 (1985) 23.
5 R. K. Saiki, D. H. Gelfand, S. Stoffel, S. J. Scharf, R. Higuchi, G. T. Horn, K. B. Mullis and H. A. Erlich, *Science*, 239 (1988) 487.
6 G. R. Uhl, H. H. Zingg and J. F. Habener, *Proc. Natl. Acad. Sci. U.S.A.*, 82 (1985) 5555.
7 R. J. Britten, D. E. Graham and B. R. Neufeld, *Methods Enzymol.*, 29 (1974) 363.

8 J. Eisinger, *Biochem. Biophys. Rès. Commun.*, 43 (1971) 854.
9 S. K. Nigyogi and C. A. Thomas, Jr., *J. Biol. Chem.*, 243 (1968) 1220.
10 J. A. Abraham, A. Mergia, J. L. Whang, A. Tumulo, J. Friedman, K. A. Hjerrild, D. Gospodarowicz and J. C. Fiddes, *Science*, 233 (1986) 545.
11 M. Jaye, R. Hawk, W. Burgess, G. A. Ricca, I.-M. Chiu, M. W. Ravera, S. J. O'Brien, W. S. Modi, T. Maciag and W. N. Drohan, *Science*, 233 (1986) 541.
12 C. Dickson and G. Peters, *Nature (London)*, 326 (1987) 833.
13 M. Guthridge, J. Bertolini and M. T. W. Hearn, in preparation.
14 G. Copolla, J. Underwood, G. Cartwright and M. T. W. Hearn, *J. Chromatogr.*, 476 (1989) 269.

Journal of Chromatography, 476 (1989) 455–466
Elsevier Science Publishers B.V., Amsterdam — Printed in The Netherlands

CHROMSYMP. 1633

SEPARATION OF TWO MOLECULAR FORMS OF HUMAN ESTROGEN RECEPTOR BY HYDROPHOBIC INTERACTION CHROMATOGRAPHY

GRADIENT OPTIMIZATION AND TISSUE COMPARISON

SALMAN M. HYDER[a,*] and JAMES L. WITTLIFF

Hormone Receptor Laboratory, Department of Biochemistry, James Graham Brown Cancer Center, University of Louisville, Louisville, KY 40292 (U.S.A.)

SUMMARY

High-performance hydrophobic interaction chromatography (HPHIC) was used to separate and characterize two molecular forms of estrogen receptor with a SynChropak propyl hydrophobic column (300 Å pore size). The linear gradient utilized earlier with a polyether-bonded column (2 to 0 *M*) ammonium sulfate in 40 min, gave poor resolution with the propyl column. However, resolution was maximized with either an initial ammonium sulfate concentration of 1 *M* (40-min gradient) or with a two-phase gradient (2 to 0.5 *M* in 10 min, 0.5 to 0 *M* in 30 min). This indicated that the propyl column was more hydrophobic than the polyether column. Estrogen receptor separated into two isoforms, either in the presence [MI, retention time (t_R) = 13–14 min; MII, t_R = 20–21 min] or absence (I, t_R = 21–23 min; II, t_R = 31–33 min) of the estrogen receptor stabilizing reagent, sodium molybdate. Similar isoforms were observed in cytosols from human breast tumors, uterus, and MCF-7 breast cancer cells. Unlike others, MCF-7 estrogen receptor did not show MI. Since MCF-7 cells contain 90 000 dalton heat shock proteins (HSP-90), HSP-90 is probably not directly involved in MI formation. Sodium molybdate selectively interacted with isoform II and converted it to MI. All isoforms appeared to be high-molecular-weight proteins (> 60 Å) when subsequently analyzed by high-performance size-exclusion chromatography. Interestingly, when estrogen receptor was immobilized on the stationary phase, no change was detected in either hydrophobicity or steroid-binding capacity. After 16–18 h, immobilized receptor was eluted with a slightly longer t_R. During incubation on the column, component MI was converted into I and/or II. HPHIC appears to be a rapid, yet gentle procedure for isolating large receptor complexes in significant quantities with high recoveries. This allows one to discern the complicated structure–function relationships of estrogen receptor and associated non-receptor proteins and provides information about the on-column behavior of complex proteins.

[a] Present address: Department of Pharmacology, University of Texas Medical School, P.O. Box 20708, Houston, TX 77225, U.S.A.

0021-9673/89/$03.50

INTRODUCTION

Previous analyses of estrogen receptors from either human breast tumors or rat uterus by high-performance hydrophobic interaction chromatography (HPHIC) revealed the presence of two hydrophobic species of the ligand-binding form of the protein[1–8]. The two hydrophobic forms of receptors were detected either in the absence or presence of the receptor-stabilizing reagent, sodium molybdate[3,7]. Furthermore, one of the two isoforms of estrogen receptor detected contained an associated protein kinase activity[2] when immunoprecipitated with monoclonal Antibody D547, which was raised against the estrogen receptor molecule[9]. A thorough analysis of the detailed kinase reaction revealed that this is not an intrinsic property of receptor[3], although our earlier results suggested this[2,10,11]. In support of the latter observation, some estrogen receptor negative human breast tumors demonstrated the kinase reaction while other estrogen receptor positive tumors did not[3]. The consistent appearance of similar isoforms from several different samples of human breast tumors indicated that the presence of two molecular forms is not an artifact, nor are they dependent upon protein kinase activity.

Our analysis of estrogen receptor from a SynChropak propyl column revealed that both were hydrophobic isoforms of high molecular weight (> 65 Å), as judged by their elution in high-performance size-exclusion chromatography (HPSEC)[7,12,13]. Since the proteolyzed form of estrogen receptor did not aggregate, we concluded that the high-molecular-weight isoforms eluted from the hydrophobic column must contain the 60 000-dalton estrogen receptor molecule complexed with other cellular molecules, such as the heat-shock proteins and protein kinase(s)[2–4,7,13]. Similar evidence of this effect has been cited recently for androgen receptors[14].

In this paper we present data related to (a) optimization of the ammonium sulfate gradient conditions on a propyl-based hydrophobic column for the separation and resolution of estrogen receptor, based on their hydrophobicity; (b) the effect of sodium molybdate on selective interaction with the most hydrophobic form of estrogen receptor, converting it to the least hydrophobic form, (c) the effect of time on the HPHIC profile of the receptor, (d) the uniformity of hydrophobic elution patterns of estrogen receptor among different tissues, and (e) the usefulness of the hydrophobic column for storing receptors at 4°C in the immobilized form.

EXPERIMENTAL

Materials

Ammonium sulfate, (HPLC-grade) was obtained from Bio-Rad Labs. (Richmond, CA, U.S.A.). The ligand, [16α-^{125}I]iodoestradiol-17β (IE_2) (*ca.* 2200 Ci/mmol) was obtained from DuPont/New England Nuclear Products (Boston, MA, U.S.A.). Sodium molybdate, disodium ethylenediaminetetraacetic acid (EDTA) and glycerol were purchased from Fisher Scientific (Louisville, KY, U.S.A.). Unlabeled diethylstilbestrol (DES), which was used as an estrogen inhibitor, Norit A, Dextran T-70 and dithiothreitol (DTT) were obtained from Sigma (St. Louis, MO, U.S.A.).

Human breast tumor tissues from patients were provided by the various surgeons and pathologists at the local hospitals, cooperating with the Hormone Receptor Laboratory. The tissues were brought to the laboratory on dry ice and kept frozen

at −86°C until analyzed. Only residual tissue from clinical receptor analyses was used in this study.

Residual tissue from human uteri was obtained following hysterectomy for a variety of clinical conditions through the cooperation of the Pathology Departments at Norton Kosair Children's Hospital and at Humana Hospital University (Louisville, KY, U.S.A.). These tissues were weighed and immediately placed on ice and transported to the laboratory. Samples were taken for histopathology, and the remainder was stored at −86°C until utilized. A pilot study conducted in our clinical laboratory determined the status of estrogen receptor and progesterone receptor in these tissues by the titration assay[15,16].

Cell culture

MCF-7 cells were grown in Dulbecco's Modified Eagle Medium (DMEM) supplemented with 10% fetal calf serum (FCS). Cells were cultured in a humidified atmosphere of 5% carbon dioxide in air at 37°C. Cultures were again fed the same medium at intervals of 2–4 days; cells were subcultured at weekly intervals. Cells were grown to a density of approximately 60–70% confluency and kept with DMEM-containing 1 mg/ml bovine serum albumin (BSA) for 24 h before the start of an experiment. Confluent cells were harvested with the addition of trypsin EDTA solution (Sigma) and collected after centrifugation. The cells were washed once with P_{10}EDG buffer [10 m*M* potassium phosphate (pH 7.4), containing 1.5 m*M* EDTA, 1 m*M* DTT and 10% (v/v) glycerol] and collected. The cells were resuspended in P_{10}EDG and sonicated for 2 × 10 s at a setting of 60 in a Fisher Sonicator Model 300. The supernatant from high-speed centrifugation (105 000 *g*) was then prepared as described below.

Preparation and labeling of soluble estrogen receptor

All subsequent procedures were performed at 4°C in a Puffer–Hubbard cold box (Ashville, NC, U.S.A.). Human breast tumors and uterine tissue (*ca.* 200–400 mg/ml) were homogenized in P_{10}EDG. Homogenization was performed with two 10-s bursts in a Brinkman Polytron homogenizer (Westbury, NY, U.S.A.).

Soluble fractions were prepared by centrifugation of the homogenate for 30 min at 40 000 rpm in a Beckman Ti 70.1 rotor (Palo Alto, CA, U.S.A.). The supernatant was removed carefully, avoiding the layer of fat at the top. The soluble fractions were labeled with 2–3 n*M* IE_2 in the presence and absence of a 200-fold excess of DES for 2–4 h at 4°C. Free steroid was removed with dextran-coated charcoal after centrifuging the sample for 5 min at 1000 *g*. Cytosol protein concentrations were determined by the method of Bradford[17], using BSA as the standard. The protein concentrations generally ranged from 4 to 8 mg/ml.

HPHIC

All buffers were filtered under vacuum through Millipore (Bedford, MA, U.S.A.) 0.45-μm HAWP filters before use. Free steroid or estrogen receptor complexes were applied to the 10 cm × 4.6 mm I.D. silica-based SynChropak propyl column, obtained from SynChrom (Lafayette, IN, U.S.A.), using an Altex Model 210 sample injection valve (Beckman Instruments, San Ramon, CA, U.S.A.). Elution was carried out with a Beckman Model 114 delivery module, including a Model 421 system controller.

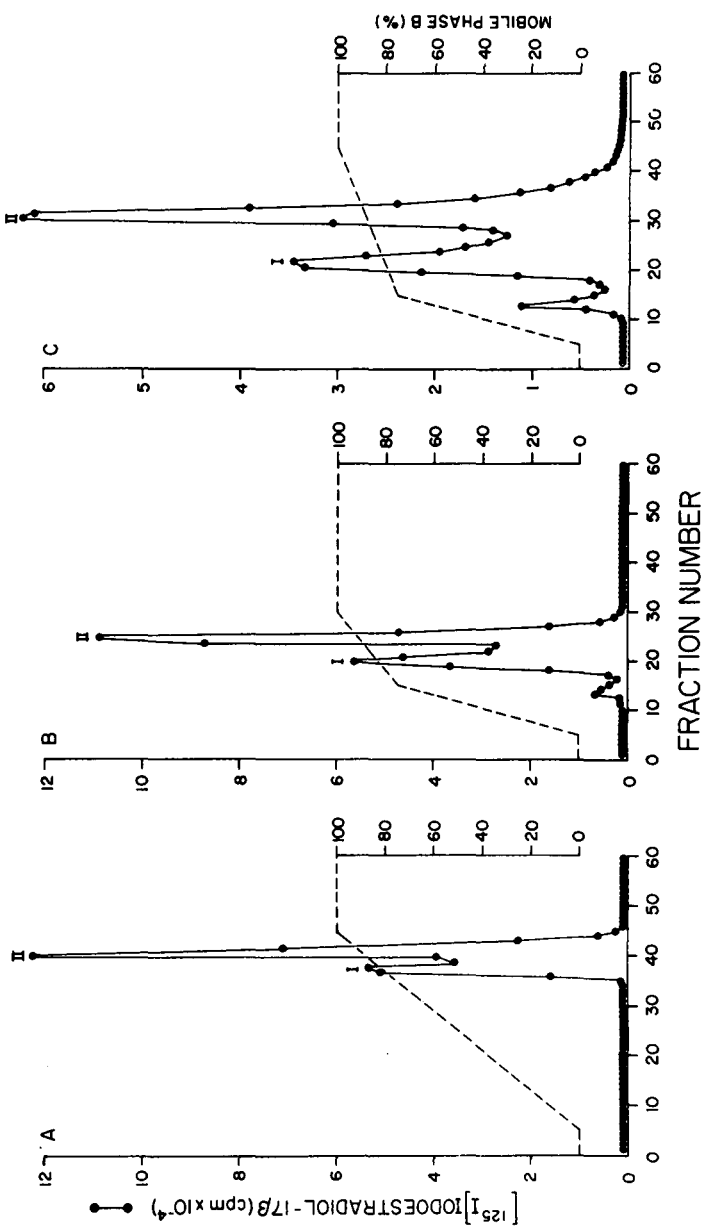

Fig. 1. Influence of gradient development time on HPHIC separation of estrogen receptor isoforms from human breast cancer. Dextran-coated charcoal-treated human breast tumor cytosol was injected into the SynChropak propyl column and chromatographed with gradient times reaching (A) 100% eluent B in 40 min, (B) 75% B in 10 min followed by 100% B in next 15 min and (C) 75% B in 10 min, followed by 100% B in 30 min. All samples were adjusted to 1.5 *M* ammonium sulfate prior to injection. Eluent A in this experiment was P_{10}EDG, containing 2 *M* ammonium sulfate; eluent B was P_{10}EDG. For clarity, only total cpm/fraction (●) are shown.

Unless otherwise stated, the gradient program for elution consisted of an starting eluent A (P_{10}EDG containing 2 *M* ammonium sulfate, pH 7.4) at a flow-rate of 1 ml/min and, following sample injection, a linear, descending salt gradient reaching 75% P_{10} EDG (eluent B) in 10 min, followed by 100% B in the next 30 min. Eluent B was maintained for the next 15 min before switching to 100% eluent A for reequilibration of the column.

In the initial phase of this study, other experimental gradients were developed. The conditions for these separations are listed in the individual figure legends.

Following chromatography, 1-ml fractions were collected, and free and protein-bound steroids were detected radiometrically in a Micromedics 4/600 gamma radioisotope detector (Rohm & Haas, Cleveland, OH, U.S.A.). The counting efficiency was 65%. Since the non-specific binding (radioactive steroid bound to cytosols labeled in the presence of DES) showed primarily base-levels, representing no more than 5–10% of the total binding, these are not shown in the figures. Recovery of specifically bound radioactive steroid was 80–100%.

HPSEC

Analytical size-exclusion columns (Spherogel TSK-3000 SW), particle size 10μm (600 × 7.5 mm I.D.) from Beckman Altex Instruments, were used for steroid receptor separation, as described previously[15,18]. HPLC was performed at 4°C with a Beckman 114 solvent delivery module, including a Model 421 system controller and injector block. Cytosol were applied in 100–200 μl volumes with a Hamilton syringe. The elution buffer (pH 7.4) at 4°C, was $PEDGK_{100}$ [10 m*M* potassium phosphate buffer (pH 7.4), 1.5 m*M* EDTA, 1 m*M* DTT, 10% (v/v) glycerol, 100 m*M* potassium chloride]. All buffers were filtered through a 0.45-μm filter (Millipore). Elution was carried out at a flow-rate of 0.7 ml/min. Fractions were collected at 0.5-min intervals in 12 × 75 mm tubes. Recoveries were in the range of 75–100%.

RESULTS AND DISCUSSION

The usefulness of HPHIC in the separation and analysis of proteins without denaturation has been discussed earlier[4,6,19] and we have applied this technique to the detailed characterization of estrogen receptor previously[1–8,11–13]. These analyses were performed on both a polyether-linked silica-based stationary phase, which is non-ionic in nature, and on a propyl column with a mobile phase containing organic solvent. To extend these studies and rule out the possibility of column-induced effects, a mobile phase without organic solvent was designed to be employed with a three-carbon chain (proprietary chemistry) hydrophobic column (SynChrom propyl).

Gradient optimization

When HPHIC was performed on the SynChrom propyl column under the same conditions as those used with the polyether-bonded phase, 2 to 0 *M* ammonium sulfate in 40 min, estrogen receptor was eluted with a longer retention time (t_R = 38 min for peak I and t_R = 41 min peak II) from the propyl column (Fig. 1A) than (t_R = 26 min for peak I and t_R = 34 min for peak II) from the polyether-based column[3]. Although the resolution on the propyl was not optimal under these conditions, the results were in agreement with previous experiments, where two receptor isoforms

were observed. This confirms that the propyl column is more hydrophobic in nature than the polyether-based column, yet estrogen receptor was not denatured.

To enhance resolution of the estrogen receptor isoforms, the gradient conditions were modified to reach 75% B in 10 min and, in a second phase, to reach 100% B in 15 min (Fig. 1B). This increased the relative resolution slightly. Also, a minor third peak (t_R = 13 min) was observed, which had been ignored initially. However, the majority of molybdate-stabilized receptor, which we have termed MI was eluted at this retention time (see Discussion below). A better resolution of receptor isoforms was observed when the second phase of the gradient was extended to reach 100% eluent B in 30 min (Fig. 1C).

Since the propyl column was more hydrophobic, the effect of starting the gradient at a lower ionic strength was analyzed on the basis of the retention of the estrogen receptor molecule. Fig. 2A demonstrates that when the initial ionic strength of ammonium sulfate was 1 *M*, the separation of estrogen receptor was comparable to that with 2 *M* ammonium sulfate as the starting buffer (Fig. 1C). The sample concentration was also adjusted to 1 *M* ammonium sulfate prior to injection. However, when the initial concentration of eluent A was lowered to 0.5 *M* ammonium sulfate, a considerable proportion of receptor protein was not bound to the bonded phase. This occurred regardless of whether the sample concentration was adjusted to 0.5 *M* ammonium sulfate (Fig. 2B) or to 1.0 *M* ammonium sulfate (Fig. 2C) prior to sample application. Therefore, it is imperative that a critical ammonium sulfate concentration be reached both in eluent A and in the receptor preparation to insure immobilization of the proteins on the bonded phase. This probably reflects the removal of water molecules associated with the receptor protein, which is known to be ionic[11,20] or water molecules from associated proteins.

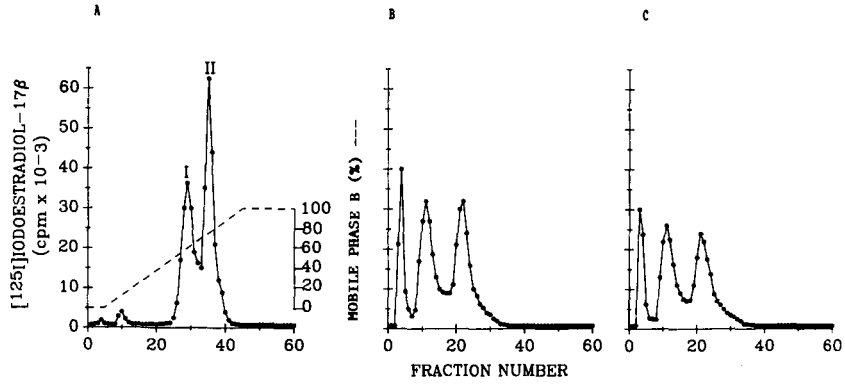

Fig. 2. Influence of the initial ionic strength on the separation of estrogen receptor isoforms in human breast tumor cytosol. Human breast tumor cytosol was injected into the SynChropak propyl column and chromatographed with a 1 to 0 *M* ammonium sulfate gradient in 40 min with prior adjustment of cytosol to 1 *M* ammonium sulfate (A). In (B) the same cytosol was chromatographed with a 0.5 to 0 *M* ammonium sulfate gradient with adjustment of the cytosol to 0.5 *M* ammonium sulfate. In (C) the conditions were the same as in (B), except that the cytosol was adjusted to 1.0 *M* ammonium sulfate prior to injection. ● = total cpm/fraction.

Effect of sodium molybdate on the hydrophobic properties of estrogen receptor

A previous study[3] indicated that once estrogen receptor was bound to the polyether-bonded hydrophobic column, only one of the two isoforms (isoform II) was displaced by molybdate-containing buffers and converted to MI. This behavior of isoform II was also observed for the propyl column (Fig. 3). It indicates that only one of the two receptor isoforms contains a molybdate-sensitive contact site, which may be near the DNA-binding domain. The sequence of estrogen receptor indicates that a small hydrophobic region exists in this domain[21]. It should be stressed that MI has been observed even in the absence of molybdate (*e.g.*, Fig. 3), suggesting that the receptor first exists in this least hydrophobic form on the column and then either dissociates into II or assumes another conformation (expressed as II), which is more hydrophobic.

Influence of time on HPHIC and HPSEC of estrogen receptor isoforms

In agreement with our observations with the polyether column[2], the hydrophobic properties of estrogen receptor from human breast cancer changed when this receptor was incubated overnight in the presence of IE_2 at 4°C (Fig. 4A and B). When analyzed after a short incubation with the steroid, the receptor was eluted as isoforms I and II. The longer incubation (18–24 h) at 4°C, converted isoform II into isoform I. Since the receptor may have been proteolyzed with time, resulting in the elution of receptors as the single peak I, receptor size was monitored by HPSEC. Trypsinized or proteolyzed receptor was eluted as a single, sharp peak at 25–30 Å which retained the steroid-binding domain[5]. The receptor is known to dissociate from other complex macromolecules, such as HSP-90[20,22] with time, to produce a non-proteolyzed form.

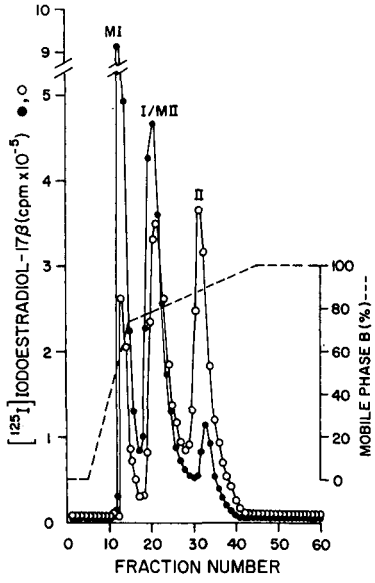

Fig. 3. Comparison of estrogen receptor isoforms separated by HPHIC in the absence and presence of 10 m*M* sodium molybdate. Breast cancer cytosol was prepared in buffer lacking molybdate. Samples were injected into the propyl column and eluted with buffers lacking (○) or containing (●) 10 m*M* sodium molybdate.

which is also eluted in the 25–30 Å range in HPSEC and is difficult to separate from the proteolyzed form[20]. This process can be accelerated with potassium chloride in buffers. Although some of the 65-Å receptor complex was transformed to the 30-Å species during a 24-h incubation (Fig. 4C and D), this conversion cannot be responsible for the extensive change in receptor hydrophobicity (Fig. 4A and B). This suggests that receptor size and hydrophobicity are unrelated.

Tissue distribution of estrogen receptor isoforms

Estrogen receptors from both human uterus and human breast cancer cells in culture were analyzed for their hydrophobic properties. Estrogen receptor separated into two isoforms, whether obtained from uterus (Fig. 5A) or from breast cancer cells (Fig. 5B). The retention times of the isoforms were the same as those of receptors separated from human breast tumor cytosols. This indicates that estrogen receptor in different tissues undergoes similar post-translational modifications and associates with similar proteins[20]. A protein known to interact with estrogen receptor is HSP-90, which has been detected in many different tissues[23]. Using monoclonal antibody raised against HSP-90 from chick oviduct, HSP-90 was detected only in the MI isoform[23].

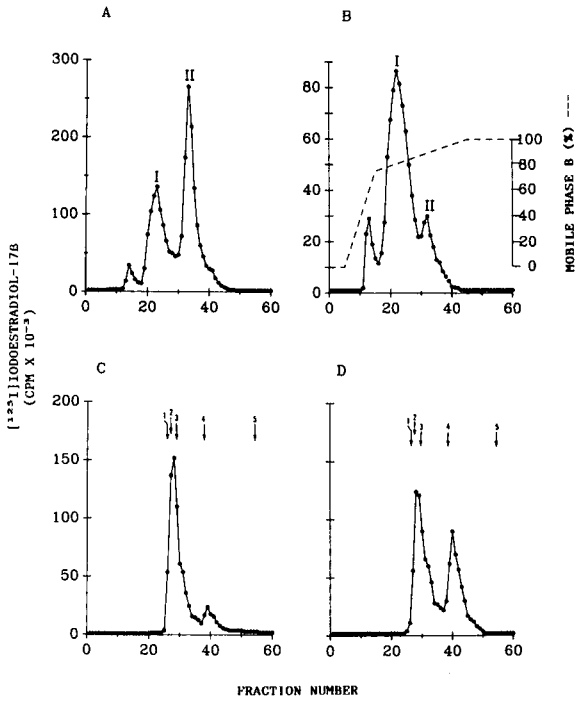

Fig. 4. Influence of time on HPHIC and HPSEC profiles of estrogen receptor isoforms. Human breast cancer cytosol was prepared as described in the Experimental section and incubated with IE_2. Following a 3-h incubation at 4°C, samples were injected simultaneously into (A) the propyl column and (C) the TSK-3000 SW size-exclusion column. A second sample was injected following a 24-h incubation of the cytosol into (B) the propyl and (D) the size-exclusion column. For details of methods see Experimental. The void volume is represented by (1). Markers used were ferritin (2), catalase (3), hemoglobin (4) and cytochrome *c* (5).

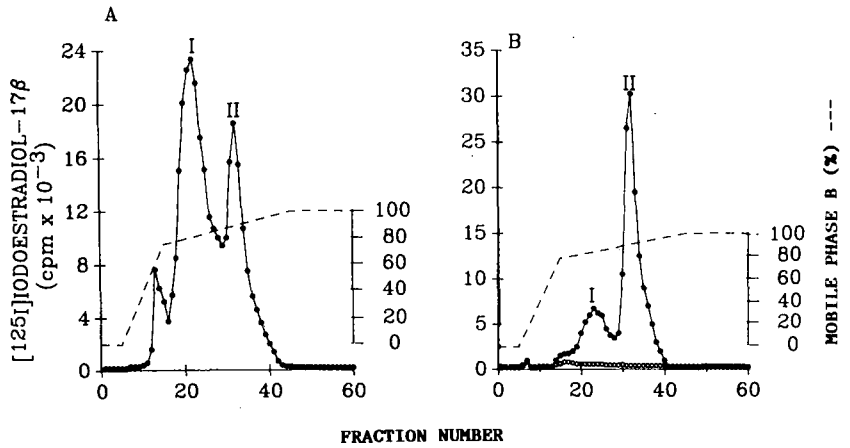

Fig. 5. HPHIC of estrogen receptor from human uterine tissue (A) and MCF-7 human breast cancer cells (B). Extraction and labelling conditions for estrogen receptor were as described in the Experimental section. Separation conditions were the same as described in the legend to Fig. 1.

We made the interesting observation that estrogen receptor, obtained from MCF-7 cells, exhibits little (5%) isoform MI when homogenized in the presence of sodium molybdate (Fig. 6). Since MCF-7 cytosol contained HSP-90[23], isoform MI was expected to be in the form of an estrogen receptor–HSP-90 complex[8]. It now appears that HSP-90 itself is not the contact domain for isoform MI. Rather, the receptor protein interacts with the stationary phase directly, or the equilibrium conditions for estrogen receptor–HSP-90 association in the MCF-7 cell cytosol are different. Nevertheless, hydrophobic heterogeneity of receptor isoforms from MCF-7 cells was observed. Collectively, these results suggest a common mechanism of steroid hormone receptor assembly in normal and neoplastic tissues, as judged by surface hydrophobicity.

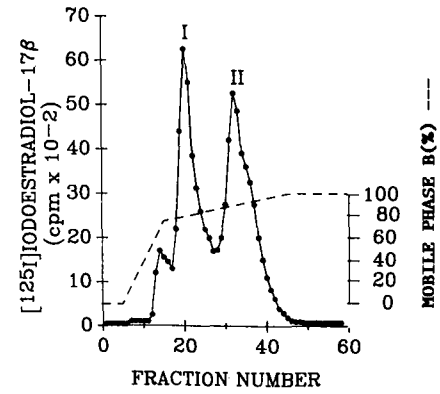

Fig. 6. Influence of sodium molybdate on HPHIC of estrogen receptor from human breast cancer cells. The extraction and labelling conditions for estrogen receptor were as described in the Experimental section, except that the extraction buffers contained 10 m*M* sodium molybdate. Samples were injected into the propyl column and eluted with buffers containing 10 m*M* sodium molybdate.

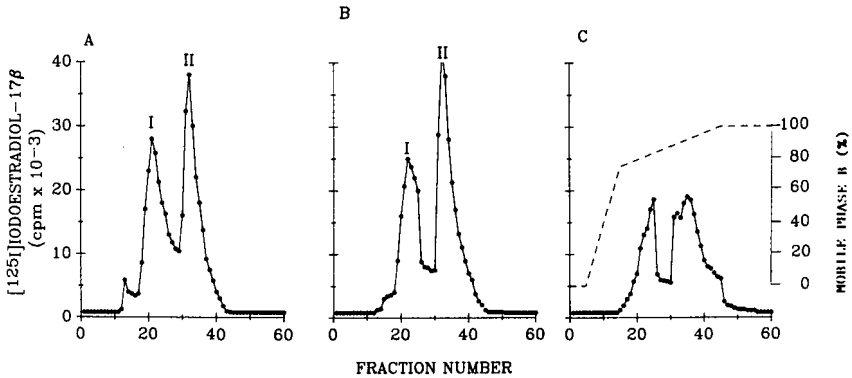

Fig. 7. Influence of contact time of stationary with estrogen receptor on HPHIC separation of estrogen receptor isoforms from human breast cancer cytosol. Dextran-coated charcoal-treated cytosol was injected into the propyl column and eluted with a 2 to 0 *M* ammonium sulfate gradient. (A) control, (B) elution after 90 min, (C) elution after 16 h contact with the stationary phase. After 16 h, the total loss of receptor concentration in the cytosol was 30% of the control. Recoveries of radioactive steroid in all the cases were 80–100%.

Influence of contact time of receptor with the stationary phase

Steroid receptors are known to be labile proteins, found in very small amounts in target cells. This makes their isolation and study extremely difficult[4,6,8,16]. Properties of the hydrophobic stationary phase were investigated for separation and characterization of estrogen receptor isoforms and as a means of storing receptor protein without denaturation for short and long periods. Fig. 7 illustrates a representative experiment demonstrating that estrogen receptor eluted as isoforms I and II in control cytosol (Fig. 7A) and retains its chromatographic characteristics when immobilized on the stationary phase for 90 min at 4°C (Fig. 7B). However, when the receptor was in contact with the stationary phase for 16 h at 4°C, the peak characteristics and elution patterns were altered (Fig. 7C). Curiously, both isoform I and isoform II were eluted with t_R values that were 3 min longer than those observed for the control. Since the experimental conditions were identical, except for the holding time, these results suggest unfolding of the protein with an increase in hydrophobicity. It is intriguing that both receptor forms showed a similar change in hydrophobicity, suggesting a common event. Both receptor isoforms retained their ligand-binding properties, indicating that extensive denaturation did not occur.

CONCLUSION

In several of our previous publications[4,6,8,16] we discussed the usefulness of high-performance liquid chromatography (HPLC) for the rapid separation of steroid receptor isoforms. The synthesis of several hydrophobic bonded phases allows separating labile proteins, such as the estrogen receptor, without obvious denaturation[4]. Separation of two different high-molecular-weight proteins, based on their relative hydrophobicity, was a novel finding[7,13]. Although a single high-molecular-weight receptor species was observed by HPSEC[2,7], we demonstrated that this peak is composed of two distinct hydrophobic isoforms[7,12,13]. The basis of this polymorphism is of interest, since the sequence of the cloned gene predicts only a single 65 000-dalton

component[21]. Steroid receptors are known to be phosphoproteins[24]. Therefore, different degrees of phosphorylation would alter surface ionic properties, allowing the formation of different complexes, even with non-receptor proteins. Also, the modified receptors themselves may interact directly with the bonded phase. Further purification of individual isoforms is required to elucidate the nature of interaction of the receptor protein(s) with the bonded phase.

Another novel finding reported in this paper is that different human tissues, such as the breast, uterus, and MCF-7 breast cancer cells in culture show a remarkably similar hydrophobic isoform distribution in the absence of molybdate. Our previous analysis with rat uterine estrogen receptor gave identical results[2,3]. This indicates that (i) the post-translational modifications of estrogen receptor are common in different tissues and (ii) a single homologous gene is responsible for expression of estrogen receptor. The gene for estrogen receptor from several sources has been cloned and appears similar in sequence[21,25]. Although alternative initiation sites on DNA or alternate splicing of mRNA could give rise to different steroid receptor protein isoforms, accounting for receptor polymorphism, this has been ruled out in the case of the progesterone receptor[26]. It has been shown for the latter that proteolysis may account for these differences. Proteolysis does not appear to contribute to the formation of the two hydrophobic forms of estrogen receptor, since overnight incubation of receptor gives rise to the same isoforms (judged on the basis of size) as those observed in the control cytosol. Proteolyzed receptor is eluted from a size-exclusion column as a single, sharp peak[27] at 25–30 Å.

It is unclear why isoform II from human breast cancer cells was not converted to MI in the presence of sodium molybdate. In rat and human breast tumor cytosol, interconversion was consistent[2,3]. Since molybdate prevents DNA binding of the receptor, isoform II interconversion is attributed to the interaction of the oxy anion with the DNA-binding domain of the receptor. The transformation process should be a common event. The lack of MI in the HPHIC elution pattern of estrogen receptor from human breast cells is puzzling, particularly since MCF-7 cells contain HSP-90[23]. Perhaps molybdate associates with another domain on the receptor molecule, permitting the formation of different complexes.

Finally, immobilization of estrogen receptor from human breast cancer tissues on the hydrophobic column exhibited no change in the hydrophobicity of either isoform for up to 90 min. Longer retention (16–24 h) resulted in slight alteration of hydrophobicity of both receptor isoforms. With improved conditions, one may be able to transport the receptor in this immobilized form from one laboratory to another for analyses, such as protein sequencing.

An interesting observation was made here with respect to receptor interconversion. When the receptor is left overnight in solution, it is transformed into a single peak. In the immobilized form, this conversion does not take place even after 16–24 h of incubation. This indicates that a significant hydrophobic transformation takes place in solution due to an enzymatic process, such as protein phosphorylation/dephosphorylation, ribosylation, or acetylation, which is inhibited on the column. The inhibition of such an enzymatic activity could be due either to binding of the enzyme to the stationary phase with its catalytic site rendered inaccessible to substrate (receptor) or to the binding of the receptor to the column with the proteolytic domain hidden at the contact site.

The complexity of steroid receptor proteins with multiple binding domains for steroid, DNA and associated proteins and their labile nature hinder their investigation in small specimens, such as cultured cells. HPHIC, as developed in our laboratory, using estrogen receptor as a model protein, provides a sensitive means of working with femtomolar quantities of a specific regulatory protein without destroying its biological activity. This study shows that surface properties of proteins may be used to distinguish subtle alterations in receptor configurations which may relate to the mechanism of action of steroid receptors. Changes in receptor hydrophobicity appear to reflect several events in the natural history of the receptor as it is synthesized on the endoplasmic reticulum, during the process of receptor activation which brings about its ability to bind DNA and to initiate gene transcription, its dissociation from the DNA, and its subsequent turnover.

ACKNOWLEDGEMENTS

This research was supported in part by grants from Phi Beta Psi Sorority and from National Cancer Institute CA-42154.

REFERENCES

1 S. M. Hyder, R. D. Weihle, D. W. Brandt and J. L. Wittliff, *J. Chromatogr.*, 327 (1985) 237.
2 S. M. Hyder, N. Sato and J. L. Wittliff, *J. Chromatogr.*, 397 (1987) 251.
3 S. M. Hyder, N. Sato, W. Hogancamp and J. L. Wittliff, *J. Steroid Biochem.*, 29 (1988) 197.
4 S. M. Hyder and J. L. Wittliff, *BioChromatography*, 2 (1987) 121.
5 S. M. Hyder and J. L. Wittliff, *J. Chromatogr.*, 44 (1988) 225.
6 S. M. Hyder and J. L. Wittliff, in F. Ausubel, R. Brent, R. Kingsdon, D. Moore, J. A. Smith, J. Seidman and K. Struhl (Editors), *Current Protocols in Molecular Biology*, Greene Publishing, New York, 1987, p. 10.15.1.
7 S. M. Hyder and J. L. Wittliff, *J. Steroid Biochem.*, (1989) in press.
8 J. L. Wittliff, J. Allegra, T. Day, Jr. and S. M. Hyder, in V. K. Moudgil (Editor), *Steroid Receptors in Health and Disease*, Plenum Press, New York, 1988, p. 287.
9 G. L. Greene, C. Nolan, J. P. Engler and E. V. Jensen, *Proc. Natl. Acad. Sci. U.S.A.*, 77 (1980) 5115.
10 A. Baldi, D. M. Boyle and J. L. Wittliff, *Biochem, Biophys. Res. Commun.*, 135 (1986) 597.
11 J. L. Wittliff, R. D. Wiehle and S. M. Hyder, in A. Kerlavage (Editor), *Receptor Biochemistry and Methodology*, Alan R. Liss, New York, in press.
12 S. M. Hyder and J. L. Wittliff, *70th Endocrine Society Meeting, New Orleans, LA, 1988*, p. 348.
13 S. M. Hyder, N. Heer and J. L. Wittliff, presented at *8th International Symposium on HPLC of Proteins, Peptides and Polynucleotides, Copenhagen, 1988.*
14 Y. Ohara-Nemoto, T. Nemoto, N. Sato and M. Ota, *J. Steroid Biochem.*, 31 (1988) 295.
15 S. M. Hyder, F. P. Kohrs and J. L. Wittliff, *J. Chromatogr.*, 397 (1987) 269.
16 J. L. Wittliff, in W. Donegan and J. Spratt (Editors), *Steroid Receptor Analysis, Quality Control and Clinical Significance*, W. B. Saunders Co., Philadelphia, PA, 1988, p. 303.
17 M. M. Bradford, *Anal. Biochem.* 72 (1976) 248.
18 R. D. Wiehle, G. E. Hofmann, A. Fuchs and J. L. Wittliff, *J. Chromatogr.*, 307 (1984) 39.
19 N. T. Miller, B. Feibush, K. Corina, S. P. Lee and B. L. Karger, *Anal. Biochem.*, 148 (1985) 510.
20 S. M. Hyder, N. Shahabi and J. L. Wittliff, *BioChromatography*, 3 (1988) 216.
21 R. M. Evans, *Science (Washington, D.C.)*, 240 (1988) 889.
22 W. P. Sullivan, B. T. Sullivan, V. J. Vroman, R. K. Bauer, R. M. Puri, G. R. Pearson and D. O. Toft, *Biochemistry*, 24 (1985) 6586.
23 D. Toft, personal communication.
24 V. K. Moudgil (Editor), *Steroid Receptors in Health and Disease*, Plenum Press, New York, 1988.
25 L. A. Shepel and J. Gorski, *BioFactors*, 1 (1988) 71.
26 M. Misrahi, H. Loosfelt, M. Atger, C. Merid, V. Zerah, P. Dessen and E. Milgram, *Nucleic Acids Res.*, 16 (1988) 5459.
27 N. Sato, S. M. Hyder, L. Chang, A. Thais and J. L. Wittliff, *J. Chromatogr.*, 359 (1988) 475.

Journal of Chromatography, 476 (1989) 467–475
Elsevier Science Publishers B.V., Amsterdam — Printed in The Netherlands

CHROMSYMP. 1605

HIGH-PERFORMANCE LIQUID CHROMATOFOCUSING AND COLUMN AFFINITY CHROMATOGRAPHY OF *IN VITRO* ^{14}C-GLYCATED HUMAN SERUM ALBUMIN

DEMONSTRATION OF A GLYCATION-INDUCED ANIONIC HETEROGENEITY

P. VIDAL*
Hagedorn Research Laboratory, 6 Niels Steensensvej, DK-2820 Gentofte (Denmark)
T. DECKERT
Steno Memorial Hospital, 2 Niels Steensensvej, DK-2820 Gentofte (Denmark)
and
B. HANSEN and B. S. WELINDER
Hagedorn Research Laboratory, 6 Niels Steensensvej, DK-2820 Gentofte (Denmark)

SUMMARY

High-performance liquid chromatofocusing of human serum albumin (HSA) after *in vitro* glycation with purified [^{14}C]glucose has shown that with increasing glycation time a progressive increase in two major anionic fractions (p*I* 4.8 and 4.65) occurs, while the p*I* 4.9 fraction decreases in parallel. As early as after 5 days of glycation time, the [^{14}C]glucose content in the anionic fractions was markedly higher than in the p*I* 4.9 fraction. After 10 and 15 days of glycation, a considerable heterogeneity of 10–15 components could be demonstrated. In addition, phenylboronic acid (PBA) affinity chromatography was applied and an enrichment of the more glycated species could be obtained using this method. We conclude that, in contrast to previous reports, glycation of HSA induces anionic heterogeneity (in accordance with the theoretically expected loss of positively charged amino groups) and, although the efficiency in separating non-glycated from monoglycated HSA was found to be very low, an enrichment of these anionic species can be achieved using PBA affinity chromatography.

INTRODUCTION

In previous studies we have demonstrated a different renal clearance of glycated[a] and non-glycated albumin in diabetics with incipient nephropathy[2,3]. The reason for this difference could be a varying surface charge of glycated and non-glycated albumin

[a] According to the recomendations of the IUB (International Union of Biochemistry) and IUPAC (International Union of Pure and Applied Chemistry)[1], "glycation" is used instead of "glycosylation" or "glucosylation" to refer to the non-enzymatic reaction between glucose and free amino groups of proteins.

0021-9673/89/$03.50

or of the glomerular barrier. As a cationic charge heterogeneity of glycated albumin has been reported[4–7], which, however, is different from that theoretically expected, we have studied the electrical charge of glycated human serum albumin after 0–15 days of *in vitro* glycation with purified [^{14}C]glucose. In a previous study[8] we have demonstrated an anionic heterogeneity (using isoelectric focusing, pH 4–6.5) contradictionary to other studies[4–7], and in this paper we report the results obtained by using high-performance liquid chromatofocusing (HPLCF) before and after phenylboronic acid (PBA) affinity chromatography.

EXPERIMENTAL

Purification of [^{14}C]glucose

Fast-reacting contaminants of [U-^{14}C]glucose (Amersham International, Amersham, U.K.) were removed by incubation with human serum albumin coupled to a vinyl sulphone agarose matrix (Mini-Leak; Kem-En-Tec, Hellerup, Denmark) for 36 h at 37°C in 0.1 M phosphate buffer (pH 7.4) containing 0.15 M NaCl and 0.02% NaN_3 as described[8].

In vitro glycation of albumin

Crystalline human serum albumin (HSA) (Behringwerke, Marburg, F.R.G.) was dissolved in 0.1 M phosphate buffer (pH 7.4) containing 0.15 M NaCl, 0.02% NaN_3 and 50 mM [^{14}C]-D(+)-glucose (specific activity 6 μCi/mg). The solution was filtered through a 0.22-μm Millex filter (Millipore, Tåstrup, Denmark) and incubated for 0–15 days at 37°C in a shaking bath (30 cycles/min). Albumin samples incubated without glucose and with non-labelled glucose were also included. Salts, glucose and non-covalently bound glucose were separated from the HSA using a 95 × 2.5 cm I.D. Sephadex G-50 column eluted with 0.1 M ammonium hydrogen carbonate (pH 8.0) at 28 ml/h. Incubation of HSA for 0, 5, 10 and 15 days resulted in an activity of 0.9, 19.9, 47.5 and 70.3 · 10^3 dpm per mg of protein.

Affinity chromatography

Prepacked microcolumns containing 1 ml of aminophenylboronic acid immobilized to agarose (Glycogel B) (Pierce, Rockford, IL, U.S.A.) were used as described[9] for the separation of glycated and non-glycated albumin. As it has been reported that column overloading might influence this separation[10], 5 mg in addition to 0.01–0.08 mg of protein were loaded on the affinity columns. Fractions of 0.5 ml were collected and 50 μl of each fraction, mixed with 2.5 ml of Hi-Safe Optiphase scintillation cocktail (LKB, Hillerød, Denmark), were analysed for radioactivity in a Tri-Carb 460 liquid scintillation counter (Packard, Downers Grove, IL, U.S.A.). The counting efficiency was >95%. UV absorption at 280 nm was measured in 450 μl of each fraction diluted 1:1 in elution buffer using a Uvicon 810 spectrophotometer (Kontron, Zurich, Switzerland).

High-performance liquid chromatofocusing

HPLCF was performed on a 200 × 5 mm I.D. Mono P HR 5/20 column (Pharmacia, Hillerød, Denmark), equilibrated with different non-denaturing and denaturing buffers at several pH ranges between 4 and 8, followed by Polybuffer 74

(Pharmacia) in a more acidic range (above pH 4.0). The non-denaturing buffers used were 0.025 M Bis–Tris–HCl, 0.025 *M* imidazole–HCl and 0.025 *M* methylpiperazine–HCl. As denaturing buffers, 7 *M* urea, 50% ethylene glycol or 50% glycerol were used. The best separation was achieved using 12 ml of 0.025 *M* methylpiperazine–HCl (pH 5.7) followed by 27 ml of Polybuffer 74, diluted 1:10, at pH 4.39. An SP 8700 chromatograph (Spectra-Physics, Santa Clara, CA, U.S.A.) plus a U6K injector (Millipore Waters, Milford, MA, U.S.A.) were used throughout. The flow-rate was 0.5 ml/min and the absorption at 280 nm was monitored continously using a UV-VIS 200 detector (Linear Instruments, Reno, NE, U.S.A.). Fractions of 250 μl were mixed with 2.5 ml of HiSafe-Optiphase and analysed for radioactivity as described above. Before HPLCF, samples obtained from the phenylboronic acid affinity chromatography were desalted using Sephadex G-25 microcolumns (PD-10 columns from Pharmacia). Samples were eluted with 0.1 *M* ammonium hydrogencarbonate, lyophilized and dissolved in HPLCF equilibrating buffer before injection.

RESULTS

With increasing glycation time a progressive increase in two major anionic fractions of HSA (*ca.* p*I* 4.8 and 4.65) could be demonstrated using HPLCF (Figs. 1 and 2), while the p*I* 4.9 fraction decreased in parallel. Under denaturing conditions (*e.g.*, 7 M urea) similar patterns were found, but at a markedly higher pH range, approximately one pH unit higher (data not shown).

When the radioactivity corresponding to [^{14}C]glucose incorporated into HSA was analysed, the main increase in radioactivity, from 0 to 15 days of glycation, was found in the anionic components, and a considerable heterogeneity (more than ten components) could be demonstrated after 10–15 days of incubation (Fig. 2).

After PBA affinity chromatography of the same samples (from 0 to 15 days of glycation) a progressive increase in the bound fraction could be demonstrated (Fig. 3A). Further, the specific activity [^{14}C]glucose/mg HSA) of the bound fraction increased with increasing glycation time, but a parallel increase in specific activity was found in the unbound fraction (Fig. 3B). Even when minimal amounts of protein were

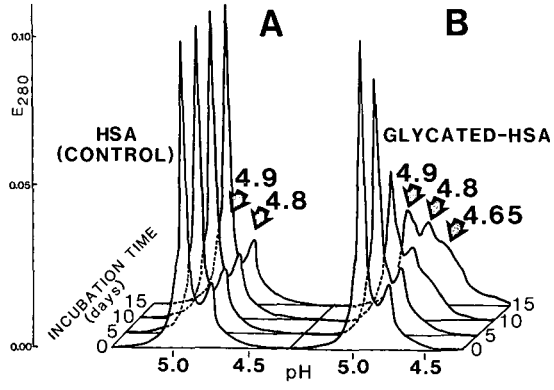

Fig. 1. HPLCF of HSA after 0–15 days of *in vitro* glycation, showing a progressive increase in two main fractions (p*I* 4.8 and 4.6) at the expenses of the first (p*I* 4.9). (A) HSA incubated without glucose; (B) HSA incubated with glucose.

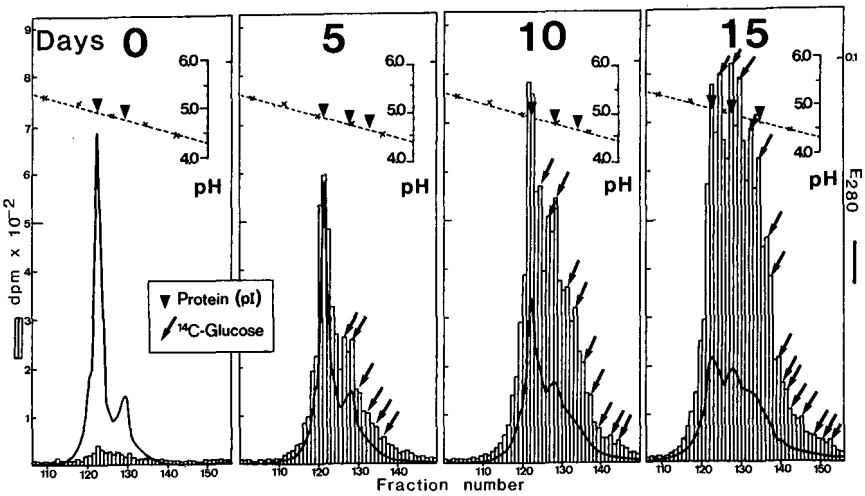

Fig. 2. UV and radioactivity HPLCF profiles of HSA after *in vitro* glycation with purified [^{14}C]glucose, showing the progressive increase in the [^{14}C]glycosyl adducts in the anionic range with, in addition, a considerable heterogeneity.

applied (in order to avoid column overloading), approximately half of the total radioactivity applied was found in the unbound fraction (Fig. 4). By adding the corresponding percentage of glycated protein present in the unbound fraction (calculated from the radioactive profiles and after correction of the column overloading) to the percentage of glycated HSA obtained from the protein profile,

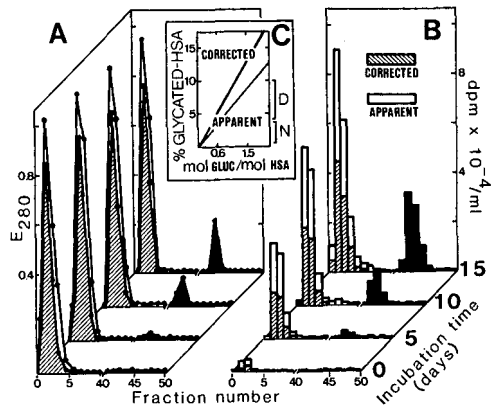

Fig. 3. Glycogel B affinity chromatography of 5 mg of *in vitro* [^{14}C]glycated HSA before and after correction for column overloading. Calculations were made using peak areas instead of peak height. (A) UV-profiles (A_{280}); (B) radioactive profiles (dpm/ml); "apparent", obtained by Glycogel B chromatography alone; "corrected", after elimination of the column overloaded protein. (C) indicates the underestimation of glycated HSA (percentage) obtainable by Glycogel B affinity chromatography used alone ("apparent") and that calculated from the radioactivity profiles after correction for column overloading ("corrected"). N and D, range of glycated HSA in normals and diabetics, respectively (as reported using the same chromatographic matrix[11–13]).

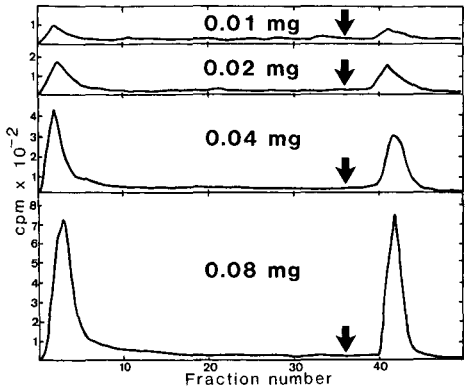

Fig. 4. Glycogel B affinity chromatography of 0.01–0.08 mg of 15-day glycated HSA. Arrows indicate buffer change.

a noticeable underestimation of the glycation extent could be demonstrated when the PBA chromatography was used alone (Fig. 3A–C).

In Fig. 5, the glucose content calculated for the PBA and HPLCF fractions is shown. Even at the pathophysiological glycation range observed in HSA (*i.e.*, an average glucose content of below 1 mol per mol HSA, according to refs. 2, 3 and 14), it is possible to demonstrate the presence of glycated HSA in the PBA-unbound fraction (Fig. 5A). Nevertheless, the glucose content in this fraction did not rise above 1 mol per mol HSA during the incubation time studied here. Parallel to this analysis, a higher glucose content in the anionic fractions (p*I* 4.8 and 4.65) could be demonstrated using HPLCF, while the p*I* 4.9 had a markedely lower glucose content (Fig. 5B).

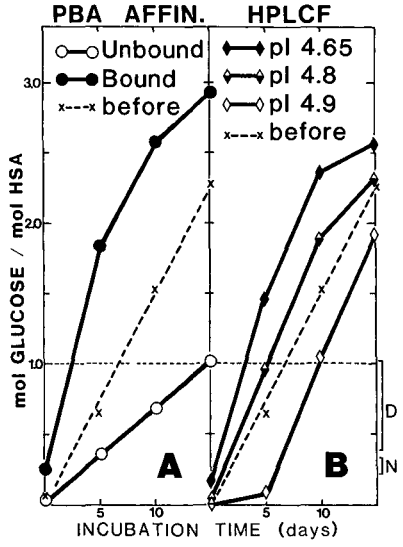

Fig. 5. Glucose content in different fractions of glycated HSA after (A) PBA affinity chromatography and (B) HPLCF. PBA-unbound values have been corrected for protein overloading. N and D indicate the range of glucose contents reported in normals and diabetic patients[2,3,14] using the furosine method.

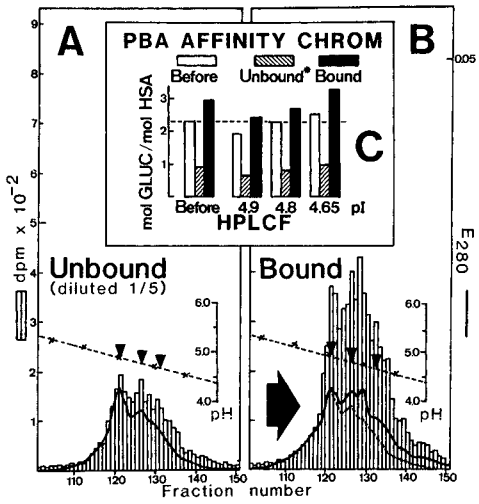

Fig. 6. Protein and radioactive HPLCF profiles of 15-day glycated HSA after PBA affinity chromatography. (A) Unbound fraction; (B) bound fraction. A dashed profile indicates the protein pattern obtained in A for comparison (arrowed). (C) indicates the glucose content of the HPLCF subfractions from PBA chromatography. * The PBA-unbound values have been corrected for column overloading.

When the bound and unbound fractions after PBA affinity chromatography were analysed separateley by HPLCF, noticeable amounts of radioactivity were also found to remain in the unbound fraction (Fig. 6A). Although radioactivity corresponding to the column overloading was included in this fraction, a larger amount of anionic species was found in the bound than in the unbound fraction (Fig. 6B). These anionic species were found to contain an increased heterogeneity (Fig. 6B) and a progressively increasing amount of glucose (Fig. 6C).

DISCUSSION

The present results confirm our previous studies using isoelectric focusing[8], but conflicts with other reports[4–7] because the observed heterogeneity is shown to be an anionic heterogeneity: more than ten anionic components were demonstrated after 15 days of glycation when the [^{14}C]glucose incorporated into the albumin was analysed. The demonstration of an increased amount of anionic fractions of glycated albumin is in accord with the theoretically expected loss of positively charged amino groups due to glycation[15].

We have previously demonstrated a reduced clearance of glycated albumin compared with the non-glycated albumin in diabetic patients with incipient nephropathy[2,3], and this reduced clearance of the glycated HSA may now be better explained by the interaction between a more heterogeneously anionic glycated albumin (as has been demonstrated above) and a less anionic glomerular barrier, owing to a loss of anionic charge in the glomerular membrane, possibly resulting from reduced incorporation of heparan sulphate[16].

An increased p*I* of albumin analysed under denaturating conditions is in accord

with previous data[17,18], and may be explained by changes in the three-dimensional structure (*i.e.*, partial or total unfolding), leading to a different surface charge distribution.

It should be noted that considerable amounts of glycated albumins (expressed as radioactivity of [^{14}C]glucose) were found in the unbound fraction after PBA chromatography, even when minimum amounts of albumin were loaded on the column. Apart from the often reported column overloading problem due to sensitivity reasons[9–13], the limitted efficiency of the PBA matrix in the separation of glycated from non-glycated HSA (see above) may explain the markedly lower estimates of glycation rates reported using this matrix[11–13] compared with other techniques (*e.g.*, the thiobarbituric acid method, CM-cellulose chromatography or the furosine method[3,19,20]). These observations agree with our previous findings[8] and a recent report[21] on the lack of specificity of PBA chromatography. A possible explanation[21] could be that the bound fraction corresponds to HSA glycated in more than one site, probably Lys-525 and Lys-199[15], and that this structure can be easily recognized by the affinity matrix due to steric accessibility.

From the present results (where calculations of glucose content in the PBA fractions are in good agreement with those reported by Johnson and Baker[21]), we find that even after 15 days of glycation the glucose content in the PBA-unbound fraction does not exceed 1 mol per mol HSA (Fig. 5A). In the PBA-bound fraction, the average glucose content increases to *ca.* 3 mol per mol HSA (Fig. 5A). The two anionic forms of HSA were found to contain more glucose than the p*I* 4.9 fraction, showing, in addition, a p*I* relationship (Fig. 5B). In similar terms, the glucose content of these two fractions, when they contained more than 2 mol glucose per mol HSA, could be noticeably enriched by using PBA chromatography, and the extent of this enrichment was also found to be p*I*-related (Fig. 6C).

All this is consistent with the postulated requirement of 2 mol glucose per mol HSA to bind PBA. However, in disagreement with Johnson and Baker[21], we believe that HSA with less than 2 mol glucose can also bind to PBA, although with a lower affinity. This is supported by the finding of the p*I* 4.9 fraction in the 15-day glycation sample after PBA chromatography (Fig. 6B) where, despite its glucose content of more than 2 mol per mol HSA (Fig. 6C), its p*I* remains at 4.9. This might indicate the presence of glucose bound to lysine groups other than Lys-199 and the (supposed) primarily involved Lys-525. Such lysine groups (*i.e.*, Lys-281 or Lys-439)[22] might be easily accesible for glycation, but not for interaction with the PBA matrix. On the other hand, a relatively low affinity for the p*I* 4.65 fraction to the PBA matrix might be explained by conformational changes in the HSA molecule (*i.e.*, disulphide breakdown, cross-linking, condensation), which could interfere with the interaction between the 2 mol glucose-containing epitopes from the HSA and the double-site recognition structures from the matrix. Conformational changes collaborating in a surface charge modification of HSA after glycation might be expected, as a lower glucose content was required to produce a p*I* variation from 4.8 to 4.65 compared with that from 4.9 to 4.8.

Consequently, we suggest that addition of 2 mol glucose per mol HSA is a sufficient but not necessary condition for PBA binding; HSA molecules with 2 mol glucose (in Lys-525 and Lys-199) will have a high-affinity binding to PBA and they might be easily enriched with a high yield by using this technique. In contrast, HSA molecules containing 1 mol glucose (in Lys-525) or more than 2 mol (in Lys-525,

Lys-199 and Lys-281 or/and Lys-439) will bind to the matrix with a lower affinity and, consequently, be enriched with a lower yield.

In vivo, including normal and diabetic ranges, the average glucose content in HSA is generally below 1 mol per mol HSA[2,3,14]. As this is a mathematical average, some HSA molecules with more than a single glucose are probably present. From the relatively small number of HSA molecules containing some glycosyl adduct (usually $< 10\%$ for humans), Lys-525 from HSA is the first glycation site involved (according to Garlick and Mazer[15]), but probably not the only one. *In vitro*, a higher extent of glycation can easily be achieved and a large number of HSA molecules with glycosyl adducts in Lys-199 can be strongly expected. This is in good agreement with the inhibitory effect on glycation of acetylsalicylic acid (ASA), involving a competitive acetylation in Lys-199[19]. The involvement of a secondary glycation-site may explain the only partial effect obtainable by using such a drug or its analogues[19,23]. Nevertheless, this effect of ASA, which was preported to be especially evident when PBA chromatography was used[23], is in accord with the above-mentioned necessity for a double recognition site for this matrix.

In addition to the effect of column overloading and (potential) conformational changes, a large number of substances may bind to the HSA and interfere with the glycation and the binding to the PBA matrix. Fatty acids, as they are present before glycation (probably in the p*I* 4.8 fraction) (Figs. 1 and 2), may interfere with glycation[24,25], although glycation does not interfere with binding of fatty acids[26], and the role of Lys-525 in this equilibrium has been particularly emphasized[24]. The effects of ASA-related compounds and fatty acids on the glycation of HSA and on its measurement are currently being investigated.

ACKNOWLEDGEMENTS

This study was supported by the Nordisk Insulinlaboratorium Foundation. P.V. is a post-doctoral fellow from the University of Santiago (Spain), granted by the Spanish Xunta de Galicia.

REFERENCES

1 Nomenclature Committee of IUB (NC-IUB) and IUB–IUPAC Joint Commission on Biochemical Nomenclature (JCBN), *Hoppe-Seyler's Z. Physiol. Chem.*, 365 (1984) I.
2 B. S. Welinder, P. Vidal, T. Deckert and B. Hansen, *Diabetes. Res. Clin. Pract.*, Suppl. 1 (1985) 599.
3 A. Kverneland, B. Feldt-Rasmussen, P. Vidal, B. S. Welinder, L. Bent-Hansen and T. Deckert, *Diabetologia*, 29 (1986) 634.
4 G. M. Ghiggeri, G. Candiano, G. Delfno, G. Pallavicini and C. Queirolo, *Diabete Metab.*, 11 (1985) 157.
5 G. Candiano, G. M. Ghiggeri, G. Delfino and C. Queirolo, *Diabetologia*, 25 (1983) 145.
6 G. Candiano, G. M. Ghiggeri, G. Delfino, C. Queirolo, E. Ginazza and P. G. Righetti, *Electrophoresis*, 5 (1984) 217.
7 G. M. Ghiggeri, G. Candiano, G. Delfino, F. Bianchini and C. Queirolo, *Kidney Int.*, 25 (1984) 565.
8 P. Vidal, B. S. Welinder, T. Deckert and B. Hansen, in C. Schafer-Nielsen (Editor), *Proceedings of the VIth Meeting of the International Electrophoresis Society*, VCH, Cambridge,1988, p. 468.
9 M. Rendell, G. Kao, P. Mecherikunnel, B. Peterson, R. Duhaney, J. Nierenberg, K. Rasbold and D. Klenk, *Clin. Chem.*, 31 (1985) 229.
10 B. J. Gould, P. M. Hall and J. G. H. Cook, *Ann. Clin. Biochem.*, 21 (1984) 16.
11 M. Rendell, G. Kao, P. Mecherikunnel, B. Petersen, R. Duhaney, J. Nierenberg, K. Rasbold, D. Klenk and P. K. Smith, *J. Lab. Clin. Med.*, 105 (1985) 63.

12 P. Painter, J. Evans, W. Law, J. Eaddy, J. Cope and J. Smith, *Clin. Chem.*, 31 (1985) 945.
13 R. Ducrocq, B. Le Bonniec, O. Carlier, R. Assan and J. Elion, *J. Chromatogr.*, 419 (1987) 75.
14 E. Schleicher and H. Wieland, *J. Clin. Chem. Clin. Biochem.*, 19 (1981) 81.
15 R. L. Garlick and J. S. Mazer, *J. Biol. Chem.*, 258 (1983) 6142.
16 T. Deckert, B. Feldt-Rasmussen, E. R. Mathiesen and L. Baker, *Diabetic Nephropathy*, 3 (1984) 83.
17 M. R. Salaman and A. R. Williamson, *Biochem. J.*, 122 (1971) 93.
18 K. Wallevik, *Biochim. Biophys. Acta*, 420 (1976) 42.
19 J. F. Day, S. R. Thrope and J. W. Baynes, *J. Biol. Chem.*, 259 (1979) 595.
20 C. E. Guthorow, M. A. Morris, J. F. Day, S. R. Thrope and J. W. Baynes, *Proc. Natl. Acad. Sci. USA*, 76 (1979) 4258.
21 R. N. Johnson and J. R. Baker, *Clin. Chem.*, 34 (1988) 1456.
22 N. Iberg and R. Fluckiger, *J. Biol. Chem.*, 261 (1986) 13542.
23 M. Rendell, J. Nierenberg, C. Brannan, J. L. Valentine, P. M. Stephen, S. Dodds, P. Mercer, P. K. Smith and J. Walker, *J. Lab. Med.*, 108 (1986) 286.
24 K. A. Mereish, H. Rosenberg and J. Cobby, *J. Pharm. Sci.*, 71 (1982) 235.
25 N. Shaklai, R. L. Garlick and H. F. Bunn, *J. Biol. Chem.*, 259 (1984) 3812.
26 M. H. Murthiashaw and K. H. Winterhalter, *Diabetologia*, 29 (1986) 366.

Journal of Chromatography, 476 (1989) 477–485
Elsevier Science Publishers B.V., Amsterdam — Printed in The Netherlands

CHROMSYMP. 1625

COMPARISON OF ION-EXCHANGE HIGH-PERFORMANCE LIQUID CHROMATOGRAPHY COLUMNS FOR PURIFICATION OF SENDAI VIRUS INTEGRAL MEMBRANE PROTEINS

S. WELLING-WESTER*, R. M. HARING and H. LAURENS
Laboratorium voor Medische Microbiologie, Oostersingel 59, 9713 EZ Groningen (The Netherlands)
C. ÖRVELL
Deparment of Virology, Karolinska Institute, School of Medicine and Department of Virology, National Bacteriological Laboratory, S-10521 Stockholm 1 (Sweden)
and
G. W. WELLING
Laboratorium voor Medische Microbiologie, Oostersingel 59, 9713 EZ Groningen (The Netherlands)

SUMMARY

The recovery and separation of the integral membrane proteins, the haemagglutinin-neuraminidase (HN) and the fusion protein (F), from a Sendai virus detergent extract were compared on three different ion-exchange high-performance liquid chromatography (IE-HPLC) columns: Mono Q, TSK DEAE-NPR and Zorbax BioSeries SAX. The detergent, either 1-O-*n*-octyl-β-glucopyranoside (octylglucoside) or decyl polyethylene glycol-300 (decyl PEG-300), used for extraction of HN and F proteins from the virions, was also present in the elution buffers at a concentration of 0.1%. Recovery of HN and F proteins was primarily dependent on the detergent present in the eluent, resulting in yields of HN varying from 18 to 28 and 56 to 67%, when octylglucoside and decyl PEG-300, respectively, were used. The highest yield for HN protein was obtained by separation on either a Mono Q or a TSK DEAE-NPR column with decyl PEG-300 as the additive. Yields of F protein were lower, and the highest recovery of 46% was found in the presence of decyl PEG-300 by separation on the Mono Q column. Analysis of the fractions by sodium dodecyl sulphate-polyacrylamide gel electrophoresis and by size-exclusion HPLC indicated that the HN protein eluted in the presence of decyl PEG-300 from the Mono Q and the TSK DEAE-NPR columns was obtained in pure form, while the F protein was slightly contaminated with HN. Analysis of the fractions with monoclonal antibodies directed against conformational epitopes of HN and F proteins indicated that after IE-HPLC the conformation of the proteins is largely retained.

INTRODUCTION

Ion-exchange high-performance liquid chromatography (IE-HPLC) has been applied to the isolation of viral proteins, either alone or in combination with other

0021-9673/89/$03.50

modes of HPLC[1–10]. Differences in the electrostatic interaction between the column ligands and charged groups on the proteins are the basis for the separation. Many types of IE columns are commercially available[11]. They consist of porous or non-porous silica or polymeric particles with different charged ligands, *e.g.*, diethyl aminoethyl or trimethyl aminomethyl groups, resulting in a medium anion exchanger and a strong anion exchanger, respectively. Proteins are generally eluted by a salt gradient under physiological conditions (pH near 7). Therefore, IE-HPLC is particularly suitable for purification procedures where it is important to retain the biological activity of a protein.

Prior to purification, viral proteins must be solubilized. Detergents (surfactants) are widely used for this purpose[12–14]. To avoid aggregation of membrane proteins during purification, detergents are added to eluents as well. Non-ionic detergents generally do not affect the native conformation and electrostatic properties of proteins, and therefore they are preferentially used as additives in elution buffers for IE-HPLC. Some non-ionic detergents (Berol, Nonidet, Triton) absorb UV light and interfere with the spectrophotometric determination of proteins at 280 nm, while others, like octylglucoside and alkyl polyoxyethylene ethers, do not.

We studied the separation of integral membrane protein present in a detergent extract of Sendai virus particles on three different columns: two porous columns, Zorbax BioSeries Sax (Du Pont) and Mono Q (Pharmacia), and a non-porous column, TSK DEAE-NPR (Toyo Soda) with either 1-O-*n*-octyl-β-glucopyranoside (octylglucoside) or decyl polyethylene glycol-300 (decyl PEG-300) in the eluent. Sendai virus is a paramyxovirus of mice and belongs to the same family as the human parainfluenza, measles and mumps viruses. These virus particles are enclosed in a loose and fragile envelope, a lipid bilayer in which two integral membrane proteins are embedded. These proteins are the haemagglutinin-neuraminidase protein HN (M_r = 68 000) and the fusion protein F (M_r = 65 000). In the mature virus particles the HN protein is probably present only as the dimer and tetramer (HN_2 and HN_4, respectively) and can be converted into the monomeric form (HN) by treatment with a reducing agent. Occasionally, truncated forms of the HN protein (HN_4- and HN_2-), without the membrane-spanning region, are observed, due to degradation during the extraction procedure. The F protein consists of two components, F_1 (M_r = 50 000) and F_2 (M_r = 13 000–15 000), which are connected by disulphide bridges. Multimeric forms of the F protein have been described[15], depending on the medium used for solubilization. The HN and F proteins are present as spikes on the outside of the virus particle.

In this study, the separation, recovery and immunological activity of Sendai virus HN and F proteins were compared after IE-HPLC on the three different columns.

EXPERIMENTAL

Detergent extracts of Sendai virus particles

Sendai virus was grown in 10-day-old embryonated eggs. The allantoic fluid was harvested 72 h after infection. Cell debris was removed by low-speed centrifugation (30 min at 2000 *g*, 5°C), and virus particles were pelleted from the supernatant by ultracentrifugation (1 h at 70 000 *g* at 5°C). The virus pellet was resuspended in 10

m*M* Tris-HCl (pH 7.2), supplemented with 10% sucrose and stored at −80°C. The protein concentration of the virus pellet was determined according to Lowry *et al.*[16].

Extraction of Sendai virus glycoproteins was performed with the detergents octylglucoside (Boehringer, Mannheim, F.R.G.) and decyl PEG-300 (Kwant-Hoog Vacolie Recycling and Synthese, Bedum, The Netherlands). Briefly, to a Sendai virus pellet suspension, containing 40 mg protein per ml buffer (10 m*M* Tris–HCl, pH 7.2), the same volume of buffer, containing 4% detergent, was added. The final detergent concentration was 2% and there were 40 mg viral proteins in 2 ml buffer. After incubation for 20 min at room temperature, the extraction procedure was terminated by ultracentrifugation for 1 h at 70 000 *g* at 5°C. The extracted HN and F proteins are present in the supernatant, which was stored in 200-μl portions at −80°C. The decyl PEG-300 extract of Sendai virus contained 298 μg HN protein and 400 μg F protein per 200 μl, and the octylglucoside extract 232 μg HN protein and 396 μg F protein per 200 μl.

Ion-exchange and size-exclusion HPLC

Chromatography was performed with a system consisting of a M 6000A pump (Waters, Etten-Leur, The Netherlands) or a 2150 pump (LKB, Zoetermeer, The Netherlands), a Rheodyne 7125 injector (Inacom, Veenendaal, The Netherlands) and a Waters 441 detector or a Pye Unicam LC-UV detector (Philips, Eindhoven, The Netherlands).

Anion-exchange HPLC was performed with a Mono Q HR 5/5 (50 mm × 5 mm I.D.) column (Pharmacia, Uppsala, Sweden), with trimethyl aminomethyl groups and consisting of hydrophilic polymer beads with a particle size of 10 μm and pores of 80 nm; a TSK DEAE-NPR (35 mm × 4.6 mm I.D.) column (Toyo Soda, Tokyo, Japan), with diethyl aminomethyl groups and consisting of a non-porous hydrophilic resin with a particle size of 2.5 μm (ref. 17) and a Zorbax BioSeries SAX (80 mm × 6.2 mm I.D.) column (Du Pont, Wilmington, DE, U.S.A.), with trimethyl aminomethyl groups and consisting of zirconium oxide-stabilized silica with a particle size of 6 μm and a pore size of 30 nm. The protein capacities of the Zorbax BioSeries SAX and Mono Q columns, as reported by the supplier, are 42 and 26 mg per ml column volume, respectively. The capacity of the TSK DEAE-NPR column is 8.6 mg per ml column volume[17].

After injection of an octylglucoside extract of Sendai virus (439 and 900 μg of protein) or a decyl PEG-300 extract (342 and 698 μg of protein), the column was eluted isocratically for 5 min. The proteins retained were eluted with a linear 12-min gradient from 20 m*M* Tris–HCl (pH 7.8), containing 0.1% detergent, to 0.5 *M* sodium chloride in the same buffer. The detergent (either oxtylglucoside or decyl PEG-300) used for the extraction of HN and F proteins from the virions was also present in the elution buffers. The gradient was generated by a low-pressure mixing system[18]. The flow-rate was 1 ml/min, and the absorbance was monitored at 280 nm. Fractions were collected manually in Minisorp tubes (Nunc, Roskilde, Denmark). Aliquots of each fraction were taken for analysis by sodium dodecyl sulphate-polyacrylamide gel electrophoresis (SDS-PAGE). The remaining part of the fraction was dialyzed overnight against water by covering the tubes with a square piece of dialysis membrane tubing, and the tubes were closed by fitting a slice of silicone rubber tubing over the dialysis membrane. After dialysis, the fractions were freeze-dried in the

tubes. The freeze-dried fractions were used to determine the recovery of proteins HN and F, and they were analyzed in an enzyme-linked immunosorbent assay (ELISA) for reaction with conformation-dependent monoclonal antibodies against HN and F proteins.

Size-exclusion (SE) HPLC was performed on two Zorbax GF 450 (250 mm × 9.4 mm I.D.) columns (Du Pont) in tandem, to determine the amounts of HN and F proteins present in the fractions collected during IE-HPLC. The IE-HPLC fractions (freeze-dried after dialysis) were dissolved in 100 μl water. Of the dissolved fraction, 20 μl were taken (the remainder was used in the ELISA), and SDS was added to a final concentration of 4%. The fractions were heated for 3 min in a bath of boiling water and subjected to analysis by SE-HPLC. The proteins were eluted with 50 m*M* sodium phosphate (pH 6.5), containing 0.1% SDS, at a flow-rate of 1 ml/min. The absorbance was monitored at 280 nm. The recovery of HN and F proteins was calculated from the peak height, using the elution pattern of a mixture of 50 μg bovine serum albumin (BSA), 50 μg ovalbumin and 50 μg trypsin inhibitor as a standard.

SDS-PAGE

Samples of the eluate fractions (50 μl) were prepared for SDS-PAGE[19] on 8% gels under non-reducing conditions by the addition of ten-fold concentrated sample buffer (15 μl) without reducing agent. After electrophoresis, the gels were fixed and silver-stained as described[20].

ELISA

The IE-HPLC fractions were analyzed for the presence of structurally intact HN and F proteins by determination of the reaction with conformation-dependent monoclonal antibodies HN 851 and F 1.216. The production of these monoclonal antibodies, directed against HN and F proteins, and their characterization as conformation-dependent has been described[21,22]. For coating of the ELISA trays, the remaining part (80 μl) of the IE-HPLC fractions, dissolved in water, was diluted in coating buffer (50 m*M* sodium carbonate, pH 9.6) to concentrations of 10, 2 and 0.5 μg protein per ml. Plates were coated with 100 μl per well of these three concentrations. After coating overnight at 4°C (or 2 h at 37°C), plates were washed three times for 5 min with phosphate-buffered saline (pH 7.2), containing 0.2 *M* sodium chloride, 0.3% Tween 20 and 1 mg SDS/l (washing buffer). The coated proteins were allowed to react with monoclonal antibodies HN 851 and F 1.216, diluted 1:1000 in washing buffer supplemented with 0.5% BSA (dilution buffer). After incubation at room temperature for 1 h and washing (three times for 5 min), peroxidase-labelled anti-mouse immunoglobulin G (IgG) (conjugate), diluted 1:1000, was added and the plates were incubated for 1 h at 37°C. After washing, the peroxidase activity was visualized by adding 100 μl substrate, consisting of 0.2 mg *o*-phenylenediamine dihydrochloride (Eastman Kodak, Rochester, NY, U.S.A.)–0.006% (v/v) H_2O_2 in 2% methanol–50 m*M* sodium phosphate (pH 5.6) per well. The reaction was terminated by adding 50 μl 2 *M* sulphuric acid per well. The optical density at 492 nm was measured in a microplate photometer. Optical density values below 0.2 were considered as negative.

RESULTS AND DISCUSSION

In Fig. 1 the elution profiles of a decyl PEG-300 extract of Sendai virus, separated on the Mono Q, TSK DEAE-NPR and Zorbax Bio Series SAX columns (Fig. 1a, b and c, respectively), are shown. The elution profiles after IE-HPLC of decyl PEG-300 and octylglucoside extracts for the Mono Q and the Zorbax BioSeries SAX columns showed many sharp peaks and one broad peak, while the peaks from the TSK DEAE-NPR column were generally broader. Analysis by SDS-PAGE of the IE-HPLC fractions showed that, despite differences in elution profiles, the separation of the Sendai virus proteins was rather similar (data not shown). In Fig. 2, the elution pattern of a decyl PEG-300 extract, separated on the Mono Q colum, together with the analysis by SDS-PAGE, is shown as an example. The first peak fractions that were eluted did not contain protein material. Then the multimeric forms of the HN protein (first HN_2-, and thereafter a mixture of HN_4, HN_2 and HN_2-) were eluted, followed by a broad peak of the F protein. These peaks do not entirely reflect the different multimeric forms of HN (HN_4, HN_2 and HN_2-, respectively) and F protein, but may be due to different aggregate forms in the extract and probably also to differences in charge, caused by partial glycosylation. Eighteen percent of the oligosaccharides from the HN protein are acidic, while more than 75% of the oligosaccharides from the F protein are acidic[23]. In addition to this general separation pattern, IE-HPLC of octylglucoside extracts of Sendai virus with the same detergent added to the eluent often showed HN_2- protein in one of the first peaks. The data obtained by SDS-PAGE of the fractions from the different IE-HPLC columns show that the time

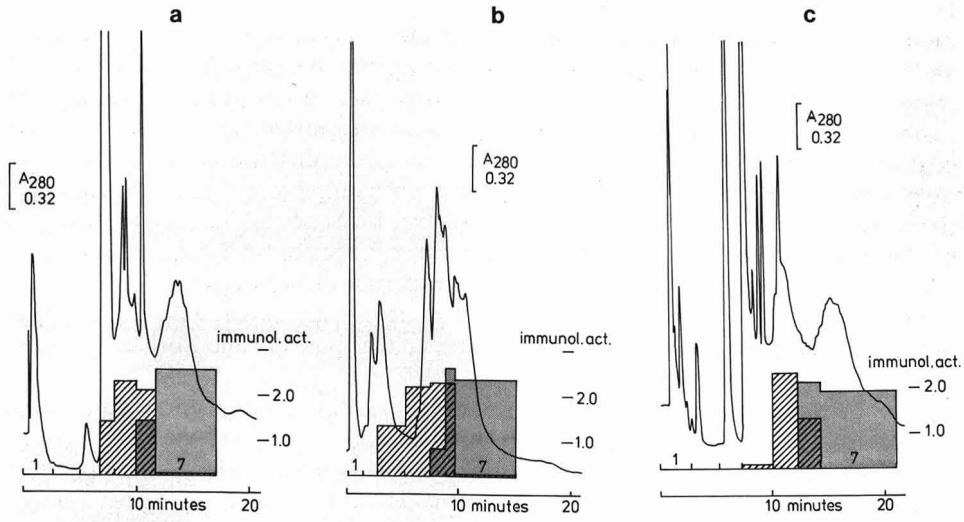

Fig. 1. IE-HPLC of a decyl PEG-300 extract of Sendai virions, containing 298 μg HN and 400 μg F protein, separated on Mono Q (a), TSK DEAE-NPR (b) and Zorbax BioSeries SAX (c) columns. Elution was performed with a 12-min gradient from 20 m*M* Tris-HCl (pH 7.8), containing 0.1% decyl PEG-300, to 0.5 *M* sodium chloride in the same buffer. The flow-rate was 1 ml/min and the absorbance was monitored at 280 nm. The fractions were collected as indicated. Amounts of 0.2 μg of each fraction were investigated for reactivity with monoclonal antibodies HN 851 (hatched area left), directed against intact HN protein, and with monoclonal antibodies F 1.216 (hatched area right), directed against intact F protein.

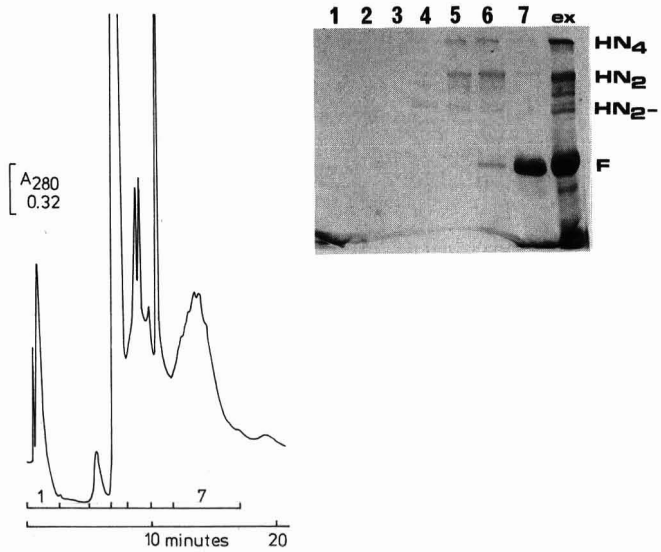

Fig. 2. IE-HPLC of a decyl PEG-300 extract of Sendai virus membrane proteins on a Mono Q column. Elution was performed as in Fig. 1. The flow-rate was 1 ml/min; the absorbance was monitored at 280 nm. Fractions were collected as indicated, and samples were analyzed by SDS-PAGE (8% gel) under non-reducing conditions. Lane numbers of the gel refer to IE-HPLC fractions; ex = the decyl PEG-300 extract; HN_4, HN_2, HN_2- and F are the tetramer of HN, dimer of HN, truncated form of the HN dimer and the F protein, respectively.

at which the multimeric forms of HN and F proteins were eluted is different. HN and F proteins were eluted from the Mono Q and Zorbax BioSeries SAX column after starting the salt gradient. In contrast, HN was partially eluted from the non-porous TSK DEAE-NPR column before the salt gradient was started. This can be explained by the medium-strong anion-exchange properties of this diethylaminoethyl-functionalized support, compared to the strong anion-exchange properties of the trimethyl aminomethyl groups in the Mono Q and Zorbax BioSeries SAX columns. The HN and F proteins were eluted later from the Zorbax BioSeries SAX column than from the Mono Q column. The anion-exchange properties of both types of columns are rather similar. The retarded elution of the proteins may be caused by the slower diffusion of the proteins HN and F from the smaller pores of the Zorbax BioSeries SAX packing.

The recovery of HN and F proteins after IE-HPLC on the various columns in the presence of octylglucoside and decyl PEG-300 was quantitated by analysis of the IE-HPLC fractions using SE-HPLC. In Fig. 3 this is illustrated by the analysis of fractions 4-7, obtained after IE-HPLC on the Mono Q column in the presence of decyl PEG-300. Peak 1 is an aggregate peak, which contains no proteins, peaks 2 and 3 contain the tetramer and dimer of HN protein, respectively, peak 4 contains the F protein. Fraction 4 contains mainly HN_2 forms (12 μg) and small amounts of HN_4 and F proteins (3 μg of each). In fraction 5 the amounts of HN_2 and HN_4 are increased to 36 and 42 μg, respectively, while the amount of F protein is still small (5 μg). Fraction 6 contains 33, 26 and 16 μg of HN_4, HN_2 and F proteins, respectively,

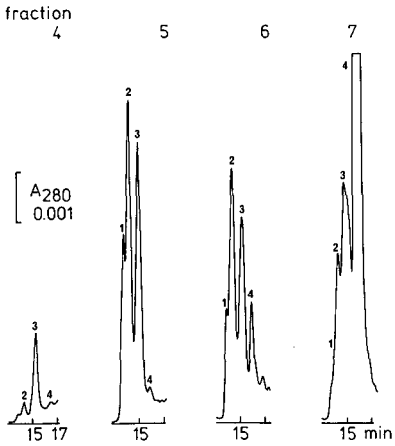

Fig. 3. Size-exclusion HPLC of fractions 4–7 of the IE-HPLC shown in Fig. 2. Samples of the fractions were made 4% in SDS and heated for 3 min in a bath of boiling water prior to analysis on two tandem-linked Zorbax GF-450 columns. The elution was performed with 50 m*M* sodium phosphate buffer (pH 6.5), containing 0.1% SDS. The flow-rate was 1 ml/min, and absorbance was monitored at 280 nm. Peaks: 1 = nonproteinaceous material; 2 = tetramer of HN; 3 = dimer of HN; 4 = F protein.

while in fraction 7 predominantly F protein (193 μg) is eluted. Table I summarizes the recoveries for HN and F proteins obtained after IE-HPLC on the various columns. The recovery is mainly determined by which detergent is present in the elution buffer. Values for HN and F proteins are approximately three times higher with decyl PEG-300 in the buffer than with octylglucoside in the eluents and are independent of the amount of protein injected. The highest recovery (28%) of HN in the presence of octylglucoside is obtained by separation on the TSK DEAE-NPR column, while with decyl PEG-300 in the eluents the recoveries of HN (67%) are similar for the Mono Q and the TSK DEAE-NPR columns. The recoveries of F protein are lower than those

TABLE I

PERCENT RECOVERY OF HN AND F PROTEINS FROM DIFFERENT IE-HPLC COLUMNS WITH OCTYLGLUCOSIDE AND DECYL PEG-300 AS DETERGENTS IN THE ELUTION BUFFERS

Column type	*HN protein*		*F protein*	
	Octylglucoside[a]	*Decyl PEG-300*[b]	*Octylglucoside*[a]	*Decyl PEG-300*[b]
Mono Q HR 5/5	20	67	12	46
TSK DEAE-NPR	28	67	12	27
Zorbax BioSeries SAX	18	56	< 10	34

[a] Two different amounts of an octylglucoside extract of Sendai virus (containing 162 and 332 μg of HN protein, and 277 and 568 μg F protein, respectively) were separated with a linear salt gradient from 0 to 0.5 *M* sodium chloride in 20 m*M* Tris–HCl (pH 7.8) with 0.1% octylglucoside.

[b] Two different amounts of a decyl PEG-300 extract of Sendai virus (containing 146 and 298 μg HN protein, and 196 and 400 μg F protein, respectively) were separated with a linear salt gradient from 0 to 0.5 *M* sodium chloride in 20 m*M* Tris-HCl (pH 7.8) with 0.1% decyl PEG-300.

of the HN protein for all three columns investigated. IE-HPLC in the presence of 0.1% octylglucoside results in a recovery of 12% F protein from the Mono Q and TSK DEAE-NPR columns; for the Zorbax BioSeries SAX column the recovery was less than 10%. With 0.1% decyl PEG-300 as additive the recoveries are higher, 46, 34 and 27% for the Mono Q, Zorbax BioSeries SAX and TSK DEAE-NPR, respectively. Relatively low recoveries with oxtylglucoside in the eluent have also been described by others[24,25]. Various viral membrane proteins have been successfully isolated by IE-HPLC from detergent extracts, *e.g.*, polypeptides of 84 000, 90 000 and 105 000 daltons from bovine viral diarrhea virus (BVDV)[5,7], a membrane protein gp 340 from Epstein-Barr virus (EBV)[8] and the haemagglutinin (H protein) protein from measles virus[10]. The BVDV proteins were separated on a TSK DEAE-5PW column in the presence of 0.5% Berol 185 with a recovery of 60–70%. The recovery of gp 340 from EBV was 77% after IE-HPLC on a Mono Q column with 0.5% MEGA-9 in the eluent. The H protein of measles virus, related to the HN protein of Sendai virus, was purified on a Mono Q column in the presence of 0.03% Triton X-100, with a recovery of 55%. The recoveries of the above-mentioned viral membrane proteins range from 55 to 77%. These values are comparable to the recoveries of 56–67% of the HN protein obtained in the presence of decyl PEG-300. The recoveries (46–27%) of F protein in the presence of decyl PEG-300 are slightly lower than those reported for other viral membrane proteins. Results from SE-HPLC in combination with SDS-PAGE analysis of the IE-HPLC fractions indicated that only small quantities of HN protein (fractions 3 in Fig. 1a and b) that were eluted in the presence of decyl PEG-300 from the Mono Q and the TSK DEAE-NPR columns were obtained in pure form. F Protein was always slightly contaminated with HN protein. A second IE-HPLC of appropriate fractions probably may result in pure HN and F proteins.

The structural alterations possibly resulting from IE-HPLC were measured by determination of the immunological activity of the HN and F proteins in the eluate fractions. In Fig. 1 the immunological activity of the fractions is shown together with the elution profiles in the presence of 0.1% decyl PEG, for the Mono Q, TSK DEAE-NPR and Zorbax BioSeries SAX columns. Amounts of 1, 0.2 and 0.05 μg of each fraction were used to investigate the reaction with two conformation-dependent monoclonal antibodies: HN 851, directed against protein HN, and F 1.216, directed against F protein. Both monoclonal antibodies reacted with the fractions collected during IE-HPLC (Fig. 1), indicating that the native structure of a considerable number of the HN and F molecules is preserved during the chromatographic procedure. A high reactivity of the monoclonal antibodies with either HN or F protein does not imply that there may not be small, local changes, distantly located from the epitopes to which the monoclonal antibodies are directed. However, large structural changes in any part of the protein molecule are expected to have long-range effects and will therefore affect the reactivity of the monoclonal antibodies. In agreement with this is the observation that the reaction of a mixture of conformation-dependent monoclonal antibodies, directed against different epitopes, is identical with the reaction of one conformation-dependent monoclonal antibody HN 851 (unpublished results). In an earlier study[22] we have described the immunological activity of proteins HN and F after SE-HPLC with 0.05% sarkosyl in the eluent. After SE-HPLC, amounts of 1 mg of the eluate fractions were necessary to obtain the same level of immunological activity as is present in 0.2 μg of the IE-HPLC fractions described here. This indicates

that, in this particular study, after IE-HPLC more protein molecules have the native conformation than after SE-HPLC.

CONCLUSIONS

The results show that IE-HPLC is a relatively mild separation method yielding structurally intact viral membrane proteins. Recovery is largely determined by the detergent present in the eluent, and to a lesser extent by the type of IE-HPLC column used. The highest recovery of HN protein was obtained by using either a Mono Q column of a TSK DEAE-NPR column, while the highest recovery of F protein was obtained after chromatography on the Mono Q column. Differences observed in the elution profiles of the IE-HPLC columns (Mono Q, TSK DEAE-NPR and Zorbax BioSeries SAX) were more likely due to the anion-exchange properties and pore sizes of the supports than to their porous or non-porous character.

ACKNOWLEDGEMENTS

We are indebted to Dr. Y. Kato, Central Research Laboratory, Toyo Soda Mfg., Tonda Shinnanyo, Japan, for supplying the TSK DEAE-NPR column and to Dr. A. Dams, Du Pont, 's-Hertogenbosch, The Netherlands, for providing the Zorbax BioSeries SAX column.

REFERENCES

1 G. W. Welling, G. Groen and S. Welling-Wester, *J. Chromatogr.*, 266 (1983) 629.
2 G. W. Welling, J. R. J. Nijmeijer, R. Van der Zee, G. Groen, J. B. Wilterdink and S. Welling-Wester, *J. Chromatogr.*, 297 (1984) 101.
3 M. Green and K. H. Brackmann, *Anal. Biochem.*, 124 (1982) 209.
4 M. Waris and P. J. Halonen, *J. Chromatogr.*, 397 (1987) 321.
5 P. Kårsnäs, J. Moreno-Lopez and T. Kristiansen, *J. Chromatogr.*, 266 (1983) 643.
6 L. Ho-Terry and A. Cohen, *Arch. Virol.*, 84 (1985) 207.
7 J. G. Mohanty and Y. Elazhary, *J. Chromatogr.*, 435 (1988) 149.
8 E. M. David and A. J. Morgan, *J. Immunol. Methods*, 108 (1988) 231.
9 M. L. Gallo, D. H. Jackwood, M. Murphy, H. S. Marsden and D. S. Parris, *J. Virol.*, 62 (1988) 2874.
10 D. Gerlier, F. Garnier and F. Forquet, *J. Gen. Virol.*, 69 (1988) 2061.
11 O. Mikes, *High-performance Liquid Chromatography of Biopolymers and Biooligomers*, Part A, Elsevier, Amsterdam, 1988, p. A173.
12 A. Helenius and K. Simons, *Biochim. Biophys. Acta*, 415 (1975) 29.
13 A. Helenius, D. R. McCaslin, E. Fries and C. Tanford, *Methods Enzymol.*, 56 (1979) 734.
14 L. M. Hjelmeland and A. Crambach, *Methods Enzymol.*, 104 (1984) 305.
15 O. Sechoy, J. R. Phillipot and A. Bienvenue, *J. Biol. Chem.*, 262 (1987) 11519.
16 O. H. Lowry, N. J. Rosebrough, A. L. Farr and R. J. Randall, *J. Biol. Chem.*, 193 (1951) 265.
17 Y. Kato, T. Kitamura, A. Mitsui and T. Hashimoto, *J. Chromatogr.*, 398 (1987) 327.
18 R. van der Zee and G. W. Welling, *J. Chromatogr.*, 292 (1984) 412.
19 U.K. Laemmli, *Nature (London)*, 227 (1970) 680.
20 W. Wray, T. Boulikas, V. P. Wray and R. Hancock, *Anal. Chem.*, 118 (1981) 197.
21 C. Örvell and M. Grandien, *J. Immunol.*, 129 (1982) 2779.
22 S. Welling-Wester, B. Kazemier, C. Örvell and G. W. Welling, *J. Chromatogr.*, 443 (1988) 255.
23 H. Yoshima, M. Nakanishi, Y. Okada and A. Kobata, *J. Biol. Chem.*, 256 (1981) 5355.
24 Y. Kato, T. Kitamura, K. Nakamura, A. Mitsui, Y. Yamasaki and T. Hashimoto, *J. Chromatogr.*, 391 (1987) 395.
25 H. Ikigai, T. Nakae and Y. Kato, *J. Chromatogr.*, 322 (1985) 212.

Journal of Chromatography, 476 (1989) 487–490
Elsevier Science Publishers B.V., Amsterdam — Printed in The Netherlands

CHROMSYMP. 1603

Note

High-performance liquid chromatographic assay for nicotinamide–adenine dinucleotide kinase

MARIO PACE, PIER LUIGI MAURI, CLAUDIO GARDANA and PIER GIORGIO PIETTA*
Dipartimento di Scienze e Tecnologie Biomediche, Sez. Chimica Organica, University of Milano, Via G. Celoria 2, 20133 Milan (Italy)

The phosphorylation of nicotinamide–adenine dinucleotide (NAD) to the corresponding phosphate (NADP) is a process occurring in animals[1,2], algal cells[3,4] and in higher plant leaves and seedlings[5,7]. In plants it is a light-dependent process connected with the energy exchange in chloroplasts where the NAD kinase activity plays an important role in the photoregulation of the nicotinamide coenzyme levels. The enzyme responsible for this phosphorylation is a NAD kinase (E.C. 2.7.1.23) which is generally activated by Ca^{2+} and calmodulin and requires a nucleoside triphosphate as a phosphate donor, according to the reaction:

$$NAD + ATP \xrightarrow{\text{NAD kinase}} NADP + ADP$$

Even though the enzyme is often called ATP/NAD^+ 2′-phosphotransferase, it is not highly specific for this phosphate donor. Other nucleoside triphosphates, such as GTP, ITP and UTP , are also very effective[8].

The measurement of enzyme activity is a time-consuming procedure which requires an additional enzyme (glucose-6-phosphate dehydrogenase or isocitrate dehydrogenase) for the determination of NADP produced during the kinase reaction. On the other hand, high-performance liquid chromatography (HPLC) is a technique which provides a simple and direct determination of substrate(s) and product(s)[9–11] and therefore is an efficient method for the assay for NAD kinase which is more rapid than the common method and does not require consecutive reactions.

EXPERIMENTAL

Materials

NAD^+ and $NADP^+$ were obtained from Boehringer (Mannheim, F.R.G.); NAD kinase, GTP and GDP were from Sigma (St. Louis, MO, U.S.A.); thymine from Fluka (Buchs, Switzerland), and calmodulin from veal brain was a gift from Dr. Graziano Zocchi (Istituto di Chimica Agraria, University of Milano). All other chemicals were of analytical reagent grade. Methanol was of HPLC grade (Baker Chemicals, Deventer, The Netherlands). Water was distilled in a glass apparatus and filtered through a 0.45-μm membrane (Type HA; Millipore, Bedford, MA, U.S.A.) before use.

0021-9673/89/$03.50

Chromatographic conditions

HPLC analyses of the enzyme-catalysed reaction were performed with a Waters Assoc. apparatus (Milford, MA, U.S.A.) consisting of a Model 590 pump, equipped with a Model U6K universal injector, a Lambda-Max Model 480 ultraviolet detector and a Model 730 data module. Separations were accomplished on a μBondapak C_{18} column (300 mm × 3.9 mm I.D.) with a C_{18} Corasil precolumn (35 × 3.9 mm I.D.) (both from Waters). Elution was performed with 0.1 *M* potassium dihydrogenphosphate buffer pH (6.1) containing 5% methanol at a flow-rate of 2.0 ml/min and the eluent was monitored by UV absorption at 254 nm (0.05 a.u.f.s.).

A typical chromatogram of the reaction mixture is shown in Fig. 1.

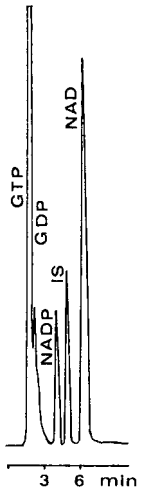

Fig. 1. Typical HPLC chromatogram of the reaction mixture, indicating GTP, GDP, thymine (IS), NAD and NADP. The amounts of NAD, NADP and thymine injected after 10 min of reaction were 2.9, 0.61 and 2.0 nmol respectively. The elution was monitored at 254 nm (0.05 a.u.f.s.).

Assay of enzyme activity

2 m*M* NAD in 0.1 *M* Tris–HCl (pH 7.6) was allowed to react with 3 m*M* GTP and NAD kinase in the presence of 0.1 m*M* $CaCl_2$ and 4.5 μg of calmodulin in a total volume of 1 ml. The enzyme was pre-incubated with calmodulin at 37°C for 2 min, and the reaction was started by adding NAD. At 10-min intervals, 10 μl of the reaction mixture were pipetted into 40 μl of 20 m*M* HCl, containing 10 nmol of thymine as an internal standard, then 10 μl of this solution were injected into the HPLC apparatus. Alternatively, the reaction mixture contained also 0.4 m*M* NADP, *i.e.*, the product of the reaction, and the samples were diluted in only 20 m*M* HCl. When NADP was added to the reaction mixture the product formed during the enzyme-catalysed reaction was calculated as previously described[12], according to

$$\text{nmol NADP} = \frac{P_0\left[\dfrac{A_s(0) - Y_s}{A_p(0) - Y_p} - \dfrac{A_s(t) - Y_s}{A_p(t) - Y_p}\right] \cdot R}{\left[\dfrac{A_s(t) - Y_s}{A_p(t) - Y_p} \cdot R\right] + 1}$$

where: P_0 = amount of product initially present in the injected sample, $A_s(0)$ = peak area of the substrate (NAD) at time zero, $A_p(0)$ = peak area of the product (NADP) at time zero, $A_s(t)$ = peak area of NAD at time t, $A_p(t)$ = peak area of NADP at time t, R = ratio of the slopes of the calibration graphs, NADP/NAD, Y_s and Y_p = peak areas of NAD and NADP respectively at zero concentration calculated from the calibration graphs obtained without the internal standard.

An activity unit is defined as the amount of enzyme which phosphorylates 1.0 nmol of NAD to NADP per min at 37°C, pH 7.6, and in the presence of calcium ions and calmodulin.

RESULTS AND DISCUSSION

GTP was chosen as the phosphate donor since it did not overlap NADP, as did ATP under the chromatographic conditions used, and because it is even more effective than ATP[8]. However, while GTP overlapped the peak of GDP, another product of the reaction, this did not affect the analysis, since the assay was based mainly on the determination of NADP. When the column was not exhaustively washed in the course of the analysis, the NAD peak tended to shift toward the internal standard (thymine) and an appropriate reequilibration of the column (about 30 min) led to a delay in the total assay. This inconvenience was circumvented by eliminating thymine from the dilution medium and using NADP itself as the internal standard according to the procedure described.

Reproducible results (S.D. = 4.2%) were obtained in the assay of the specific activity of three different amounts of enzyme (3.7 units/mg). In the calibration graphs, the detector responses for NAD and NADP standard samples were linear in the range of 0.5–10 nmol (r = 0.999) and 0.2–4.5 nmol (r = 0.999) respectively.

The activity measured by means of the internal standard method indicated no difference from that determined with NADP and the use of the equation reported above, as shown in Fig. 2. This means that the concentration of NADP in the assay

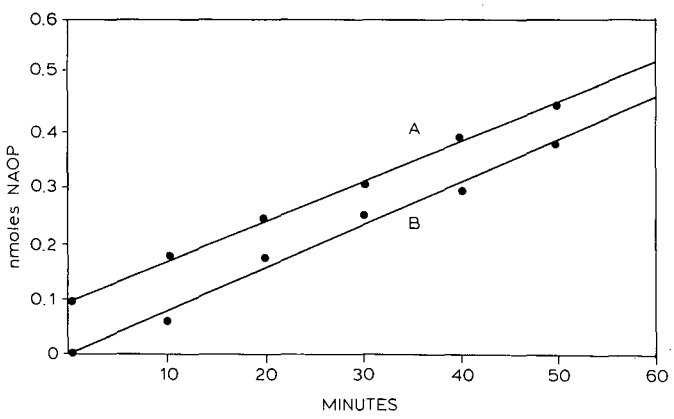

Fig. 2. Comparison of the activities of a sample of NAD kinase determined by the internal standard method (A) and the equation given in the text (B). The values of the constants in the equation were P_0 = 0.08 nmol, R = 0.8, Y_s = 484.8 and Y_p = −0.05. The specific activities were 3.6 and 3.8 units/mg respectively.

sample does not cause any product inhibition but is able to provide a more rapid assay than the use of an internal standard, which requires prolonged washing of the column (about 30 min). Moreover, the specific activity of NAD kinase was linearly related to the amount of enzyme used as demonstrated with three different quantities of enzyme.

In conclusion, the HPLC assay proposed here for NAD kinase activity represents a precise and rapid method without the need of a second enzyme for the determination of the reaction product (NADP).

REFERENCES

1 C. Blomqvist, *J. Biol. Chem.*, 248 (1973) 7044.
2 D. Epel, C. Patton, R. W. Wallace and W.-Y. Cheung, *Cell*, 23 (1981) 543.
3 T. Oh-hama and S. Miyachi, *Biochim. Biophys. Acta*, 30 (1959) 202.
4 H. Matsumura-Kadota, S. Muto and S. Miyachi, *Biochim. Biophys. Acta*, 679 (1982) 300.
5 J. M. Anderson and M. J. Cormier, *Biochem. Bipohys. Res. Commun.*, 84 (1978) 595.
6 S. Muto, *FEBS Lett.*, 147 (1982) 161.
7 P. Simon, M. Bonzon, H. Greppin and D. Marme, *FEBS Lett.*, 167 (1984) 332.
8 A. E. Chung, *J. Biol. Chem.*, 242 (1967) 1182.
9 D. E. Blume and J. A. Saunders, *Anal. Biochem.*, 114 (1981) 97.
10 P. G. Pietta, M. Pace and F. Menegus, *Anal. Biochem.*, 131 (1983) 533.
11 P. G. Pietta, P. L. Mauri and M. Pace, *J. Chromatogr.*, 411 (1987) 498.
12 M. Pace, P. L. Mauri, P. G. Pietta and D. Agnellini, *Anal. Biochem.*, 176 (1989) 437.

Journal of Chromatography, 476 (1989) 491–498
Elsevier Science Publishers B.V., Amsterdam — Printed in The Netherlands

CHROMSYMP. 1593

HETEROGENEITY OF HUMAN PEPSIN 1, AS SHOWN BY HIGH-PERFORMANCE ION-EXCHANGE CHROMATOGRAPHY

K. PEEK, N. B. ROBERTS* and W. H. TAYLOR
Department of Chemical Pathology, Royal Liverpool Hospital, Liverpool L7 8XW (U.K.)

SUMMARY

We have shown that pepsin 1 can be prepared in milligram quantities from human gastric juice by semi-preparative high-performance ion-exchange chromatography. Further investigation into the elution of this enzyme using linear chloride gradients have shown it to be a heterogeneous mixture, the components of which all have peptic activity, but differing specific activities. These components are changed in number and retention time by incubation with hyaluronidase and aryl sulphatase, but not by neuraminidase or acid phosphatase, implying the presence of a sulphated proteoglycan.

INTRODUCTION

Pepsin 1 is present in human gastric juice in relatively low amounts, but is increased in patients with peptic ulcer disease[1]. It has different enzymic properties from the major human pepsin 3, particularly in its action on gastric mucoprotein[2] and bovine collagen[3]. We have shown that pepsin 1 contains up to 40–50% carbohydrate by weight[4], in contrast to human pepsins 3 and 5. "Fast" and "slow" moving components of pepsin 1 have been described[5], and subsequently Ryle and Foltmann[6] suggested that pepsin 1 is a mixture of pepsin–carbohydrate complexes produced as a result of differing amounts of carbohydrate attached to a common protein.

We now describe an investigation by high-performance ion-exchange chromatography (HPIEC) into the heterogeneity of pepsin 1 and the effect after pre-incubation with enzymes which might hydrolyse its carbohydrate component and any attached phosphate or sulphate groups.

EXPERIMENTAL

Chemicals

The chemicals used were of AnalaR grade (British Drug Houses, Poole, U.K.). Agarose was obtained from Oxoid (London, U.K.). DEAE-cellulose, naphthalene black, bovine haemoglobin, bovine globin, swine pepsin, acid phosphatase, neuraminidase, hyaluronidase, and aryl sulphatase were obtained from Sigma (Poole, U.K.).

0021-9673/89/$03.50

Apparatus

The ion-exchange column used was 7.5 × 0.75 cm, TSK DEAE 5PW 10 μm (Toyo Soda Manufacturing, Tokyo, Japan), connected with a guard column containing TSK guard gel DEAE 5PW. The high-performance liquid chromatographic (HPLC) system included a CM4000 low-pressure mixing ternary pump (Milton Roy, Stone, U.K.). The eluent was monitored at 280 nm with a SM4000 variable wavelength detector (Milton Roy). Samples were injected automatically with a Gilson 231 autosampler (Anachem, Bedford, U.K.) through a 500-μl loop.

Sample preparation

Human gastric juice, obtained from patients undergoing routine Pentagastrin tests, was pooled and concentrated five times, using a Sartorious tangential flow ultrafiltration apparatus (V. A. Howe, London, U.K.). Approximately 1 l of concentrated gastric juice was then dialysed against 10 l of 50 m*M* sodium acetate (pH 4.1) for 16 h and mixed with 100 gm of DEAE cellulose, which had been equilibrated with 50 m*M* sodium acetate (pH 4.1). The slurry was stirred for 1 h at +4°C, allowed to settle, and the supernatant was discarded. The DEAE-cellulose was washed with 750 ml of 50 m*M* sodium acetate (pH 4.1), containing 0.25 *M* NaCl and the supernatant was discarded. The pepsin 3- and 1-rich fraction was then eluted with 750 ml of 50 m*M* sodium acetate (pH 4.1), containing 1 *M* NaCl, and concentrated in 200 ml aliquots to 10 ml by ultrafiltration, using stirred cells (Amicon, Stonehouse, U.K.). The concentrates were dialysed for 16 h against 1 l of 50 m*M* sodium acetate (pH 4.1), filtered through a 0.45-μm filter, and the pepsins isolated by HPIEC with gradient 1 (Table I). The purified pepsin 1 fractions were pooled, dialysed against 1 l of 50 m*M* sodium acetate (pH 4.1) for 16 h and then used for HPIEC studies. All the preparative and dialysis procedures were carried out at +4°C.

High-performance ion-exchange chromatography

The heterogeneity of pepsin 1 was investigated, using gradients 2 and 3 (Table I). The flow-rate was 1 ml/min and the back-pressure less than 10 bar. All solvents were filtered through a 0.45-μm filter under vacuum and purged with helium for 10 min before use. After use, the HPIEC system was flushed with methanol, followed by deionised water for 10 min each. For the proteolytic activity profiles, 0.5-ml fractions

TABLE I

ELUTION PROFILES FOR THE SEPARATION OF HUMAN PEPSIN 1

Solvent A = 50 m*M* sodium acetate (pH 4.1). Solvent B = A + 1 *M* NaCl. Linear gradients.

Gradient 1			*Gradient 2*			*Gradient 3*		
Time (min)	*A (%)*	*B (%)*	*Time (min)*	*A (%)*	*B (%)*	*Time (min)*	*A (%)*	*B (%)*
0	100	0	0	100	0	0	100	0
5	100	0	5	100	0	5	100	0
30	70	30	25	0	100	95	0	100
30.1	0	100	40	0	100	97	100	0
40	0	100	42	100	0			
42	100	0						

were collected into 5-ml plastic tubes on ice and assayed for protein[7] and for proteolytic activity, using bovine haemoglobin at pH 2.0 (ref. 8) (calibrated with a swine pepsin standard). Specific activity was expressed as the proteolytic activity in swine pepsin equivalents per mg of protein.

Agar gel electrophoresis

Agar gel electrophoresis was performed at pH 5.0 using a Panagel electrophoresis unit (Millipore, London, U.K.) for 1.5 h at 150 V and 40 mA on 1.5% w/v agar gels at +4°C, containing 25 m*M* sodium acetate (pH 5.0) as described by Newton *et al.*[9], and the pepsins were visualised after incubation with bovine globin at pH 2.0 (ref. 8).

Treatment of pepsin 1 with hydrolytic enzymes

Acid phosphatase (wheat germ, E.C. 3.1.3.6), neuraminidase (*Clostridium perfringens*, E.C. 3.2.1.18), hyaluronidase (bovine testes, E.C. 3.2.1.35), and aryl sulphatase (limpet, E.C. 3.1.6.1) were freshly prepared (1 mg/ml) in 50 m*M* sodium acetate (pH 4.1). Each enzyme was incubated with pepsin 1 (1:1, w/w; total volume 2 ml) for 1 h at 37°C. Immediately after incubation, the mixture was chromatographed in the HPIEC system; enzyme and pepsin 1 alone were used as controls.

RESULTS

Fig. 1 shows the purification of pepsin 1 (*ca.* 14% of the total pepsin content) from a pepsin 3- and 1-rich fraction by HPIEC. Pepsin 1 is well resolved from pepsin 3,

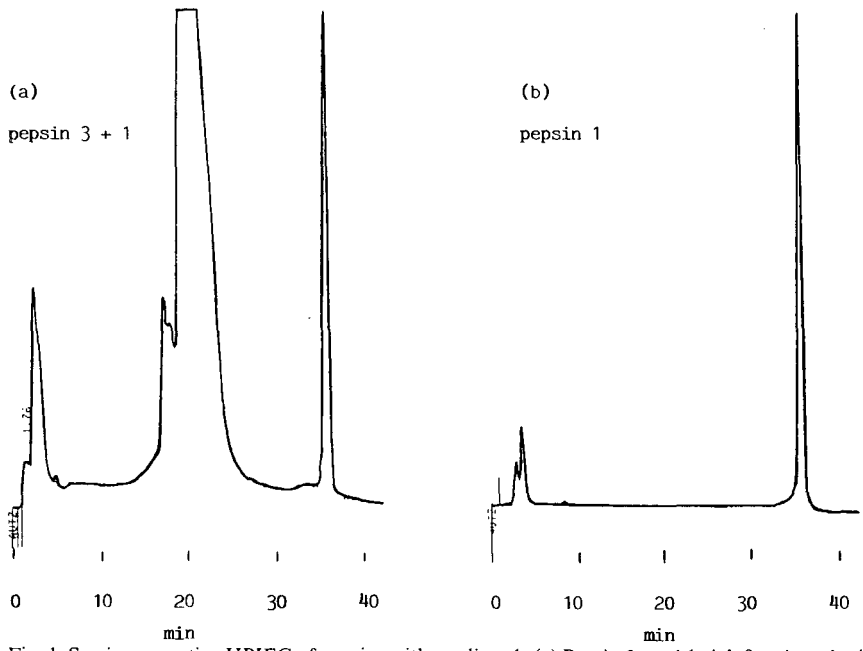

Fig. 1. Semi-preparative HPIEC of pepsins with gradient 1. (a) Pepsin 3- and 1-rich fraction obtained from concentrated gastric juice by the DEAE-cellulose preparative method, is shown to contain only pepsins 3 and 1. A 500-μl sample was injected, containing 15 mg of protein. (b) The pepsin 1 fraction obtained from Fig. 1a was rechromatographed to confirm its purity. A 500-μl sample was injected containing 1 mg of protein. UV 280 nm, 2.0 a.u.f.s.

and upon reinjection it was eluted as a single peak. This peak, when chromatographed with gradient 2 (Fig. 2), was eluted as a broad peak, consisting of several unresolved peaks. All fractions taken through this peak showed proteolytic activity against bovine haemoglobin (Fig. 2), but with differing specific activities (mean 0.2 ± 0.13 S.D.).

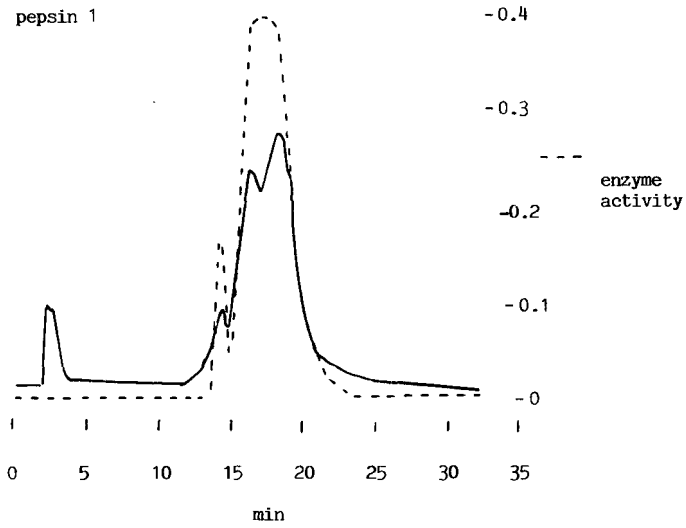

Fig. 2. HPIEC of purified pepsin 1 with gradient 2. (———) UV 280 nm, 0.2 a.u.f.s.; (– – –) proteolytic activity. A 500-μl sample was injected containing 500 μg of protein.

When the chloride gradient was extended to 95 min with gradient 3 (Fig. 3a), the elution of pepsin 1 extended over 33 min in at least six unresolved peaks.

Chromatography of pepsin 1 after treatment with various acid hydrolases is shown in Fig. 3. Neuraminidase and acid phosphatase had no effect on the elution profile of pepsin 1 (Fig. 3b and c). However, hyaluronidase changed the retention time and the elution profile, which now consisted of four large but still unresolved peaks eluted at a lower chloride concentration (Fig. 3d). When the hyaluronidase–pepsin 1 mixture was electrophoresed on agar gel, a slower migration to the anode was observed than for with pepsin 1 alone (Fig. 4). Aryl sulphatase (Fig. 3e) did not affect the onset of elution of pepsin 1, but significantly reduced the time for complete elution from 33 min to *ca.* 20 min. When the hydrolytic enzymes were chromatographed alone, no peaks were eluted in the pepsin 1 region.

DISCUSSION

Pepsin 1 can be readily obtained in milligram quantities by a combination of DEAE-cellulose batch adsorption and HPIEC. Pepsin 1 is observed as a single proteolytic zone on agar gel electrophoresis, but extended gradients in HPIEC show it to be heterogeneous, being eluted as a broad band, in which proteolytic activity can be detected in all fractions.

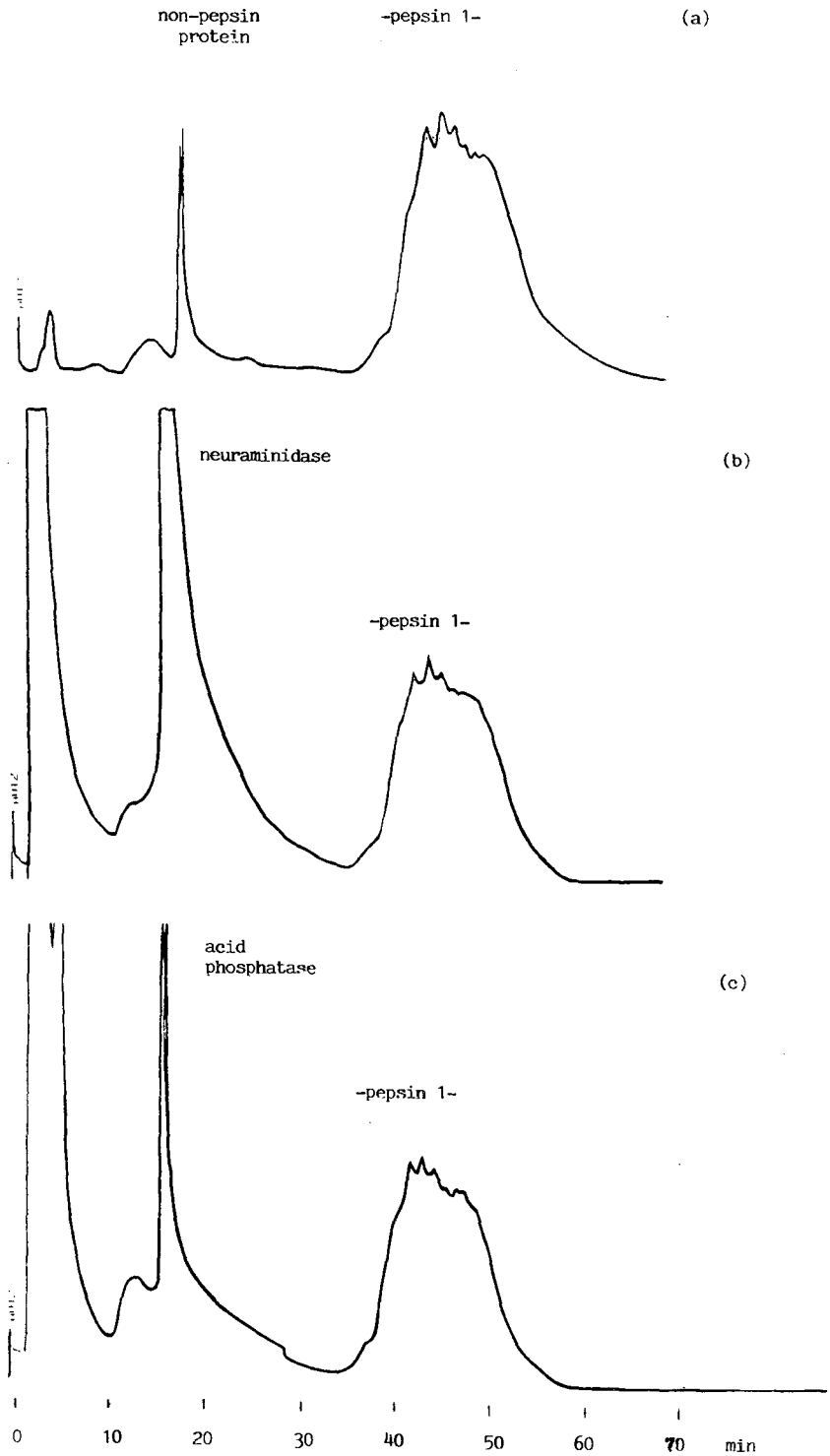

Fig. 3.

(Continued on p. 496)

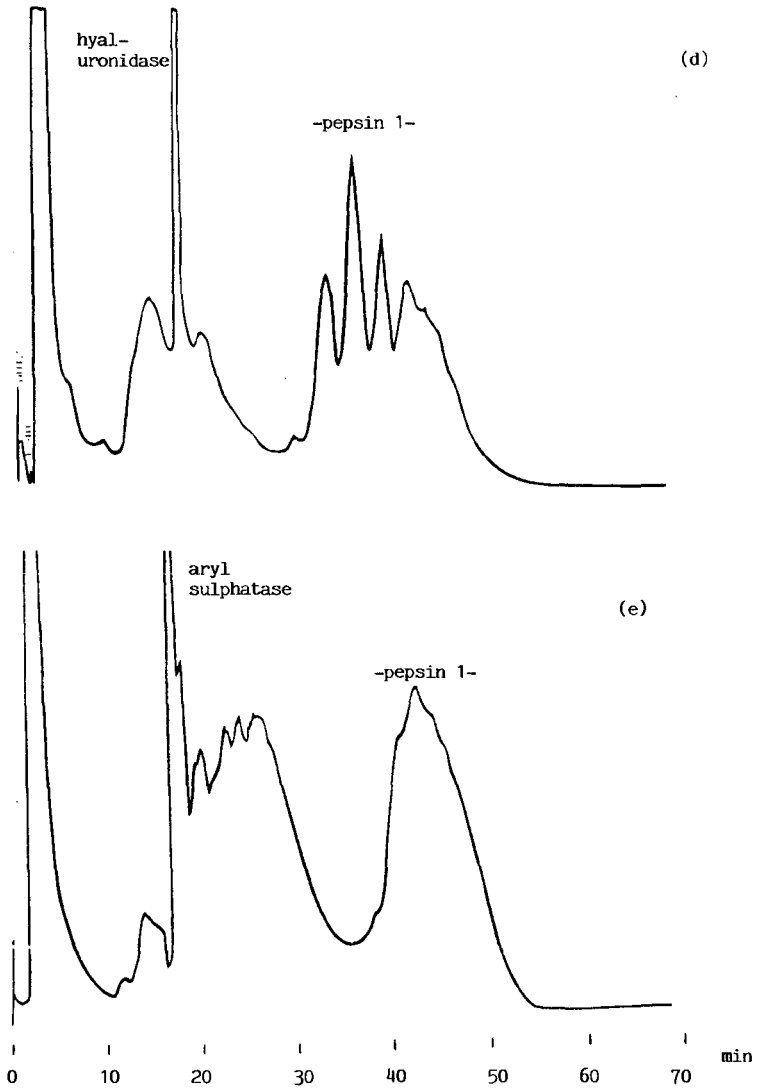

Fig. 3. Chromatogram of pepsin 1 with gradient 3 after pre-incubation with: (a) pepsin 1 control, (b) neuraminidase, (c) acid phosphatase, (d) hyaluronidase and (e) aryl sulphatase. UV 280 nm, 0.02 a.u.f.s. A 500-μl sample was injected containing 250 μg of pepsin 1.

Pepsin 1 is known to contain up to 50% carbohydrate[4], and Ryle and Foltmann[6] suggest that the variable substitution of carbohydrate onto a common protein may account for the heterogeneity observed on agar gels. We have investigated the action of various acid hydrolases on pepsin 1; aryl sulphatase and hyaluronidase had striking effects. In particular, hyaluronidase changed the elution profile and retention time of pepsin 1. Ryle and Foltmann[6] were the first to observe the effect of hyaluronidase on the electrophoretic mobility of pepsin 1, and showed that fragments were removed in association with a reduction in molecular weight.

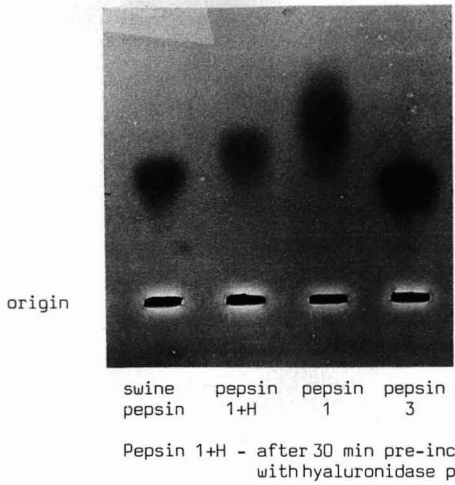

Fig. 4. Agar gel electrophoresis at pH 5.0 of pepsin 1 after treatment with hyaluronidase. Enzymic activity is shown as zones of unstained areas (dark in the photograph) as a result of depletion of the substrate (bovine globin) contained in the gel.

Initial studies by Pearson *et al.*[4] on the sugar analysis of the pepsin 1 complex showed the presence of uronic acid, N-acetylglucosamine, N-acetylgalactosamine and neutral sugars. In addition, they separated a proteoglycan from pepsin 1 by equilibrium centrifugation in a caesium chloride gradient containing 4 *M* guanidium chloride. They concluded that pepsin 1 was a complex of protein and proteoglycan, interacting ionically.

Hyaluronidase will degrade both hyaluronic acid and chondriotin sulphate, and the evidence we present indicates that pepsin 1 may contain one or both of these glycosaminoglycans. In addition, the action of aryl sulphatase would imply the presence of a sulphated proteoglycan.

The high electrophoretic mobility and strong adsorption on anion-exchange resins may thus result not only from the presence of phosphate[10], but from the presence of a proteoglycan moiety in which acidic sugars and sulphate groups produce an increased negative charge. The formation of this highly charged species may also affect the activity of pepsin 1 by interacting ionically with the substrate and allow more efficient proteolysis[2,3].

REFERENCES

1 W. H. Taylor, *Nature (London)*, 227 (1970) 76.
2 J. P. Pearson, R. Ward, A. Allen, N. B. Roberts and W. H. Taylor, *Gut*, 27 (1986) 243.
3 D. J. Etherington and W. H. Taylor, *Clin. Sci.*, 58 (1980) 30.
4 J. P. Pearson, A. Allen, N. B. Roberts and W. H. Taylor, *Clin. Sci.*, 72 (1987) 33p.
5 N. B. Roberts and W. H. Taylor, *Biochem. J.*, 169 (1978) 607.
6 A. P. Ryle and B. Foltmann, in V. Kostka (Editor) *Aspartic Proteinases and their Inhibitors*, Walter de Gruyter, Berlin and New York, 1985, p. 97.

7 O. H. Lowry, N. J. Rosenbrough, N. J. Farr and R. J. Randall, *J. Biol. Chem.*, 193 (1937) 265.
8 D. J. Etherington and W. H. Taylor, *Biochem. J.*, 113 (1969) 663.
9 C. J. Newton, N. B. Roberts and W. H. Taylor, *J. Chromatogr.*, 417 (1987) 391.
10 N. B. Roberts, *Ph.D. Thesis,* University of Liverpool, Liverpool, 1975.

Journal of Chromatography, 476 (1989) 499–511
Elsevier Science Publishers B.V., Amsterdam — Printed in The Netherlands

CHROMSYMP. 1619

REVERSED-PHASE LIQUID CHROMATOGRAPHY OF PROTEINS WITH STRONG ACIDS

GÉRALDINE THÉVENON and FRED E. REGNIER*
Department of Biochemistry, Purdue University, West Lafayette, IN 47907 (U.S.A.)

SUMMARY

Small organic acids are generally used as pairing agents at less than 1% concentration in reversed-phase chromatography (RPC) of proteins. When the protein is very hydrophobic and insoluble, as in the case of membrane proteins, up to 60% aq. formic acid has been used. This paper reports a study of the influence of acid concentration on both chromatographic retention and protein structure in RPC.

Chromatographic retention increases in proportion to the concentration of organic acid in the mobile phase up to some intermediate concentration. Use of still higher concentrations of acid results in a sharp drop in chromatographic retention with a change in selectivity. The data indicate that the structure of proteins in strong acids are different from that in weak acids. This work examines the reason for this decrease in chromatographic retention at formic and trifluoroacetic acid concentrations above 30% (v/v). Spectroscopic studies show that protein conformation continuously changes with the addition of acid.

INTRODUCTION

Retention and elution of proteins in reversed-phase chromatography (RPC) involves conformational changes of the solute and generally denaturation. The nature of the solvents used in this chromatographic mode, and the interaction of the polypeptides with the sorbent are the main causes for this denaturation[1]. The most popular solvents for RPC consist of a very acidic aqueous solution and a gradient of organic solvent, particularly when silica-based materials are employed as the sorbent. Protonation of the residual silanol groups on the support diminishes ionic interactions with the basic amino acid residues of the proteins. Moreover, small organic acids form ion pairs with these basic sites. Recently, a large-pore poly(styrene–divinylbenzene) material has become commercially available that can be used for RPC of biological compounds[2,3]. The chemical stability of this material is an advantage in work with strong acids and bases[4]. Moreover, this new packing does not contain silanol groups. It should be noted, however, that the use of trifluoroacetic acid (TFA) at concentrations of 0.1 to 1% with acetonitrile as modifying solvent often gives the best chromatographic results, even with organic resins which contain no silanol groups[5].

0021-9673/89/$03.50

The process by which proteins are denatured in RPC has been a subject of intense investigation in the past few years. The response to the denaturants both in solution and on the column varies with each protein[6,7]. As determined by coupling RPC with other chromatographic modes, even the rate of unfolding and the extent of denaturation following the removal of acids and organic solvents is protein-specific[8,9]. Depending on the degree of unfolding and the reversibility of the process, proteins may be eluted with multiple or broad peaks, as has been shown in several studies[10–12].

All of the work cited above has been done with dilute acids (0.1–1%). However, these conditions are of limited utility in the chromatography of large, hydrophobic proteins. Cell membranes or viral envelopes are not soluble under such conditions, and cannot be eluted[13]. It is necessary to work at very high acid concentrations to solubilize the proteins in these cases. Formic acid at concentrations ranging up to 60% has been found of much greater utility than the more hydrophobic TFA normally used[14,15]. To date, little work has been done to understand why such conditions are more successful for the chromatography of these proteins. Obviously, such severe conditions must have a profound effect on protein structure. This work examines the influence of high concentrations of acid on protein chromatography. Maximum retention was obtained for all the proteins studied at intermediate acid concentrations. Solvent effects or conformational changes could induce such a phenomenon. Spectroscopic methods were employed to determine whether conformational changes of proteins occur in such media. This paper will show that the conformation of proteins changes with the concentration of acid in the mobile phase. The balance between hydrophobic and hydrophilic amino acid residues at the surface of the protein seems the main cause for the retention changes of the polypeptides in RPC.

MATERIALS AND METHODS

Equipment

The chromatographic system consisted of a Varian 5500 gradient pumping system (Varian, Walnut Creek, CA, U.S.A.), a Valco (Houston, TX, U.S.A.) Model C6U injector with a 2-, 40- or 100-μl sample loop and an LC 85B variable-wavelength UV detector (Perkin Elmer, Norwalk, CT, U.S.A.) operated at 280 nm. A Hewlett-Packard (HP) (Palo Alto, CA, U.S.A.) Model 1040A photodiode-array detector was used for the determination of absorbance ratios and second-derivative spectroscopy. This detector was equipped with an HP85B personal computer, an HP 9121 P/S disc drive, and an HP 7470A graphics plotter. Second derivatives were processed with the HP Data Evaluation II software. The flow-rate was 1 ml/min unless otherwise specified.

RPC was performed on poly(styrene–divinylbenzene) PLRP-S, 8 μm, 300 Å (1000 Å for IgG) (Polymer Labs., Shropshire, U.K.). Columns were packed in 2-propanol, at 3000 p.s.i. with a Shandon column packer (Sewickley, PA, U.S.A.). Dimensions of the columns were 5 × 0.46 cm I.D. Elution was achieved with linear gradients of 40 min for all the retention measurements and 20 min for the spectroscopic measurements. Except for Fig. 1, eluent B was pure acetonitrile in all RPC experiments. The amount of protein injected varied between 10 and 20 μg for all proteins, except IgG, where 250 μg were injected. Each retention value is the result of at least two reproducible values.

Cation-exchange chromatography was performed on a SynChropak CM 300 column, 15 × 0.41 cm I.D., from SynChrom (Lafayette, IN, U.S.A.).

Reagents

HPLC-grade acetonitrile came from American Burdick & Jackson (Muskegon, MI, U.S.A.). TFA (99%) was from Aldrich (Milwaukee, WI, U.S.A.). Formic acid 88%, from Fischer Scientific (Fair Lawn, NJ, U.S.A.) was used for all the experiments, except for the determination of absorbance ratios and second-derivative spectroscopy, where 99% formic acid from Aldrich was employed. Proteins and peptides were purchased from Sigma (St. Louis, MO, U.S.A.). Acid solutions were filtered through a Whatman GF/C (1.2 μm) filter (Hilboro, OR, U.S.A.).

Buffers for cation exchange were prepared with mono- and dibasic potassium phosphate (Mallinckrodt, Paris, KY, U.S.A.) and sodium chloride (Fischer Scientific). Solutions were filtered through a Rainin Nylon-66 (0.45 μm) filter (Woburn, MA, U.S.A.) and degassed. Recovery of IgG was determined with the Bio-Rad (Richmond, CA, U.S.A.) protein assay reagent.

Ribonuclease A and IgG recoveries

Protein fractions were collected after RPC. Solutions containing 60% and 80% aq. formic acid were dialyzed overnight against 200 and 400 volumes of water, respectively. Samples were then dialyzed twice for 5 h against 200 volumes of 10 m*M* phosphate buffer. The fraction collected with 0.1% acid was dialyzed directly against phosphate buffer, as described above. All dialysates were then lyophilized and resolubilized in water. Protein concentrations were determined by the Bio-Rad micro assay. The 100% control was prepared by disconnecting the column and collecting the protein sample directly after the injection valve.

Refolding of ribonuclease A and ovalbumin

The procedure used for the collection, dialysis, and lyophilization was identical to that for IgG. Samples were chromatographed on an ion-exchange column with a 30-min gradient from 10 m*M* phosphate buffer (pH 7) to 1 *M* sodium chloride in 100 m*M* phosphate buffer (pH 7). Ribonuclease A activity was measured by the method recommended by the enzyme supplier with the exception that the solutions used were fifteen times more concentrated than specified by the supplier.

RESULTS AND DISCUSSION

Chromatographic results

Fig. 1 reports the retention of various proteins as a function of formic acid concentration. The retention of all proteins examined gradually increased to a maximum and then began to decline slowly, with the exception of ovalbumin (OVA). The longer a protein was retained, the higher the concentration of acid required before its retention began to decrease. The normal practice in RPC of polypeptides is to add acid to both the aqueous and organic solvent. When the concentration of acid is low ($< 1\%$), the addition of acid to the organic eluent does not significantly change its concentration. In contrast, addition of 30–80% aq. formic acid to the organic solvent drastically changes it. This make it difficult to interpret the results at high concentra-

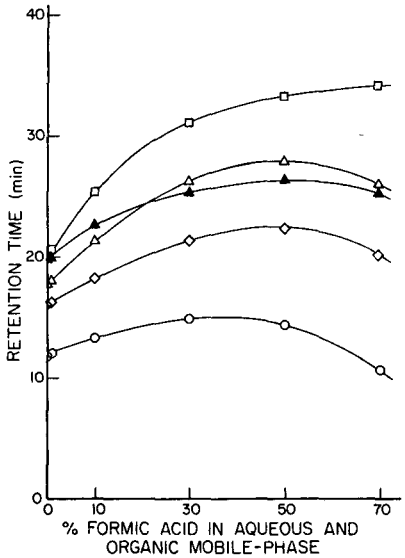

Fig. 1. Retention of various proteins and heme *vs.* the percentage of formic acid in the aqueous and organic mobile phases. For chromatographic conditions see Materials and Methods section. □ = Ovalbumin; ▲ = heme; △ = apomyoglobin; ◇ = lysozyme; ○ = ribonuclease A.

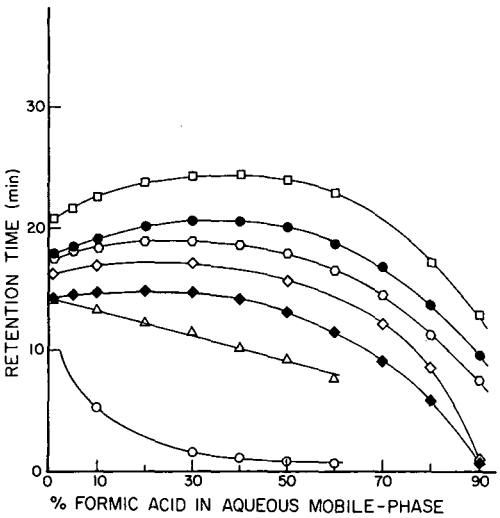

Fig. 2. Retention of various proteins and peptides *vs.* the percentage of formic acid in the aqueous mobile phase. For chromatographic conditions see Materials and Methods section. □ = Ovalbumin; ● = α-chymotrypsinogen-A; ⬡ = soybean trypsin inhibitor; ◇ = lysozyme; ◆ = cytochrome *c*; △ = hippuryl-L-phenylalanine; ○ = N-acetyl-L-tyrosine.

tions of acid. Therefore, the same experiment was repeated without acid in the organic mobile phase (Fig. 2).

When no acid was added to the organic mobile phase, maximum in retention of all proteins was achieved with *ca.* 30% aq. formic acid in the mobile phase. Maxima of these curves, as determined by the first derivative, are given in Table I and reveal that the position of the maximum is related to the retention magnitude (and size) of the protein.

The retentions of two small peptides, hippuryl-phenylalanine and N-acetyl-L-tyrosine, are also shown in Fig. 2. The retentions are maximal at low concentrations of formic acid and decrease with increasing amounts of acid. This is probably because the solvophilic power of formic acid is slightly higher than that of water. Therefore, the increasing retention observed for the proteins studied cannot be explained easily by this solvent phenomenon.

In Fig. 3 the lysozyme retention is plotted against the acid concentration when formic acid is substituted by TFA. TFA is a well-known pairing agent, used in RPC[16] and in size-exclusion chromatography (SEC), where retention is related to the size and charge of the proteins[17]. These curves reveal two phenomena: (i) the curve shape is similar for these two acids and (ii) the increase in retention is larger with TFA than with formic acid. The similarity in curve shapes indicates that the phenomenon observed is not specific for formic acid. One explanation for the second observation may be that the hydrophobicity of TFA is higher than that of formic acid. The more hydrophobic the ion-pairing agent, the higher the retention in RPC[18,19].

The ion pairs formed by acids with the protonated amine groups of the proteins could explain the initial retention increase. The hydrophobic part of the ion-paired acid would increase the surface contact of the solute with the stationary phase and, concomitantly, the retention. Another explanation could be based on a denaturation effect. The more acid is added, the more the proteins are denatured. The hydrophobic interior of the proteins would become more accessible to the stationary phase at high concentrations of acid and this increases chromatographic retention. Retention would continue to increase with the addition of acid until the protein has reached some maximum state of acid-induced unfolding. The decrease in retention at still higher concentrations of acid could be explained by the greater solvophilic power of formic acid relative to water.

To further confirm the ion-pairing and protein unfolding roles of these acids at

TABLE I

PERCENT ACID AT RETENTION MAXIMUM FOR VARIOUS PROTEINS

For chromatographic conditions see Fig. 2.

Proteins	*MW*	*Formic acid (%)*
Ovalbumin	45 000	38 ± 2
α-Chymotrypsinogen A	25 000	35 ± 2
Soybean trypsin inhibitor	20 100	27 ± 2
Apomyoglobin	17 500	28 ± 2
Lysozyme	14 300	26 ± 2
Cytochrome *c*	12 200	22 ± 2

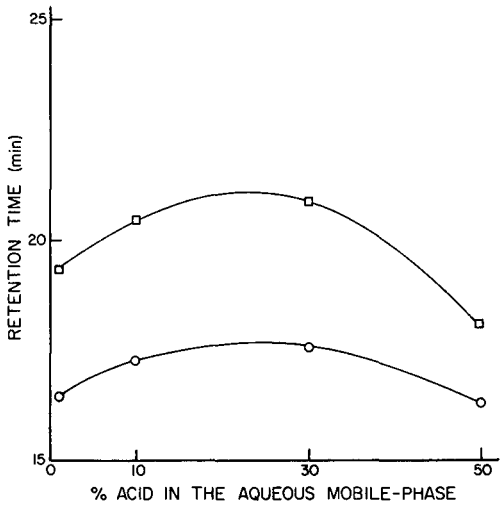

Fig. 3. Retention of lysozyme *vs.* the percentage of acid in the aqueous mobile phase. For chromatographic conditions see Materials and Methods section. □ = TFA; ○ = formic acid.

high concentration, we studied the influence of acid on the retention of a solute possessing a rigid three-dimensional structure in strong acid. It is well known that under acidic conditions, in the presence of organic solvent, myoglobin loses its heme[20]. Consequently, this protein gives two peaks in RPC, one corresponding to the apoprotein, the other corresponding to the free heme (solute possessing a rigid three-dimensional structure). In Fig. 4, the retention of these two solutes are plotted against the concentration of formic acid. Two different retention curves are obtained. While the curve obtained for apomyoglobin is similar to the one obtained for the proteins

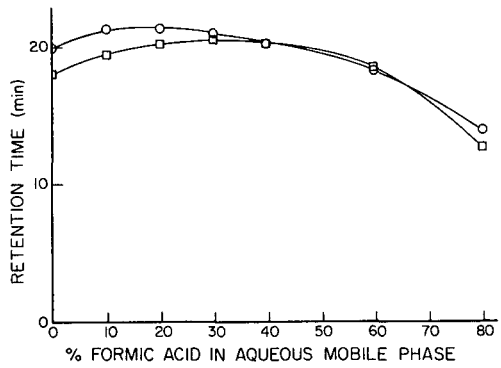

Fig. 4. Retention of apomyoglobin and its heme *vs.* the percentage of formic acid in the aqueous mobile phase. For chromatographic conditions see Materials and Methods section. □ = Apomyoglobin; ○ = heme.

previously studied, it differs for the heme. Its retention first increases with acid concentrations, this is probably due to its ability to bind acid ligands[21], but the maximum retention is reached at a lower acid concentration (10%) than for the proteins. Moreover, the shape of the curve after the maximum is somewhat different from that observed for the proteins in Fig. 2. The same curve shape and maximum retention were obtained with polylysine, a polypeptide capable of forming a large number of ion pairs (data not shown).

These results show that, even if the ion-pairing effect increases when acid is added to the mobile phase, this does not explain the retention of proteins when the concentration of acid is higher than 10%. It is probable that protein structure plays a role in the increase in retention observed at acid concentrations higher than 10%.

Spectroscopic studies

Absorbance ratio measurements. When conformational changes occur in a protein, different amino acid residues become more or less exposed to the solvent. If the aromatic residues are affected by these changes, the UV absorbance of the polypeptide will vary. Consequently, these variations can be monitored by observing the shifts induced in the UV spectrum of the protein. Each of the three aromatic amino acid residues in proteins has a different UV spectrum[22]. If two wavelengths are selected at the absorbance maximum of the aromatic amino acid residues, a ratio of the two will indicate which amino acids become exposed to the surface and which are inside the protein. This technique has previously been applied successfully in following the unfolding of β-lactoglobulin in hydrophobic-interaction chromatography[23]. That work[22,23] has shown that the contributions of the three aromatic amino acid residues to the UV spectra were: 292 nm, tryptophan only; 274 nm, tryptophan and tyrosine; 254 nm, tryptophan, tyrosine, and phenylalanine.

The ratios of these wavelengths have been calculated for various proteins, at different concentrations of acid. The two proteins used in this study contain different relative amounts of the aromatic amino acid residues (Table II). Ribonuclease A was chosen because it lacks tryptophan. The strong absorbance of this aromatic amino acid usually prevents the observation of any changes for phenylalanine. Consequently, this protein allowed studies of changes in the environment of phenylalanine. Lysozyme has a ratio Trp/Tyr of 2, which allows studies of changes in the exposure of these two aromatic amino acid residues to the surface, as seen in Fig. 5. A reorientation of aromatic amino acids seems to occur at an acid concentration around 30%, as seen in all the curves.

TABLE II

AROMATIC AMINO ACID RESIDUES IN VARIOUS PROTEINS

Protein	*Number of residues*		
	Phe	*Tyr*	*Trp*
Ribonuclease A[27]	3	6	0
Lysozyme[27]	3	3	6
Ovalbumin[26]	20	9	3

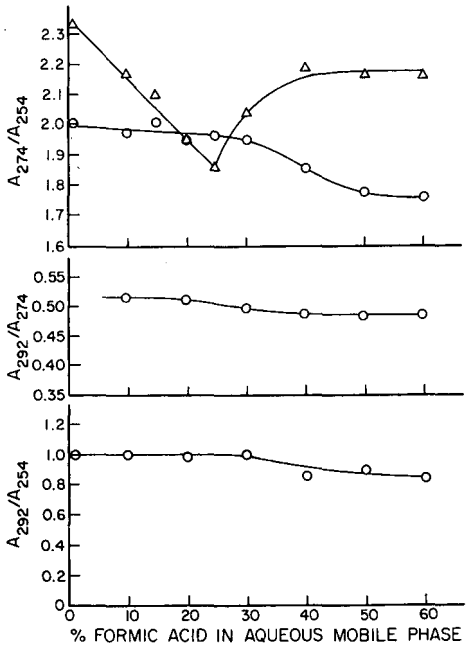

Fig. 5. Influence of the amount of formic acid on the spectroscopic properties of various proteins. For chromatographic conditions see Materials and Methods section. △ = Ribonuclease A; ○ = lysozyme.

With ribonuclease A, the A_{274}/A_{254} ratio decreased when the initial amount of formic acid was added. This suggests a change in conformation, resulting in phenylalanine residues becoming more exposed at the surface of the protein. This is expected in denaturation. At formic acid concentrations higher than 25%, the ratio suddenly increased and remained stable. This suggests either an increase of the absorbance at 274 nm or a decrease at 254 nm. Either exposure of tyrosine residues to the surface or movement of the phenylalanine residues back into the interior of the protein, or both, could result in such a spectral change. The data do not allow us to decide which of these phenomena are occurring.

Lysozyme contains all three aromatic amino acid residues, interpretation of the results obtained with this protein is consequently more complex. However, a drop in the A_{274}/A_{254} ratio was noticeable when the level of acid was higher than 30%. Recognition that the tyrosine residues do not move to the interior of the protein could suggest that tryptophan residues do. The two other ratios, A_{292}/A_{274} and A_{292}/A_{254} showed a decrease for a concentration of acid near 30%. Both suggest a greater exposure of the tyrosine or a lower exposure of the tryptophan residues to the mobile phase.

Second-derivative spectroscopy. One major inconvenience in the use of absorbance ratios is the overlapping of the tryptophan band with the tyrosine and phenylalanine spectra. Second-derivative spectroscopy has been shown to be an effective tool for differentiating between contributions of each amino acid residue to the UV spectra of proteins[24]. More recently, it has been applied to the determination of

tyrosine exposure in proteins[25]. This technique has also been used to obtain information on conformational changes of proteins during chromatography[23]. The limitation of this method is that in order to obtain satisfactory precision in the observation of tyrosine movement, it is necessary that the protein contains twice as much tyrosine as tryptophan. Of the proteins studied in this work, OVA fulfills this requirement (Table II). Table III gives the results obtained for the measurement of the *a/b* ratio for different acid concentrations, where *a* and *b* indicate the peak-to-peak distances between the maximum at 288 nm and the minimum at 283 nm and the maximum at 296 nm and the minimum at 292 nm, respectively. This ratio has been shown to reflect the exposure of tyrosine to the surface[25]. Each value is the average of at least four measurements. The maximum difference obtained between them is also reported in this table. These data reveal a slight increase in the *a/b* ratio, which reflects an increase in the exposure of tyrosine residues to the exterior of the protein. These results are in agreement with the one obtained above in the measurement of absorbance ratios.

It is now possible to state that for acid concentrations higher than 30%, the decrease in protein retention is not due only to the higher solvophilic power of formic acid relative to water but also to various conformational states of the proteins. Spectroscopic measurements display a decrease in the A_{292}/A_{274} and A_{292}/A_{254} absorbance ratios. This observation, plus the increase in the *a/b* ratio obtained in second-derivative spectroscopy, reveals the movement of the tyrosine residues to the exterior of the protein. It is not possible to visualize the movement of any of the aliphatic amino acid residues, but it is probable that the behavior of tyrosine is representative for most of the residues containing a polar group. This largely influences the solubility of the proteins in the chromatographic eluent, and their retention. These results are consistent with the fact that high concentrations of acid are effective in the chromatography of large, hydrophobic proteins.

Refolding of proteins

A major concern in any chromatographic method is the conservation of the activity of the proteins. In RPC, the nature of the eluents causes the unfolding of polypeptides. However, it is possible for some proteins to regain their activity when the acid and organic solvent are removed. Ribonuclease A is well known for its refolding capability and OVA for its irreversible unfolding. Luiken *et al.*[9] have used

TABLE III

SECOND-DERIVATIVE SPECTROSCOPY OF OVALBUMIN (*a/b* RATIOS FOR DIFFERENT FORMIC ACID CONCENTRATIONS)

Formic acid concentration	*a/b Ratio*
10	0.79 ± 0.06
30	0.71 ± 0.04
60	0.84 ± 0.04
80	0.94 ± 0.04

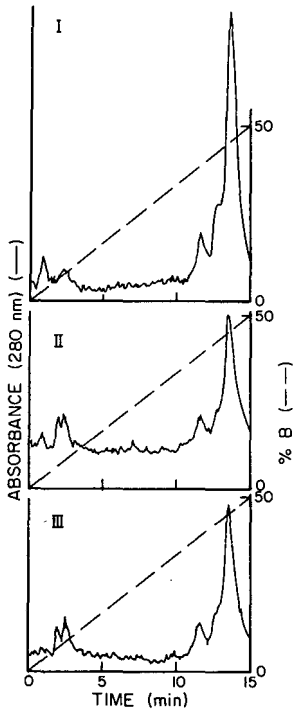

Fig. 6. Chromatographic pattern of ribonuclease A in cation-exchange chromatography. (I) native enzyme, (II) after RPC, 0.1% formic acid, (III) after RPC with 80% formic acid. For chromatographic conditions see Materials and Methods section.

ion-exchange chromatography to demonstrate the structural changes observed in these proteins after RPC. The same technique has been applied in our work for proteins eluted with 0.1% and 80% aq. formic acid. The treatment applied to the proteins collected after RPC is described in the Methods section.

For ribonuclease A, the chromatographic profiles obtained in cation-exchange chromatography are the same for native enzyme and the protein eluted from the RPC column with 0.1 and 80% aq. formic acid (Fig. 6). Furthermore, the measurement of the regain of activity (*a*) for ribonuclease A was comparable for 80% and 0.1% aq. formic acid elution. A ratio of $a_{80}/a_{0.1}$ of 95% was obtained, confirming that the high concentration of formic acid does not compromise the refolding of this protein. For OVA, the precipitate obtained after lyophilization of the fractions collected in both acid concentrations could not be solubilized in phosphate buffer.

These results show that the use of harsh conditions, like 80% aq. formic acid, still allows the refolding of some proteins. Perhaps the renaturation of proteins denatured with high concentrations of formic acid will not be more difficult than that of proteins denatured with 0.1% TFA.

Chromatography of IgG

IgG is a large protein (150 kD) whose analysis by RPC is difficult due to its

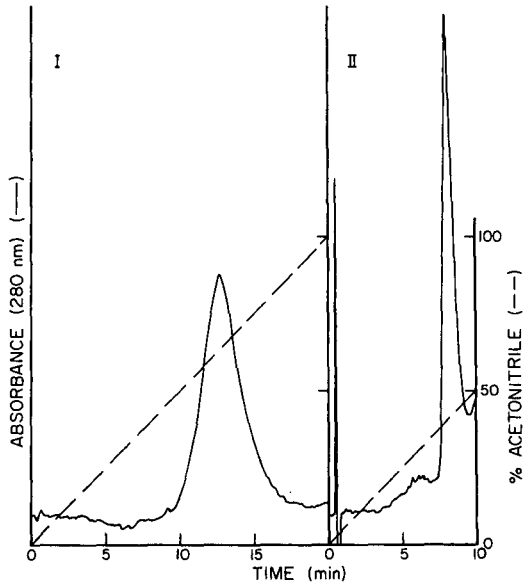

Fig. 7. Chromatographic pattern of IgG with (I) 0.1% formic acid, (II) 80% formic acid and a 20-min linear gradient of acetonitrile.

hydrophobicity. Usually, standard RPC elution with 0.1% TFA or 0.1% formic acid in acetonitrile results in a broad peak, as shown in Fig. 7. The improvement in the efficiency at 80% aq. formic acid is obvious.

An important consideration in any chromatographic method is solute recovery. Recovery of IgG from RPC columns with 0.1% TFA–acetonitrile can be very low. It was of interest to determine whether the improvement in peak shape was accompanied by a better protein recovery. Table IV reveals that the recovery is comparable for 0.1 and 80% aq. formic acid. However, better peak shape, and no additional loss in recovery make the use of 80% of formic acid a useful procedure in the RPC of IgG.

Stability of the chromatographic sorbent

All results presented in this paper have been obtained with poly(styrene–divinylbenzene). The use of high concentrations of acid had little effect on the chroma-

TABLE IV

RECOVERY OF RABBIT IgG FOR VARIOUS FORMIC ACID CONCENTRATIONS

Formic acid concentration	*Recovery (%)*
0.1	73
60	75
80	69

tographic performance of the column. Retention and peak shape for proteins were identical before and after this study[28].

CONCLUSIONS

Our results suggest that the role of acid in reversed-phase chromatography of proteins is dependent on its concentration. At concentrations of less than 10%, the acid acts both as a denaturant and as an amine pairing agent. This induces an increase in the retention of the protein when the acid concentration increases. At higher concentrations of acid, ranging from 10–30%, further denaturation of proteins occurs, with a migration of hydrophobic residues from the interior of the protein to more accessible regions on the exterior of the structure. The overall effect of this migration is an increase of the hydrophobicity of the solute and, consequently, an increase in retention. At concentrations of acid greater than 30%, the solution becomes so polar that hydrophobic residues begin to migrate into the interior of some highly denatured structure. Both, absorbance ratio measurements and second derivatives, have shown that tyrosine residues are more exposed to the exterior of the protein when the acid concentration increases. Accumulation of hydrophilic amino acids on the exterior of the molecule, plus the higher solvophilic power of formic acid compared to water result in a decrease in proteins retention. In general, this means that alterations in the hydrophobic amino acids of a protein will be most easily detected at intermediate acid concentrations; *i.e.*, 10–30%. These studies also suggest that, unless a polypeptide contains hydrophilic amino acids that may be forced to the exterior, high concentrations of acid will not be particularly effective in increasing solubility.

ACKNOWLEDGEMENTS

We thank Polymer Labs for their gift of PLRP-S poly(styrene–divinylbenzene). This work was supported by NIH Grant number GM 25431. This is paper No. 11844 of the Purdue University Agricultural Experiment Station.

REFERENCES

1 F. E. Regnier, *Science (Washington, D.C.)*, 238 (1987) 319.
2 K. A. Tweeten and T. N. Tweeten, *J. Chromatogr.*, 359 (1986) 111.
3 D. P. Lee, *J. Chromatogr.*, 443 (1988) 143.
4 D. P. Lee, *J. Chromatogr. Sci.*, 20 (1982) 203.
5 K. D. Nugent, W. G. Burton, T. K. Slattery, B. F. Johnson and L. R. Snyder, *J. Chromatogr.*, 443 (1988) 381.
6 A. J. Sadler, R. Micanovic, G. E. Katzenstein, R. V. Lewis and C. R. Middaugh, *J. Chromatogr.*, 317 (1984) 93.
7 G. E. Katzenstein, S. A. Vrona, R. J. Wechsler, B. L. Steadman, R. V. Lewis and C. R. Middaugh, *Proc. Natl. Acad. Sci. U.S.A.*, 83 (1986) 4268.
8 S. Y. Lau, A. K. Taneja and R. S. Hodges, *J. Chromatogr.*, 317 (1984) 129.
9 L. Luiken, R. van der Zee and G. W. Welling, *J. Chromatogr.*, 284 (1984) 482.
10 S. A. Cohen, K. P. Benedek, S. Dong, Y. Tapuhi and B. L. Karger, *Anal. Chem.*, 56 (1984) 217.
11 S. A. Cohen, K. P. Benedek, Y. Tapuhi, J. C. Ford and B. L. Karger, *Anal. Biochem.*, 144 (1985) 275.
12 X. M. Lu, A. Figueroa and B. L. Karger, *J. Am. Chem. Soc.* 110 (1988) 1978.
13 F. E. Regnier, *J. Chromatogr.*, 418 (1987) 115.
14 J. Heukeshoven and R. Dernick, *J. Chromatogr.*, 252 (1982) 241.

15 J. Heukeshoven and R. Dernick, *J. Chromatogr.*, 326 (1985) 91.
16 W. C. Mathoney and M. A. Hermodson, *J. Biol. Chem.*, 255 (1980) 1199.
17 G. B. Irvine and C. Saw, *Anal. Biochem.*, 155 (1986) 141.
18 H. P. J. Bennett, C. A. Browne and S. Solomon, *J. Liq. Chromatogr.*, 3 (1980) 1353.
19 W. C. Mahoney, *Biochim. Biophys. Acta*, 704 (1982) 284.
20 L. Stryer, *Biochemistry*, W. H. Freeman, New York, 2nd ed., 1981, p. 57.
21 J. E. Falk, *Porphyrins and Metalloporphyrins* (*B.B.A. Library*, Vol. 2), Elsevier, Amsterdam.
22 C. Balestrieri, G. Colonna, A. Giovane, G. Irace and L. Servillo, *Eur. J. Biochem.*, 90 (1978) 433.
23 S. L. Wu, K. Benedek and B. L. Karger, *J. Chromatogr.*, 359 (1986) 3.
24 T. Ichikawa and H. Terada, *Biochim. Biophys. Acta*, 494 (1977) 267.
25 R. Ragone, G. Colonna, C. Balestrieri, L. Servillo and G. Irace, *Biochemistry*, 23 (1984) 1871.
26 J. R. Whitaker and S. R. Tannenbaum, *Food Proteins*, AVI Puslishing Company, Westport, CN, 1977, pp. 218–219.
27 A. L. Lehninger, *Biochemistry*, Worth Publishers, New York, 2nd ed., 1975, pp. 27, 101.
28 G. Thévenon, Y. B. Yang and F. E. Regnier, in preparation.

Author Index

PUBLICATION SCHEDULE FOR 1989

Journal of Chromatography and Journal of Chromatography, Biomedical Applications

MONTH	J	F	M	A	M	J	J	A	S	
Journal of Chromatography	461 462 463/1	463/2 464/1	464/2 465/1 465/2	466 467/1 467/2	468 469 470/1 470/2	471 472/1 472/2 473/1	473/2 474/1 474/2 475	476 477/1 477/2		The publication schedule for further issues will be published later
Bibliography Section		486/1		486/2		486/3		486/4		
Biomedical Applications	487/1	487/2	488/1 488/2	489/1 489/2	490/1 490/2	491/1	491/2	492 493/1	493/2	

INFORMATION FOR AUTHORS

(Detailed *Instructions to Authors* were published in Vol. 445, pp. 453–456. A free reprint can be obtained by application to the publisher, Elsevier Science Publishers B.V., P.O. Box 330, 1000 AH Amsterdam, The Netherlands.)

Types of Contributions. The following types of papers are published in the *Journal of Chromatography* and the section on *Biomedical Applications*: Regular research papers (Full-length papers), Notes, Review articles and Letters to the Editor. Notes are usually descriptions of short investigations and reflect the same quality of research as Full-length papers, but should preferably not exceed six printed pages. Letters to the Editor can comment on (parts of) previously published articles, or they can report minor technical improvements of previously published procedures; they should preferably not exceed two printed pages. For review articles, see inside front cover under Submission of Papers.

Submission. Every paper must be accompanied by a letter from the senior author, stating that he is submitting the paper for publication in the *Journal of Chromatography*. Please do not send a letter signed by the director of the institute or the professor unless he is one of the authors.

Manuscripts. Manuscripts should be typed in double spacing on consecutively numbered pages of uniform size. The manuscript should be preceded by a sheet of manuscript paper carrying the title of the paper and the name and full postal address of the person to whom the proofs are to be sent. Authors of papers in French or German are requested to supply an English translation of the title of the paper. As a rule, papers should be divided into sections, headed by a caption (*e.g.*, Summary, Introduction, Experimental, Results, Discussion, etc.). All illustrations, photographs, tables, etc., should be on separate sheets.

Introduction. Every paper must have a concise introduction mentioning what has been done before on the topic described, and stating clearly what is new in the paper now submitted.

Summary. Full-length papers and Review articles should have a summary of 50–100 words which clearly and briefly indicates what is new, different and significant. In the case of French or German articles an additional summary in English, headed by an English translation of the title, should also be provided. (Notes and Letters to the Editor are published without a summary.)

Illustrations. The figures should be submitted in a form suitable for reproduction, drawn in Indian ink on drawing or tracing paper. Each illustration should have a legend, all the *legends* being typed (with double spacing) together on a *separate sheet*. If structures are given in the text, the original drawings should be supplied. Coloured illustrations are reproduced at the author's expense, the cost being determined by the number of pages and by the number of colours needed. The written permission of the author and publisher must be obtained for the use of any figure already published. Its source must be indicated in the legend.

References. References should be numbered in the order in which they are cited in the text, and listed in numerical sequence on a separate sheet at the end of the article. Please check a recent issue for the layout of the reference list. Abbreviations for the titles of journals should follow the system used by *Chemical Abstracts*. Articles not yet published should be given as "in press" (journal should be specified), "submitted for publication" (journal should be specified), "in preparation" or "personal communication".

Dispatch. Before sending the manuscript to the Editor please check that the envelope contains three copies of the paper complete with references, legends and figures. One of the sets of figures must be the originals suitable for direct reproduction. Please also ensure that permission to publish has been obtained from your institute.

Proofs. One set of proofs will be sent to the author to be carefully checked for printer's errors. Corrections must be restricted to instances in which the proof is at variance with the manuscript. "Extra corrections" will be inserted at the author's expense.

Reprints. Fifty reprints of Full-length papers, Notes and Letters to the Editor will be supplied free of charge. Additional reprints can be ordered by the authors. An order form containing price quotations will be sent to the authors together with the proofs of their article.

Advertisements. Advertisement rates are available from the publisher on request. The Editors of the journal accept no responsibility for the contents of the advertisements.